GL01310

DIC

General GP

Geology and Geophysics of the Southern Raft River Valley Geothermal Area, Idaho, USA

PAUL L. WILLIAMS, DON R. MABEY,
ADEL A. R. ZOHDY, HANS ACKERMANN
DONALD B. HOOVER, KENNETH L. PIERCE,
STEVEN S. ORIEL
U.S. Geological Survey, Denver, Colorado 80225, USA

ABSTRACT

The Raft River valley, near the boundary of the Snake River plain with the Basin and Range province, is a north-trending late Cenozoic downwarp bounded by faults on the west, south, and east. Pleistocene alluvium and Miocene-Pliocene tuffaceous sediments, conglomerate, and felsic volcanic rocks aggregate 2 km in thickness. Large gravity, magnetic, and total field resistivity highs probably indicate a buried igneous mass that is too old to serve as a heat source. Differing seismic velocities relate to known or inferred structures and to a suspected shallow zone of warm water. Resistivity anomalies reflect differences of both composition and degree of alteration of Cenozoic rocks. Resistivity soundings show a 2 to 5 ohm·m unit with a thickness of 1 km beneath a large part of the valley, and the unit may indicate partly hot water and partly clayey sediments. Observed self-potential anomalies are believed to indicate zones where warm water rises toward the surface.

Boiling wells at Bridge, Idaho are near the intersection of north-northeast normal faults which have moved as recently as the late (?) Pleistocene, and an east-northeast structure, probably a right-lateral fault. Deep circulation of ground water in this region of relatively high heat flow and upwelling along faults is the probable cause of the thermal anomaly.

INTRODUCTION

A flow of about 2000 l/min of water at bottomhole temperatures of 147°C has been produced from a 1526-m-deep well completed in the Raft River valley, southern Idaho, early in 1975. The well was drilled after an integrated geologic, geophysical, and hydrologic exploration program begun a year and a half earlier by the U.S. Geological Survey (USGS) in cooperation with the Energy Research and Development Administration (ERDA). Drilling of additional wells is now (May 1975) in progress.

The southern Raft River valley near Bridge, Idaho (Fig. 1), was designated a Known Geothermal Resource Area (KGRA) in 1971 by the USGS (Godwin et al., 1971) on the basis of two shallow wells—Bridge and Crank—that flow boiling water (Fig. 2). The boiling wells and geochemical thermometry suggesting temperatures of about 150°C at depth had sparked ERDA's interest in the area as a potential site for an experimental binary-fluid geothermal power plant. The USGS studies were undertaken to provide a scientific framework for evaluation of the resource and to test the applicability of various geophysical and geologic techniques to the study of geothermal resources, and to aid in siting test wells.

The Raft River valley is part of an area mapped geologically

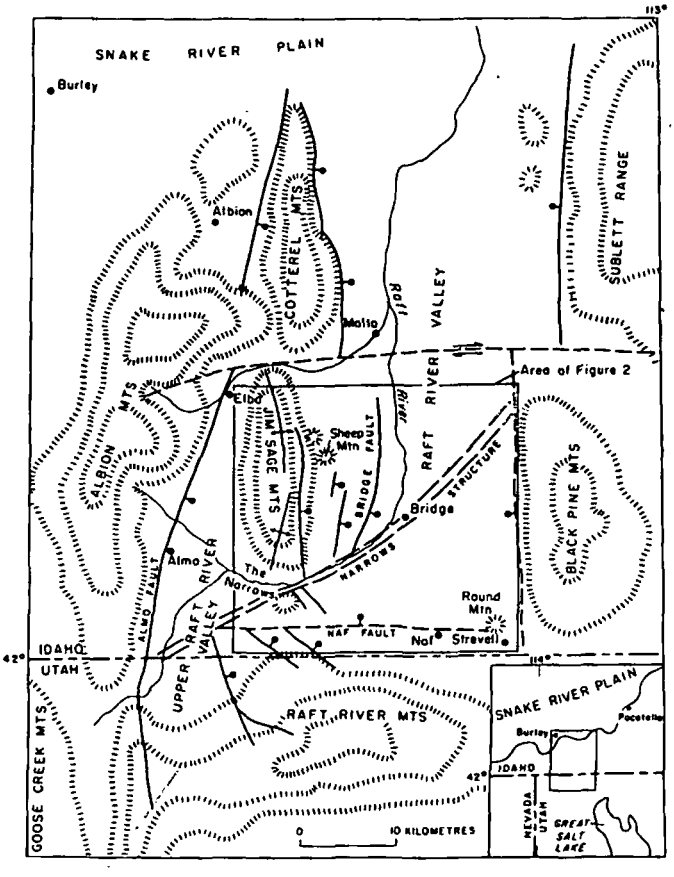

Figure 1. Map of the Raft River valley region, Idaho and Utah, showing major faults (bar and ball on downthrown side; arrows indicate relative direction of movement) and anitclines (Jim Sage Mountains only).

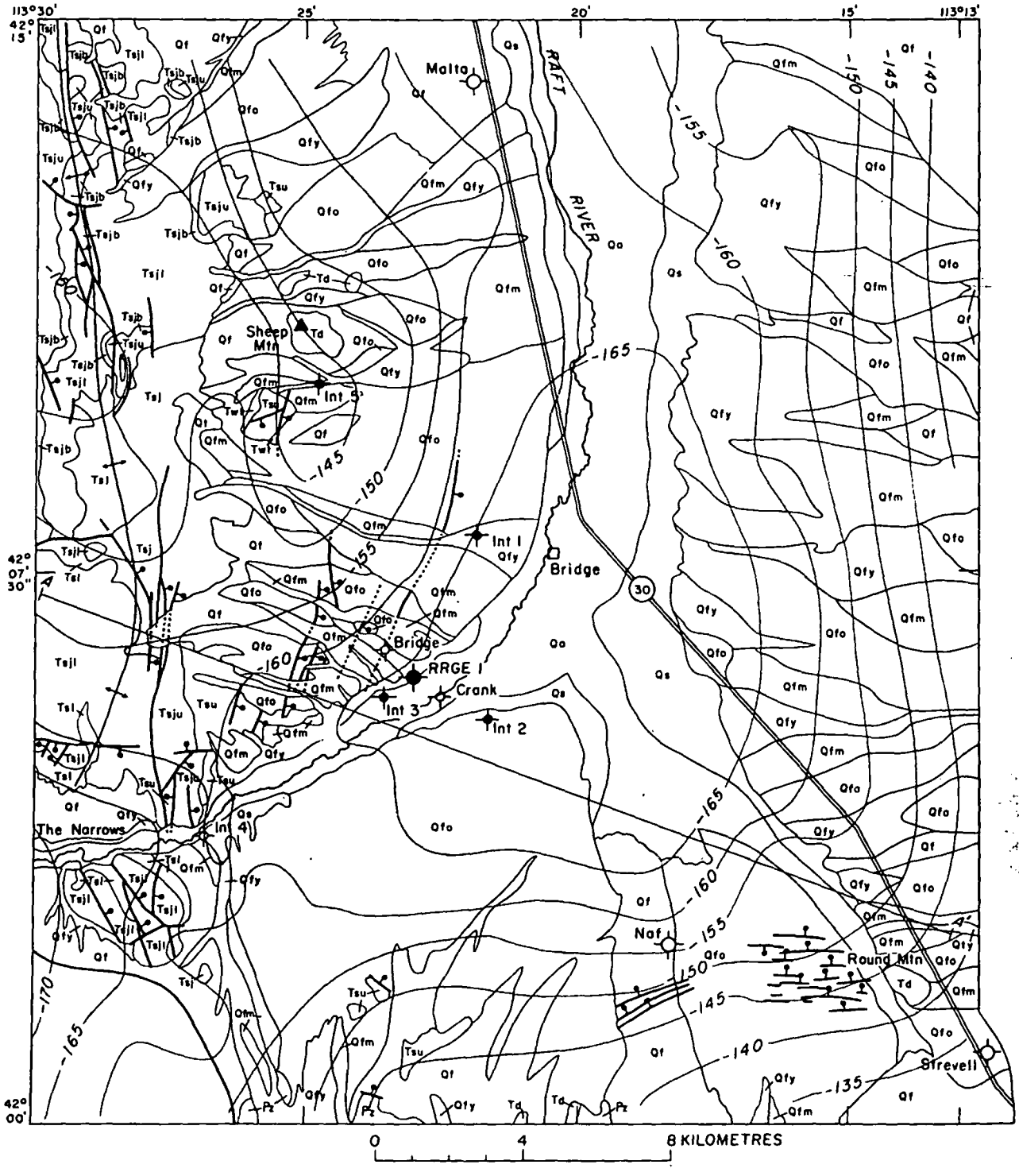

Figure 2. Geologic and gravitational features of the southern Raft River valley. *Left*, area map showing Bouguer gravity units in the area map and the cross section and a key to

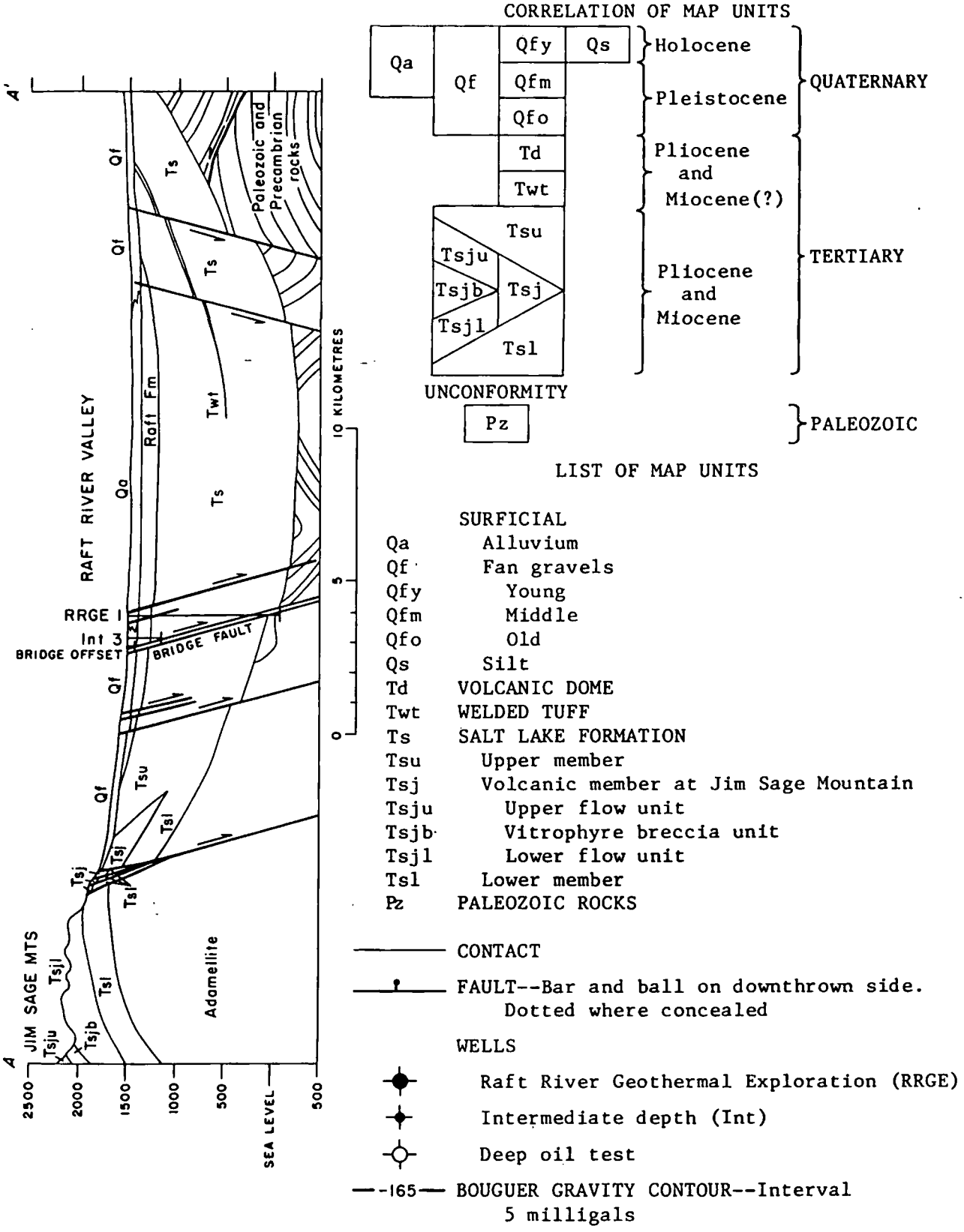

contours, wells and geology. *Right,* cross section through AA' on the area map. *Far right,* correlation and list of geologic map symbols. Geology based on Williams et. al. (1974).

in reconnaissance by A. L. Anderson (1931). Ground-water studies by the USGS have been carried out over a period of four decades (Stearns, Crandall, and Steward, 1938; Nace et al., 1961; Mundorff and Sisco, 1963; and also Walker et al., 1970, in cooperation with the Idaho Department of Water Administration). Geochemistry of the water from the Bridge and Crank wells is described by Young and Mitchell (1973).

SURFACE MANIFESTATIONS AND EXPLORATION

The presence of a geothermal reservoir in the southern Raft River valley is evident in only a few places. There is a warm seep (38°C) near Intermediate depth well (Int) in The Narrows (Fig. 2), and altered alluvium around the Bridge well marks the site of a former hot spring. Total dissolved solids in water from the Bridge and Crank wells are 1720 and 3360 ppm, respectively; aquifer temperatures inferred from the silica and Na-K-Ca geothermometers (Young and Mitchell, 1973) are nearly the same as the maximum temperature (147°C) measured in the first deep exploration well, RRGE 1. There are no tufa or sinter mounds. Gray Tertiary tuffaceous sediments are altered to light green and locally weather to yellow; accumulations of chalcedony locally are present. Lava and flow breccia exposed in The Narrows are altered from black and brown to yellow along faults and fractures, but plagioclase feldspars remain fresh. The green and yellow colors probably indicate formation of montmorillonitic clays, proving definite but weak and nonpervasive hydrothermal alteration (C. R. Nichols, oral commun., 1974).

The limits of the geothermal reservoir remain undefined. Warm water flows from several irrigation wells throughout the Raft River valley, and temperatures of 70°C were measured on the surface in water leaking from a completed but nonproductive oil test drilled near Malta (Fig. 1). Water temperatures of 60 and 38°C, respectively, were measured in wells northeast of Albion and near Almo (Fig. 1); (Young and Mitchell, 1973).

Initial shallow drilling was begun by the USGS cooperatively with ERDA in 1974 to determine temperatures and flow in the shallow aquifer. A total of 32 auger holes were drilled to depths of about 30 m in and near the Raft River flood plain between Bridge and The Narrows. An offset to the Bridge well was drilled to a depth of 123 m. In 1974 and early 1975, five core holes were drilled in cooperation with Idaho Department of Water Administration to intermediate depths of 76 to 434 m to test hydrological, geophysical, and geologic models; the deepest of these, No. 3, encountered water at 90°C near the bottom. The first deep hole, Raft River Geothermal Exploration (RRGE) 1, was drilled by a commercial contractor for ERDA, and was completed early in April 1975 to a depth of 1526 m. The Bridge fault zone was intersected between 1240 and 1300 m, and yielded a flow of about 40 l/sec at subsurface temperatures of 140 to 147°C. Cuttings from oil tests near Malta, Naf, and Strevell (Fig. 1) also yielded valuable information on the geology of the basin.

GEOLOGIC SETTING

The lower Raft River valley in southern Idaho lies in a north-trending basin both warped and downfaulted in late Cenozoic time. The basin is in the northern part of the Basin and Range province near its boundary with the Snake River plain. About 60 km long and 20 to 24 km wide, with an average surface elevation of 1400 m, the basin is filled with Cenozoic sediments to an inferred depth of 1800 to 2000 m. The Raft River flows northward through the basin, which opens onto the Snake River plain. North of the Raft River basin is the prominent Great Rift system of open fractures in very young basalt flows that extends northward 50 km to Craters of the Moon National Monument. The basin is flanked on the west, east, and south by mountain ranges made up of Tertiary, Paleozoic, and Precambrian rocks, respectively. On the east are the Sublett Range (higher elevations about 2000 m) and the Black Pine Mountains (2900 m) consisting mainly of faulted Pennsylvanian and Permian sedimentary rocks (R. L. Armstrong and J. F. Smith, Jr., oral commun., 1974). On the west, the Cotterel and Jim Sage Mountains (2500 m), formerly grouped as the Malta Range, are made up of Tertiary rhyolites and tuffaceous sediments, which in the Jim Sage Mountains define a broken antiform structure, as first noted by Martin Pruatt (oral commun., 1973). Directly to the west of the Cotterel and Jim Sage Mountains, and separated from them by a narrow fault valley, lie the Albion Mountains (3000 m). Rising southward from the basin are the Raft River Mountains (3000 m), one of the few east-trending mountain ranges in the North American Cordillera. The Albion and Raft River Mountains expose gneiss-dome complexes of Precambrian (2.4 billion years) adamellite (quartz monzonite) mantled by Precambrian and lower Palcozoic metasedimentary rocks and by allochthonous upper Paleozoic sedimentary rocks (Felix, 1956; Armstrong, 1968; Compton, 1972). Drill data are demonstrating that the metamorphic complex directly underlies extensive parts of the Cenozoic fill of the Raft River basin. Borehole cuttings from the Malta and Strevell oil tests indicate the presence of metamorphic units resembling those in the Raft River Mountains, and not a thick succession of unmetamorphosed Paleozoic rocks that would have been inferred from outcrops.

Rock units and surficial deposits recognized in the southern Raft River basin and adjacent ranges are summarized in Table 1. Pre-Tertiary units are those described by Compton (1972); most of these units do not crop out in the mapped area (Fig. 2).

GEOPHYSICAL STUDIES

Gravity Measurements

Gravity stations were established at 330 points in the area of Figure 2. The data were reduced to the complete Bouguer anomaly assuming a density of 2.45 g/cm^3. The procedures used were designed to produce Bouguer anomaly values accurate to 0.2 mgal (milligal) except in areas of high local topographic relief where the uncertainty in the terrain correction may be as large as 0.4 mgal. The gravity map of the region (Mabey and Wilson, 1973) shows a series of lows along the entire course of the Raft River; the low in the southern Raft River basin is one of these. Bouguer anomalies rise toward highs over the Black Pine and Raft River Mountains and a high centered over the alluvium south of Sheep Mountain in the eastern Jim Sage Mountains. The gravity low is produced mostly by the density contrast between the Cenozoic sedimentary and volcanic rocks, calculated from the data to be about 2 km thick, and the

Table 1. Rock units and surficial deposits of the southern Raft River basin and adjacent ranges. Letter symbols refer to map units in Figure 2.

Age	Description
Quaternary	
Holocene and Pleistocene	Alluvial and eolian silt (Qs). Alluvium of major drainage (Qa)
	Fan alluvium: Coarse to fine, moderately well-sorted subangular gravel on piedmont slopes. Young gravels (Qfy) deposited during last pluvial episode; middle gravels (Qfm) deposited during last 2 or 3 pluvial episodes; old gravels (Qfo) older than third oldest pluvial episode; age of undivided gravels (Qf) was not determined.
Pleistocene	*Raft Formation: Sand, gravel, silt and clay beneath Raft River Valley (Fig. 2)
Tertiary	
Pliocene and Miocene (?)	Volcanic domes (Td). Extrusive and shallow intrusive glassy and lithoidal rhyolite domes containing plagioclase phenocrysts at and north of Sheep Mountain, at Round Mountain, and along south edge of map area. Radiometric ages are: Sheep Mountain dome, 7.8 ± 1.1 m.y. (zircon fission-track, C. W. Naeser, U.S.G.S.) and 8.42 ± 0.20 m.y. (K-Ar feldspar, J. D. Obradovich, U.S.G.S.); Round Mountain dome, 8.3 ± 1.7 m.y. (zircon fission-track, C. W. Naeser).
	Welded tuff (Twt). Thin glassy rhyolite ash-flow tuff on Cedar Knoll, and in Malta and Naf wells. Radiometric age, 7.0 ± 2.0 m.y. (zircon fission-track, C. W. Naeser). Intercalated in upper member of Salt Lake Formation.
Pliocene and Miocene	Salt Lake Formation. Total thickness, about 1800 m. In western part of basin, divided by volcanic member at Jim Sage Mountain into upper and lower members. Tuffaceous sandstone, siltstone and conglomerate. In RRGE 1, the upper 670 m is light-green and gray tuffaceous sandstone and siltstone and coarse-grained sandstone and conglomerate; the lower 570 m is light-green bedded tuff, tuffaceous siltstone and sandstone, and tan calcareous siltstone and laminated shale. In the Naf well, the upper 1000 m is dominantly gray and tan tuffaceous sandstone and siltstone; the lower 260 m is mostly conglomerate and sandstone.
	Upper member (Tsu); Gray and light-green tuff, tuffaceous sandstone and siltstone, and buff and gray conglomerate.
	Volcanic member at Jim Sage Mountain: Consists of rhyolite flows (Tsj), divided into upper (Tsju) and lower (Tsjl) units where separated by a vitrophyre breccia unit (Tsjb). Flows 1 to 50 m thick of black glassy and red-brown porphyritic-aphanitic calc-alkali rhyolite containing phenocrysts of oligoclase-andesine and pigeonite; upper unit has normal magnetic polarity; most flows in lower unit are magnetically reversed. Vitrophyre breccia unit consists of black glass clasts a few centimeters to 2 m in diameter in a yellow and orange matrix of hydrated glass; rare tongues of glassy lava have reversed magnetic polarity; unit replaced laterally by bedded tuff in southern Jim Sage Mountains. Radiometric dates on upper flow unit: 9.2 ± 0.5 m.y. (K-Ar whole rock, Armstrong, Leeman, and Malde, 1975); 9.4 ± 1.6 m.y. (zircon fission-track, C. W. Naeser).
	Lower member (Tsl): Gray and white, thin-bedded to massive, tuff and tuffaceous sandstone, white to light-green shale and siltstone, and sparse beds of fine-grained conglomerate.
Permian and Pennsylvanian	Oquirrh Formation: Dark-gray sandy limestone and calcareous sandstone
Pennsylvanian and Mississippian	*Manning Canyon (?) Shale: Dark-gray phyllite
Ordovician	*Fish Haven (?) Dolomite: Gray and cream-colored metamorphosed dolomite
	*Eureka (?) Quartzite: White metaquartzite
	Pogonip (?) Group, Undivided: Tan-weathering impure marble
Cambrian (?)	*Schist of Mahogany Peaks: Dark-brown biotite-muscovite schist
	*Quartzite of Clarks Basin: Quartzite with thin muscovite-biotite schist interbeds
Precambrian (?)	*Schist of Stevens Springs: Fine-grained muscovite-quartz schist and graphite phyllite
	*Quartzite of Yost: White, locally green, muscovitic and hematitic quartzite
	*Schist of upper Narrows: Dark-brown biotite quartzofeldspathic schist and gneiss; occurs in RRGE 1 from 1390 to 1433 m
	*Elba Quartzite: White to pale-tan muscovitic quartzite. Occurs in RRGE 1 at 1433 to 1518 m
Precambrian	*Older schist: Brown mica schist
	*Adamellite: Bodies of massive and gneissic porphyritic adamellite; in part intrusive into Precambrian (?) metamorphic rocks and in part older than those rocks. Forms gneiss domes in western Raft River Range and Albion Range. Occurs in RRGE 1 below 1518 m

* Unit does not crop out in map area, but is present in nearby area and/or in subsurface.

more dense pre-Cenozoic "basement" rocks. Relatively small variations in the gravity field superimposed on the large low may reflect mass anomalies within the Cenozoic rocks or within the basement rocks.

Aeromagnetic Data

An aeromagnetic survey of part of the area was flown with north-south flight lines 800 m apart and 1800 m above sea level. The magnetic data are shown as a residual map in Figure 3. On the east side of the Jim Sage Mountains the magnetic anomalies correlate with the mapped distribution of volcanic rocks. Major highs and lows are associated with normally and reversely magnetized units. A general correlation between magnetic intensity and the gravity high south of Sheep Mountain suggests that the basement rock is slightly magnetic. The absence of large magnetic anomalies within the area of the major gravity low suggests that volcanic rock is not a major part of the basin fill. Two elongate magnetic highs south and east of Sheep Mountain may be produced either by volcanic rocks or by magnetic units within the basement rocks.

Seismic Refraction Measurements

Seismic refraction spreads were obtained in an area extending from the large gravity low in the central part of the Raft River valley (Fig. 4) southwestward into The Narrows and westward from the low, across alluvial fans east of the Jim Sage Mountains. All spreads were shot from both directions, but complete reverse basement coverage was obtained on only part of the spreads.

Three major velocity units were mapped: 5.2 to 6.7 km/sec for the pre-Tertiary basement rocks, about 4 km/sec for Tertiary volcanic rocks, and less than 4 km/sec for Tertiary sedimentary rocks.

Three areas of different seismic velocities that correlate well with geologic and topographic features were defined in the Cenozoic rocks. One area is confined largely to the central part of the valley, but it also extends lower parts of the alluvial fans. In most places the velocity sections are typical of those expected from a basin containing a thick succession of poorly consolidated sediments. The second area is confined to the alluvial fans. Velocities in the range expected for lava flows (higher than those encountered at comparable depth in the first area) occur at depths

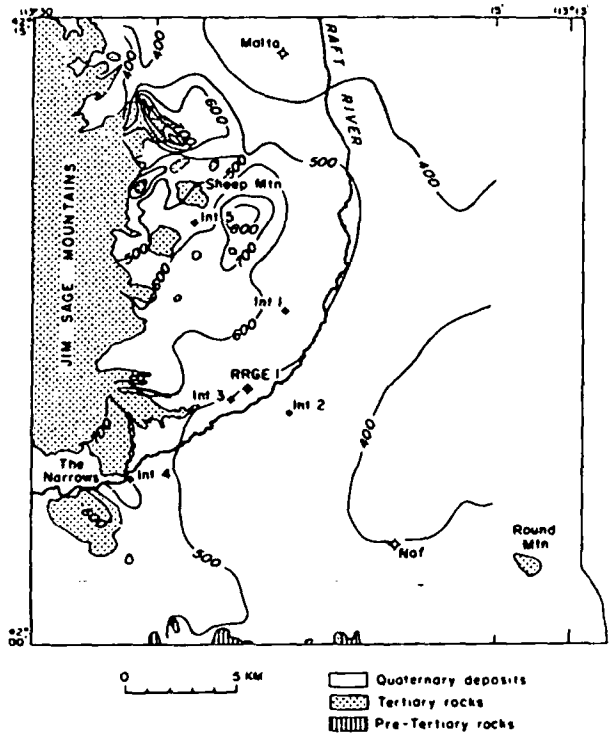

Figure 3. Aeromagnetic map of the southern Raft River valley. *Contour interval 100 gammas.*

less than 400 m. The third area is in and near The Narrows where high-velocity rocks (volcanics) are near the surface.

A typical velocity regime for water-saturated unconsolidated or partly consolidated basin fill is a gradual velocity increase with depth from about 1.5 to 2.5 km/sec. Much of the valley area is underlain by rocks of these velocities; nowhere do interpreted velocities exceed 3.0 km/sec. From the Bridge fault to The Narrows in a strip about 1.5 km wide, layers with 2.5 km/sec velocities are within a few tens of meters below the surface, suggesting hydrothermal induration of the sediments.

Basement velocities vary between approximately 5.2 and 6.7 km/sec, probably indicating lithologic differences or local fracturing.

Audiomagnetotelluric Soundings

Sixty-eight audiomagnetotelluric (AMT) sounding stations were occupied in the southern Raft River valley. At each station two soundings were made, one for a north-south and the other for an east-west orientation of the telluric line. Scalar resistivities were calculated at each of 10 frequencies in the range 8 to 18600 Hz to define the sounding curves, and maps were prepared for several of the frequencies to delineate areas of anomalous conductivity. The station spacing of 2 to 3 km defines only the gross conductivity variations in the area.

Figure 5 shows two AMT apparent-resistivity maps made at 26 Hz for each orientation of the telluric line. Differences in the maps reflect the presence of lateral resistivity variations near the sounding site. The range in apparent resistivity values is from about 2 to 200 ohm·m at 26 Hz. The skin depths (which are the approximate exploration depth) for these resistivities at 26 Hz are 140 to 1400 m.

Examination of the two AMT maps shows that the most prominent resistivity high is just east of The Narrows. This correlates with a north-trending structural high seen on the gravity map and a correlative high in the total field data. The differences in apparent resistivity between the two orientations indicate that the edge of the body was close to the station, and together with the gravity anomaly imply a narrow body. Fair correlation is evident between the AMT high and the gravity high near Sheep Mountain. The largest AMT low, in the vicinity of the hot wells, is defined by the 14-ohm·m contour.

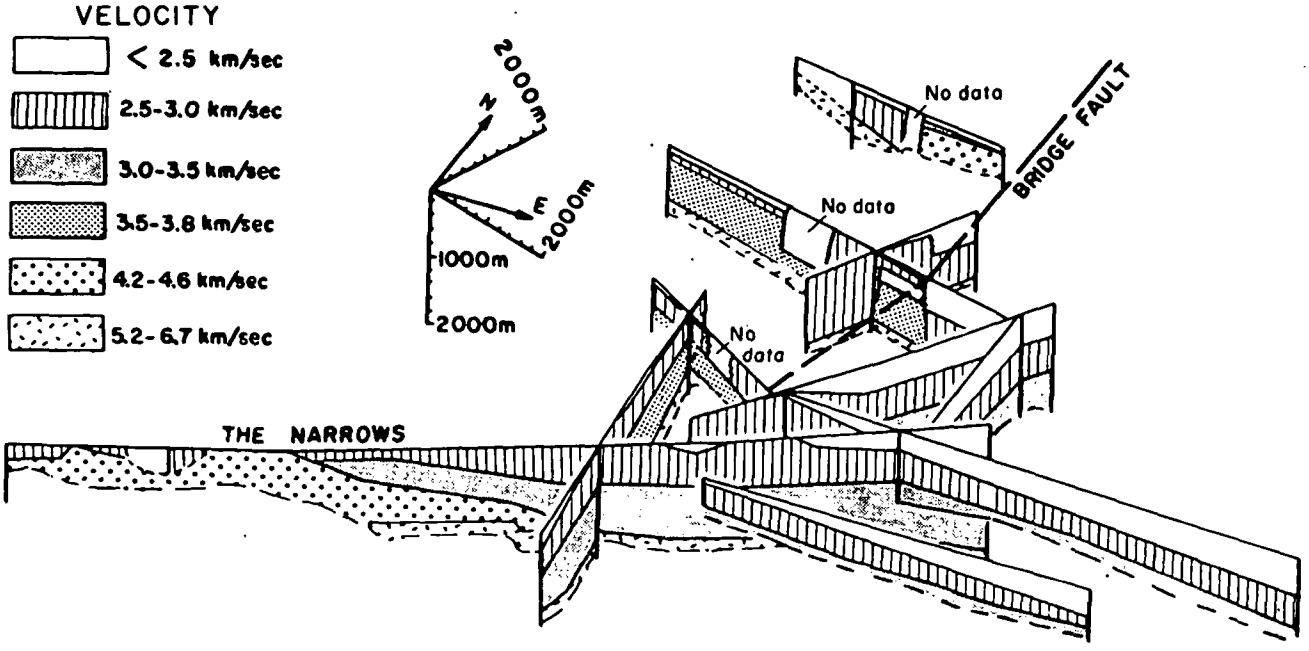

Figure 4. Seismic profiles of the southern Raft River valley.

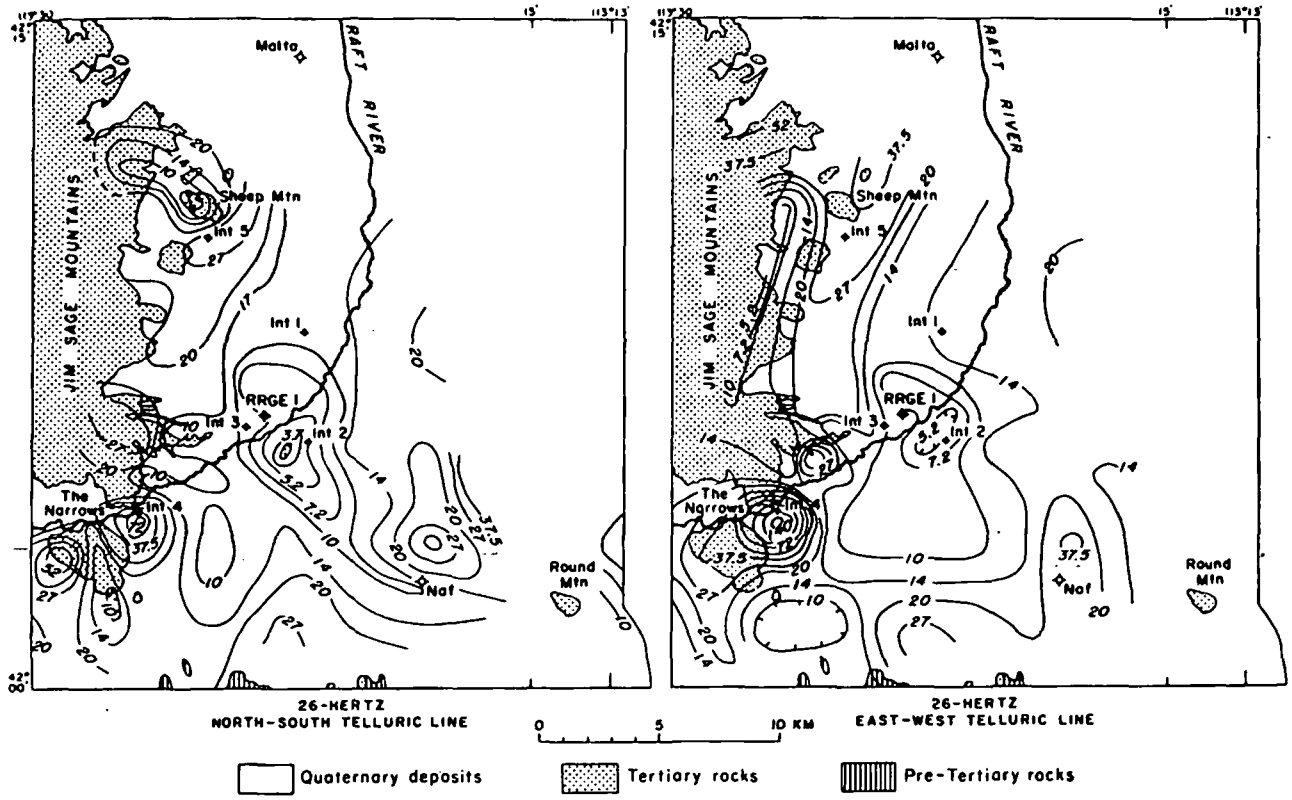

Figure 5. Audiomagnetotelluric apparent-resistivity maps of the southern Raft River valley. Resistivity contours shown are a logarithmic interval in ohm·meters.

Direct-Current Resistivity Survey

A bipole-dipole total field resistivity survey consisting of 269 total field stations occupied about a current bipole 3.22 km long. At each station the potential differences were recorded between three potential electrodes (M, N, and N') placed at the corners of a triangle and the electric field components were calculated from the approximations.

$$E_{MN} = \frac{V_{MN}}{MN}, \quad E_{MN'} = \frac{V_{MN'}}{MN'}, \quad E_{NN'} = \frac{V_{NN'}}{NN'}$$

These three components were added vectorially, using polar plots, to obtain the direction and the magnitude of the total electric field E_T. The lengths of the sides of the measured triangle ranged roughly from 30 to 100 m. Electric currents in the range of 40 to 60 A were provided from a 40-kVA truck-mounted generator, and the differences in potential at the field stations were measured on potentiometric chart recorders.

Figure 6 shows the normalized (or reduced) apparent-resistivity map which is obtained by calculating the ratio between the observed and theoretical apparent resistivities for horizontal layering beneath the center of the current bipole (Zohdy, 1973; Zohdy and Stanley, 1974). In general, areas outlined by values greater than unity indicate that the section contains more resistive materials or that basement rocks are shallower than at a sounding made at the current bipole, or both. Conversely, areas outlined by contour values less than unity designate the opposite. It should be noted, however, that false lows and highs may be caused by the

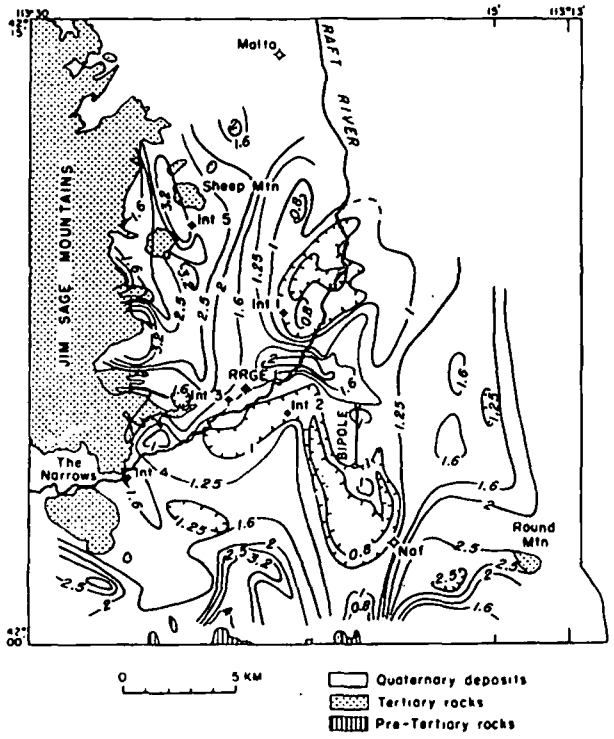

Figure 6. Normalized bipole-dipole resistivity map of the southern Raft River valley. Resistivity contours shown are a logarithmic interval in ohm·meters.

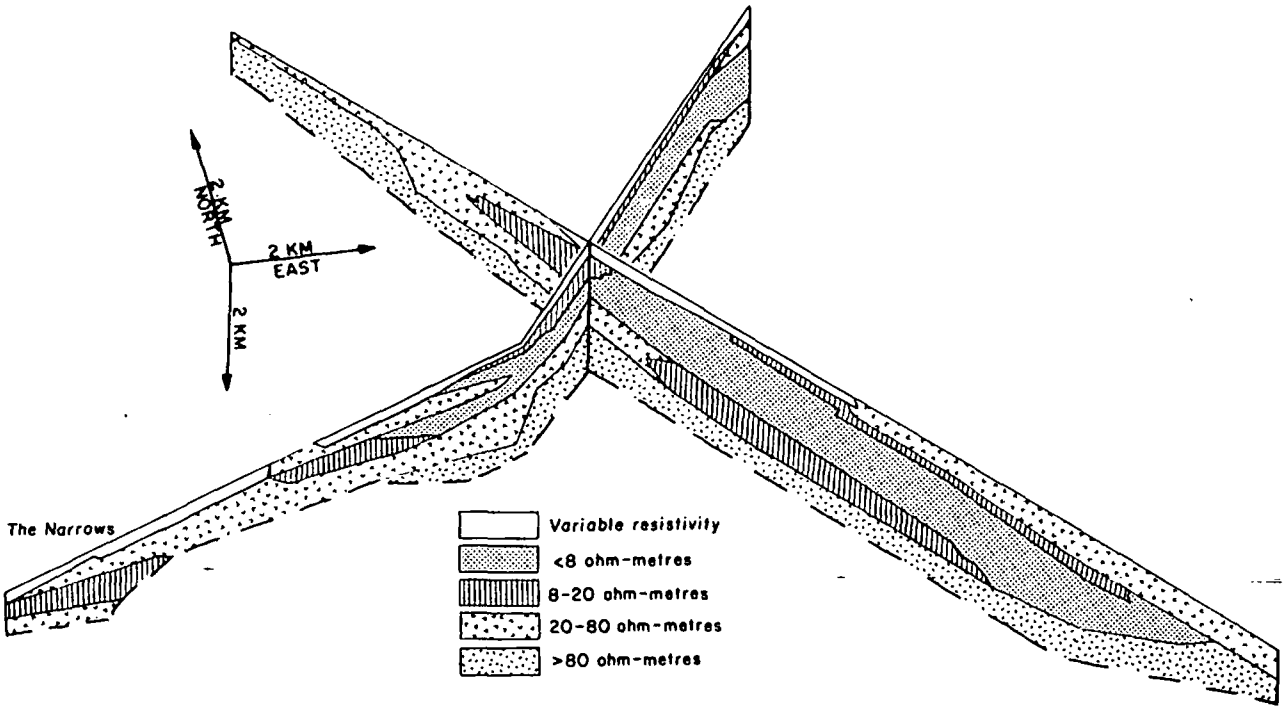

Figure 7. Resistivity profiles of the southern Raft River valley.

presence of steeply dipping faults separating media of large differences in resistivity.

Seventy-nine symmetric Schlumberger soundings were made. The maximum electrode spacing ($AB/2$) for most soundings ranged from $AB/2$ = 914 m (3000 ft) to $AB/2$ = 3660 m (12000 ft). All the soundings were automatically processed and interpreted (Zohdy, 1974a, 1975; Zohdy, Jackson, and Bisdorf, 1975) using a DEC-10 digital computer and a Hewlett Packard 7203A graphic plotter. Equivalent solutions to the automatically obtained ones were derived by adjusting the corresponding D. Z. (Dar Zarrouk) curves (Zohdy, 1974b).

Figure 7 shows two resistivity sections based on some of these soundings. The high-resistivity material (>80 ohm·m) underlying most of the section is pre-Cenozoic basement rock. Resistivities between 20 and 80 ohm·m probably reflect volcanic rock or coarse clastic sediments. Resistivities below 20 ohm·m are probably finer-grained sediments. In the middle part of both sections is a low-resistivity layer (3 to 8 ohm·m) in the Salt Lake formation with an average thickness of about 1 km. Drilling data indicate that this layer is fine grained, consisting of silt and clay, and is weakly hydrothermally altered.

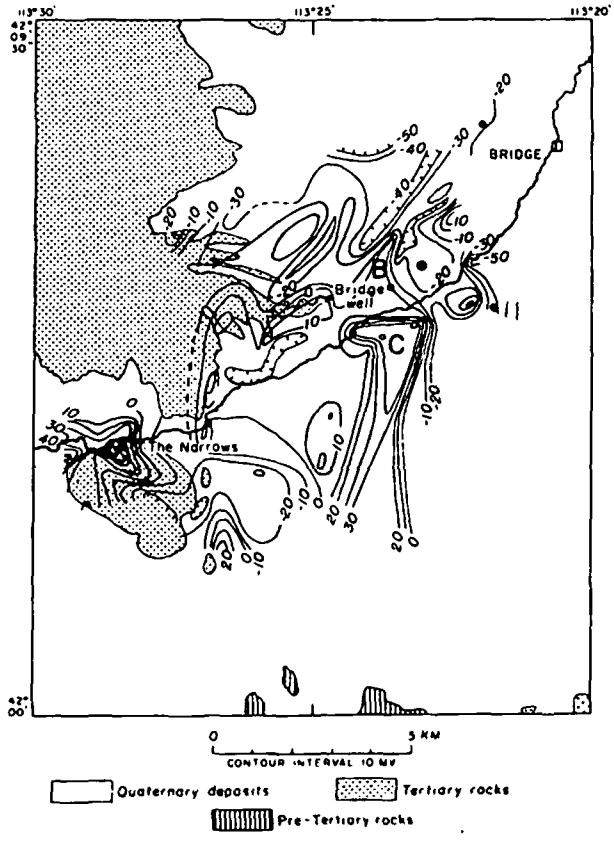

Figure 8. Self-potential map of part of the southern Raft River valley.

Self-Potential Measurements

A self-potential (SP) survey was made in the area of known hot wells and warm seeps, from The Narrows to the vicinity of Bridge. The SP map (Fig. 8) was made with an electrode spacing of 500 m and so does not define short-wavelength anomalies. No large-amplitude anomalies were found; the maximum observed was about 60 mV, and anomalies are in part masked by topographic effects seen as more negative potentials as one goes higher up the pediment slopes.

Two regions show positive SP anomalies in areas of known near-surface hot water. One is a narrow north-trending zone just east of The Narrows (A). The other (B) extends through the Bridge well and trends north-northeast; it is flanked for about 2 km of its length by associated negative zones which presumably are due to the deeper negative source pole. This anomaly correlates with the Bridge fault which

is assumed to be a major conduit for the near-surface hot water in the area.

A large positive anomaly (C) found just south of the area of hot wells on the south side of the Raft River does not appear to correlate with other geophysical data. However, it is coincident with a depositional segment of an alluvial fan and is at the junction of lineaments seen on aerial photographs. The significance of this anomaly is not yet clear.

Geophysical Summary

In summary, the gravity data show accurately the gross structure of the basin, and yield an approximate thickness of the Cenozoic basin fill. Magnetic anomalies are related primarily to the volcanic rocks and are useful in inferring their distribution and structure. The AMT survey provided a preliminary indication of the resistivity anomalies related to lithology and structure. The seismic refraction and direct-current resistivity surveys provide information about the thickness and lithology of basin fill and the location of major faults. The significance of the self-potential survey results has not been determined, but anomalies may be related to near-surface circulation of hot water along faults.

An evaluation of the geothermal resources of the southern Raft River valley and similar areas requires an understanding of the geology in three dimensions. This can be obtained only through knowledge of the regional geology and geophysics, detailed geologic mapping in the immediate area of interest, intensive geophysical surveys, and test drilling. We have not discovered any geophysical technique for the direct detection of thermal waters.

STRUCTURE

The geometry of the Raft River basin is well-defined by the gravity survey. Thicknesses of the Cenozoic basin fill predicted from gravity, resistivity, and seismic data are in close agreement and are confirmed by drilling at RRGE 1, where Precambrian rocks were encountered at a depth of 1390 m. The concealed basement high east of Sheep Mountain (Mabey and Wilson, 1973) trends northwest across the northern Jim Sage Mountains and apparently is an extension of the Big Bertha gneiss dome of the Albion Mountains (Armstrong, 1968). Intermediate drill-hole No. 5 encountered Precambrian (?) adamellite at 210 m, a depth predicted from the gravity study.

The Cenozoic rocks, including Pleistocene fan gravels, are cut by numerous faults that in a general way parallel the east, west, and south basin margins (Fig. 1). The faults with greatest displacement, as determined from steep gravity gradients and steep gradients of normalized total-field resistivity are (1) the north-trending Bridge fault; (2) a fault system along the west front of the Black Pine Mountains; and (3) a concealed east-west fault, the Naf fault, in the southern part of the basin at about the latitude of Round Mountain (Fig. 1). Generally, the faults show downward displacement toward the center of the basin; eastward dips in bedding of 15 to 30 degrees on the east flank of the Jim Sage Mountains anticline augment basinward stratigraphic throw on the faults. Faults are inferred to dip 60 to 70 degrees based on measurement of fractures in the core from Intermediate drill hole No. 3, direct measurement of an exposed fault plane in the volcanic member of the Salt Lake formation at Jim Sage Mountain, gravity expression, and the geometry of intersection of the Bridge fault in RRGE 1.

Age of latest movement on the faults is inferred from study of loessal soils mantling the alluvial fans. The north-trending faults near Bridge cut "older" fan surfaces mantled by as much as 3 m of loess reflecting at least four depositional-weathering episodes, indicating an age older than the fourth pluvial interval before the present. The same faults do not cut, and are covered by, fans of "middle" age, which are mantled by 0.6 to 1.5 m of loess deposited in two or three pluvial episodes. If the fourth-from-youngest pluvial is middle Pleistocene, then the most recent movement on the faults was several hundred thousand years before present.

Known occurrences of thermal waters above 100°C in the southern Raft River basin are located near the intersection of the north-trending normal faults with the Narrows structure (Fig. 1), a northeast-trending linear feature with regional geophysical expression, probably a basement shear, that passes just south of the Jim Sage Mountains. Nearly coincident with this structure is a concealed northeast to east-northeast fault through The Narrows that separates widely different structural styles in the Salt Lake formation, and is expressed by gravity and resistivity. The Bridge fault and other north-trending fault sets do not cross this structure.

The drill site for RRGE 1 was selected near the intersection of the Narrows structure with the Bridge fault, and the well was predicted to intersect the Bridge fault and produce hot water at or below 1400 m; actually, the fault zone and flow of water was encountered between 1240 and 1320 m. Seismic and resistivity studies predicted penetration of basement rocks in the well at a depth of about 1600 and 1400 m respectively; actual depth to basement is 1390 m. The seismic study had showed low-velocity basement under the well site, due probably to fractured rock, and this proved to be so.

GEOTHERMAL MODEL

Geochemical and other data suggest that the Raft River geothermal system is typical of low-temperature hot water systems as described by White, Muffler, and Truesdell (1971). The system apparently is self-sealing. Masses of secondary silica and calcite do not occur at the surface, but a silica caprock was encountered at a depth of 1370 to 1373 m in RRGE 1; many fractures in cores from the intermediate-depth wells are filled with chalcedony and calcite. The high chloride content of the waters (1000 ppm and more) and aquifer temperatures lower than 150°C clearly indicate a hot-water rather than vapor-dominated system.

The southern Raft River valley geothermal system is probably the result of deep circulation of meteoric water along major faults. The most recent igneous activity in the southern part of the basin apparently took place between 7 and 10 million years ago, and any related intrusive masses are too old to be an important heat source. We propose a model in which meteoric water from the Albion, Goose Creek, and Raft River Mountains, which have relatively high precipitation of about 800 m/yr, collects in deep Cenozoic fill in the upper Raft River basin west of The Narrows and in the southernmost Raft River valley, perhaps with minor contributions from ranges east of the basin. Some of this water descends along faults to depths sufficient

to heat it to 145°C. Heat-flow values of 2 to 3 $\mu cal/cm^2/sec$ occur in the southern flank of the Snake River plain (Urban and Diment, 1975), which permits heating to 145°C at depths of 3 to 5 km. Heated water then migrates upward along The Narrows structure and north-trending faults, and is tapped by wells intersecting these structures. Faults are doubtless only parts of a conduit system that includes permeable aquifers in the Salt Lake formation, fractured zones in the Precambrian rocks, and perhaps, gently dipping thrust faults in Paleozoic and Precambrian rocks.

ACKNOWLEDGMENTS

We thank the following Geological Survey colleagues: L. J. P. Muffler gave varied and generous support throughout the study; E. G. Crosthwaite, Eugene Shuter, and W. Scott Keys made drill core and hydrological data immediately available to us; H. R. Covington, D. H. McIntyre, and P. W. Schmidt contributed to surface mapping and subsurface studies; D. B. Jackson and J. E. O'Donnell did part of the resistivity study and a telluric current survey, respectively.

Others who contributed valuable information, data and assistance are C. R. Nichols, Boise State University; John Griffith, ERDA; J. F. Kunze, Lowell Miller, and Roger Stoker, Aerojet Nuclear Company; and Jack A. Barnett, Sherl L. Chapman, and Edward Schlender, Raft River Rural Electrical Co-operative. The sustained informal support of ERDA's Idaho Operations, Idaho Falls, is gratefully acknowledged.

This report is preliminary and has not been edited or reviewed for conformity with U.S. Geological Survey standards.

REFERENCES CITED

Anderson, A. L., 1931, Geology and mineral resources of eastern Cassia County, Idaho: Idaho Bur. Mines and Geology Bull. 14, 69 p.

Armstrong, R. L., 1968, Mantled gneiss domes in the Albion Range, southern Idaho: Geol. Soc. America Bull., v. 79, p. 1295.

Armstrong, R. L., Leeman, W. P., and Malde, H. E., 1975, K-Ar dating, Quaternary and Neogene volcanic rocks of the Snake River plain, Idaho: Am. Jour. Sci., v. 275, p. 225.

Compton, R. R., 1972, Geologic map of the Yost quadrangle, Box Elder County, Utah, and Cassia County, Idaho: U.S. Geol. Survey Misc. Geol. Inv. Map I-672.

Felix, C. E., 1956, Geology of the eastern part of the Raft River Range, Box Elder County, Utah, *in* Guidebook to the Geology of parts of northwestern Utah: Utah Geol. Soc., no. 11, p. 76-97.

Godwin, L. H., Haigler, L. B., Rioux, R. L., White, D. E., Muffler, L. J. P., and Wayland, R. G., 1971, Classification of public lands valuable for geothermal steam and associated geothermal resources: U.S. Geol. Survey Circ. 647, 17 p.

Mabey, D. R., and Wilson, C. W., 1973, Bouguer gravity anomaly map of the southern Raft River area, Cassia County, Idaho: U.S. Geol. Survey open-file rept.

Mundorff, M. J., and Sisco, H. G., 1963, Ground-water in the Raft River Basin, Idaho, with special reference to irrigation use, 1956-60: U.S. Geol. Survey Water-Supply Paper 1619-CC, 23 p.

Nace, R. L., et al., 1961, Water resources of the Raft River basin, Idaho-Utah: U.S. Geol. Survey Water-Supply Paper 1587, 138 p.

Stearns, H. T., Crandall, L., and Steward, W. G., 1938, Geology and ground-water resources of the Snake River Plain in southeastern Idaho: U.S. Geol. Survey Water-Supply Paper 774, 268 p.

Urban, T. C., and Diment, W. H., 1975, Heat flow on the south flank of the Snake River Rift: Geol. Soc. America, Abs. with Programs, v. 7, no. 5, p. 648.

Walker, E. H., Dutcher, L. C., Decker, S. O., and Dyer, K. L., 1970, The Raft River Basin, Idaho-Utah as of 1966: A reappraisal of the water resources and effects of ground-water development: Idaho Dept. Water Admin. Water Inf. Bull. 19, 95 p.

White, D. E. Muffler, L. J. P., and Truesdell, A. H., 1971, Vapor-dominated hydrothermal systems compared with hot-water systems: Econ. Geology, v. 66, p. 75.

Williams, P. L., Pierce, K. L., McIntyre, D. H., and Schmidt, P. W., 1974, Preliminary geologic map of the southern Raft River valley, Cassia County, Idaho: U.S. Geol. Survey open-file rept.

Young, H. W., and Mitchell, J. C., 1973, Geothermal investigations in Idaho—Part 1, Geochemistry and geologic setting of selected geothermal waters: Idaho Dept. Water Admin. Water Inf. Bull. 30, 43 p.

Zohdy, A. A. R., 1973, Total field resistivity mapping (abs.): Geophysics, v. 38, p. 1230.

——, 1974a, A computer program for the automatic interpretation of Schlumberger sounding curves over horizontally stratified media: Springfield, Va., U.S. Dept. Commerce, Natl. Tech. Inf. Service, PB-232 703, 25 p.

——, 1974b, The use of Dark Zarrouk curves in the interpretation of VES data: U.S. Geol. Survey Bull. 1313-D, 41 p.

——, 1975, Automatic interpretation of Schlumberger curves using modified Dar Zarrouk function: U.S. Geol. Survey Bull. 1313-E, 39 p.

Zohdy, A. A. R., and Stanley, W. D., 1974, A computer program for the calculation of bipole-dipole apparent resistivity maps over horizontally stratified media: Springfield, Va., U.S. Dept Commerce, Natl. Tech. Inf. Service, PB-273 727, 10 p.

Zohdy, A. A. R., Jackson, D. B., and Bisdorf, R. J., 1975, Schlumberger soundings and total field measurements in the Raft River geothermal area, Idaho: U.S. Geol. Survey open-file rept. 75-130, 5 p.

Geophysical Studies in Sarayköy-Kızıldere Geothermal Field, Turkey

A. K. TEZCAN
Maden Tetkik ve Arama Enstitüsü, Ankara, Turkey

ABSTRACT

This work presents the results of the resistivity and gravity studies and their evaluations, made prior to drillings in the Sarayköy-Kızıldere geothermal field. The geothermal area is covered by Neogene formations overlying a metamorphic basement. Possible reservoir rocks are the marbles in the metamorphic basement and middle Miocene limestones in the Neogene formations. The Bouguer gravity map revealed the topography of the metamorphic basement. The existing Kızıldere thermal manifestations were found to be located on the south flank of a metamorphic uplift which was delineated by an east-west trending gravity high.

The resistivity survey was carried out over an area covering this flank. Electrical soundings with a Wenner electrode array resulted in sounding graphs with two- or three-layer curves; the resistive bottom layer of these curves reflects the relief of the metamorphics. The low resistivity values in the resistivity maps of different electrode spacings were correlated with the hot water. Therefore, the low resistivities were due to the existence of hot water in the Neogene rocks. It was assumed that this was due to an underlying, geologically possible, main reservoir in the marbles, by a feeding and/or heating process.

The drillings made in the low-resistivity area to the depth of the resistive bottom layer produced a steam-water mixture from the Neogene formations and, more powerfully, from the metamorphic marbles.

INTRODUCTION

Combined geophysical studies of hot-water areas, in order to develop them as geothermal fields, started with the study of the small İzmir-Agamemnon thermal area in 1962. The positive results of the test drills made there have placed the geophysical studies in an important position in the exploration of geothermal fields in Turkey. Sarayköy-Kızıldere or Denizli-Kızıldere geothermal field has been one of the largest of these fields (Fig. 1).

This article presents the results of geophysical, gravity, and, in a more detailed form, resistivity studies made in the Sarayköy-Kızıldere field, prior to drilling. It discusses what had been expected of those studies and what sort of picture of the geothermal field had been inferred as the result. The results are quoted here, with some minor modifications in their presentation, as they were submitted in the report prepared in 1967, before the drillings were started. To complete the presentation and to allow the reader to make a comparison, the results of the subsequent test and development drillings are added at the end.

GEOLOGY

The Kızıldere and Tekke Hamam areas are situated on a Neogene-filled basin surrounded by high topographic level metamorphics of the Menderes massif and, respectively, on the north and south of the east-west trending B. Menderes graben. The outcropping formations (Uysallı, 1967) from young to old are (Fig. 2): (1) alluvium; (2) Pliocene-Pleistocene; (3) Pliocene (marls, sandstones); (4) upper Miocene (marls intercalated with sandy, clayey limestones); (5) middle Miocene (marly limestones and limestones); and (6) metamorphics (schists, gneiss, marbles).

Alluvium appears all along the B. Menderes River cutting east-west through the basin on the lowest topography. To the north and south from the river, as the topography gets higher, the older formations start to outcrop in sequence except the Pleistocenes which are distributed over the area as patches over all kinds of older formations. The outcrop-

Figure 1. Denizli-Sarayköy region, Turkey.

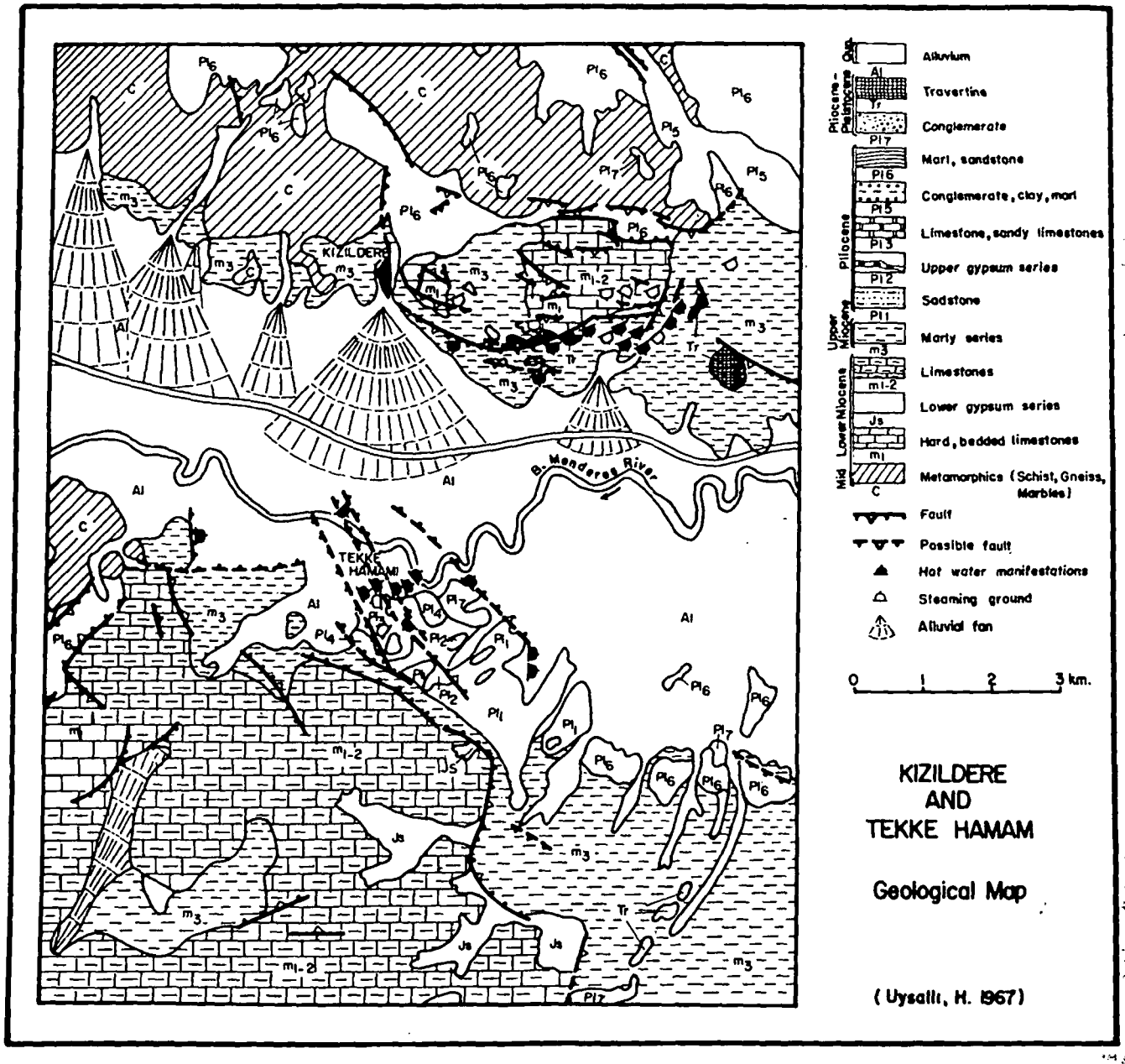

Figure 2. Detailed geology of Kızıldere and Tekke Hamam (Uysallı, 1967).

ping metamorphic rocks constitute the highest topographical portion of the region (Fig. 3).

The observed faults (Fig. 2) are mostly parallel to the east-west trending formation boundaries and topographic contours. Horsts (Uysallı, 1967) might exist under the cover of Neogene formations. The hot-water and steam manifestations are distributed all along the northern and southern parts of the B. Menderes River where the topography starts to rise.

Possible reservoir rocks (Uysallı, 1967) are fractured marbles and middle Miocene limestones. All the other Neogene formations have clayey constituents or are interbedded with clays and marls. Thus, they have the properties of caprocks.

GEOPHYSICAL STUDIES AND OBJECTIVES

The first geophysical survey was the gravity survey covering an area of 1500 km^2, used to disclose the general character of the basin and the region. The instrument used was the Frost type of gravimeter. The area of the resistivity survey was selected according to the results of the geology and the gravity studies. Its objectives were based on experience at İzmir-Agamemnon and local conditions. The area of study is covered by Neogene formations which have a predominantly marly and clayey constitution. The hot-water samples taken from the springs had given low resistivity values (Table 1). Therefore, the part of the Neogene formations containing this sort of water in its pores and/or the part heated by an underlying source would also have low resistivity values.

Based on these observations and facts, the objectives of the survey were (1) to reveal and locate the distribution of low-resistivity mediums which would lead to the discovery of the reservoir; (2) to delineate the Neogene-covered metamorphic substratum quantitatively; and (3) to obtain other information where possible. The resistivity instrument used was a Gish-Rooney dc potentiometer. The survey was

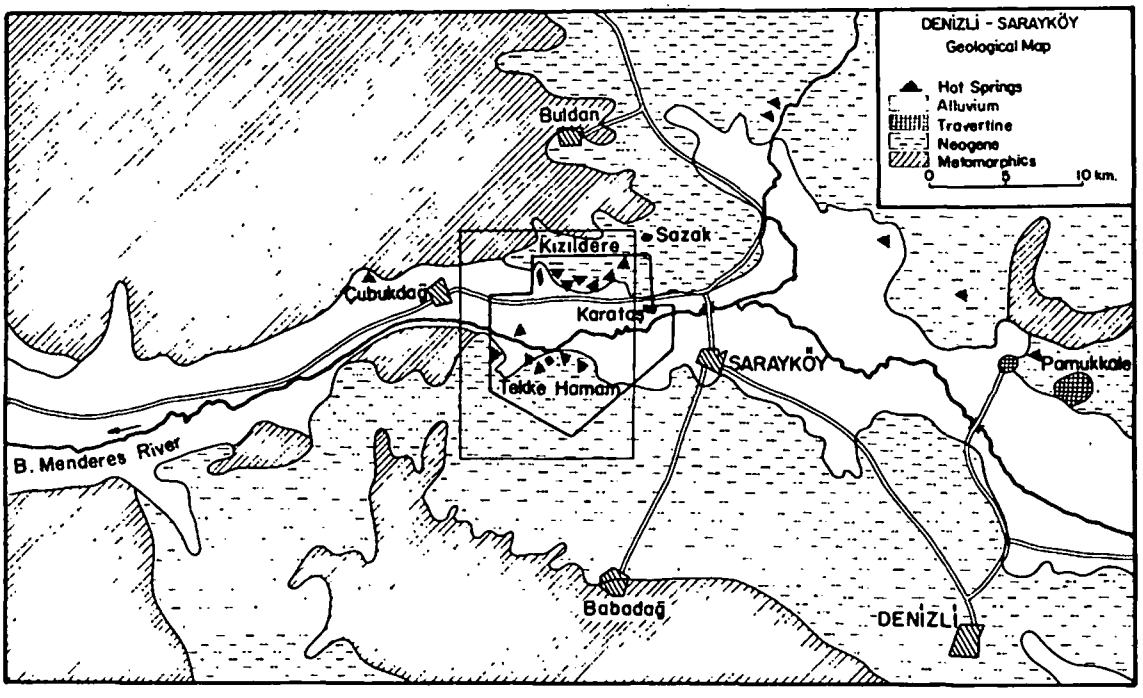

Figure 3. Geology of Denizli-Sarayköy region and the areas of detailed geology and resistivity surveys.

Table 1. Hot waters and formation resistivities.

Formations		Resistivities (Ohm-m)
Schists and Gneiss		80-300
Marly Limestones (m_{1-2})		80-2000
Marls (m_3)		15-20
Waters		
Hot Waters of Kızıldere	(95-100 C°)	2-2.5 (at 50 C°)
" " " Tekke Hamamı	" " "	" " " "
" " " Ortakçı	(45 C°)	6.0 " "
Water of B. Menderes River		10.0 " "

carried out as electrical soundings with a Wenner array by using a maximum current-electrode separation of 3000 m. The survey covered an area of approximately 40 km^2.

Results of the Gravity Survey

The gravity observations were converted to Bouguer anomaly and second-derivative maps and sections. By comparing the Bouguer anomaly and its second-derivative maps with the known geology (Figs. 4 and 5), it is seen that the high-topographic-level formations, the metamorphics, raise the Bouguer values considerably with respect

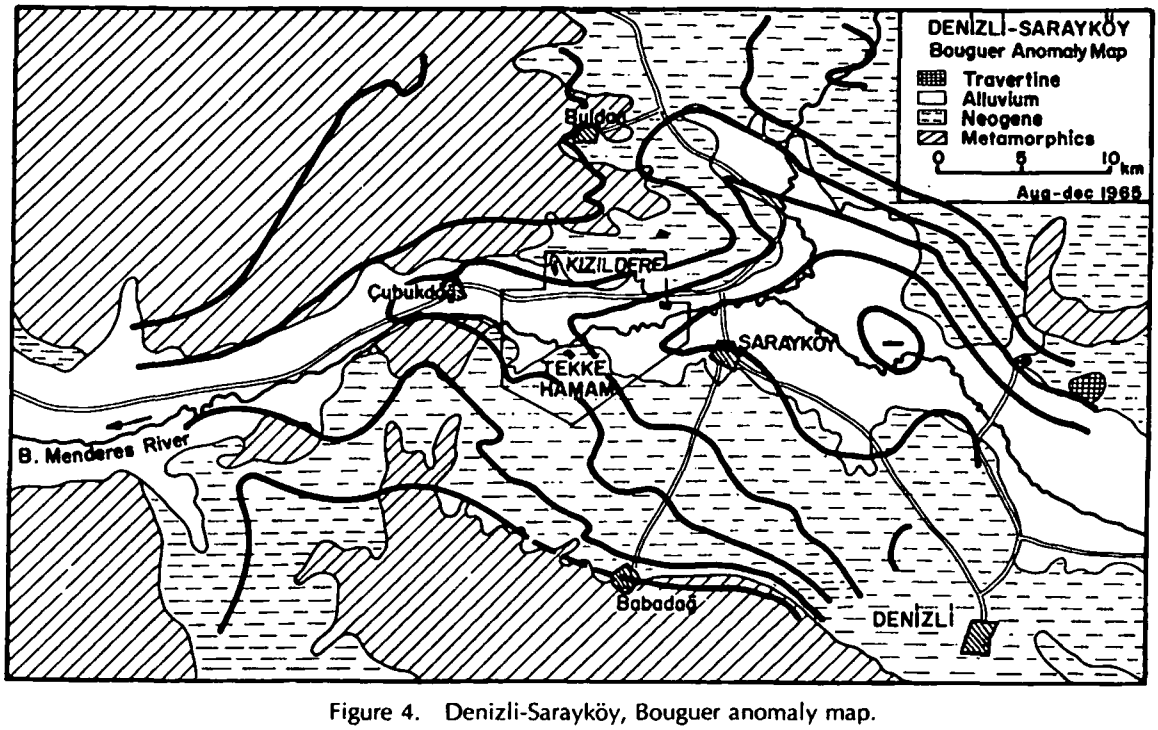

Figure 4. Denizli-Sarayköy, Bouguer anomaly map.

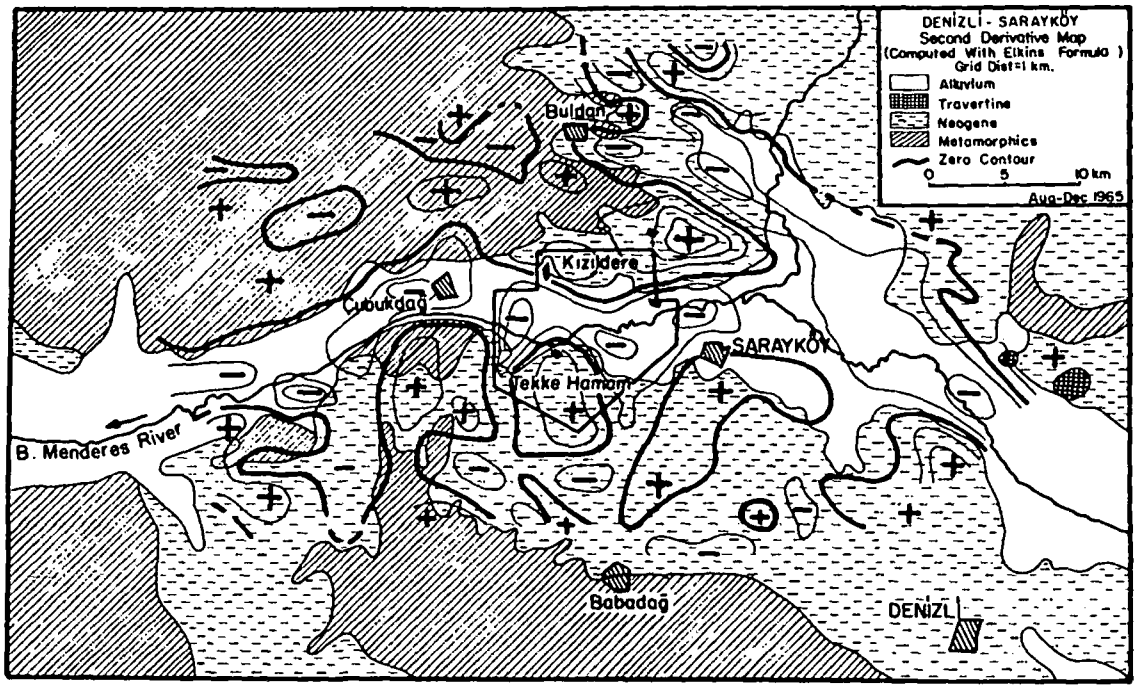

Figure 5. Denizli-Sarayköy, the second-derivative map.

to the low-level Neogene formations. Therefore, the Bouguer values reflect the metamorphic topography under the Neogene cover. Any Bouguer anomaly variations in the area of Neogene cover can easily be attributed to the topographic variations of the underlying metamorphic substratum. Where thin middle Miocene limestones exist, some modifications were also expected.

Two large, clearly identifiable highs are outstanding in the Bouguer and second-derivative maps (Figs. 4, 5)—one is situated between Kızıldere and Buldan with an east-west.

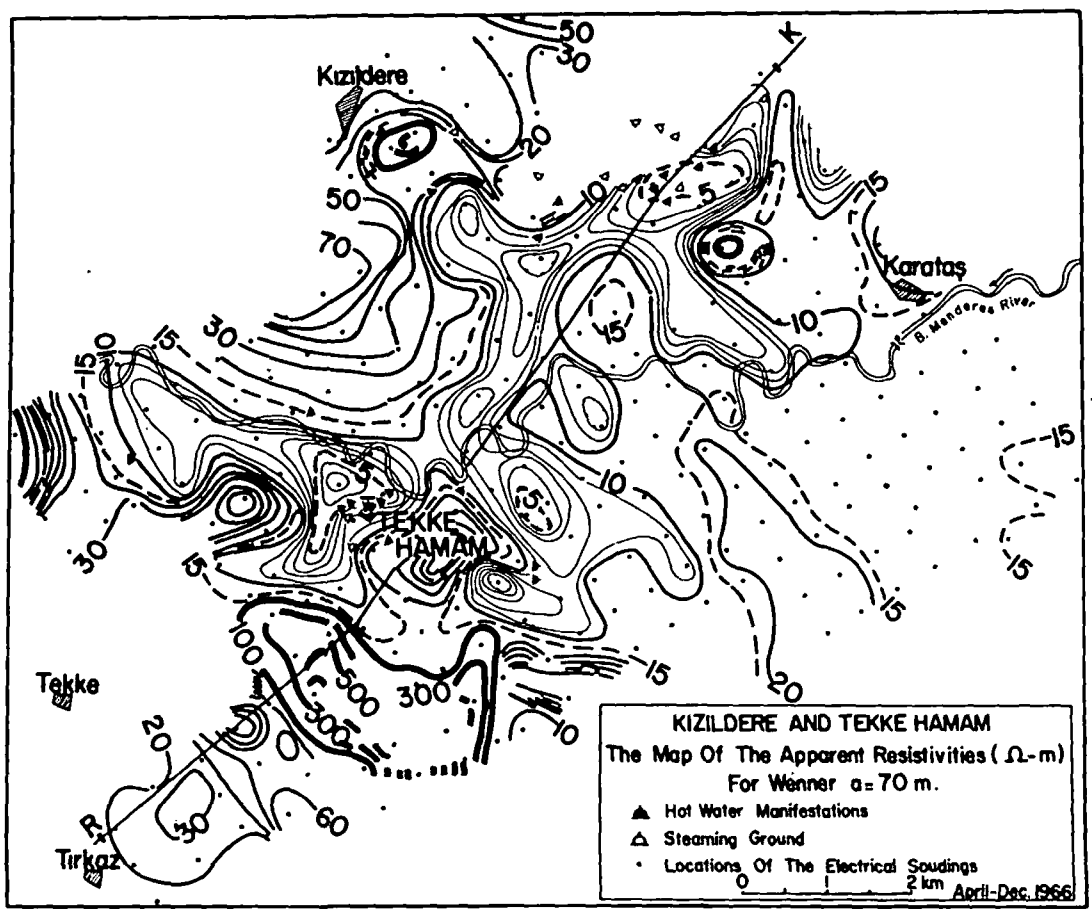

Figure 6. Apparent resistivities, Wenner a = 70 m, Kızıldere and Tekke Hamam.

trend; the other is south of Tekke Hamam. They were interpreted and selected as two important uplifts because all the major hot-water and steam manifestations are associated with them and are situated, respectively, on their south and north flanks. The resistivity survey was made to study those flanks and their neighboring areas.

Results of the Resistivity Survey

The observations of the resistivity survey were plotted as apparent-resistivity maps of different electrode separations, apparent-resistivity sections, and electrical-sounding graphs. The hot-water resistivities were measured and the formation resistivities were determined for the outcrops (Table 1). The evaluations of the resistivity studies have been made in two stages: in the first, the resistivity maps and sections were studied; in the second, the electrical sounding graphs were considered.

Inspection of the maps (Figs. 6, 7, 8, 9, 10) and the section (Fig. 11) clearly shows that there are two large low-resistivity areas situated parallel to the extension of hot-water manifestations of Kızıldere and Tekke Hamam, on the northern and southern parts of the B. Menderes River. On the map of resistivity with a 70-m separation (Fig. 6), both the low-resistivity areas and the area of hot-spring manifestations coincide with each other. The coincidence can be seen better on the section of Figure 11. Many of the hot springs appear to be outcrops of the two large low-resistivity mediums in the Neogene formations. The contour patterns have also shown that they are connected at several depths.

There is no low-resistivity water other than the hot waters, and no other low-resistivity constituents of the Neogene have been detected in the surveyed area. Under these conditions, the stated association of the low-resistivity mediums with the hot waters have led us to conclude that they have been created by the inclusion of hot waters into the Neogene formations. Therefore, the vertical and horizontal distributions of those mediums reflect the distribution of hot waters in the porous and fractured constituents of the Neogene formations. Since the area is in an active earthquake region, fracturing is quite possible, even in the clayey constituents near the active faults of the graben.

When the field curves of electrical soundings (Figs. 12, 13) have been inspected, there is no indication of the high-resistivity substratum of the metamorphics or the middle Miocene limestones in the localities around the B. Menderes River. It has been understood that they are quite deep in the middle of the basin—more than 1000 m deep.

Toward the Kızıldere and Tekke Hamam uplifts, where the low-resistivity mediums start to appear, a resistive bottom layer also starts to show in the curves. This layer comes nearer to the surface as it comes nearer to the metamorphic and the limestone outcrops. Therefore, it has been correlated with them. Its depths have been determined and mapped (Fig. 12). (Figure 12 actually shows the bottom of the low-resistivity layers; the deeper layer has been interpreted this way since it conformably approaches the surface and outcrops as metamorphics or limestones.)

All these findings have been combined to infer the nature and structure of the Kızıldere geothermal field as described below.

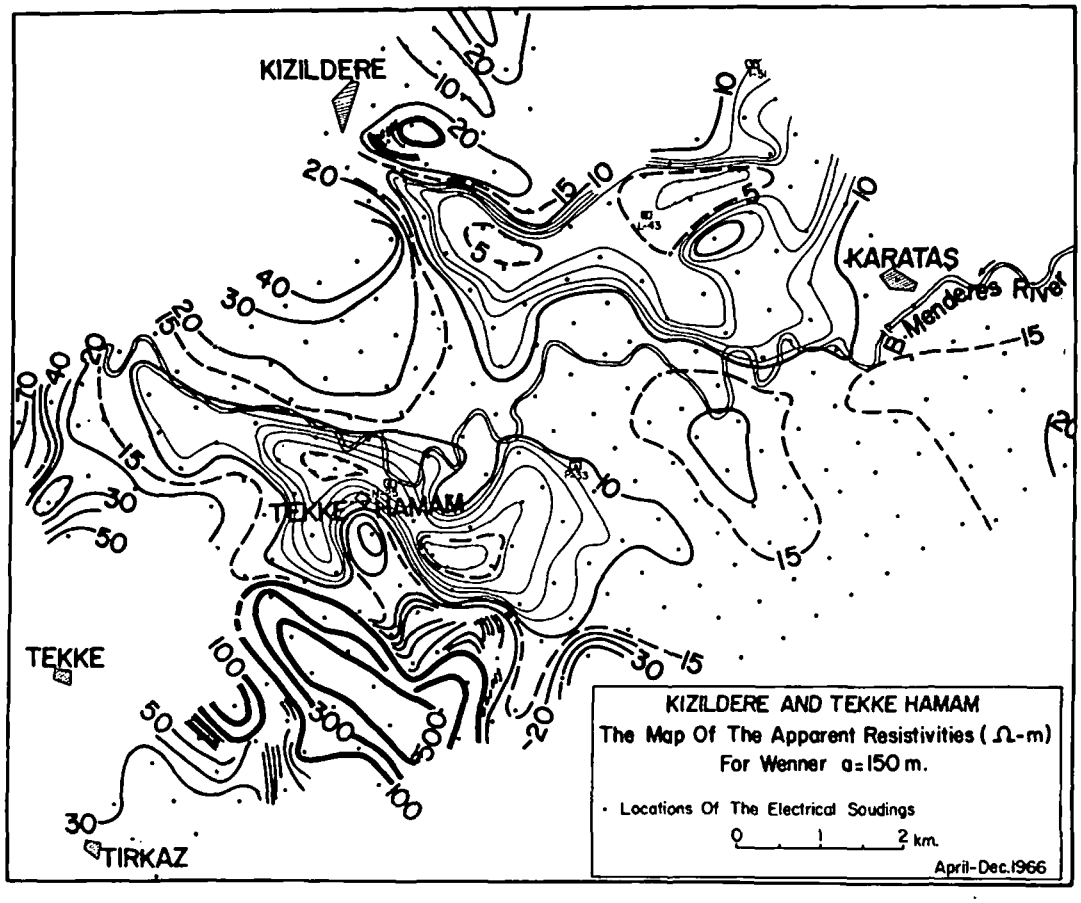

Figure 7. Apparent resistivities, Wenner a = 150 m, Kızıldere and Tekke Hamam.

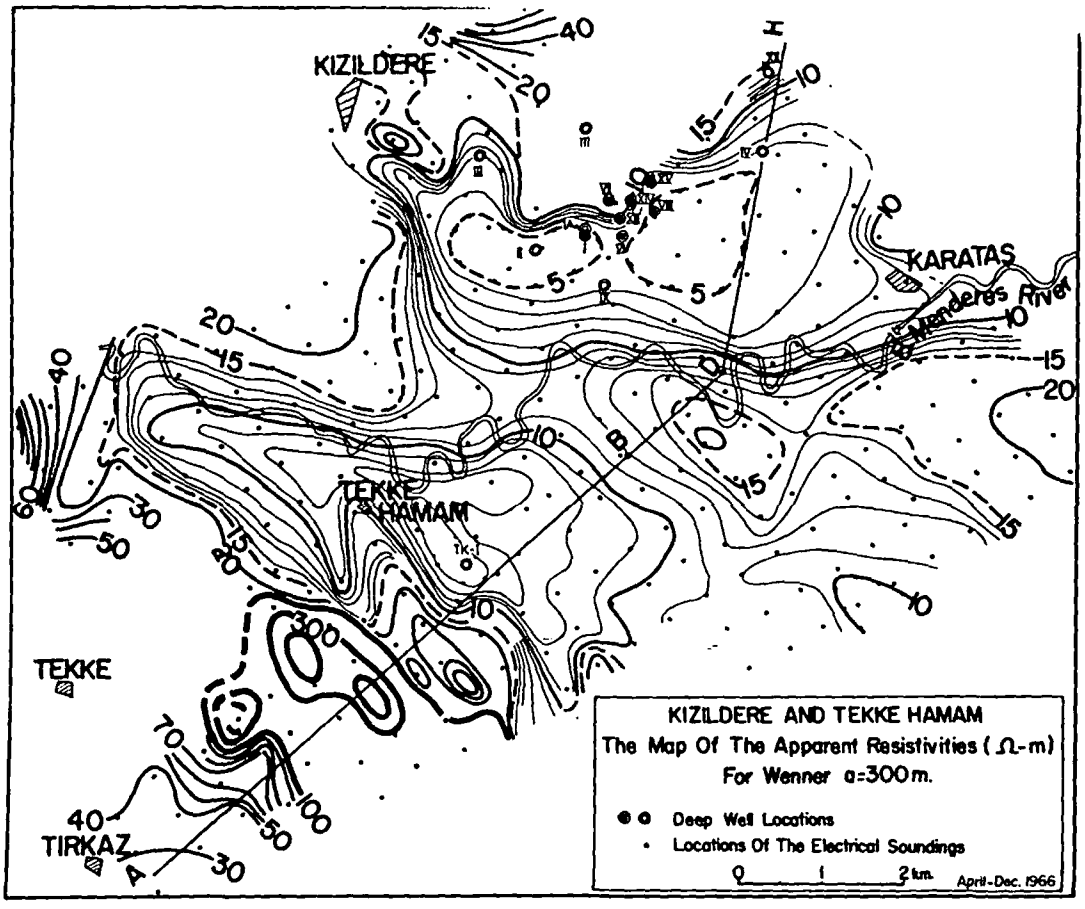

Figure 8. Apparent resistivities, Wenner a = 300 m, Kızıldere and Tekke Hamam.

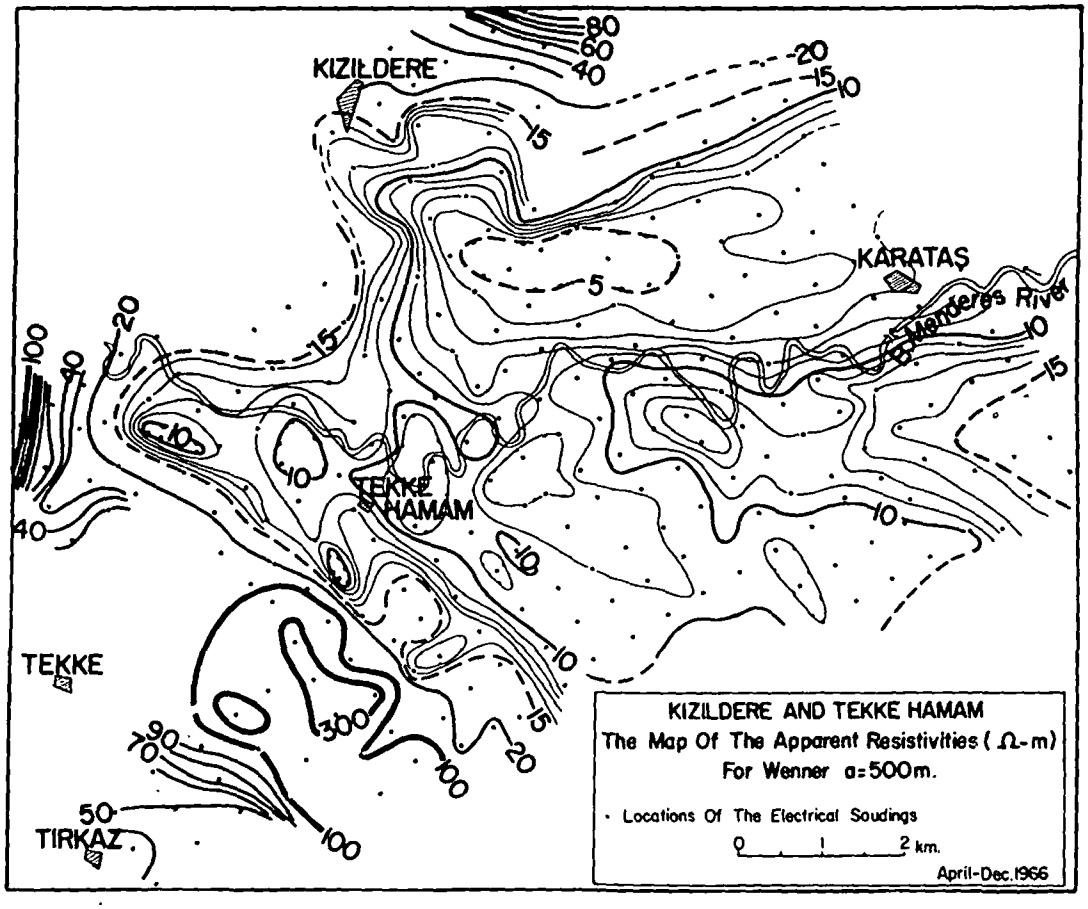

Figure 9. Apparent resistivities, Wenner a = 500 m, Kızıldere and Tekke Hamam.

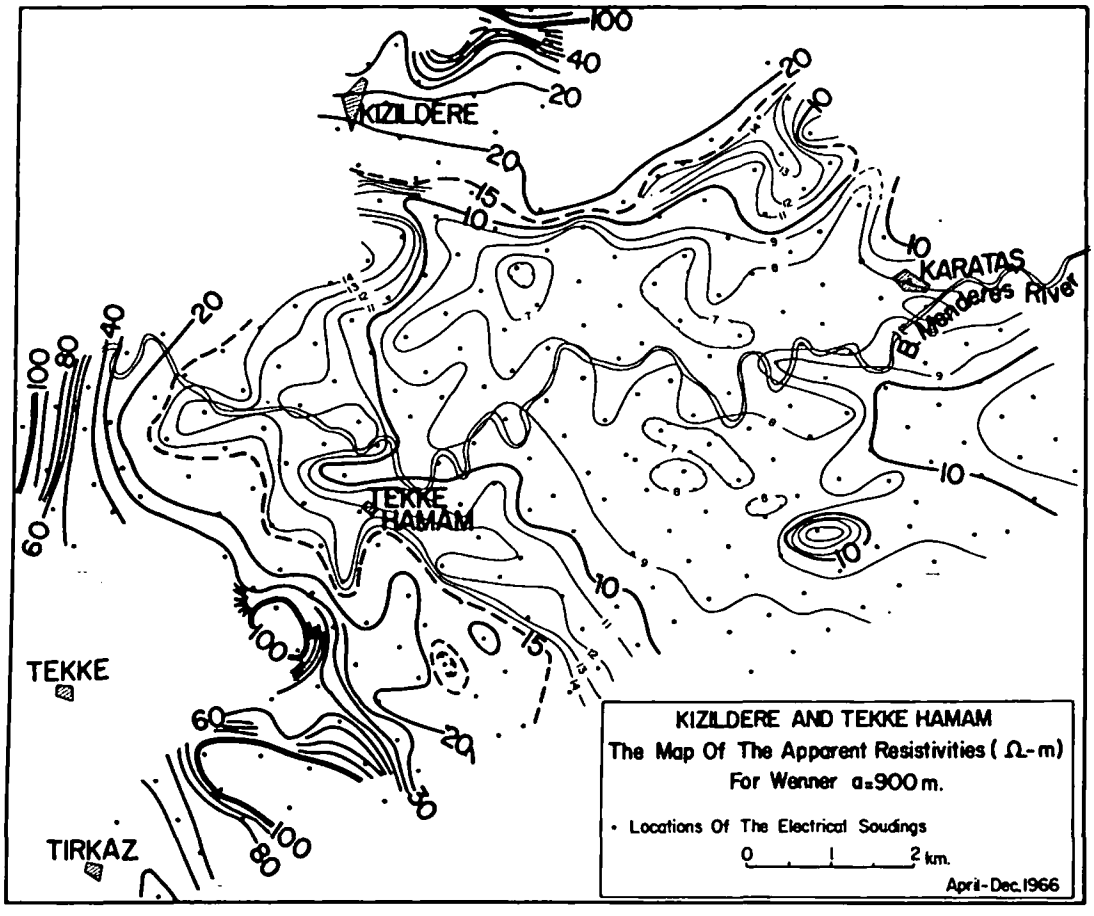

Figure 10. Apparent resistivities, Wenner a = 900 m, Kızıldere and Tekke Hamam.

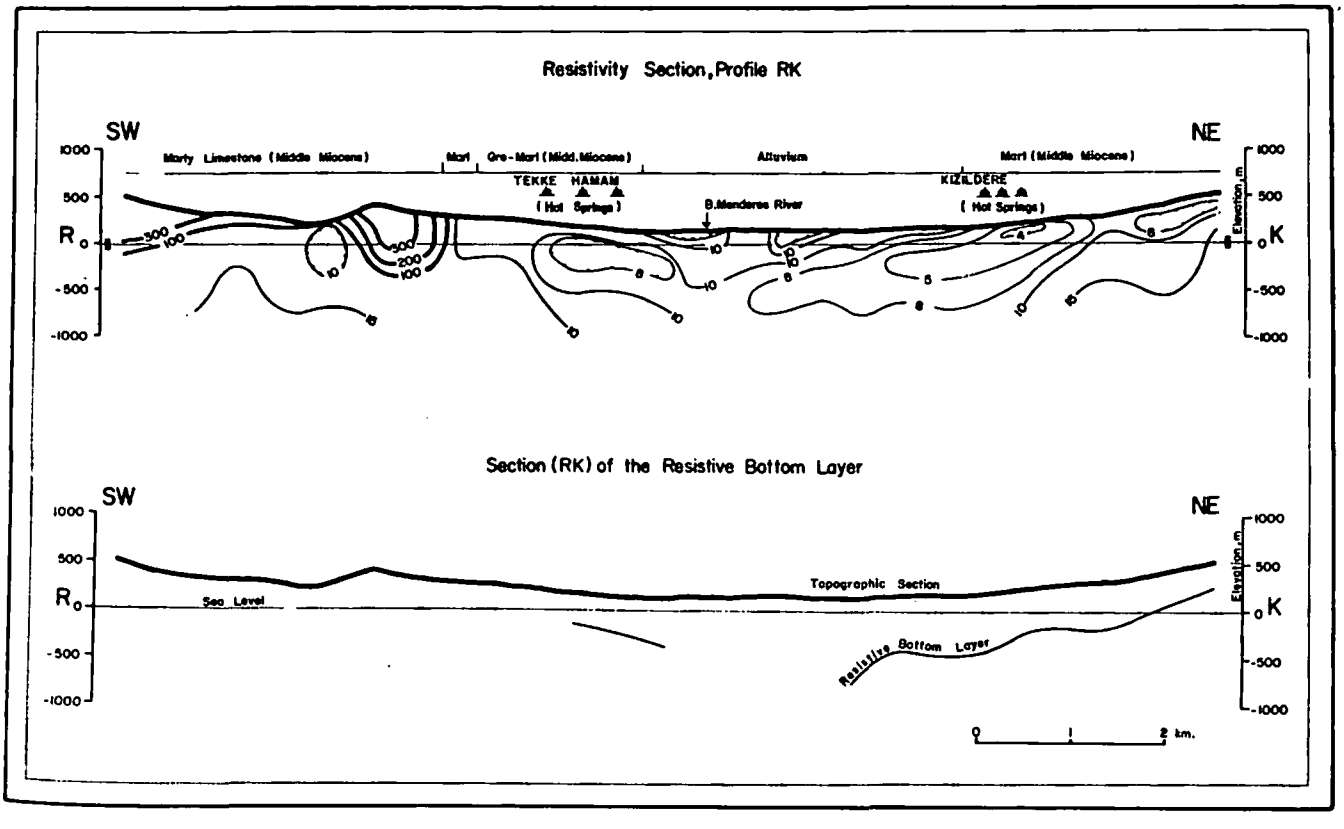

Figure 11. Resistivity section, profile 'RK,' Kızıldere and Tekke Hamam.

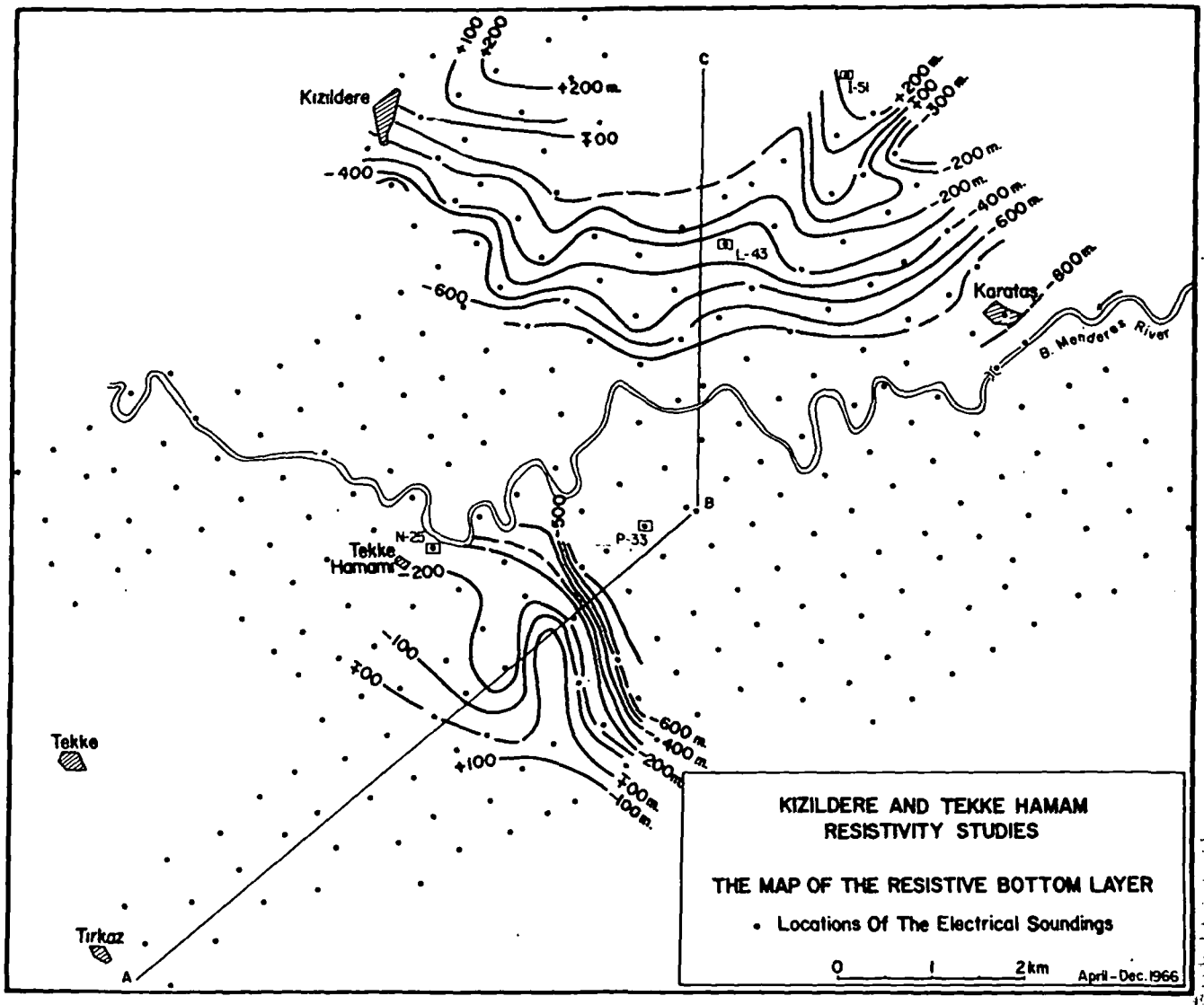

Figure 12. Map of the resistive bottom layer, Kızıldere and Tekke Hamam.

Nature and Structure of Kızıldere Field

The gravity and resistivity surveys have revealed the morphology of the metamorphic substratum; but the resistivity survey has determined it quantitatively as the resistive bottom layer. The upper surface of this layer, as explained above, divides the ground into two parts, one on top of the other. The constituents of the upper part are the Neogene formations, in which a hydrothermal distribution has taken place as revealed by the low-resistivity mediums. It occupies quite a large volume and produces all the hot springs of Kızıldere and Tekke Hamam. The lower part corresponds to the resistive base of the Neogene formations and/or the metamorphics.

It can be concluded that the nature and the origin of hot waters in the Neogene formations can only be produced by feeding and/or heating by the underlying geologically possible marble reservoir in the metamorphic layer. Since the permeabilities in the Neogene formations were not expected to be very high, the two large low-resistivity mediums detected in the Neogene formations should rest immediately over the supposed underlying main reservoir.

Thus the Kızıldere and Tekke Hamam fields must have hot water originating from, and conducted through, the permeable portions of the Menderes massif. The fractures in the two metamorphic uplifts defined by gravity surveys should control the transport of the hot water to the geothermal fields to produce the hydrothermal distributions described above.

SUGGESTED SUBSEQUENT WORK

Drillings were the principal suggested work for checking whether the low-resistivity mediums in the Neogene formations and the underlying resistive bottom layer were reservoirs. Some locations were especially fixed at its elevated parts to increase the chance of getting dry steam. This subject is dealt with in another article (Tezcan, 1975). For fixing the extent and the thermal nature of the fields, some geothermal work was also suggested.

LATER WORK

Later work, started in 1967, consisted of geothermal gradient measurements, and deep test and development drills. So far, 16 holes have been drilled, 15 at Kızıldere

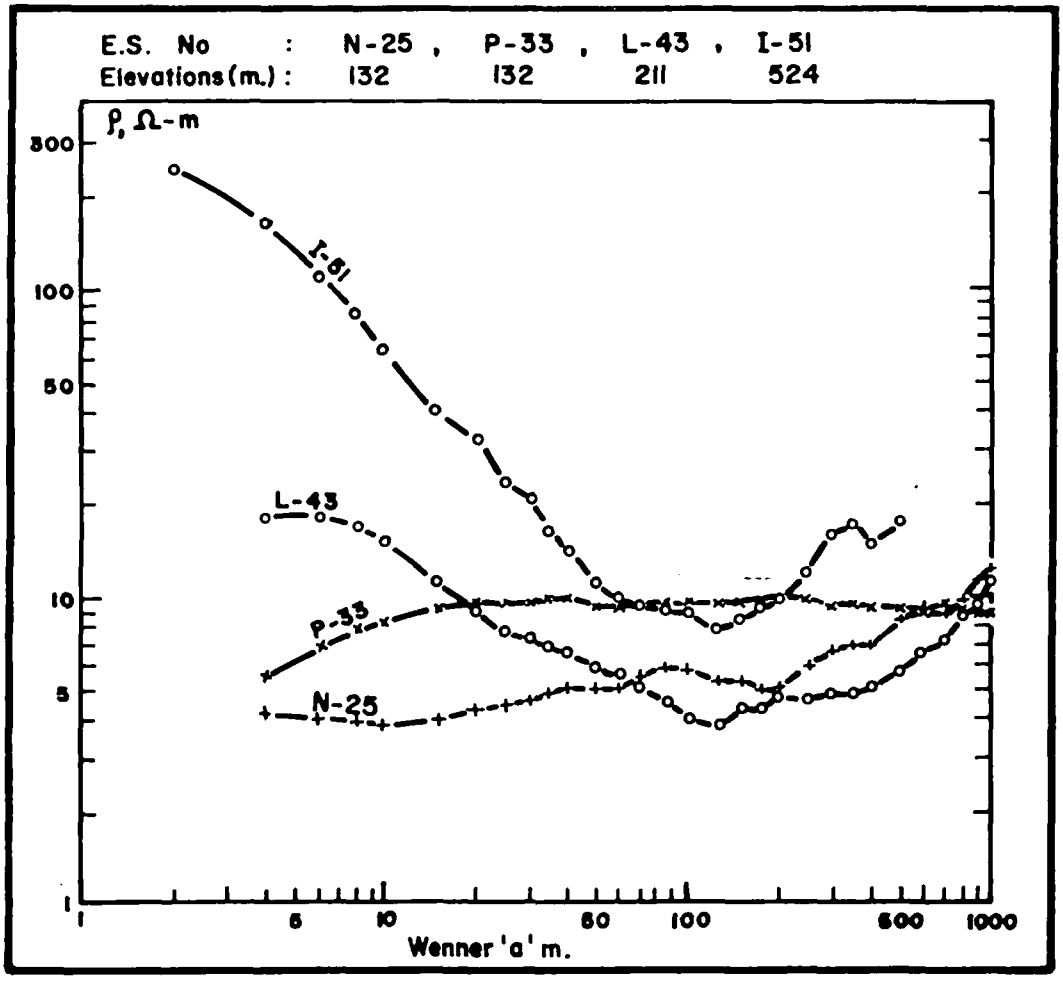

Figure 13. Typical electrical sounding curves, Kızıldere and Tekke Hamam.

and 1 at Tekke Hamam. All of them, except one, produced steam-water mixtures from the rigid fractured components (including middle Miocene limestones) constituting the base of the Neogene formations and, more powerfully, from the underlying metamorphic marbles.

In Kızıldere, the Neogene reservoir has a temperature of 165 to 175°C; the lower, main reservoir in the marbles has a temperature of 195 to 205°C. Where the drilling has been done, the depth of the first reservoir is 300 to 800 m and of the second is 400 to 1100 m.

The single deep drill hole in Tekke Hamam is 700 m in depth and produced steam-water mixtures from the metamorphic reservoir. Its temperature was 114°C. The depth of the resistive bottom layer has been found to correspond to the resistive, rigid, fractured part of the Neogene formation (Ten Dam and Erentöz, 1970) immediately over the metamorphic layer and the metamorphic layer itself where that Neogene layer does not exist. The resistive bottom layer has proved to be the productive horizon in either case.

The hot waters produced from the Neogene or the metamorphic reservoirs have similar geochemical compositions (Dominco and Şamilgil, 1970). The observations made in the holes in Kızıldere have shown that for the whole field, the hot waters have a common static level (Tezcan, 1975). Consequently, it can be concluded that all the reservoirs are connected, and the fields are producing hot water originating in the metamorphic rocks of the Menderes massif.

CONCLUSION

The application of the resistivity survey to the exploration of the Kızıldere and Tekke Hamam geothermal fields has made contributions in two respects. The first contribution was to fix low-resistivity mediums which are produced by the hot water forced into the pores of the Neogene formations by the underlying marble reservoir so that a kind of print has been produced. This gives the locations of the reservoirs. Secondly, it has helped to determine the depths of the hot-water-producing horizon, either as the base of the Neogene or the metamorphic formations.

This manner of field use and evaluation can be applied to locate and to delineate geothermal reservoirs covered with caprocks of sedimentary or volcanic origin having similar characteristics.

ACKNOWLEDGEMENT

I am grateful to Dr. S. Alpan, General Director of the Mineral Research and Exploration Institute, Turkey; to Dr. S. Kavlakoğlu, Director of the Geophysics Department of the same Institute, for their kind support and encouragement in my work on this subject; and to all the crew members and colleagues who contributed to the several stages of the field and office work.

REFERENCES CITED

Burgassi, R., 1962, L'expérience Italienne de l'utilisation des fluides endogènes comme source d'énergie électri-

que: 6th World Power Conference, Melbourne.

Dominco, E., and Şamilgil, E., 1970, The geochemistry of the Kızıldere geothermal field, in the framework of the Sarayköy-Denizli geothermal area: UN Symposium on the Development and Utilization of Geothermal Resources, Pisa, Proceedings (Geothermics, Spec. Iss. 2), v. 2, pt. 1, p. 553.

Erentöz, C., and Kurtman, F., 1970, Géologie des provinces géothermique de l'Anatolie occidental: UN Symposium on the Development and Utilization of Geothermal Resources, Pisa, Proceedings (Geothermics, Spec. Iss. 2), v. 2, pt. 2, p. 1067.

Facca, G., and Tonani, F., 1964, Theory and technology of a geothermal field: Bull. Volcanol.

Kavlakoğlu, S., 1970, Origin of geothermal waters or natural steam: UN Symposium on the Development and Utilization of Geothermal Resources, Pisa, Proceedings (Geothermics, Spec. Iss. 2), v. 2, pt. 2, p. 1250.

Marinelli, G., 1961-1962, L'énergie géothermique en Toscane: Soc. Géol. Belgique Annales, t. 85.

Ten Dam, A., and Erentöz, C., 1970, Kızıldere geothermal field, western Anatolia: UN Symposium on the Development and Utilization of Geothermal Resources, Pisa, Proceedings (Geothermics, Spec. Iss. 2), v. 2, pt. 1, p. 124.

Tezcan A. K., 1963, İzmir-Agamemnun sıcaksu araştırmaları, rezistivite, termik ve S.P. etüdleri: Ankara, M.T.A. Rap. no. 3214 (unpub.).

——, 1967, Denizli-Sarayköy jeotermik enerji araştırmaları gravite ve rezistivite etüdleri: Ankara, M.T.A. Rap. no. 3896.

——, 1975, Dry steam possibilities in Sarayköy-Kızıldere geothermal field, Turkey: Second UN Symposium on the Development and Use of Geothermal Resources, San Francisco, Proceedings, Lawrence Berkeley Lab., Univ. of California.

Uysallı, H., 1967, Tekke Hamam-Kızıldere (Denizli-Sarayköy) sıcaksu sahalarının jeolojik etüdü ve jeotermik enerji imkânları: Ankara, M.T.A. Rap. no. 3874 (unpub.).

The Useful Heat Contained in the Broadlands Geothermal Field

W. J. P. MACDONALD

Geophysics Division, Department of Scientific and Industrial Research, P.O. Box 8005, Wellington, New Zealand

ABSTRACT

Measurements in the Broadlands geothermal field indicate that, below the casing, at depths greater than 730 m the water is not boiling. It is inferred that the fall in temperature is caused by a lateral inflow of cold water. Because of this cold inflow it is possible to extract all of the useful heat (2.9×10^{18} J) stored in the rocks of the reservoir between depths of 600 and 2600 m. This heat, together with the heat in the water of the reservoir and the small amount of heat introduced from below, should give a minimum for the generation of electric power of 200 MW for 47 years.

INTRODUCTION

The Broadlands geothermal field in the central volcanic region of the North Island of New Zealand was initially delineated by an electrical resistivity survey in 1964. Since then the field has been extensively investigated using geological, geochemical, and geophysical techniques. Twenty-eight holes have been drilled to date ranging in depth from about 760 m to almost 2400 m. At present the measured output of the field is about 120 MW of generated electricity. However the total useful power will depend upon the size of the field, the temperature, and the availability of water to enable the heat to be extracted from the ground.

MEASUREMENTS

Resistivity

The horizontal dimensions of the field have been found at several depths by resistivity methods. These methods have been discussed in a number of papers, and Figure 1 is derived from Risk, Macdonald, and Dawson (1970, Fig. 11) and Hatherton, Macdonald, and Thompson (1966, Fig. 6). The figure shows the position of the boundaries of the field, which appear from the resistivity measurements to be approximately vertical. The length of the bars delineating the boundary indicates the resistivity gradient—the shorter the bars the steeper the gradient. This means that the distance between hot and cold ground should be proportional to the length of the bars.

Gravity

The relatively flat topography of the area and the finding of the greywacke basement in some drill holes has enabled the gravity survey to be interpreted with confidence. The results in the form of a residual anomaly map are given in Figure 2 which is taken from Macdonald and Hatherton (1968).

The gravitational pattern is thought to be caused by two effects (Hochstein and Hunt, 1971), the minor one being due to the Broadlands and Ohaki dacite and rhyolite, and the major one being caused by an increase in density of the rocks through alteration and deposition from ascending hot waters. The similarity to the resistivity pattern in Figure 1 should be noted.

Drill Hole Temperatures

At present there are 27 drill holes between 760 and 1200 m and there is one hole 2368-m deep.

The degree to which the temperature and pressure measured in the hole is representative of the surrounding country is open to argument. However, provided that the measurements are made below the solid casing and that the hole has been standing closed for some time, the measured values are the best obtainable estimates for the surrounding ground.

The boiling temperature at any depth will depend not only on the hydrostatic pressure but also on the partial pressure of any gas present. The main gas in the field is CO_2, and Mahon and Ellis (1968) give a figure of 250 millimoles CO_2 per 100 moles of water for the deep waters of the Broadlands field. With this value, and an initial water temperature of 310°C, the partial pressure of the gas lowers the boiling point by 3°C at 300°C. When the temperature has been reduced to 260°C, the effect is 1°C.

Inspection of the temperature and pressure measurements shows that boiling in the bottom 100 m of the hole is possible in only two deep bores, No. 17, 1070 m, and No. 25, 1250 m. There are two shallower holes, No. 8 and No. 11 (770 m and 760 m respectively) where boiling at the bottom is also possible. However the temperatures in all the bores, on the average, decrease with decrease in depth, but the rate of decrease is often irregular, and occasionally there is an increase in temperature with decrease in depth.

If the water does not boil, the drop in temperature with decrease in depth must be due to the sharing of the heat with colder water. Loss of heat solely by horizontal conduction is ruled out because of the sharpness of the boundaries. Therefore by assuming an initial temperature for the deep water and taking the measured temperature at a given level, it is possible to calculate the amount of cold water that

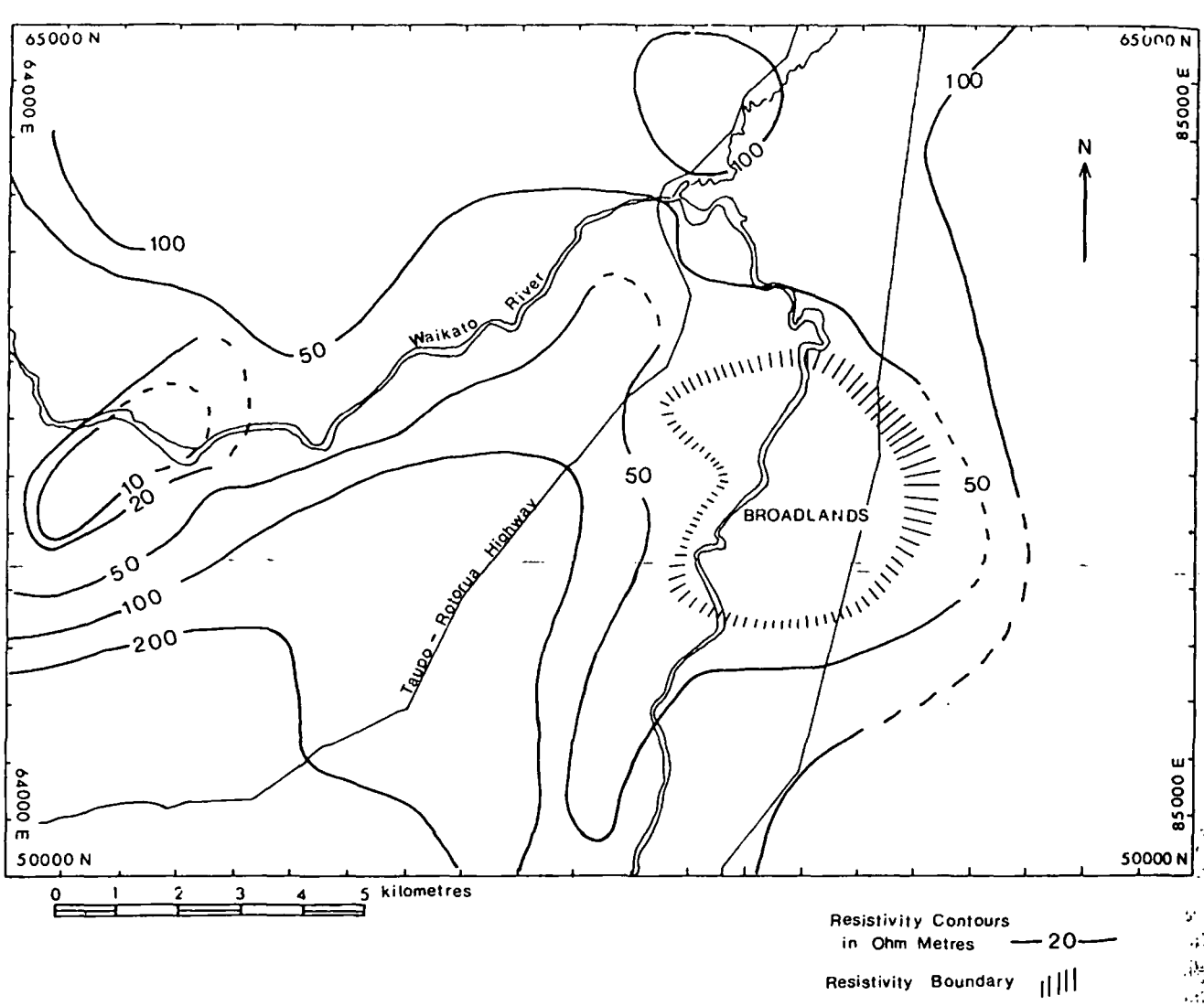

Figure 1. Map showing the resistivity pattern around the Broadlands geothermal field. Measurements are for a Wenner-type traverse with electrode spacing of 550 m. The boundary of the field found by resistivity measurements is indicated by bars.

has been added to the system up to that level.

The highest temperature measured in the Broadlands field is about 307°C, so a temperature of 310°C has been assumed for the deep water. Any difference between the assumed and real temperature would add a constant to the value of the calculated ratio of hot to cold water. The enthalpy of the hot water is taken as 140 kJ/kg, and the cold water entering the field is assumed to have a temperature of 21°C and an enthalpy of 100 kJ/kg. The minimum depth considered is 730 m, as the solid casing in most of the holes does not extend beyond this depth.

Using these assumptions, the amount of cold water that must be added to the system to reduce the temperature of each unit mass of deep water to that of the measured values at 1000 m and 730 m has been calculated. These values have been contoured and are shown in Figures 3 and 4. Both figures show elongated northwest-southeast trending contours, the values for the 730 m depth, Figure 4, being about double those of the 1000 m depth, Figure 3. This indicates that most of the horizontal inflow of cold water occurs at depths of less than 1000 m.

Natural Heat Flow

The estimation of the natural heat output from the Broadlands field has proved a difficult task. Most authors suspect that there is a considerable discharge of hot water into the Waikato River, but as this river has a flow of more than 57 $m^3 s^{-1}$, even a large inflow of hot water would lead to only a very small increase of temperature of the river. Estimates of the heat flow range from 73 MW by Dickinson (1968) to 188 MW (Dawson and Dickinson, 1970) and 204 MW (Mahon, personal commun.). These values seem low when compared with Wairakei, 426 MW, and Waiotapu, 560 MW (Dawson and Dickinson, 1970).

DISCUSSION

Geophysical methods show that there is a column of hot water rising vertically, or nearly vertically, from some depth in excess of 2.5 km. The surface output of heat appears to be lower than expected when compared with Wairakei (426 MW) and Waiotapu (560 MW).

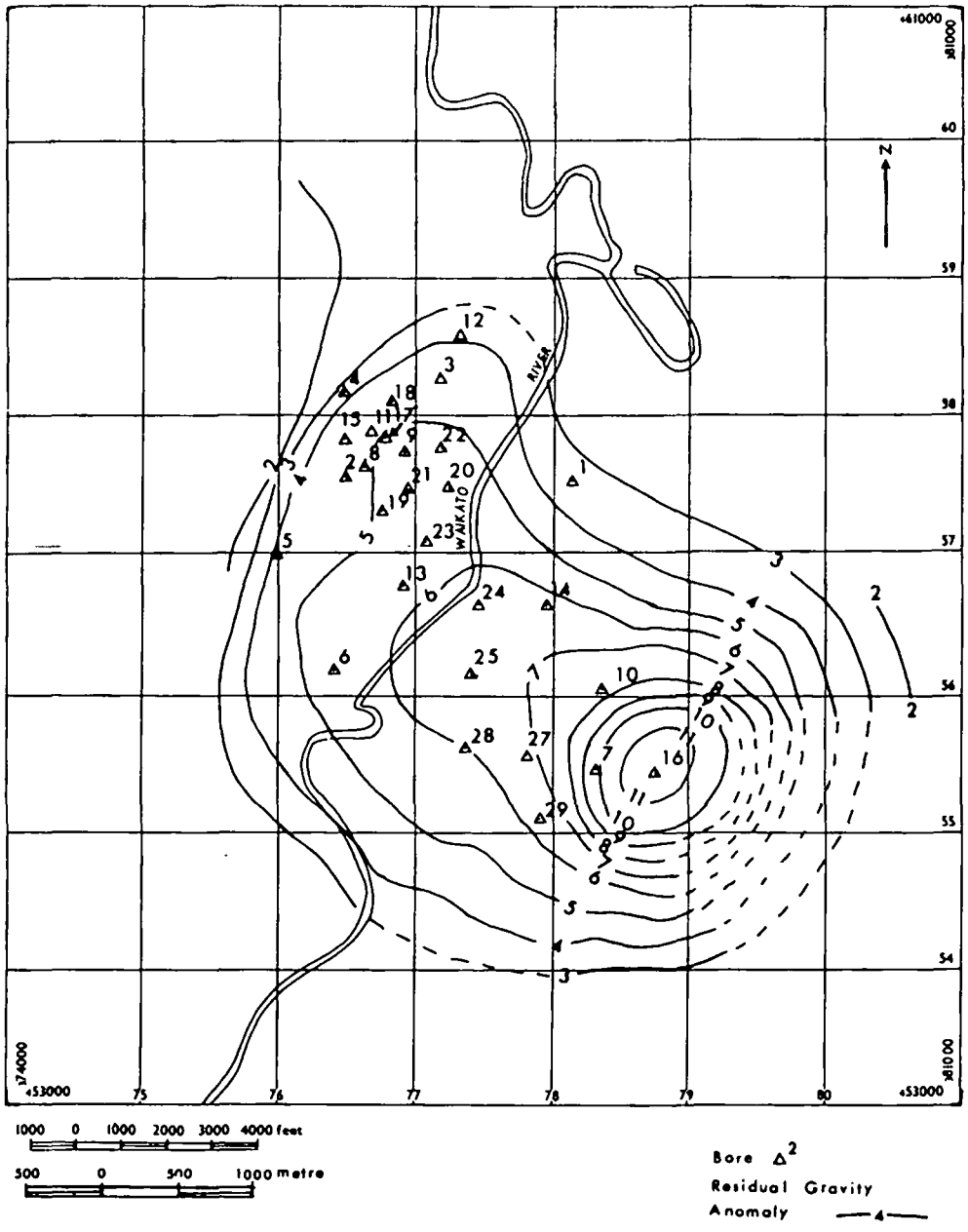

Figure 2. Residual gravity map of the Broadlands field after the removal of the effect of the greywacke basement. The contour values are 10 $\mu N \cdot kg^{-1}$ (milligals).

However the probable explanation is that the tongue of resistivities of less than 50 ohm·m shown in Figure 1, following along the course of the Waikato River both up- and downstream, indicates a subsurface outflow of hot water from the field, which mixes with cold water in the general water table of the area. It is likely that relatively impermeable layers in the Huka Falls formation provide a leaky capping layer to the Broadlands field, as there is some surface activity within the field, but there is also artesian warm water that rises in a 150-m drill hole on the banks of the Waikato River 15 km downstream.

Thus it appears that within about 100 m of the surface the hot water of the rising column strikes a rather impermeable layer which causes some of the hot water to flow horizontally below it, along the course of the Waikato River, where the hot water is mixed with the cold ground water of the area.

Temperature and pressure measurements in drill holes show that in only 2 of the 26 deep holes is boiling in the bottom 100 m possible. This means that there is little possibility of the water boiling at greater depth. Because the inflow of cold water decreases with increasing depth, the temperature of the water that reaches the surface is unlikely to exceed 320°C at depth.

Within the field there is a complicated pattern of flows of hot and cold water, and in places there will be separate flows of hot and cold water. Throughout the field there will be conductive transfer of heat between the hot water, rock, and cold water, and in parts there will be mixing of the hot and cold water. Indications of separate flows are given where the temperature-depth curve gradient changes rapidly. Bore 6, Figure 5, is an extreme example of this. Examples of mixing of hot and colder water are given in Figures 6 and 7 for bores where the temperature

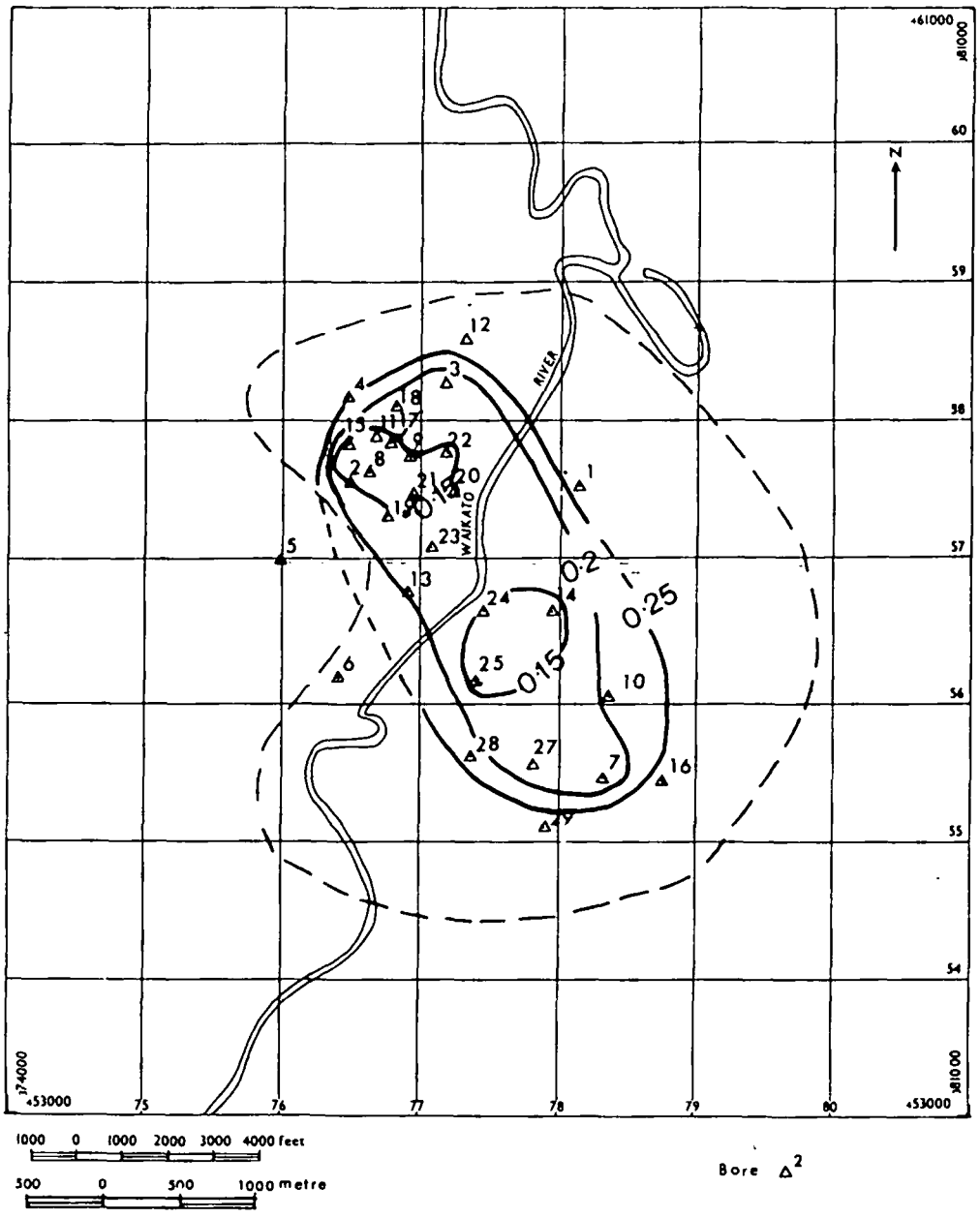

Figure 3. Map of the Broadlands field. The contours show the ratio of the rate of inflow of cold water to hot water from great depth to a depth of 1000 m.

shows regular change of gradient, and the temperature is well below the boiling point for the measured pressure. Bore 23 also shows the effect of a larger flow of cold water between 600 and 420 m.

Hence the simple model given by the geophysical methods has to be refined to include the detail from the bore measurements. The model now becomes a column of hot water with an initial temperature not much greater than 320°C rising approximately vertically. As the column rises, cold water enters from the sides. Within the field there will be a complicated pattern of flows of hot and cold water, such that temperatures generally lie below the boiling point for the actual pressure.

POWER POTENTIAL

The energy available from the field can be divided into two types: the energy stored in the hot rock and water in the reservoir, and the energy of the hot water moving into the reservoir from the heating source.

The stored energy can be estimated by measuring the volume and temperature of the reservoir. The estimate of heat added from the source is more difficult, but a minimum value can be obtained by estimating the natural heat loss from the reservoir. However, experience at Wairakei has shown that the amount of additional heat can be increased by exploitation of the field.

Stored Energy

The cross-sectional area of the Broadlands field according to resistivity measurements is 13 km^2. As the average length of solid casing is about 600 m and the deepest hole is about 2400 m, the reservoir is taken to lie between 600 and 2600 m. These values result in a volume of exploitable stored energy of 26×10^9 m^3. The temperature at 2600 m is

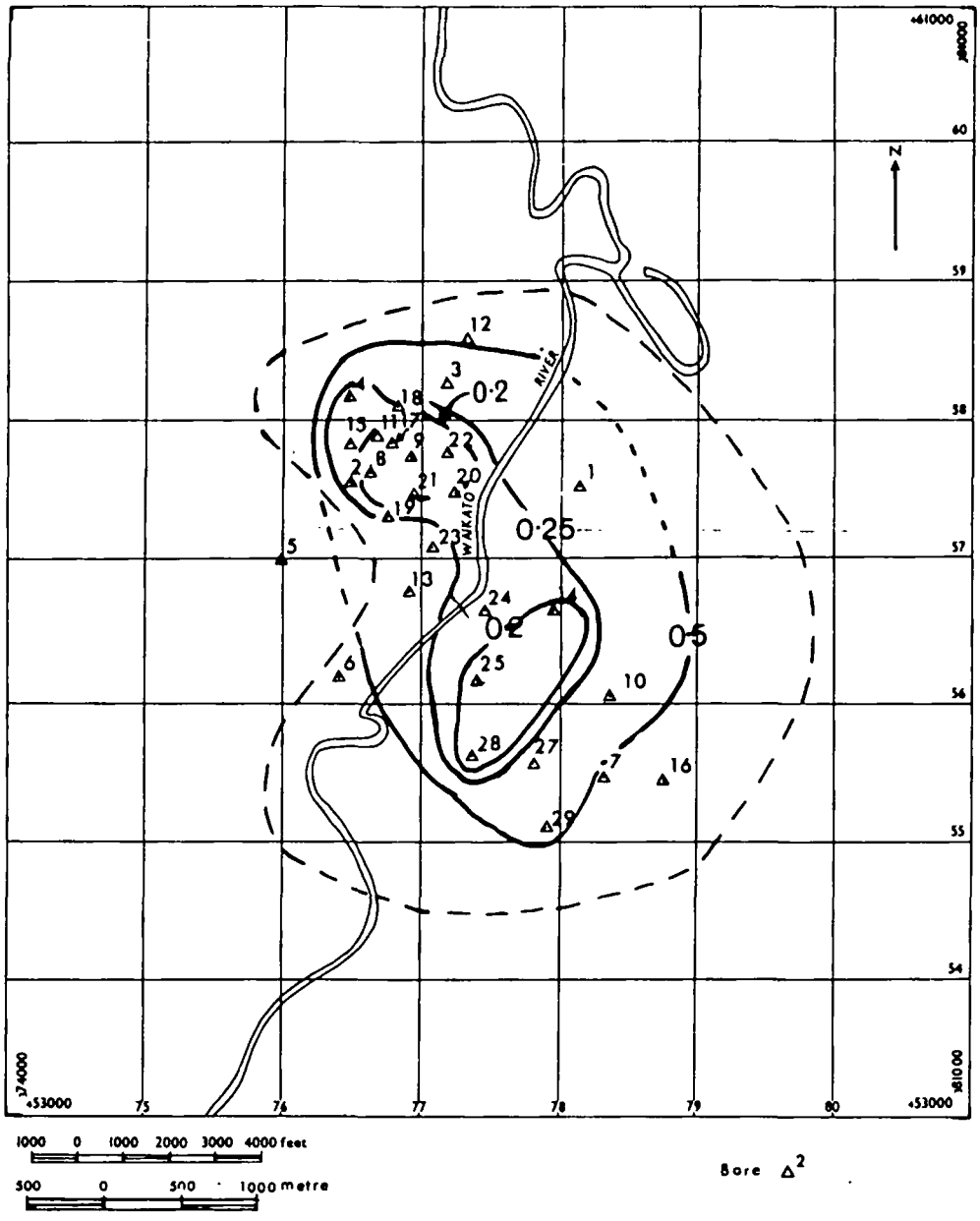

Figure 4. Map of Broadlands field. The contours show the ratio of the rate of inflow of cold water to hot water from a great depth to a depth of 730 m.

estimated to be 310°C and a temperature of 232°C at 600 m is the average of the measured temperatures in all bores, weighted by area. Porosity of 15% has been found by measurements of drill cores.

Because of practical considerations, the minimum usable temperature in the ground is taken to be 200°C, although the water that reaches the surface can be used down to 46°C.

With the above values the usable heat contained in the water of the system is 7.1×10^{17} J. The heat in the rock can be extracted by the colder water coming into the field horizontally. Assuming a starting temperature of 21°C for the cold water, 2.9×10^{18} J of the heat of the rock can be used. This makes a total of 3.6×10^{18} J.

At present it is reasonable to assume an efficiency of about 8% for conversion from heat to electricity. This means that Broadlands has a potential output of electrical energy, derived from stored heat only, of 2.9×10^{17} J or 9.2×10^{3} MW·yr.

Input Heat

Broadlands in its unexploited state appears to be a stable system, and hence the input of heat equals the output. It is likely that the natural heat output has been underestimated because there is an outflow of heat about 100 m below the surface, but it is not possible at present to forecast the increased input that should follow exploitation.

However, if measurements of gravity and ground level are made before exploitation, it is possible by repeating surveys over a period of years to calculate the net mass lost from the system (Hunt, 1970). If at the same times the position of the boundary is measured as suggested by Risk (in press) it should be possible to decide whether heat

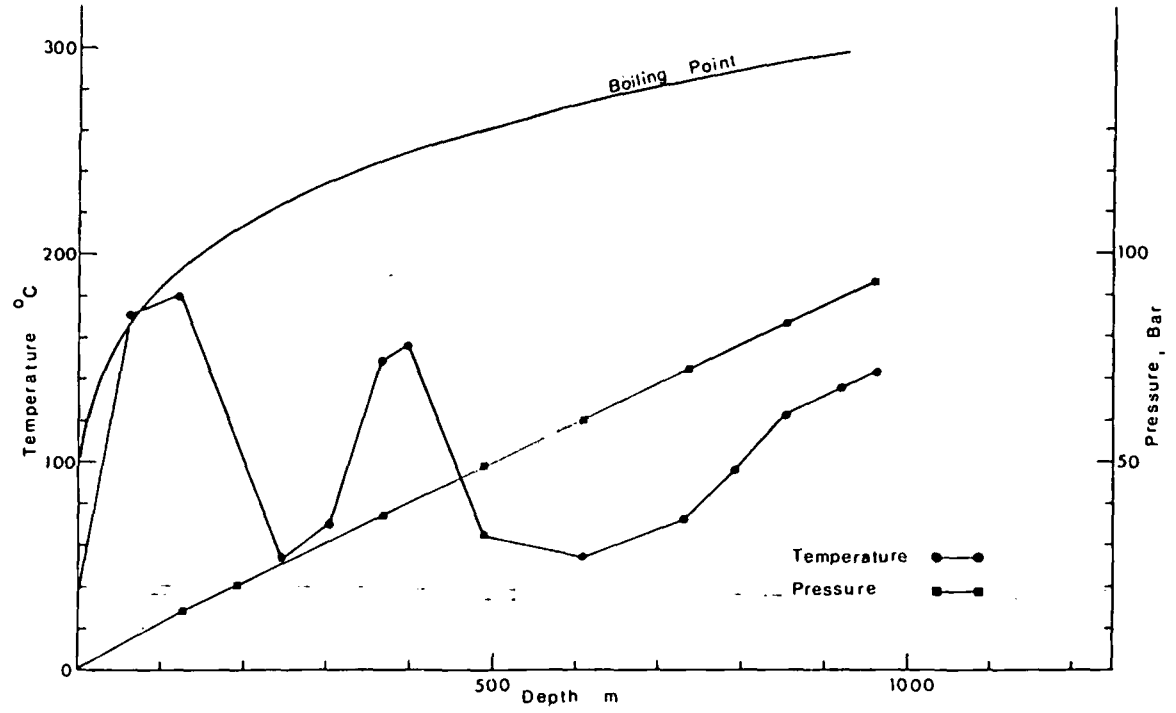

Figure 5. Temperatures and pressures measured in bore 6. The boiling-point curve is calculated from the measured pressures and allows for a gas content of 250 millimoles CO_2 per 100 moles of water at an original temperature of 310°C.

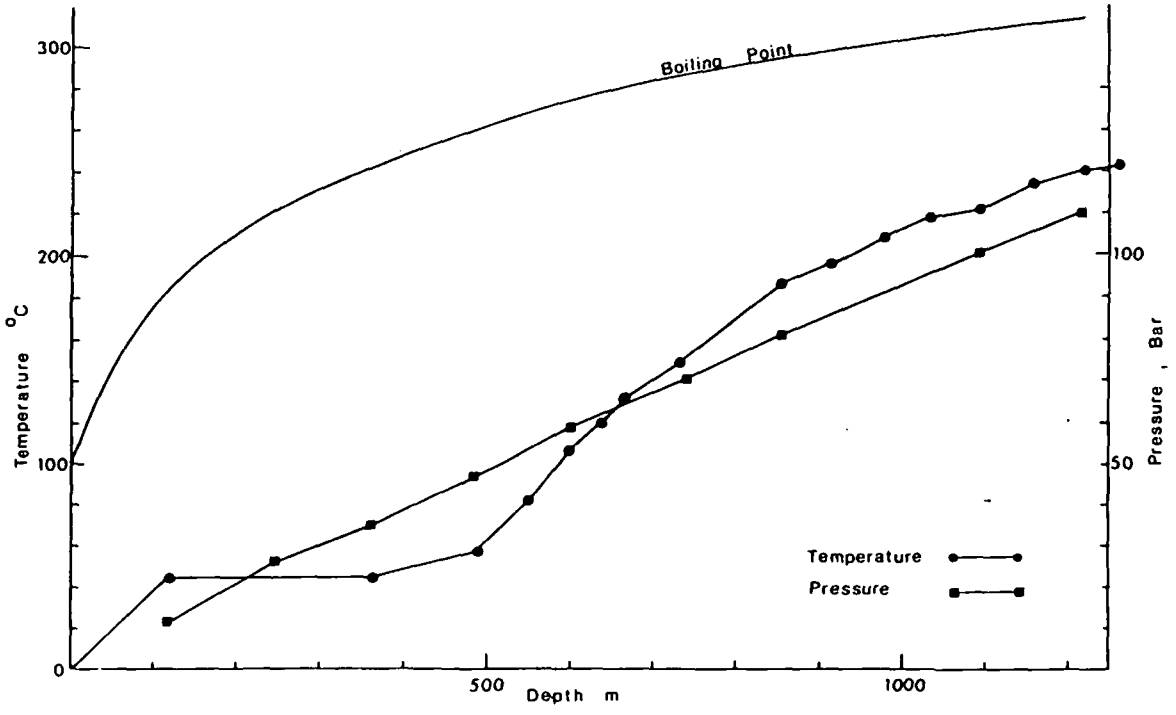

Figure 6. Temperatures and pressures measured in bore 5, Broadlands. Boiling-point curve calculated as for Figure 5.

is being replenished by increased inflow from the source.

The natural inflow using Dawson and Dickinson's value of 188 MW to 12°C, is equivalent to about 13 MW of generated electricity. This is a very low figure but it should be emphasized that this value is likely to be greatly exceeded when the field is exploited.

CONCLUSIONS

The Broadlands geothermal field is of the hot-water type. It is unlikely that the water that reaches the surface has ever been hotter than 320°C.

The drop in temperature with decreasing depth is caused

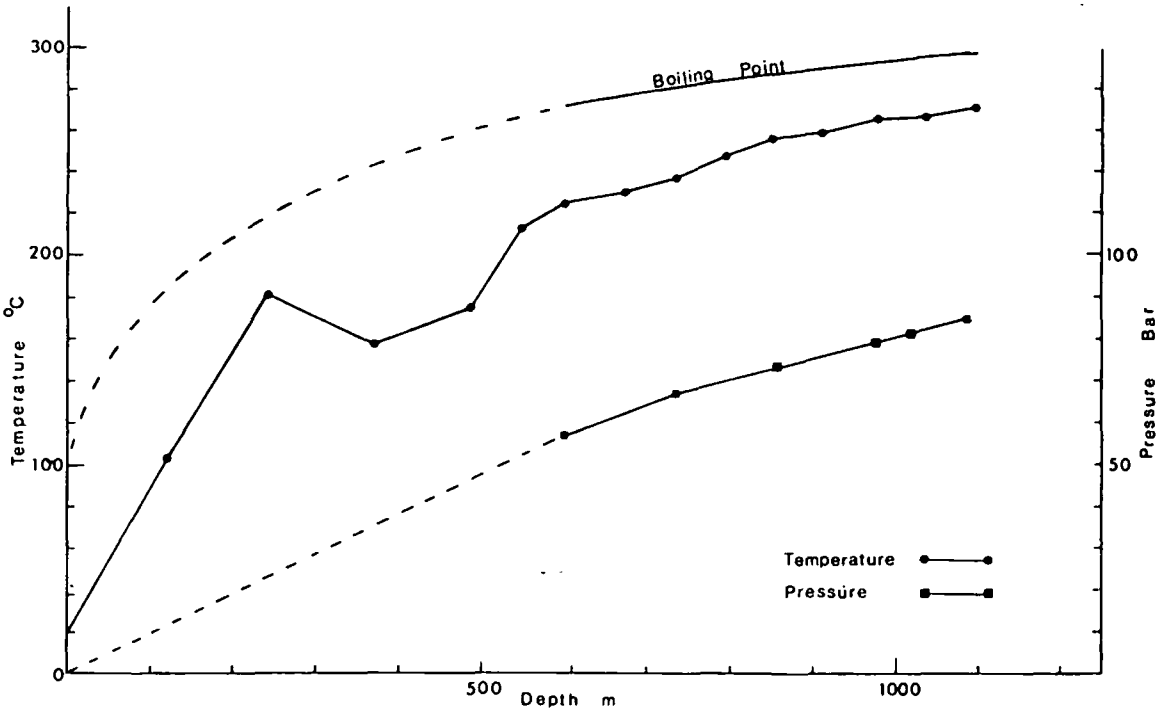

Figure 7. Temperatures and pressures measured in bore 23, Broadlands. Boiling-point curve calculated as for Figure 5.

by a horizontal inflow of cold water and not by boiling. This implies that the boundaries of the field are permeable, and that it is possible to extract all the heat from the rocks by this inflow of cold water.

The heat available from the reservoir is 3.6×10^{18} J and is equivalent to 9.2×10^{3} MW·yr of generated electricity. The measured natural heat output is only 188 MW relative to 12°C. Although at present it is not possible to predict the increase in input of heat which will result from exploitation, by analogy with Wairakei, the input should increase considerably. After the field has been exploited for several years, it will be possible to measure the increased input of heat. However, by using only the quantities of heat measured at present the most conservative estimate suggests that the Broadlands field should be capable of generating electricity at a rate of 200 MW for 47 years.

ACKNOWLEDGMENTS

The author wishes to acknowledge the help he has received from his colleagues in Geophysics Division. The temperature and pressure measurements were made by the Ministry of Works and Development.

REFERENCES CITED

Dawson, G. B., and Dickinson, D. J., 1970, Heat flow studies in thermal areas of the North Island of New Zealand: UN Symposium on the Development and Utilization of Geothermal Resources, Pisa, Proceedings (Geothermics, Spec. Iss. 2), v. 2, pt. 1, p. 466.

Dickinson, D. J., 1968, The natural heat output of the Broadlands geothermal area, 1967: New Zealand Dept. Sci. and Indus. Research, Geophysics Div. Report No. 49, p. 23.

Hatherton, T., Macdonald, W. J. P., and Thompson, G. E. K., 1966, Geophysical methods in geothermal prospecting in New Zealand: Bull. Volcanol., v. 29, p. 485.

Hochstein, M. P., and Hunt, T. M., 1971, Seismic gravity and magnetic studies, Broadlands geothermal field, New Zealand: UN Symposium on the Development and Utilization of Geothermal Resources, Pisa, Proceedings (Geothermics, Spec. Iss. 2), v. 2, pt. 1, p. 333.

Hunt, T. M., 1970, Net mass loss from the Wairakei geothermal field, New Zealand: UN Symposium on the Development and Utilization of Geothermal Resources, Pisa, Proceedings (Geothermics, Spec. Iss. 2), v. 2, pt. 1, p. 487.

Macdonald, W. J. P., and Hatherton, T., 1968, Broadlands geothermal field—geophysical investigations: New Zealand Dept. Sci. and Indus. Research, Geothermal Report No. 5, p. 44.

Mahon, W. A. J., and Ellis, A. J., 1968, The chemistry of the Broadlands geothermal field: New Zealand Dept. Sci. and Indus. Research, Geothermal Report No. 5, p. 90.

Risk, G. F., Macdonald, W. J. P., and Dawson, G. B., 1970, DC resistivity surveys of the Broadlands geothermal region, New Zealand: UN Symposium on the Development and Utilization of Geothermal Resources, Pisa, Proceedings (Geothermics, Spec. Iss. 2), v. 2, p. 287.

Inst. Invest. Geol., Santiago, Chile, 305 p.
Siegers, A., and Pichler, H., 1969, Trace element abundances in the andesite formation of northern Chile: Geochim. Cosmochim. Acta, v. 33, p. 882-887.
Trujillo, P., 1974, Castastro de recursos geotérmicos de Chile: Seminario sobre los recursos energéticos de Chile (CONICYT).
Zeil, W., 1964, Die Verbreitung des jungen Volkanismus en der Hockordillera Nordchiles: Geol. Rundschau, v. 53, p. 731-757.

Electrical

The Geothermal Field of El Tatio, Chile

A. LAHSEN
P. TRUJILLO
Proyecto Geotermico—CORFO-ONU, Casilla 14631, Correo 15, Santiago, Chile.

ABSTRACT

El Tatio geothermal field is located in the high Andes range at the northwest end of Antofagasta Province. (68°01′ latitude South, 22°20′ West Greenwich longitude). It is geologically set in volcanic rocks (ignimbrites and lavas) of the upper cenozoic overlying a basement of Cretaceous sediments, in a north-south graben originated in the recent Pliocene by expansion movements, which mainly accounts for the uplift of the Andes. Geoelectric studies have found a resistivity anomaly with values under 10 ohm·m in a surface of about 30 km², running along the main structure. This anomaly has been verified by means of 13 wells of depth between 600 and 1821 m.

The principal producing aquifer has a temperature of 265°C and is located at a depth between 800 and 900 m. From three wells now in production an amount of steam equivalent to 18 MW is being obtained. With future development programs the profitable capacity is expected to be raised to 50 MW.

By means of a pilot desalination plant, the possibility of producing fresh water from geothermal steam has been proven.

FOREWORD

El Tatio geothermal field is located at the northeastern end of Antofagasta Province, approximately 100 km east of the city of Calama and Chuquicamata copper mine, at 22°20′S. and 68°01′W. at an elevation of 4300 m above sea level (Fig. 1). (Note: All figures are in the preceding Spanish version.)

Methodical exploration began at El Tatio early in 1968 as a result of an agreement between the United Nations Development Program and the Government of Chile. Geological, geophysical, and geochemical studies that include the drilling of six slim exploration wells with depths between 600 and 750 m from 1969 to 1971 and seven production wells between 1973 and 1974 at depths that range from 870 m to 1820 m have been undertaken during this period of time.

Since September 1974 a pilot desalination plant granted by the United Kingdom has been in operation. The aim of this plant is to determine the possibility of producing fresh water from geothermal steam, as well as to study the procedures of obtaining chemical elements or compounds of economical value from the brines proceeding from the desalination process, and to carry out tests for a more suitable design of an industrial plant that would be added to the future geothermal power plants installed in El Tatio.

At present, results on the feasibility studies entrusted by the United Nations to an international consulting agency are being studied to decide on investments and development programs for the near future.

TECTONICS AND VOLCANISM IN NORTHERN CHILE

Like all the geothermal areas of northern Chile, El Tatio is located on the high ranges of the Andes Mountains, where a lively calc-alkaline volcanism occurred from the Miocene to the Recent, in accordance with the ages determined through radiometric studies by Ruiz (1965).

From the tectonic and stratigraphic point of view the upper Cenozoic volcanic activity in northern Chile has two principal episodes: (1) A pre-Pliocene or Miocene volcanism, expressed by several units of rhyolitic to dacitic ignimbrites and andesitic stratovolcanoes; and (2) A Plio-Quaternary volcanism that contains, in addition to a number of ignimbritic layers, the andesitic stratovolcanoes and rhyolitic domes which cover the highest Andean ranges (Lahsen, 1974a).

These two volcanic episodes are included in the rhyolitic formation as well as in the overlying andesitic formation of Zeil (1964), Siegers and Pichler (1969), and others. Even though these names suggest a unique chemical composition for each unit, the rhyolitic and the andestic rocks coexist with each other as it has been established above.

The oldest volcanic episode began at least 18.7 millon years ago as has been shown by radiometric ages (Ruiz, 1965). The lavas and ignimbrites of this episode were folded in the upper Miocene, during the last compressive phase of the Andean tectonic cycle. The volcanic activity decreased or probably stopped during this compressive phase and appeared again during the east-west expansion that followed

and probably is still developing (Lahsen, 1974a).

The Plio-Quaternary expansion, which had its principal intensity in the upper Pliocene, originated block movements through a system of nearly north-south faults that produced the most important morphostructural features of the area: (1) the Chile-Perú trench; (2) the coastal ranges; (3) the central depression (valley); and (4) the Andean occidental ranges (Fig. 1).

The Plio-Quaternary expansion has been in turn correlated with the present oceanic spreading activity that began 10 m.y. ago (Charrier, 1973) and in which the main volcanic activity characteristic of the Andean mountain ridges developed.

It is possible that the Plio-Quaternary volcanism of this Circum-Pacific margin has developed as a result of the subduction of the oceanic lithosphere (Nazca plate) along the zone of Benioff, which in this latitude has a slope between 20° and 30°, and whose intermediate and deep seismic foci are located just beneath the highest Andean elevations.

The earth's crust below the highest parts of the Andes has a thickness between 60 to 70 km (Dragnicević, 1974). The thickness of the crust and the inclination of the Benioff plane would be the determinant agents of the nature and characteristics of Plio-Quaternary volcanism in northern Chile.

GEOLOGY OF EL TATIO

Mesozoic Basement

Jurassic and Cretaceous rocks outcrop toward the west of El Tatio, mainly on the occidental slope of the Tucle-Loma Lucero horst and in those places where the erosion of the overlying ignimbrites has exposed it.(Fig. 2).

The oldest rocks of this basement correspond to a sequence of Middle Jurassic shallow marine sediments, called Lomas Negras formation (Lahsen, 1969, unpub. rept.). These strata are formed by sandstones and multicolor shales strongly silicified and pierced by andesitic and lamprofiric dikes. It is displayed in tight NW-SE folded structures, produced by the compressive movements imputed to the Nevadian orogenesis (Upper Jurassic). These sediments are overlayed uncomformably by the Agua Fresca formation of likely Upper Jurassic-Early Cretaceous age (Lahsen, 1969, unpub. rept.). This formation is composed mainly of strongly epidotized amphilbole andesites due to a regional metamorphism and strong hydrothermal activity that have originated a number of copper mineralizations. Probably due to the inter-Senonian orogenic movements the Jurassic series are overlayed by Cretaceous deposits by means of a strong fold and erosion unconformity. These deposits are represented by the Quebrada de Justo formation, which is formed by a well-stratified sequence of sandstones and pink tuffaceous limolites, with basal conglomerates that include a great number of fragments belonging to the underlying Jurassic rocks. According to its stratigraphic position and its tectonic characteristics, these sediments are imputable to the Upper Cretaceous; this formation has been affected by the diastrophic movements attributable to the Laramide orogenesis that originated the inverse faulting and the folds with N-S trends.

Upper Cenozoic Volcanism

Over this basement of strongly faulted, folded, and eroded Mesozoic rocks, the deposition of a thick layer of volcanic material that ranges from the Miocene to the Pleistocene began.

Miocene

The oldest upper Cenozoic rocks correspond to the Río Salado volcanic group; they crop up mainly in the Tucle-Loma Lucero horst. This group includes two densely welded ignimbrite sheets, separated by a variable thickness of unwelded tuffs and pumice breccias. Locally, in the central part of the Serrania de Tucle, the ignimbrites are covered by a dark andesite and pink tuffaceous breccias with big volcanic bombs. These andesites and volcanic agglomerates were probably erupted from a volcanic center located near the west ridge of the Tucle horst (Lahsen, 1974b).

The thickness of this formation varies from place to place according to the pre-existing landforms over which it was deposited; accordingly, it presents in its base a changeable thickness of tuffaceous breccias, especially thick in those places which were depressions. This basal member has been called Peñaliri formation by Trujillo (1973, unpub. rept.) and constitutes an important permeable layer at the southwest end of the field.

The Río Salado volcanic group is covered by the Sifon ignimbrite, defined by Guest (1969), formed by strongly welded gray or light brown dacitic tuffs, containing crystals that are smaller in size and amount than the underlying ignimbrites. The thickness and distribution of Sifon ignimbrite is controlled by the topography of the Mesozoic rocks and it may reach to a slab of up to 100 m of thickness. It outcrops especially in the Serrania de Tucle and in the Toconce-Caspana area about 10 km west of El Tatio. This unit could not be recognized underground and it probably was mistaken from the wells for the Salado ignimbrite.

These two formations are assumed to correspond to the lower Miocene because they are older than the subvolcanic domes of Copacoya and Piedras Grandes. The latter has been dated at 7.35 m.y. by Rutland in 1965. They occur slightly folded, forming structures with North 20° to 30° trend; the compressive phase that originated these movements is considered to be of upper Miocene age; that is to say, of the last compression of the Andean tectonic cycle.

Toward the northwest the Sifon ignimbrite is spread over a series of tuffs and alluvial and pyroclastic sediments, called the Toconce formation (Lahsen, 1969). It is composed of a lower member of pumiceous tuffs and moderately welded rhyolitic breccias, with a maximum thickness of 100 m upstream in the Toconce River; an intermediate member that includes up to 50 m of well-stratified sands and gravels interbedded with pumice layers and thin diatomaceous strata, deposited only locally in the Aiquina-Caspana area; and an upper member formed by approximately 30 m of grayish to white, very badly welded tuffs, inconsistent in places. This formation could not be recognized through the drilled wells.

The Miocene volcanism culminates with the placing of the dacitic subvolcanic domes of Piedras Grandes and Copacoya along a N-S fault system located in the west margin of the Tatio graben. It is probable that these domes

are the last result of an acid magmatism, turned more viscous due to degasification, after an explosive phase that would have originated some of the ignimbrite units of the area (Lahsen, 1969, unpub. rept.; 1974b). According to the age determination by radiometric methods carried out by Rutland and others in 1965, the age for the Piedras Grandes dome is 7.35 m.y., which permits an attribution of an upper Miocene age to it.

Pleistocene-Holocene

This volcanic episode begins with the deposition of the Puripicar ignimbrite, a name given by Guest (1969) to a series of welded light gray or pink dacitic tuffs with a high content of phenocrysts, among which big crystals of biotite of up to 3 mm and an amatrice-type pink quartz are remarkable. At the base of this unit a white pumiceous breccia of widely varying thicknesses commonly appears.

The Puripicar ignimbrite is one of the most important producing levels of El Tatio; its permeability is mainly due to the cooling cracks and fractures of tectonic origin. In 1965 Rutland and others assigned an age of 4.24 m.y. to these rocks according to radiometric determinations. This allows us to locate it in the lower Pliocene.

The Puripicar ignimbrite is overlayed by a number of pyroclastic sediments, tuffs, and lavas named the Tucle volcanic group. These materials have a good permeability and form one of the most superficial aquifers of the reservoir, especially the Tucle dacites.

Following, we have the Tatio ignimbrite (Healy, 1969; unpub. rept.; Lahsen, 1969, unpub. rept.) that corresponds to the youngest sheet of ignimbrites of the area. It is composed of moderately welded tuffs, with a low content of crystals and fragments of rhyolitic pumice especially abundant and large in the upper layers of this unit. The Tatio ignimbrite is restricted only to the eastern part of the Tucle-Loma Lucero uplifted block which blocked the way of the flow toward the west. This structural range was originated by the E-W distensional movements initiated in the Pliocene.

The volcanic activity in this area ends with the El Tatio volcanic group, formed by a series of andesitic stratovolcanoes and rhyolitic domes, that top the Andes Mountains in this latitude. This volcanic system reaches a height of 5000 m above sea level, and is located on the eastern margin of El Tatio, along the N-S fractures of the Plio-Quaternary expansion phase. We are not sure if this line of volcanoes marks the eastern margin of the Tatio graben or if it extends more toward the east.

STRUCTURE

El Tatio geothermal field is located in the sunken block (Tatio graben) oriented approximately N-S for about 20 km. It is limited to the west by the horst of Serrania de Tucle-Loma Lucero. Its dimension toward the east is unknown; however, it could be limited by the band of volcanoes of the El Tatio volcanic group (Fig. 2) up to where it reaches a medium width of about 7 km. The horst of Tucle, as well as its lengthening toward the north through Loma Lucero, and the graben Tatio have originated in the Plio-Quaternary extension that allowed the gradual displacements of blocks along the almost N-S fault systems. These vertical block movements developed at the same time as volcanic activity, with principal emission centers located along these fractures.

The size of the settlement of the Tatio graben, considering the thickness in meters of the volcanic formation of the upper Cenozoic that refilled it plus the difference in height of the Serrania de Tucle compared with the Tatio valley, varies approximately between 800 m in the area of Well No. 1 and 2000 m in the area of Well No. 9.

Outcrops of the Jurassic and Cretaceous are found in the positive structure of the Serrania de Tucle and Loma Lucero. In this way the permeable upper Cenozoic volcanic series are in touch with the argillaceous rocks of the Quebrada de Justo formation, constituting the west margin of faults of the Tatio graben, a natural barrier that restrains the movements of the geothermal fluids toward the west (Fig. 3).

Along the fault system of the eastern border of the Tucle horst, the magma was periodically channeled, allowing the shedding of volcanic material of some of the units described above. Among the units with emission centers in this area are the upper levels of the Tucle volcanic group and the subvolcanic domes of Copacoya and Piedras Grandes.

The volcanic centers of El Tatio would have been channeled through nearly N-S fractures also belonging to the distensive system of the Plio-Quaternary. These are mainly in a N-S line toward the east of El Tatio graben.

The N-S system is associated with secondary transcurrent NW-SE and NE-SW fault systems, which were especially active during the Pleistocene. In fact, only these two systems of fractures have affected the Tatio ignimbrite, deposited when the Tucle horst already formed an important positive block, blocking the ash flows toward the west.

The NE-SW and NW-SE fault systems caused the subdivision of the main structures in two minor blocks. In this way the block of Loma Lucero has been displaced toward the west in relation with the Serrania de Tucle, as well as the southern portion of the Copacoya hill. In its turn the Tatio graben subdivided itself in different blocks, with horizontal as well as vertical movement with respect to its N-S position, which makes the well site selection for production drill bores very difficult.

The surface hydrothermal activity of El Tatio is displayed essentially along NW-SE and NE-SW fractures. Some of these features can be inferred by the alignment of the thermal manifestations. The movement of the thermal fluids is controlled by the N-S fracture system and by the Pleistocene secondary systems.

The temperatures recorded through the wells have helped to determine the movement of the fluid at different depths. In fact, the wells located in the western area of the field (Figs. 3 and 10) show a decrease of the temperature with depth; this would prove that the heat in this area is not uniformly transmitted from below by conduction. This phenomenon is not found at the NE end of the field, where the highest temperatures have been recorded (Table 1).

This has been interpreted (Lahsen, 1971, unpub. rept.) as an area where thermal fluids rise vertically through N-S fractures or probably along the intersection points with the Pleistocene fracture systems from where they feed the permeable levels, and through which the fluids move horizontally toward the north and northwest.

Shallow Hydrothermal Activity

The thermal activity at El Tatio is scattered over an area of about 30 km^2. It occurs preferably in the upper levels of the Tatio graben, at about 4100 m above sea level.

The area of the largest thermal activity concentration is found at the sources of Salado River which springs from it. In this zone covering a surface of about 10 km^2 the thermal activity includes geysers, fumaroles, boiling water and mud ponds, mud volcanoes, "soffioni," steam soils, and others.

From the waters discharged by these springs, great quantities of salts are precipitated, mainly composed of chlorides and silica that originate significant sinter cones and terraces formed around the geysers. These hot springs form small brooklets that flow through gorges, converging in the Salado River which drains El Tatio valley across a narrow gorge carved in the Serrania de Tucle. The water discharged by the thermal manifestations varies between 250 and 500 l/sec according to seasonal changes.

Other smaller localities with hydrothermal activities are generally situated at higher levels (4600 m above sea level) southeast of the main area (Fig. 3).

In general, the temperature of these hot springs reaches 86°C, which corresponds to the water boiling point for this altitude; higher temperatures have been found in some geysers and fumaroles.

Heat Loss

The total heat loss of El Tatio, determined by direct methods from the natural discharge, has been estimated as 26 × 10^6 cal/sec (Hochstein, 1971) and 50 × 10^6 cal/sec (Trujillo, 1974).

The difference observed in these values may be due to different criteria used for its estimation or by actual variations produced by seasonal changes during rainfalls.

Actually, precipitation as well as the superficial aquifers control the size of thermal manifestations such as steam soils, geysers, hot springs, or fumaroles.

By means of chemical techniques based on chloride content, Mahon (1970) estimates a heat loss between 40 to 60 × 10^6 cal/sec. In 1972 the same author in warmer periods with little or no rainfall, found a heat loss between 25 to 28 × 10^6 cal/sec (Table 2).

According to the abovementioned data the mean heat loss for El Tatio could be considered to be about 35 to 40 × 10^6 cal/sec. Comparing this value with those corresponding to other parts of the world, El Tatio heat loss is higher than the Japanese thermal areas (from 2 to 20 × 10^6 cal/sec, according to Fukada et al., 1970) and lower than most of the New Zealand hydrothermal areas (from 20 to 135 × 10^6 cal/sec; Dawson and Dickinson, 1970).

In accordance with the heat loss determined for El Tatio and comparing it with other geothermal areas of the world, Trujillo (1974), has estimated a power of generation of about 100 MW as being developed in this geothermal field.

GEOCHEMISTRY

The geochemistry of El Tatio geothermal field appears in detail in the paper by Cusicanqui et al. presented in this Symposium. For that reason we will limit ourselves to only a brief review of the essential geochemical characteristics observed in this field.

The hot water and steam discharged by the thermal manifestations and the drilled wells correspond to an approximately neutral solution (mean pH = 7.2) with the following main components: NaCl, KCl, $CaCl_2$, B and SiO_2 (Table 1). It also presents some concentrations of Li, Rb, and Cs. The principal dissolved gases are H_2S and CO_2 (Ellis, 1969; Mahon, 1970; Table 2).

The mean chloride content is about 7500 ppm; however, through sampling at different depths in the wells, levels with more than 2000 ppm of Cl^- have been found (mainly Wells 2 and 9).

The average SiO_2 content is 450 ppm in the wells, whereas in the hot springs it is about 210 ppm.

The variations in content of the dissolved solids observed in the different hot springs and in the wells are indicative of a mixture of aquifers (Mahon, 1970) at different temperatures and with various salt contents. According to this and considering the geological structure of the field, Lahsen (1971, unpub. rept.) determined the existence of thermal water flows which, after a long and deep run, rise through fractures to the permeable levels of the field, from where they move toward the west and northwest, mingling in different proportions with the more superficial water flows, and with waters recently infiltrated through the fractured modern volcanic rocks (Figs. 2 and 12).

Before the wells were drilled, the contents of SiO_2 and the Na/K ratio were used to determine a minimum underground temperature of about 190°C (Ellis, 1969). The significant temperatures recorded in the wells may also be considered as indicative of such dilutions with colder superficial waters containing inferior quantities of dissolved solids.

The concentrations of deuterium and oxygen 18 measured in the different types of water of the area indicate their meteoric origin.

GEOPHYSICS

Geophysical explorations, based only on geoelectrical methods, have been used to determine the extension of geothermal reservoir in the subsurface. The low resistivity values of the rocks with hot salty water have been used to determine the limits of the field and to obtain a pattern of the movements of the geothermal fluids in El Tatio.

With geoelectrical prospections a resistivity anomaly of about 30 km^2 with 10 ohm·m has been found in the Tatio graben, and within it, a zone of 14 km^2 with 5 ohm·m. Enclosed in the abovementioned region there are two little areas of 3 ohm·m, one toward the north of 3.5 km^2, and the other one in the central part of 2.5 km^2 (Hochstein, 1971).

This anomalous zone exhibits a N-S elongation, comparable to the Tatio basin shape, presenting a widening toward the west in its central part, coinciding with the Rio Salado gorge. Likewise there are two continuations westward, one in the northern part (N. 534 000) and the other one in the south (N. 528 000).

Three resistivity surveys have been done covering the major part of the geothermal field; for this purpose the Schlumberger array with AB/2 = 250 500, and 1000 m was used with DC commuted every 10 seconds, in addition to resistivity soundings with Schlumberger arrays up to 1000 m of penetration, and measurements with dipole method for depths over 2 km (Figs. 7, 8, and 9). The high contact

Table 1. Chemical composition of thermal springs and wells of El Tatio.

Sample	Date	pH 25°C	COMPOSITION in ppm Li	Na	K	Rb	Cs	Ca	Mg	Sr	NH_3	Cl	F	SO_4	B	SiO_2	CO_2	HCO_3	H_2S	Molecular ratios Na/K	Na/Li	Cl/B	Cl/SO_4	C/Cs
Hole 1*	Jan. 70	7.22	3.14	4.300	440	10.0	16.5	297	1.24	3.2	1.2	7.738	2.75	38.0	179.3	392	1.4	19.5	1.0	16.6	38.0	13.3	560	1.780
2	3 Dec. 71	7.38	43.0	5.070	640	8.3	17.0	276	0.69	—	2.17	9.037	2.92	42.0	195.0	450	3.0	65.0	—	13.3	35.5	14.1	586	1.960
4	8 Sep. 71	7.74	29.8	4.700	282	3.14	17.9	238	1.50	—	—	8.016	—	70.0	194.0	385	3.5	77.5	—	28.3	47.8	12.6	310	1.674
Hole 7*	Jan. 74	7.15	45.0	4.890	840	0.6	17.3	211	0.08	—	3.0	8.870	—	29.0	203	750	3.2	39.0	—	9.9	32.8	13.3	828	1.924
9	Jan. 74	6.55	22.5	8.952	467	0.9	3.8	4.418	68.0	—	1.2	22.355	—	29.0	—	—	8.5	27.0	—	31.9	120.0	36.5	2.088	22.515
10	Jan. 74	7.05	43.4	4.745	740	8.3	16.7	277	0.89	—	2.7	8.705	—	39.0	—	—	5.3	40.0	—	10.9	33.0	13.1	605	1.948
Spring 103	Nov. 69	5.9	33.0	3.360	170	—	10.3	247	0.3	—	1.8	5.924	—	67.0	139	162	—	17.0	0.2	34.0	31.0	13.0	240	2.150
157	Nov. 69	6.35	—	3.320	190	—	11.1	256	—	—	—	5.660	—	48.0	130	151	22	37.0	5.0	30.0	—	13.3	320	1.910
172	Nov. 69	7.75	27.0	2.780	241	—	9.9	202	—	—	1.8	4.811	—	39.0	110	154	1	58.0	7.0	19.5	31.0	13.3	330	1.820
226	Nov. 69	7.0	47.0	4.540	530	—	13.1	162	—	—	2.3	8.233	2.4	44.0	186	260	5	29.0	6.0	14.5	29.0	13.5	510	2.350
241	Nov. 69	7.38	45.0	4.320	525	—	—	278	—	—	—	7.874	—	26.0	170	280	1	21.0	11.0	14.0	29.0	14.1	820	—
331	Nov. 69	6.22	46.0	4.580	525	—	13.0	269	—	—	—	8.037	2.9	32.0	182	221	22	30.0	12.0	14.8	30.0	13.4	680	2.310

Analyzed by H. Cusicanqui and/or A. Mahon. * Sampling pressure: 8.7 psig.—Not analyzed.

Table 2. Steam analysis of El Tatio wells *

Well No.	Date	WHP psig	S.P psig	Enthalpy Btu/lb	Gas in steam at sampling pressure milimoles/100 moles in ppm Co_2	H_2S	Gas in total discharge milimoles/100 moles in ppm CO_2	H_2S	% by weight of gas CO_2	% in total steam discharge CO_2	$\frac{CO_2}{H_2S}$ molar
1	19 Jan 70	208.0	30.0	408	132.0	0.03	23.4	0.005	0.32	0.057	4.400
2	21 Jul 71	168.7	164.7	402	400.0	1.30	29.5	0.096	0.98	0.072	308.0
4	16 Dec 70	87.7	74.7	366	790.0	0.42	77.6	0.041	1.93	0.16	1.885
7	21 Nov 73	187.7	88.7	474	79.4	1.20	15.8	0.238	0.19	0.38	66.5
10	7 Jan 74	38.7	18.7	463	98.6	1.21	27.7	0.341	0.24	0.068	81.2

* Analyzed by A. Mahon and/or H. Cusicanqui

Table 3. Drilled production wells and their reached depths.

Well	Spudded	Finished	Total depth m CHF
7	9. 1.73	3. 5.73	873
8	25. 5.73	1. 8.73	1.590
9	18. 8.73	15.10.73	1.821
10	5.11.73	1.12.73	1.010
11	26.12.73	2. 2.74	900
12	14. 2.74	25. 3.74	1.421
13A	25. 5.74	7. 7.74	1.000

resistivity, the high value of noise to signal ratio, and the low resistivities observed have made this survey very exigent from the instrumental point of view.

The apparent resistivities that correspond to AB/2 = 250, AB/2 = 500 and AB/2 = 1000, respectively, are shown in Figures 4, 5, and 6. By comparing these maps, the way that resistivity changes with depth may be observed (Hochstein, 1971).

Resistivities between 800 ohm·m and 30 ohm·m have been detected in the different lithologic units existing in the area, but out of the geothermal field they vary from 30 ohm·m in the Quebrada de Justo formation (Cretaceous) up to 800 ohm·m in the andesities of the modern volcanoes. The ignimbrites present a mean resistivity of 400 ohm·m (Marinović and Fernandez, 1970, unpub. rept.).

AB/2 = 250 m. Three areas of low apparent resistivity were determined with this spacing; they concur with the zones of superficial hydrothermal activity. The major one is located in the central part of El Tatio together with two smaller ones found north and southeast respectively; separated by zones of high resistivity (Fig. 4).

The zones of high resistivity near to areas of low resistivity can be explained by changes in the permeability of the rocks due to fractures. Likewise the areas of low resistivity, according to this penetration, show the distribution of shallow hot aquifers.

AB/2 = 500 m. The isoresistivity map obtained with this survey (Fig. 5) has in general AB/2 = 250 m. However, the zones of low resistivity have spread and the north and central areas of anomaly join. The zones of high resistivity that previously divided the field have decreased in surface and in values.

AB/2 = 1000 m. The zones of smaller than 3 ohm·m appear in two well-defined places, at the central and northern parts of the field (Fig. 6).

The anomaly opens toward the west in the area where the Salado River cuts the Tucle horst. This may indicate that the river was excavated along relatively deep NE-SW fractures that let the hot fluids pass beyond the limit permitted by the Tucle horst in the rest of the field. Another opening shown by the anomaly of low resistivity is toward the southeast. It corresponds to the place where the hot fluids ascend through fractures and are transmitted horizontally toward the northeast.

In the southwest part of the anomaly at AB/2 = 1000 m the discontinuities found in AB/2 = 250 and 500 m do not persist. This may be interpreted as caused by the existence of salty levels at depths of more than 500 m which disguise small changes in temperature of the fluids. This has been evident in well No. 9 where Cl^- contents up to 22 000 ppm were measured. The existence of this salty level suggests a trapping of the fluids in this locality due to vertical block movements.

Schlumberger Soundings

Some of the electrical soundings done with Schlumberger arrays up to AB/2 = 1000 m each 250 m are presented in Figures 7, 8, and 9, which correspond to the zone where the production wells are located. In them a clear arrangement of the isoresistivity lines may be appreciated, with values normally growing toward the east in the deeper zones, besides a zone of very low resistivity (1.5 ohm·m) in the upper parts of the profiles, corresponding to the permeable layer of the Tucle dacites, and including a high water content at the mean temperature of 160°C.

DRILLED WELLS

Between 1969 and 1971 six exploratory wells 4 inches diameter were drilled at a mean depth of 600 m. They crossed a permeable zone, determined by the loss of circulation during the drilling; by the injection of cold water and its following temperature rise with the well closed and through temperature and pressure profiles during the discharge (Figs. 10 and 11).

The principal permeable layers were found at a depth between 225 and 650 m, preferably in the Puripicar ignimbrite, in a smaller proportion in the Tucle volcanic group, and only occasionally in the Río Salado ignimbrites.

The discharge of these wells corresponds to a mixture of steam and water with a dryness that varies between 8 and 21%. The temperatures measured in Wells 1, 2, and 4 (Fig. 6), located in the west and northwestern portion of the field, show maximum temperatures of 212 to 230°C decreasing toward the bottom. On the other hand, in Wells 3 and 6, located in the southeastern part of the field, this inversion in temperature does not exist. In all the wells the maximum temperature coincides with the Puripicar ignimbrite, except in Well 6 where it was not reached. In Well 3 a maximum temperature of 254°C was reached but it did not cut permeables zones of importance. This is common in permeabilities produced by tectonic fracturing or by cooling of volcanic rocks showing great variabilities from one place to another.

The seven production wells drilled were located in the SE part of the field (Fig. 6) where it is supposed that the fluids rise and move horizontally toward the northeast (Fig. 12). The dates and depths reached by these wells appear in Table 3.

All these wells flowed with air lift after a certain period of heating, discharging a mixture of water and steam. Bores 8 and 9 were blocked due to the collapsing of their walls, preceded by the expulsion of a large quantity of rocks.

The determination of the characteristics of the fluid discharged by Wells 7, 10, and 11 was done by means of a 42 inch cyclone separator and also based on the measurements of lip pressures. The results of these measurements are displayed in Table 4, where a great proportion of the water content of the mixture may be observed. The useful potential calculated for these bores corresponds to 75% of the total measured capacity.

Table 4. Well Fluids: Capacity and characteristics.

Well	T°C WH†	WHP* ata	Mass (kg/hr)	Water (kg/hr)	Steam (kg/hr)	Dryness (%)	Power MW Total	Usable
7	174.5	9.0	276.000	227.700	48.300	17.5	9.10	6.37
10	169.6	8.0	131.790	107.541	24.249	18.4	4.14	3.32
11	169.6	8.0	264.370	215.726	48.644	18.4	8.87	6.21
							22.11	15.90

*Well head pressure. †Well head.

Table 5. Permeable levels crossed in the 8 inch diameter wells.

Well	Depth	Formation	T°C	Depth	Formation	T°C	Depth	Formation	T°C
7	170/245	Tucle*	160	480/530	Puripicar	228	745/890	Peñaliri*	260
8	Impermeable			450/500	Puripicar†	225	950/970	Peñaliri†	213
9	141/180	Tucle*	160	550/600	Puripicar†	224	1150/1580	Peñaliri†	200
10	150/190	Tucle*	160	550/600	Puripicar†	230	700/800	Peñaliri	235
11	150/190	Tucle*	156	500/550	Puripicar	228	700/800	Peñaliri Salado*	240

†low permeability. *high permeability.

With these bores three permeable levels have been detected: the upper one located in the Tucle dacites at depths that vary between 150 to 250 m, the middle one between 450 and 600 m located in the Puripicar ignimbrite, and the lower one at the base of the Rio Salado volcanic group from which well production is obtained (Table 5), since the upper levels are cased out.

The permeability of the strata cut by the bores is of the secondary type, originated by tectonic fracturing or by the rapid cooling of volcanic rocks. In the case of the Tucle volcanic group the possibility exists that some levels formed by volcanic sands and gravel have a relatively high primary permeability. It is important to note the good permeability encountered in the contact between the ignimbrites of the Rio Salado volcanic group and the breccias of the lower member (Peñaliri formacion).

The fact that most of the zones of high permeability are found in the Puripicar ignimbrite and not in the Rio Salado ignimbrite is somewhat strange since the latter is much more fractured according to the surface studies. A possible explanation of this phenomenon could be the fact that the Rio Salado ignimbrite, due to the block tectonics, may have been put in contact with impermeable rocks of the Quebrada de Justo formation, blocking the horizontal flow of the fluids.

REFERENCES CITED

Armbrust, G. A., Arias, J., Lahsen, A., y Trujillo, P., 1974. Geochemistry of the hydrothermal alteration at the El Tatio geothermal field, Chile: IAVCEI, International Symposium on Volcanology, Santiago, Chile (pre-print).

Charrier, R., 1973. Interruptions of spreading and compressive tectonic phases of the Meridional Andes: Earth and Planetary Sci. Letters, v. 20, p. 242–249.

Cusicanqui, H., Mahon, W. A. J., and Ellis, A. J., 1976. The geochemistry of the El Tatio geothermal field, northern Chile: Second United Nations Geothermal Symposium Proceedings, Lawrence Berkeley Laboratory, Univ. of California, Berkeley, California.

Dawson, G. B., and Dickinson, D. J., 1970. Heat flow studies in thermal areas of the north of New Zealand: First United Nations Symposium on the Development and Utilization of Geothermal Resources, Pisa, Italy.

Dragnicević, M., 1974. Carta Gravimetrica de América del Sur: Dept. de Geof., U. de Chile, Pub. 167.

Ellis, A. J., 1969. Preliminary geochemistry report El Tatio geothermal field, Antofagasta Province: UN Project Report.

Fukuda, M., and others, 1970. Some geothermal measurements at the Otake geothermal area: First United Nations Symposium on the Development and Utilization of Geothermal Resources, Pisa, Italy.

Guest, J. E., 1969. Upper Tertiary ignimbrites, northern Chile: Geol. Soc. America Bull., v. 80, p. 337–362.

Hochstein, M. P., 1971. Geophysical survey of the El Tatio Geothermal area, results up to December 1970: UN Project Report.

Lahsen, A., 1974a. Geothermal exploration in northern Chile: Circum-Pacif. En Min. Res. Cof. Honolulu.

——— 1974b. Antofagasta-Tatio-Laco Volcano Guide Book, Exc A 2 (AVCE): International Symposium on Volcanology, Santiago, Chile.

Mahon, W. A. J., 1970. A geochemical assessment of the El Tatio geothermal field with particular reference to the fluids discharged from Holes, 1, 2, 3, and 4: UN Project Report.

——— 1972. Geochemical survey of the El Tatio geothermal area, summary of results, January, February, 1972: UN Project Report.

Ruiz, C., 1965. Geología y yacimientos metalíferos de Chile: Inst. Invest. Geol., Santiago, Chile, 305 p.

Siegers, A., and Pichler, H., 1969. Trace element abundances in the andesite formation of northern Chile: Geochim. Cosmochim. Acta, v. 33, p. 882–887.

Trujillo, P. 1974. Castastro de recursos geotérmicos de Chile: Seminario sobre los recursos energéticos de Chile (CONICYT).

Zeil, W., 1964. Die Verbreitung des jungen Volkanismus en der Hockordillera Nordchiles: Geol. Rudschau, v. 53, p. 731–757.

Following are the captions for the illustrations referred to in this paper. The illustrations may be found in the Spanish version which immediately precedes this English translation.

Figure 1. Principal morphostructural features of northern Chile, with the location of Quaternary volcanism and hydrothermal areas.

Figure 2. Geologic map of El Tatio. 1. Thermal manifestations; 2. Deposits (a) aluvial, (b) morenic; 3. Sediments; 4. El Tatio volcanic group—upper Pleistocene–Holocene—(a) andesites, (b) rhyolites; 5. Tatio Ignimbrite (lower Pleistocene); 6. Tucle Volcanic Group—(upper Pliocene)—(a) dacitic strata volcanoes, (b) dacitic lavas and andesitic domes, (c) pyroclastics and tuffs; 7. Puripicar Ignimbrite (lower Pliocene); 8. Copacoya (upper Miocene) subvolcanic domes; 9. Toconce formation (upper Miocene); 10. Sifon ignimbrite (middle Miocene); 11. Rio Salado volcanic group (lower Miocene); 12. Quebrada de Justo Formation (Upper Cretaceous); 13. Aqua Verde Formation (Upper Jurassic); 14. Lomas Negras Formation (Middle Jurassic).

Figure 3. Tectonic Scheme of El Tatio and its hydrothermal activity.

Figure 4. Resistivity of El Tatio, AB/2 = 250 m.

Figure 5. Resistivity of El Tatio, AB/2 = 500 m.

Figure 6. Resistivity of El Tatio, AB/2 = 1000 m.

Figure 7. E-W Profile (528 750 N) resistivity soundings Schlumberger array up to AB/2 = 1000 m.

Figure 8. E-W Profile (528 500 N) resistivity soundings Schlumberger array to to AB/2 = 1000 m.

Figure 9. E-W Profiles (528 250 N) resistivity soundings Schlumberger array up to AB/2 = 1000 m.

Figure 10. NW-SE geological cross section through wells 1, 4, 9, and 7.

Figure 11. Temperature profile and permeable zones throu wells 1, 4, 9, and 7.

Figure 12. E-W schematic profile of El Tatio. (a) Geolo (b) Movement of the geothermal fluids in the system.

Good paper

Electrical

Geophysical Exploration of the Kawah Kamojang Geothermal Field, West Java

MANFRED PAUL HOCHSTEIN

Geology Department, University of Auckland, Private Bag, Auckland, New Zealand

ABSTRACT

The Kawah Kamojang field in West Java lies at an altitude of about 1500 m on top of an elongated volcanic massif and stands about 600 to 900 m above the plains of the Garut Valley and the Bandung Plateau. A dc-resistivity reconnaissance survey showed the existence of a coherent low-resistivity structure which encloses on its eastern margin a natural discharge area where acidic sulfate waters are also being discharged. Since no trace of chloride waters as found in springs on the flanks of the massif, it was inferred that the Kawah Kamojang field is a vapor-dominated system and that the low-resistivity structure represents a condensate layer enriched with sulfate waters. The thickness of the condensate layer was determined by dc-resistivity soundings, and the true resistivity of the layer was found to be between 2 to 5 ohm·m. The condensate layer is underlain at a depth of about 200 to 500 m by a coherent layer with intermediate resistivities greater than 10 ohm·m which was interpreted to be the top of a deeper reservoir containing some vapor. The field covers an area of about 14 km^2.

To obtain some independent information about the lateral extent of the field, a number of shallow holes (20 to 50-m deep) were drilled and temperature gradient measurements were taken. However, no reliable information could be obtained since most measurements were disturbed by near-surface ground-water movement.

Two exploratory deep holes were drilled recently in the field outlined by the resistivity measurements. The results of downhole measurements confirm the geophysical model.

INTRODUCTION

Geophysical, geological, and geochemical investigations of the Kawah Kamojang area in West Java were made between 1972 and 1973. The studies were part of a bilateral aid project (Colombo Plan project) between the governments of Indonesia and New Zealand. In addition to Kawah Kamojang, other geothermal fields in west Java and Bali were also investigated. In this paper only the results of the geophysical exploration of the Kawah Kamojang area are presented, but reference to some results of the other studies will be made.

The aim of the project was originally to assess the feasibility of producing electric power from suitable geothermal fields in west Java and Bali. The project was extended at the end of 1973 to include drilling of exploratory holes in some prospects, drilling of production wells, and the construction of a pilot power plant of originally 5 MW capacity (now enlarged to 30 MW) in one field.

The Kawah Kamojang geothermal field lies on top of a broad, east-west trending volcanic massif which is part of a long volcanic chain in West Java. Gunung Guntur, an active volcano about 7 km to the east of the center of the field lies at the east end of the chain. The term geothermal field will be used in this paper to describe the upper part of a reservoir with thermal fluids as it is outlined by geophysical measurements. The shape of the massif along a north-south section is shown in Figure 1; the crest (altitude about 1500 m) stands about 600 to 900 m above the plains of the Garut Valley in the south and the Bandung Plateau in the north and controls the hydrological setting of the field.

Small active thermal areas occur near the northeast margin of the field at an elevation of about 1650 m (Fig. 2). The surface manifestations have been described by Stehn (1929) and Neumann von Padang (1951). The most active discharge features, which include fumaroles, steaming ground, turbid hot lakes, and mud pools, lie at the locality Kawah Kamojang, which has lent its name for all active areas in the northeast part of the field. The only other thermal discharge in the area occurs in a valley on the south flank, 2.5 km south of the Kawah Kamojang thermal area.

A general geological description of the whole area has been given by Taverne (1926) who interpreted a shallow depression as a relict of a caldera or set of calderas. The near-surface rocks consist of a series of pyroclastics which are intensely weathered. Outcrops outside the field indicate a sequence of andesites, andesitic tuffs, and breccias lying beneath the weathered pyroclastics (J. Healy, personal commun.). Most of the area is covered by dense jungle.

The existence of a steam reservoir at shallow depths in the northeast part of the field was proved by drilling (max. depth 128 m) in the Kawah Kamojang thermal area as early as 1926 (Stehn, 1929). One well (Well 3 in Fig. 3) is still discharging superheated steam from a depth of probably less than 50 m.

GEOPHYSICAL MEASUREMENTS

Chemical analyses of thermal waters from the Kawah Kamojang thermal area and from hot springs 2.5 km to

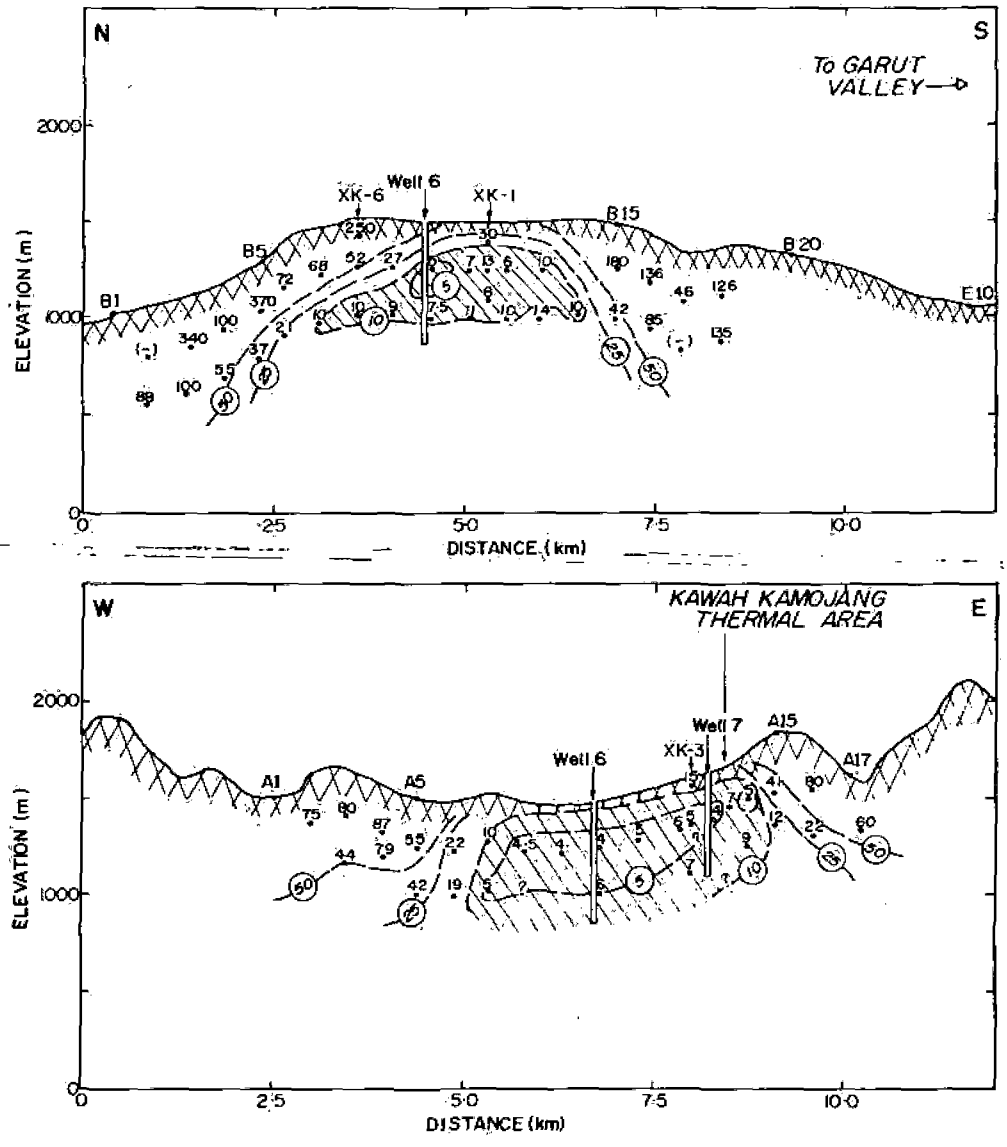

Figure 1. Sections of apparent resistivity plotted versus depth (depth arbitrarily chosen as $AB/4$) along two profiles crossing the Kawah Kamojang field in a north-south direction (*top*) and an east-west direction (*bottom*); for the position of the field stations see Figure 2.

the south were available at the beginning of the geophysical survey. The results showed that these waters contain practically no chlorine but a large amount of sulfates (Kawah Kamojang) and some bicarbonates (southern springs). The pH values of the sulfate-rich waters are low (2 to 4) and presumably are brought about by the oxidization H_2S rising from deeper parts of the field. Hence, it was postulated that the Kawah Kamojang field is a vapor-dominated system as defined by White, Muffler, and Truesdell (1971), at least down to the level of the southern springs, that is, down to 1350 m.

Not much had been published about the geophysical exploration of vapor-dominated systems when we started with our measurements in October 1972. In Italy, for example, resistivity measurements had been unsuccessful in outlining the reservoir of such systems located in sedimentary rocks, except for the mapping of the high-resistivity basement structure beneath some of these fields (Alfano, 1961). More successful were measurements of the temperature gradient in shallow holes (Calamai et al., 1970), which defined the approximate size of some fields. In 1972 we did not know whether geophysical methods were suitable for the exploration of vapor-dominated systems located in young volcanics although we had heard that rocks with low resistivities occur in the direct vicinity of such systems in the United States and probably also in Kenya. On the other hand, we had experience with the exploration of hot-water systems in young volcanics in New Zealand and also South America by dc-resistivity methods (Banwell and Macdonald, 1965; Hatherton, Macdonald, and Thompson, 1966; Risk, Macdonald, and Dawson, 1970; Healy and Hochstein, 1973). Hence, for the exploration of geothermal prospects in west Java we chose dc-resistivity and thermal-gradient methods.

To find out whether a significant resistivity anomaly occurs at Kawah Kamojang and whether such an anomaly is typical for similar systems, reconnaissance resistivity traverses were made not only across the Kawah Kamojang area but also over the nearby Kawah Manuk thermal area using linear arrays ($AB/2 = 500$ m). The center of the Kawah Manuk field (Darajat field) lies about 10 km southwest of that of the Kamojang field. The surface manifestations and the

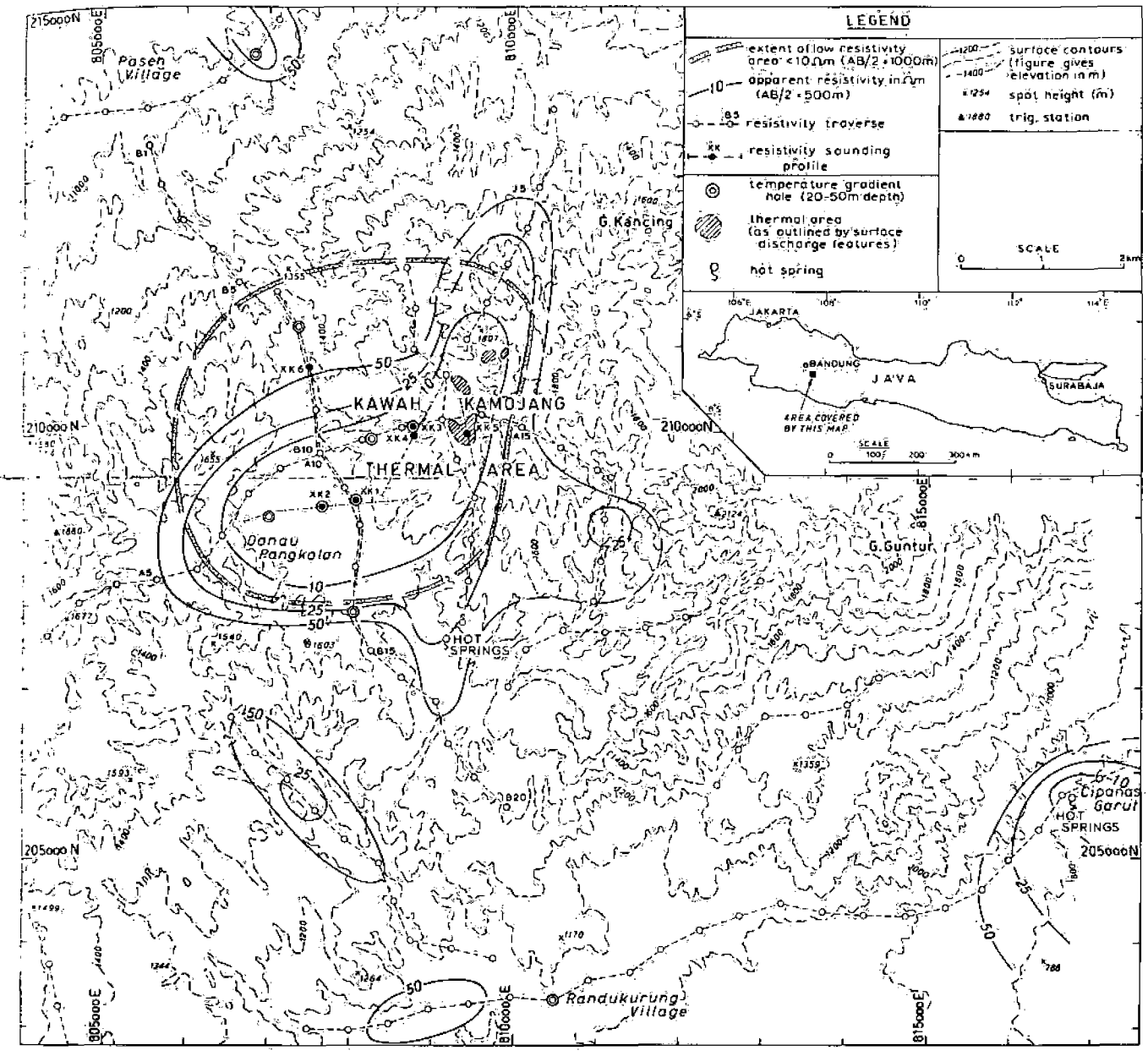

Figure 2. Map of the Kawah Kamojang region showing location of resistivity traverses, resistivity sounding profiles and temperature gradient holes.

chemistry of the discharged fluids at Kawah Manuk are similar to those at Kamojang, that is, Kawah Manuk is probably also a vapor-dominated system. The resistivity traverses showed that in both areas low apparent resistivities, typically between 5 and 10 ohm·m, occur around the thermal areas whereas further away, values between 50 to 300 ohm·m were found.

Shallow holes (up to 50 m deep) were then drilled inside and outside the low-resistivity area. Downhole measurements showed that temperatures in holes inside the low-resistivity area were significantly higher than those in holes outside which implies that the low resistivities are connected with a thermal reservoir. Resistivity sections were then determined by resistivity soundings with spacings up to $AB/2 = 1000$ m. The lateral extent of the low-resistivity rocks at greater depths was mapped by linear arrays with spacings of $AB/2 = 1000$ m. Later studies also included an assessment of the total natural heat discharge. At the end of 1973 we were in a position to predict that the resistivity structure at Kawah Kamojang is connected with the reservoir of a vapor-dominated system and that the resistivity structure provides a drilling target for exploratory holes. Drilling of exploratory holes down to about 600-m depth at Kawah Kamojang was started in the later part of 1974. Results of the geophysical measurements are discussed in detail in the following paragraphs.

RESISTIVITY MEASUREMENTS

All measurements were made using a small portable resistivity device consisting of a dc-power unit (0.5 kW) and a high input impedance voltmeter (Hewlett-Packard model 420) for monitoring of the drop voltage. Reproducibility tests showed that the error was usually less than 5%.

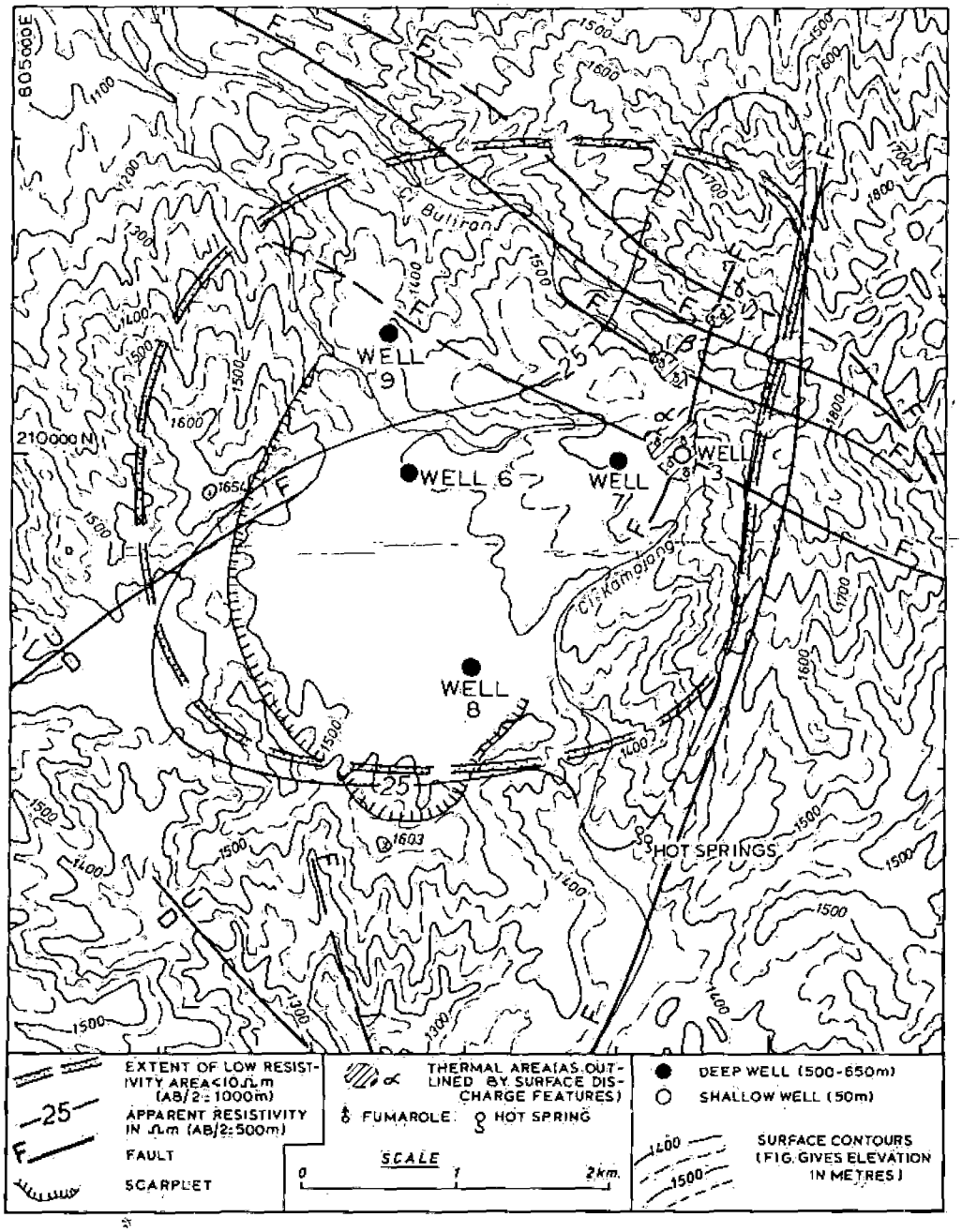

Figure 3. Map of the Kawah Kamojang geothermal field showing extent of the field as outlined by the area with low apparent resistivities, the position of lineaments and faults, and the location of deep exploratory holes.

Systematic errors, however, occurred during the wet season because of leakage from the power unit and cable drums. Erroneous readings showed up with high drop voltages, nonsymmetrical with respect to the center of the potential electrodes. Suspect readings were always repeated. Precautions were also taken to place the potential electrodes in smooth terrain, thus avoiding distortion of the equipotential lines. The resistivity was measured at about 140 stations covering an area of almost 100 km^2; in addition, resistivity soundings were made at six stations.

Resistivity Traverses

Results of the reconnaissance traverses with a Schlumberger array of $AB/2 = 500$ m are shown in Figure 2. It can be seen that a coherent area with apparent resistivities of less than 10 ohm·m occurs between the thermal areas and the Danau Pangkalan depression. Lobes in the resistivity contours point to a structure which trends about north-northeast, bisecting the thermal areas and a less well-defined feature with an east-southeast trend. These directions are similar to those of ill-defined lineaments and inferred faults (J. Healy, personal commun.) shown, for example, in Figure 3.

The low resistivities over the depression led us initially to believe that the resistivity pattern was confined to the postulated caldera structure (Taverne, 1926), but subsequent measurements using arrays with a spacing of $AB/2 = 1000$ m showed that at greater depths resistivities extend further to the north. The area over which values less than 10 ohm·m were observed covers about 14 km^2 and is outlined by a dashed double line in Figure 2.

Results of resistivity traverses along a north-south and an east-west profile (B and A lines in Fig. 2) are shown in form of pseudo-resistivity sections in Fig. 1; the profiles intersect at the approximate center of the resistivity structure. The observed resistivity values were plotted at depths equal to half of the nominal depth penetration (that is, at 250 m for an array with $AB/2 = 500$ m). If interbedded high-resistivity layers are absent, which is true for most of the field, this presentation gives a pattern which is similar to that of a true resistivity section. Figure 1 shows that the low-resistivity structure underlying the Kawah Kamojang area has a lensoidal shape with steeper boundaries in the east-west section than in the north-south section.

Resistivity Soundings

To obtain information about the changes of true resistivities with depth inside the low-resistivity structure and to find out whether this structure is connected with the thermal structure of the field, several resistivity soundings were made also using Schlumberger arrays with spacings up to $AB/2 = 1000$ m. The soundings were taken along profiles shown in Figure 2. The profiles were all positioned inside the resistivity low as outlined by the $AB/2 = 500$-m traverses to avoid any adverse boundary effects with the exception of sounding XK-6. The observed resistivities are shown by sequence of dots and circles in Figure 4.

For the interpretation of the soundings it was assumed that the resistivity structure inside the low-resistivity area away from the boundaries can be approximated by a sequence of nearby horizontal layers, an assumption which is justified on the evidence of the sections shown in Figure 1. The auxiliary point method (Ebert, 1943; Zohdy, 1965) and standard three-layer curves (Rijkswaterstaat, 1969) were used to obtain approximate solutions which were then refined by computing a set of theoretical sounding curves using a program similar to that described by Argelo (1967) until a good fit between observed and computed data was obtained. In computing the best fit curves, which are shown as solid lines in Figure 4, we overcame the problem of equivalent strata by assuming that the resistivities of the deeper layers were similar and that simple models which give a good fit are preferable to models which require a more detailed structure. No attempt was made to reconcile any resistivity interface at shallow depths with the shallow water table observed in the temperature holes, since such modification does not affect our findings about the deeper resistivity structure and also since recent drilling has shown that in some parts of the field the shallow water table is perched.

Resistivity Section Inside the Low-Resistivity Area

The various resistivity layers of the best fit models shown as sections in the bottom half of Figure 4 were then correlated with rock types, abundance of conductive minerals, and nature of thermal fluids. The dry surface layer consisting of partly weathered ash and lapilli (200 to 2000 ohm·m) is underlain by similar water-saturated material (about 100 ohm·m). In the Pangkalan depression the upper 20 m in hole XK-2 (Fig. 5) were found to consist of wet clays and weathered pyroclastics which have a resistivity of about 10 to 20 ohm·m as verified by laboratory measurements of the resistivity of cores from the bottom of the hole. Hence, similar material likely occurs down to 110 m at sounding XK-2 and probably between 30 and 250 m at XK-1.

The center of sounding XK-5 was over steaming ground with ground temperatures of 90 to 95°C at 0.7 m depth and was about 50 m west of the old well mentioned in the introduction which produces dry steam (T = 140°C) from a depth of presumably less than 50 m. The surface layer at XK-5 consists of hot but still moist thermal clays (kaolinite) and weathered ash. The surface resistivity layer of 8 ohm·m at XK-5 was therefore correlated with hot, but still hydrated, thermal clays and weathered ash. Similar resistivities were observed in the laboratory in samples from this layer when heated up to 75°C. From old drill logs it can be inferred that the same material also occurs down to depths of about 60 m. The resistivity (25 ohm·m) of the underlying layer between 8 to 24 m depth is likely caused by partly or completely dehydrated clays, the dehydration being brought about by vapor. Similar resistivity values (25 to 40 ohm·m) were also found at similar depths at the nearby Kawah Manuk field over steaming ground near discharge features issuing superheated steam.

The low-resistivity layer (2 to 4 ohm·m) was interpreted

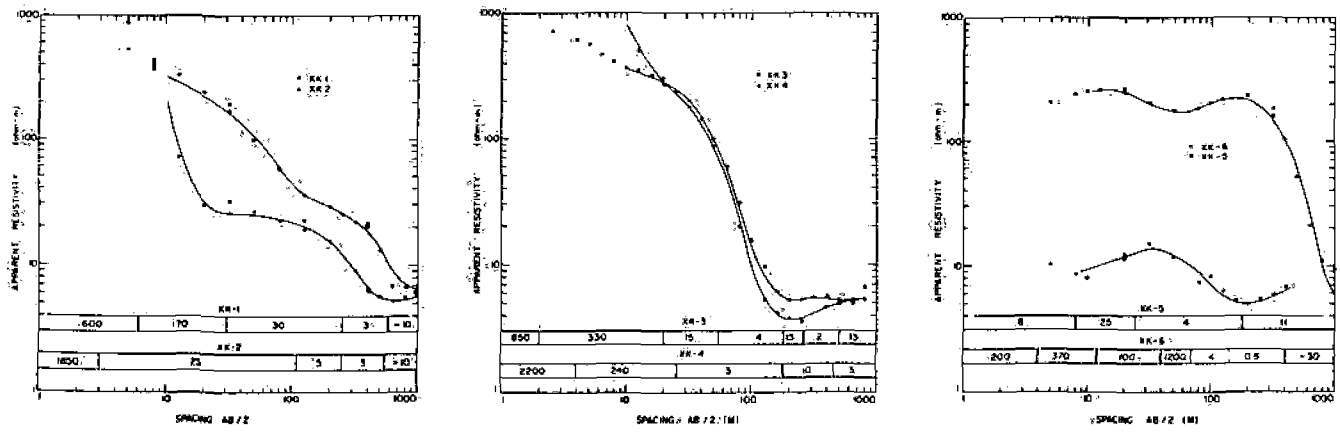

Figure 4. Resistivity sounding curves at stations XK-1, XK-2 (*left*); XK-3, XK-4 (*middle*); XK-5, XK-6 (*right*). For the location of the stations and the orientation of the sounding profiles, see Figure 2. Observed apparent resistivities are shown by dots and circles, computed resistivities of best fit models are shown by solid lines; the best fit models are shown as resistivity sections in the lower part, numbers refer to the true resistivity of a certain layer in ohm·m.

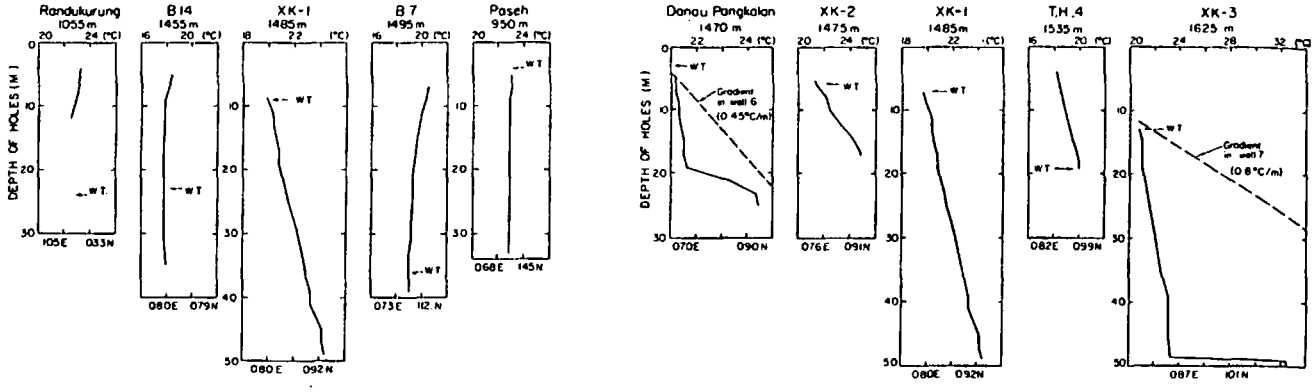

Figure 5. Temperature profiles in shallow drill holes; for the location of the holes see Figure 2. Drill hole XK-1 is shown twice. Holes shown in the left half of the figure stand in ground with high apparent resistivity (except XK-1), holes shown in the right half stand in ground with low apparent resistivities. W.T. refers to the water table. The dashed lines give the observed (Well 6) or inferred (Well 7) temperature gradient in the upper 200 m of nearby deep exploratory holes.

as a layer made up of volcanics and pyroclastics which contains hydrated alteration minerals and which is saturated with diluted sulfate waters. The concentration of these waters near the discharge area is presumably less than 0.5×10^3 ppm. Some evidence for this interpretation comes from measurements in hole XK-3 which just penetrated the low-resistivity layer (4 ohm·m) at a depth of about 50 m (Fig. 6). It was found that the pore fluids of the low-resistivity rocks at the bottom of this hole consisted of very diluted warm sulfate waters (pH ≈ 6). Mineralogical studies of cores from the bottom showed that alteration minerals started to occur (P. Browne, personal commun.). Hence, the low resistivity of 4 ohm·m at the bottom of this hole is primarily related to the presence of hydrated alteration minerals rather than to diluted sulfate waters. The same explanation also holds if the sulfate waters attain concentrations of about 0.5×10^3 ppm (pH ≈ 3.3), assuming that the pore fluids are made up by a dissociated H_2SO^4 solution of similar concentration. In this case the resistivity of the pore fluids in the temperature range of 100 to 200°C is >20 ohm·m. Treating the rock matrix as an insulator and making allowance for the porosity (formation-factor)

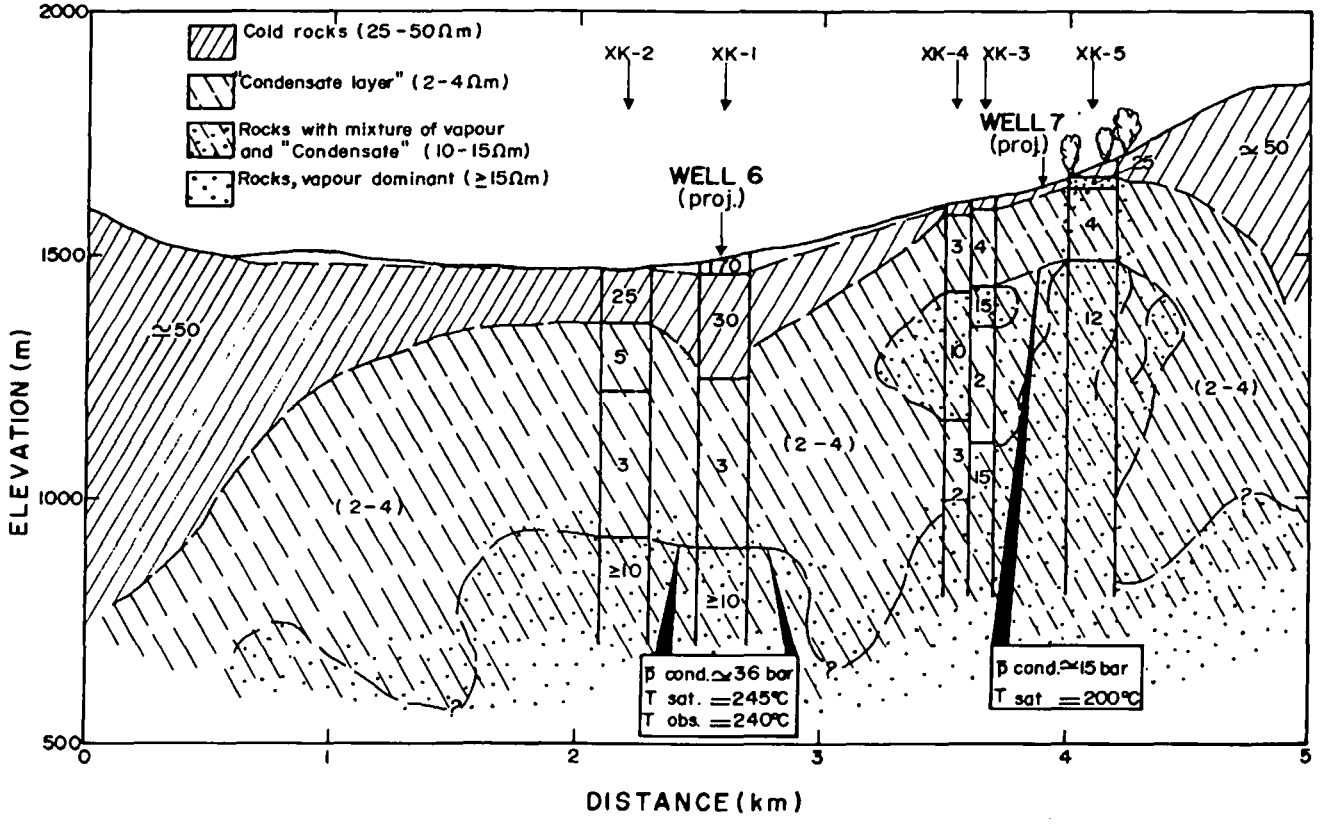

Figure 6. Idealized resistivity section across the field along a line joining sounding stations XK-5 and XK-2 (see Figure 2). The exact position of the lower boundary of the low resistivity layer (2 to 4 ohm·m) is uncertain; the position of the inferred descending low-resistivity tongues is hypothetic.

(Keller and Frischknecht, 1966) of the rocks, it can be shown that solutions > 10^4 ppm are required to obtain resistivities of less than 5 ohm·m for these rocks.

A unifying explanation for the low-resistivity layer can be given if one assumes that the conductivity brought about by hydrated alteration minerals is the dominant conductance mechanism in the low-resistivity layer. Any changes in concentration of the sulfate waters with depth would therefore not alter significantly the conductivity of this layer as long as the bulk percentage of the alteration minerals—or better, the exchange capacity of these minerals per unit volume—remains constant with depth.

The low-resistivity layer in turn is underlain at XK-5, also at XK-3 and XK-4, by a layer with intermediate resistivities of 10 to 15 ohm·m at a depth of about 180 m. In the western half of the field the low-resistivity layer occurs down to depths of 400 to 600 m where it is also underlain by a substratum with intermediate resistivities greater than 10 ohm·m and which is well documented, for example, by the increase in apparent resistivity at spacings greater than 500 m in sounding XK-2 (Fig. 4). Since it is unlikely that the bulk percentage of alteration minerals decreases significantly beneath an active discharge area, it was inferred that the intermediate resistivities at the bottom of the low-resistivity layer are caused by a partial or complete dehydration of the alteration minerals due to a partial or complete replacement of the pore fluids by vapor, as is the case in layer 2 at XK-5. If one accepts this explanation for intermediate resistivities at a depth of about 180 m at XK-3, XK-4, and XK-5, it follows that the same explanation is also applicable for the intermediate resistivities of the substratum at 400 to 600 m depth at XK-1, XK-2, and XK-6. Resistivity soundings over the nearby Kawah Manuk field produced similar results and lend support for the model, which has far-reaching implications.

For hydrological stability it is, for example, necessary that the vapor pressure at the bottom of the low-resistivity layer is such that it can support the hydrostatic column above. Since condensation of vapor will take place continuously at the bottom of the low-resistivity layer unless the temperature is near saturation temperature, a large upflow of vapor is required to maintain the position of the deepest interface. On the other hand, any inflow of colder water would result, especially near the boundaries of the field, in deep descending tongues of condensates. The bottom part of the low-resistivity layer is therefore likely made up by a layer filled with condensates; and to emphasize the likely origin of the low-resistivity layer, it is called from now on the condensate layer.

There were several uncertainties in the geophysical model of the field. For example, we had no clear idea about the degree of condensation in the substratum nor the amount of vapor present in the pores. No satisfactory explanation could be given for the changes in thickness of the low-resistivity layer beneath the vapor-filled layer with a resistivity of 10 to 15 ohm·m at XK-3 and XK-4. We were also aware that the position of the top of the condensate layer near the boundaries of the field is unstable without any impedance in the layer which would restrict outflow.

Despite these uncertainties, at the end of 1973 we postulated a geophysical model which combined all the facts and inferences discussed so far and which was similar to that shown in Figure 6. The important features of the model are:

1. The low apparent resistivities as shown in Figures 1, 2, and 4 delineate the lateral extent of the condensate layer.
2. The condensate layer has a thickness of 500 ±150 m in the center of the field and decreases in thickness to 150 to 180 m in the vicinity of the area with surface manifestations.
3. The condensate layer is underlain by a layer or substratum which contains vapor.
4. The lateral extent of hot rocks at depth is approximately given by the extent of the condensate layer.

The condensate layer of the Kawah Kamojang field is unusually thick compared with a thickness of about 100 m reported for other vapor-dominated systems such as The Geysers (McNitt, 1963) and the mud volcano field in Yellowstone Park (Zohdy, Anderson, and Muffler, 1973). The results of geophysical studies of the mud volcano field were published after our studies at Kawah Kamojang were finished. Since the resistivity structure of the mud volcano field was found to be similar to that of the Kamojang field we became confident that our model of the gross structure of the Kamojang field was essentially correct.

TEMPERATURE MEASUREMENTS AND HEAT LOSS

Before the geophysical model of the field was tested by deep drilling, a series of shallow holes (up to 50 m depth) were drilled. The aim of this program was to find out whether the low-resistivity layer, further away from the area with surface manifestations, also contains hot water. Although the alteration minerals in the low-resistivity layer were thought to be responsible for the conductance of this layer, these minerals could still have been produced during an earlier thermal history of the field.

The shallow holes were made by hand at sites shown in Figure 2. Downhole temperatures were measured after a standing time of at least one month using a thermocouple. Several runs were made over a period of one year, and the observed stable temperatures are shown in Figure 5. It can be seen that in holes which lie outside the low-resistivity area temperatures are constant with depth and are near the mean annual temperature, whereas temperatures increase gradually with depth in holes which lie inside the low resistivity area (Fig. 6). Heat transfer in the latter ones, however, is not by conduction as indicated by the sudden increase in temperature at the bottom of holes at Danau Pangkalan and at XK-3. As mentioned in the previous section, the hole XK-3 reached the top of the low-resistivity layer which explains also the increase in temperature at the bottom of this hole. A similar rise in temperature at the bottom of the Danau Pangkalan hole cannot be correlated with the low-resistivity layer which lies at much greater depth. The absence of any significant rise in temperature at the same level in the nearby hole XK-1 and the increase in temperature in hole XK-2, however, indicate that thermal waters are rising to the surface beneath the depression. Since the likely source of these waters is the low-resistivity layer, the results give some support for the assumption that thermal waters occur throughout the low-resistivity layer.

An assessment of the total heat discharged at the surface of the thermal areas was included in the geophysical exploration of the Kamojang field. The methods used for measurement of the output of the various discharge features

were similar to those described by Dawson (1964) except for the measurement of the mass flow of fumaroles for which a pressure transducer was used. The total heat discharge rate of the Kawah Kamojang thermal area was found to be about 9×10^7 J/sec (90 MW) of which nearly 50% is due to evaporative losses of hot lakes and pools in the south area (area α in Fig. 3). The heat transfer rate through the whole system is probably significantly greater if condensation at the bottom and outflow at the top of the condensaten layer takes place.

TEST BY DEEP DRILLING

The geophysical model of the field developed earlier has been tested by several exploratory wells down to depths of about 600 m; these wells were encased down to about 300 m depth. The first hole, Well 6, was sited in the center of the field as outlined by the condensate layer (Fig. 3); the hole reached a depth of 612 m. Downhole measurements showed that the top of the condensate layer occurs at a depth of about 150 m as given by the level of fluids in the well at zero wellhead pressure; the temperature at this depth is about 100°C. Temperatures were found to increase linearly to about 215°C at 400 m depth where a significant change in gradient occurs; the temperature at the bottom of the hole (580 m) is 239°C. Pressures were hydrostatic throughout, given by the mean density of the hot water column (K. Holyoake, personal commun.). Mineralogical studies of cuttings (P. R. L. Browne, personal commun.) showed that below 160 m depth rocks are thermally altered and contain thermal clays (illites, for example). Although certain sections were less altered, on the whole, the degree of alteration does not change significantly below 160 m depth. The sulfate concentration of fluids in the well decreases with depth (0.2×10^3 ppm at the bottom) as shown by downhole sampling prior to discharging of the well (W. A. J. Mahon, personal commun.). Since discharging, the well has continued to produce dry steam probably from a depth of about 410 m.

The above-listed results from Well 6 confirm important features predicted by the geophysical model, namely the existence of a thick conductive layer filled with hot water, the condensate layer, and the position of the upper boundary of this layer. The lower boundary is diffuse; however, the approximate temperatures and pressures at the bottom of the inferred condensate layer are similar to those observed at the bottom of the hole. Taking for example an average thickness of 400 m for this layer at Well 6 (as indicated by the average thickness of the low resistivity layer at XK-1 and XK-2), the hydrostatic pressure at the bottom of this layer would be about 36 bar neglecting the influence of noncondensable gases. For the boundary to be stable, the temperature of the vapor must be near saturation temperature which for a pressure of 36 bar is 245°C, similar to the observed temperature of 239°C at 580 m depth. Some indication for the diffuse nature of the lower boundary of the condensate layer is given by the observation that all temperatures between 400 and 580 m depth are near the saturation temperature of vapor, and it is possible that some vapor occurs at these depths. Such a diffuse, presumably over 200-m-thick, boundary zone, however, could not be predicted from our sounding data.

The second hole, Well 7, was drilled in the vicinity of the thermal area α (Fig. 3) and lies halfway between soundings XK-5 and XK-3 (XK-4). The overall confirmation of the geophysical model of the field by the results of Well 6 led us to predict certain characteristics of Well 7 using data shown in Figure 6. Since the average thickness of the condensate layer at Well 7 is about 160 m and the inferred hydrostatic pressure of the hot water column at the bottom of this layer is about 15 bar (which points to a vapor saturation temperature of about 200°C) it was predicted that the temperature at about 200 m depth would be slightly below 200°C. Assuming that vapor is the dominant phase in the substratum with intermediate resistivities, it was postulated that temperatures would change only gradually with depth below 200 m and that pressures would be nonhydrostatic; hence any production from below 200 m depth should be in the form of dry steam.

Since zero wellhead pressure could not be attained, no representative temperatures could be measured in the upper half of the well, neither could the depth to the top of the condensate layer be determined. Incomplete temperature runs, however, showed that the temperature at 200 m depth is at least 180°C and that temperatures increase only slightly from 215°C at 300 m depth to about 224°C at 520 m depth. Pressure runs were also incomplete. Initially the pressure gradient in the bottom part of the hole was significantly smaller than the hydrostatic gradient; pressures also decreased significantly with time but stabilized later, reaching a hydrostatic gradient (K. E. Seal, personal commun.). The alteration of rocks between 50 to 250 m is apparently similar to that in Well 6 although lower-temperature alteration minerals tend to occur below 250 m (P. R. L. Browne, personal commun.). On opening, the well discharged wet steam which presumably comes from a zone where large circulation losses had occurred during drilling and into which about 2×10^3 m^3 of cold water had been pumped.

These results imply that vapor is not dominant in the two-phase mixture beneath the condensate layer and one has to assume that large fingers or columns of condensate are penetrating into the substratum as, for example, shown in Figure 6. Such a configuration of descending columns of condensate would also explain the resistivity structure below the condensate layer at soundings XK-3 and XK-4, assuming that the sounding profile XK-3 runs over an inferred column of condensate which is absent beneath sounding profile XK-4 (Fig. 6). The boundary zone at the bottom of the condensate layer beneath Well 7 is therefore probably 250 m thick.

The success of Wells 6 and 7 affected the siting of the next exploratory holes, which originally were sited in a small area to the north of Well 7 using the conventional approach that exploratory holes in a geothermal field also have to prove the production of thermal fluids. Such holes are usually drilled in zones of inferred permeability, that is, near faults in the vicinity of surface discharge areas. At Kawah Kamojang, Well 8 and Well 9, however, were sited to prove the extent of the reservoir as predicted by the geophysical model (Fig. 3). Recent incomplete measurements in Well 8 indicate that although hot rocks occur at the bottom, temperatures are significantly lower (about 180°C) than those at the bottom of Well 6 (K. E. Seal, personal commun.); this might indicate that the condensate layer is significantly thicker towards the margin of the field.

Keeping in mind that the geophysical model only outlines the gross structure of the field and that the validity of any model has to be assessed by the predictions, it can be

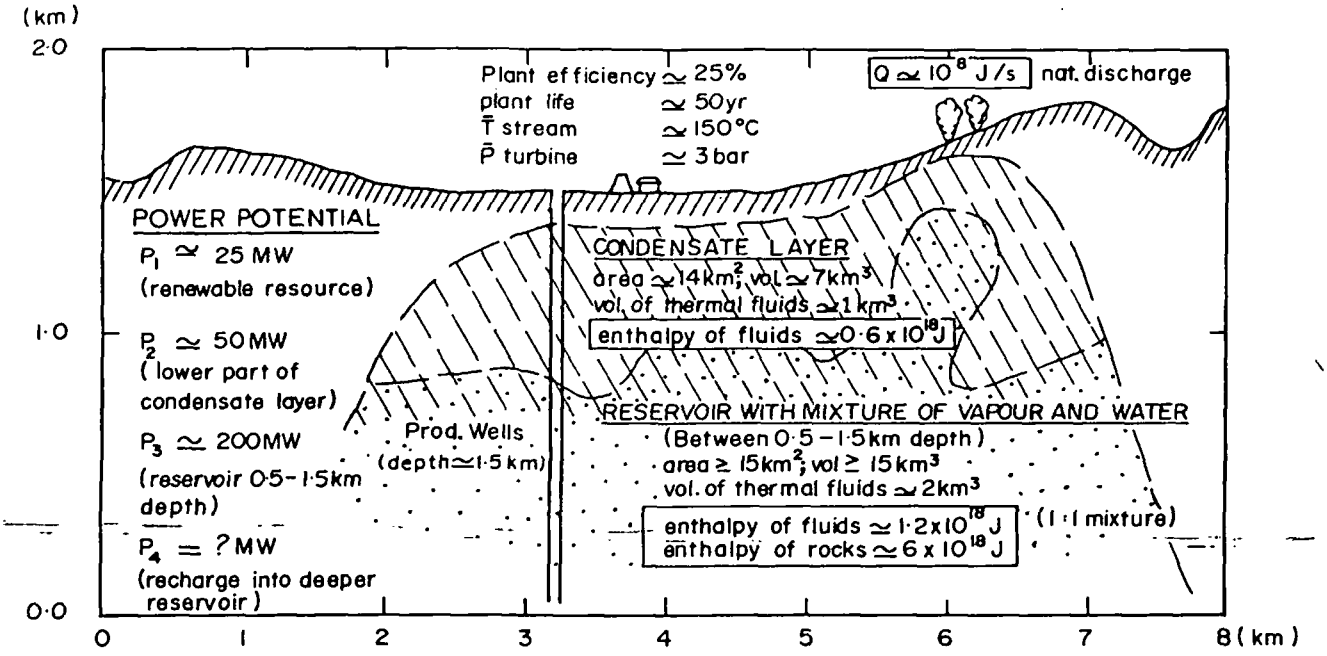

Figure 7. Schematic section of the Kawah Kamojang field summarizing parameters from which the power potential of the field has been assessed.

concluded that the geophysical model of the Kawah Kamojang field is essentially correct. The model can also be used to estimate the magnitude of the stored heat and the power potential of the reservoir.

POWER POTENTIAL OF THE FIELD

Since the reservoir of the field is outlined by the geophysical model and since some information about the temperature and the nature of fluids is available, an estimate of the power potential can be given. Such an estimate is of some use for the planning of the likely scale of the various phases of exploitation and is at this stage more useful than an assessment based on the output of numerous production wells. For the assessment it was assumed that the total power potential of the field is given by the energy of: (1) fluids continuously transferred through the system; (2) fluids stored in the condensate layer; (3) fluids in the reservoir beneath the condensate layer down to the likely depth of production wells; and (4) hot rocks, assuming that some induced recharge might occur (see Fig. 7).

The minimum energy continuously transferred through the system is about 10^8 J/sec, that is, about 100 MW, as given by the natural heat discharge rate. Assuming that under ideal conditions fluids transporting this heat can be tapped and that the heat can be transported in the form of steam of about 150°C to a powerhouse at an inlet pressure of about 3 bar, that is, that the plant efficiency would be about 25%, the power potential of the field, if exploited as a renewable resource, would be about 25 MW.

The enthalpy of the fluids in the condensate layer is about 0.6×10^{18} J, assuming an average thickness of about 0.5 km and an average porosity of about 15% for this layer. Production of fluids from beneath the condensate layer will induce a downward movement of the condensates, that is, the condensates will presumably act as a buffering recharge. Using a plant life of 50 years (1.6×10^9 sec) and assuming that about half of the fluids can be extracted, one can infer a potential of about 50 MW for this layer.

Any estimate of the total enthalpy of fluids stored in the reservoir below the condensate layer is uncertain at this stage since we have no information about the average ratio of the two-phase mixture of fluids in this important part of the field. If one assumes that there is a 1:1 mixture of vapor and water, one obtains a total enthalpy of about 1.2×10^{18} J for these fluids. The power potential of the reservoir between 0.5 to 1.5 km depth would therefore be about 200 MW, although in the worst case, namely if all voids below the condensate layer are filled with vapor, this figure would drop to about 20 MW.

Hot rocks of the deeper reservoir have a total enthalpy of about 6×10^{18} J. However, extraction of this energy will be possible only if colder fluids enter this part of the reservoir. Any estimate of the amount of energy which can be extracted is unrealistic at this stage, since no information about recharge and efficiency of total heat transfer from rocks to fluids is available.

The figures cited here also allow an estimate of the total energy stored in the reservoir which is of the order of 10^{19} J down to a depth of 1.5 km. From the ratio of total energy stored and present rate of energy transfer one obtains a minimum static lifetime of the field of about 10^{11} sec (3000 years) which would be required to transport all the heat into the reservoir, assuming that the input rate is similar to that of the present discharge rate. Although the input rate might have been significantly greater, our estimate shows that the Kawah Kamojang field is an old system.

SUMMARY

Geophysical studies presented in this paper together with some results from other disciplines have been used to show that the Kawah Kamojang geothermal field is a vapor-dominated system which is capped by a 200 to 500-m-thick

condensate layer. The condensate layer shows up with true resistivities of 2 to 5 ohm·m which are likely brought about by hydrated conductive alteration minerals. The lower boundary of the layer is diffuse, and it is likely that large tongues of condensates descend into the deeper reservoir which contains a two-phase mixture of fluids and where some dehydration of alteration minerals probably takes place as reflected by the higher resistivities of 10 to 15 ohm·m. The temperature at the bottom of the condensate layer is near the saturation temperature of vapor which indicates quasi-stable conditions. Measurements in recently drilled exploratory holes showed that the gross structure of the field as summarized holds here. Since the geophysical model gives an outline of the reservoir of the field, a rough estimate of the stored energy and the power potential of the field can be given. It was found that the power potential is about 100 to 250 MW. Since thermal fields with a similar structure have been found elsewhere in West Java, it is likely that vapor-dominated systems in young volcanic rocks are far more common than believed so far.

ACKNOWLEDGEMENTS

Permission for presentation of the results was given by R. Tonkin of Geothermal Energy N.Z., Ltd.; G. B. Dawson of the New Zealand Department of Scientific and Industrial Research (DSIR) and M. Davis (Geothermal Energy N.Z. Ltd.) participated in the field program; efficient help in the field was also provided by various members of the Geological Survey of Indonesia. Information cited under personal communication was provided by the project manager, K. E. Seal and K. Holyoake (both Geothermal Energy N.Z. Ltd.), as well as by J. Healy, W. A. J. Mahon and P. R. L. Browne (all DSIR).

REFERENCES CITED

Alfano, L., 1961, Geoelectrical explorations for natural steam near "Monte Amiata": Quad. Geofisica Appl., v. 21, p. 3.

Argelo, S. M., 1967, Two computer programs for the calculation of standard graphs for resistivity prospecting: Geophys. Prosp. [Netherlands], v. 15, p. 71.

Banwell, C. J., and Macdonald, W. J. P., 1965, Resistivity surveying in New Zealand thermal areas: Commonwealth Mining & Metallurgy Congress, eighth, Australia and New Zealand, Paper 213, p. 1.

Calamai, A., Cataldi, R., Squarci, P., and Taffi, L., 1970, Geology, geophysics and hydrogeology of the Monte Amiata geothermal field: Geothermics, Special Issue, v. 1, p. 1.

Dawson, G. B., 1964, The nature and assessment of heat flow from hydrothermal areas: New Zealand Jour. Geology and Geophysics, v. 7, p. 155.

Ebert, A., 1943, Grundlagen zur Auswertung geoelektrischer Tiefenmessungen: Beitr. Angewandten Geophysik, v. 10, p. 1.

Hatherton, T., Macdonald, W. J. P., and Thompson, G. E. K., 1966, Geophysical methods in geothermal prospecting in New Zealand: Bull. Volcanol., v. 29, p. 485.

Healy, J., and Hochstein, M. P., 1973, Horizontal flow in hydrothermal systems: Jour. Hydrology [New Zealand], v. 12, p. 71.

Keller, G. V., and Frischknecht, F. C., 1966, Electrical methods in geophysical prospecting: Oxford, Pergamon Press, 519 p.

McNitt, J. R., 1963, Exploration and development of geothermal power in California: California Div. Mines and Geology Special Report 75.

Neumann von Padang, M., 1951, Catalogue of the active volcanoes of the world including solfatara fields, part 1: Naples, Italy by International Volcanological Association.

Rijkswaterstaat, 1969, Standard graphs for resistivity prospecting: European Assoc. of Exploration Geophysicists.

Risk, G. F., Macdonald, W. J. P., and Dawson, G. B., 1970, DC-resistivity surveys of the Broadlands geothermal region, New Zealand: UN Symposium on the Development and Utilization of Geothermal Resources, Pisa, Proceedings (Geothermics, Special Issue 2), v. 2, pt. 1, p. 287.

Stehn, C. E., 1929, Kawah Kamojang: Pacific Science Congress, fourth, Java, Excursion C. 2, p. 1.

Taverne, N. J. M., 1926, Vulkaanstudien op Java: Vulkanologische Mededeelingen van den Dienst van den Mijnbouw, v. 7, p. 27.

White, D. E., Muffler, L. J. P., and Truesdell, A. H., 1971, Vapor-dominated hydrothermal systems compared with hot-water systems: Econ. Geol., v. 66, p. 75.

Zohdy, A. A. R., 1965, The auxiliary point method of electrical sounding interpretation and its relationship to the Dar Zarrouk parameters: Geophysics, v. 30, p. 644.

Zohdy, A. A. R., Anderson, L. A., and Muffler, L. J. P., 1973, Resistivity, self-potential, and induced-polarization surveys of a vapor-dominated geothermal system: Geophysics, v. 38, p. 1130.

Geothermal Resources Council, TRANSACTIONS Vol. 4, September 1980

GEOPHYSICAL INVESTIGATIONS AT MOMOTOMBO, NICARAGUA

Ulrich J. Cordon and Ernst G. Zurflueh

International Engineering Company, Inc. (IECO)
San Francisco, CA 94105

ABSTRACT

The Momotombo geothermal field in Nicaragua was investigated in three exploration stages, using a number of geophysical techniques. Stage 1 of the investigations by Texas Instruments, Inc., (1970) located and delineated a potential geothermal field, with the dipole mapping surveys and electromagnetic soundings being most effective. Stage 2 of the investigations, performed in 1973 by the United Nations Development Program (UNDP), outlined the resistivity anomalies in the area west of the previously selected field; Schlumberger VES soundings and constant depth profiling (SCDP) proved most useful. During Stage 3 of the investigations, Electroconsult (ELC) performed 20 additional Schlumberger VES soundings as part of the 1975 plant feasibility studies. Results of these geophysical techniques are summarized and their effectiveness briefly discussed.

STAGE 1

Eight Schlumberger soundings were performed in the southern slopes of the Momotombo volcano. The resulting curves were interpreted in terms of a sequence of horizontal layers, but, as Banwell (1971) points out, this has very little resemblance to the true underground distribution of resistivity in the area. There is little evidence of correlation between pseudo-layering found in neighboring soundings and little similarity between the results of soundings taken at nearly the same points. Low resistivities (< 1 ohm-m) were found near the hydrothermally altered areas and the maximum depths interpreted from the soundings range between 300 m and 400 m. This depth is insufficient to reach the low resistivity formation which lies at 1400 m to 1700 m, as indicated by the electromagnetic soundings. The result of the two dipole mapping surveys is shown in Figure 1. Even though this method was used in Broadlands, New Zealand, to outline the boundaries of the field, the limited coverage at Momotombo did not produce a satisfactory boundary mapping of the area. Signal levels were not high enough to permit accurate detection beyond 4 km from the source dipole which crossed a pair of vertical faults affecting the apparent resistivity pattern (Banwell, 1971).

The results of the three electromagnetic soundings are in general agreement. A hot water reservoir, now designated as the 'deep reservoir', was indicated and lying at depths of 1400 m to 1700 m. Keller (1971) classifies this technique as superior to the resistivity soundings because of the insensitivity to problems caused by resistant surface rocks. A brief audio-magnetic-telluric (AMT) survey showed a rough correlation between the high temperature areas and low resistivity. The local variation in structure, however, as noted by Banwell (1971), could readily mask any relationship or explain disagreements. The limitation of the maximum penetration depth of 400 m does not enable this sounding to check the presence of the suspected reservoir. Data from a reconnaissance gravity-magnetic survey consisting of 23 stations have no direct bearing on the geothermal conditions in the area.

STAGE 2

Most of the geophysical survey was done using Schlumberger constant depth profiling (SCDP) with a Lee partition added to detect any lateral inhomogeneities and to check the validity of the results. The measurements were useful in detecting zones of low resistivity to be later investigated with VES soundings. Little contrast was detected in the entire region, with Zones C, D, and E in Figure 2 showing the lowest resistivity.

Schlumberger VES soundings provided subsurface information such as thickness of certain conductive layers and variation in resistivity between adjacent formations. Results of these soundings are shown in Figure 2. Some irregular results were caused by the limitation on the applicability of the VES method in volcanic regions such as Momotombo, where the layers are irregular and the measured sounding curve cannot be matched to any theoretical model.

The roving dipole method was not extensively used since it showed little depth control and some of the results remained unclear. The placement of the current electrodes near Lake Managua caused some of the current to flow through the lake rather than being uniformly distributed through the ground; this caused lower resistivities to be recorded (Carriere, et al., 1974).

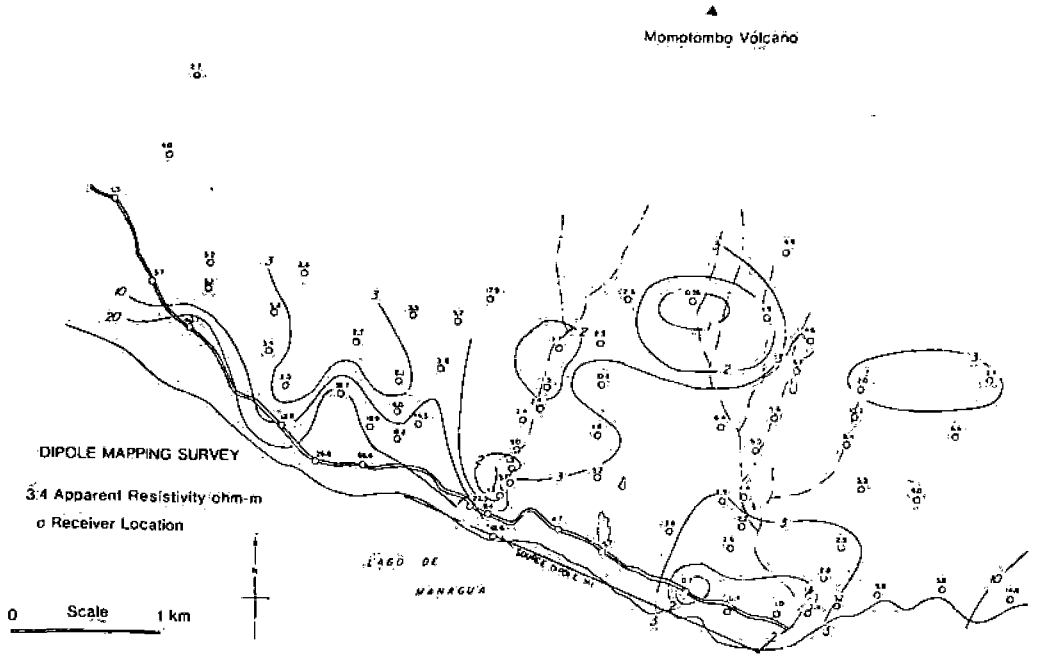

Fig. 1 Results of dipole mapping survey (Texas Instruments, 1971). Two regions of low resistivity were detected: one parallel to the lakeshore, and the other lying about 1.5 km up the volcanic slope, parallel to the first. No indication of closure of the low resistivity contours was obtained.

One frequency domain sounding and a dipole-dipole survey were performed on a test basis, and no conclusive results were obtained.

Self-potential measurement data gave information about the near surface hydrothermal system, but the anomalies are small and can be easily confused with other effects. Studies by Corwin and Hoover (1979) indicate no consistent pattern to the anomalies caused in 13 different geothermal areas and a number of factors which affect data quality. There is some indication that such measurements, however, may be used to locate faults.

STAGE 3

Twenty Schlumberger soundings were performed with electrode separations of 2 km to 3 km; larger separations gave inaccurate results due to the high resistivity of surface layers. Contact resistance was high, requiring eight potential electrodes for all readings greater than AB/2 = 300 m and using up to 500 l of water for the current electrodes (Electroconsult, 1977). The progress was eventually slow and costly. Results are shown in the cross section of Figure 3.

A gravity survey consisting of 200 stations was performed over an area of approximately 300 sq.km. The usual problems of access and topography affected the distribution of the stations and consequently limited the interpretation accuracy. A new corrected version of the Bouguer anomaly map is presented in Figure 4.

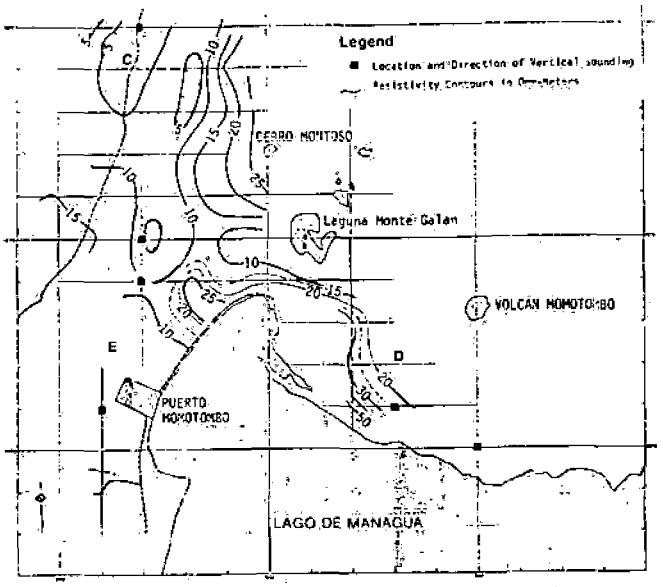

Fig. 2 Results of VES soundings (UNDP, 1974). A sounding in Zone C was interpreted as a 2-layer curve with the second layer having an estimated resistivity of less than 5 ohm-m. Zone D soundings point to a low resistivity zone existing at shallow depths (> 70 m) to the east. Results of soundings in Zone E are irregular due to the expansion of the array into soils on one side and volcanics on the other (Carriere, et al., 1974).

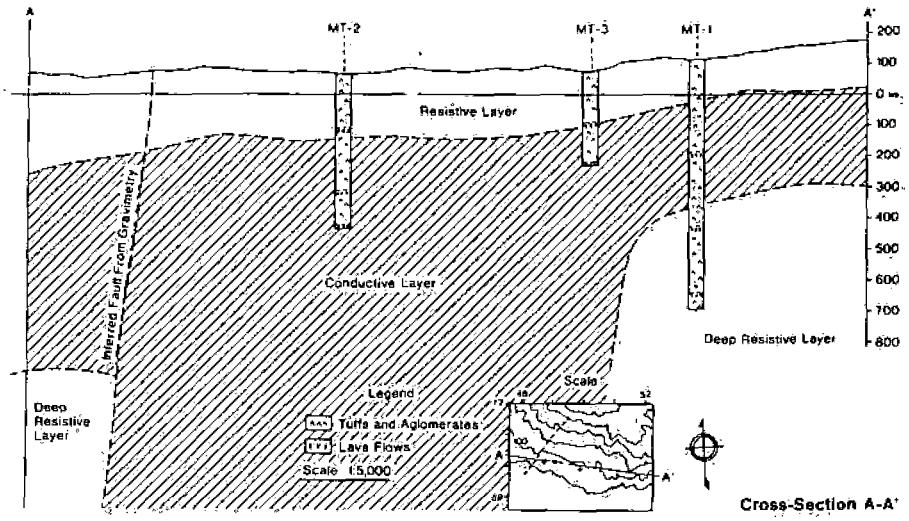

Fig. 3 Three formations were encountered which exhibited different resistivities. The zone in the central portion shows resistivities less than 5 ohm-m (Electroconsult, 1977).

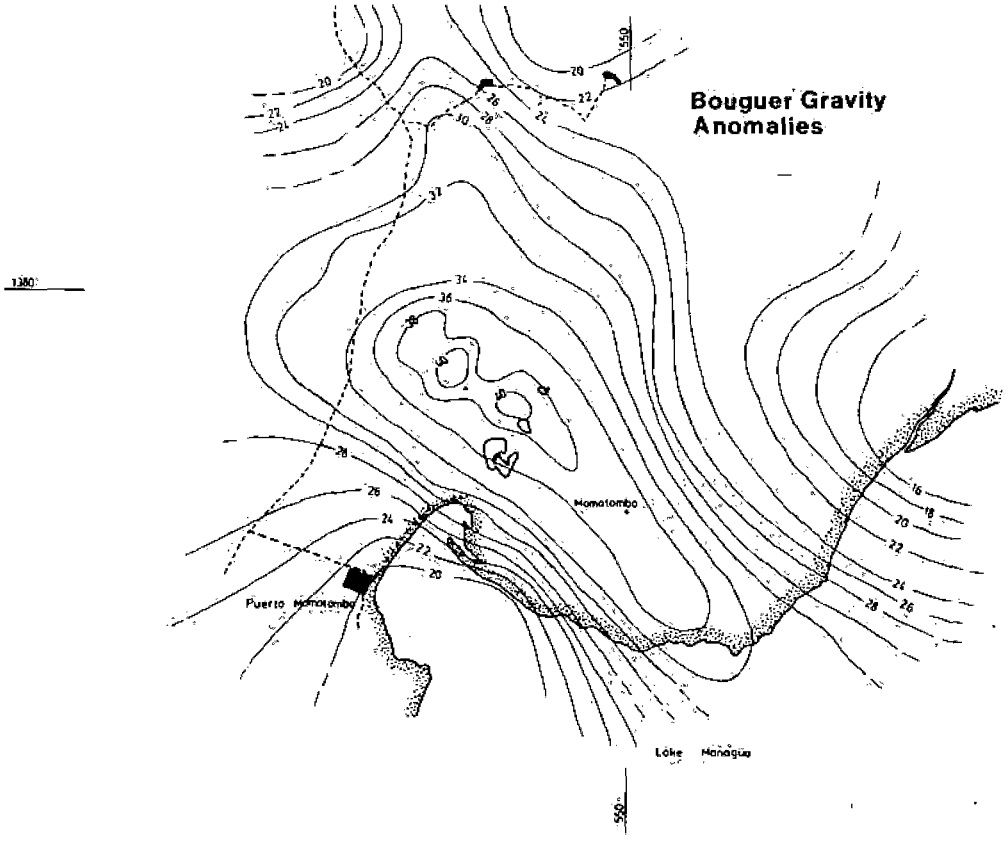

Fig. 4 Correct version of the Bouguer anomaly map for the vicinity of the Momotombo volcano.

• The Momotombo case history study is supported under DOE Contract PRDA No. DE-RA07-79ET27077. International Engineering Company, Inc., is grateful to Instituto Nicaraguense de Energia, and especially its Director, Dr. Emilio Rappacioli, for giving International Engineering Company, Inc., permission to publish Momotombo geothermal field data. Ms. Ingrid Han was of considerable help in both editing and typing this paper.

REFERENCES

Banwell, C. J., 1971, Electrical geophysical survey, Nicaragua; evaluation of methods. Project Report WR-13, UNDP Geothermal Resources Development. unpub.

Carriere, D. R., and Klein, J., 1974, Report on geophysical investigations for geothermals, Nicaragua - on behalf of the United Nations Development Program. unpub.

Corwin, R. F., and Hoover, D. B., 1979, The self-potential method in geothermal exploration, Geophysics v. 44, no. 2, p. 226-245.

Electroconsult, 1977, Momotombo geothermal field feasibility report; Prospeccion Geoelectrica, Reporte GNI-D-3508 and Gravimetric Survey, Report GNI-D-3772. unpub.

Keller, G. V., 1971, Summary evaluation of geophysical survey results; Final report, Nicaragua Geothermal Resources Project - Stage 1, Part 10 - Appendix C. Texas Instruments, Inc. unpub.

Texas Instruments, Inc., 1971, Final report, Geothermal Resources Project - Stage 1. Parts 6 and 7. unpub.

Geothermal Resources Council, TRANSACTIONS Vol. 4, September 1980

not very useful

MOMOTOMBO FIELD MODELS AT SIX STAGES IN TIME

Ulrich J. Cordon

International Engineering Company, Inc. (IECO)
San Francisco, California 94105

ABSTRACT

Conceptual models of the Momotombo Field were developed after each exploration stage through a detailed study of all technical data generated. These, in turn, single out methods that were most effective in outlining the field structure when compared to a final model.

As additional geologic, geochemical and geophysical data become available, the earth system model is refined, obtaining a better understanding of subsurface conditions and increasing the probability of drilling a successful well. At Momotombo only Stage 4 model was developed after investigations.

Fig. 1 Stage 1 Model. The objective of these investigations was to delimit the field by geological and geophysical methods. Geologic field mapping and photogeologic interpretation aided in delineating lineaments and faults. Temperature-gradient holes confirmed the presence of high temperatures (> 90°C) at depth; one 1995-foot borehole confirmed the existence of a steam-water mixture at a depth of 780 feet. Cuttings enabled a limited description of subsurface rocks. Electromagnetic soundings indicated a hot water reservoir about 1500 m deep over an electrical basement detected approximately at 2000 m. (Model developed from Texas Instruments, 1971.)

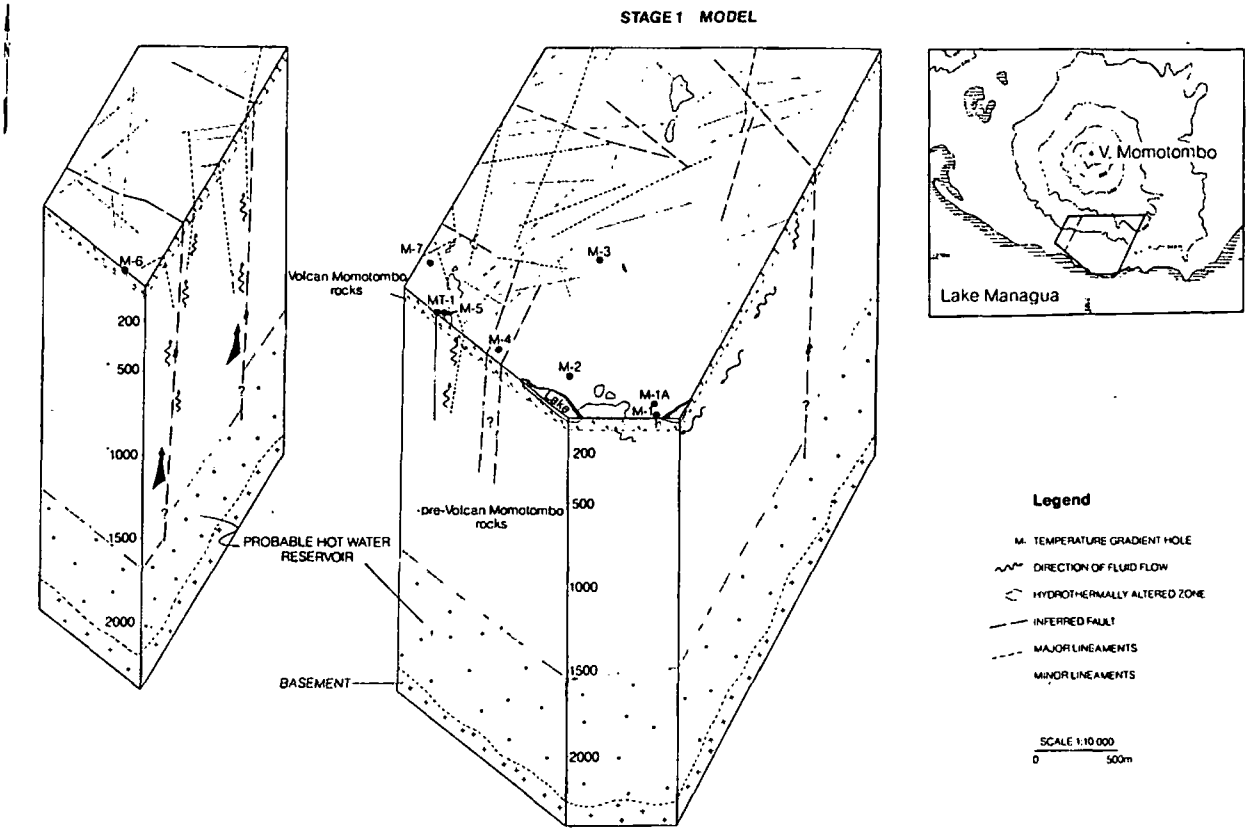

Fig. 2 Stage 2 Model. This model was devised from geological, geochemical, and few geophysical measurements. The most significant contribution was provided by geochemical data that suggested an upflow of thermal waters originating in a deep, high-temperature reservoir. Fluids rise to shallow, permeable layers where they flow downslope toward the lake. It was suggested that drilling anywhere within the area of surface activity would encounter thermal fluids at shallow depth and deeper drilling might encounter the reservoir. (Model developed from United Nations Development Program Reports, 1973).

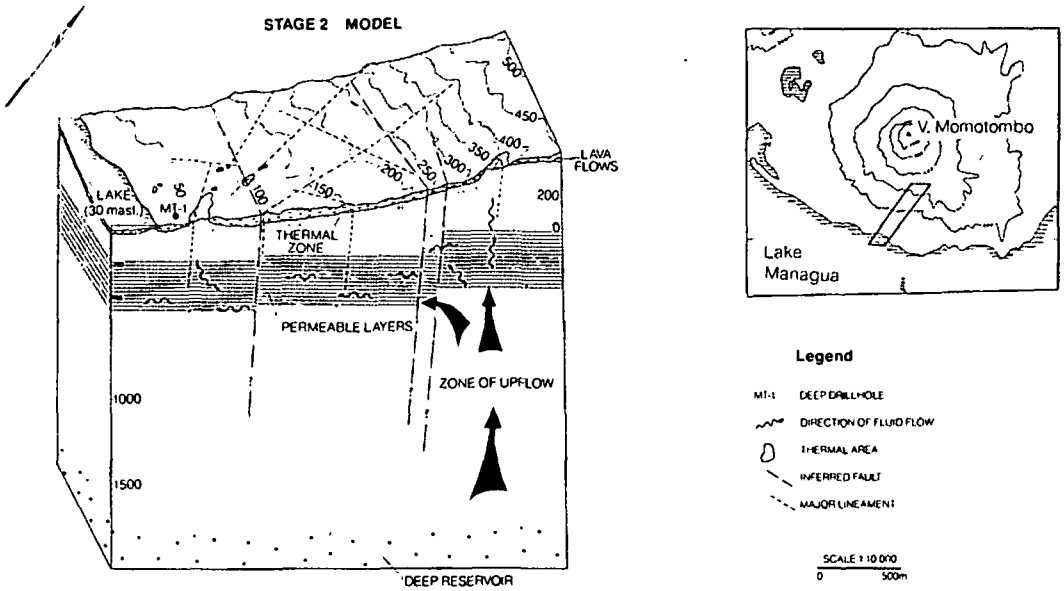

Fig. 3 Einarsson Model. S. Einarsson, senior technical adviser to the United Nations, devised this model based on the analyses of temperature distribution in drillholes. This illustration depicts the first inferred heat source and recharge of the system. The NE trending fault governs the upflow feeding of the shallow reservoir and acts as the NW field boundary. The convective system controls the maximum transport of fluids and, subsequently, the steam production potential; this limited system narrows the field to approximately 2 sq. km. (Model developed from Einarsson, 1977).

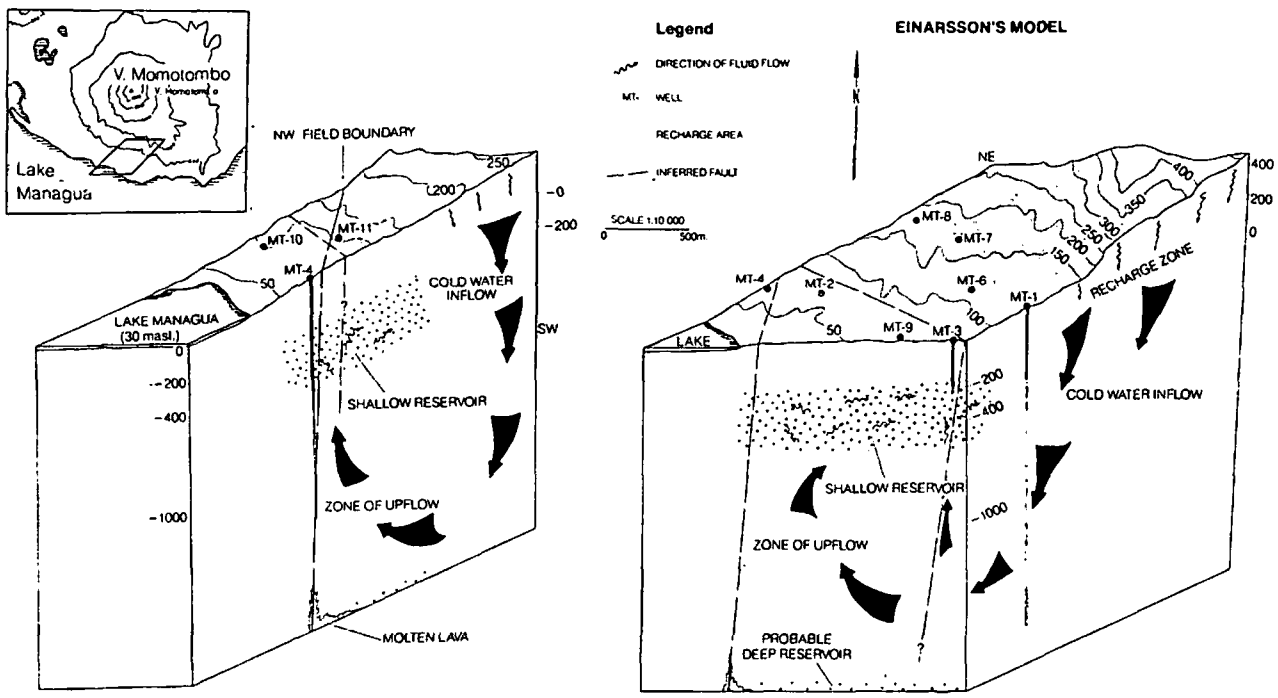

Fig. 4 Electroconsult Model. Stage 3 isotope analyses suggested the existence of two reservoirs and a convective cell developing within permeable formations. Hydrothermally altered pyroclastics act as a cap rock for the system. Recharge of the deep reservoir occurs from an area about 10 km south; fluids move northwesterly, following a channel formed by the Nicaraguan Depression and are eventually heated by the shallow magmatic chamber of Momotombo Volcano. Some cold water inflow from the east partially feeds the shallow reservoir. (Electroconsult, 1977.)

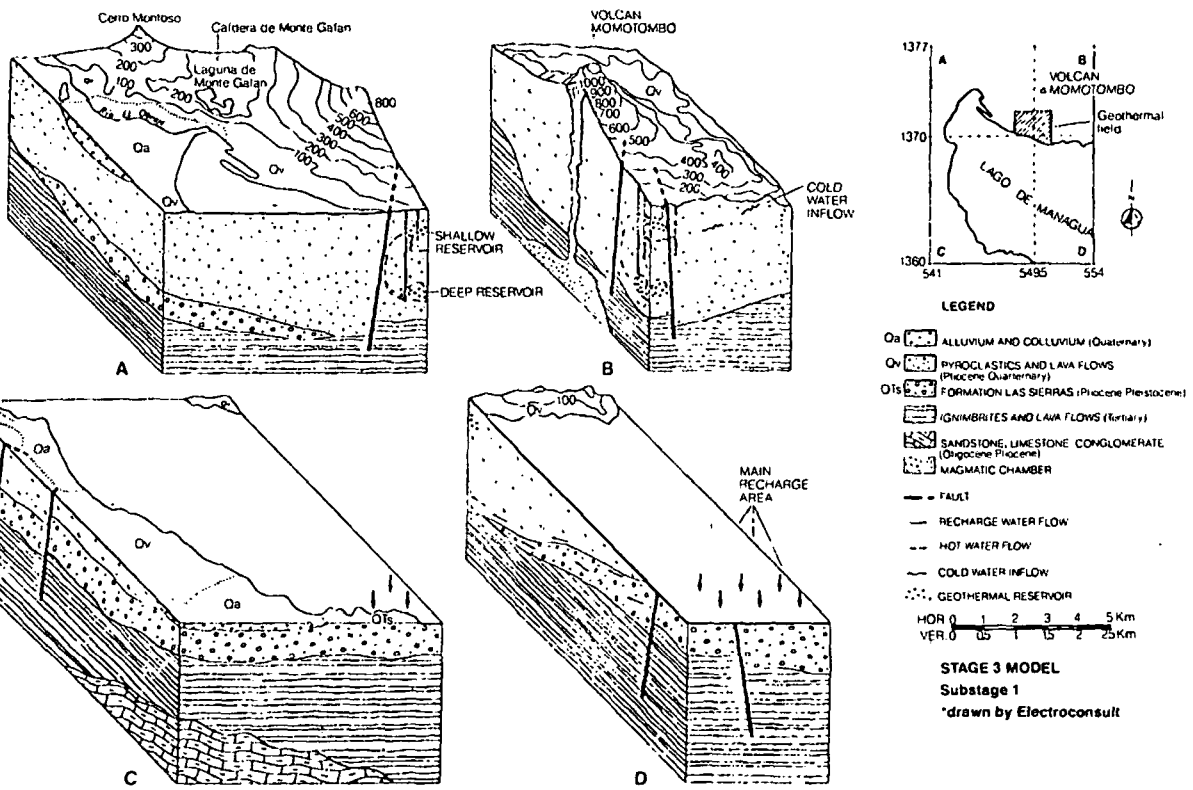

Fig. 5 Stage 4 Model. Stage 4 investigations included analyses of temperature measurements and geological observations from thirty-three wells. The first stratigraphic column was presented. The two wedge-shaped, fault-fracture systems are surface expressions of deep-seated faults serving as conduits for fluid flow, and their intersection serves as the major zone of upflow. Fluids migrate to the east within a tephra cone composed of units Id, Ie, and II. (Model developed from California Energy Company, Inc. Reports. 1979.)

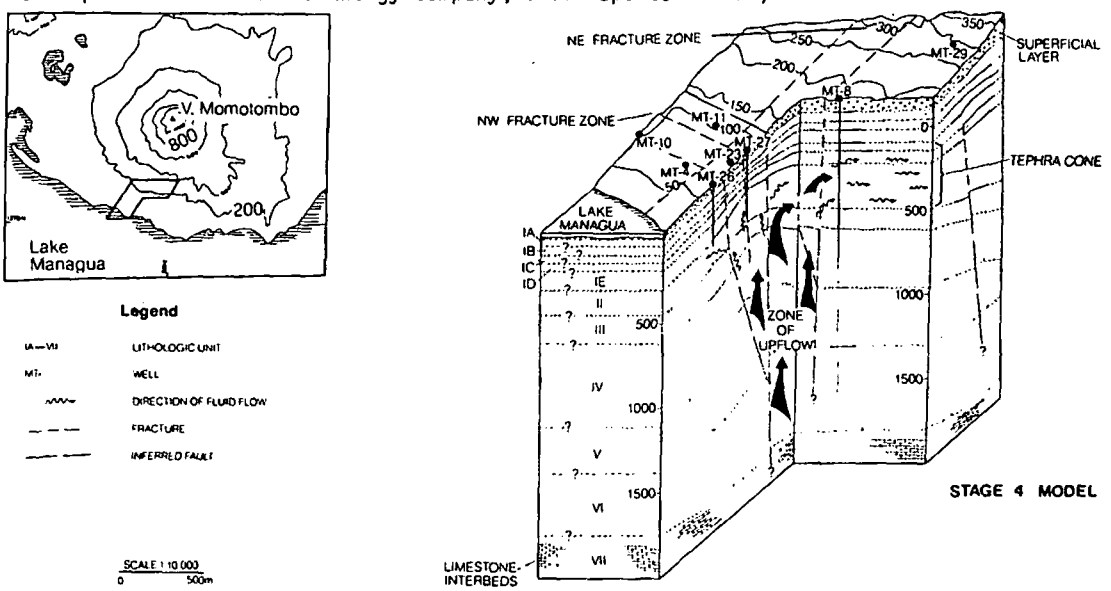

Fig. 6 IECO Model. This model was developed from analyses of subsurface temperature distribution and from previous findings by various companies. A broad, northeasterly trending fault-fracture zone resembling a graben structure controls fluid flow. Probable recharge of the deep reservoir occurs from the south. Thermal fluids rise to the surface within the fracture zone and move eastward in the productive horizon until encountering cold water inflow, which bounds the eastern and probably northeastern portion of the hydrothermal system. The deep reservoir extends to the west with increasing depth, but has an abrupt temperature drop near the eastern margin of the fracture zone due to cold water inflow. The shallow reservoir is controlled by fracture permeability within the 200 m to 500 m. depth range.

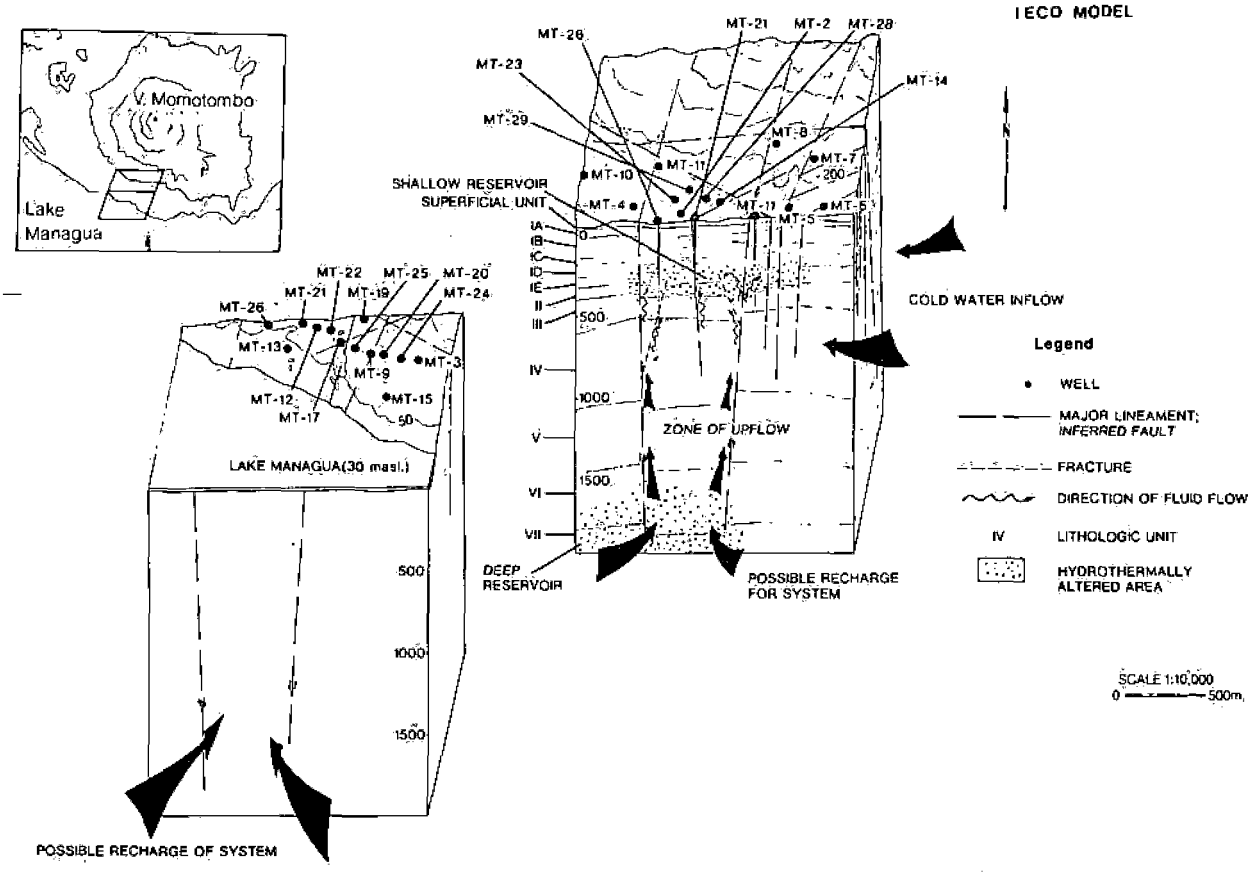

REFERENCES

California Energy Company, Inc., 1979, Geology and temperature distribution of the Momotombo Geothermal Field, Nicaragua. unpub.

Einarsson, S., 1977, Study of the temperature distribution in the geothermal reservoir at Momotombo and its implication: United Nations Development Program (UNDP), Geothermal Resources Development, Nic/74/003. unpub.

Electroconsult, 1977, Momotombo Geothermal Field Feasibility Report: unpub.

Texas Instruments, Inc., 1971, Final Report; Geothermal Resources Project-Stage 1. Parts 1-10. unpub.

United Nations Development Program, 1973, Geothermal Resources Development, Nicaragua: Reports WR 08, 10. unpub.

Electrical
County

PROCEEDINGS

Second United Nations Symposium on the Development and Use of Geothermal Resources

San Francisco, California, USA
20–29 May 1975

Investigaciones Recientes en el Campo Geotérmico de Ahuachapán

ALBERTO VIDES

Consultora Técnica S.A., Alameda Roosevelt 2940, San Salvador, El Salvador

RESUMEN

Nuevos estudios geológicos, geofísicos y geoquímicos indican que el área geotérmica de Ahuachapán-Chipilapa-El Salitre es una sola, existiendo además la posibilidad que esta área esté comunicada con el campo de Los Toles-Guayapa-El Durazneño.

Se ha continuado con las tareas de perforación realizándose nuevos pozos exploratorios, de gradiente térmico y de producción. Además se han retrabajado los pozos Ah-5 y Ah-7 incrementándose su producción.

Se analiza las diversas alternativas para eliminar las aguas de desperdicio. Debido a que la construcción de una canaleta de descarga al mar está atrasando el desarrollo del campo, se han reiniciado las pruebas de reinyección. Se presenta un programa de reinyección que podría solucionar a un costo reducido el problema de la eliminación de las aguas de desperdicio.

INTRODUCCIÓN

El proyecto geotérmico de El Salvador principió hace aproximadamente diez años, a finales de 1965, con la ayuda de las Naciones Unidas, ayuda que se prolongó hasta junio de 1971, habiendo quedado como asesor de la Comisión Ejecutiva Hidroeléctrica del Río Lempa, el señor Sveinn Einarsson, hasta el 31 de marzo de 1972.

En noviembre de 1971 se firmó un contrato con la firma italiana ELC Electroconsult S.p.A., para la construcción de la primera unidad geotérmica de 30 MW de capacidad. Se contaba para ese entonces con cuatro pozos productores, denominados Ah-1, Ah-5, Ah-6 y Ah-7, los cuales producían un flujo de agua salina con temperatura de 232°C en el reservorio. La producción total de esos pozos medida a diferentes presiones era del orden de 1080 ton/hora (2 381 000 lb/hr), producción que separada a 6 ata podría dar unas 162 ton/hora de vapor, o sea una producción estimada de 20 600 kW.

Para confirmar los estudios realizados previamente, se midieron cuatro perfiles de sondeos eléctricos con configuración Schlumberger de 4 km de separación entre electrodos y una serie de puntos de gravimetría, estudios que confirmaron las conclusiones de Naciones Unidas-CEL.

Después se firmó con la misma compañía italiana una adición al contrato, para realizar los estudios geotérmicos en el área norte-noroeste de Ahuachapán, que cubrían los siguientes aspectos: (1) seis perfiles de resistividad eléctrica con sondeos de 4 a 5 km de separación entre electrodos; (2) confirmación de la geología de la zona de los resultados obtenidos por métodos fotogeológicos; (3) estudios gravimétricos y magnetométricos; (4) el inventario de los puntos de agua; (5) análisis de aguas y gases de los manantiales; y (6) la perforación de 18 a 20 pozos de gradiente, todo ello sobre una superficie de 700 km^2. Todos estos trabajos serían hechos por ingenieros salvadoreños, siguiendo las instrucciones y bajo la dirección de los ingenieros italianos, quienes harían también la interpretación de los resultados.

Posteriormente fueron ampliados estos estudios, para ver si era posible la reinyección, ya que el costo de la canaleta de las aguas de desperdicio hacia el mar es muy superior al estimado, debido a la topografía y clases de terrenos encontrados y al incremento mundial de los precios.

El primer contrato que se firmó, bajo la asesoría de ELC Electroconsult, fue para la perforación de pozos profundos, con la firma francesa Foramines, S.A. El objeto del contrato sería afianzar la potencia de 30 MW de la primera unidad de media presión y la perforación de los pozos de la segunda unidad de media presión y como resultado de estas dos unidades, la tercera unidad de baja presión, también de 30 MW para alcanzar 90 MW, que es el total del proyecto del campo geotérmico de Ahuachapán.

GEOLOGÍA

Debido a la existencia de un mapa fotogeológico bastante bueno, se decidió que se debía únicamente comprobar el contacto Terciario-Cuaternario con los perfiles que se muestran en la Figura 1, la cual es una reducción del mapa original. Se adjuntan seis perfiles (Figs. 2 a 7) de los 18 que se realizaron mostrando las fallas principales y algunas secundarias del área. Estas fallas principales forman parte de la falla regional de El Salvador.

En la Figura 8 a 10 se hacen las comparaciones de los pozos perforados en el área de Ahuachapán-Chipilapa, por medio de perfiles litológicos esquemáticos, y se mira que hay correspondencia en toda el área, por la naturaleza de las rocas, según comunicación del geólogo Mario Jiménez.

GEOFÍSICA

En los meses previos a la contratación de ELC, se hicieron unos estudios de resistividad eléctrica en la zona conocida por Los Toles, donde existen fumarolas y nacimientos de

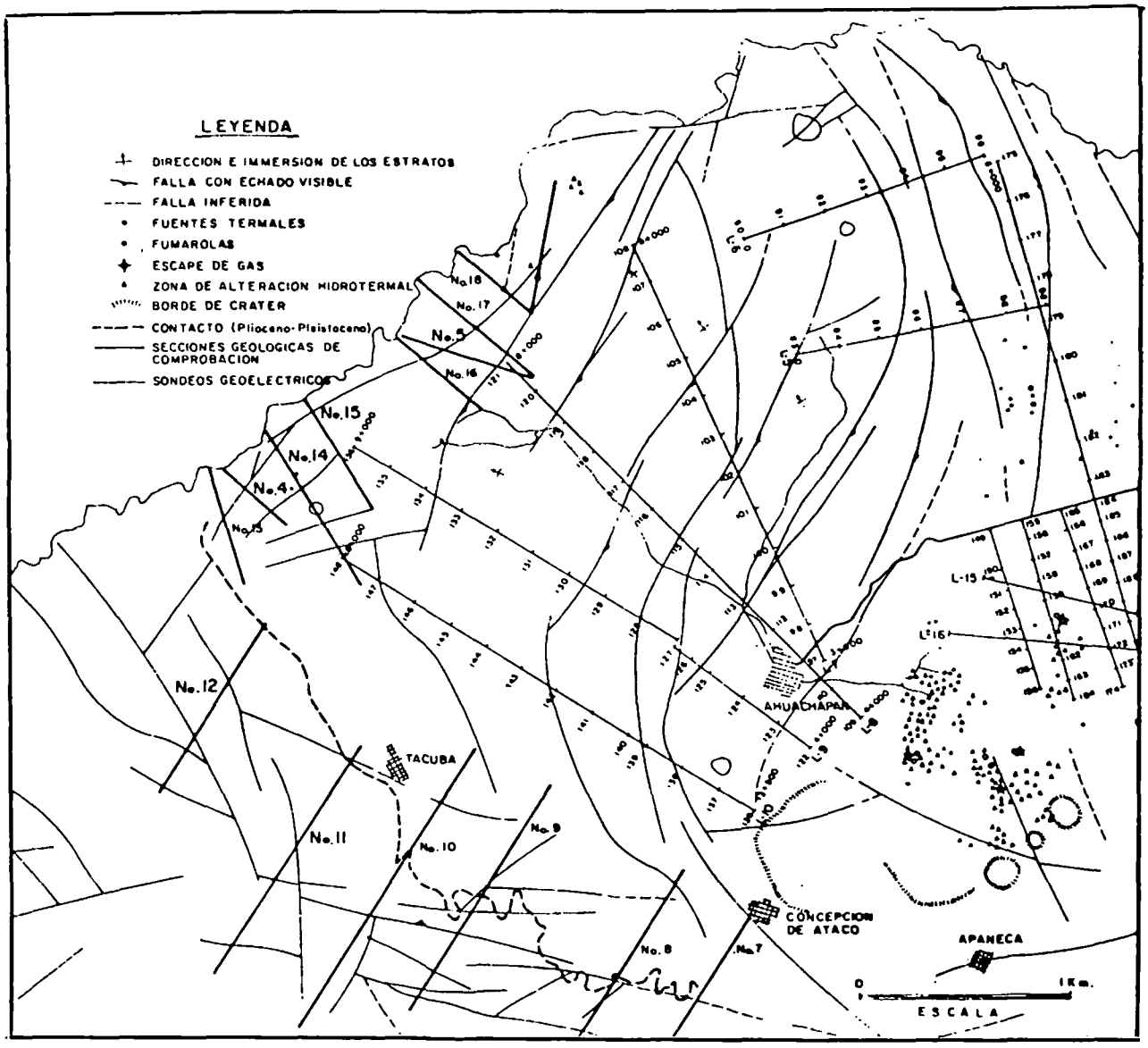

Figura 1. Mapa del área de Ahuachapán, indicando ubicación de perfiles geológicos y sondeos geoeléctricos.

agua caliente, los resultados de estos estudios son mostrados en la Figura 11, los estudios se descontinuaron, pues el personal pasó a realizar los sondeos de comprobación en las líneas 1, 2, 3 y 4 que aparecen en la Figura 12.

Como se puede apreciar en la Figura 11, la composición química de las fuentes de agua de Los Toles, Guayapa y El Durazneño son muy similares entre sí y corresponden al análisis típico del agua del reservorio de los pozos profundos, según comunicación del Dr. Gustavo Cuéllar.

La resistividad eléctrica aparente y la similitud en la composición química, hacen pensar en una posible conexión entre ambos campos, no por la parte del graben formado entre las cordilleras de la era Terciaria y de la era Cuaternaria, sino que por la falla regional de El Salvador, sobre la cordillera más reciente y que es conocida como la falla de Humboldt. Hasta la fecha no se han hecho mediciones geoeléctricas para confirmar esta aseveración, pero es de suponer que los sondeos de la segunda etapa de geoeléctrica estarán encaminados a ese fin.

Los estudios geoeléctricos son además muy interesantes en la zona de Chipilapa, ya que muestran con las líneas de los sondeos 11, 12, 13, 14, 15 y 16, además de los antes citados, que hay una conexión directa entre el área geotérmica de Chipilapa y la de Ahuachapán, sin haberse podido establecer hasta la fecha un límite hacia el sur del campo Ahuachapán-Chipilapa. Quedando sobre este rumbo la falla de Humboldt. Ver Figura 12.

Los estudios gravimétricos muestran además que existen zonas de anomalías Bouguer positivas alternadas con zonas de anomalías negativas, lo que podría explicar que no se hayan encontrado resistividades eléctricas bajas en el graben, por no coincidir las líneas de sondeo con las fallas posibles, como la encontrada en el área Los Toles-El Durazneño en las mediciones anteriores. Aún cuando esto se puede interpretar como la existencia de un dique que no permite el flujo de agua subterránea caliente hacia la frontera de Guatemala, según comunicación del Ing. Luciano Baldo de ELC Electroconsult. Ver la Figura 13, hecho con densidad terrestre tan baja como 2.00.

Los estudios magnetométricos, como en estudios previos, parecen ser un reflejo de las curvas isométricas, lo que posiblemente se debe al hecho de que existen coladas de

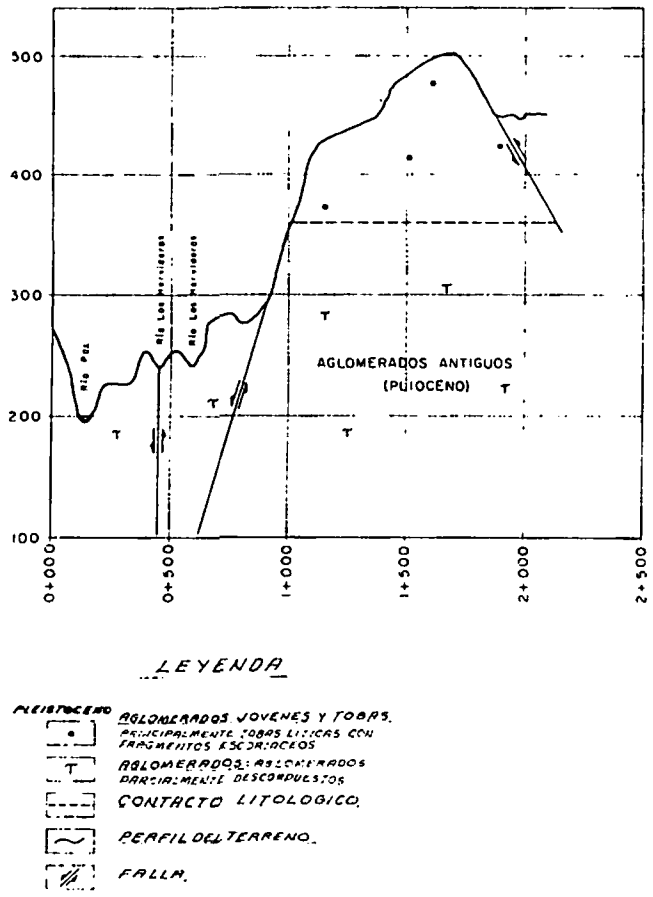

Figura 2. Perfil geológico No. 4, Ahuachapán.

lava muy próximas a la superficie del terreno, las que influyen grandemente en las mediciones de magnetometría de un aparato de componente vertical solamente. La gravedad específica y la composición química de las rocas que afloran a la superficie o que están de 10 a 200 m de profundidad, es casi la misma. La Figura 14 muestra las curvas isomagnetométricas.

GEOQUÍMICA

Según comunicación del Dr. Gustavo Cuéllar, las conclusiones a las que se ha llegado por medio del muestreo y análisis geoquímico de los puntos de agua caliente y fumarolas, son las siguientes:

1. El quimismo de las aguas y gases de Chipilapa, El Salitre y de la zona Los Toles-Guayapa-Durazneño, demuestra que lo más seguro es que provengan de una fuente común; sin embargo, en la zona últimamente mencionada existe un marcado incremento en sulfatos, lo que puede ser debido a reacciones secundarias en esa zona.
2. No se ha finalizado el muestreo y análisis químicos de los puntos de agua.

GEOTERMIA

Para los estudios del gradiente geotérmico se programaron 14 pozos de diámetro NX, con profundidades entre 60 y 150 m, y dependiendo del resultado de éstos, se perforaría de cuatro a seis pozos integrativos, con profundidades hasta de 300 m, de estos últimos solo se perforó un pozo y de los 14 primeros se profundizó uno de ellos. En todas estas perforaciones se encontró gradiente normal, la Tabla 1 muestra los resultados de los pozos y sus profundidades y la Figura 15 la ubicación de las perforaciones y las isotermas correspondientes.

POZOS PROFUNDOS

En las perforaciones profundas se pueden distinguir tres etapas, por así decirlo: (1) las perforaciones localizadas por técnicos de UN y CEL; (2) las perforaciones para delimitar el campo; y (3) las perforaciones para la producción de la segunda unidad, localizadas por el suscrito. En la Tabla 2 se dan los resultados de acuerdo a la clasificación anterior y a la secuencia cronológica en que fueron perforados.

Los pozos Ah-1, Ah-5, Ah-6, Ah-7, Ah-9 y Ah-10 se incluyen en la Tabla 2 a pesar de haber sido perforados en campañas de perforación previas a las investigaciones recientes, pues algunos de estos pozos serán usados para la generación de la primera unidad, juntamente con el pozo Ah-4. A los pozos Ah-5 y Ah-7 se les extrajo el liner y ambos aumentaron la producción, el Ah-5 en un 5% y el Ah-7, el cual fue además profundizado, aumentó su capacidad en un 70% (de 174 a 295 ton/hr).

En la Figura 16 aparece la ubicación de los pozos del área de Ahuachapán y se puede notar claramente que las isotermas definen el campo en los bordes norte y oeste, y no así hacia el sur y hacia el este, aún cuando no se ha obtenido producción en algunos pozos y que la producción es irregular en otros, no se ha podido delimitar el campo y la falta de producción se debe a problemas de otra índole.

Según mi opinión, la temperatura del reservorio nos indica la presión a que debían fluir estos pozos, si el nivel hidrostático estuviera a la boca del pozo, pero siendo que el nivel está a unos 200 m debajo de la superficie y que la presencia de gases en el campo es mínima y por lo tanto no disminuye el peso de la columna, al tener que levantar una columna de agua mayor (entre 50 y 80 m), se pierde la presión que normalmente se tiene para la producción y ésta no se realiza o es irregular.

La terminación mecánica de los pozos se había aumentado de 9-5/8 pulg. a 13-3/8 pulg. o.d., en la tubería de producción, como se muestra en la Figura 17, lo cual tenía

Tabla 1. Temperaturas medidas en los pozos de gradiente geotérmico.

Pozos de gradiente	Profundidad (metros)	Temperatura (°C)
A	288.00	En calentamiento
B	101.30	25.7
C	102.00	26.3
D	102.50	28.5
E	101.17	25.4
F	101.88	25.3
G	94.36	26.5
H	100.86	26.2
I	100.83	29.6
O	102.00	26.8
P	101.57	31.4
L	100.57	28.5
M	100.80	27.2
N	100.49	28.7
R	202.27	29.2

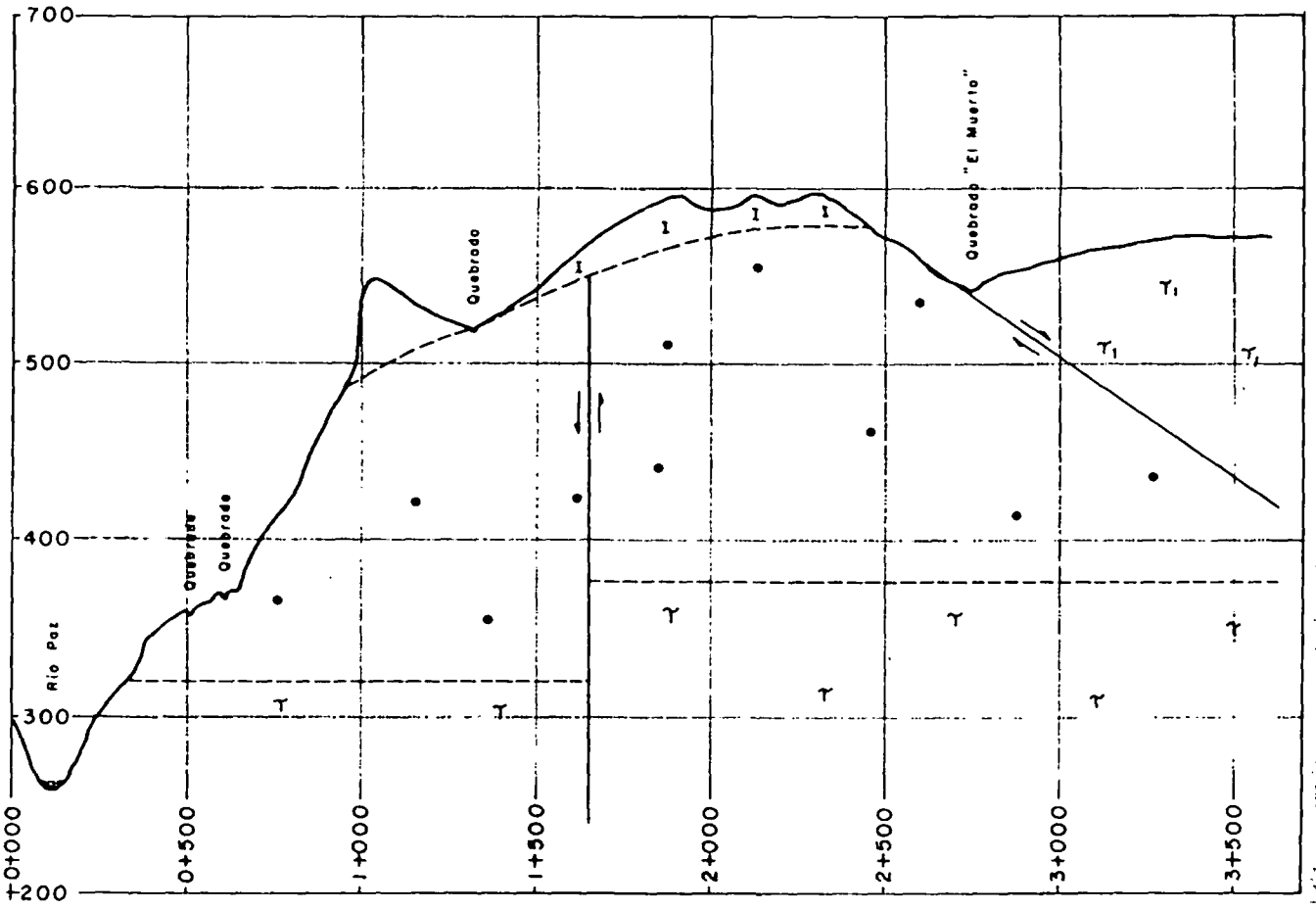

LEYENDA

HOLOCENO — T1 — TOBAS CAFE: Material Piroclástico, joven principalmente polvo volcánico, pómez, lapilli, arenas y ceniza

PLEISTOCENO — I — IGNIMBRITAS: Eventualmente tobas fundidas.

• — AGLOMERADOS JOVENES: Principalmente tobas líticas con inclusiones de fragmentos de material escoriáceo, oscuro; además, tobas líticas aglomeráticas, aglomerados jovenes etc. cerca del contacto con los aglomerados antiguos aparecen pequeñas coladas de lava andesítica. (Andesitas Basales).

PLIOCENO — T — AGLOMERADOS ANTIGUOS: Constituyen el basamento de todas las unidades de esta región.

FALLA

NIVEL DEL TERRENO

CONTACTO

Figura 3. Perfil geológico No. 5, Ahuachapán.

por objeto el aumento de la producción por pozo a un costo un poco mayor. Debido a la escasez de materiales, especialmente tuberías de revestimiento, se ha vuelto a reducir el diámetro de las perforaciones.

PROBLEMA CON LAS AGUAS DE DESPERDICIO

El campo de Ahuachapán está situado en el graben con la cordillera cuaternaria entre el campo en sí y el mar. La única comunicación directa entre el campo y el mar, por la que se podría evacuar las aguas a un costo moderado, sería por medio del Río Paz, pero este río es fronterizo entre Guatemala y El Salvador y por los problemas que la contaminación de las aguas podría originar, además de los problemas ecológicos, se decidió hacer las pruebas de reinyección en el pozo Ah-5, inyectándole primero el agua del pozo Ah-1 y luego las del pozo Ah-1 sumadas a las del pozo Ah-6, con flujos de 91 l/seg y de 164 l/seg en un período de aproximadamente un año. Estas experiencias están explicadas en otro trabajo presentado por Einarsson et al. en este Simposio.

La desventaja de este método según se suponía es que

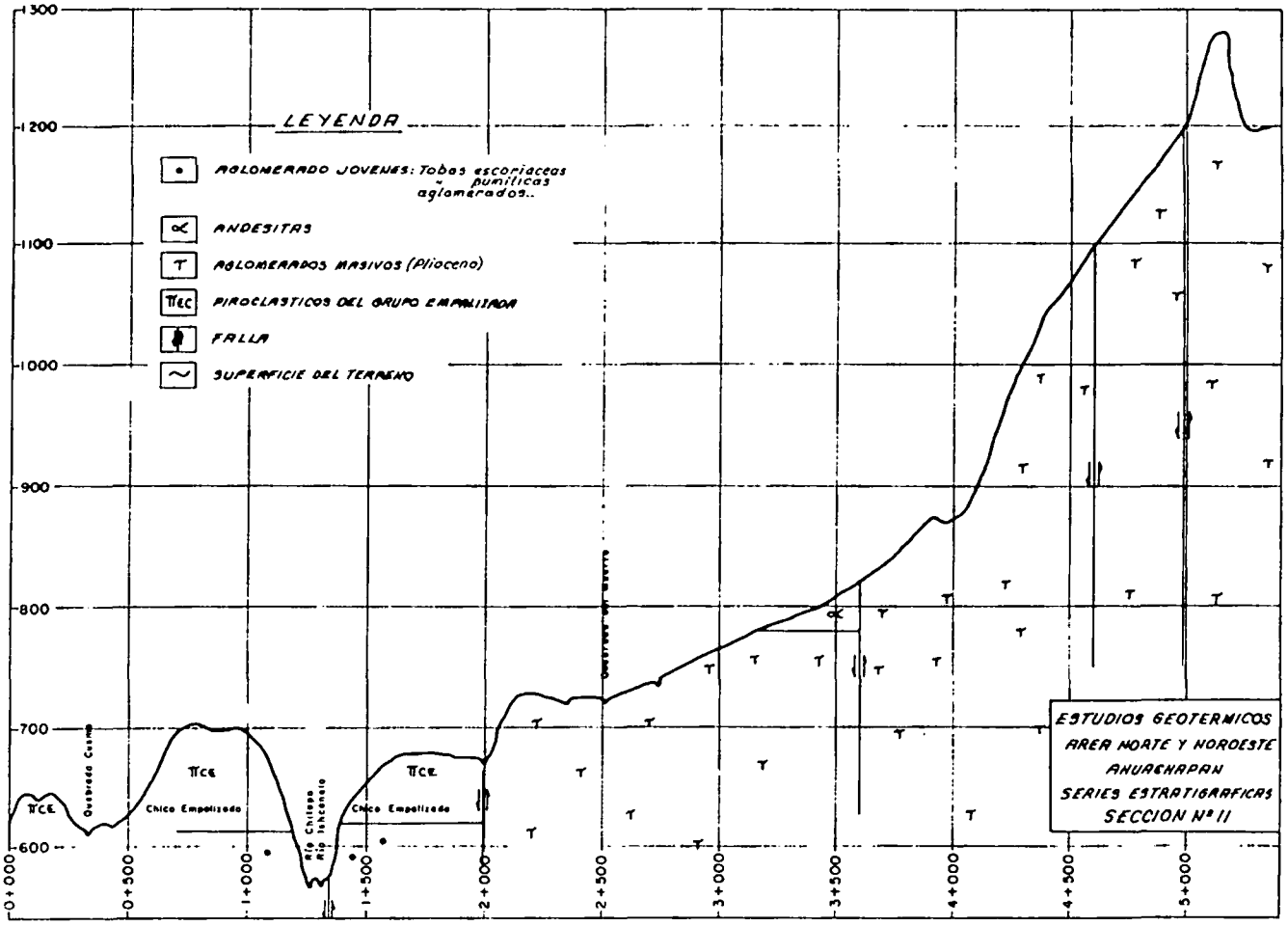

Figura 4. Perfil geológico No. 11, Ahuachapán.

Tabla 2. Características de los pozos perforados en las tres etapas del programa de perforación.

Pozo No.	Elevación m.s.n.m.	Profundidades en metros abajo del cabezal 26" ϕ	20" OD	17-1/2" ϕ	13-3/8" OD	12-1/2" ϕ	9-5/8" OD	8-1/2" ϕ	7"	ϕ Tubería producción (pulg.)	Presión producción (kg/cm² g)	Temp. (°C)	Producción ton/hora
1	802.79	—	—	37	24.38	491	486	1205	—	8	10.2	232	338
5	789.45	—	—	104.6	98.2	468.8	456.9	951.6	—	7	7.1	230	208
6	782.97	—	—	95.3	90.7	455.2	454.3	591.2	—	10	7.0	232	360
7	804.79	—	—	103.6	96.7	484.3	483.4	950	—	7	5.2	232	295
9	871.33	—	—	94.6	90.8	488.1	484.5	1424	1424	7	—	237	Irregular
10	723.78	—	—	102.1	96.4	492.9	485.6	1525	1524	—	—	145	Nada*
4	812.23	110	56	485	481	640	—	—	—	12	6.2	234	475
8	810.99	110	107	467	464	988	723	—	—	8	Varía	232	Irregular†
11	759.30	100	96	464	462	943	—	—	—	—	—	185	Impermeable
12	758.80	100	96	500	496	600	—	1003	—	—	—	135	Impermeable
3	855.50	105	80	475	472	802	696	737	—	7	Varía	235	Irregular
2	808.00	96	94	700	686	900	—	—	—	—	—	232	Nada‡
13	859.60	98	97	490	480	831	812	—	—	6	Varía	232	Irregular
14	821.77	97	96	500	348	570	465	800	698	—	—	230	Nada§
16	868.76	101	100	510	506	700	698	—	—	7	Varía	232	Irregular
15	772.68	90	98	505	495	704	—	—	—	—	—	110?	Colapsado
20	792.00	86	84	453	448	600	—	—	—	8	En proceso	232	En proceso
21	795.00	96	94	487	472	669	—	—	—	10	En proceso	232	En proceso
22	842.00	—	—	93	90	510	509	659.5	—		En proceso	232?	En proceso
23	818.50	Plataforma en construcción											
24	803.10	—	—	98	95	En perforación							
25	Plataforma en construcción												

*Fue perforado para reinyección y no tiene permeabilidad.
†La presión en el cabezal sube hasta 14 kg/cm². En la primera abertura se colapsó y fue intervenido.
‡No fluye probablemente a la profundidad de la tubería de revestimiento. Será usado para reinyección.
§No ha sido estimulado convenientemente aún. Está bastante lejos de la Central.
Los pozos Ah-3, Ah-13 y Ah-16 tienen temperatura y permeabilidad, pero fluyen irregularmente debido a su elevación.
Los pozos Ah-20, Ah-21 y Ah-22 están en proceso de medición los dos primeros y de calentamiento el tercero.
El Pozo Ah-24 está siendo perforado.

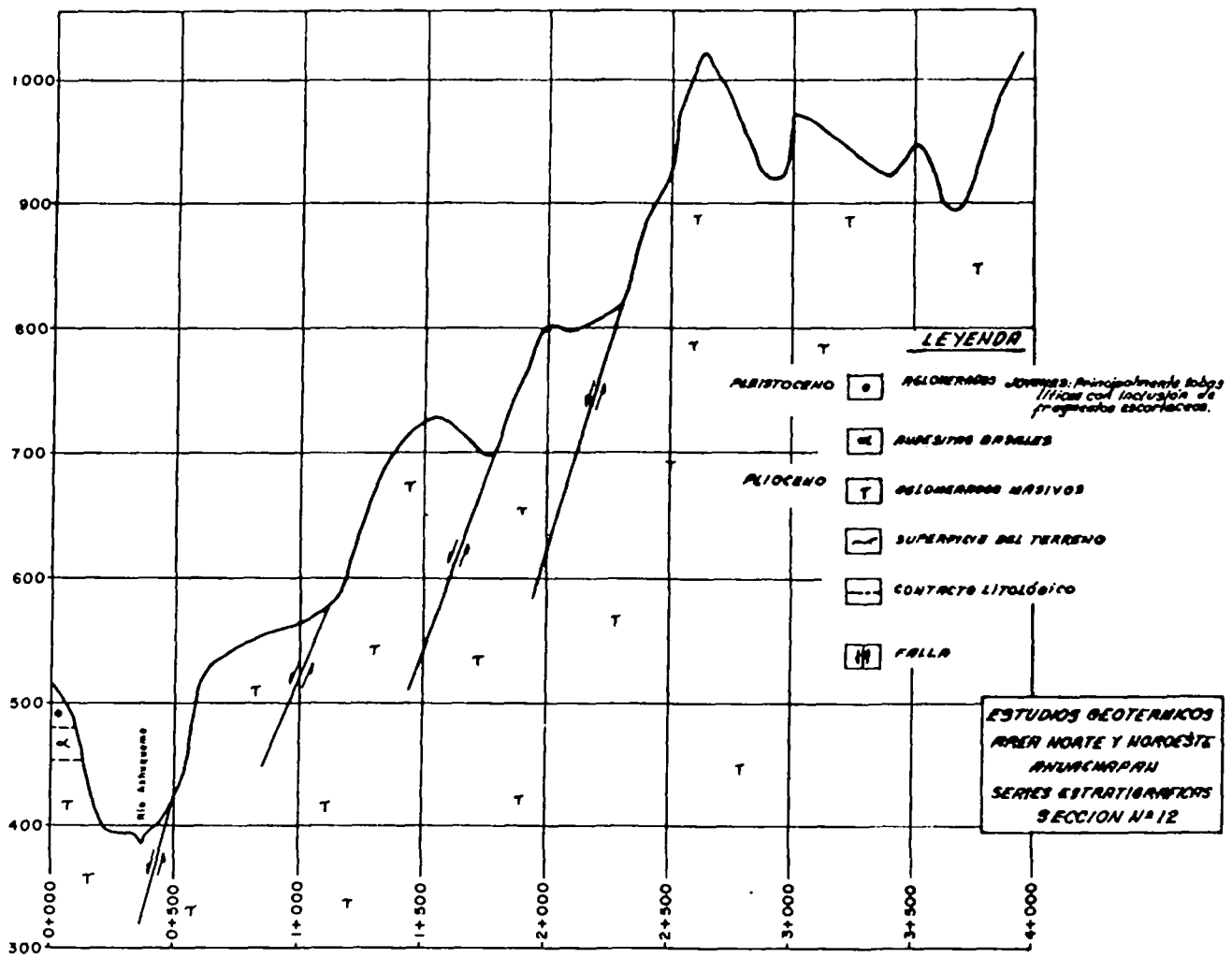

Figura 5. Perfil geológico No. 12, Ahuachapán.

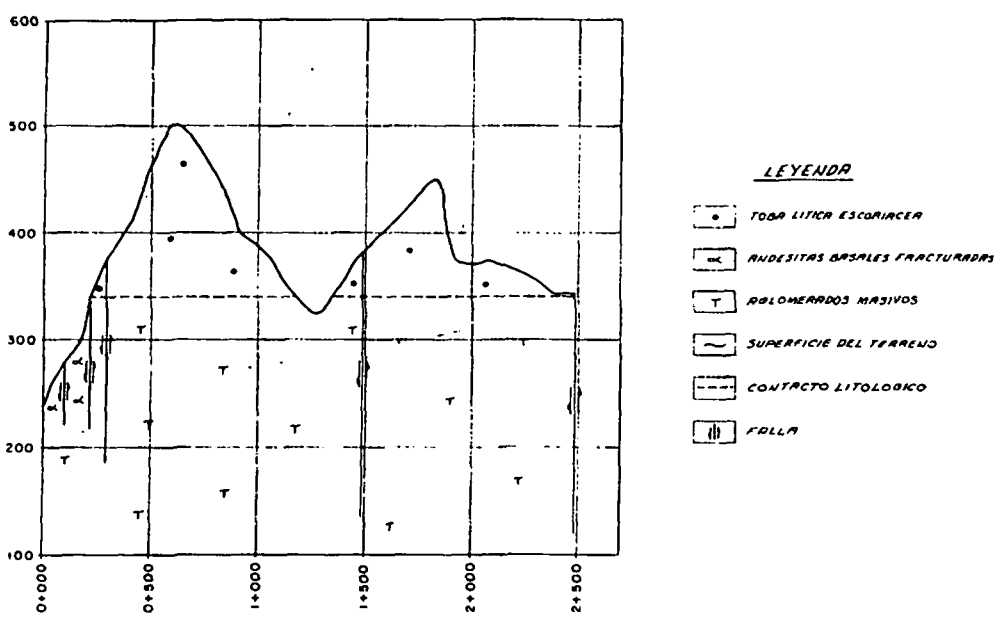

Figura 6. Perfil geológico No. 14, Ahuachapán.

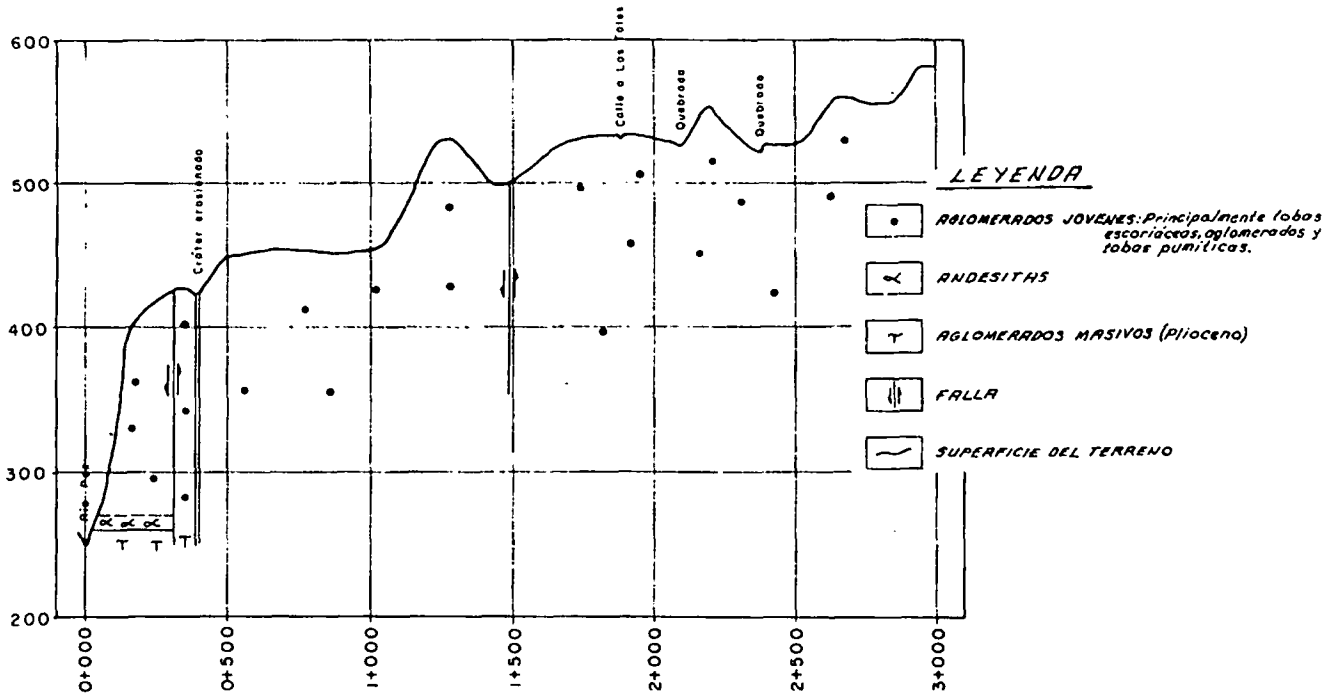

Figura 7. Perfil geológico No. 15, Ahuachapán.

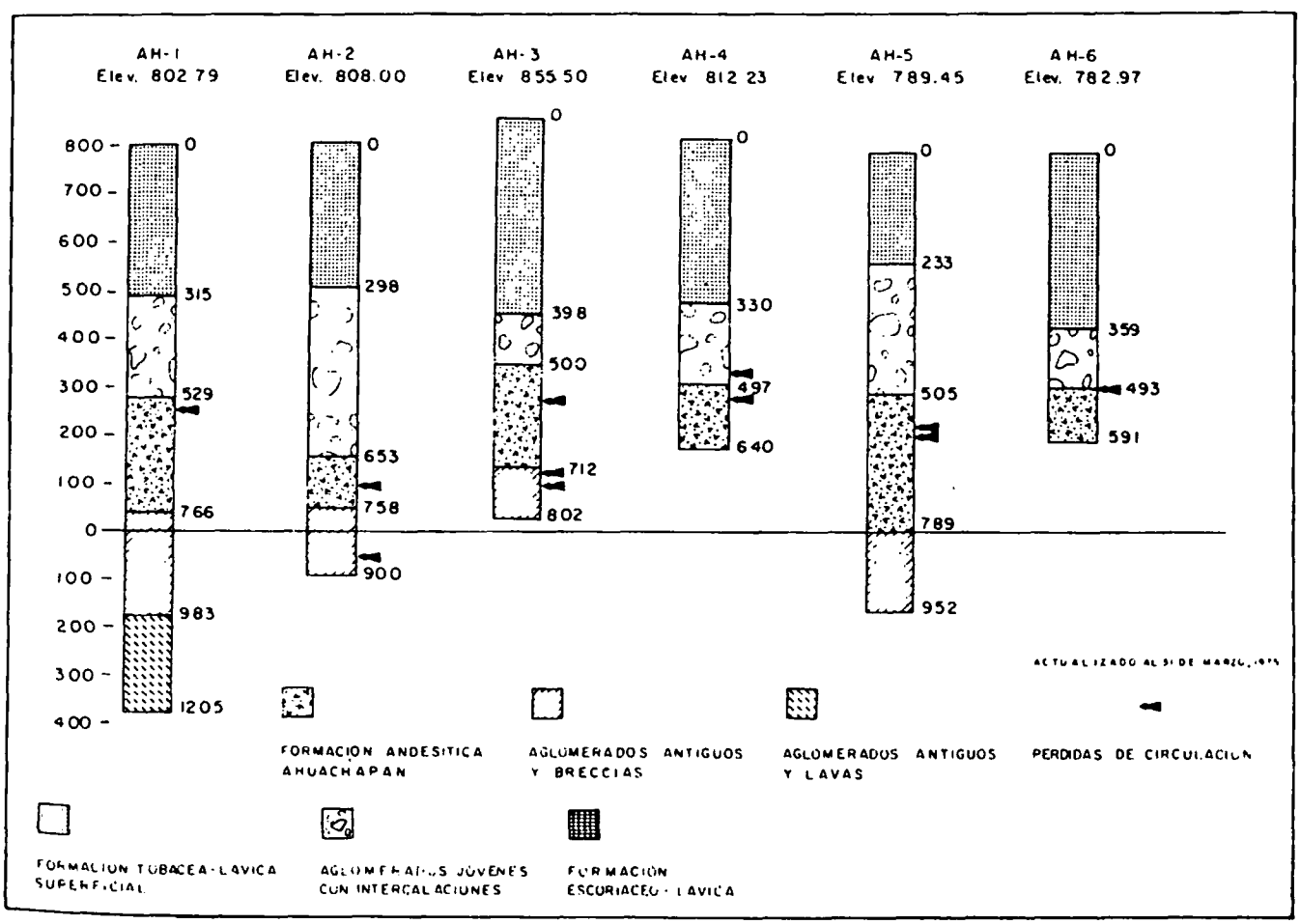

Figura 8. Columnas estratigráficas, pozos Ah-1 a Ah-6, Ahuachapán.

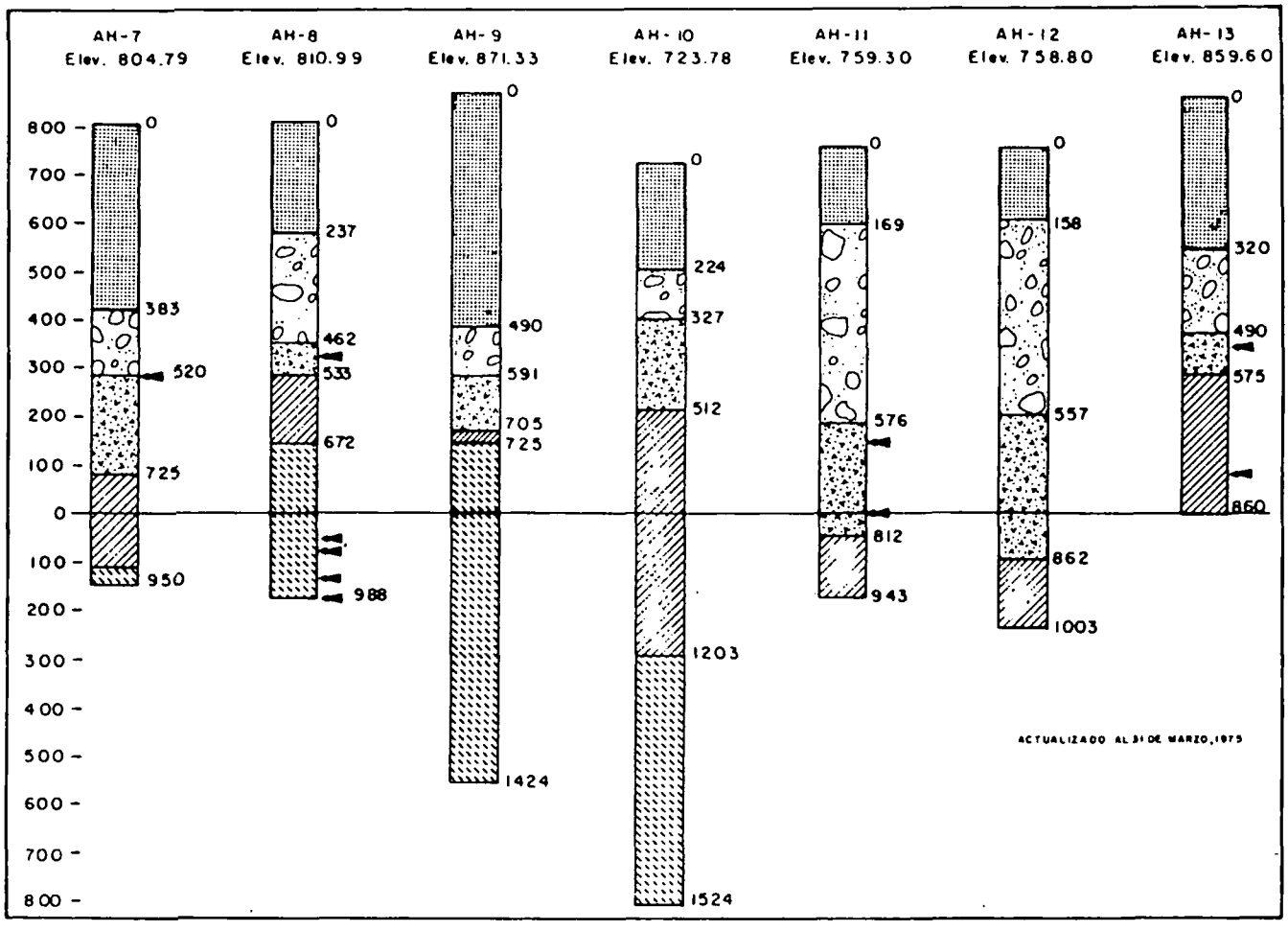

Figura 9. Columnas estratigráficas, pozos Ah-7 a Ah-13, Ahuachapán.

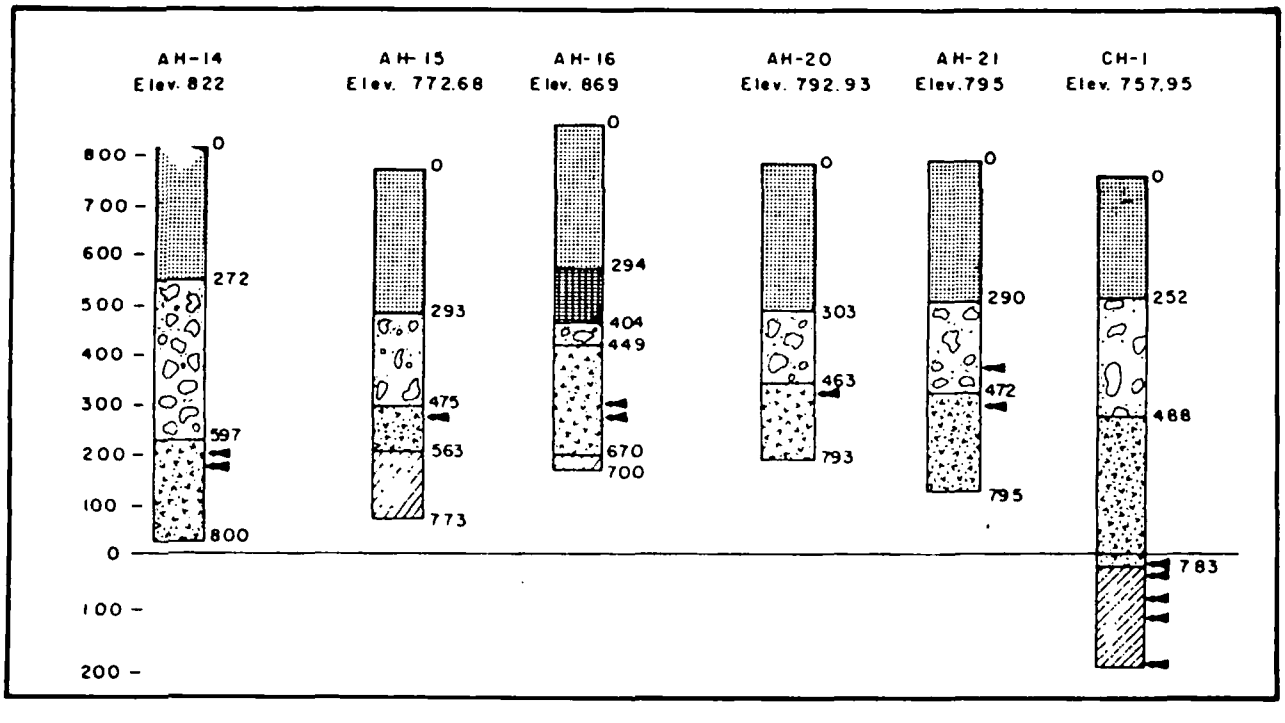

Figura 10. Columnas estratigráficas, pozos Ah-14, Ah-15, Ah-16, Ah-20, Ah-21, y Ch-1, Ahuachapán y Chipilapa.

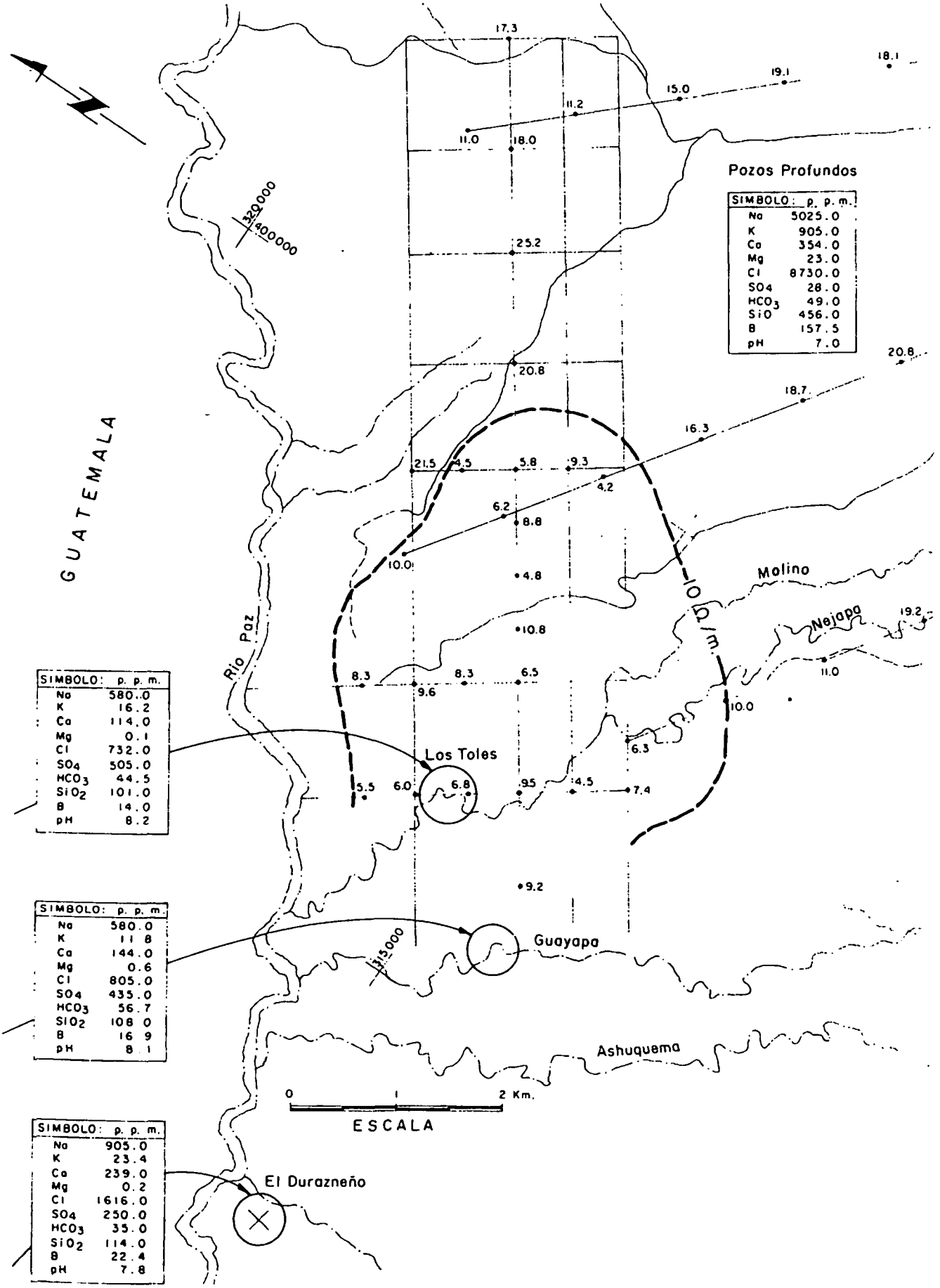

Figura 11. Resistividad eléctrica aparente (AB/2 = 500 m); composición química de aguas.

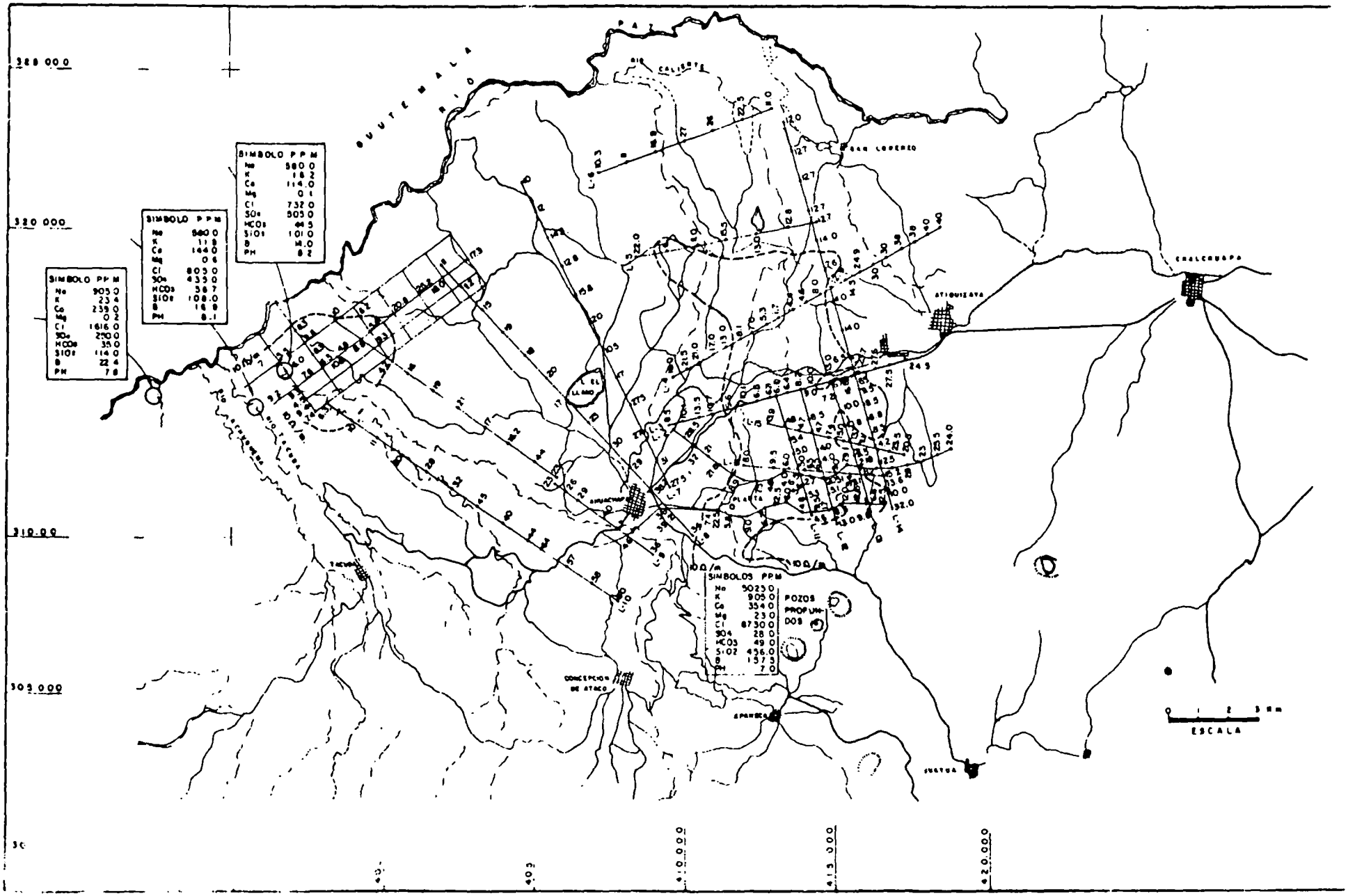

Figura 12. Resistividad eléctrica aparente (configuración Schlumberger); composición química de aguas.

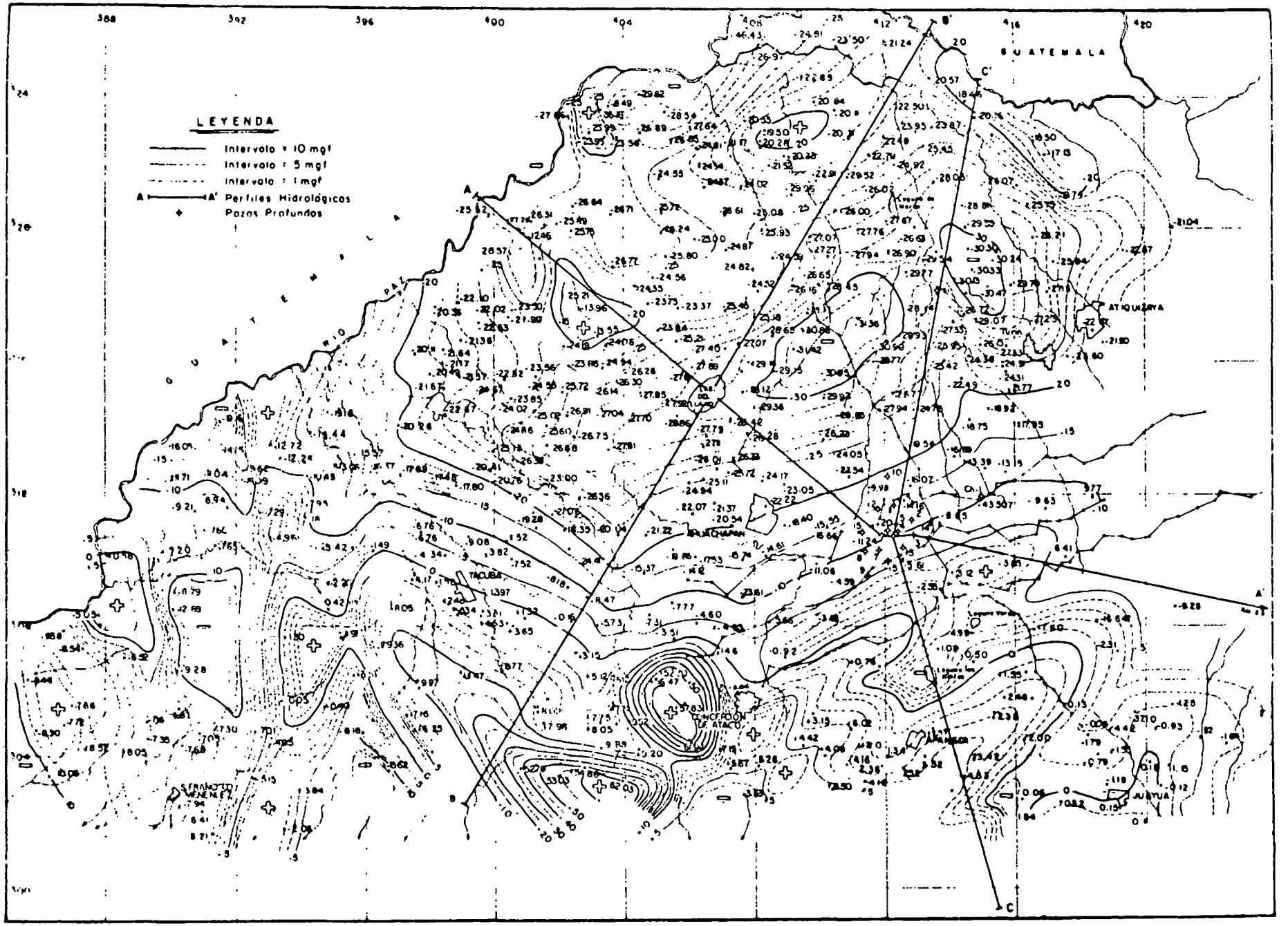

Figura 13. Curvas isogravimétricas; densidad = 2.00.

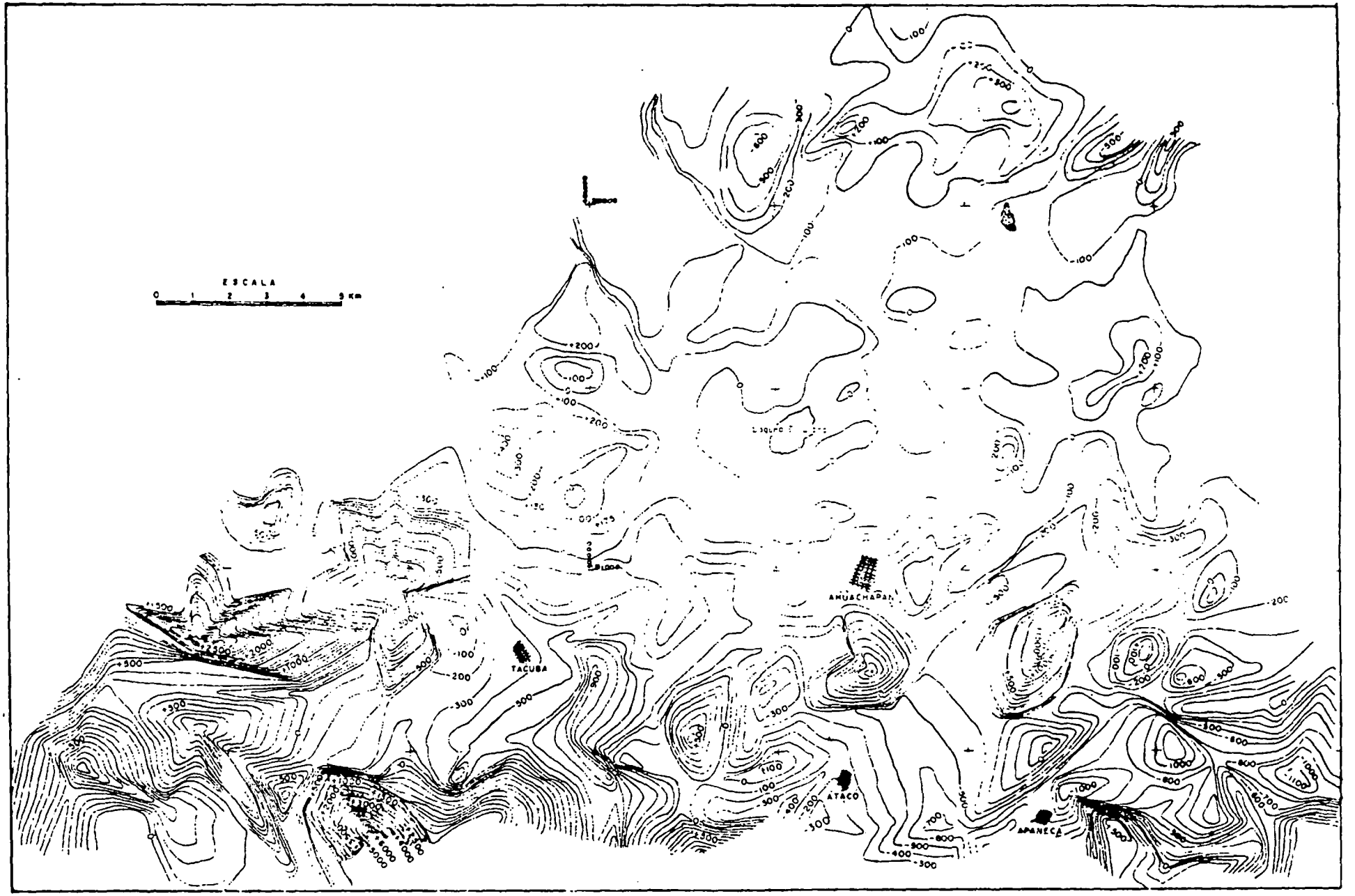

Figura 14. . Curvas isomagnetométricas de componente vertical.

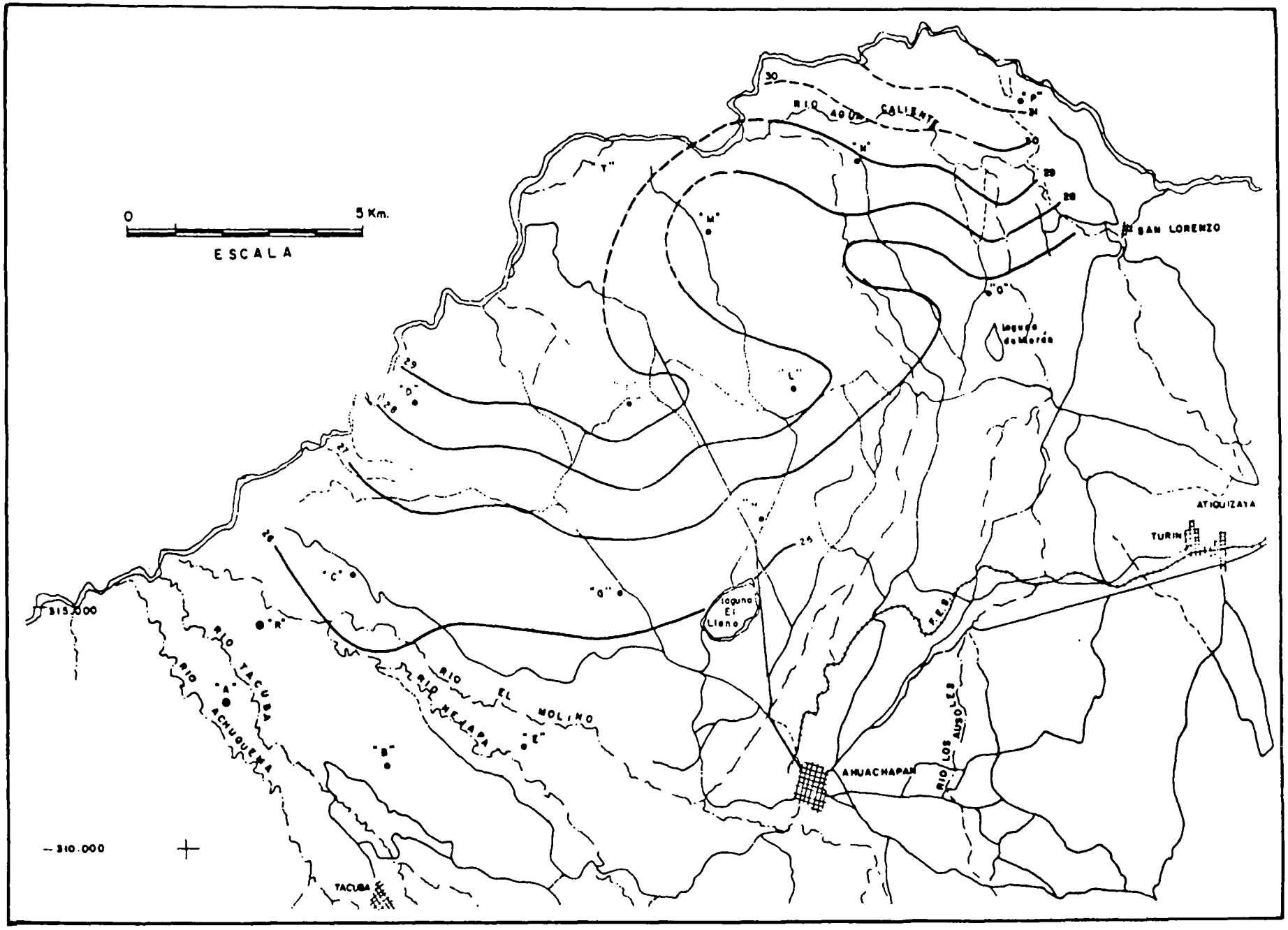

Figura 15. Curvas isotérmicas y ubicación de pozos de gradiente térmico.

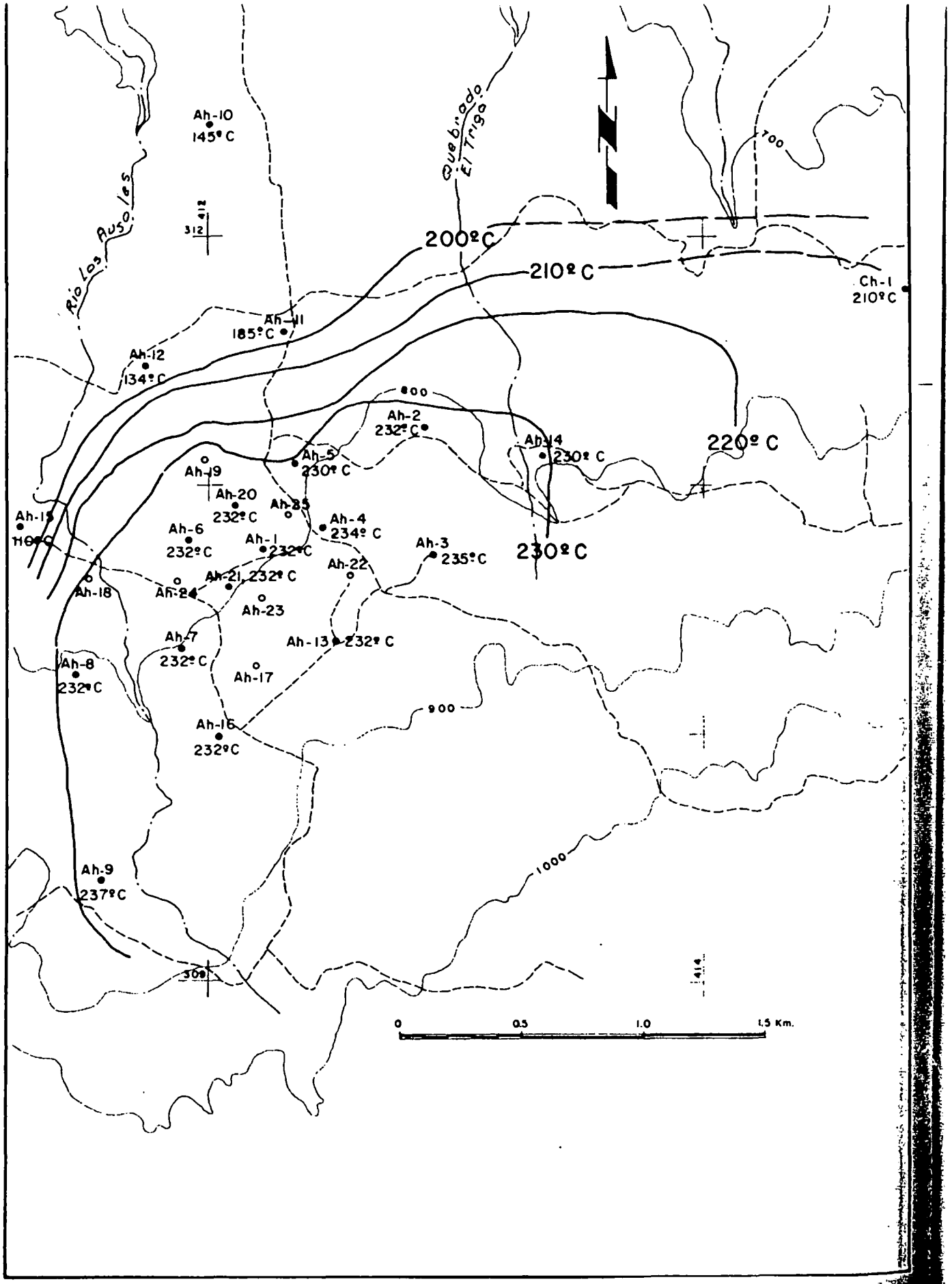

Figura 16. Temperaturas del reservorio geotérmico y ubicación de pozos, Ahuachapán.

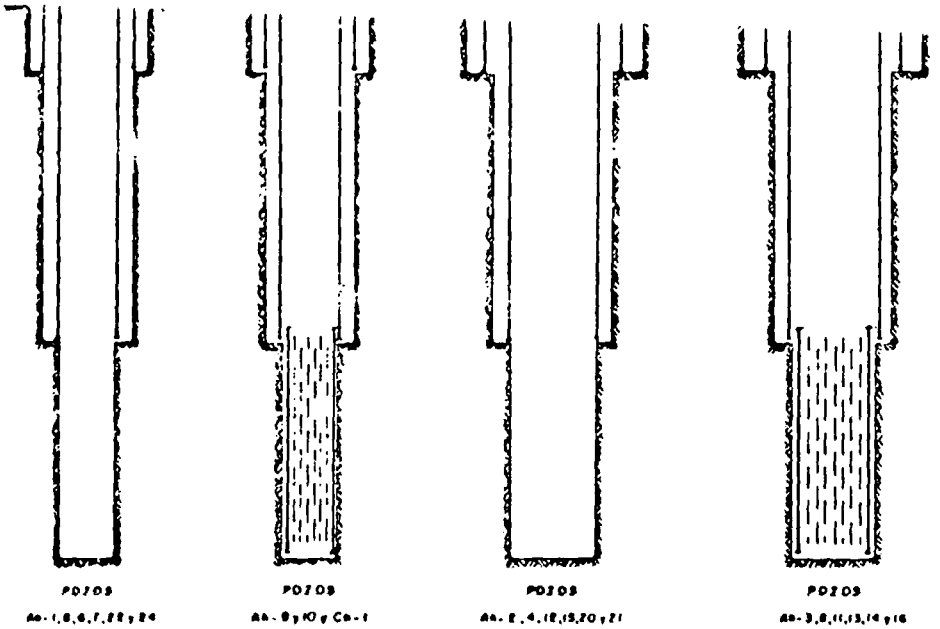

Figura 17. Terminación mecánica de los pozos de Ahuachapán (ver Tabla 2).

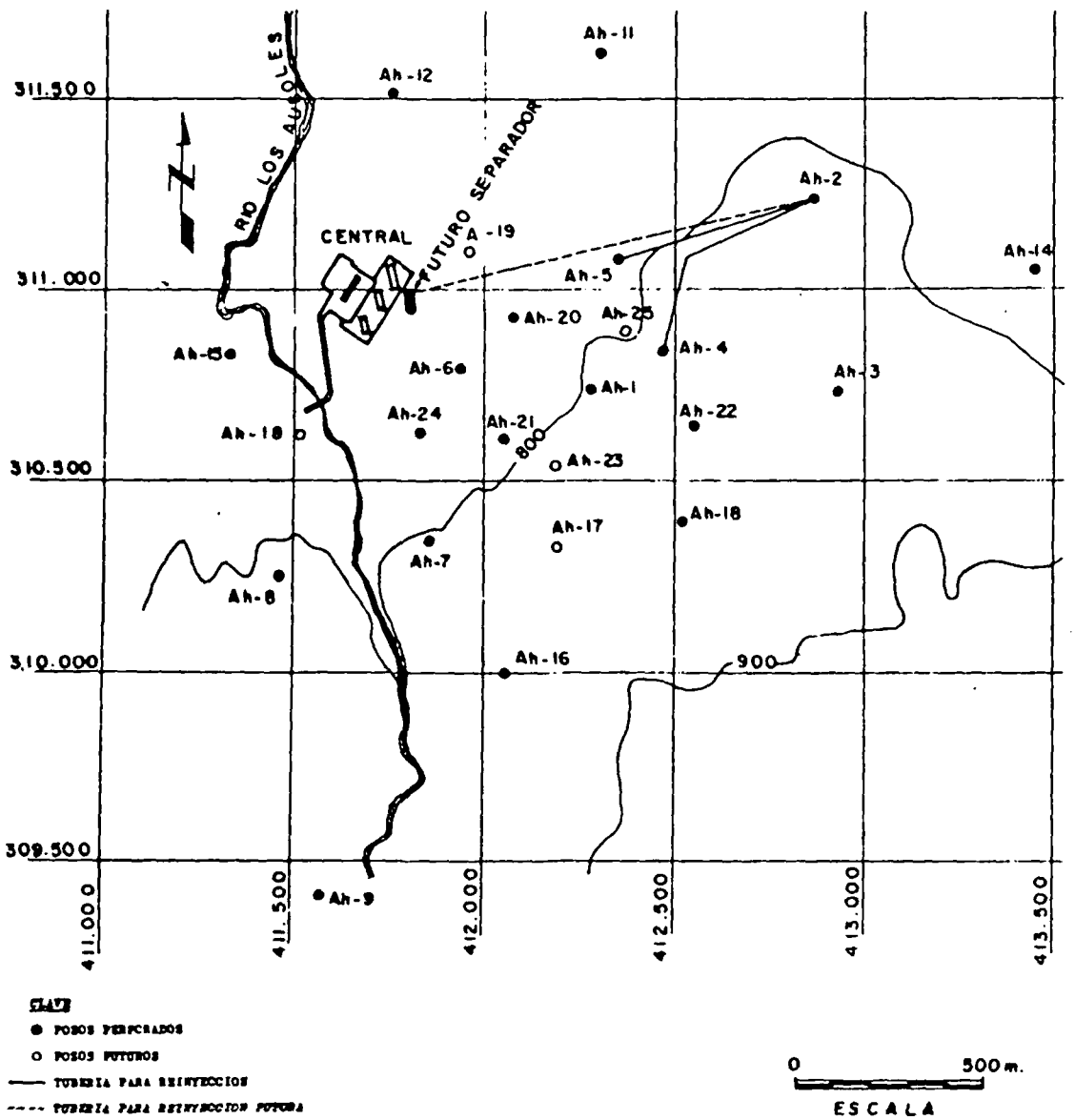

Figura 18. Ubicación de los pozos a ser utilizados en las experiencias de reinyección.

había que inyectar el agua a temperaturas del orden de los 150°C, por motivos de la depositación de sílice y por consiguiente, no se podía pensar en la tercera unidad de baja presión, lo cual significaría una pérdida del 50% de la capacidad.

Según comunicación del Dr. Russell James, sus experiencias le han demostrado que es posible conseguir la *no* depositación de sílice en tuberías, si el agua geotérmica no entra en contacto con el aire, aún a temperaturas tan bajas como 40°C. Estas experiencias serán presentadas posiblemente en otro trabajo de este Simposio.

Otra importante comunicación del Dr. James es que según los científicos del Department of Scientific and Industrial Research of New Zealand (DSIR) el frente químico debido a la reinyección llegaría primero que el frente frío a los pozos en producción. Es decir, que habría primero un cambio en el quimismo de las aguas, antes de que se llegara a detectar un cambio en la temperatura de las mismas.

Los costos de la canaleta al mar, que parecía ser la solución al problema, se han incrementado enormemente y además es un trabajo de ingeniería bastante complicado, lo cual está atrasando todo el proyecto. Por estos motivos se ha dispuesto regresar a hacer una prueba de reinyección en el pozo Ah-2, con las aguas de desperdicio de los pozos Ah-4 y Ah-5 y aplicando las teorías del Dr. James, siempre se podría tener la tercera unidad de 30 MW de baja presión.

En el caso de Ahuachapán, debido al incremento de caudal del Río Paz, durante la estación lluviosa, se podría alternar reinyección con evacuación de las aguas por medio del río, es decir, seis meses de reinyección y seis meses de flujo al Río Paz, que, por su caudal no se vería afectado por el efluente de las aguas geotérmicas.

La experiencia de reinyección será realizada por etapas, de modo que si fuese posible inyectar el agua por gravedad, como se hizo previamente, los beneficios de la experiencia serían mayores, de otra manera, habría que instalar bombas para realizar la reinyección. Las etapas de la experiencia serían las siguientes:

1. Prueba de reinyección por gravedad, las alturas de los pozos en metros sobre el nivel del mar son las siguientes: Ah-2, 808.00; Ah-4, 812.23; y Ah-5, 789.45. En la experiencia anterior las elevaciones fueron: Ah-5, 789.45; Ah-1, 802.79; y Ah-6, 782.97. Ver Figura 18 y Tabla 3.
2. Si esta prueba no diese resultado se utilizarían las dos bombas de turbina impulsadas por vapor, que fueron traídas a El Salvador por UN para la primera experiencia, y las cuales no hubo necesidad de utilizar, y así realizar la reinyección.
3. Al entrar en funcionamiento la tercera unidad de baja presión, se tiene previsto separar las aguas residuales de todos los pozos cerca de la central geotérmica a 1.5 ata, para economizar tuberías de gran diámetro. En este caso se deberán usar las bombas para llevar el agua desde la central hasta el pozo Ah-2 y otro u otros que se destinen a tal efecto.

Tabla 3. Ubicación y elevación de los pozos en Ahuachapán.

Pozo	Latitud	Longitud	Elev.
1	310740.58	412228.10	802.79
2	311228.86	412885.54	808.00
3	310719.15	412925.84	855.50
4	310835.13	412470.45	812.23
5	311081.09	412367.66	789.45
6	310784.22	411926.01	782.97
7	310342.10	411863.14	804.79
8	310251.43	411475.71	810.99
9	309411.93	411578.57	871.33
10	312447.81	412014.72	723.70
11	311619.32	412319.08	759.30
12	311493.50	411768.13	758.80
13	310428.40	412479.68	859.60
14	310934.58	413706.56	821.77
15	310847.34	411260.82	772.68
16	309945.09	412106.16	869.76
17	310360	412200	
18	310625.25	411520.15	
19	311100	411980	
20	310921.64	412087.46	792.00
21	310600.15	412067.04	795.00
22	310632.21	412668.65	842.00
23	310545.45	412194.76	818.50
24	310616.04	411852.48	803.10
25	310887.24	412808.68	
Central	310969.90	411628.79	768.50

CONCLUSIONES

El área Ahuachapán-Chipilapa-El Salitre es una sola como se había supuesto anteriormente, y las aguas que fluyen por los pozos perforados en el área tiene una fuente de calor lejana que debe hallarse ubicada en la cordillera cuaternaria. Esta aseveración está confirmada por los perfiles de resistividad eléctrica aparente y por el quimismo de las aguas y gases el cual indica el origen común de las mismas. Existe en proceso de estudio un muestreo isotópico el cual podría hacer más valedera la afirmación o negarla.

Existe además la duda razonable de una comunicación por medio de la misma falla regional entre el campo Ahuachapán-Chipilapa-El Salitre con el campo geotérmico Los Toles-Guayapa-El Durazneño. Esta duda podría ser eliminada con estudios geoeléctricos a lo largo y a través de la cordillera cuaternaria y además por los estudios isotópicos en proceso.

El programa de reinyección tal como lo he planteado en este trabajo se podría realizar a un costo reducido y en mi opinión sería la solución al problema de las aguas de desperdicio. Este programa lo expuse previamente a la CEL y creo que a estas horas estarán ya haciendo los preparativos necesarios para realizarlo.

moderately useful

Recent Developments of Geothermal Exploration in the Travale-Radicondoli Area

PIERDOMENICO BURGASSI
GIAN CARLO STEFANI
ENEL-Compartimento di Firenze, 54 Lungarno Colombo, Florence, Italy
RAFFAELE CATALDI
ENEL-Centro di Ricerca Geotermica, 14 Piazza Bartolo da Sassoferrato, Pisa, Italy
ARISTIDE ROSSI
PAOLO SQUARCI
LEARCO TAFFI
CNR-Istituto Internazionale per le Ricerche Geotermiche, 55 Lungarno Pacinotti, Pisa, Italy

ABSTRACT

Based on a reinterpretation of the previously acquired data relative to the old Travale field, a program was set up in 1969 for extending geothermal exploration to the surrounding area. This program consists of a series of geological and geophysical surveys and a number of deep wells.

In 1971, the Travale 22 well was drilled 2 km northeast of the previously drilled area, providing a production of 314 t/h of steam, with a delivery pressure of 8.07 ata, a temperature of 185°C, and a gas-steam ratio in gas percentage of 9 by weight. The shut-in pressure was 60 ata. Since July 1973 this well has been supplying a 15-MW exhausting-to-atmosphere power plant (specific consumption 12 kg/kWh).

Subsequently, the R1, R2, and R4 wells were drilled in an area within 1 km from Travale 22. Below the cap rock, R1 and R2 encountered temperatures of 250 to 270°C in very low permeability rocks. R4 has produced 108 t/h of gas-steam mixture, with a delivery pressure of 3.02 ata, a temperature of 151°C and a gas-steam ratio in gas percentage of 64 by weight. The shut-in pressure was 62 ata.

A step-fault structure with a total throw of about 700 m separates Travale 22 and R4 reservoirs, thereby justifying the considerable differences in the characteristics of the fluids produced by these two wells.

INTRODUCTION

The area of Travale-Radicondoli is one of the areas where geothermal exploration has been most concentrated over the past five years. This area is located 10 to 15 km east-southeast of Larderello, in the southwestern part of Tuscany (Fig. 1). As regards this area, the National Electric Energy Agency (ENEL) and the National Research Council (CNR), through its International Institute for Geothermal Research, set up a joint research group, aimed at studying the behavior of the wells in the old Travale field and at establishing how and to what extent geothermal exploration may be developed in the surrounding region.

The geological and geophysical situation of the old Travale field, as well as production and hydrogeological dynamics of the wells until 1969, were summarized and discussed by Cataldi et al. (1970).

After 1969, based on the general revision of all data collected until that date for the old production area, a research program was set up to cover, by means of up-to-date geological and geophysical prospecting, a larger area than the one previously investigated. This research program, carried out mainly during the 1969 to 1970 period, led to the discovery of a new area located several kilometers northeast of the old field.

The first exploratory well drilled in this area (T22) produced 314 t/h of steam, with a delivery pressure of 8.07 ata, a wellhead temperature of 185°C and a gas-steam ratio of 9% by weight. The shut-in pressure was 60 ata. Since July 1973 this well has been feeding a 15-MW exhausting-to-atmosphere power plant, with a specific fluid consumption of 12 kg/kWh. The well has been kept producing at a constant flow rate of 180 t/h; its delivery pressure was 42 ata in July 1973 and diminished to 25 ata in March 1975 with a rapid drop in the initial production phase.

During the past three years, the exploration of the new Travale-Radicondoli area has continued with the drilling of five other wells (R1, R2, R3, R4, and C1). R3 was not completed for technical reasons and C1, which replaces R3, is in progress. Though the R1 and R2 wells encountered temperatures of 250 to 270°C in very low permeability formations below the cap rock, they proved to be nonproductive. R1, however, initially delivered a modest amount of fluid. The fluid produced by R4 (108 t/h, with a delivery pressure of 3.02 ata, a wellhead temperature of 151°C, a gas-steam ratio of 64% by weight, and a shut-in pressure

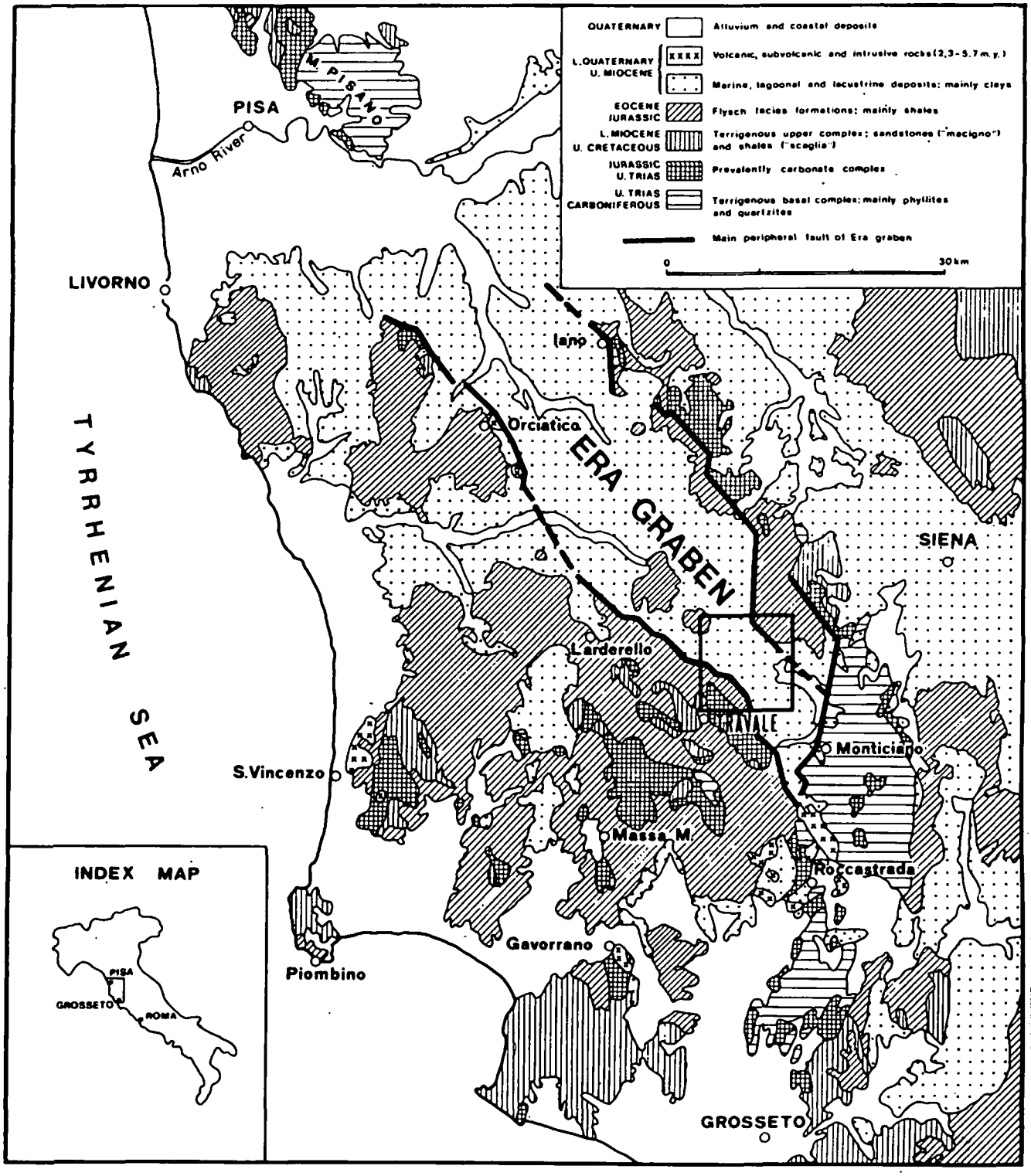

Figure 1. Map showing location of the Travale-Radicondoli geothermal area and general geology of southwestern Tuscany.

of 62 ata) indicates that this well is fed by a geological layer which, through a step fault having a total throw of about 700 m, is separated from the layer feeding T22.

While exploration is continuing, this paper provides up-to-date information on the geology, geophysics, and drilling carried out in the Travale-Radicondoli area during the past five years.

GEOLOGICAL OUTLINE

The area of Travale-Radicondoli is part of a geological region (southern Tuscany, Fig. 1) where, even in the past, numerous geological studies were conducted. More recently, detailed geological surveys were performed in areas where geothermal fields have been exploited for a long time, such as Larderello (Mazzanti, 1966; Lazzarotto, 1967), or where

exploitation is starting, such as Travale-Radicondoli (Lazzarotto and Mazzanti, 1974).

Stratigraphy

From the top down, the stratigraphic sequence can be schematized as follows (Figs. 1 and 2):

1. Recent alluvial, coastal deposits, and travertines.
2. Magmatic rocks, having an age between 2.3 and 5.7 m.y. They include intrusive rocks (granites of S. Vincenzo and Gavorrano), subvolcanic rocks (selagites of Orciatico), and effusive rocks (rhyodacites of S. Vincenzo and rhyolites of Roccastrada).

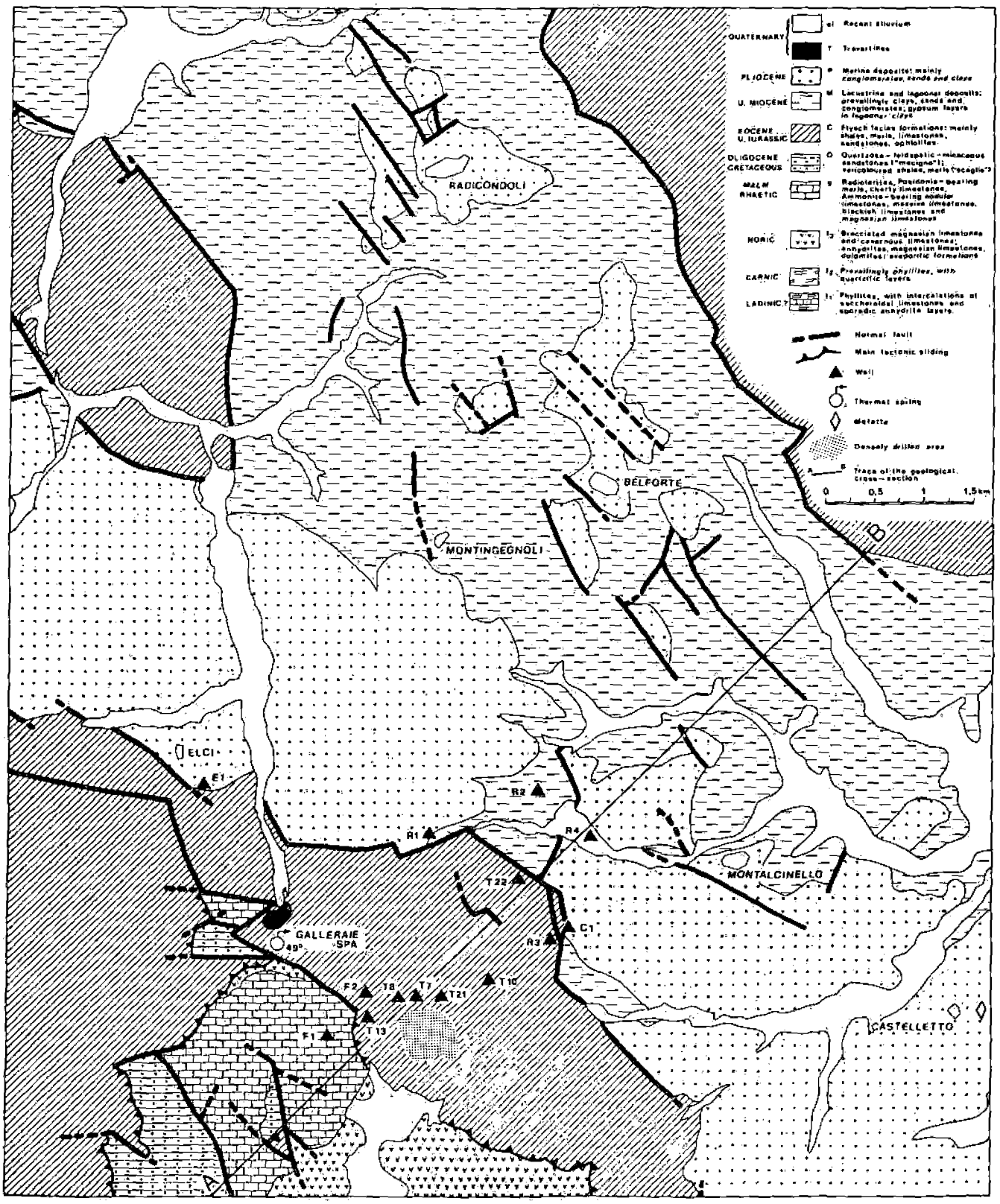

Figure 2. Geological map of the Travale-Radicondoli geothermal area (partly drawn from Lazzarotto and Mazzanti, 1974).

3. Marine, lagoonal, and lacustrine deposits of Quaternary, Pliocene, and Miocene age. Transgressive clays, sands, conglomerates, and organogenic limestones, overlie the oldest complexes. They represent the filling of the sedimentation basins (graben), initially lacustrine, then lagoonal, and finally marine, which formed starting during the late Miocene and continued until the Pliocene. In the post-Pliocene period, the region underwent intense upheaval movements, except at the Tyrrhenian coast belt, where marine sedimentation continued until the Calabrian.
4. Flysch-facies formations (Eocene to Upper Jurassic), predominantly made up of shales, marls, sandstones, and ophiolites. These formations tectonically rest on any of the following complexes.
5. Upper terrigenous complex (lower Miocene to Upper Cretaceous), including, in the upper part, a predominantly arenaceous formation ("macigno") and, in the lower part, variegated shales ("scaglia").
6. Carbonate complex (Jurassic to Upper Triassic), including radiolarites, Posidonia-bearing marls, cherty limestones, ammonite-bearing nodular limestones, massive limestones, black stratified limestones, cavernous limestones and breccias, alternations of anhydrites and magnesian limestones (evaporitic formations).
7. Basal terrigenous complex (regional basement of the Upper Triassic to Palaeozoic), consisting mainly of phyllites, quartzites, sandstones, and quartzose conglomerates. It prevalently outcrops in the M. Pisano-Jano-Monticiano-Roccastrada ridge (Fig. 1) and is known in the area only through drilling (Fig. 3). It has an upper transgressive part (Upper Triassic) and a lower part (Carboniferous and pre-Carboniferous) which was involved in the Hercynian orogeny.

Tectonics

The structures of the Tuscan region are ascribable to a tectogenetic compressive phase followed by a distensive one (Giannini, Lazzarotto, and Signorini, 1971). The former developed mainly from the upper Oligocene to the upper Miocene and caused the partial overthrusting, beyond the Jano-Monticiano-Roccastrada ridge, of the upper terrigenous and carbonate complexes, as well as the arrival of flysch-facies formations from the Tyrrhenian area.

The distensive phase is characterized by direct faulting and horst-graben combinations which involve all previous structures. This phase may be related to the spreading which occurred in correspondence to the Tyrrhenian Sea, which is interpreted as a basin tardily formed behind the compressive margin of the Apennines (Elter et al., 1975).

This distensive phase started in the late Miocene with the formation of subsident sedimentation basins, initially lacustrine, then lagoonal, and finally marine, where subsidence continued throughout the Pliocene. At the end of this period, the upheaval in the region began and attained its maximum in the area of Larderello-Travale.

Additionally, starting from the late Miocene, a prevalently acid magmatism developed in the region, which originated the intrusive, subvolcanic, and volcanic manifestations previously described (Barberi, Innocenti, and Ricci, 1971).

The Travale-Radicondoli area is located in correspondence to the southernmost part of the Era graben, some 20 km north of the Roccastrada volcanic outcrop.

Hydrogeological Complexes

In the Travale-Radicondoli area, the various outcropping or buried terrains can be grouped as follows, according to their permeability and geometric position:

1. Upper complex, including Pliocene and Miocene marine, lagoonal, and lacustrine deposits, flysch-facies formations, and, locally, the "macigno" and "scaglia" formations. It is impermeable on the whole and represents the cap-rock of the geothermal reservoir.
2. Lower complex, including Mesozoic carbonate formations, and, locally, the terrains of the regional basement (phyllites, quartzites, and intercalations of saccharoidal limestones and anhydrites). This complex, permeable by fracturation, represents the potential reservoir of geothermal fluids. However, where this complex outcrops, it constitutes an absorption area, controlling hydrostatic pressure in the confined aquifer.

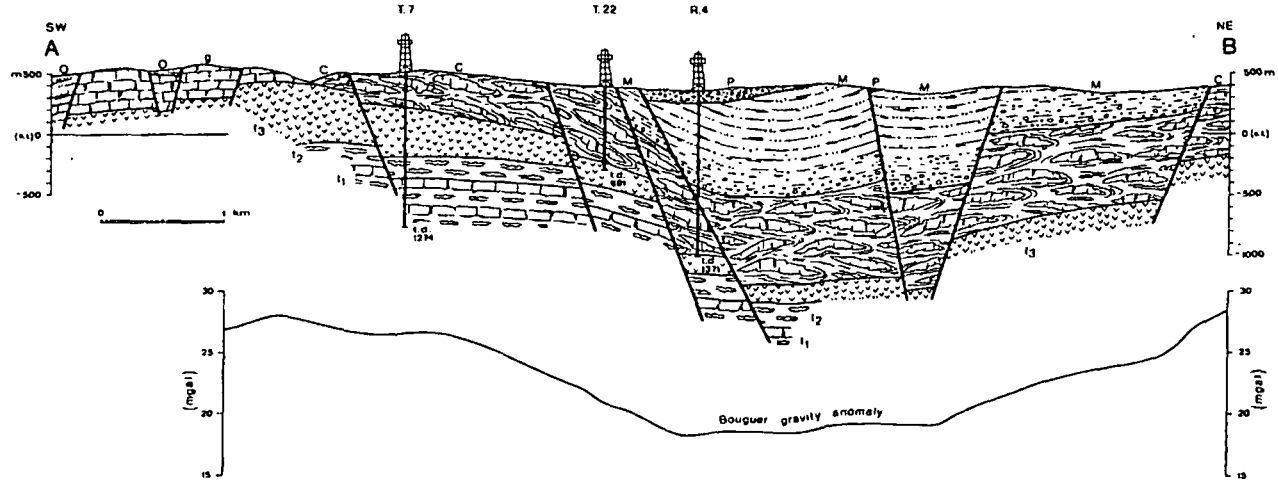

Figure 3. Geological and gravimetrical cross section of the Travale-Radicondoli geothermal area (for explanation of symbols see Figure 2).

GEOPHYSICAL SURVEYS

Geophysical prospecting has been carried out in the Travale-Radicondoli area since 1969, and the main results achieved can be summarized as follows.

Gravity Prospecting

The regional gravity survey of the whole area of Larderello, conducted in 1963, also marginally covered the geothermal area of Travale with a density of about 1.5 measuring points per square kilometer. The extension of geothermal research northeast of the old field, started in 1969, required more detailed gravity prospecting, capable of providing sufficiently detailed information as to the local structural situation. A new gravity survey was thus performed only for the area northeast of the old field of Travale, over a surface of about 70 km^2, with 210 measuring stations.

The Bouguer anomaly map (worked out with a constant density of 2.25) exhibits a significant negative anomaly corresponding to the graben located northeast of the old Travale field (Fig. 4). This graben appears as the dominating feature of the whole area, has a northwest-southeast trend,

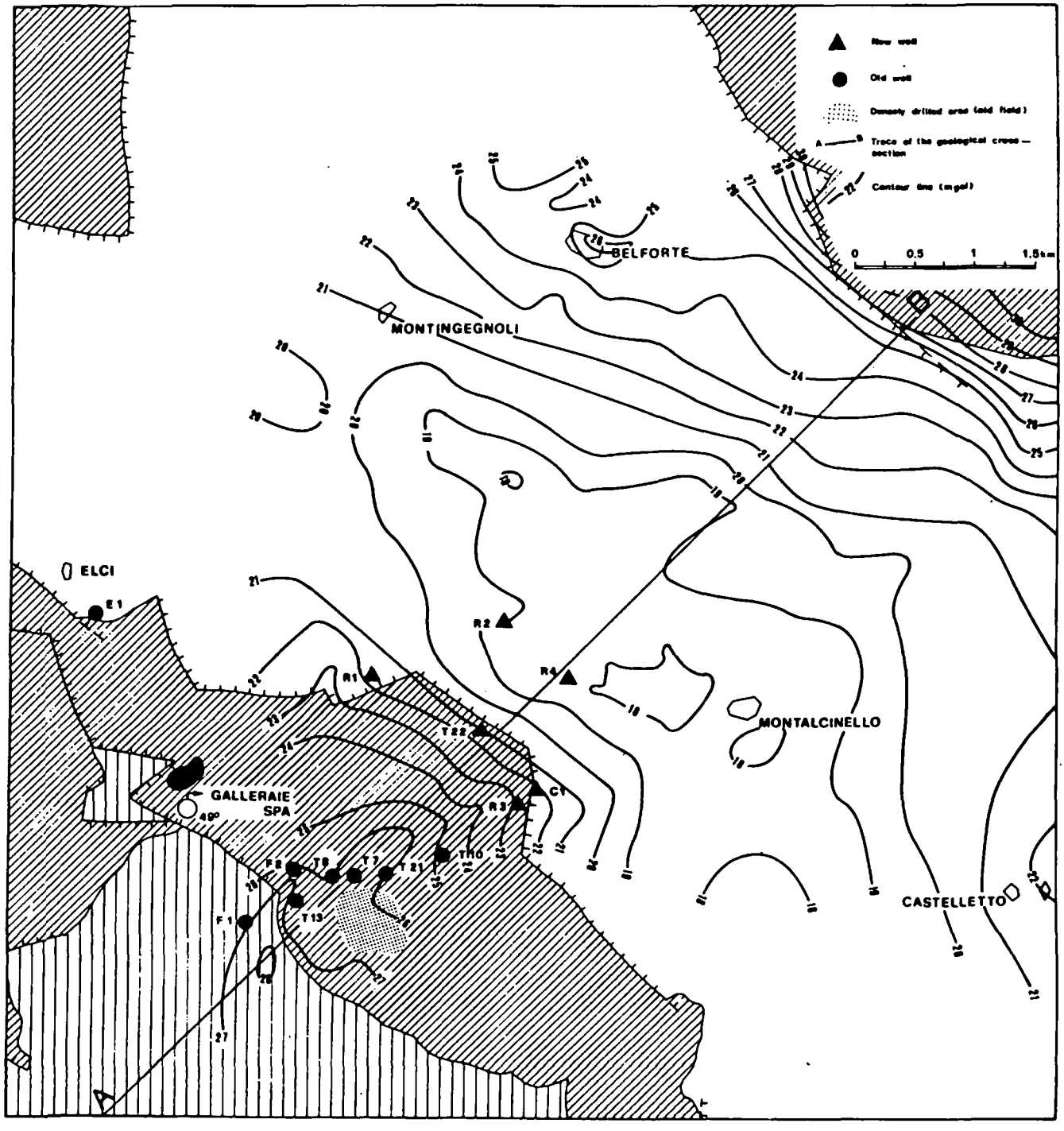

Figure 4. Map showing Bouguer anomaly and sketch of geological structure of the Travale-Radicondoli geothermal area (for explanation of other symbols, see Figure 5).

is delimited by faults with a considerable throw and is indented by transversal faults.

Inside the graben, small positive features of gravity appear, which can be referred to the presence of superficial or shallow masses (essentially conglomerates), having a density higher than that used for preparing the Bouguer map.

Finally, the maps of regional and residual anomalies (not presented here) allow us to recognize a subcircular feature at the southwestern margin of the area involved, in correspondence to Castelletoto, where some gas manifestations exist (CO_2 prevalently and H_2S).

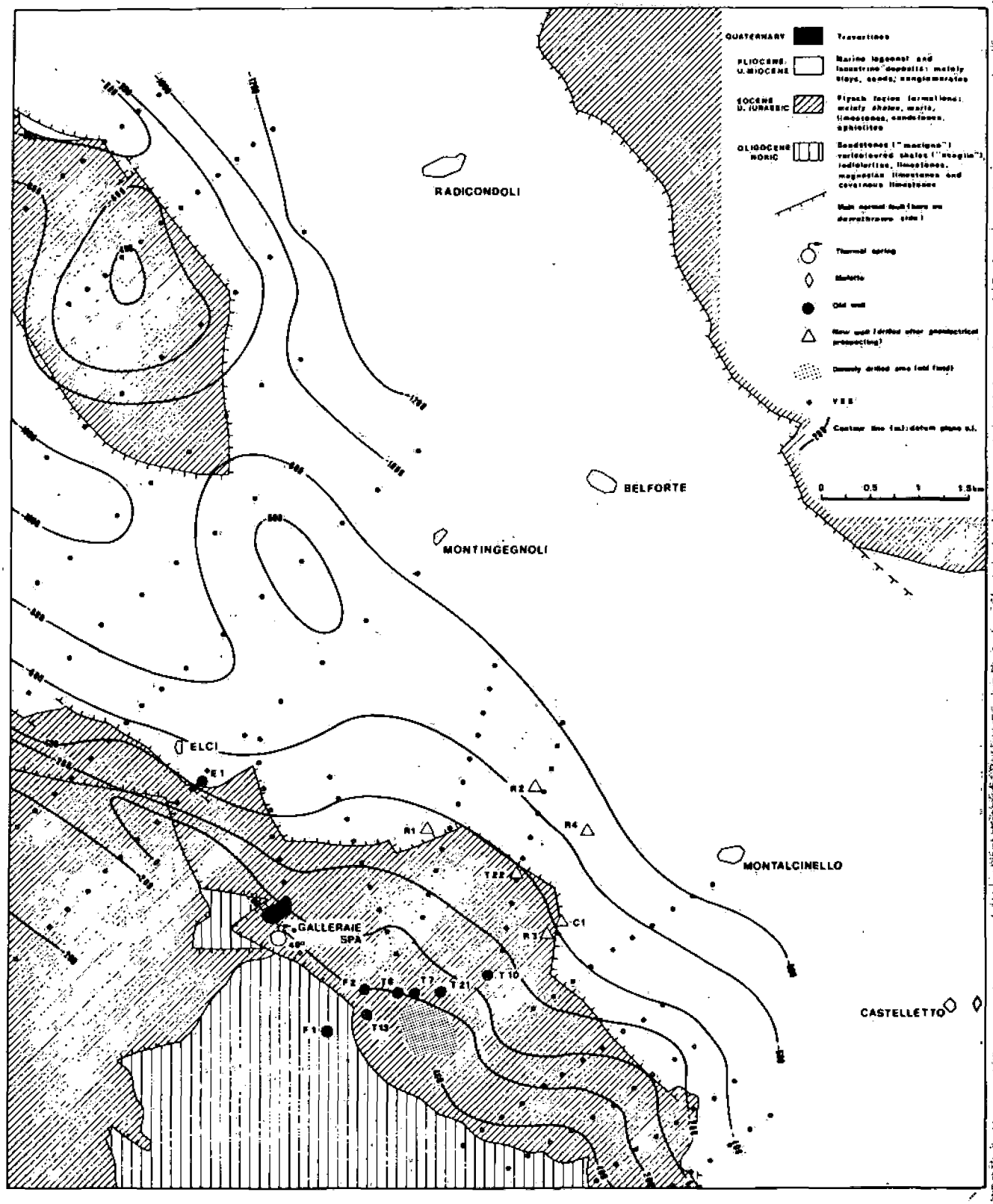

Figure 5. Map showing resistive substratum and sketch of geological structure of the Travale-Radicondoli geothermal area.

Geoelectrical Prospecting

The area was geoelectrically prospected (quadripole Schlumberger configuration) in order to establish the attitude of the top of the geological formations making up the potential geothermal reservoir.

The geoelectrical method was applied because of the limited depth of the potential reservoir (especially near the uplifted step of the graben) and of the lithologic nature of the formations in the area. Indeed, lithologic differences between cap rock and potential reservoir entail strong resistivity contrasts (most frequent values: 5 to 40 ohm·m in the cap rock, and more than 100 ohm·m in the underlying rocks).

The results of geoelectrical prospecting, which includes 170 vertical electric soundings (VES) scattered on profiles with an *AB* of 2000 to 8000 m, are shown in Figure 5. This shows an attitude of the resistant substratum in substantial agreement with the structural frame obtained by surface geology and gravity prospecting.

The depth of the resistive substratum (which generally corresponds to the reservoir formations) was given with good approximation by the geoelectrical survey, especially at the uplifted margin of the graben. Nevertheless, the resistant substratum does not always correspond to the top of the reservoir rocks, owing to the presence of resistive layers in the basal part of the cap rock.

At the margin of the graben, the presence of step faults with a considerable throw determines lateral effects which geoelectrically result in an attenuation of the differences relative to dislocation of the various blocks. Toward the central part of the graben, finally, depth does not allow us to obtain, with the geoelectrical method, correct quantitative indications about the thickness of the conductive cover.

Thermal Gradient and Heat Flow

Surveys for determining geothermal gradient and heat flow in the Travale-Radicondoli area concerned a surface of about 70 km², where 27 measurement holes were drilled. The depth of such holes varies from about 25 to 200 m, with a general average around 75 m.

In most cases, terrains where platinum resistance thermoprobes were located (and from which cores were extracted for laboratory measurements of thermal conductivity with the Maxell-Von Herzen needle probe), include Neogenic

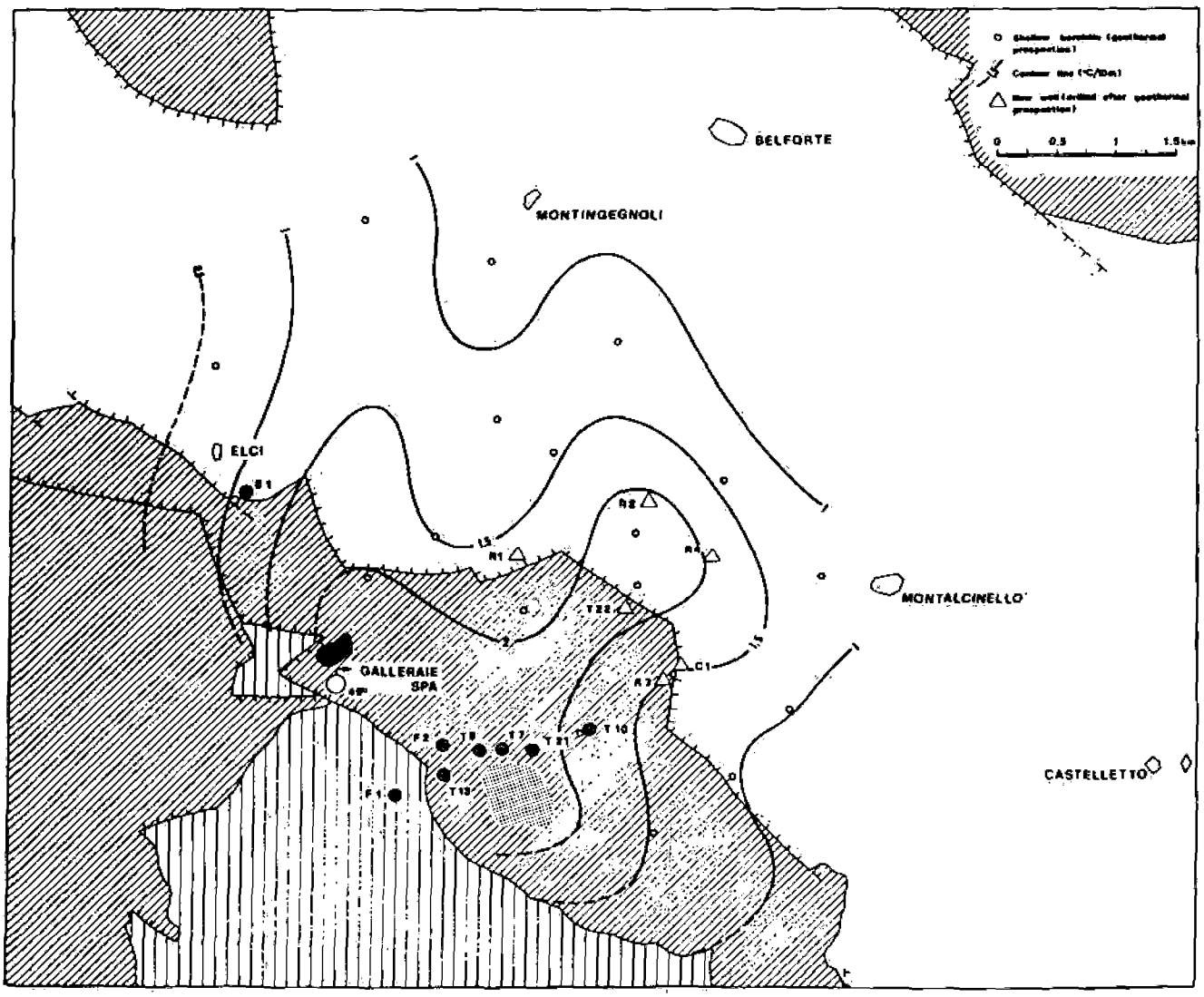

Figure 6. Map showing thermal gradient and sketch of geological structure of the Travale-Radicondoli geothermal area (for explanation of other symbols, see Figure 5).

clays and shales of flysch-facies formations. In a few cases, the terrains involved were of the sandy-clayey or marly type. Anyway, measures were always taken in impervious terrains and observations were prolonged for a period sufficient to attain thermal equilibrium in the hole. The results obtained are partly shown in Figures 6 and 7 for geothermal gradient and heat flow, respectively.

First of all, an optimum correspondence is noted in the attitude of isogradient and isoflow curves. This is in accord with the fact that the thermal conductivity measured, though ranging between the extremes of 3 and 5 $\times$ 10^{-3} cal/°C·cm·sec approximately, has over 80% of the values comprised in the interval 3.3 to 4.2 $\times$ 10^{-3} cal/°C·cm·sec.

The comparative examination of these two figures evidences an area of regional thermal anomaly, which covers a surface of roughly 20 km^2. Inside it, a local anomaly stands out, which is delimited by the 1.5°C/10 m isogradient and 5 μcal/cm^2·sec isoflow curves. Even if this local anomaly is not well-defined in the southwestern part (where permeable formations outcrop), it encloses both the old field of Travale, with the nearby thermal springs of Galleraie, and the new exploration area around the T22 well, over a total surface not exceeding 7 to 8 km^2.

Additionally, outside the local anomaly area, the flow map exhibits a rapid drop of values, while inside the 5-μcal/cm^2·sec and 1.5-°C/10-m curves for flow and gradient, respectively, the local anomaly appears separated in two main branches. The first branch has a north-south trend, and the second one, a northeast-southwest trend. The second branch shows, for both gradient and, especially, flow, a substantial thermal continuity between the new exploration area and the old field.

We should recall that deep wells drilled in the new area (T22, R1, R2, R3, R4, and C1) substantially confirmed the values of temperature at the bottom of the cap rock foreseen on the basis of the geothermal gradient map.

Magnetotelluric Prospecting

With a view to locating high-permeability areas of the potential reservoir, the magnetotelluric method with five components and exponential solutions (Musé, 1973) was used in experiments. Field work was performed in 1973 with 84 measuring stations over about 50 km^2 (Fig. 8). The results of the prospecting are reported by Celati et al. (1973). As these authors emphasized, the significant elements

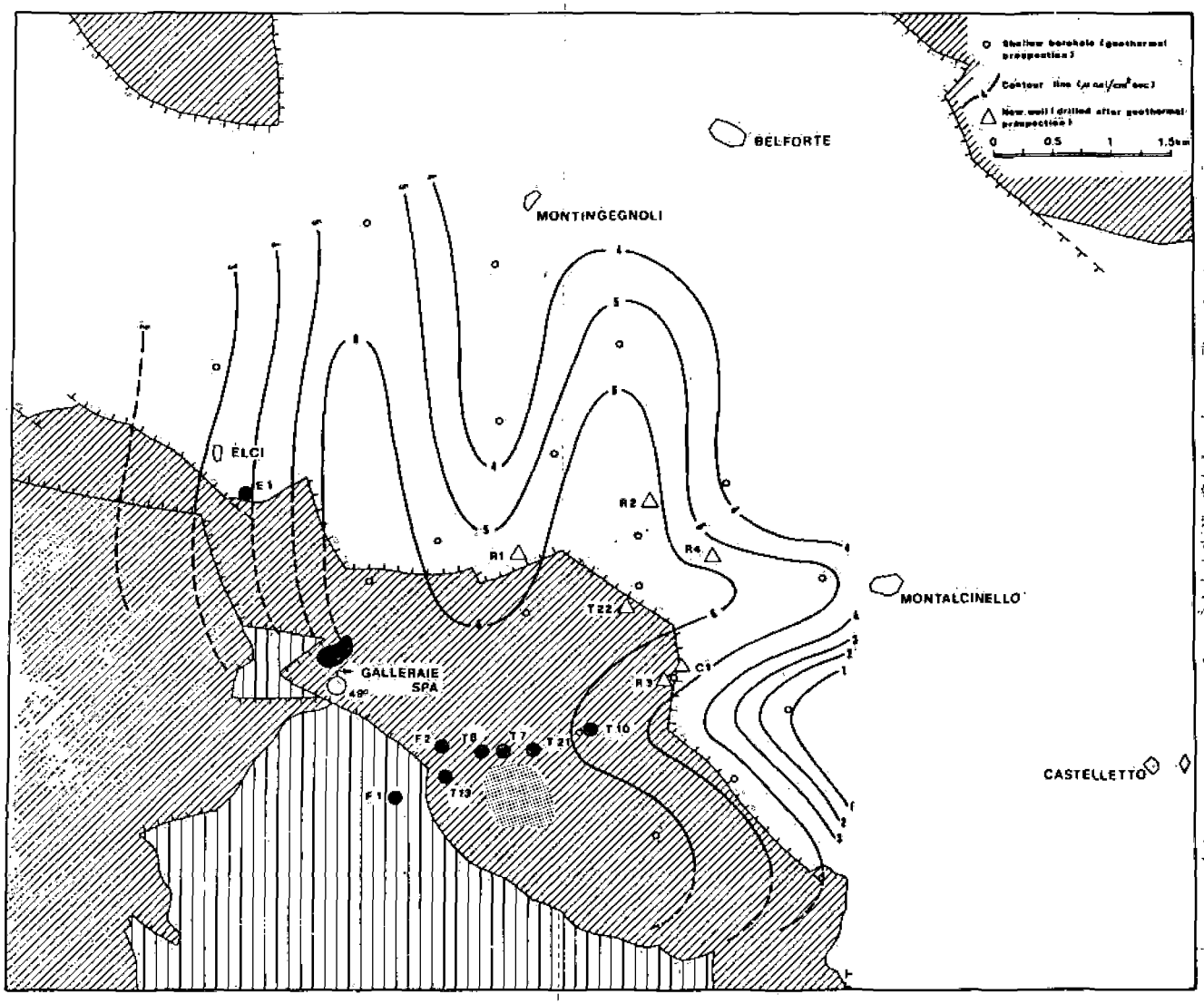

Figure 7. Map showing heat-flow values and sketch of geological structure of the Travale-Radicondoli geothermal area (for explanation of other symbols, see Figure 5).

derived from this survey are the following. First of all, the conductance anomalies have a prevalent northeast-southwest trend, contrasting with the main northwest-southeast trend evidenced by the elongation of the carbonate outcrop and of the graben. Secondly, the significant contrast in the values of longitudinal conductance measured at the different stations, often very close to one another, results in narrow and elongated conductive areas separating resistant areas. Thirdly, it should be emphasized that at some measuring points electric conductance is extremely high.

The paper by Celati et al. (1973) attempts a first interpretation of prospecting results in the light of the data acquired from drilling (old field, T22, R1). Subsequently, three other wells were drilled (R2, R3, R4) and a fourth well is being drilled (C1). The R2 well, situated on a conductance low, encountered rocks of very low permeability in the potential reservoir. The R4 well located instead on a conductance high, encountered highly permeable fractured rocks in the reservoir. This would seem to confirm the hypothesis that resistant areas correspond, in first approximation, to low-

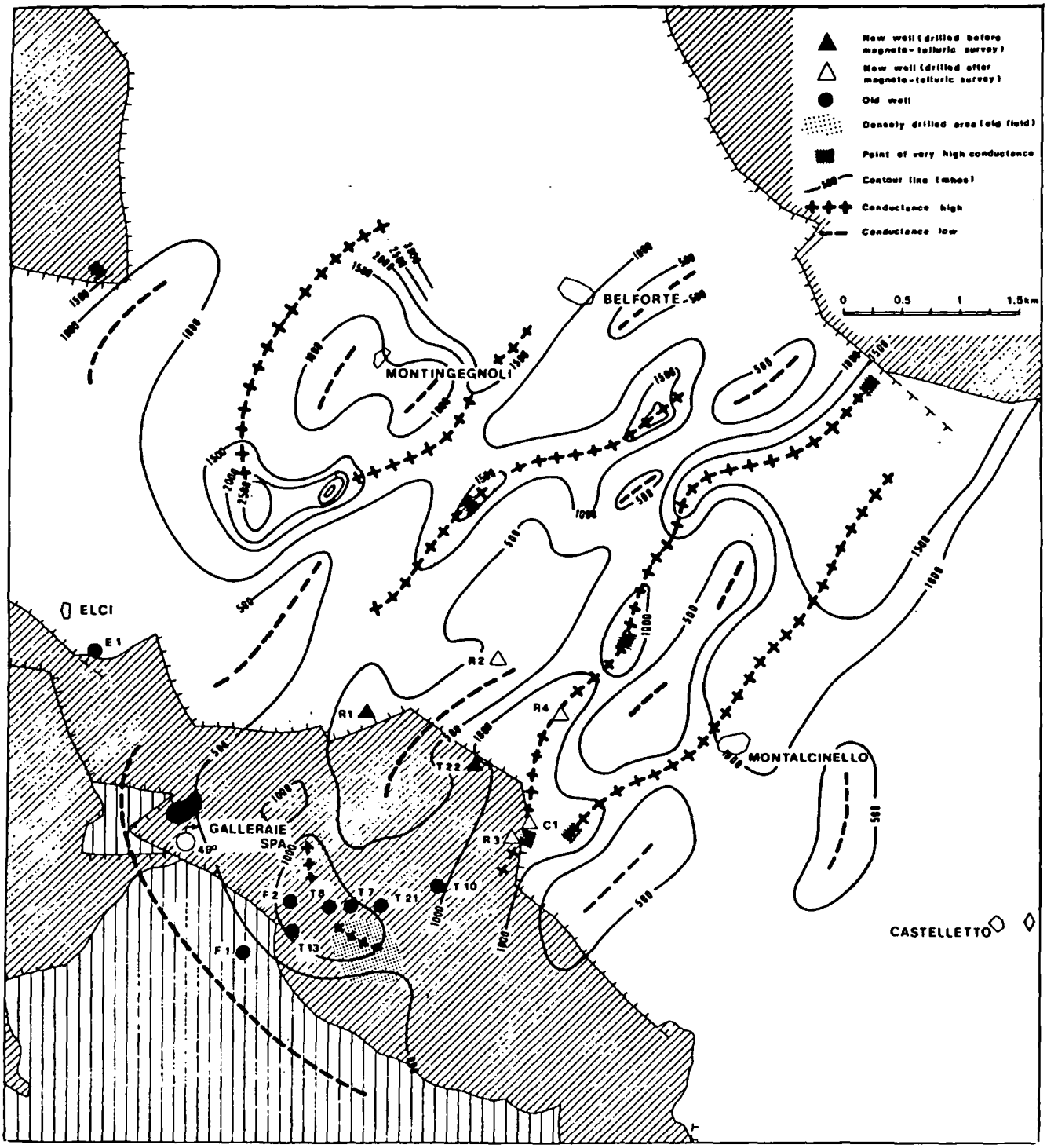

Figure 8. Map showing longitudinal conductance and sketch of geological structure of the Travale-Radicondoli geothermal area (for explanation of other symbols, see Figure 5).

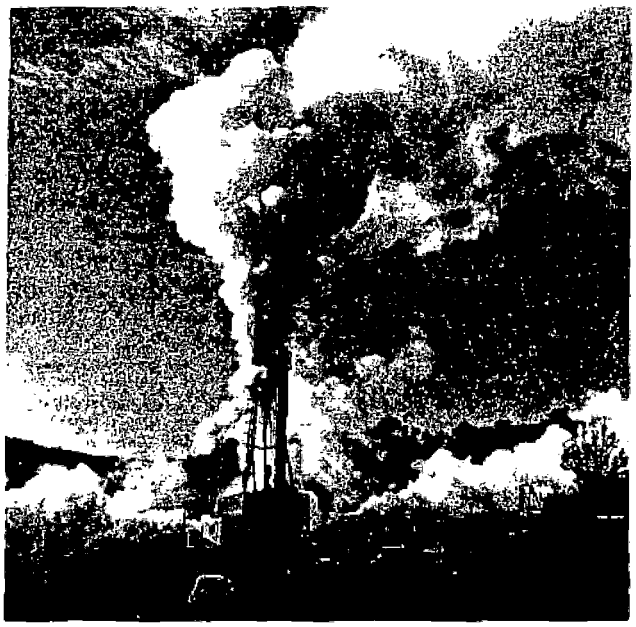

Figure 9. Travale 22 after blowout.

Table 2. Production characteristics of wells T22 and R4.

Characteristic	T22	R4
Three months after completion		
Date of completion	1/1972	8/1974
Total flow rate (t/h)	314	108
Delivery pressure (ata)	8.07	3.02
Temperature (°C)	185	151
Gas/steam (weight %)	9	64
Shut-in pressure (ata)	60	62
March 1975		
Total flow rate (t/h)	176	91
Delivery pressure (ata)	25	5.90
Temperature (°C)	239	166
Gas/steam (weight %)	10.3	66
Shut-in pressure (ata)	on stream	open for measurement

permeability rocks, and conductive areas to highly permeable rocks.

The R3 and C1 wells, drilled in correspondence to one of the points where conductance proved to be extremely high (see grid areas in Figure 8), failed to clarify the physical meaning of such points. The well C1, indeed, even though it is not yet completed, has found high permeability layers at the top of the potential reservoir.

One of the next targets is to establish whether conductance values obtained with magnetotelluric prospecting are controlled by relatively shallow rocks (1000 to 2000 m) or by deeper rocks, not explored by drilling. This information is expected from a study under way which resorts to bidimensional models.

SUMMARY OF DRILLING AND CONCLUSIONS

The main technical details and production characteristics of the new wells drilled from 1971 to 1975 in the Travale-Radicondoli area are reported in Tables 1 and 2, respectively.

As shown in Table 1, exploration started with the drilling of well T22, located in correspondence to the area with the highest geothermal gradient and heat flow, at the uplifted margin of the graben. The extremely favorable result of this well led to concentrating exploration in the surrounding area to speed up its development for production of electric power.

Only two out of the five wells completed found high-permeability layers at the reservoir top and proved to be

Table 1. Technical details of new wells. N = Neogenic deposits; F = flysch-facies formations; M = sandstones ("macigno") and shales ("scaglia"); E = evaporitic formation: anhydrites, and so forth; B = phyllites, quartzites, and so forth.

Well	Elevation a.s.l. (m)	Terrains crossed initial and final depth (m)	Production casing depth (m)	Production casing diameter (in.)	Circulation loss depth (m)	Circulation loss quantity (m^3/h)	Max. temp. in reservoir (°C)	Result
T 22	380	0–640 (F) 640–691 (E)	636	13-3/8	642	≥50	264*	productive
R 1	418	0–15 (N) 15–890 (F) 890–1130 (M) 1130–1280 (E) 1280–1500 (B)	1147	9-5/8	—	—	252	†
R 2	370	0–430 (N) 430–1430 (F) 1430–1460 (M) 1460–1550 (E) 1550–1841 (B)	1480	9-5/8	1500	2	269	nonproductive
R 3	420	0–720 (F) 720–1018 (E)	719	13-3/8	799	3	220‡	§
R 4	340	0–820 (N) 820–1365 (F) 1365–1371 (E(	1350	9-5/8	1365	>40	197‖	productive
C 1	425	0–20 (N) 20–693 (F) 693–1305 (E) 1305–1830 (B)	698	13-3/8	702	>50	>230	#

*Shut-in temperature value with 56.6 ata. †This well initially produced intermittently a gas-steam mixture along with debris; ‡Nonstabilized value. Extrapolated value is about 250°C; §Technical difficulties prevented completion of this well; ‖Shut-in temperature with 59 ata; #In progress: 1830 m on April, 30, 1975.

productive (T22 and R4). The sixth well (C1) is being drilled. The three other wells, though penetrating the reservoir for some hundreds of meters, encountered instead rocks of very low-permeability. These wells, however, always found very high temperatures. Indeed, except for well R4 (whose fluid has a very high CO_2 content), the other wells showed, below the cap-rock, temperatures up to 270°C.

The different compositions of the fluid from two wells quite close to each other (T22 and R4) should certainly be related to the presence of a step-faulted feature, which results in the hydrogeologic discontinuity between the uplifted and downlifted blocks of the potential reservoir (Fig. 3).

In addition to the influence of the structure, an attenuation of the thermal anomaly in the central part of the graben is also likely to determine the different physico-chemical characteristics of the fluid in the reservoir. If so, prospects of evolution of the fluid delivered by well R4 are limited.

If, on the contrary, the thermal anomaly is not attenuated in this direction, gas accumulation around well R4 is to be attributed only to the structural feature which prevented gas drainage by natural manifestations and by the wells in the old field. In this case, the continuing production of well R4 would cause, with gas drainage, a progressive steam enrichment of the mixture, together with a temperature rise. The fluid produced by well R4 may even tend to acquire characteristics similar to those of T22.

Independent of the production possibilities on the steps of and within the graben and regardless of the evolution possibilities of such wells as R4, the fact remains that, over an area not greater than 1 km^2, all wells evidenced significantly high temperature, but generally low permeability.

The explored area of Travale-Radicondoli presents, therefore, conditions suitable for stimulation experiments. These can attempt to enlarge or to artificially create fractures, which would allow either drainage of existing fluid or recovery of heat through an artificial water loop.

REFERENCES CITED

Barberi, F., Innocenti, F., and Ricci, C. A., 1971, La Toscana meridionale, il magmatismo: Soc. Italiana Mineralogia i Petrografia Rend., v. 27, fasc. spec., p. 169.

Cataldi, R., Rossi, A., Squarci, P., Stefani, G., and Taffi, L., 1970, Contribution to the knowledge of the Larderello geothermal region: Remarks on the Travale Field: UN Symposium on the Development and Utilization of Geothermal Resources, Pisa, Proceedings (Geothermics, Spec. Iss. 2), v. 2, pt. 1, p. 587.

Celati, R., Musé, L., Rossi, A., Squarci, P., Taffi, L., and Toro, B., 1973, Geothermal prospecting with magneto-telluric method (M.T.-5-E.X.) in the Travale area (Tuscany, Italy): Geothermics, v. 2, nos. 3-4.

Elter, P., Giglia, G., Tongiorgi, M., and Trevisan, L., 1975, Tensional and compressional areas in the recent (Tortonian to present) evolution of the northern Apennines: Boll. Geofisica Teor. ed Appl.

Giannini, E., Lazzarotto, A., and Signorini, R., 1971, La Toscana meridionale, lineamenti di stratigrafia e tettonica: Soc. Italiana Mineralogia i Petrografia Rend., v. 27, fasc. spec., p. 33.

Lazzarotto, A., 1967, Geologia della zona compresa fra l'alta Valle del Fiume Cornia ed il Torrente Pavone (Prov. di Pisa e Grosseto): Soc. Geol. Italiana Mem. v. 6, fasc. 2, p. 151.

Lazzarotto, A., and Mazzanti, R., 1974, Carta geologica dell'Alta Val di Cecina (Prov. di Pisa-Siena-Grosseto): Litografia Artistica Cartografica, via del Romito, 11-13r, Firenze.

Mazzanti, R., 1966, Geologia della zona di Pomarance-Larderello (Prov. di Pisa): Soc. Geol. Italiana Mem., v. 5, fasc. 2, p. 105.

Musé, L., 1973, A five-component magneto-telluric method in geothermal exploration, the M.T.-5-E.X.: Geothermics, v. 2, no. 2, p. 41.

good, orig
General GP

The Mesa Geothermal Anomaly, Imperial Valley, California: A Comparison and Evaluation of Results Obtained from Surface Geophysics and Deep Drilling

CHANDLER A. SWANBERG

New Mexico State University, Box 3D, Las Cruces, New Mexico 88003, USA

ABSTRACT

To date, a range of geophysical and geochemical surveys and five deep geothermal wells have been completed at the Mesa anomaly. The geophysical surveys all outline the same general area as having abnormally high subsurface temperatures, making the Mesa anomaly an ideal area for comparison and evaluation of geothermal exploration techniques. The origin of the anomaly is an active fault which acts as a conduit for ascending geothermal fluids. Dipmeter logs from the geothermal wells indicate that this fault has been active during the deposition of the most recent 2 km of sediments. The geothermal wells were sited so as to obtain stratigraphic and thermal data from various parts of the anomaly, both for comparison with surface geophysical data, and to determine the ultimate size, shape, and production potential of the geothermal reservoir. The geothermal reservoir is confined beneath a clay cap, roughly 600 m thick and consisting of about 60% clay. This clay cap is an effective seal as there are no surface manifestations of geothermal activity at the Mesa anomaly, and waters collected from shallow wells (<400 m) located within and away from the high heat-flow area yield similar Na-K-Ca estimated temperatures. The stratigraphic interval 600 to 750 m is a transition zone between the clay cap and the geothermal reservoir. Over this interval the clay content drops to about 25% and the geothermal gradient drops from over 150°C/km to less than 40°C/km. The reservoir itself is at least 1400 m thick and has a surface manifestation ($q > 5$ hfu) of 40 km^2 and a base temperature of 200°C. The sediments within the reservoir are essentially flat-lying, loosely consolidated continental deposits. The sands (75%) have a mean porosity of 20% and a modal permeability of 100 md. The geothermal fluids are of a sodium chloride type with a total dissolved solids content of 2500 mg/liter or less.

INTRODUCTION

The Mesa anomaly is one of several promising geothermal prospects located in the Imperial Valley, California. A considerable amount of research has been conducted on the Mesa anomaly including the drilling and testing of five geothermal wells and a wide range of geophysical, hydrologic, geochemical, and geologic studies (Combs and Muffler, 1973; Dutcher, Hardt, and Moyle, 1972; Rex et al., 1971; Rex et al., 1972; USBR, 1971; 1973a; 1973b; 1974; 1975; Swanberg, 1974a; 1974b; Coplen, 1974). The purpose of the present manuscript is to synthesize this vast amount of data, develop a physical model of the system, discuss its origin and potential, and evaluate the results obtained from surface geophysics in terms of what has been learned from deep drilling. The wells themselves, their flow characteristics, and their production potential are discussed by Mathias (1975). An overview of the program of the U.S. Bureau of Reclamation (USBR) in the Imperial Valley is presented by Fernelius (1975).

There are several features of the Mesa anomaly which make it an ideal locality to present a case history for geothermal exploration and development.

1. A vast amount of information is available on the Mesa anomaly and this information can be synthesized into a reasonably simple model. All of the surface geophysical techniques that have been applied to the Mesa anomaly have not only been individually successful but all give essentially the same results, although they differ in detail. If production wells were to be drilled on the basis of heat flow, residual gravity, seismic ground noise, microearthquake epicenters, or electrical resistivity, the holes would all fall within a few hundred meters of one another, and all would fall within the zone suitable for geothermal development as defined by the 5-hfu heat-flow contour.
2. The Mesa anomaly is a "blind" geothermal field, there being no surface manifestations of geothermal activity such as geysers, hot springs, fumaroles, travertine deposits, and so on. Such fields present the greatest challenge in the exploration for geothermal deposits.
3. Of the geothermal fields which have been developed for power generation, all are either vapor-dominated or liquid-dominated with very high base temperatures (~300°C). The Mesa anomaly is an example of an intermediate temperature (base temperature ~200°C) liquid-dominated field, and such fields are more common and present a much greater potential resource.
4. Several predevelopmental environmental studies have been conducted at the Mesa anomaly including ground motion studies (Lofgren, 1974) and seismic studies (Hill et al., 1974; Combs, 1974). Repetition of these studies during

successive stages of development will help to determine the true environmental impact of geothermal development.

I will start with a physical description of the anomaly as interpreted from the logs and temperature-gradient surveys in the five geothermal wells and then discuss the anomaly's origin and dimensions. Then I will present the results of the surface geophysics, placing particular attention on the parameters measured by each technique, and show how the surface geophysics is consistent with the preliminary model. Finally I shall present an analysis of the potential of the anomaly.

GEOLOGIC SETTING

The Mesa anomaly is located in the Imperial Valley, California, on the eastern flank of the Salton trough, the sediment-filled structural depression that forms the northern extension of the Gulf of California and the East Pacific Rise. Seismic refraction profiling and regional Bouguer gravity data (Biehler, Kovach, and Allen, 1964; Kovach, Allen, and Press, 1962) show the maximum thickness of sediments in the trough to be about 6.4 km at a point located just south of the international border, with the basement becoming shallower both to the south and north. In the vicinity of the Mesa anomaly, the total thickness of sediments is about 3.5 km (Kovach, Allen, and Press, 1962). The sediments in the Salton trough consist largely of terrestrial sandstones, siltstones, and clays that comprise the delta of the Colorado River (Merriam and Bandy, 1965; Muffler and Doe, 1968). Analysis of hydrogen and oxygen isotopic compositions on well waters, surface waters, geothermal brines, and local precipitation (Coplen, 1972) indicate that most of the subsurface water in the Salton trough originated from the Colorado River, although ground water near the margin of the trough originated from local precipitation during recent times.

The Imperial Valley is a tectonically active area with most of the present seismic activity centered on the Imperial fault (Hill et al., 1974). Ground-motion studies by Lofgren (1974) show natural subsidence on the order of 6.5 cm/yr to be occurring near the Salton Sea. Lofgren (1974) also reports right lateral displacement of about 5 mm/yr on the Brawley fault. The structure and volcanism of the Imperial Valley and the relationship between the Imperial Valley and the East Pacific Rise are discussed by Elders et al. (1972).

DATA FROM DEEP DRILLING

To date, one injection and four production wells have been completed on the Mesa anomaly and their locations are shown in Figure 1. A full description of these wells including drilling specification, flow characteristics, chemical quality, geology, and other pertinent information has been published by the U.S. Bureau of Reclamation (1973a, 1974), Mathias (1975), and Fournier (1973). The distribution of temperature with depth for the five wells is shown in Figure 2. Perhaps the most obvious feature of these temperature-depth plots is the break in gradient which occurs in all wells at a depth of about 600 to 900 m. Gradients in the upper 600 m of the wells are about 150°C/km whereas the gradients below 900 m are about 29°C/km. This change in gradient is too large to result strictly from changes in thermal conductivity of the rock and indicates a change in the primary mode of heat transfer from a conductive to a convective regime. This is a significant point as convective regions can be expected to produce far greater quantities of water and energy than regions in which heat is transferred primarily by conduction.

To understand the reason for this shift from conductive to convective heat flow in the 600 to 900-m range it is necessary to examine the nature of the sediments penetrated by the geothermal wells. Figure 2 gives a breakdown of the relative abundances of clay and sand for five different depth ranges for each of the five wells. Also, the distribution of permeability within the sands is shown in Figure 2. Each histogram shows the relative frequency of clay and of sands in the permeability ranges 0 to .9, 1 to 9, 10 to 90, 100 to 900, and greater than 1000 millidarcys (md). The permeabilities were taken from the Saraband log, a computer-processed sandstone analysis developed by Schlumberger Ltd. The reliability of the low-permeability values is demonstrated by comparing the computed values to those measured in laboratory tests (Table 1). The high-permeability values could not be so verified because the unconsolidated nature of the sediments precluded the taking of core material.

It is readily apparent from the data in Figure 2 that the upper 600 m of each well—that portion of the wells in which heat is transferred primarily by conduction—is dominated by clay material. This clay is apparently acting as a caprock, confining the geothermal fluids below about 600 m. This clay cap is apparently an effective barrier to vertical migration of ground water as there are no hot springs or other surface manifestations of geothermal activity in the vicinity of the Mesa anomaly. A similar clay cap of approximately the same thickness confines the Salton Sea geothermal field, located about 55 km northwest of the Mesa anomaly (Helgeson, 1968).

The depth range 600 to 750 m represents a transition region between the clay-dominated caprock and the sand-dominated geothermal reservoir. As shown in Figure 2 all five wells show a marked decrease in clay content over this depth range and a corresponding increase in the more permeable sand horizons.

The depth range 750 to 900 m represents the upper portion of the geothermal reservoir. This depth range is characterized by permeable sands, the most common having a permeability in the range 100 to 1000 md, and a total clay concentration of only 20 to 25%. Furthermore, the temperatures at this depth are 85 to 90% of the value at total depth. According to the data in Figure 2 it should be possible to complete a successful geothermal well at almost any depth between 750 and 2175 m.

The depth ranges 900 to 1525 m and 1525 to 2175 m constitute the remainder of the geothermal reservoir. These ranges are essentially similar to the 750 to 900-m interval, the principle difference being a shift to less permeable sands, a shift which undoubtedly results from the increasing overburden pressure and exposure to geothermal fluids.

Only one well, Mesa 6-1, has penetrated below 1900 m and the data in Figure 2 indicate the possibility of another sedimentary break at about 2175 m. Below 2175 m, there is a marked increase in clay content, a significant increase of very low-permeability sands (<1 md), a decline of reservoir pressure (see USBR, 1974, Table 3), a slight increase in temperature gradient, and the near-absence of promising production zones. These data indicate that the

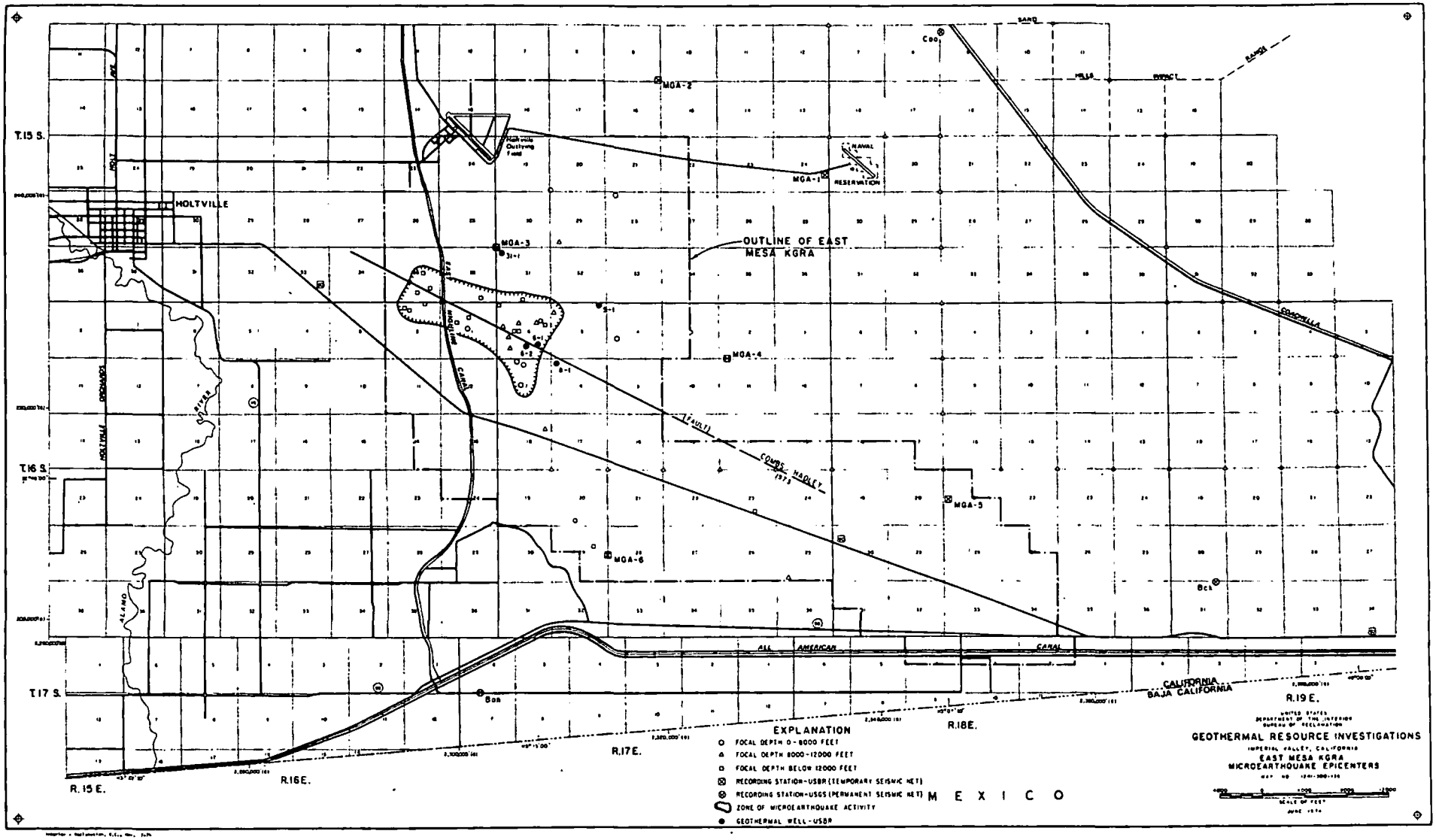

Figure 1. Location map of the Mesa anomaly showing the positions of the geothermal wells with respect to microearthquake epicenters. The open circles, triangles, and squares represent microearthquake focal depths of respectively 0 to 2.4 km (approximate depth of deepest well), 2.4 to 3.5 km (within the sedimentary section), and greater than 3.5 km (the basement). Seismic data from Combs (1974).

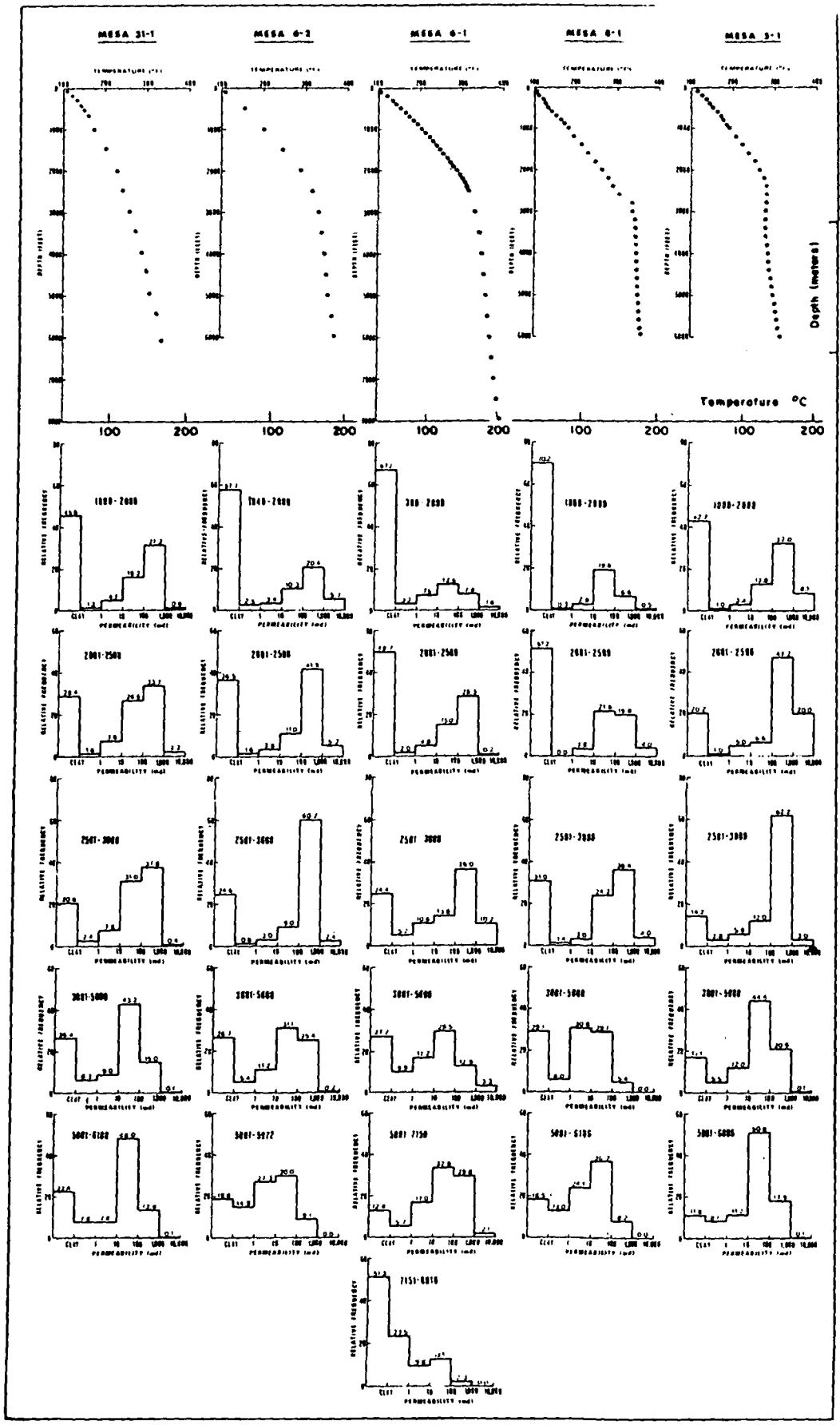

Figure 2. Distribution of temperature, clay, and sand permeability with depth for five geothermal wells. The depth ranges are shown in feet and correspond to the clay cap (0 to 600 m), the transition zone (600 to 750 m), the upper portion of the geothermal reservoir (750 to 900 m), two additional segments of the reservoir (900 to 1525 m and 1525 to 2175 m), and below the reservoir (2175 to 2448 m).

Table 1. Comparison of porosity and permeability for samples from geothermal well Mesa 6-1.

Depth (m)	Vertical permeability (md) Laboratory	Vertical permeability (md) Computed	Porosity (%) Laboratory	Porosity (%) Computed
1356.1–1356.4	0.40	0.35	10.6	10.75
1358.2–1358.5	1.3	1.5	15.5	13.45
2135.8–2136.1	0.011	clay	17.2	clay
2136.4–2136.7	0.11	clay	20.2	clay

Note: The laboratory determinations were performed by Core Laboratories Inc. of Dallas, Texas, and the computed determinations were values averaged from the Saraband log of Schlumberger Ltd. of New York.

geothermal reservoir may have a bottom below which production would be controlled by the availability of fractures. These data also show why the original well completion design for Mesa 6-1, in which selected sands below 2238 m were screened for production, did not yield encouraging production tests and why uphole perforation in the range 2075 to 2179 m vastly improved production. This subject is treated in detail by Mathias (1975).

Another important property of the geothermal reservoir and one of interest to reservoir engineers is the physical nature of the rock material. Fournier (1973) has conducted an x-ray and optical study of the cuttings from Mesa 6-1 and characterizes the sediments as chiefly siltstones, with varying amounts of interbedded sandstones ranging from very fine to very coarse sand size. Some information regarding the mechanical strength of the rock can be gleaned from the core recovery record. Table 2 shows that the only material from Mesa 6-1 which has sufficient mechanical strength to permit coring are the clays and impermeable sands (<1 md) and that the sands having a permeability of more than 10 md are either unconsolidated or highly friable. Comparing the data in Table 2 and Figure 2 indicates that about 70% of the geothermal reservoir consists of these unconsolidated materials. These observations may have significant bearing on the design of downhole heat exchangers (Rogers Engineering Co., 1972), the problem of sand production in the goethermal wells, and the possibility for land subsidence as a consequence of removal of geothermal fluids (Swanberg, 1975).

DATA FROM SURFACE GEOPHYSICS

In the previous section I discussed the nature of the Mesa anomaly as interpreted from the five geothermal wells. In this section, I shall present the principle results obtained from surface geophysics and develop a model for the origin of the anomaly.

Table 2. Core record from Mesa 6-1.

Depth range (m)	Total interval cored (m)	Total core recovered (m)	Total clay + impermeable sand (<1 md) from the Saraband log (m)	Description of core: USBR (1973)
776.6–794.3	17.7	5.5	0.6*	firm hard claystone
1350.9–1365.5	14.6	7.6	8.2	4.6 m hard shale: 3.0 m very fine, silty, clayey, calcareous sand
2129.9–2147.3	17.4	6.4	7.3	3.7 m hard shale. 2.7 m hard sandy silt

*Another 4.3 meters fall in the permeability range 1 to 10 md.

Heat Flow

Heat flow is perhaps the most effective method of geothermal exploration in that there are fewer assumptions between the measured parameters and the required information—that is, knowledge of the subsurface distribution of temperature. A full analysis of the heat flow at the Mesa anomaly and the technique used in its determination are presented by Swanberg (1974b) and summarized in Figure 3. Background heat-flow values range from 1.4 to 2.4 hfu (1 hfu = 10^{-6} cal/cm^2·sec) and are typical of those throughout the Basin and Range province (Roy, Blackwell, and Birch, 1968). Heat-flow values for the anomaly itself (northwest lobe of the East Mesa Known Geothermal Resource Area, or KGRA) are as high as 7.9 hfu, with the highest values located near gravity and seismic noise maxima and electrical resistivity minima (Fig. 4).

The three pronounced contours in Figure 3 are the 3-, 5-, and 7-hfu contours. The 3-hfu contour roughly outlines the extent of anomalously high heat flow. Areas outside this contour are only marginally above the regional background and such areas cannot be expected to yield a successful production well, although they might well prove ideal for disposal of geothermal brine. The area within the 5-hfu contour can be considered the production area. Any place within this contour should yield a successful production well, provided of course that suitable production horizons are encountered. For the Mesa anomaly, over 40 km^2 of land fall within this contour.

Also shown in Figure 3 are the three faults postulated for the Mesa anomaly. One of these faults (Combs, 1974) is currently active and was located during microseismic monitoring at the Mesa anomaly. The correlation between the fault traces and the heat-flow contours is obvious, and this correlation suggests a tectonic origin for the anomaly. That is, the faults act as conduits, allowing the rise of geothermal fluids from the deep igneous heat source into the geothermal reservoir. Note also that the heat-flow values decrease with distance very rapidly west of the zone of maximum heat flow but decrease very slowly to the east. This indicates that the faults either dip to the east or alternatively, that the predominant flow of water in the geothermal reservoir is to the east, away from the faults.

Gravity

A complete Bouguer gravity map of the Imperial Valley has been prepared by Biehler (1971) who notes the correlation between positive gravity anomalies and areas of high surface heat flow. The Mesa anomaly itself is associated with a 4-mgal residual anomaly closure, and this closure is shown in Figure 4 along with the heat-flow contours. The close relation between the maxima of heat flow and residual gravity is obvious and indicates a cause-and-effect relation. The lack of an obvious magnetic anomaly associated with the Mesa anomaly (USBR, 1971) would seem to preclude the presence of the type of rhyolite plugs which crop out near the Salton Sea. It is more likely that the gravity anomaly results from cementation (and possibly silicification) and low-grade metamorphism of the sediments as a consequence

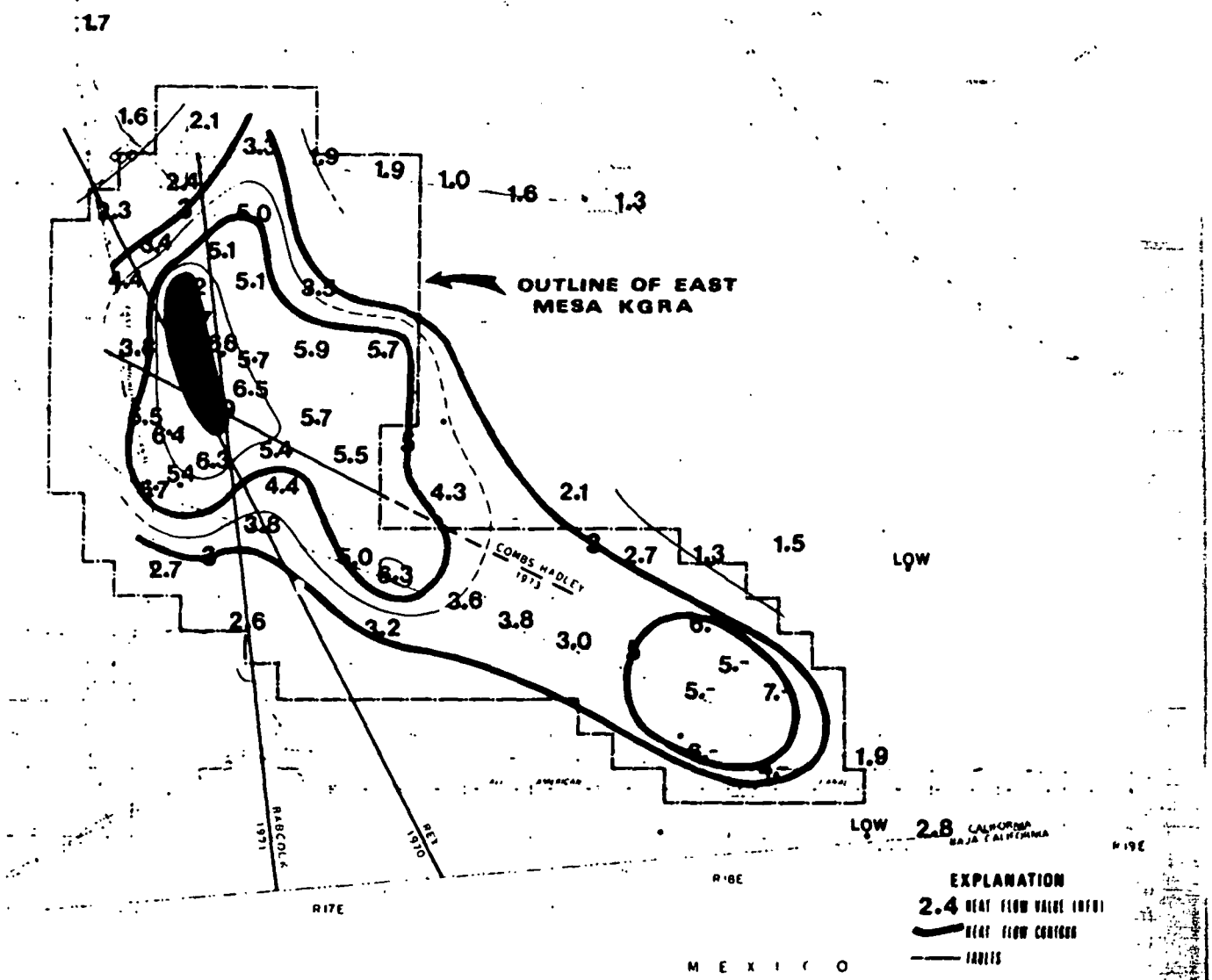

Figure 3. Distribution of heat flow over the Mesa anomaly (northwest lobe of the East Mesa KGRA) and the border anomaly (southeast lobe). Data from Swanberg (1974b), USBR (1974).

of exposure to geothermal fluids. The close agreement of the residual gravity and the faults which control the ascending geothermal fluids would seem to substantiate this hypothesis.

Biehler (1971) has applied a simple half-width calculation to the residual gravity (spherical symmetry) and obtained a maximum depth to the center of mass of about 3.6 km. Assuming a density contrast of 0.15 gm/cm^3, this mass would have a radius of 2.7 km which would place it well within the depth range penetrated by the geothermal wells (Biehler, 1971). In an attempt to verify this model, the densities for the five wells were estimated from the gamma-gamma density log. The densities for the three wells within the maximum residual contour are similar to the densities for the two wells outside the contour (Table 3), indicating that the anomalous mass must be deeper than the 1.8 km penetrated by four of the wells, and that the density contrast be greater than 0.15 gm/cm^2. Mesa 6-1 shows a sharp increase in density below 2.1 km, but this cannot be conclusively linked to the origin of the gravity anomaly. since the other wells do not penetrate to this depth, and the data of Biehler, Kovach, and Allen (1964) show the presence of a regional seismic velocity increase occurring at about the same depth.

Microseismic Data

Microseismic monitoring in the Mesa anomaly area is currently being conducted on a regional basis (Hill et al., 1974) and on a detailed basis near the anomaly itself (Combs, 1974), and the results show considerable seismic activity associated with the anomaly. This monitoring is of interest from an environmental standpoint in that it establishes the background seismicity of the area prior to development, and has also made it possible to locate geothermal injection well Mesa 5-1 in a seismically stable part of the anomaly (Swanberg, 1975). This monitoring is also of use in developing a model for the geothermal system. The zone of principle seismic activity and the right lateral strike-slip fault (Mesa fault) thereby defined are shown in Figure 4. The correlation between the Mesa fault and the heat-flow contours indicates that both lobes of the East Mesa KGRA exist due to geothermal fluids ascending along this fault.

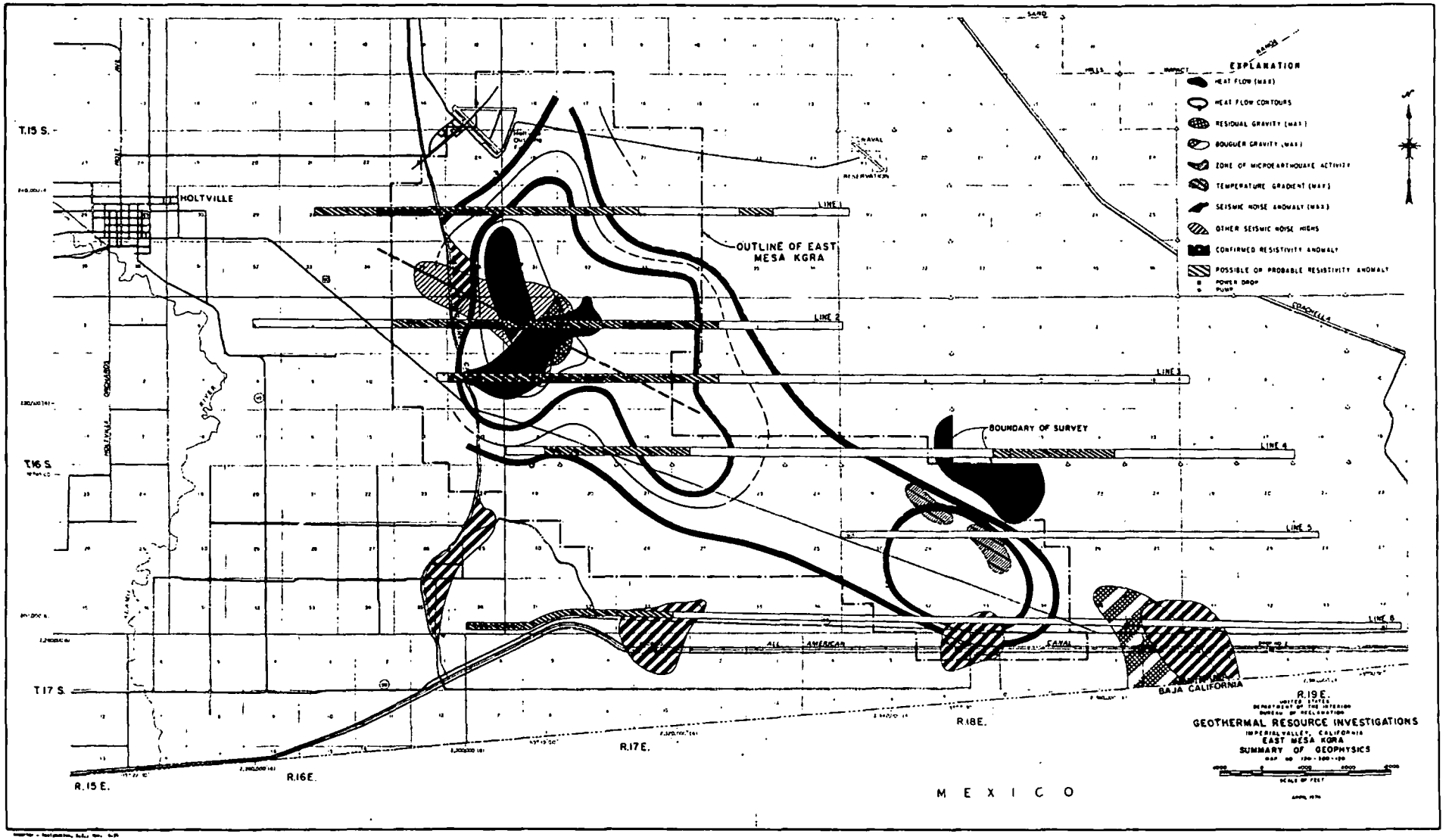

Figure 4. Summary of geophysical data for the Mesa anomaly. Data from USBR (1974), Swanberg (1974b), Biehler (1971), Combs (1971; 1974), Teledyne-Geotech (1972), McPharr Geophysics (1974).

Table 3. Distribution of density throughout the five geothermal wells as taken from the γ-γ density log.

Depth (m)	Geothermal Well Mesa 6-1	Mesa 5-1	Mesa 31-1	Mesa 6-2	Mesa 8-1	Average of wells 6-1, 6-2, 8-1	Average of wells 31-1, 5-1
0–152					1.88		
152–305	2.09				1.97		
305–457	2.13	2.01	2.07	1.94	2.07	2.05	2.04
457–610	2.17	2.10	2.14	2.07	2.14	2.13	2.12
610–762	2.21	2.12	2.16	2.09	2.13	2.14	2.14
762–914	2.09	2.16	2.15	2.13	2.18	2.13	2.16
914–1067	2.21	2.21	2.22	2.18	2.28	2.22	2.22
1067–1219	2.22	2.24	2.22	2.26	2.40	2.29	2.23
1219–1372	2.14	2.26	2.21	2.23	2.35	2.24	2.24
1372–1524	2.04	2.29	2.26	2.23	2.33	2.20	2.28
1524–1676	2.29	2.30	2.26	2.37	2.41	2.36	2.28
1676–1829	2.27	2.28	2.31	2.36	2.38	2.34	2.30
1829–1981	2.34						
1981–2134	2.31						
2134–2286	2.39						
2286–2438	2.52						
2286–2438	2.52						
2438–2448	2.60						
Average for the interval (305–1829)	2.18	2.20	2.20	2.19	2.27	2.21	2.20

Note: The last two columns represent average values for the wells inside and outside the residual gravity closure.

Information regarding the total displacement of the fault cannot be determined by applying conventional structural analysis. Detailed studies of the cuttings from Mesa 6-1 (Fournier, 1973) and analysis by the author of the geophysical logs from all five wells have failed to delineate any marker horizons which might be used to determine displacement. The dipmeter logs which were run in four of the wells, however, provide some information on the history of the fault. Figure 5 shows a contoured, stereo net plot of dip direction and magnitude for various depth intervals within the four wells. The strata in Mesa 5-1, an injection well deliberately drilled well away from the Mesa fault, are essentially flat-lying throughout the total depth penetrated. There is a slight tendency for the beds to dip to the west; this is expected, since the Mesa anomaly lies on the east flank of the Salton trough. Mesa 31-1, also several kilometers from the fault, shows this same general tendency although considerable more scatter exists. However, the strata penetrated by Mesa 6-2 and Mesa 8-1, two wells which lie very near the Mesa fault (see Fig. 1), show this tendency only in the upper 600 m. Below 600 m there is a tendency for the beds to dip to the southeast, parallel to the fault, and this tendency becomes more apparent with increasing depth. There is also a tendency for the dip angle to increase with increasing depth for these two wells. These data are consistent with deposition during faulting and indicate that the Mesa fault is not only currently active but also that it has been active during the deposition of the most recent 2 km of sediments.

Seismic Ground Noise

A seismic ground-noise survey of the Mesa anomaly area has been prepared by Teledyne-Geotech (1972), and the maximum (>30 dB) total power contour in the 3 to 5 Hz pass band is shown in Figure 4. Considerable care must be exercised in interpreting seismic ground-noise data because cultural activity may introduce considerable noise in the 3 to 5 Hz pass band. In particular, two of the seismic noise highs in the southern portion of the map area relate directly to power drops along the All American Canal. Also, the noise highs along the East Highline Canal may relate to water movement in the canal, the presence of pumps, or agricultural activity in the cultivated regions of the Imperial Valley to the west. The seismic ground-noise anomalies which cannot be attributed to cultural activity are shown in Figure 4.

The data in Figure 4 show the presence of a seismic noise high associated with the Mesa anomaly. There are two plausible origins for the seismic noise anomaly, both pertaining indirectly to geothermal activity. The first pertains to the movement of geothermal fluid, either vertically along the Mesa fault or horizontally within the geothermal reservoir. The spacial proximity among the ground-noise maxima, the Mesa fault, and the zone of maximum heat flow are consistent with this hypothesis. A second possible origin of the seismic ground-noise high has been presented by Combs (1974) who notes the resemblance between areas of high seismic noise and areas of microearthquake activity. Thus the enhanced levels of seismic ground noise may be wave phenomena associated with the continuously occurring nanoearthquakes in the Mesa anomaly area (Combs, 1974).

Electrical Resistivity

Electrical and electromagnetic techniques have been used by a number of workers to delineate geothermal fields and are based on the fact that increasing temperature greatly reduces the electrical resistance of porous, water-saturated rocks. Imperial Valley, however, is a rather hostile environment for the utilization of electrical methods. The high regional heat flux and the high salinity of the ground water throughout much of the valley combine to create a low background level of resistivity, leading to a reduced resistivity contrast between the geothermal fields and the nongeothermal adjacent areas. Contact resistance at the electrodes,

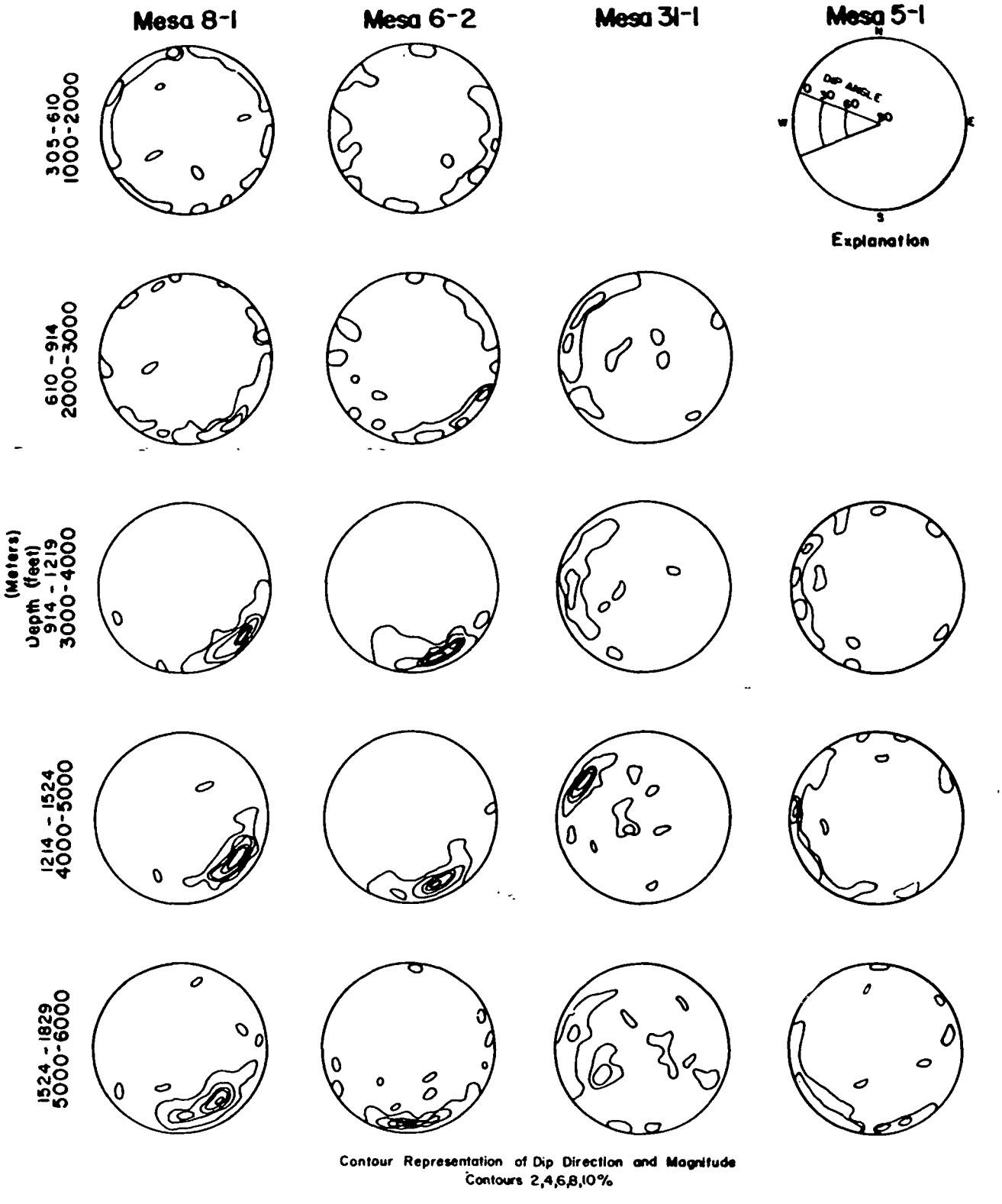

Figure 5. Stereo net plots of dip direction and magnitude.

which must frequently be placed in dune sand, is frequently high. Despite these problems, electrical resistivity soundings have been successfully employed in the Mesa anomaly area by Meidav and Furgerson (1972) and McPhar Geophysics (1974). The former study utilized the Schlumberger array with AB/2 ranging from 300 to 2500 m and showed a 5-ohm·m closure over the Mesa anomaly. This study was of a reconnaissance nature, however, and the large distance between data points did not provide an accurate determination of the boundaries of the geothermal field. The latter study utilized the dipole-dipole technique with 600-m dipoles extended out to N = 5, giving a maximum depth of penetration of approximately 1.5 km. Six east-west profiles were run across the anomaly; the zones of confirmed and suspected anomalous surface temperatures are shown in Figure 4. There is a very close agreement between the

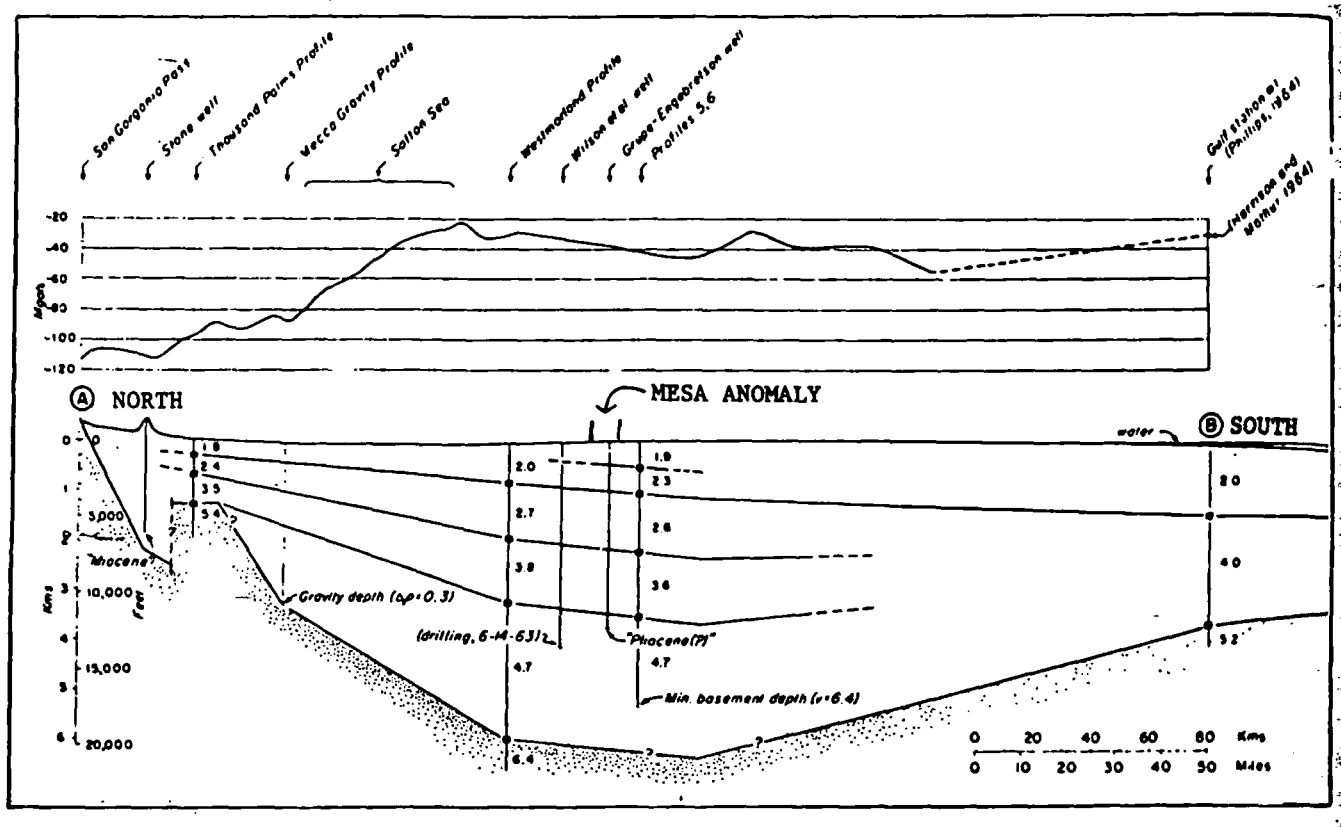

Figure 6. Seismic refraction profile of the Imperial Valley, California. Modified from Biehler, Kovach, and Allen (1964).

anomalous areas as depicted by the resistivity lows and the 5-hfu contour, indicating that dipole-dipole resistivity is a valuable tool in locating and defining the boundaries of geothermal areas in the Imperial Valley, California.

Seismic Refraction

Seismic refraction profiles in the Imperial Valley have been conducted by Biehler, Kovach, and Allen (1964), and their north-south profile, which passes about 10 km west of the Mesa anomaly, is reproduced in Figure 6. Biehler, Kovach, and Allen (1964) report the presence of several through-going velocity zones but were unable to correlate these zones with known stratigraphic units. These velocity zones, however, correlate quite well with the stratigraphic data presented in Figure 2. The bottom of the clay cap, which confines the geothermal fluids to depths below about 600 m, is located at about the same depth as the 1.9 to 2.3 km/sec velocity contrast, a contrast which is also apparent on the sonic logs from the five wells, although the break is transitional and varies slightly in depth among the five wells. This velocity contrast occurs only in the vicinity of the Mesa anomaly (Fig. 6); and if this is not a coincidence, then a potentially powerful geothermal exploration technique is suggested. For a geothermal field to exist, there must be a source of geothermal fluids and a caprock to confine them. If potential clay caps can be located by seismic refraction, and if faults act as conduits for ascending geothermal fluids, then the coincidence of a caprock and a fault would be a promising geothermal prospect. As shown in Figure 2, there is a marked change in the lithology penetrated by Mesa 6-1 at a depth of 2175 m. This depth corresponds to the 2.6 to 3.6 km/sec velocity break shown in Figure 6.

Geochemical Data

Geochemical studies of the Imperial Valley have been conducted by Dutcher, Hardt, and Moyle (1972) and Rex et al. (1971, 1972). The chemistry of the geothermal brines from the Mesa anomaly has been summarized by the Bureau of Reclamation (USBR 1973a, 1974). In general, the brines are of a sodium chloride variety and contain roughly 2500 mg/liter total disolved solids, although samples collected below 2238 m in Mesa 6-1 have up to 22 000 mg/liter (Table 4).

Perhaps the only geothermal exploration technique attempted at the Mesa anomaly that has not been successful is the use of the Na-K-Ca geothermometer (Fournier and Truesdell, 1973) to detect areas of abnormally high subsurface temperatures, although this method has been successful in other areas (Coplen, 1974; Swanberg, 1975b). The Na-K-Ca geothermometer applied to 74 ground-water samples in nongeothermal portions of the Imperial Valley yields an average estimated temperature of 83°C (data from Coplen, 1974). This value compares with an average value of 90°C for six samples of ground water located within the 5-hfu heat-flow contour of the Mesa anomaly. Although the near-surface waters (46 to 400 m in depth) over the Mesa anomaly give slightly higher estimated temperatures, this difference is not deemed significant. These data emphasize the fact that the clay cap overlying the Mesa anomaly geothermal reservoir is a very effective barrier to vertical ground-water movement.

Several different geothermometers have been applied to the geothermal brines from the Mesa anomaly and the results are summarized in Table 4. The estimated and observed temperatures are in fair agreement with all three geothermometers, showing an average discrepancy of about 20°C.

Table 4. Comparison of observed temperatures and temperatures estimated by the silica and the sodium-potassium-calcium geothermometers.

Well	Sample number	Observed T(°C)	Quartz conductive (°C)	Quartz adiabatic (°C)	Na-K-Ca (°C)	Total dissolved solids (mg/l)
Mesa 6-1	W30.3		186.5	173.5	231.8	16180
	W84.4		166.4	157.1	231.6	19360
	W1033		197.7	182.5	254.7	21967
	Average	204	183.5	171.0	239.4	
Mesa 6-2	W609.3		180.0	168.1	227.5	2130
	1032		209.6	192.1	225.9	2687
	Average	187	194.8	180.1	226.7	
Mesa 5-1	1059	157	180.3	168.4	166.6	1575
Mesa 8-1	1235	179	199.4	183.9	170.9	2463
Mesa 31-1	1226	154	130.2	126.8	136.6	2311
	Average difference (°C)		19.5	17.1	23.6	

Note: All samples except Mesa 5-1 represent unflashed formation fluid. Observed temperature is bottom-hole temperature. Data from USBR (1974).

Table 5. Summary of information necessary to compute the potential of the Mesa anomaly.

Parameter	Magnitude	Source of data
Areal extent	40 km^2	Heat flow (Fig. 3)
Verticle extent	750–2175 m	Seismic refraction: Saraband log (Figs 6,2)
Temperature	170°C	Temperature surveys (Fig. 2)
Total sand	75%	Saraband log (Fig. 2)
Porosity of sand	20%	Saraband log (USBR, 1973a)
Total volume of water in sands	8.6×10^9 m^3	
Production from Mesa 6-1 (wellhead T = 127°C)	$8.8 \times 10^7 \frac{m^3}{century}$	Flow test (USBR, 1974)
Production from Mesa 6-1 (wellhead T = 166°C)	$1.6 \times 10^7 \frac{m^3}{century}$	Flow test (USBR, 1974)

More significant, however, is the lack of any systematic error. The Na-K-Ca geothermometer overestimates the observed temperature in three cases, but underestimates in the other two. This geothermometer also gives the most accurate temperature in two cases, but the least accurate in two others. A similar lack of systematic error is also present for both silica geothermometers. Thus there appears to be little advantage in attempting to refine these geothermometers, and any estimated temperature based on these geothermometers will be subject to a maximum total uncertainty of up to 40°C.

POTENTIAL OF THE MESA ANOMALY

As the U.S. Bureau of Reclamation's program for development of the Mesa anomaly is to provide new sources of fresh water by desalting geothermal brines, a first step in estimating the potential of the anomaly is to estimate the total amount of geothermal brine available. Table 5 summarizes the required parameters.

Table 5 shows that the Mesa geothermal reservoir contains 8.6×10^9 m^3 of geothermal brine at an average temperature of 170°C, and this volume of water is contained within sand horizons having a mean porosity of 20% and a modal permeability of 100 md. Taking the flow data from Mesa 6-1 (USBR, 1974) and assuming that wellhead temperatures of 166°C will be necessary to operate the desalting plant, then roughly 500 wells operating continuously for 100 years would be required to produce this volume of fluid. If ground-water recharge is considered—and recharge is likely to be quite large as the isotope data of Coplen (personal commun.) show the Mesa anomaly to be a rather "open" system—an even greater number of wells (or additional time) would be required to produce this volume of fluid. There seems little use in extending this approach further. The volume of geothermal brine available for production is far in excess of what can be physically produced, leading to the speculation that the Mesa anomaly is very nearly an infinite resource. Another conclusion to be drawn from the data in Table 5 is that the use of geophysical data to estimate production potential will generally lead to overestimates. Thus the true potential of the Mesa anomaly can best be determined by the flow testing of the wells, by observing the decline of wellhead pressure with time, and by observing the interactions among wells during production.

ACKNOWLEDGEMENTS

Much of the work was completed while the author was employed by the U.S. Bureau of Reclamation, Boulder City, Nevada, and I wish to thank the following personnel—M. K. Fulcher, W. A. Fernelius, K. E. Mathias, and W.

Whitbread. The manuscript has benefited greatly from discussions with J. Combs, T. Coplen, W. Elders, S. Biehler, and D. Bird.

REFERENCES CITED

Biehler, S., 1971, Gravity studies in the Imperial Valley, *in* Rex, R. W., et al., Cooperative geological-geophysical-geochemical investigations of geothermal resources in the Imperial Valley area of California: Riverside, Univ. of California, p. 29-42.

Biehler, S., Kovach, R. L., and Allen, C. R., 1964, Geophysical framework of northern end of Gulf of California structural province, *in* Van Andel, T., and Shor, G., eds., Marine geology of Gulf of California: Am. Assoc. Petroleum Geologists Mem. 3, p. 126-143.

Combs, J., 1971, Heat flow and geothermal resource estimates for the Imperial Valley, *in* Rex, R. W., et al., Cooperative geological-geophysical-geochemical investigations of geothermal resources in the Imperial Valley area of California: Riverside, Univ. of California, p. 5-27.

——, 1974, Microearthquake investigation of the Mesa geothermal anomaly, Imperial Valley, California: Final report to the U.S. Bureau of Reclamation: Riverside, Univ. of California, Inst. Geophys. and Planet. Phys., 37 p.

Combs, J., and Muffler, L. J. P., 1973, Exploration for geothermal resources, *in* Kruger, P., and Otte, C., eds., Geothermal energy: Resources, production, stimulation: Stanford, California, Stanford Univ., p. 95-128.

Coplen, T. B., 1972, Origin of geothermal waters in the Imperial Valley of southern California, *in* Rex, R. W., et al., Cooperative investigation of geothermal resources in the Imperial Valley area and their potential value for desalting of water and other purposes: Riverside, Univ. of California, Inst. Geophys. and Planet. Phys, p. E1-E33.

——, 1974, Imperial Valley investigations: Geothermal Energy, v. 2, n. 2, p. 32-34.

Dutcher, L. C., Hardt, W. F., and Moyle, W. R., Jr., 1972, Preliminary appraisal of ground water in storage with reference to geothermal resources in the Imperial Valley area, California: U.S. Geol. Survey Circ. 649, 57 p.

Elders, W. A., Rex, R. W., Meidav, T., Robinson, P. T., and Biehler, S., 1972, Crustal spreading in southern California: Science, v. 178, p. 15-24.

Fernelius, W. A., 1975, Production of fresh water by desalting geothermal brines: A pilot desalting program at the East Mesa geothermal field, Imperial Valley, California: Second UN Symposium on the Development and Use of Geothermal Resources, San Francisco, Proceedings, Lawrence Berkeley Lab., Univ. of California.

Fournier, R. O., 1973, An x-ray and optical study of cuttings from the U.S. Bureau of Reclamation Mesa 6-1 drillhole, Imperial County, California: U.S. Geol. Survey Open-File Rept., 35 p.

Fournier, R. O., and Truesdell, A. H., 1973, An empirical Na-K-Ca geothermometer for natural waters: Geochim. et Cosmochim. Acta, v. 37, p. 1255.

Helgeson, H. C., 1968, Geologic and thermodynamic characteristics of the Salton Sea geothermal system: Am. Jour. Sci., v. 266, p. 129.

Hill, D. P., Peake, L., Mowinckel, P., and Hileman, J. A., 1974, Seismicity of the Imperial Valley, California, 1973: EOS (Am. Geophys. Union Trans.), v. 55, no. 4, p. 346.

Kovach, R. L., Allen, C. R., and Press, F., 1962, Geophysical investigations in the Colorado delta region: Jour. Geophys. Research, v. 67, no. 7, p. 2845.

Lofgren, B. E., 1974, Measuring ground movement in geothermal areas of the Imperial Valley, California: Conference on Research for the Development of Geothermal Energy Resources, Pasadena, California Inst. Tech., Jet Prop. Lab., Proceedings, p. 128.

Mathias, K. E., 1975, The Mesa geothermal field: A preliminary evaluation of five geothermal wells: Second UN Symposium on the Development and Use of Geothermal Resources, San Francisco, Proceedings, Lawrence Berkeley Lab., Univ. of California.

McPhar Geophysics Inc., 1974, Report on the reconnaissance resistivity survey in the East Mesa area, Imperial County, California, for U.S. Dept. Interior, Bureau of Reclamation: 12 p.

Meidav, T., and Furgerson, R., 1972, Resistivities studies of the Imperial Valley geothermal area, California: Geothermics, v. 1, no. 2, p. 47.

Merriam, R., and Bandy, O. L., 1965, Source of upper Cenozoic sediments in Colorado delta region: Jour. Sed. Petrology, v. 35, no. 4, p. 911.

Muffler, L. J. P., and Doe, B. R., 1968, Composition and mean age of detritus of the Colorado River delta in the Salton trough, southeastern California: Jour. Sed. Petrology, v. 38, no. 2, p. 384.

Rex, R. W., Babcock, E. A., Biehler, S., Combs, J., Coplen, T. B., Elders, W. A., Furgerson, R. B., Garfunkel, Z., Meidav, T., and Robinson, P. T., 1971, Cooperative geological-geophysical-geochemical investigations of geothermal resources in the Imperial Valley area of California: Riverside, Univ. of California, 153 p.

Rex, R. W., Biehler, S., Combs, J., Coplen, T. B., Furgerson, R. B., Garfunkel, Z., Getts, T. R., Maas, J. P., and Reed, M., 1972, Cooperative investigations of geothermal resources in the Imperial Valley area and their potential value for desalting of water and other purposes: Riverside, Univ. of California, Inst. Geophys. and Planet. Phys., 10 ch.

Rogers Engineering Co. Inc., 1972, Preliminary design and feasibility study of Van Huisen downhole heat exchanger as applied to geothermal power generation: San Francisco, Rogers Engineering Co. Rept. S-72023, 34 p.

Roy, R. F., Blackwell, D. D., and Birch, F., 1968, Heat generation of plutonic rocks and continental heat flow provinces: Earth and Planetary Sci. Letters. v. 3, p. 1.

Swanberg, C. A., 1974a, The application of the Na-K-Ca geothermometer to thermal areas of Utah and the Imperial Valley, California: Geothermics, v. 3, no. 2, p. 53.

——, 1974b, Heat flow and geothermal potential of the East Mesa KGRA, Imperial Valley, California: Conference on Research for the Development of Geothermal Energy Resources, Pasadena, California Inst. Tech., Jet Prop. Lab., Proceedings, p. 85.

——, 1975a, Physical aspects of pollution related to geothermal energy development: Second UN Symposium on the Development and Use of Geothermal Resources, San Francisco, Proceedings, Lawrence Berkeley Lab., Univ. of California.

——, 1975b, Detection of geothermal components in groundwaters of Dona Ana County, southern Rio Grande rift, New Mexico, *in* 26th ann. field conf. guide-book to the Las Cruces country: New Mexico Geol. Soc.

Teledyne-Geotech, 1972, Geothermal noise survey of the East Mesa area, Imperial Valley, California: Teledyne-Geotech Tech. Rept. 72-19, 18 p.

U.S. Bureau of Reclamation, 1971, Geothermal resource investigations, Imperial Valley, California, site location report, deep geothermal test well, October 1971: Boulder City, Nevada, 11 p.

——, 1973a, Geothermal resource investigations, Imperial Valley, California, special report, test well Mesa 6-1, February, 1973: Boulder City, Nevada, 44 p.
——, 1973b, Geothermal resource investigations, Imperial Valley, California, site selection report, geothermal test well Mesa 6-2, June 1973: Boulder City, Nevada, 10 p.
——, 1974, Geothermal resource investigations, East Mesa test site, Imperial Valley, California, status report, November, 1974: Boulder City, Nevada, 64 p.
——, 1975, Geothermal reservoir and production engineering, Mesa field, Imperial Valley, California, geothermal resource investigations special report, prep. by J. S. Dodd, February, 1975: Denver, Colorado, 91 p.

Geothermal Sessions

Geothermal 1 — Techniques and Interpretation

Megasource EM Method for Detecting Deeply Buried Conductive Zones in Geothermal Exploration G1.1

George V. Keller, Kendrick Taylor, and Jose M. Souto, Group Seven, Inc.*

Application of the magnetotelluric method in geothermal exploration has indicated that in some geothermal areas, zones of unexpectedly high electrical conductivity occur in the crust at depths of only 5 to 10 km. Delineation of these features, which may represent the thermal roots of shallower exploitable geothermal systems, is difficult with the MT method because of the time required to make an individual sounding, and because of the complexity of interpretation of MT sounding curves when strong lateral variations in resistivity exist. The controlled source EM methods offer the possibility of more definitive delineation of anomalies associated with geothermal systems, providing that penetrations of 5 to 10 km can be obtained. One approach to reaching great depths in EM sounding is through the use of very intense sources, a procedure known as the Megasource EM method.

A Megasource EM survey was carried out in the Dixie Valley-Carson Sink area of northwestern Nevada. In this area, earlier MT surveys indicated the existence of anomalously conductive zones in the crust at depths as shallow as 5 to 10 km. The conductive zone is spatially related to the areas of most intense surface thermal activity in Dixie Valley and the adjacent Stillwater Mountains. Several apparently successful geothermal test wells had been drilled in this anomalous area. In the survey described here, an EM field was generated by passing a square wave current of 3000 A peak-to-peak amplitude along a 1 km grounded wire, providing a source moment of 3×10^6 amperemethers (Hence "Megasource"). The source was located on the northwest side of Carson Sink, at a distance of approximately 50 km from the target areas for exploration in Dixie Valley and south end of Carson Sink. The observation of EM fields at these distances from the source were expected to permit the determination of resistivity in the crust to depths up to 20 km. Observations of transient EM coupling using a vertical axis simulated-loop receiver were made at nearly 400 receiver locations distributed at intervals of approximately 1 km along the accessible roads in the survey area. The time interval over which the transients were recorded was from a minimum of 30 msec to a maximum of 30 sec. Many of the curves were interpreted using a one-dimensional inversion approach. The survey was successful in identifying an area where anomalously conductive rocks exist in the upper crust at depths as shallow as 7 km. This area includes locations of the successful test wells in Dixie Valley and surrounding regions. Resistivity in the anomalous zone in the upper crust is reasonably consistent, ranging from 5 to 15 Ω-m. These data might be explained by the existence of a partially moulten zone at shallow depths in the crust, but it seems more likely that the high conductivity results from extensive fracturing and a high saturation of hot water in the crust.

Experience with the EM-60 Electromagnetic System for Geothermal Exploration in Nevada G1.2 §

M. J. Wilt, J. R. Haught, N. E. Goldstein, and H. F. Morrison, Lawrence Berkeley Laboratory*

Through a joint program between the Dept. of Energy/Division of Geothermal Energy and private geothermal developers, Lawrence Berkeley Laboratory (LBL) conducted controlled-source (frequency domain) EM surveys at three geothermal prospects in northern Nevada. More than 40 receiver stations were occupied in Panther Canyon (Grass Valley), near Winnemucca; Soda Lakes, near Fallon; and McCoy, west of Austin to test and demonstrate the applicability of the EM-60 system to subsurface resistivity mapping.

The EM-60 is a frequency-domain, horizontal-loop transmitter system for which we use three-component magnetic detection. Typically, we apply ± 65 A to a 100-m diameter, four-turn loop, generating a dipole moment > 10^4 MKS over the frequency range 10^{-3} to 10^2 Hz. By virtue of this large dipole moment, we made soundings at transmitter-receiver separations of up to 5 km, thus providing a maximum depth of penetration of 5 km. Recorded spectra were interpreted by means of both simple calculations done in the field and layered-model inversions calculated in the laboratory. The EM interpretations were then compared to existing geological/geophysical data sets for the purpose of combined interpretation and method evaluation.

In comparison with other electrical-electromagnetic prospecting techniques we have used, the EM-sounding method proved to be well suited to exploration for the following reasons. It provides good depth of exploration in relation to the transmitter-receiver separation, it is relatively insensitive to distant and local lateral inhomogeneities, it provides good resolution of buried conductive bodies, and it does not require frequent movement of long wires. Experience with the EM-60 system in Nevada has shown it to be an efficient alternative to dc resistivity and magnetotellurics — and possibly more cost-effective — for geothermal exploration. An average of two soundings per field day for depths of exploration up to 2 km were obtained routinely.

Results from EM-60 at Panther Canyon compare very favorably with earlier dipole-dipole resistivity surveys. Both methods adequately outlined an irregularly shaped, buried conductive body associated with a region of high heat flow, but EM-60 provided results in just over half the field time required for dipole-dipole resistivity. At Soda Lakes, 13 high-quality EM soundings were obtained from two transmitters in 6 field days under ideal field conditions. With the EM data we were able to map the depth to and inclination of a buried conductive body associated with an area of anomalous thermal gradients. In this case, the EM results confirmed an earlier MT survey interpretation and gave additional, detailed, near-surface information. At the remote and mountainous McCoy site, data interpretation was complicated because of the locally rugged terrain. By modifying existing interpretive software, we were able to calculate the effects of tilted-source dipoles and elevation differences on soundings and thus interpret data. The EM soundings discern a conductive zone (depth 200 m) at the south end of the prospect, near a location where drilling encountered water at 100 °C. In addition, EM soundings at McCoy provided information on a deep conductor below 2 km which has yet to be drilled.

*Speaker. §Preprint available from SEG Business Office.

Interpretation of a Telluric-Magnetotelluric Survey at the Tuscarora Geothermal Exploration Unit, Elko County, Nevada § G1.3

Claron E. Mackelprang, UURI; Arthur L. Lange, Amax Exploration; Bruce S. Sibbett, UURI; and H. D. Pilkington, Amax Exploration*

Exploration at the Tuscarora geothermal prospect is being conducted by Amax Exploration, Inc. as a participant in the Dept. of Energy's industry-coupled program. The Earth Science Laboratory of the University of Utah Research Institute (ESL/UURI) has completed geologic and geochemical mapping and analysis of geophysical surveys run over the exploration unit. The Tuscarora prospect is located approximately 90 km north-northwest of Elko, Nevada, at the north end of Independence Valley — a typical basin-range graben structure. Paleozoic clastic rocks of the Western facies have been extensively covered by 35 million to 39 million-year-old tuffs and tuffaceous sediments; these, in turn, were overlain by Miocene lavas, and folded and faulted by Pleistocene tectonism. Boiling springs issue from Oligocene tuffaceous sediments near the center of an area of high heatflow (≥4h.F.U.), extending over 160 km². The springs are associated with a large mound of siliceous sinter and are presently depositing silica and calcium carbonate. Chemical geothermometers of the 95°C waters indicate a reservoir temperature over 200°C.

Five-component MT data were obtained at 11 base stations, while electric field measurements were made at 22 intervening remote stations and telemetered to the bases by Terraphysics under contract with Amax. Data quality ranged from poor to very good with the majority being fair to good.

Interpretation suggests the large conductive zone of 5 Ω-m material may be explained by alteration and mineralization associated with a liquid-dominated geothermal reservoir in the vicinity of the hot springs (station M1), by conductive valley fill near station B10, and very speculatively by a zone of partial melt at depths below about 7 km in the station interval M8 to B2. A comparison is made between interpreted resistivities obtained from 2-D modeling of the TM-mode, 1-D inversion of the TE-mode, 2-D dipole-dipole models, and a resistivity log obtained in a hole 1633 m deep drilled in the vicinity of the hot springs. The consistency in the results of these different soundings provides considerable support to the derived models.

Self-Potential Modeling From Primary Flows G1.4

William R. Sill, Univ. of Utah §

A new method for the calculation of self-potentials (SP) based on induced current sources is presented. The induced current sources are due to divergences of the *convective* current which, in turn, is driven by a primary flow, either heat or fluid. Numerical modeling utilizing this method has been implemented using a 2-D transmission surface algorithm that provides modeling capabilities for 3-D distributions of sources and 2-D structures. When the primary flow is driven by the gradient of a potential, joint modeling of the primary flow and the resultant SP is possible with this algorithm.

Examples of simple geometrical models in the presence of point sources for the primary flow are presented and discussed. In the modeling, surface boundary conditions for the primary flow problem require careful consideration as the form of the primary flow at the air-earth interface can have a profound effect on resultant electrical potentials. For example, a point source of heat flow in a homogeneous half-space produces no surface electric potential when the surface boundary condition is one of constant temperature. On the other hand, a point source of fluid flow in a homogeneous half-space produces a surface electric potential when the surface boundary condition is zero normal flux. Lastly, a field example of the joint modeling of temperature and SP data is illustrated with data from Red Hill Hot Spring, Utah.

*Speaker. §Preprint available from SEG Business Office.

The Use of Seismic Reflection Techniques in Geothermal Areas Throughout the U.S. G1.5

James K. Applegate, Vaughn S. Goebel, Prent Kallenberger, and Joerg Rossow, Colorado School of Mines*

During the past year, the Exploration Research Laboratory (ERL) of the Colorado School of Mines has acquired seismic reflection data in six areas that are either areas of geothermal exploration or near active geothermal fields. Data quality, using a variety of field parameters, has varied. However, in most cases, even though the data have not always been of typical petroleum character, it has been extremely useful in geothermal exploration. Although in apparently low temperature geothermal areas, the quality of the seismic data is similar to that obtained in any good record area. In complex geological terrain, data quality has been more variable.

The six areas where ERL has acquired data in the last year are Raft River, Idaho; Papago Indian Reservation, Arizona; Chincoteague, Virginia; Canon City, Colorado; The Geysers geothermal field; and Imperial Valley, California.

In addition, ERL has reprocessed data from Milford, Utah and the Snake River Plain, Idaho. Data quality in the Chincoteague, Virginia area was extremely high showing the classic sedimentary sequence overlying a crystal basement. The Papago Indian Reservation data, acquired to investigate the possibility of an overthrust zone in Arizona, were of excellent quality and showed below the basin fill a series of very deep structures at depths in excess of 25,000 ft. The data acquired in the Raft River geothermal area show very complex geology, perhaps suggesting that there is a decollement at a depth of approximately 6000 ft, and that the layer between the decollement and the near-surface youthful material is highly folded and faulted in classic overthrusting style. The Geysers was the only area in which ERL has acquired both *P*- and *S*-wave data. The *P*-wave data show some interesting structures while the *S*-wave data, when coupled with the *P*-wave data, may yield new information about reservoir characteristics and structure. Data in the Imperial Valley were acquired in a number of different areas. Data quality is very good, showing excellent continuity and clearly defining structure in the area. It clearly shows zones of fracturing and faulting which might be the conduits for production of geothermal fluid. Although the limited amount of seismic data acquired in the Canon City embayment is by itself not conclusive, when coupled with existing data in the area, it verified the presence of a strong subbasement reflector over 16,000 ft deep or approximately 12,000 ft below the known basement. Reprocessing of seismic data from the Milford, Utah area and the Snake River Plain showed that an appreciation of the geology aids in producing excellent seismic data in complex terrains.

In conclusion, the gathering of seismic data from a variety of geothermal provinces utilizing Vibroseis™ methodology and acquisition parameters adapted to the known geology has been successful. With correct methodology it is possible to acquire seismic data which verify the structure and potential zones of interest in geothermal reservoirs. This suggests that the seismic method will become more widely used in geothermal exploration as its utility is recognized.

™Conoco

Aeromagnetic Anomaly Inversion and Analysis of the Depth-to-Curie Isotherm G1.6

Ming-Ren Hong, Carlos L. V. Aiken, Univ. of Texas at Dallas; and Wayne J. Peeples, SMU*

Aeromagnetic data have been analyzed by several methods to determine the depth-to-Curie temperature. Limitations are associated with each approach. Spectral analysis requires data coverage over a large area and provides an average value. Use of the spectra of the anomalies of moments to define centroids of bodies or corners of vertical prisms are very complicated schemes. Comparisons of spectra of vertical cylinders with observed spectra over single anomalies require the use of symmetric anomalies.

A major criticism of the use of analysis of isolated anomalies is that it is difficult to isolate individual anomalies from interference from adjacent bodies. However, a benefit in the use of single anomalies is that they could provide point estimations of the depth-to-Curie isotherm. If estimations at specific anomalies can be found over an area, it is then possible to define an isothermal surface at the Curie temperature.

Assuming two-dimensionality, a known upper boundary of a body, a lateral extent, and a susceptibility contrast, the lower boundary can be determined by applying inversion. The observed aeromagnetic data are related to an unknown continuous function defining the lower boundary by an integral form. The method can be applied directly to the observed data consisting of magnetizations of arbitrary inclination and declination so that no manipulation of the data, such as reduction-to-pole processing, is required. A known variable upper boundary can be used to take into consideration magnetic terrain effects and different magnetic survey parameters, for example, constant barometric, mean terrain clearance, or ground magnetic surveys. Susceptibility contrast variations can be incorporated so that adjacent body interference can be taken into account.

A study of synthetic models shows that the computed solution has a very thin layer in areas where lateral susceptibility changes are required. The amplitudes will not fit if incorrect susceptibilities are employed. Adjustments of the magnitude of the susceptibilities and their lateral boundaries are necessary before predicted data converge with observed data. A kind of synthetic data from a model with a lower boundary at a depth of 20 km was successfully inverted with an error of only ± .1 km. Complicated topography on this lower boundary was obtained under ideal conditions. Due to the attenuation characteristics of magnetic effects with distance, the depth at which reasonable results are possible is limited to approximately 45 km or less.

The method has been applied to several test areas where other Curie depth estimates from magnetics, or other information on subsurface temperatures, exist. Preliminary results on the analysis of the Arizona aeromagnetic map show both deep (e.g., 25 km) and shallow (5 km) depths-to-Curie isotherm in different regions. These results are in good agreement with previous results. Curie depth studies must always consider the possibility that the thickness of a magnetic body is defined by a lithologic change rather than an isotherm.

Geothermal 2 — Techniques and Interpretation

Exploration and Interpretation of the Southwest England Geothermal Anomaly G2.1

J. Wheildon, M. F. Francis, J. R. L. Ellis, and A. Thomas-Betts, Imperial College, London*

Since 1976 geothermal energy resource appraisals have been conducted throughout the United Kingdom, and targets for low enthalpy and hot dry rock resources have been identified. The work reported here covers heat flow and heat production studies in southwest England which has emerged as the most promising area for hot dry rock development.

Twenty-three boreholes have been drilled in and around the Cornish granite batholith. In addition, almost as many boreholes drilled by mining companies and the Institute of Geological Sciences have been taken over for heat flow determinations. Temperature logs have been run and thermal conductivities determined for the majority of these boreholes. Gamma-ray spectrometric determinations of radiogenic element concentrations on several hundred borehole samples have been used to determine mean heat production values for the granites and for the enclosing country rocks.

Anomalously high values of heat flow (120 m Wm^{-2}) were observed at all sites on or adjacent to the granites, while normal heat flows (60 mWm^{-2}) were determined at sites remote from the granite. The possibility of enhancement of heat flow through convective circulation at depth, which had earlier been thought to be the case, is virtually ruled out by the uniformly high values over the entire batholith.

A 2-D finite element model has been used to explain surface heat flow along a northwest-southeast section through the Carnmenellis granite pluton, being that part of the Cornish batholith where our heat flow coverage is most detailed. The space-form of the granite is based on an interpretation of the Bouguer anomaly map produced by the Institute of Geological Sciences. Thermal conductivity and heat production values for the granites and country rocks are average values derived from boreholes in the area.

The modeled surface heat flows are in good agreement with the actual measured values. They support the conclusion that observed significant contrasts in thermal conductivity and heat production themselves explain the observed heat flow pattern, without the necessity of invoking a convective enhancement mechanism. It may therefore be concluded that the downward continuation conduction models which indicate temperatures of around 200 °C at 6 km depth are realistic, and reaffirms the Cornish granite batholith as the most favorable UK site for HDR development.

Use of Gravity, Groundwater Geochemistry, and Heat Flow in Exploring for Geothermal Resources Near Columbus, New Mexico G2.2

Chandler A. Swanberg, Paul Daggett, and Charles T. Young, New Mexico State Univ.; Paul Morgan, NASA

The city of Columbus, New Mexico, lies astride the Mexican border about 100 km (60 miles) west of El Paso, Texas. Geologically, the area lies in the southeastern part of the Mimbres basin which, along with its extension in Mexico (the Los Muertos basin) comprises the westernmost and southernmost of the deep sedimentary basins that constitute the Rio Grande rift. During 1980, we conducted a series of geophysical studies aimed at evaluating the geothermal potential of the Columbus area. Reconnaissance gravity profiling confirms that the southeastern part of the Mimbres basin is a fault-bounded graben located on the eastern flank of the broad alluvial-filled valley that lies between the Tres Hermanas and West Potrillo Mountains. The eastern bounding fault shows late Pliocene or Pleistocene movement (1-4 my). The western fault is buried beneath alluvium. Groundwaters located near both faults have chemical characteristics which suggest a component of geothermal water. Surface and airborne geoelectric data are being presented by Young et al in a companion abstract. Seventeen 35 m heat flow test holes average 52.5 °C/km with the higher values consistently located on the upthrown flanks of the graben, a feature which we attribute to thermal refraction. However, the conductivity of these alluvial sediments is low so that the heat flow is not likely to exceed the regional mean. A single 296 m temperature test hole located at the U.S.-Mexico customs facility south of Columbus has a bottom hole temperature of 33.4 °C and a conductive temperature gradient of 50.5 °C/km between 135 and 296 m. None of the data collected to date has revealed the presence of a major geothermal prospect although the regional temperature gradient may be sufficiently high for some low temperature geothermal applications if appropriate users are available.

Input and dc Resistivity Exploration for Geothermal Resources near Columbus, New Mexico G2.3 §

Charles T. Young, Michigan Tech Univ.; Chandler Swanberg, New Mexico State Univ.; and Paul Morgan, NASA*

Columbus, New Mexico is located in a zone of high heat flow, where the flux is approximately 2.5 HFU. Nearby, recent volcanoes and hot springs suggest that the deep basin west of Columbus may contain hot water. A coordinated geothermal exploration program was

*Speaker. §Preprint available from SEG Business Office.

conducted to search for this water by geophysicists from New Mexico State University. The work included dc resistivity, airborne electromagnetics, gravity, and exploratory drilling. The Input® resistivity and aeromagnetic results are reported here.

Preliminary ground dc resistivity work involved Schlumberger profiling at AB/2 spacings of 800 and 100 m. The lowest resistivities found were 2 to 3 Ω-m at AB/2 = 800m over the basin. Vertical electric soundings indicated that this zone was within 150 ft of the surface. An airborne Input and aeromagnetic survey was flown by Geoterrex to outline the anomalous area. The airborne survey found two other conductive regions in addition to the first. The Input data were converted to apparent resistivities by calculating the ration of channels 3 to 6 and applying Palacky's homogeneous half-space curves. The use of ratios reduces the effect of the drastic variations in the amplitude of channel responses caused by small variations in altitude. The later channels represent deeper penetration. The resulting apparent resistivities agree well with the ground dc resistivity data for AB/2 = 800 m. Aeromagnetic data confirm the general geologic picture of a deep basin flanked by volcanic rock.

®Barringer Research

An Integrated Geophysical Study of the Shaw Warm Spring Area, San Luis Valley, South-Central Colorado G2.4 §

Marc A. Bond, Tenneco Oil

An integrated geophysical study of the Shaw Warm Spring area located on the western edge of the San Luis Valley, a downfaulted structural depression, was undertaken to determine the nature of the geothermal system. The geophysical methods employed in the study included: time-domain electromagnetic sounding, dc resistivity survey, audiomagnetotelluric and telluric surveys, seismic reflection and refraction surveys, and gravity surveys.

A low resistivity, relatively homogeneous earth is observed, attributed to saturated volcanic flows and ruffs dipping to the east, thermal alteration, and possible warm waters. The resistivity values range from 7 to 20 Ω-m. High-angle faults associated with the Late Paleozoic and Laramide orogenesis, and then later reactivated during the Rio Grande Rift phase, are mapped. The faults extend from the near-surface through basement rock, which is located approximately 2100 to 2600 m below the surface. Greater vertical offset on the faults is observed at depth. Interbedded Tertiary volcanics and sediments unconformably overlie the Precambrian basement.

The low resistivity values observed in the study area are related to the warm geothermal waters and alteration within the volcanic section. The heat source for the geothermal waters is from deep circulation of waters through faults to a depth of a few kilometers, brought up to the surface along boundary faults. The thermal anomaly probably overlies a deep crustal feature, such as fractures, that penetrates the mantle.

§Preprint available from SEG Business Office.

Geothermal 3 Special Session — Geophysical Studies in the Cascades

Geology and Geophysics of the Cascade Range G3.1

Charles R. Bacon, U.S. Geological Survey

Quaternary volcanoes of the Cascade chain form a belt roughly parallel to the North American plate margin, opposite the subducting oceanic plate. Tertiary volcanic rocks of the Cascades occur from northern Washington to northern California and include various rock types that are considered typical of convergent boundary volcanism. Related Tertiary intrusive bodies are present from southern Oregon to southern British Columbia. Paleomagnetic studies have shown that Tertiary terranes of the Cascade region in Oregon and southern Washington have been rotated as much as ~30° in a clockwise sense. Pre-Cenozoic rocks are exposed beneath Cascade volcanic rocks north of Mount Rainier and south of Crater Lake. Seismologic studies suggest that the crust may be ~40 km thick in the intervening area.

Geologic mapping and regional geophysical data allow some tentative conclusions concerning the relation of volcanism to tectonism in the Cascade region. Northward from Glacier Peak, Quaternary volcanic centers tend to be areally restricted and widely spaced. This part of the chain constitutes a zone of normal plate convergence. South of Mount Rainier volcanic centers are far more numerous, vary widely in size and longevity, and define a broader belt. The average composition of volcanic rocks in this zone of oblique plate convergence is more mafic and the erupted volume is greater per unit length than in the zone of normal convergence. Mafic magma, similar in composition to that of other convergent plate boundaries, has been erupted throughout the length of the chain during the Quaternary.

Seismologic studies indicate that from Mt. St. Helens northward, the range is characterized by moderate seismicity and strike-slip focal mechanisms, presumably in response to tectonic shear between the Juan de Fuca and North American plates. This area is dominated by horizontal compressional stress; regional heat flow averages ~70 mW/m^2. Generally low seismicity in the Oregon Cascades suggests that plate shear is being accommodated nearly aseismically; moderate rates of seismicity in the California Cascades may be related to either volcanic, geothermal, or tectonic processes. Regional conductive heat flow in the Oregon (and probably California?) Cascades is ~100 mW/m^2; higher heat flow and lower seismicity appear to be consistent with a more extensional regional stress field in the zone of oblique plate convergence. The region between Mounts Hood and Rainier is one of transition. Late Cenozoic approximately north-trending normal and northwest-trending right-lateral strike-slip faults in the Cascades, and east-west fold axes in the Columbia Plateau, are consistent with the net north-south maximum horizontal compressive stress deduced from earthquake focal mechanisms. North-south local alignment of coeval volcanic vents in the zone of oblique convergence reflects the tendency of fluids (here, magma) to form fracture conduits whose azimuths are parallel to the axis of maximum horizontal compressive stress. Concentration of volcanic activity in specific areas may be due to weakening of the crust related to major structural discontinuities. Vertical flow of aqueous fluids in tectonic fractures may also be controlled by the regional stress field, whereas horizontal flow is dominated by highly permeable zones of fragmental material parallel to impermeable volcanic strata.

Maps of residual Bouguer gravity for the Oregon Western and High Cascades show a contiguous zone of gravity lows west of the High Cascades in central Oregon that intercepts the axis of the range near Crater Lake immediately south of Mount Hood. Anomalies on aeromagnetic maps of the Oregon Cascades that have been attributed to subsurface upper-crustal sources are oriented parallel to regional Cas-

cade structures. These gravity and aeromagnetic maps serve to define major structural trends and to delineate fault zones that may localize movement of geothermal fluids. The zone of gravity lows is particularly significant because it coincides with (1) an abrupt east-to-west decrease in heat flow from High Cascades values of ~100 to ~40 mW/m², and (2) substantial east-to-west increase in depth to the lower-crustal conductor defined by magnetotelluric soundings. This zone occurs near the geologic boundary between the Pliocene to Holocene High Cascades and older, Western Cascades volcanic rocks. Many of the hot springs in the Cascade Range are situated in the vicinity of this zone.

Petrologic studies of Cascade volcanoes provide constraints on the residence time of magma in the upper crust. Eruptive histories of polygenetic volcanoes suggest that all Cascade crustal magma reservoirs are compositionally and thermally zoned, from relatively hot mafic magma below upward to more silicic cooler magma. Common occurrence of disequilibrium phenocryst assemblages in intermediate and silic magmas suggests complicated petrogenetic histories involving crustal interaction and magma mixing. Pb isotopic data for local areas show a positive correlation between SiO_2 and radiogenic Pb, indicating a component of relatively young crustal Pb. Growth of large silicic magma chambers, such as existed at Mount Mazama before its climactic eruption and the collapse of Crater Lake caldera, that would support hydrothermal systems requires a high flux of mafic magma and its prolonged residence in the crust. Stratovolcanoes that have erupted small volumes of intermediate magma, such as Mount St. Helens, are apparently underlain by crustal magma reservoirs more akin to columns of limited areal extent, as is also suggested by studies of teleseismic *P*-wave delays and local seismicity. Such features have apparently not existed for sufficient time or have not experienced adequate supply of thermal energy in the form of mafic magma to accumulate large volumes of silicic magma and form shallow magma chambers. Consideration of the appropriate reduction density for stratocones in evaluation of gravity data indicates the presence of dense intrusive roots in the crust beneath all large Cascade volcanoes. Despite lack of evidence for abundant large shallow magma reservoirs, the recent volcanic eruptions throughout the range and the presence of active geothermal systems associated with volcanic centers at Meager Creek in British Columbia, at Lassen Peak, and beneath the floor of Crater Lake suggest that the Cascade Range has considerable potential for geothermal resources.

Evidence on the Structure and Tectonic Environment of the Volcanoes in the Cascade Range, Oregon and Washington, from Seismic Refraction/Reflection Measurements — G3.2

David P. Hill, Walter D. Mooney, Gary S. Fuis, and John H. Healy, U.S.G.S.*

As part of an integrated effort to understand the geothermal potential of the Cascade volcanoes and the volcanic processes with which they are associated, we began conducting wide-angle seismic refraction/reflection experiments around selected volcanoes during the fall of 1978. These experiments employ a recently developed seismic refraction system consisting of 100 self-contained, ultraportable recording units in conjunction with a field-ready data-processing system.

Our initial experiment, which centered on Mount Hood, defined a large variation in the velocity and thickness of the rocks of the upper 4 to 8 km of the crust that is grossly characterized by a regional thinning of the low-velocity, near-surface rocks within 5 to 10 km of the edifice of the volcano. This apparent doming of the "basement" may represent the roof of a batholith emplaced prior to the eruption of the volcanic rocks forming the contemporary mountain. Careful time-term analysis of the data shows a small (~3 percent) anisotropic component to the velocity structure in the upper 8 km with the maximum velocity trending roughly N25°W; this component may be associated with cracks controlled by the regional tectonic stress field. Data from a 270 km long profile extending south from Mount Hood to Crater Lake show that *P*-wave velocity in the crust beneath the Oregon Cascades increases systematically from 6 km/sec at the depth of 3 km to 6.5 km/sec at 25 km depth, below which the velocity is 6.8 km/sec. P_n arrivals were not identified on this profile, but reflected arrivals (P_MP) suggest that the crust may be about 40 km thick. On the basis of reconnaissance profiles in the vicinity of Mount St. Helens, it appears that this same structure extends beneath the Cascade volcanoes in southern Washington.

An extensive active seismic investigation of the crust around Mount Shasta and Medicine Lake was conducted this summer and initial results from this experiment are presented.

Structural and Thermal Implications of Gravity and Aeromagnetic Measurements Made in the Cascade Volcanic Arc — G3.3

R. Couch, M. Gemperle, G. Connard and G. S. Pitts, Oregon State Univ.*

The Cascade Mountain Range in the Pacific Northwest consists of two physiographic provinces: the Western Cascade Range and the High Cascade Range. Lava flows, pyroclastics and interbedded shallow marine sediments of Eocene to Pliocene age form the Western Cascades, and basalts, basaltic andesites, and more siliceous lavas comprise the cones that form the approximately linear belt of Quaternary composite volcanoes of the High Cascades that extend from northern California to British Columbia. High heat flow, recent volcanism and numerous hot springs suggest the Cascade Mountains contain significant geothermal resources.

Recent gravity measurements made in the Cascade Range in Oregon, when reduced with a reduction density of 2.43 gm/cm³ and after removal of anomaly wavelengths longer than 90 km, outline a contiguous series of gravity minima that extend the length of the range from Mt. Hood near the Washington border to the Klamath Graben near the California border. Outlined are the gravity minima and the location of the major composite volcanoes in Oregon. The minima lie along an arc that intersects the axis of the High Cascades near Crater Lake in southern Oregon and near Mt. Hood in northern Oregon. The gravity lows lie along the contact between the Western and High Cascade Mountain west of the Three Sisters and Mt. Jefferson in Central Oregon. We postulate that the gravity minima delineate a major fracture or brecciated zone that approximately parallels the Cascade Range in Oregon and anticipate that fractures in the zone provide access for meteoric waters to hot rocks beneath the High Cascades and control to some extent the circulation of thermal waters.

Spectral analysis applied to aeromagnetic measurements made over central and southern Oregon and northern California indicate near-surface sources cause the high-amplitude short wavelength magnetic anomalies. Source-bottom depths interpreted as Curie-point isotherm depths below the surface show minimums of 5 to 7 km in the area extending from Klamath Lake to Mount McLoughlin, 6 to 8 km in the Crater Lake and Sprague River Valley areas, and 7 to 9 km in the area extending from the Lapine Valley to Newberry Caldera. Assuming a Curie-point temperature of 580°C, these data imply vertical temperature gradients in excess of 70°C/km and heat flow values greater than 120 mW/m² along the Cascade Mountain Range where depths to the Curie-point isotherm are minimal.

Interpretation of the Heat Flow Transition Zone in the Northern Oregon Cascades — G3.4

David D. Blackwell, Southern Methodist Univ.; Richard G. Bowen, Oregon; Donald A. Hull, State of Oregon; Joseph Riccio, Nevada; John L. Steel, Southern Methodist Univ.*

A total of 75 heat flow measurements are presented for part of the Oregon Cascade Range and surrounding provinces including the Willamette Valley, the High Lava Plains, the Deschutes-Umatilla Plateau, and the Blue Mountains between 43°15'N and 45°05'N. The data document a major change in regional heat flow from values of 40 ± 2 mWm^{-2} in the Western Cascade Range and Willamette Valley prov-

*Speaker

inces to 100 ± 5 m WM^{-2} along the boundary between the High Cascade Range and Western Cascade Range provinces. Grouped heat flow profiles along the boundary show the same characteristics: a narrow transition zone between the two regions of heat flow, not exceeding 20 km at any location. The thermal gradient and heat flow values are shown for five grouped profiles form north to south along this transition zone. This thermal variation has a mean half-width of approximately 10 km and is uniform from north to south over the 150 km study area. The thermal change coincides with a north-south line of hot springs and occurs approximately 20 to 30 km west of the axis of the High Cascade Range where the major andesite stratovolcanoes (Mt. Jefferson and the Three Sisters) occur. Based on the average heat flow profile, a temperature cross-section was calculated by the method of continuation and the result is shown. The model implies very high temperature at relatively shallow depth beneath the High Cascade Range and extending approximately 10 km into the Western Cascade Range. Any one of the isotherms from the temperature cross-section could satisfy the heat flow anomaly (i.e., the source does not necessarily have to reach or exceed 700 °C). The resulting implication is that the source does have to be relatively shallow in the crust and relatively intense. Available gravity data indicate a regional change in Bouguer gravity associated with (but opposite in sign to) the heat flow data. A sharp gravity gradient (0 to 10 km west) is superimposed on a background of values decreasing to the east toward the higher elevations of the High Cascade Range and the High Lava Plains. The maximum amplitude of the anomaly is about −25 mgal. There is no similar topographic feature correlated with the heat flow and gravity gradients other than a general increase in elevation as the Cascade crest is approached. Based on the strong correlation of the heat flow and gravity gradient across the transition zone, a "common cause" source assumption was tested. Temperature data are converted to density differences which are used to create the related gravity field. The density differences were formed by subtracting a background temperature characteristic of the Western Cascade Range and multiplying the temperature differences by the coefficient of thermal expansion. The calculated "regional" value was obtained from a block extending from 20-100 km in depth with a density contrast of −0.025 g/cm^3 corresponding to the contrast between a thermally expanding lower crust and upper mantle and a nonthermally expanding section. The total thermal expansion anomaly calculated (−11.5 mgal) is too small to explain the observed of −25 mgal. If the density difference between 4 and 15 km is increased to over 0.1 g/cm^3, then the calculated gravity anomaly comes much closer to fitting the observed data. However, the density difference is much larger than could be caused by thermal expansion alone, and partial melting or a change in rock type within this depth range is required.

It is possible that complexities such as intrusive phenomena or normal faulting could generate the observed difference shallow enough to explain the rapid change in the shape of the gravity profile. In view of the close correspondence between the gravity and heat flow gradients, we prefer the thermal expansion model and interpret the gravity data to indicate that there may be a large zone of partially melted material in the upper part of the crust beneath the High Cascade Range and extending about 10 km west of the High Cascade Range boundary.

Evidence From Gravity Data on the Location and Size of Subvolcanic Intrusions: Preliminary Results — G3.5

David Williams and Carol Finn, U.S.G.S.*

We have examined the results of gravity surveys over about 20 volcanoes covering a wide range of types, sizes and ages, including long dead and eroded systems. Because of the rugged terrain associated with volcanoes, it is critical to choose the correct Bouguer reduction density; otherwise the effect of subsurface features beneath the edifice could be obscured. It is also sometimes necessary to use different reduction densities for different regions around an individual volcano. In this study we are concerned with the proper reduction density for the volcanic edifice alone.

Commonly, the Bouguer reduction density is either an assigned value (usually 2.67 g/cm^3) or is obtained by means of the Nettleton profiling method. In our study we use variations of these methods. Typically, we begin with a modification of the Nettleton profiling method, for which we create a set of gravity and topographic profiles through the volcano. On each profile we display a series of gravity curves corresponding to different reduction densities. If the wavelength of the anomaly caused by the volcanic edifice is sufficiently different from that caused by the subvolcanic stock, it is possible to pick the appropriate reduction density for the edifice. This method fails in cases where the wavelengths are too similar or if another large anomaly occurs, such as one associated with caldera fill. In these situations we have found the most useful alternative technique is to choose a reduction density by analogy to other volcanoes. The bulk densities of all the various volcanic edifices investigated so far fall in the range 2.15 to 2.35 g/cm^3. Lacking better information it is probably safer to use a density in this range than one derived from other methods.

After making careful anomaly separations for a wide range of volcano types, we have been able to make some general observations. The large silicic volcanoes, those with calderas exceding 10 km diameter, produce gravity lows. All other volcanoes produce gravity highs, usually with an anomaly wavelength shorter than that of the mountain. In fact, we have yet to find a volcano whose subvolcanic stock lacks a recognizable gravity signature. However, a small percentage of the volcanoes considered in our study have a regional gravity background so complex that we could not effectively remove them.

The interpreted source of these high and low anomalies differs considerably among the volcanoes studied. For example, in the Cascade Range the young volcanoes were built upon a layer of older volcanic rock, which in turn overlie what appear to be intrusive complexes. The positive gravity anomalies we observe over these young volcanics are probably a result of subvolcanic intrusives penetrating the less dense volcanic layer. The individual intrusive bodies are usually several km wide, but seem more limited in vertical extent. Either the body thicknesses are small or the density contrasts decrease with depth within the volcanic layer. Our interpretations are similar to those for oceanic islands where the positive gravity anomalies are attributed to intrusions emplaced within a thick volcanic pile.

Over the large silicic calderas, the broad gravity lows are caused by the negative density contrast between the granitic pluton and denser country rocks. Evidence for this is usually seen in older systems where erosion has removed the caldera fill.

These observations may be useful in exploration. For example, in the Cascade Range we see gravity highs that delineate shallow, buried plutons which could be sources of mineral or geothermal resources.

Reconnaissance Resistivity Mapping of Geothermal Regions Using Multicoil Airborne Electromagnetic Systems — G3.6

Karen R. Christopherson and Donald B. Hoover, U.S.G.S.*

In early 1981, the U.S. Geological Survey conducted further reconnaissance studies of geothermal regions using airborne EM techniques. Due to the success of a Dept. of Energy-funded 1979 study of five Known Geothermal Resource Areas (KGRAs) in the Basin and Range province using the Input™ (Barringer Research) fixed-wing airborne EM method, additional funding was allocated for studies in four geothermal areas of the Cascade Range. A helicopter-mounted electromagnetic system, Dighem II™ (Dighem Ltd.), was used since fixed-wing EM systems cannot effectively operate in the rugged terrain of the Cascades. Areas flown were Mt. Hood (Oregon), Mt. Saint Helens (Washington), and Medicine Lake Highlands and the Lassen KGRA (California). Surprise Valley, California KGRA was flown to compare with results of the Input survey flown there in 1979.

The Dighem II was flown in the "mapping" configuration using two pairs of transmitting and receiving coils to measure earth response at two different frequencies simultaneously. The standard coil pair is coaxial with the bird and transmits and receives 3600 Hz data. The "whale tail" coil pair is horizontal and measures at 900 Hz. Apparent resistivity maps can then be prepared for each frequency. Although the depth of investigation with this system is not great (maximum penetration of approximately 100m), work done in the past by the

*Speaker

U.S.G.S. using the audiomagnetotelluric (AMT) method showed that most geothermal systems do have a near-surface electrical expression which could be detectable at the Dighem II frequencies. Results of the Dighem study at the Lassen KGRA are compared with the AMT apparent resistivity map at 7.5 Hz, log-averaged for the two orthogonal electric line orientations.

The Dighem survey was flown in the east-west direction with flight lines one-half mile apart. The apparent resistivity map of Dighem data shows four major zones of low resistivity: around Sulphur Works within Lassen National Park, between Devils Kitchen and the Warner Valley, east of Stump Ranch, and the Growler Hot Springs — Doe Mountain area. A small low northeast of Ridge Lake is also evident. The AMT data at 7.5 Hz show approximately these same low resistivity regions and trends with differences due to variations in data density and the greater depth of investigation of the AMT method.

Although the Dighem system samples approximately one-tenth as deep as the AMT method at 7.5 Hz, it defined the same low resistivity trends which may be possible targets for further exploration. As shown by this comparison, an airborne EM technique appears very effective in resistivity mapping of geothermal areas, with a faster data recovery and higher density sampling than many ground reconnaissance techniques.

Magnetotelluric Survey of the Cascade Volcanoes Region, Pacific Northwest G3.7

William D. Stanley, U.S.G.S

The deep electrical structure beneath the Cascade Range volcanoes and adjacent provinces has been studied using data from 97 magnetotelluric soundings, covering frequencies from 0.0015 to 100 Hz. Widely spaced soundings on six east-west profiles spaced from Mt. Lassen on the south to Mt. Rainier on the north enabled comparison of electrical structure in the main ridge of the Cascades to that in the Klamath Mountains-Coast Range terrains, the Basin and Range terrain of eastern Oregon and northern California, and the Columbia Plateau. In addition, more detailed surveys were completed in caldera systems at Medicine Lake, Calif., and Newberry Crater, Oreg., and across the contact between the High Cascades and Western Cascades in central Oregon.

Soundings suitable for interpretation were modeled with one- and two-dimensional models. Some corrective measures were necessary for some of the data that had parallel splits between the transverse electric (TE) and transverse magnetic (TM) data covering the complete frequency range. Procedures modified from those described in Berdichevsky and Dimitriev (1976) were used to treat data with such parallel splits. Models for the MT data can be grouped for three regions: (a) Basin and Range and High Cascades of northern California and eastern Oregon; (b) Western Cascades, Klamath Mountains-Coast Range; and (c) Columbia Plateau.

In the Basin and Range province of northern California-eastern Oregon, as well as in the High Cascades, the 1-D models consist of four layers of significant thickness: (1) A surface layer of resistive volcanics (80-1000 Ω-m) with a thickness of less than 2 km and generally less than 1 km, interpreted to be mostly Quaternary volcanic rocks. (2) A second layer of low to intermediate resistivities (5-80 Ω-m), consisting of Tertiary volcanic rocks and minor amounts of sedimentary rocks. The thickness of this layer is interpreted to be 1-3 km, with an average of about 2 km. (3) A thick (8-20 km) resistive zone representing upper crustal rocks beneath the volcanic rocks of the first two layers. The resistivity values range from 80 to several hundred Ω-m, which indiates they are nonvolcanic, because resistivities in volcanic rocks tend to decrease with depth of burial or age. (4) A lower crustal conductor at depths of 10-22 km with resistivities of less than 5 Ω-m. This conductor has been mapped elsewhere in the western United States, and depths to the conductor in the Basin and Range and Cascades portions of this survey are similar to those observed in the Snake River Plain and reported in Stanley et al (1977). A plausible source for this conductor is the effect of free water at percentages below 3 percent, combined with the pressures at 10-20 km and temperatures above 500°C, which has been documented in lab samples by Olhoeft (1981). It is also possible that partial melt may be a contributing cause in some regions, notably under the ridge of Cascades volcanoes where heat flow is abnormally high and the lower crustal conductor is as shallow as 10-12 km.

A major electrical boundary separates the ridge of the High Cascades peaks on the east from the Western Cascades, Klamath Mountains, and Coast Range on the west. East of the boundary the MT data are mostly 1-D in character, but west of the boundary they are clearly 2-D, due to north-south trending blocks of alternating high and low resistivity. The blocks have cross-strike widths of 5-10 km and vertical extents of less than 5 km. The electrical boundary, which may be traced from west of Mt. Lassen to as far north as Mt. Hood, coincides with gravity, magnetic, and heat flow anomalies. Most of the hot springs in Central Oregon lie on or near this boundary, suggesting that the geothermal water is rising along zones of vertical permeability at the contact between the complex Western Cascades and the more layered, but hotter area beneath the main ridge of the High Cascades.

Models for the Columbia Plateau soundings require more than 3 km of resistive flood basalts above about 3 km or more of conductive materials that could include sediments as well as older volcanic rocks. A lower crustal conductor similar to that observed in the High Cascades and Basin and Range does not appear to exist under the Columbia Plateau.

MT studies of the caldera systems at Newberry Crater in Oregon and the Medicine Lake caldera in northern California failed to indicate the existence of large magma chambers. Furthermore, the deep electrical structure in the vicinity of the calderas was very similar to the structure in adjacent regions, but inside the calderas the surface structure is complicated, inhibiting accurate modeling of deeper zones.

An Inferred Conductivity Distribution in the Vicinity of a Cascade Volcano G3.8

Edward C. Mozley, Univ. of California, Berkeley; and Norman E. Goldstein, Lawrence Berkeley Lab

Magnetotelluric and telluric measurements were acquired in the vicinity of Mount Hood, Oregon, as part of a program to evaluate the geothermal potential of this Holocene stratovolcano, located in the High Cascade Range. The survey area is characterized by rugged topography, with deeply incised glacial valleys surrounding the volcano. The cone, consisting of pyroclastics and flows, was built upon Pliocene flows and intrusions and Miocene Columbia River basalts.

Our field procedure for data acquisition was to occupy four stations simultaneously and thus obtain a five-component magnetotelluric (MT) measurement supplemented by two remote telluric (RT) vector measurements and one remote, two-component magnetic (RTM) measurement. Ten MT sites and fourteen telluric sites were used. Quality of the data were processed using the autopower and cross-power spectral densities of the various MT and RT data sets. The remote magnetic data were used to estimate an accurate signal-to-noise ratio and thus calculate unbiased impedance tensors and tipper vectors.

Two- and three-dimensional modeling techniques were used to interpret these data. The conductivity structure which best fits the frequency response and spatial distribution of these data consists of three overlapping zones of conductivity at different depths. The first extends from the surface to a depth of approximately 2 km. This zone is extremely complex, with large lateral changes in conductivity ranging from 3 to 100 Ω-m. The intermediate zone, which extends from 2 to 12 km, is dominated by a large three-dimensional resistive structure on the southeast side of the volcano which may be a concealed Pliocene intrusive center. The third zone, below 12 km, is characterized by an elongated conductor of 1-3 Ω-m resistivity, striking N 15-20° W and enclosed in a resistive medium. Spatial sampling of the EM fields was not complete enough to provide good resolution of the width and thickness of this structure. The interpretation of the conductivity distribution in the intermediate zone was found to be consistent with the gravity, teleseismic, and seismic refraction data. The presence of the north-south striking conductor below 12 km is consistent with heat-flow data, but has not yet been identified in other geophysical studies.

Heat Flow

Heat Flow at The Geysers, California, USA

T. C. URBAN
W. H. DIMENT
J. H. SASS
U.S. Geological Survey, 345 Middlefield Road, Menlo Park, California 94025, USA
I. M. JAMIESON
Pacific Energy Corporation, 4000 Montgomery Drive, Santa Rosa, California 95405, USA

ABSTRACT

Temperature profiles in two cased holes close to thermal equilibrium, at a locality (38°48.0′ N, 122°49.9′ W) above a known part of The Geysers steam field away from areas of active steam seep, are nearly linear to the maximum depth logged (0.8 km); this indicates that heat transport is largely by conduction. Moreover, extrapolation of these temperatures to the depth of "first steam" (1.5 km at this locality) yields a temperature close to that of the steam reservoir (~240°C). This suggests that heat transport is mainly conductive in the whole interval between the surface and the steam reservoir.

Comparison of the observed temperature profiles with models calculated on the basis of conductive heat flow, a flat-topped reservoir of infinite lateral extent, and steam temperature constant over time suggests that the reservoir is at least several thousand years old and quite possibly ten or more thousands of years old. Beyond about 10 000 yr, temperatures are so close to steady state that no information as to age can be derived.

Although the rate of conductive heat loss above the steam zone is about two orders of magnitude less than the present rate of extraction of heat by producing steam wells, the total loss of heat by conduction over several thousands of years may have exceeded the annual extraction of heat from steam wells by more than a factor of ten.

Heat flow near Cloverdale (38°46.4′ N, 122°58.0′ W) about 13 km west of the holes described above and outside of the zone of known steam, is anomalously high (~4 hfu) with respect to the regional heat flow which is probably about 2 hfu. This high heat flow suggests that anomalous conditions may extend far beyond the area of the known steam field.

INTRODUCTION

The Geysers/Clear Lake region (Fig. 1) falls within the broad zone of transform faulting between the Pacific and North American plates. This zone is characterized by high heat flow (Lachenbruch and Sass, 1973), active faulting (Hearn, Donnelly, and Goff, 1975), and high seismicity (Hamilton and Muffler, 1972; Chapman, 1975). Volcanism, some of it silicic, of Pliocene to Holocene age attests to melting in the upper mantle and crust (Hearn, Donnelly, and Goff, 1975). The volcanic rocks are but a thin veneer over the Mesozoic basement rocks (McLaughlin, 1974; McLaughlin and Stanley, 1975), and no large caldera collapse structures are evident. The region may be one of incipient caldera formation (Smith and Shaw, 1973; Hearn, Donnelly, and Goff, 1975).

A large negative Bouguer gravity anomaly (Fig. 1) exists in the central part of the area (California Div. Mines Geol., 1966; Chapman, 1975; Chapman and Bishop, 1974; Chapman et al., 1974; and Isherwood, 1975). The anomaly may represent a cooling pluton below, but it is not entirely clear whether a significant part of the anomaly results from other causes. An electrical resistivity low corresponds with the gravity low (Stanley and Jackson, 1973; Stanley, Jackson, and Hearn, 1973; McLaughlin and Stanley, 1975).

The very existence of the deep steam zone (T ~240°C, P ~33 bars; White, Muffler, and Truesdell, 1971) at The Geysers (Fig. 1) requires effective sealing mechanisms in the surrounding rocks because the pressures in the steam zone are far below hydrostatic at its depth (up to 3 km or possibly more). Therefore, it is not surprising that there is a linear geothermal gradient suggestive of heat transport by conduction in the rocks above the steam field. On the other hand, it seems somewhat paradoxical that effective seals can exist in an area of such active tectonism.

DATA

The temperature measurements reported here were made with four-conductor cables, thermistors as sensors, and digital multimeters as detectors. Observations were made at discrete depths on some occasions and continuously (300 m/hr) on others. The relative accuracy is better than 0.002°C, and the absolute accuracy about 0.02°C. Some details concerning instrumentation are given by Sass et al. (1971). The high-temperature holes were logged with teflon-insulated cables with probes containing appropriate seals.

The dates of drilling and times of temperature measurement (Table 1) indicate that the thermal disturbances due to drilling subsided to an insignificant level before the last sets of temperature measurements. Flows of water along the annulus between hole and casing were effectively sealed off by cement in C-1. We are not so sure about R-3 and

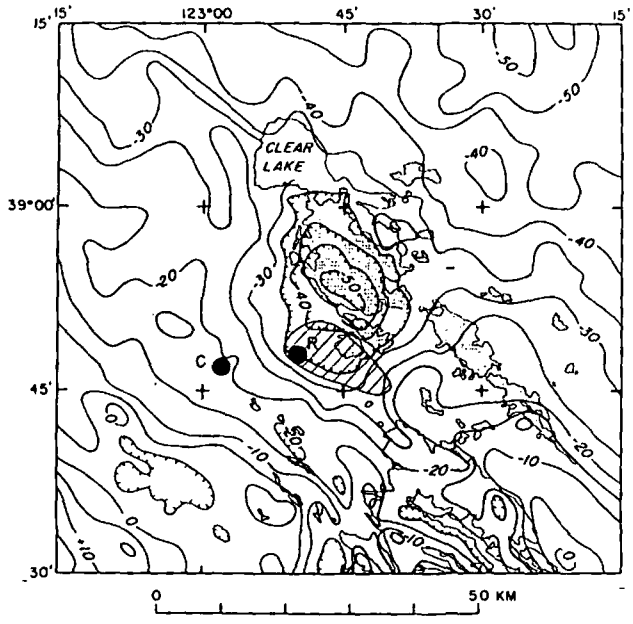

Figure 1. Map of The Geysers-Clear Lake geothermal area showing localities at which temperature measurements were made: C - Cloverdale and R - the area containing holes R-3 and R-4. The areas of Quaternary volcanic rocks (stippled) and older volcanic rock (largely Pliocene, shaded) were generalized from the Ukiah (Jennings and Strand, 1960) and Santa Rosa (Koenig, 1963) sheets of the Geologic Map of California. The approximate limit of the steam zone is hachured. Bouguer anomaly contours are from Chapman and Bishop (1974) and Chapman et al. (1974).

R-4; however, the temperature differences between these two holes are small and the last two sets, taken 10 months apart, differ by no more than a few tenths of a degree. Such differences could be attributed to differences in logging

Table 1. Details of drilling and temperature logging.

	Cloverdale 1	Rorabaugh 3	Rorabaugh 4
Location	38°46.4' N 122°58.0' W	38°48.1' N 122°49.9' W	38°48.0' N 122°49.9' W
Elevation (m)	110	532	532
Hole size (cm)	7.6	31.1	31.1
Drilling started	11/6/72	10/25/68	11/1/68
Drilling completed	11/30/72	2/11/69	2/6/69
Casing cemented in	12/4/72	–	–
Casing (O.D.-cm)	4.2	24.4	24.4
T.D. of casing (m)	250	1020	874
T.D. of hole (m)	250	2126	2200
Dates and depth logged	12/5/72 (250) 12/18/72 (250) 1/22/73 (250) 1/23/74 (250) 3/5/74 (250)	2/2/72 (740) 8/16/74 (305) 5/9/75 (152)	8/17/74 (831) 5/9/75 (152)

rates or to convective motions within the holes (Diment, 1967; Gretener, 1967).

Hole C-1 was cored into graywackes of the Franciscan formation. Samples for thermal conductivity measurement were selected at about 3-m intervals or closer in the lower part of the hole. The thermal conductivities of samples sufficiently cohesive to be machined into discs were measured with a modified divided bar apparatus (Sass et al., 1971). Those too friable to be machined were ground up, the conductivity of the fragment-water mixture was measured (Sass, Lachenbruch, and Munroe, 1971), and values of conductivity were extrapolated to zero water content (Fig. 2).

We have neither samples nor lithologic logs from R-3 or R-4. Conductivity measurements on 10 samples of Franciscan graywacke from outcrops that may be typical of the rocks penetrated in R-3 and R-4 range from 6.3 to 8.0 and average 7.1 ±0.5. The mean is probably too high because the more cohesive samples have been selected. Other rock types that may have been penetrated by these holes are

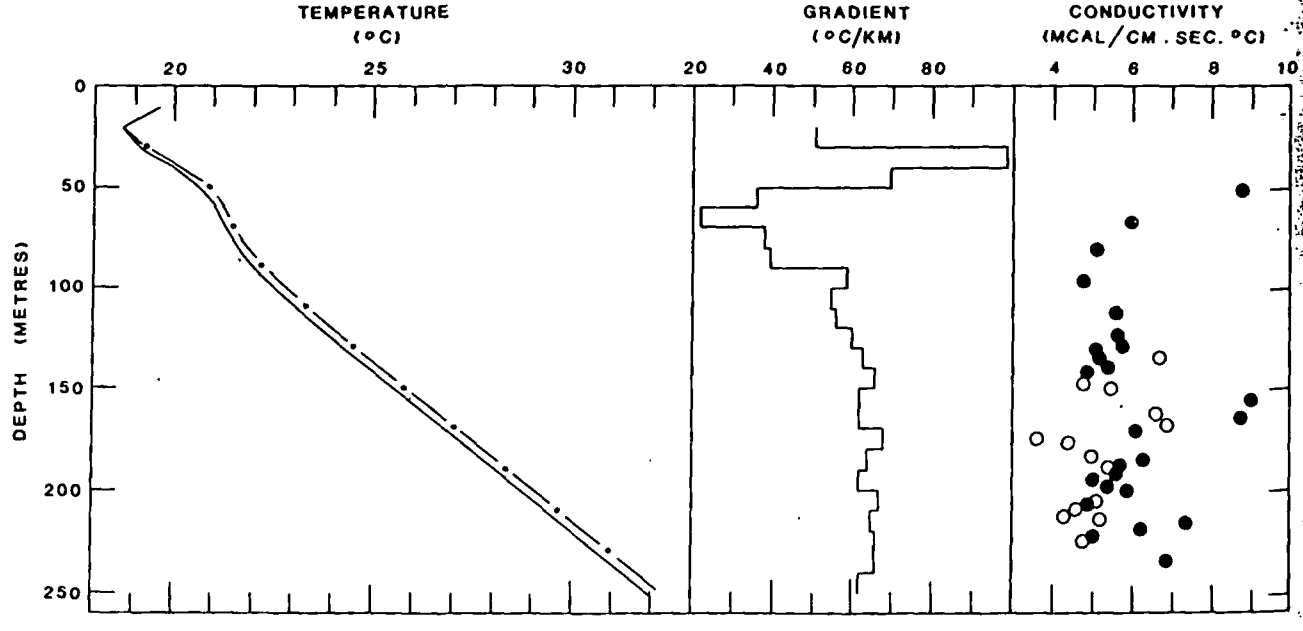

Figure 2. Data from hole C-1 near Cloverdale. The measured temperatures (——) were obtained about 2 yr after drilling (Table 1). Corrections for steady-state terrain have been applied to give corrected temperatures (·–·–·). The gradients shown are derived from the corrected temperatures. The average conductivity of samples sufficiently cohesive to be machined into discs (····) is 5.7 ±0.3 mcal/cm·sec·°C, and that of samples of fragments (°°°°) measured in a cell is 5.2 ±0.5, where the uncertainty is the standard deviation.

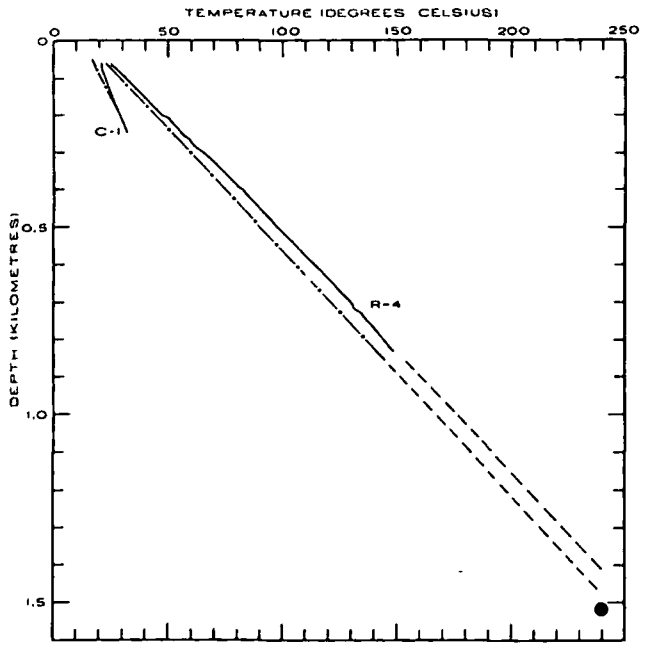

Figure 3. Temperatures in holes C-1 and R-4. Observed temperature (——), observed temperature corrected for terrain (·–·–·), temperatures extrapolated (----) to depth, and temperature of first steam (large dot) are shown.

serpentinite or metabasalts, neither of which have conductivities greatly different from the graywacke (Diment, 1964; Clark, 1966).

We think that the mean conductivity of the rocks penetrated by C-1, R-3, and R-4 lies between 5.0 and 6.5 mcal/cm·sec·°C; therefore we assign heat flows (the product of the terrain-corrected thermal gradient and the thermal conductivity) of 3.2 to 4.1 hfu for C-1 and 7.5 to 9.3 hfu for R-3 and R-4 (1 hfu = 1×10^{-6} cal/cm²·sec). These uncertainties are larger than we should like but make little difference in the particular arguments that follow.

DISCUSSION

The only "equilibrium" temperature data that we have in a locality where the depth to steam is approximately known are from the holes R-3 and R-4 (Table 1). The temperatures in these holes, which are only 87 m apart, are nearly identical and the differences are not readily discernible at the scale of Figure 3.

The depth to steam at this locality is about 1500 m below the surface as determined from steam shows in R-3, R-4, and some adjacent wells. Depth to steam is simply the depth to the first obvious manifestation of steam in an air-drilled hole and might be thought of as the depth to the first large crack in the steam reservoir. Clearly, this depth might be considerably greater than the depth to 240°C that characterizes the steam reservoir (White, Muffler, and Truesdell, 1971).

The temperature profile for R-4 (R-3 is nearly identical), when linearly extrapolated to depth, intersects the reservoir temperature (240°C) at about 1400 m, about 100 m above the depth of first steam (Fig. 3). The fact that the extrapolated temperature curve intersects the reservoir temperature close to, but slightly above, the depth to steam suggests that heat transport in the entire region above the steam reservoir is by conduction.

The extrapolation of temperature to depth was done as follows. A terrain correction was calculated, assuming that the terrain has persisted indefinitely in its present form, that the high gradient (150°C/km) associated with the steam zone extends laterally to 3000 m, and that farther away the geothermal gradient is 64°C/km as it is in C-1. Application of this correction makes the temperature profile nearly linear and permits a reasonable extrapolation to depth. In order to obtain an "observed" temperature profile in the extrapolated interval, we add the effects of terrain to the extrapolated, terrain-corrected profile. A correction for decrease in conductivity with increasing temperature (Birch and Clark, 1940) would raise the curve less than 50 m at 240°C. Although the corrections are rather primitive, they are small, and further refinement is not warranted without more information on the variation of conductivity with depth.

If the region above the steam zone is conductive, the temperature profiles reveal something about the history of the steam zone. Assuming that the top of the steam reservoir is flat and that a temperature gradient existed before the steam zone was formed, models can be constructed that illustrate the temperature history of the interval between the steam zone and the surface. The two models presented are based on an expression given by Carslaw and Jaeger (1959, p. 100, eq. 1) in which a constant thermal diffusivity is assumed (in this case 0.01 cm²/sec). The times shown are those after the formation of the steam zone which is assumed to have maintained a uniform temperature of 240°C. The two sets differ only in their initial temperature gradients (those prevailing before the formation of the steam zone). The first initial gradient (32°C/km) represents a heat flow of about 2 hfu, which is probably representative of the heat flow outside The Geysers/Clear Lake geothermal anomaly (Lachenbruch and Sass, 1973). The second initial gradient (64°C/km) corresponds to a heat flow of about 4 hfu, which has been observed at C-1 some distance west of the known limits of the steam field (Fig. 1). Such a high heat flow requires either melting within the crust or transport of heat by water or magma. In other words, we do not know whether the high heat flow at Cloverdale is a consequence of hydrothermal convection, or betrays a hot magmatic source. If it is the latter, perhaps it would be appropriate to use the higher gradient as the initial gradient for the model over the steam zone. However, the difference between the two models 25 000 yr after formation of the steam zone is negligible (Fig. 4).

Comparison of the curves for the models (Fig. 4) and the observed and extrapolated temperatures (Fig. 3) suggests that: (1) the steam zone has been in place for at least several thousand years and quite possibly 10 000 yr or more; and (2) after 10 000 yr the temperatures are so close to steady state that we could not tell the time of origin of the steam zone even if the data were nearly perfect (which they are not) and the model accurately descriptive (which it is not).

The heat flow above the steam zone is a quantity of some interest for it is a parameter in the energy balance equation of the geothermal system. Although our numbers are rather conjectural, elementary calculations give a rough idea of the size of the parameters involved. The heat flow above the steam zone is about 10 hfu or about 6 hfu above that for The Geysers/Clear Lake thermal anomaly. Assuming that the area of the steam zone is 100 km², the heat escaping by conduction is 1.8×10^{14} cal/yr. Current power production is about 5×10^{8} W (electric) or roughly 3 ×

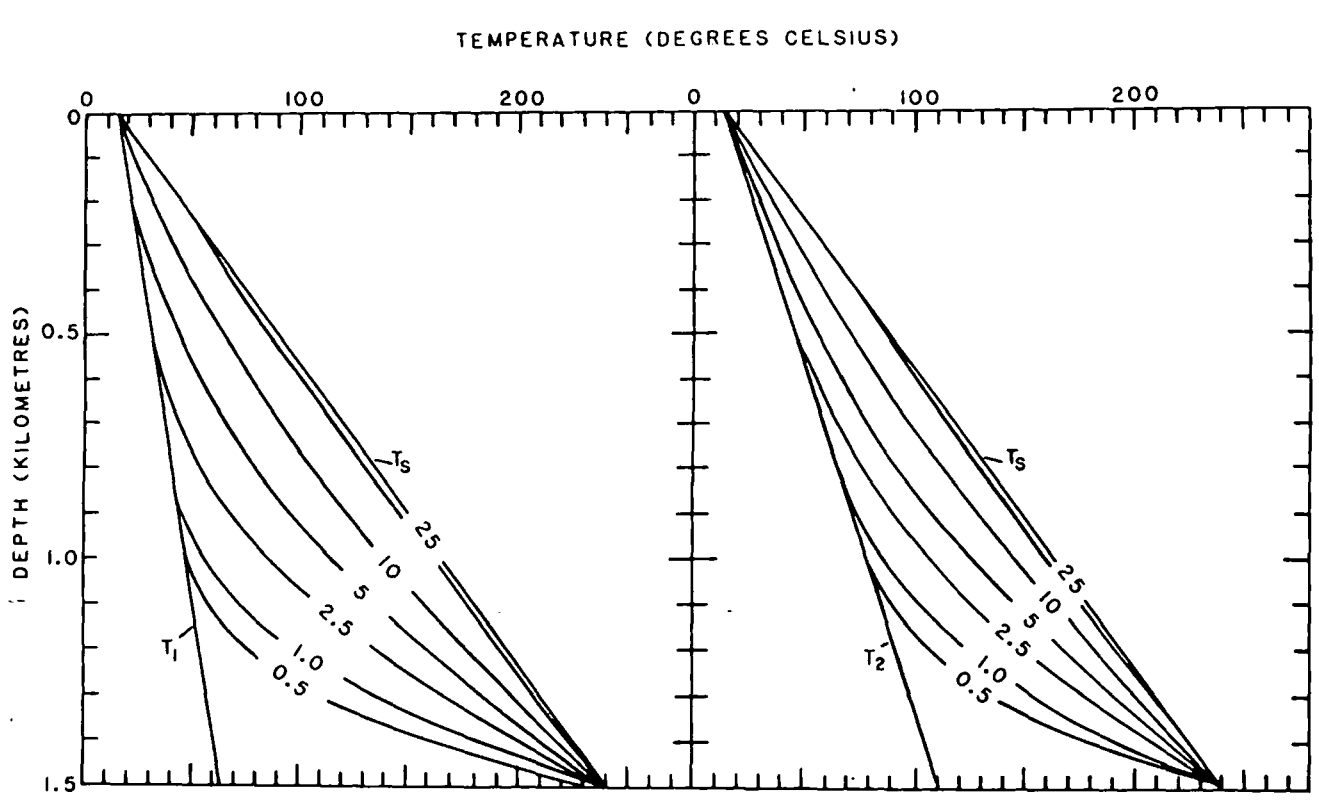

Figure 4. Graphs showing increases in temperature with time (thousands of years) after formation of steam zone (240°C at a depth of 1.5 km). A surface temperature of 14°C and a thermal diffusivity of 0.01 cm^2/sec apply to both sets of curves. The initial temperature distribution (before formation of steam zone) is T_1 = 15°C + (32°C/km)Z for the set on the left and T_2 = 15°C + (64°C/km)Z for the set on the right. T_s is the steady-state temperature.

10^9 W (thermal), which equals 2.4 × 10^{16} cal/yr for the heat extracted from the steam zone. In other words, the heat currently extracted from the ground for power production is two orders of magnitude larger than that escaping by conduction. As previously noted, however, the steam zone appears to be at least 10 000 years old and quite possibly older. If so, heat loss by natural conduction over this period of time may have equaled or exceeded by several orders of magnitude the current yearly withdrawal of energy from the steam wells.

CONCLUSIONS

We conclude that:

1. The thermal regime above the steam zone away from natural vents is conductive, at least at the one locality examined.
2. The linearity of the temperature profiles suggests that the steam zone is at least several thousand years old and quite possibly much older.
3. Although the heat escaping by conduction is two orders of magnitude less than that represented by present steam production, the total conductive loss since the origin of the steam zone may have been several orders of magnitude greater than the present annual steam production.
4. The region of highly anomalous heat flow extends far beyond the area of steam production, as evidenced by the high heat flow near Cloverdale and recent volcanism and hot springs near Clear Lake. This suggests that exploitable resources of hot water or steam may exist over a much wider area than the known steam zone.

ACKNOWLEDGMENTS

We thank R. J. Monroe for the conductivity measurements and T. H. Moses, Jr. for the temperature measurements in the Cloverdale hole and for the initial sets of temperature measurements in R-3 and R-4. A. H. Lachenbruch, L. J. P. Muffler, and Manuel Nathenson suggested significant improvements in the manuscript.

REFERENCES CITED

Birch, F., and Clark, H., 1940, The thermal conductivity of rocks and its dependence upon temperature and composition—Parts I and II: Am. Jour. Sci., v. 238, p. 529-558 and 614-635.

California Division of Mines and Geology, 1966, Gravity map of The Geysers area: Mineral Inf. Service, v. 19, no. 9, p. 148.

Carslaw, H. S., and Jaeger, J. C., 1959, Conduction of heat in solids: London, Oxford University Press, 510 p.

Chapman, R. H., 1975, Geophysical study of the Clear Lake region, California: California Div. Mines and Geology, Spec. Rept. 116, 23 p.

Chapman, R. H., and Bishop, C. C., 1974, Bouguer gravity map of California, Santa Rosa Sheet: California Div. Mines and Geology, 7 p. and map, scale 1:250 000.

Chapman, R. H., Bishop, C. C., Chase, G. W., and Gasch, J. W., 1974, Bouguer gravity map of California, Ukiah Sheet: California Div. Mines and Geology, map, scale 1:250 000.

Clark, S. P., Jr., 1966, Thermal conductivity, *in* Clark, S. P., Jr., ed., Handbook of physical constants: Geol. Soc. America Mem. 97, rev. ed., p. 459-482.

Diment, W. H., 1964, Thermal conductivity of serpentinite from Mayaguez, Puerto Rico, and other localities, *in* A study of serpentinite: The AMSOC core hole near Mayaguez, Puerto Rico: Natl. Acad. Sci.-Natl. Research Council Pub. 1188, p. 92-100.

——, 1967, Thermal regime of a large diameter borehole: Instability of the water column and comparison of air- and water-filled conditions: Geophysics, v. 32, p. 720.

Gretener, P., 1967, On the thermal stability of large diameter wells—an observational report: Geophysics, v. 32, p. 727.

Hamilton, R. M., and Muffler, L. J. P., 1972, Microearthquakes at The Geysers geothermal area, California: Jour. Geophys. Research, v. 77, p. 2081.

Hearn, B. C., Jr., Donnelly, J. M., and Goff, F. E., 1975, Geology of the Clear Lake volcanic field, California: Second UN Symposium on the Development and Use of Geothermal Resources, San Francisco, Proceedings, Lawrence Berkeley Lab., Univ. of California.

Isherwood, W. F., 1975, Gravity and magnetic studies of The Geysers-Clear Lake geothermal region, California: Second UN Symposium on the Development and Use of Geothermal Resources, San Francisco, Proceedings, Lawrence Berkeley Lab., Univ. of California.

Jennings, C. W., and Strand, R. G., 1960, Ukiah sheet: Geologic map of California: California Div. Mines and Geology, scale 1:250 000.

Koenig, J., 1963, Santa Rosa sheet: Geologic map of California: California Div. Mines and Geology, scale 1:250 000.

Lachenbruch, A. H., and Sass, J. H., 1973, Thermo-mechanical aspects of the San Andreas fault system, *in* Kovach, R. L., and Nur, A., eds., Tectonic problems of the San Andreas fault system: Stanford Univ. Pubs. Geol. Sci., v. 13, p. 192-205.

McLaughlin, R. J., 1974, Preliminary geologic map of The Geysers steam field and vicinity, Sonoma County, California: U.S. Geol. Survey Open-File Map 74-238.

McLaughlin, R. J., and Stanley, W. D., 1975, Pre-Tertiary geology and structural control of geothermal resources, The Geysers steam field, California: Second UN Symposium on the Development and Use of Geothermal Resources, San Francisco, Proceedings, Lawrence Berkeley Lab., Univ. of California.

Sass, J. H., Lachenbruch, A. H., and Munroe, R. J., 1971, Thermal conductivity of rocks from measurements on fragments and its application to heat-flow determinations: Jour. Geophys. Research, v. 76, p. 3391.

Sass, J. H., Lachenbruch, A. H., Munroe, R. J., Green, G. W., and Moses, T. H., Jr., 1971, Heat flow in the western United States: Jour. Geophys. Research, v. 76, p. 6376.

Smith, R. L., and Shaw, H. R., 1973, Volcanic rocks as geologic guides to geothermal exploration and evaluation (abs.): EOS (Am. Geophys. Union Trans.), v. 54, no. 11, p. 1213.

Stanley, W. D., and Jackson, D. B., 1973, Geoelectric investigations near The Geysers geothermal area, California [abs.]: Geophysics, v. 38, no. 6, p. 1222.

Stanley, W. D., Jackson, D. B., and Hearn, C. B., Jr., 1973, Preliminary results of geoelectrical investigations near Clear Lake, California: U.S. Geol. Survey Open-File Rept.

White, D. E., Muffler, L. J. P., and Truesdell, A. H., 1971, Vapor-dominated hydrothermal systems compared with hot-water systems: Econ. Geology, v. 66, p. 75.

Geophysical Methods in Geothermal Exploration

GUDMUNDUR PÁLMASON
Orkustofnun (National Energy Authority), Laugavegi 116, Reykjavík, Iceland

ABSTRACT

A review is given of geophysical methods used in the exploration of geothermal resources. More recent developments are emphasized, especially in the field of electric and electromagnetic surveys. Other methods discussed include heat flow (thermal gradient), aerial infrared surveys, gravity, seismic, and magnetic surveys, microearthquakes, and ground noise.

INTRODUCTION

The role of geophysics in the exploration of geothermal resources has been discussed in the past in several review papers (Banwell, 1970, 1973; Bodvarsson, 1970; Combs and Muffler, 1973). A few geophysical methods may be said to be well established in geothermal work, having proved their usefulness in numerous geothermal exploration projects. But improvements are needed, and in recent years there has been a marked effort to test new methods or new variants of older methods. This development is largely associated with the growing interest in geothermal energy following the world-wide rise in oil prices.

The strategy of geothermal exploration is often somewhat hampered by a lack of understanding of the geothermal systems, and by the variability of the geological environment (McNitt, 1970). The hot zones beneath surface thermal fields constitute the outlets of more extensive systems, about which very little is known as regards vertical and horizontal extent. Most exploration work in known geothermal fields is concerned with mapping the geometry of the relatively shallow upflow zone, but it is also possible that the deeper parts may be quite as attractive from an exploitation point of view as the shallower parts. In fact some of the deeper systems may be entirely without an upflow zone; they may be hidden. The most suitable methods of investigating such systems would in part differ from those most suitable for the shallower zones.

A further complication is the thermal state of the fluid—whether one is dealing with a vapor-dominated system (White, Muffler, and Truesdell, 1971) or a hot-water system. Some physical bulk properties of a porous rock, for example, resistivity and density, would be quite different if steam replaced the hot water in the pores. Such ambiguities, like many others in the interpretation of geophysical data, have to be resolved by drilling.

In geothermal exploration the geophysical methods used may be classified in various ways (Bodvarsson, 1970). Direct or thermal methods aim at mapping hot zones thermally and geometrically. Indirect or structural methods have as their objective the investigation of geological structures that may control the movement of the geothermal fluid. Such a classification may be of some help in clarifying the purpose of various kinds of surveys; but it is not very distinct, and many survey methods serve the purpose of thermal and structural investigations at the same time. Methods may also be classified according to the depth range they are particularly suited for, but here again there is a great deal of overlapping and many methods are suitable for a considerable range of depths.

The purpose of this paper is to review the various geophysical methods which are used in geothermal exploration work, and to comment on their usefulness in such work. The thermal and electrical methods are treated first and then the structural methods. Finally some methods which do not fit into this classification, such as microearthquakes and ground noise, are discussed. At the end a brief discussion is given on the suitability of the methods for probing to various depths.

HEAT FLOW (THERMAL GRADIENT)

Anomalous surface heat flow by conduction may be used as an indicator of water convection at depth. The heat flow can be found by drilling shallow holes and measuring the temperature profile and the thermal conductivity of the core rock. In order to interpret the heat-flow values in terms of water convection, it is necessary to know the normal regional heat flow pattern as undisturbed by hydrothermal activity. The average heat flow of the Earth is 1.5 hfu (62.7 mW/m^2), but relatively large systematic variations occur between different geological provinces. The highest values occur near diverging plate boundaries as, for example, in Iceland on the Mid-Atlantic Ridge, where "normal" values are considered to be in the range 1.7 to 7.0 hfu depending on distance from the axial zone (Pálmason, 1973, 1974). In New Zealand (Studt and Thompson, 1969) and in Japan (Uyeda, 1972) a different pattern is found with high values on one side of the volcanic zone and low values on the other side. Such a pattern appears to be characteristic of the so-called subduction zones.

Heat-flow surveys may be suitable for exploring the boundaries of a hydrothermal field. In a uniform geological environment only gradient measurements are needed, but when the thermal conductivity varies from one hole to another it may be necessary to take this into account (Sestini, 1970). In some cases variations in thermal conductivity may

be estimated from the borehole geological logs (Merkel, 1975).

When geochemical indicators of reservoir temperature are available, the gradient measurements may allow an estimate to be made of the minimum hole depth needed to reach the reservoir.

Geothermal gradient or heat-flow surveys are useful for detecting weak heat-flow anomalies, some 5 to 10 times the normal heat flow values, which may be associated with convecting water at relatively great depth. When the heat loss through the surface is greater than about 100 times the normal heat flow, as occurs within hydrothermal areas, simpler and less expensive methods may be used to map the shallow temperature field. Mapping of the temperature at a depth of, say, one meter is useful for the purpose of estimating the natural heat flux from a hydrothermal area, as has been done in great detail in New Zealand (Dawson, 1964; Robertson and Dawson, 1964). As an exploration tool for guiding site selection for deep drilling, the shallow temperature surveys are of limited value because of the low effective depth penetration. They are also rather time consuming.

Thermal gradient surveys have been used in several countries. In Italy a hole depth of about 35 m has been used (Burgassi et al., 1970; Mouton, 1969), but in Iceland a depth of about 100 m is considered necessary. The depth needed will depend on the geological conditions in each area. When the surface rocks are very permeable to a considerable depth as in many areas of active volcanism, gradient surveys may not be practicable at all.

There are several examples demonstrating the usefulness of gradient surveys in geothermal exploration. In Iceland in the low-temperature area within the capital, Reykjavík, gradient surveys have markedly guided the selection of sites for deep production drilling. The gradient surveys have outlined four areas of anomalously high surface gradient, up to 500°C/km (Fig. 1). Production drilling in three of these areas has been successful, yielding water at temperatures of 90 to 140°C, but the fourth area has not been tested yet by deep drilling.

A more recent example is from Marysville, Montana, where a heat flow anomaly was discovered in an area with no known hot-spring activity (Blackwell and Baag, 1973). A favored interpretation of the anomaly was that it was due to a cooling intrusion at depth. Subsequent drillings encountered water at 95°C, showing that the anomaly is due to convecting hot water at depth (Blackwell, personal commun.).

AERIAL INFRARED SURVEYS

At the UN Geothermal Symposium in Pisa in 1970 five papers were presented dealing with infrared aerial surveys of thermal areas in several countries (Cassinis, Marino, and

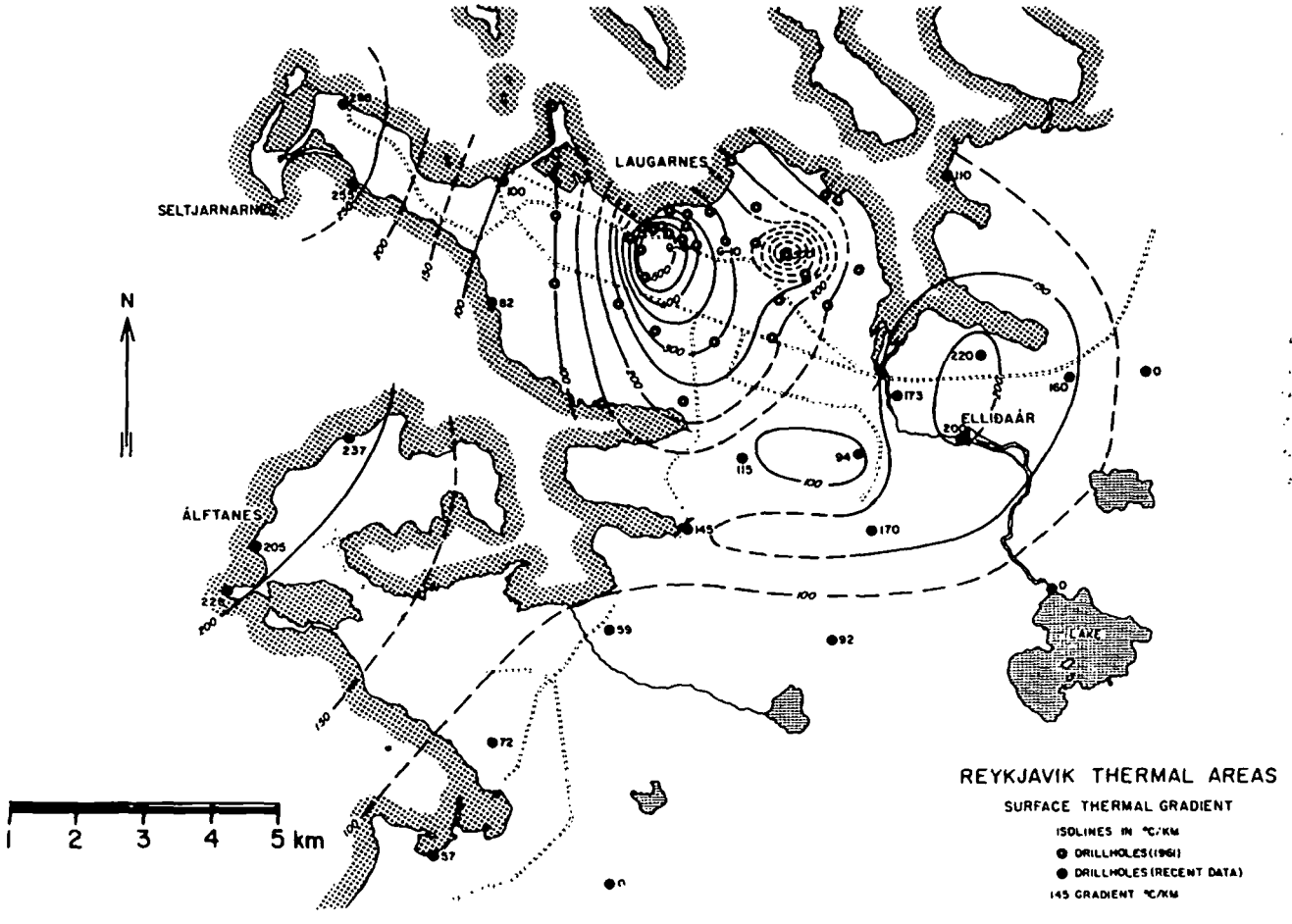

Figure 1. Thermal gradient map of the Reykjavík low-temperature fields, southwest Iceland, showing the anomalies associated with the Laugarnes, Seltjarnarnes, Ellidaár, and Álftanes fields. Based on Bodvarsson and Pálmason (1961) and later additional data.

Tonelli; Gomes Valle et al.; Hochstein and Dickinson; Hodder; Pálmason et al.; 1970). The results indicated that the threshold sensitivity of the method for detecting abnormal heat flows was in the range 150 to 700 hfu, that is, roughly one hundred times the normal heat flow. The main reason for this relatively low sensitivity is the high noise level caused by variations in the thermal properties of surface materials, which affect the thermal radiation sent out. The radiation comes from a very thin surface layer and the method has therefore practically no depth penetration.

It is possible that a more refined processing of the infrared data can lower somewhat the threshold limit for detection of geothermal anomalies. Hase (1974) on the basis of a study in Japan gives a limit of "much less than" 800 hfu.

The infrared method has an important application in mapping the surface distribution of hydrothermal activity. The imagery may be of help in relating the configuration of the hot areas to large-scale structural features, for example, faults or calderas, which may control the discharge of hot fluids to the surface. Furthermore it provides a record of surface activity which may be compared with similar records at a later date to study the effect of exploitation on the surface thermal manifestations.

ELECTRICAL RESISTIVITY SURVEYS

Electrical resistivity surveys have been used in geothermal exploration for over 25 years (Bodvarsson, 1950). Initially they were made with the classical Wenner or Schlumberger electrode configuration using dc current. The depth of penetration was small. In recent years there has been a marked effort to test various other methods, both dc and electromagnetic, partly in an attempt to increase the depth penetration under the conditions of low near-surface resistivities which usually occur in hydrothermal areas, and partly in an attempt to find faster and cheaper methods for reconnaissance surveys of relatively large areas. There is a very great variety of methods that can theoretically be used to map the subsurface resistivity distribution and the problem is to select the most suitable method from the point of view of field operations, processing of the field data, and interpreting the results.

Geothermal reservoirs are often, but not always, characterized by low resistivities. The resistivity depends on a number of parameters, the most important of which are porosity, salinity of the interstitial fluid, and temperature. The effect of a temperature change is greatest at low temperatures, less than 100°C, and becomes small above 200°C. In the deeper parts of a hydrothermal system the resistivity is therefore more affected by porosity and salinity variations than by temperature. An increasing resistivity with depth in a geothermal system may mean that the porosity changes from, for example, intergranular or vesicular porosity to fracture porosity, which is not necessarily adverse from the point of view of fluid production. The effect of temperature is probably greatest in horizontal profiling where lateral variations in resistivity are mapped.

Convenient nomograms showing graphically the relationships between rock resistivity, temperature, porosity, and salinity of the pore fluid have been given by Meidav (1970).

Controlled-Source dc Methods

These methods are the most common ones in geothermal exploration. Electric current is sent into the ground through a pair of electrodes, and the resulting potential difference across another pair or pairs of electrodes is measured. Apparent resistivities are calculated directly from relatively simple formulas. Depth soundings are carried out by varying the electrode distances, and interpretation in terms of a vertical resistivity structure is usually made by means of a set of theoretical curves.

For shallow resistivity surveys any one of the electrode arrays can be used. The Schlumberger array is the most convenient one for depth soundings. It has certain operational advantages over the Wenner array in that fewer movements of the electrodes are required. Furthermore it allows the effect of irregular lateral resistivity variations to be detected and corrected to a certain extent. This may be important in geothermal work. For horizontal profiling, the Wenner array is more convenient because of the regular electrode separations.

The practical limitation on the depth penetration of the Schlumberger array is the long wire needed for the current electrodes. If the resistivity is low, a very high current is needed to obtain a measurable voltage between the potential electrodes. Furthermore, in hydrothermal areas, a very long electrode array usually means that lateral resistivity variations are affecting the measurements, thus making interpretation difficult. Often the maximum current arm (AB/2) of the Schlumberger array is limited to 1 to 2 km in geothermal work.

Dipole arrays avoid some of the difficulties associated with deep Schlumberger soundings in geothermal areas. Very high currents are needed, several tens of amperes, but these are more safely used with short current-electrode separations than with long ones. Under favorable conditions a depth penetration of several kilometers is easily achieved.

Experience shows that apparent resistivities calculated from dipole arrays are rather sensitive to shallow lateral resistivity variations. In dipole depth soundings, care has to be taken to avoid such effects. On the other hand this may also be used to advantage in mapping lateral resistivity variations in a semiquantitative way, somewhat analogously to resistivity profiling. In this case a source "bipole" is commonly used, that is, a pair of current electrodes with a separation that is not necessarily small compared to the distance between the centers of the electrode pairs. The potential electrode pair is then moved around. This method of horizontal mapping goes under various names in the literature, such as bipole-dipole, roving dipole, or simply dipole-dipole method. A well-known example of this is from the Broadlands field in New Zealand (Risk, Macdonald, and Dawson, 1970). Theoretical calculations (Bibby and Risk, 1973) using a hemispheroidal reservoir model have made possible an estimate of the thickness of the low-resistivity reservoir beneath the Broadlands field from the dipole data.

As a general comment regarding the use of dipole methods for depth soundings, it may be said that shallow resistivity mapping is required to properly interpret the dipole soundings. For horizontal reconnaissance surveys, the dipole methods have certain operational advantages, since a relatively large area can be mapped from a single source dipole. This may be especially important in rugged terrain. The calculated apparent resistivities, however, do not necessarily correspond to real resistivities in the underlying formations.

Controlled-Source Electromagnetic Methods

In recent years a considerable effort has been made to test the suitability of various electromagnetic methods in

the exploration for geothermal resources (Keller, 1970; Keller and Rapolla, 1974). These methods have been used in mineral exploration for a long time. In geothermal work the requirement of depth penetration is usually greater than in mineral exploration. This means that lower frequencies have to be used and consequently the equipment becomes somewhat bulkier.

Primary external electromagnetic fields induce eddy currents and secondary fields in a conducting earth. The secondary fields can be detected by a variety of source-receiver arrangements (Keller and Frischknecht, 1966; Vanyan, 1967). Depth soundings are made by varying either the source-receiver distance or the frequency. Interpretation is usually carried out by a comparison with calculated models, often consisting of horizontal layers. The depth penetration may be expressed by the "skin depth" $d = 0.5\sqrt{\rho/\nu}$ km. A plane electromagnetic wave of frequency ν Hz in a medium of resistivity ρ ohm·m is attenuated to 37% of its original amplitude in a distance equal to the skin depth. The expression for the skin depth shows that the electromagnetic methods are particularly suitable for probing through high-resistivity surface materials, but have lower penetration in conductive surface materials.

A two-coil moving source-receiver arrangement ("electromagnetic gun") has been used in New Zealand and in Chile to map resistivity variations to a depth of the order of 30 meters (Lumb and Macdonald, 1970). This method appears to be an attractive alternative to a shallow temperature survey or conventional shallow resistivity profiling, because of its low cost and high speed. The field procedure is straightforward, and apparent resistivities are obtained from calculated curves. The resistivities obtained in the Broadlands field agree reasonably well with those obtained from a Wenner survey.

A somewhat similar shallow test survey was recently carried out by Ward et al. (1975) in a geothermal area in Utah. It was concluded from a comparison of Schlumberger soundings with electromagnetic soundings that the latter are less affected by lateral inhomogeneities than the Schlumberger soundings. A better definition of a shallow low-resistivity area may thus be possible with the electromagnetic method. Deeper soundings to a depth of 1 to 3 km are also discussed in the paper and it is concluded that here also much smaller transmitter-receiver distances are required than the corresponding current electrode separations in the Schlumberger array.

An interesting possibility in electromagnetic soundings is the use of a transient method (time-domain technique). This method, which is based on theoretical work by Vanyan (1967), has been developed further at the Colorado School of Mines, and tested mainly around the Kilauea Volcano in Hawaii (Jackson and Keller, 1972; Keller and Rapolla, 1974). A step-current is introduced into the ground through a pair of electrodes, and the voltage induced in a coil by the time-varying magnetic field is measured as a function of time. Apparent resistivity is obtained as a function of time. It may be shown that early-time resistivity is characteristic of shallow depth and late-time resistivity, characteristic of deeper layers. The method thus has a certain appeal in that information on resistivity variation with depth is obtained in a single measurement. This advantage, however, may be more than offset by the rather complicated processing that is needed to obtain the resistivities, involving synchronous stacking, deconvolution, and smoothing of the recorded signal. Furthermore the interpretation in terms of resistivity variation with depth is not as straightforward as in the dc methods. It appears that the transient method needs to be further tested in geothermal areas by a comparison with more conventional methods before its merits in geothermal exploration can be judged.

Natural Field Methods

Natural electromagnetic fields caused by thunderstorm activity (frequency >1 Hz) and micropulsations in the Earth's magnetic field (frequency <1 Hz) are affected near the surface by the resistivity distribution in the underlying rocks. The depth effect depends on the frequency. Where and when these fields are sufficiently strong in the frequency range of interest, they can be used to explore the resistivity distribution in the depth range of importance in geothermal exploration.

There are essentially three variants of the natural field methods which have been used and appear to be promising in geothermal exploration. They are (1) the ordinary low-frequency magnetotelluric method, utilizing frequencies below about 1 Hz; (2) the audio-frequency magnetotelluric (AMT) method, which utilizes frequencies above 1 Hz, mainly in the range 8 Hz to 20 kHz, and (3) the telluric method. The first two are depth-sounding methods. They might perhaps be classified together, but because of the different frequency ranges the measuring techniques are different. The third method is a horizontal profiling method primarily.

In the magnetotelluric methods one measures the two perpendicular horizontal components of the electric and magnetic fields in the incoming radiation. After spectral analysis or narrow-band filtering an apparent resistivity is calculated from the formula $\rho_a = (0.2/\nu)(E/B)^2$, where E (mV/km) and B (gammas) are the two perpendicular components of the electric and the magnetic field, and ν is frequency (Hz). This relationship is based on the assumption that the resistivity varies only in a vertical direction. Where there are significant lateral resistivity variations, a more complicated relationship is obtained involving the so-called impedance tensor.

The ordinary or low-frequency *magnetotelluric method* is useful for probing to very great depths, from a few to one hundred km or more. Its place is therefore mainly in regional work where information is sought on deep crustal resistivity which may be related to temperature and possible heat sources. The method has been used for this purpose, for example, in Iceland (Hermance and Grillot, 1970, 1974; Hermance, 1973; Björnsson, 1975; Thayer and Hermance, 1975) and gives results in good agreement with those predicted from regional heat flow studies and model calculations (Pálmason, 1973).

A good description of the experimental, analytical and interpretative techniques used in magnetotelluric surveys was given by Vozoff (1972).

In geothermal exploration the direct usefulness of the low-frequency magnetotelluric method is limited because of the large probing depth and a consequent insensitivity to shallower resistivity variations. A much more promising method appears to be the audio-frequency magnetotelluric (AMT) method which employs frequencies mainly in the range 8 Hz to 20 kHz (Keller, 1970; Keller and Rapolla, 1974). The lower part of this range appears to be especially

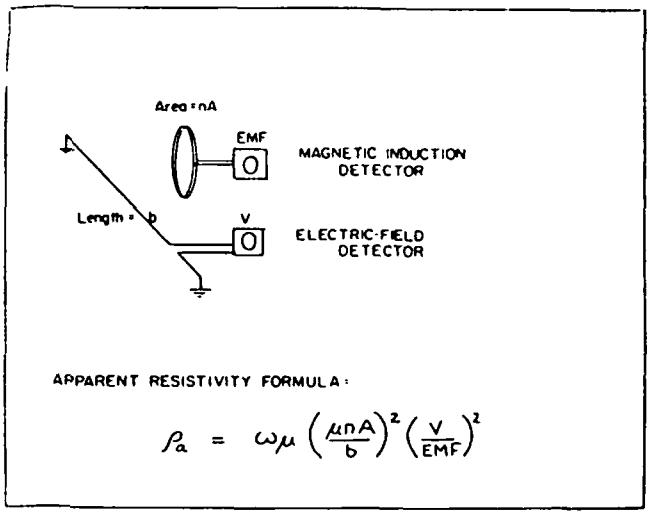

Figure 2. The audio-frequency magnetotelluric method of resistivity mapping (from Keller and Rapolla, 1974).

suitable under the conditions commonly found in geothermal areas. Surveys with this method have been reported from geothermal areas in New Zealand, Hawaii, and Nicaragua.

The instrumentation for an AMT survey is relatively simple, consisting of two narrow-band tuned voltmeters of high sensitivity, measuring the output from a pair of electrodes and from an induction coil (Fig. 2). By varying the tuning frequency, a set of apparent resistivity values are obtained, which can be interpreted by a comparison with theoretical curves, or, approximately, using the skin depth as a depth indicator. Where the electromagnetic noise in the audio-frequency range is sufficiently strong and continuous, the AMT method appears to be a rapid and inexpensive tool for reconnaissance surveys of geothermal areas.

The third natural field method, the *telluric method*, is mainly suitable for reconnaissance of horizontal resistivity variations. It is based on the assumption that telluric currents flowing in extensive sheets are affected by lateral variations in the resistivity structure, which can be caused, for example, by variations in geological structure or by hydrothermal systems. The method requires the simultaneous measurement of the telluric electric field at two stations. From the ratio of the amplitudes of the electric field at the two stations, inferences may be drawn about variations in the underlying resistivity structure. By keeping the base station fixed and moving a field station about, one can thus map resistivity variations in a qualitative way.

The method has been used in geothermal exploration in Nevada (Beyer, Morrison, and Dey, 1975) and in Iceland (Thayer and Hermance, 1975). It appears to be a convenient method for regional surveys in order to detect areas worthy of more detailed exploration by dipole methods.

The three natural field methods that have been mentioned, that is, the low-frequency magnetotelluric method, the audio-frequency magnetotelluric method, and the telluric method all depend on the presence of natural electromagnetic fields that may be of variable intensity in space and time. This dependence is a disadvantage in practical exploration work. On the other hand nature provides the source equipment for these fields so that the field instrumentation required in an exploration program is simpler than with some other methods. Present experience indicates that the telluric profiling method may be useful in regional surveys, and that the audio-frequency magnetotelluric method may be very convenient in more detailed work.

The Schlumberger, dipole, and magnetotelluric methods may be combined to obtain a continuous section from shallow to relatively great depths. An example from a survey across the volcanic zone in northern Iceland through the Námafjall high-temperature field is shown in Figure 3.

SELF-POTENTIAL SURVEYS

A natural field method which may be useful in the study of hydrothermal areas is the self-potential method. Recent

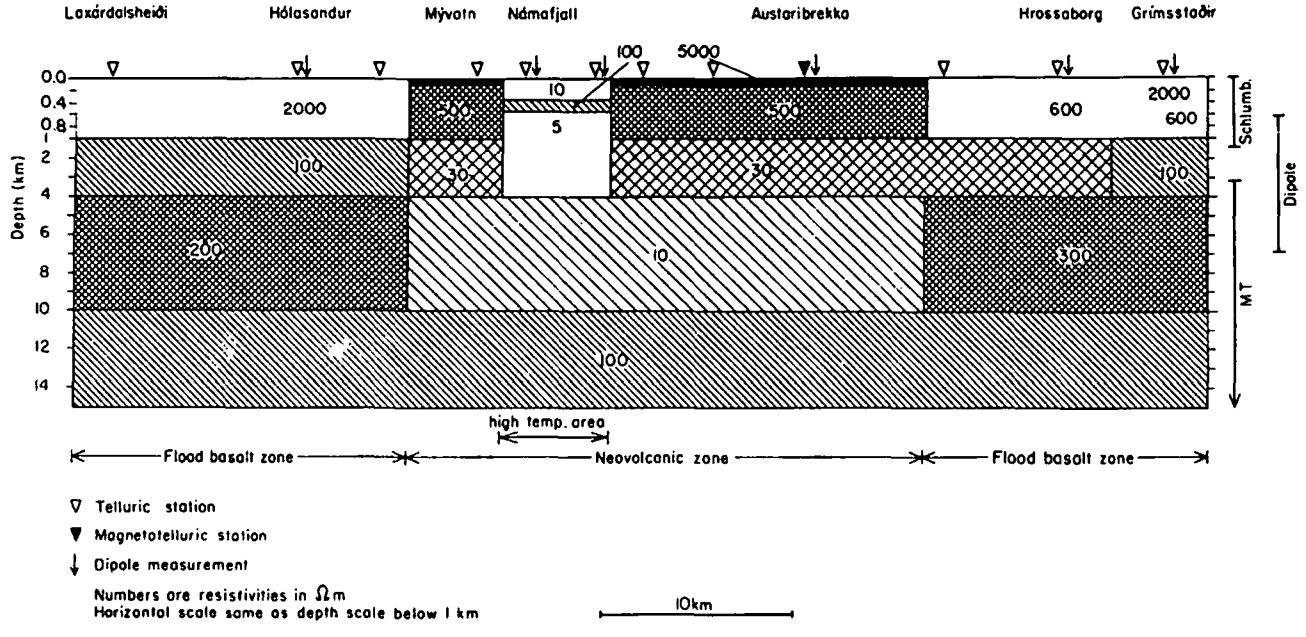

Figure 3. A schematic resistivity section across the volcanic zone in northern Iceland through the Námafjall high-temperature field. Based on Schlumberger, dipole, and magnetotelluric measurements from a joint survey by Brown University, Rhode Island, USA, and the National Energy Authority, Reykjavík (A. Björnsson).

surveys in several hydrothermal areas (Zohdy, Anderson, and Muffler, 1973; Anderson and Johnson, 1973; Rapolla, 1974) have established that electrical dc field anomalies are commonly found associated with hydrothermal activity. One explanation of such electric fields is that they are associated with the movement of conducting geothermal fluids (streaming potentials), when cation enrichment of the water takes place by preferential adsorption of the anions by the rock, leading to a positive self-potential anomaly over a zone of upward-moving water. Although the electric potentials may also be affected by other factors, such as variations in the electrical properties of altered rocks, it appears that further studies of self-potential anomalies associated with hydrothermal areas would be worthwhile in order to evaluate their usefulness in geothermal exploration.

STRUCTURAL METHODS

Gravity, Seismic, and Magnetic Survey Methods

In geothermal exploration the gravity, seismic, and magnetic survey methods are often classified together as structural methods in contrast to the thermal and electrical methods whose main purpose is to outline the geometrical and thermal parameters of a hydrothermal system. In this sense the structural methods are primarily an extension of geological mapping. But there is also considerable evidence showing that some of the anomalies mapped by the structural methods in geothermal areas may be directly caused by the effect of the hydrothermal system on the host rock. The electrical methods, on the other hand, may also be called structural, to the extent that the resistivity variations are caused by variations in porosity. This shows that there is no sharp distinction possible between methods which map the thermal and the structural parameters of a hydrothermal system.

Gravity surveys. These are relatively easy to make in the field, but they are dependent on good elevation control, and this may be the main cost item in the collection of the data. In areas of rugged topography the terrain corrections may be large and time-consuming to make. Therefore the gravity survey method is most suitable in areas of smoothly varying relief. One of the more useful properties of gravity anomalies is that they allow an estimate to be made of the total anomalous mass causing the anomaly, even though absolute density contrasts are not known.

Gravity surveys in geothermal areas in different geological environments appear to indicate that the sources of gravity anomalies may be (1) hydrothermal alteration of reservoir rocks; (2) a high proportion of intrusives; and (3) structural features, for example, faults, calderas, basement structure.

In the New Zealand geothermal areas, positive gravity anomalies are considered to be due to rhyolitic domes and to hydrothermal alteration of the reservoir rocks (Hochstein and Hunt, 1970; Macdonald and Muffler, 1972). In the Imperial Valley of California a correlation has been noted between positive gravity anomalies and high heat flow (Meidav, 1970); the gravity effect is considered to be due to metamorphism of the sedimentary reservoir rocks. In Iceland the high-temperature areas are often associated with major volcanic centers, and positive gravity anomalies commonly found in such areas have been interpreted to be due either to a high proportion of intrusives or to metamorphism, or both.

There appear to be sound arguments for including a gravity survey in any major geothermal exploration program, in particular in areas of smooth relief and poor geological exposures.

One other important use of gravity measurements in geothermal work is connected with exploitation. Withdrawal of fluid from a hydrothermal system may lead to net mass transfers that affect the gravity values measured in the area. Such changes can be very conveniently monitored by measuring the gravity values at a set of fixed bench marks in the area under exploitation, as has been done at Wairakei (Hunt, 1970). The method is cheap and rapid, and is likely to become a standard procedure in any major exploitation of geothermal fields.

Seismic reflection method. This is a major geophysical method in oil exploration, but it has found relatively little use in geothermal work. This is mainly due to the different geological environments of these two energy resources. Most of the geothermal fields that have been explored so far are in volcanic areas where smooth sedimentary series are absent, or are highly disturbed by intrusions. The only case known where the reflection method appears to have been used with some success is in the Matzukawa field in Japan (Hayakawa, 1970).

Seismic refraction method. On the other hand, seismic refraction appears to be quite useful in volcanic areas, especially for structural studies in conjunction with gravity surveys, since the two physical properties, density and seismic velocity, are empirically related. If a gravity survey shows an anomalous mass distribution, it cannot be unambiguously interpreted in terms of structure without further information. A seismic refraction survey is likely to provide such information, for example, on the depth to the anomalous mass.

Refraction profiles have been measured across some of the high-temperature areas in Iceland as part of a regional survey of seismic crustal structure (Pálmason, 1971). A seismic boundary at a depth of about 1 km has been correlated with a geological section in a drill hole in the Reykjanes thermal field. It is of some interest that aquifers appear to be more abundant in a deeper higher-velocity ($v_p = 4.2$ km/sec) material than in a shallower lower-velocity material ($v_p = 3.0$ km/sec) which is more porous (Björnsson, Arnórsson, and Tómasson, 1970, 1972). A similar result, that the highest-porosity rocks are not always the most productive ones, has been reported from the Kawerau geothermal field in New Zealand (Macdonald and Muffler, 1972).

A disadvantage of the seismic refraction method is that explosives or equivalent sources of seismic waves are needed in the field. It is advisable that refraction surveys be preceded by gravity surveys, which may indicate anomalous structures as well as help in planning the refraction survey.

Magnetic surveys. These have been carried out in many geothermal fields. Their use can be either as a structural method or as a method of mapping changes in the magnetization of rocks caused by the hydrothermal fluids. Magnetic anomalies in New Zealand geothermal fields have been interpreted as being due to a conversion of magnetite to

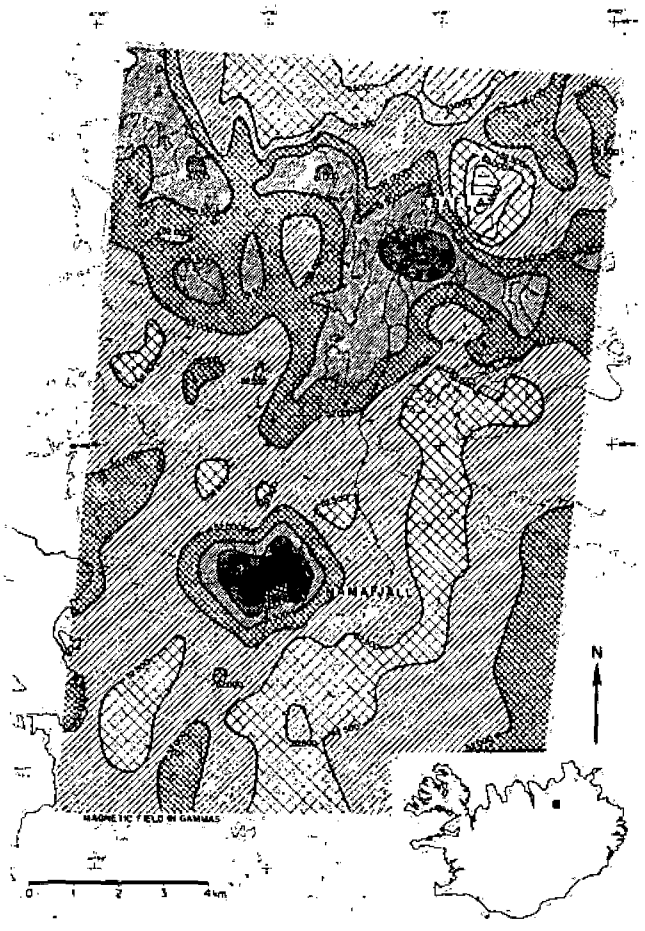

Figure 4. An aeromagnetic map of the Námafjall and Krafla high-temperature fields in northern Iceland, showing negative anomalies associated with the hydrothermal fields (survey by Th. Sigurgeirsson).

pyrite (Studt, 1964). Such an effect would remain in extinct hydrothermal systems.

Opinion has been divided on the usefulness of magnetic surveys in geothermal exploration (Cheng, 1970; Banwell, 1970). The magnetization of different rock units may be quite variable, especially in volcanic areas. Alteration effects in a hydrothermal system would affect a large volume of rock, and the best way to detect such effects is by an aeromagnetic survey, which is less affected by near-surface rocks than a ground survey would be.

There is no doubt that distinct magnetic anomalies are associated with many high-temperature geothermal fields. Examples of this are the Námafjall and Krafla fields in northern Iceland (Fig. 4); but it is also known from other areas that such anomalies are not always present. Test profiles on the ground should therefore be made before one decides on an extensive aeromagnetic survey in a geothermal exploration program.

Magnetic ground surveys have been used extensively in low-temperature fields in Iceland for tracing hidden dykes and faults that often control the flow of thermal water to the surface. Drill holes are then sited so as to cut the dyke at a certain depth. In some cases the dykes or faults act as barriers to horizontal flow and may then form a boundary of the hydrothermal system in one direction.

MICROEARTHQUAKE SURVEYS

Surveys of microearthquake activity (magnitude −1 to 3) in some tectonically active and volcanic areas have shown that geothermal fields are often characterized by a relatively high level of such activity (Ward, Palmason, and Drake, 1969; Lange and Westphal, 1969; Ward and Björnsson, 1971; Ward, 1972; Hamilton and Muffler, 1972). A very extensive study of this kind has been made in the Reykjanes peninsula in southwest Iceland (Björnsson and Einarsson, 1974).

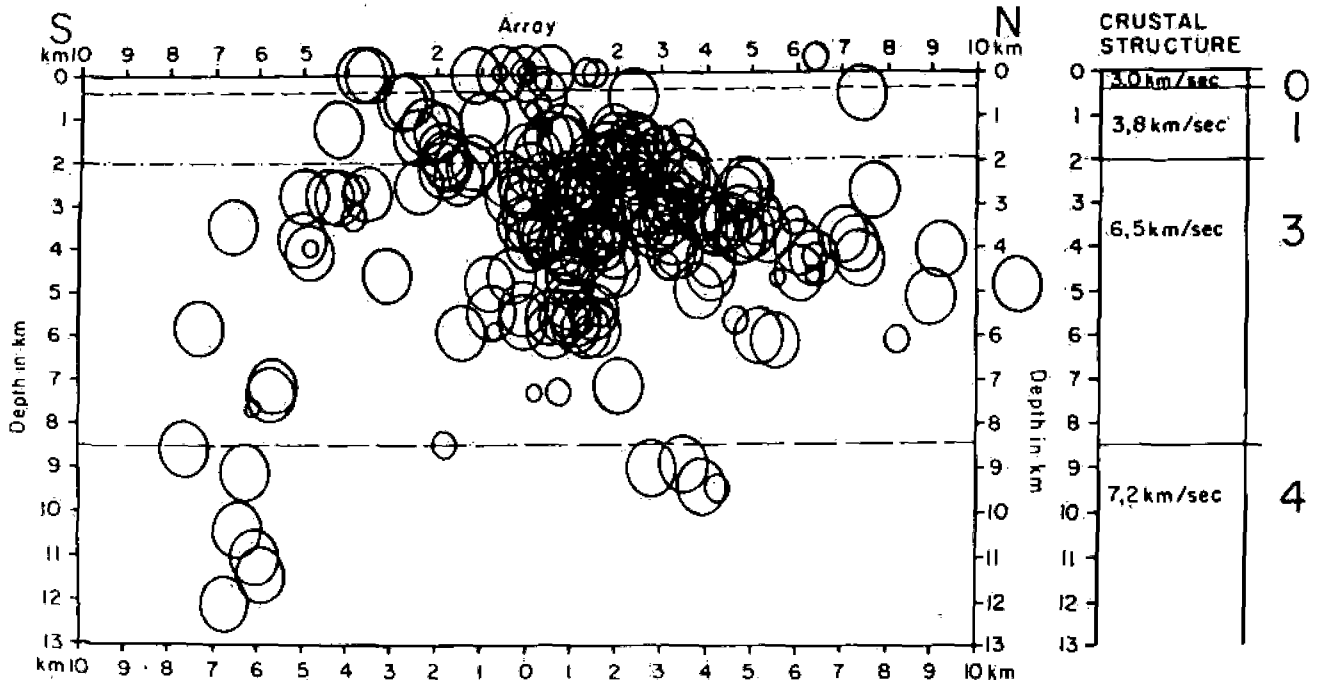

Figure 5. Distribution of microearthquake foci beneath the Krísuvík high-temperature field in southwest Iceland (Ward and Björnsson, 1971).

This area is a part of the axial zone of the Mid-Atlantic Ridge, and includes three high-temperature geothermal fields. Continuous recordings for more than three years have confirmed the earlier indications that the geothermal fields have a fairly consistent microearthquake activity of 3 to 30 events/day, with a focal depth range of 2 to 6 km. The intermediate parts of the axial zone also have a high microearthquake activity, but here the events are more distributed in swarms, with quieter periods in between. Figure 5 shows the distribution of foci beneath the Krisuvik high-temperature field in southwest Iceland (Ward and Björnsson, 1971).

The value of microearthquake surveys for geothermal studies is at present somewhat limited by a lack of understanding of the mechanism causing these events. The microearthquakes may be tectonic in origin, and their depth distribution controlled by the temperature distribution. It is also conceivable that they are somehow related to a penetration of water into hot rock (Lister, 1974). At the present time it appears that the main use of microearthquake surveys may be to try to predict the depth of water circulation in hydrothermal systems, something which cannot easily be done with other methods.

GROUND NOISE SURVEYS

Since the pioneering work of Clacy (1968) on ground noise in a geothermal area in New Zealand, a number of similar studies have been undertaken by others (Whiteford, 1970; Goforth, Douze, and Sorrells, 1972; Luongo and Rapolla, 1973; Cappello, Lo Bascio, and Luongo, 1974; Iyer and Hitchcock, 1974). A high noise level is invariably found in geothermal fields, decreasing with distance from the surface activity. Spectral analysis of the noise shows that surface activity produces noise with frequencies above about 10 Hz. An example is Old Faithful with a spectral range of 8 to 24 Hz. Lower frequencies, down to about 1 Hz, are also usually found and are postulated to be due to deeper water convection. In high heat-flow areas in the Imperial Valley, which are without surface thermal activity, most of the noise energy is in the frequency range 0.5 to 5 Hz.

All the above-mentioned ground noise surveys have been made in areas where hydrothermal activity is known from surface manifestations or other geophysical surveys. If ground noise surveys are to be useful as an exploration tool, the source of the noise must be understood. Douze and Sorrells in 1972 developed a model to explain the spatial distribution of noise in the Mesa area of the Imperial Valley. It involves pressure variations (3 Hz) of about 1 mbar at 1500 m depth. Perhaps such models could be further tested by measurements of the ground noise at various depths in deep boreholes.

APPLICABILITY TO DIFFERENT DEPTH RANGES

The geophysical methods used in geothermal exploration can be discussed and compared on the basis of various criteria such as rapidity, cost, simplicity of field operations, data processing, interpretation, and so on. It appears to be useful also to discuss them in relation to the depth range that each one is suitable for probing. Such a division will of course not be distinct, but may still be of some use. The depth ranges will be denoted as shallow (0 to 200 m), intermediate (200 to 2000 m), and deep (more than 2000 m).

For shallow investigations, the greatest variety of methods is available. Such investigations aim to define the area of hot ground associated with surface thermal activity. They have no place in the search for hidden reservoirs.

An aerial infrared survey is the most convenient and rapid method of mapping surface activity, especially in areas that are little known and are not masked by vegetation. The shallow temperature field is best explored with conventional Schlumberger resistivity profiling. A rapid, low-cost reconnaissance may also be provided by the electromagnetic (EM gun) and the audio-frequency magnetotelluric (AMT) method, although at the present time there is less experience available with these methods in geothermal work than with the conventional dc resistivity methods.

At intermediate depths, the Schlumberger and dipole dc methods appear to be the most suitable ones for outlining low-resistivity zones. The dipole methods can be used either as depth-sounding or as profiling methods. Considerable experience has been gained in using them and in interpreting the measurements. Electromagnetic controlled-source methods may prove to be suitable also, but much less experience has been gathered so far with them. Of the natural field methods the telluric profiling appears to be an effective reconnaissance tool. Aeromagnetic surveys may be feasible if test profiles on the ground indicate variations in the magnetic field that may be associated with a thermal zone at depth.

Heat-flow or gradient surveys are particularly suitable in the search for hidden reservoirs or for exploring the boundaries of a thermal field. They are expensive because drill holes are needed, but they give unambiguous indications of thermal anomalies. They are effective only where the surface rocks are of low permeability.

All of the structural methods may be useful for mapping anomalies whose sources are at intermediate depth. Their usefulness depends on the particular geological environment under consideration.

For deep investigations of hydrothermal reservoirs several methods can be used, but their resolution is smaller than at shallower levels. Gradient surveys for predicting temperature at depth are suitable in impervious surface rocks, and dipole dc methods are suitable for probing the resistivity to a depth of a few kilometers if the shallower resistivities are laterally not very inhomogeneous. The low-frequency magnetotelluric method permits probing resistivity variations from a few kilometers to very great depths.

Of the structural methods, the gravity and seismic refraction methods are particularly suitable for studying deep structures, which may be of importance for controlling the flow of water, or as heat sources. A gravity survey would normally come first because it is cheaper. If major structural anomalies are indicated, they can be studied further by seismic methods. An interpretation based on both gravity and seismic measurements is much more reliable than if based on only one of these methods.

In connection with deep investigations the microearthquake survey should be mentioned. As mentioned earlier, focal depths of microearthquakes may give an indication of the depth of circulation of hot water, although this needs to be confirmed by independent methods. It appears that in order to have a reliable estimate of the average behavior of microearthquake activity, a recording time of several months may be needed.

REGIONAL SURVEYS

Geophysical surveys of geothermal resources are often restricted to the immediate neighborhood of surface thermal activity, as this is the most likely area for the siting of drill holes. It is fairly common knowledge, however, that geothermal systems are more extensive at depth than near the surface. When deep investigations are conducted, they should therefore cover a considerably larger area than would be indicated by the near-surface hot zones. Such regional surveys are also very useful when interpreting data from a more detailed survey near the thermal manifestations. A geological map of a thermal field is more useful when viewed in its regional setting than by itself. The same reasoning applies to geophysical surveys. The added cost of collecting some regional data may well be returned in a more reliable interpretation of the main bulk of the data.

REFERENCES CITED

Anderson, L., and Johnson, G., 1973, The application of self-potential method in the search for geothermal energy (abstract): Geophysics, v. 38, no. 6, p. 1190.

Banwell, C. J., 1970, Geophysical techniques in geothermal exploration: UN Symposium on the Development and Utilization of Geothermal Resources, Pisa, Proceedings (Geothermics, Spec. Iss. 2), v. 2, pt. 1, p. 32.

——, 1973, Geophysical methods in geothermal exploration, *in* Geothermal energy; Review of research and development: UNESCO, p. 41–48.

Beyer, H., Morrison, H. F., and Dey, A., 1975, Electrical exploration of geothermal systems in north central Nevada (abstract): Geophysics, v. 40, p. 174.

Bibby, H. M., and Risk, G. F., 1973, Interpretation of dipole-dipole resistivity surveys using a hemispheroidal model: Geophysics, v. 38, p. 719.

Björnsson, A., 1975, Electrical resistivity of layer 3 in the Icelandic crust: Greinar, V., Soc. Sci. Islandica.

Björnsson, S., Arnórsson, S., and Tómasson, J., 1970, Exploration of the Reykjanes thermal brine area: UN Symposium on the Development and Utilization of Geothermal Resources, Pisa, Proceedings (Geothermics, Spec. Iss. 2), v. 2, pt. 2, p. 1640.

——, 1972, Economic evaluation of the Reykjanes thermal brine area: Am. Assoc. Petroleum Geologists Bull., v. 56, p. 2380.

Björnsson, S., and Einarsson, P., 1974, Seismicity of Iceland, *in* Kristjánsson, L., ed., Geodynamics of Iceland and the North Atlantic area: Holland, D. Reidel, p. 225.

Blackwell, D. D., and Baag, C. G., 1973, Heat flow in a "blind" geothermal area near Marysville, Montana: Geophysics, v. 38, no. 5, p. 941.

Bodvarsson, G., 1950, Geophysical methods in the prospecting for hot water in Iceland (in Danish): Verkfraedingafélags Islands Timarit (Jour. Eng. Assoc., Reykjavik), v. 35, p. 49.

——, 1970, Evaluation of geothermal prospects and the objectives of geothermal exploration: Geoexploration, v. 8, p. 7.

Bodvarsson, G., and Pálmason, G., 1961, Exploration of subsurface temperature in Iceland: UN Conference on New Sources of Energy, Rome, Geothermal Energy; 1, v. 2, p. 91.

Burgassi, P. D., Ceron, P., Ferrara, G. C., Sestini, G., and Toro, B., 1970, Geothermal gradient and heat flow in the Radicofani region (east of Monte Amiata, Italy): UN Symposium on the Development and Utilization of Geothermal Resources, Pisa, Proceedings (Geothermics, Spec. Iss. 2), v. 2, pt. 1, p. 443.

Cappello, P., Lo Bascio, A., and Luongo, G., 1974, Seismic noise survey at Solfatara crater, Phlegraean Fields, Italy: Geothermics, v. 3, no. 2, p. 76.

Cassinis, R., Marino, C. M., and Tonelli, A. M., 1970, Ground and airborne thermal imagery on Italian volcanic areas: UN Symposium on the Development and Utilization of Geothermal Resources, Pisa, Proceedings (Geothermics, Spec. Iss. 2), v. 2, pt. 1, p. 413.

Cheng, W. T., 1970, Geophysical exploration in the Tatun volcanic region, Taiwan: UN Symposium on the Development and Utilization of Geothermal Resources, Pisa, Proceedings (Geothermics, Spec. Iss. 2), v. 2, pt. 1, p. 262.

Clacy, G. R. T., 1968, Geothermal ground noise amplitude and frequency spectra in the New Zealand volcanic region: Jour. Geophys. Research, v. 73, p. 5377.

Combs, J., and Muffler, L. J. P., 1973, Exploration for geothermal resources, *in*, Kruger, P., and Otte, C., eds., Geothermal energy: Stanford, California, Stanford Univ. Press, p. 95–128.

Dawson, G. B., 1964, The nature and assessment of heat flow from hydrothermal areas: New Zealand Jour. Geology and Geophysics, v. 7, p. 155.

Goforth, T. T., Douze, E. J., and Sorrells, G. G., 1972, Seismic noise measurements in a geothermal area: Geophys. Prosp., v. 20, p. 76.

Gomes Valle, R., Friedman, J. D., Gawarecki, S. J., and Banwell, C. J., 1970, Photogeologic and thermal infrared reconnaissance surveys of the Los Negritos-Ixtlan de los Hervores geothermal area, Michoacan, Mexico: UN Symposium on the Development and Utilization of Geothermal Resources, Pisa, Proceedings (Geothermics, Spec. Iss. 2), v. 2, pt. 1, p. 381.

Hamilton, R. M., and Muffler, L. J. P., 1972, Microearthquakes at The Geysers geothermal area, California: Jour. Geophys. Res., v. 77, p. 2081.

Hase, H., 1974, Geologic remote sensing of the Kausatsu-Manza geothermal area, Central Japan: Japan Geol. Survey Rept. no. 252, 56 p.

Hayakawa, M., 1970, The study of underground structure and geophysical state in geothermal areas by seismic exploration: UN Symposium on the Development and Utilization of Geothermal Resources, Pisa, Proceedings (Geothermics, Spec. Iss. 2), v. 2, pt. 1, p. 347.

Hermance, J. F., 1973, An electrical model for the sub-Icelandic crust: Geophysics, v. 38, p. 3.

Hermance, J. F., and Grillot, L. R., 1970, Correlation of magnetotelluric, seismic, and temperature data from southwest Iceland: Jour. Geophys. Research, v. 75, p. 6582.

——, 1974, Constraints on temperature beneath Iceland from magnetotelluric data: Physics Earth and Planetary Interiors, v. 8, p. 1.

Hochstein, M. P., and Dickinson, D. J., 1970, Infra-red remote sensing of thermal ground in the Taupo region, New Zealand: UN Symposium on the Development and Utilization of Geothermal Resources, Pisa, Proceedings (Geothermics, Spec. Issue 2), v. 2, pt. 1, p. 420.

Hochstein, M. P., and Hunt, T. M., 1970, Seismic, gravity and magnetic studies, Broadlands geothermal field, New Zealand: UN Symposium on the Development and Utilization of Geothermal Resources, Pisa, Proceedings (Geothermics, Spec. Iss. 2), v. 2, pt. 1, p. 333.

Hodder, D. T., 1970, Application of remote sensing to geothermal prospecting: UN Symposium on the Development and Utilization of Geothermal Resources, Pisa, Proceedings (Geothermics, Spec. Iss. 2), v. 2, pt. 1, p. 368.

Hunt, T. M., 1970, Net mass loss from the Wairakei geothermal field, New Zealand: UN Symposium on the Development and Utilization of Geothermal Resources,

Pisa, Proceedings (Geothermics, Spec. Iss. 2), v. 2, pt. 1, p. 487.

Iyer, H. M., and Hitchcock, T., 1974, Seismic noise measurements in Yellowstone National Park: Geophysics, v. 39, no. 4, p. 389.

Jackson, D. B., and Keller, G. V., 1972, An electromagnetic sounding survey of the summit of Kilauea Volcano, Hawaii: Jour. Geophys. Research, v. 77, p. 4957.

Keller, G. V., 1970, Induction methods in prospecting for hot water: UN Symposium on the Development and Utilization of Geothermal Resources, Pisa, Proceedings (Geothermics, Spec. Iss. 2), v. 2, pt. 1, p. 318.

Keller, G. V., and Frischknecht, F. C., 1966, Electrical methods in geophysical prospecting: New York, Pergamon Press, 519 p.

Keller, G. V., and Rapolla, A., 1974, Electrical prospecting methods in volcanic areas, *in* Civetta, L., et al., eds., Physical volcanology: Amsterdam, Elsevier Sci., p. 133.

Lange, A. L., and Westphal, W. H., 1969, Microearthquakes near The Geysers, Sonoma County, California: Jour. Geophys. Research, v. 74, p. 4377.

Lister, C. R. B., 1974, On the penetration of water into hot rock: Royal Astron. Soc. Geophys. Jour., v. 39, p. 465.

Lumb, J. T., and Macdonald, W. J. P., 1970, Near-surface resistivity surveys of geothermal areas using the electromagnetic method: UN Symposium on the Development and Utilization of Geothermal Resources, Pisa, Proceedings (Geothermics, Spec. Iss. 2), v. 2, pt. 1, p. 311.

Luongo, G., and Rapolla, A., 1973, Seismic noise in Lipari and Vulcano Islands, southern Tyrrhenian Sea, Italy: Geothermics, v. 2, no. 1, p. 29.

Macdonald, W. J. P., and Muffler, L. J. P., 1972, Recent geophysical exploration of the Kawerau geothermal field, North Island, New Zealand: New Zealand Jour. Geology and Geophysics, v. 15, no. 3, p. 303.

McNitt, J. R., 1970, The geologic environment of geothermal fields as a guide to exploration: UN Symposium on the Development and Utilization of Geothermal Resources, Pisa, Proceedings (Geothermics, Spec. Iss. 2), v. 2, pt. 1, p. 24.

Meidav, T., 1970, Application of electrical resistivity and gravimetry in deep geothermal exploration: UN Symposium on the Development and Utilization of Geothermal Resources, Pisa, Proceedings (Geothermics, Spec. Iss. 2), v. 2, pt. 1, p. 303.

Merkel, R. H., 1975, The generation of thermal-conductivity and heat-flow logs from conventional borehole logs (abstract): Geophysics, v. 40, p. 176.

Mouton, J., 1969, Contribution des méthodes de prospections géothermique, electrique et gravimétrique á l'étude des champs géothermiques de Toscane: Bull. Volcanol., v. 33, p. 165.

Pálmason, G., 1971, Crustal structure of Iceland from explosion seismology: Soc. Sci. Islandica, Publ. 40, 187 p.

——, 1973, Kinematics and heat flow in a volcanic rift zone, with application to Iceland: Royal Astron. Soc. Geophys. Jour., v. 33, p. 451.

——, 1974, Heat flow and hydrothermal activity in Iceland, *in* Kristjánsson, L., ed., Geodynamics of Iceland and the North Atlantic area: Holland, D. Reidel, p. 297.

Pálmason, G., Friedman, J. D., Williams, R. S., Jr., Jónsson, J., and Saemundsson, K., 1970, Aerial infrared surveys of Reykjanes and Torfajökull thermal areas, Iceland, with a section on cost of exploration surveys: UN Symposium on the Development and Utilization of Geothermal Resources, Pisa, Proceedings (Geothermics, Spec. Iss. 2), v. 2, pt. 1, p. 399.

Rapolla, A., 1974, Natural electric field survey in three southern Italy geothermal areas: Geothermics, v. 3, no. 3, p. 118.

Risk, G. F., Macdonald, W. J. P., and Dawson, G. B., 1970, D.C. resistivity surveys of the Broadlands geothermal region, New Zealand: UN Symposium on the Development and Utilization of Geothermal Resources, Pisa, Proceedings (Geothermics, Spec. Iss. 2), v. 2, pt. 1, p. 287.

Robertson, E. I., and Dawson, G. B., 1964, Geothermal heat flow through the soil at Wairakei: New Zealand Jour. Geology and Geophysics, v. 7, p. 134.

Sestini, G., 1970, Heat-flow measurement in non-homogenous terrains; its application to geothermal areas: UN Symposium on the Development and Utilization of Geothermal Resources, Pisa, Proceedings (Geothermics, Spec. Iss. 2), v. 2, pt. 1, p. 424.

Studt, F. E., 1964, Geophysical prospecting in New Zealand's hydrothermal fields: UN Conference on New Sources of Energy, Proceedings, v. 2, pt. 1, p. 380.

Studt, F. E., and Thompson, G. E. K., 1969, Geothermal heat flow in the North Island of New Zealand: New Zealand Jour. Geology and Geophysics, v. 12, no. 4, p. 673.

Thayer, R. E., and Hermance, J., 1975, Geothermal exploration with the telluric-magnetotelluric method in northern Iceland (abstract): Geophysics, v. 40, p. 177.

Uyeda, S., 1972, Heat flow, *in* The crust and upper mantle of the Japanese area, Part I: Earthquake Research Institute, Univ. of Tokyo, Tokyo, p. 97.

Vanyan, L. L., 1967, Electromagnetic depth soundings: New York, Consultants Bureau, 312 p. (Transl. by G. V. Keller).

Vozoff, K., 1972, The magnetotelluric method in the exploration of sedimentary basins: Geophysics, v. 37, no. 1, p. 98.

Ward, P. L., 1972, Microearthquakes: Prospecting tool and possible hazard in the development of geothermal resources: Geothermics, v. 1, no. 1, p. 3.

Ward, P. L. and Björnsson, S., 1971, Microearthquakes, swarms and the geothermal areas of Iceland: Jour. Geophys. Research, v. 76, p. 3953.

Ward, P. L., Pálmason, G., and Drake, C., 1969, Microearthquake survey and the Mid-Atlantic Ridge in Iceland: Jour. Geophys. Research, v. 74, p. 665.

Ward, S. H., Glenn, W. E., Smith, B. D., and Rijo, L., 1975, Electromagnetic soundings in the geothermal environment (abstract): Geophysics, v. 40, p. 177.

White, D. E., Muffler, L. J. P., and Truesdell, A. H., 1971, Vapor-dominated hydrothermal systems compared with hot-water systems: Econ. Geol., v. 66, p. 75.

Whiteford, P. C., 1970, Ground movement in the Waiotapu geothermal region, New Zealand: UN Symposium on the Development and Utilization of Geothermal Resources, Pisa, Proceedings (Geothermics, Spec. Iss. 2), v. 2, pt. 1, p. 478.

Zohdy, A. A. R., Anderson, L. A., and Muffler, L. J. P., 1973, Resistivity, self-potential, and induced-polarization surveys of a vapor-dominated geothermal system: Geophysics, v. 38, p. 1130.

DOE/ID/12079-108
Geothermal Resources Council
Special Report No. 13
May, 1983, p. 121-157

GEOPHYSICAL STUDIES OF ACTIVE GEOTHERMAL SYSTEMS IN THE NORTHERN BASIN AND RANGE

Stanley H. Ward

Earth Science Laboratory/University of Utah Research Institute
420 Chipeta Way, Suite 120
Salt Lake City, Utah 84108

ABSTRACT

Most of the geophysical data in the public domain, acquired in exploration for high temperature geothermal systems in the Northern Basin and Range Province, have been reviewed. Sufficient data are available to compare 14 methods at 13 sites, but only 110 entries occur in the 14 by 13 matrix whereas 182 entries would have been optimum. Only four of the sites studied are believed to be capable of production of commercial electricity while three others probably will be placed in this category in the next few years. For three additional systems believed to be capable of commercial production, insufficient geophysical data are available, in the public domain, to permit review.

On a rating scale of 1 equals good through 4 equals poor, no geophysical method has a mean ranking of 1. Five methods rank about 2, six rank about 2.5, and three rank about 3, while none ranks 4. This ranking system is subjective, but uniformly applied to the question, "what contribution has the method made to understanding the reservoir or the presumed reservoir, at site X". The averages of the evaluations at each site are the rankings given above. No combination of any four methods has been successful at more than one site where "successful" means a ranking of 1 or 2. The most useful of the methods, judging by their average rankings, are heat flow, microearthquakes, gravity, resistivity, and self-potential. The least effective methods are earth noise, reflection seismology, magnetics, magnetotellurics and tellurics. The radiometric and induced polarization methods were excluded from the comparative study due to a paucity of data. The CSAMT method has been included with CSEM for purposes of this comparative study.

Twenty-three applications of geophysical techniques were judged to be good, 29 were judged to be fair, 48 were judged to be questionable, while 10 were judged to be poor. Only 52 of 110 entries in the 14 by 13 matrix were judged to be fair or good; i.e. 53 percent of the geophysical applications gave questionable or poor results. Of the 58 applications where questionable or poor ratings were assigned, 41 applications were judged to be simple failure of the geophysical method to solve the problem at hand. However, 17 of the applications could have been better if improved technology or interpretation were available; some poor technology was applied in the middle of the 1970-80 decade.

Overall, this review provides a somewhat discouraging picture. This may be due in part to inadequate subsurface control and to inadequate survey design, execution and interpretation as a result of lack of experience. I would tend to use heat flow, microearthquakes, gravity, resistivity (or CSAMT), and self-potential methods at all prospects. Once these data were interpreted and correlated, I would then decide whether or not additional geophysical surveying was required and/or justified. All geophysical surveys should be designed and executed only after the geology has been mapped carefully, an integrated interpretation has been made of any and all other available earth science data, and one or more specific questions have been formulated for the survey to answer. The surveys should be designed with one or more conceptual geological models in mind and the density and extent of the geophysical coverage should be designed to provide adequate cover of the area dictated by such conceptual geologic models.

Within this manuscript, I have discussed the advantages and limitations of all of the geophysical methods considered; such a discussion is essential to their evaluation. Examples of overlapping geophysical data sets are given for three igneous-related geothermal systems and for two systems without obvious igneous relationships. No systematic difference in the past application to geophysical exploration for igneous-related systems versus those with no obvious igneous relationships is evident.

1.0 OBJECTIVES

Heat is the essence of a geothermal resource, and its role in the development of such resources, the theme of this symposium, is fundamental. However, this leads to the question of how much surface manifestation of heat is necessary to define a geothermal prospect worthy of exploration. Clearly, heat flow specialists at this conference will attempt to address this question directly. I have been asked to address it indirectly and to concentrate on the other geophysical methods used

in geothermal exploration and to provide a "common thread" among geophysical results for prospect-sized areas of 10 to 1000 square miles.

The objective of this paper, accordingly, is to focus on a comparative study of the problems and successes encountered with the gravity, magnetic, passive seismic, active seismic, self-potential, resistivity, passive electromagnetic, and active electromagnetic methods. Such a comparative study would be incomplete if I failed to draw conclusions as to the cost-effectiveness and preferred role of each of the methods listed above. At the risk of criticism from special interest groups, I shall draw such conclusions. The extent to which I am able to justify my conclusions must be judged by the individual reader in relation to his own experience. With the passing of time and further drilling, my conclusions undoubtedly will be modified. At least, however, I shall have provided a datum to which further analyses may be referenced.

For the purposes of this paper, I use Edmiston's (1982) definition of the Northern Basin and Range Province (Fig. 1). The number and evaluation of geothermal prospects in Figure 1 differs, however, from that given by Edmiston (1982). It is my intent to convey an overview of the contributions made by each geophysical method to understanding the geothermal reservoir of most of the prospects of Figure 1, independent of whether the prospect may now be classified as a discovery or otherwise. In this process, I shall use examples of geophysical data from only a few of the prospects. This permits the paper to be reasonably concise and yet illustrative. The zone of enhanced extension, shown in Figure 1, is my own interpretation.

2.0 DISTRIBUTION OF KNOWN HIGH TEMPERATURE RESOURCES

As noted by Edmiston (1982), "The northern Basin and Range Geologic Province of the western U.S.A. has been widely recognized as a highly prospective area for high-temperature geothermal reservoirs. Yet, only six apparent discoveries resulted from the drilling of 53 geothermal wildcat wells in this area from 1974 through 1981. This relatively lower success rate can be partly attributed to the difficulty of developing accurate geological and geophysical models in this area prior to drilling. However, it may also indicate that large, high-temperature geothermal reservoirs may be less common in this area than thought previously." Mansure and Brown (1982) support Edmiston's observations by forecasting (Figure 2) that the rate of drilling of geothermal wells through the year 2000, will be about the same for northern Nevada as for Roosevelt Hot Springs or Valles Caldera. If this forecast is correct, then the electric power generated by geothermal energy in northern Nevada will indeed be modest, i.e. of the order of 500 MWe. One might conclude, from the works of Edmiston (1982), Mansure and Brown (1982), and Benoit and Butler (1983), that for the whole of the northern Basin and Range Province there will be electrical production, by the year 2000, only at Beowawe, Coso, Desert Peak, Dixie Valley, Humboldt House, Roosevelt Hot Springs and Steamboat Springs. Soda Lake and Long Valley should possibly be added to this list. All of these potential resources lie in the eastern and western margins of the northern Basin and Range Province as Figure 1 shows; these are regions of enhanced crustal extension. Of course, moderate- to low-temperature geothermal resources are much more widespread.

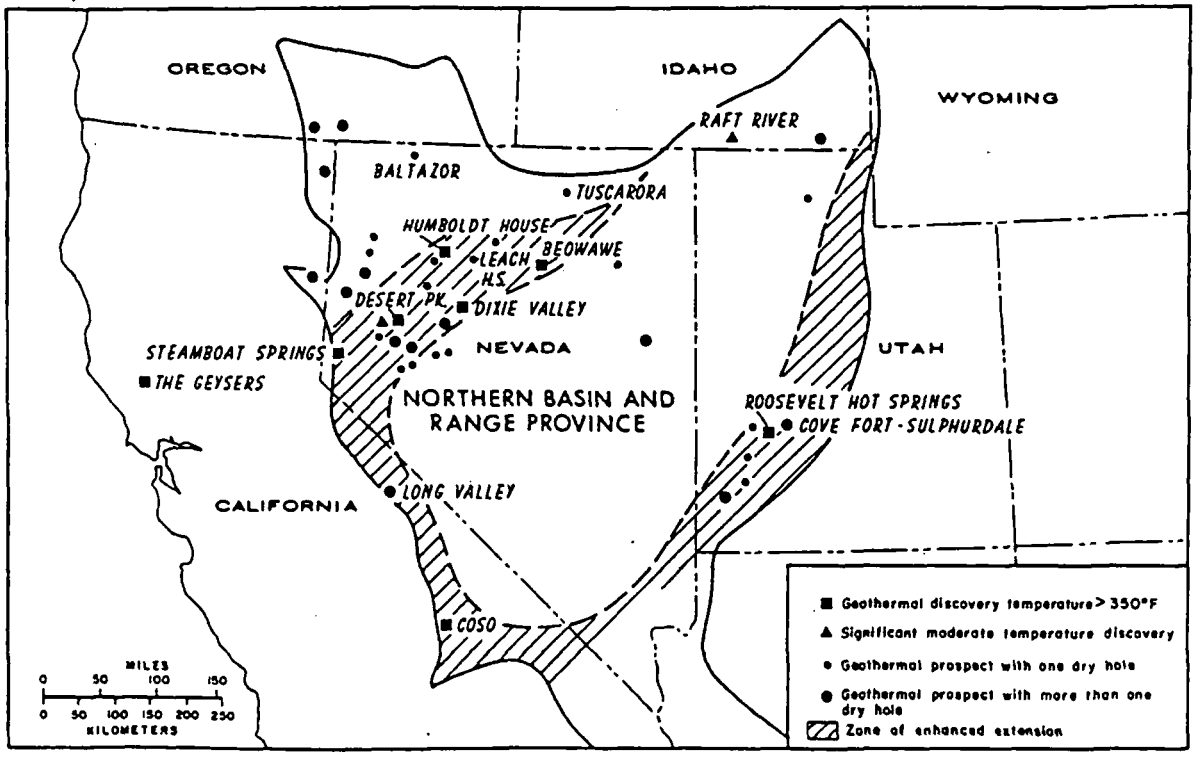

Figure 1. Map showing the location of geothermal discoveries and unsuccessful geothermal wildcat wells in the northern Basin and Range Province (after Edmiston, 1982).

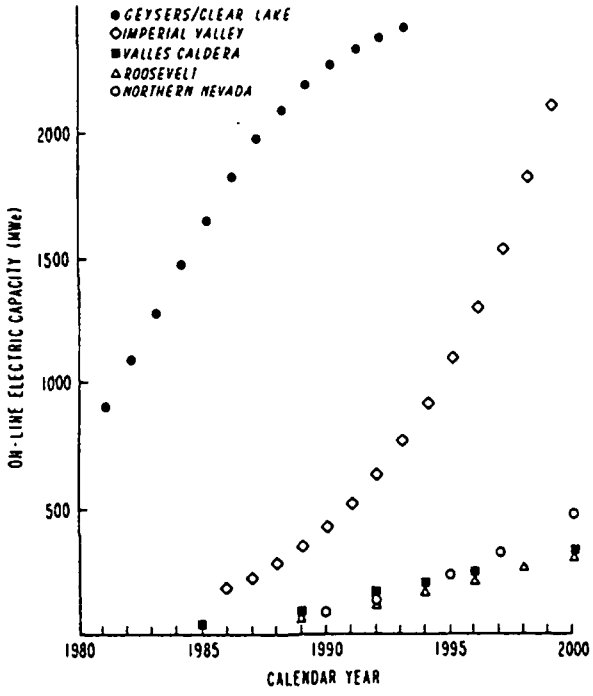

Figure 2. Forecast of geothermal electric power capacity (after Mansure and Brown, 1982).

Is this distribution of known, high temperature resources due to the geologic environment created by enhanced crustal extension, or is it because, in part, that we have not developed geophysical techniques capable of detecting and delineating high temperature resources when these resources are hidden? One would certainly have expected more than one exploitable high temperature resource along the eastern margin of the Basin and Range, if high heat flow, thin crust, and Quaternary volcanism are the key indicators of prime prospecting ground.

3.0 GEOPHYSICAL METHODS FOR GEOTHERMAL EXPLORATION

In the Northern Basin and Range Province, the basic target for geophysical surveys in most cases is a fracture and fault system filled with thermal fluids. The reservoir itself may be relatively near surface as in parts of Roosevelt Hot Springs, or it may be 5,000 to 10,000 feet deep as at Beowawe or Desert Peak. Many geophysical techniques are only capable of delineating the top of the plumbing system and this may or may not contribute to understanding the reservoir (C.M. Swift Jr., pers. com.). With this thought in mind, let us turn to the geologic feature or features each method is usually directed toward, as listed in Table 1. A brief discussion of each target, in relation to the appropriate method, follows.

earth noise

Earth noise is associated with hot spring activity, fluid circulation, and fluid phase changes in geothermal systems, i.e. active hydrothermal processes, and can be a direct indicator of the presence of a geothermal system. This noise, and noise generated in other ways, may also be used to map the three dimensional distribution of velocity and attenuation (Iyer and Hitchcock, 1975; Liaw and McEvilly, 1979; Liaw and Suyenaga, 1982).

microearthquakes

Microearthquakes are associated with active faulting. They can occur more or less continuously, but more frequently they are episodic. Hypocenter locations give information on regions where faults are active and can help determine strike and dip. Fault-plane solutions can yield information on direction of movement. The three-dimensional distribution of seismic wave attenuation may be mapped. By measuring both compressional and shear wave velocities, Poisson's ratio can be computed; it is expected to be low over a vapor-dominated system and high over a fractured, liquid-dominated system. The source parameters seismic moment, stress drop, fault slip, and source radius may be estimated, but their value in reservoir definition and delineation is unknown at present. Minimum hypocentral depth of microearthquakes is useful in estimating the thermal regime surrounding geothermal reservoirs (Ward, R.W. et al., 1979, Majer and McEvilly, 1979).

teleseisms

If a sufficiently distant earthquake is observed with a closely spaced array of seismographs, changes in P-wave travel-time from station to station can be taken to be due to velocity variations near the array. Travel-time residuals are computed as the observed arrival time minus that calculated for a standard earth. A magma chamber beneath the geothermal system would give rise to low P-wave velocities and hence to late observed travel times (Iyer et al., 1979; Reasenberg et al., 1980; Robinson and Iyer, 1981).

refraction and reflection

The seismic refraction and reflection methods can be used to map the depth to the water table, stratigraphy, faulting, intrusions, and geologic structure in general. They may also yield the subsurface distribution of seismic P-wave and S-wave velocities, attenuations and Poisson's ratio. Detection of a characteristic attenuation or a "bright" spot, as found over reservoirs in petroleum exploration, would be a useful feature (Ward, R.W. et al., 1979; Applegate et al., 1981), but this has not been reported clearly for any prospect in the northern Basin and Range province.

gravity

Density contrasts among rock units permit

Table 1.

GEOPHYSICAL TARGETS IN GEOTHERMAL EXPLORATION

METHOD	TARGETS
SEISMIC	
EARTH NOISE	Active hydrothermal processes, distribution of velocity and attenuation.
MICROEARTHQUAKES	Active faulting, fluid filled fracturing.
TELESEISMS	Deep magma chamber.
REFRACTION	Structure, distibution of velocity and attenuation.
REFLECTION	Structure, distibution of velocity and attenuation.
GRAVITY	Structure, alteration, densification, intrusions, distribution of density.
MAGNETICS	Structure, hydrothermal alteration, intrusives, extrusives.
ELECTRICAL	
RESISTIVITY	Faulting, brines, hydrothermal alteration.
INDUCED POLARIZATION	Hydrothermal alteration.
CSEM & SCALAR AMT	Faulting, brines, hydrothermal alteration.
MT / AMT	Structure, deep reservoir, magma chamber ?, partial melt in deep crust or upper mantle.
SELF POTENTIAL	Fluid and heat flow.
TELLURICS	Faulting, brines, hydrothermal alteration.
RADIOMETRIC	Alteration, ^{226}Radon, ^{222}Radium.
HEAT FLOW	Reservoir temperature.

use of the gravity method to map intrusions, faulting, deep valley fill, and geologic structure in general. A subsurface distribution of densities can be obtained in the interpretation process. Densification of porous sediments gives rise to gravity highs over some geothermal systems (Isherwood and Mabey, 1978).

magnetics

Magnetic susceptibility contrasts in the subsurface permit use of the aeromagnetic and ground magnetic methods to map the distribution of magnetite. In some instances, this distribution may be related to rock type, and hence rock units can be mapped. This can be useful in structural studies. In some convective hydrothermal systems, alteration will lead to destruction of magnetite and hence the magnetic method can be used to map zones of active hydrothermal alteration. It can also used to determine the depth to the Curie isotherm (Isherwood and Mabey, 1978).

resistivity, controlled source electromagnetics (CSEM), controlled source audiomagnetotellurics (CSAMT), tellurics and scalar audiofrequency magnetotellurics

These electrical methods are capable of delineating low resistivity associated with brine-saturated and hydrothermally altered rocks in geothermal systems. Usually, the brine and alteration occur predominantly along faults, so these methods may map faults controlling a fractured reservoir. Alternatively, they may map a stratigraphic unit that contains thermal brines and/or alteration. By virtue of resistivity contrasts among rock units, each of these methods can map faults, stratigraphy, intrusions, and geologic structure in general, independent of the presence of brine or alteration (Hoover et al., 1978; Ward, S.H. and Sill, 1982).

induced polarization

The induced polarization method is theoretically capable of mapping the distribution of pyrite and clays, alteration products in convective hydrothermal systems (Zohdy et al., 1973; Risk, 1975a; Chu et al., 1983).

MT/AMT

The tensor magnetotelluric/audiofrequency magnetotelluric method is usually too expensive to be used for mapping the resistivity distribution in the shallow parts of a geothermal system. Hence, it is more logically used to map regional structure, to map the deeper parts of convective hydrothermal systems, to attempt to map magma chambers, and to detect and delineate zones of partial melt in the deep crust and upper mantle (Ward, S.H. and Wannamaker, 1983).

self-potential

Self-potential anomalies over convective hydrothermal systems arise from electrokinetic and

thermoelectric effects. Accordingly, the self-potential method can give information on fluid flow and on the distribution of heat sources in the subsurface. This measurement can be made in the static state or dynamically when an injection experiment is under way (Anderson and Johnson, 1976; Corwin and Hoover, 1979; Sill, 1982a,b,c; Sill, 1983a,b).

radiometric

Gamma-ray spectrometry may be used to map the areal distributions of ^{40}K, ^{238}U, and ^{232}Th. The gamma-ray peaks used are at 1.46 MeV for ^{40}K, 1.76 MeV (^{214}Bi) for ^{238}U, and 2.62 MeV (^{208}Tl) for ^{232}Th. If ^{226}Rn or ^{222}Ra are present in a geothermal system, they will be detected in the ^{214}Bi peak, since they also are daughter products of ^{238}U decay (Ward, S.H., 1981). "An examination of hot-spring waters in Nevada indicates the presence of [^{226}Rn and ^{222}Ra], in varying abundances, in spring systems where $CaCO_3$ is the predominant material being deposited. Systems where silica predominates are relatively low in radioactivity" (Wollenburg, 1975). The use of alpha-cup detectors for radon emanating from geothermal systems has been reported by Wollenburg (1975) and Nielson (1978).

heat flow

Measurement of thermal gradients in holes drilled to 100 m provide shallow temperature data which may be direct evidence of a major source of heat at depth. However, flattening or reversal of thermal gradients frequently occurs so that the data from shallow holes may be misleading. For this reason, temperature gradient holes of 1000 m or greater are frequently employed (Blackwell, this volume).

4.0 THE PRINCIPAL PROBLEMS WITH GEOPHYSICAL METHODS IN GEOTHERMAL APPLICATIONS

The following discussion covers the principal problems encountered in applying geophysical methods in geothermal exploration. To facilitate understanding the problems, the elementary basis for each method is described where considered necessary. The amount of space devoted to each method largely reflects the author's experience. For example, someone who has been directly involved in applying reflection seismology in geothermal exploration would undoubtedly expand upon the section I have written. However, it is expected that most of the significant problems encountered in applying geophysical methods are at least mentioned here.

earth noise

The velocity V, frequency f, wavelength λ, and wavenumber k, of seismic waves are related through the equations

$$V = f\lambda = \frac{2\pi f}{k} \quad . \qquad (1)$$

It has been demonstrated by several workers (e.g. Liaw and Suyenaga, 1982) that hydrothermal processes deep in the reservoir radiate seismic body waves in the frequency band 1 to 100 Hz. Contours of noise power on the surface should delineate these reservoir-associated sources of noise, i.e. the noise radiating from a deep reservoir ought to be evident as body waves of high phase velocity (Liaw and McEvilly, 1979).

Noise in the 1 to 100 Hz band also arises in nearby sources such as freeway traffic, trains, rivers, canals, waterfalls, pipelines, wind, cattle, interfering seismic wavetrains, etc. There is also a distant source of noise of unknown origin. Thus, there is always an ambient noise background upon which any seismic radiation due to hydrothermal processes is superimposed. This ambient noise exhibits a diurnal variation, being lowest in the early morning hours. It may be, in part, related to the diurnal solar heating cycle.

It is well known that seismic noise amplitudes are usually higher over alluvium and soft sedimentary basins than over hard rock. (Iyer and Hitchcock, 1975). Thus, noise power anomalies may merely reflect a local increase in sediment cover. The noise in valley alluvium is dominantly of high-wavenumber, i.e. low velocity, (Liaw and McEvilly, 1979) and is propagated as fundamental-mode Rayleigh waves with the alluvium serving as a waveguide.

An array of geophones spaced on 100 m centers, as commonly used in ground noise studies in the past, would give spurious results because spatial aliasing folds high-wavenumber noise into low-wavenumber noise. The spatial aliasing results in the appearance of noise of erroneously high velocity, such noise being interpreted as body waves, whereas in reality they are surface waves of low velocity. From equation (1), one can see that aliasing of k implies aliasing of V.

If a geophone array is sufficiently dense that wavenumber aliasing is avoided, then the fundamental mode Rayleigh waves can be used to obtain the three-dimensional distributions of velocity and attenuation. These distributions may be used with the horizontal component of the vector wavenumber, via ray tracing, to locate a source region of radiating microseisms (Liaw and McEvilly, 1979). Random directions of propagation (i.e. random vector wavenumbers) are characteristic of low velocity waves (Iyer and Hitchcock, 1975).

Liaw and Suyenaga (1982) detected high-

velocity body waves at Beowawe, but did not detect any body waves at Roosevelt Hot Springs. Liaw and McEvilly (1979) failed to find any body waves at Grass Valley. Thus, even when full f-k analysis is performed, high-velocity body waves may not be detected because they are not generated in all geothermal systems.

microearthquake (MEQ)

Microearthquakes, those having magnitudes between -2 and +3, frequently are closely related spatially to major geothermal systems. Accurate locations of these earthquakes can provide data on the locations of active faults that may channel hot water toward the surface (Ward, P.L. et al., 1969; Lange and Westphal, 1969; Ward, P.L. and Bjornsson 1971; Ward, P.L., 1972; Hamilton and Muffler, 1972).

From the arrival times of P and S waves at 8 to 12 geophones, spaced several kilometers apart, the source location, i.e. hypocenter of a seismic event, is calculated. The locus of many hypocenters may define a fault zone. Using first motion polarities, a fault-plane solution may indicate the type of motion along the fault, i.e. dip-slip vs. strike-slip, etc.

P- and S-wave velocities are retrievable from microearthquake data. Majer and McEvilly (1979) report locally high P-wave velocities in the production zone at The Geysers as determined from refraction surveys. Gupta et al. (1982) used microearthquake data to obtain regional P- and S-wave velocities for The Geysers. Usually, detailed velocity models, obtained from refraction surveys, are used to control the hypocenter determinations of the microearthquakes.

Measurement of either the absorption coefficient or a differential attenuation number called the "Q" may reveal the presence of exceptionally lossy materials in a reservoir due to fluid-filled fractures, or it may reveal the presence of low-loss materials due to steam-filled fractures or to silica- or carbonate-filled fractures. Majer and McEvilly (1979) found a shallow, high Q in the production zone at The Geysers from refraction and microearthquake surveys while they found a deeper, lower Q from the refraction survey. Majer (1978) reported that a refraction survey yielded high Q at Leach Hot Spring due to silica densification of sediments. Gertson and Smith (1979) found high Q over the geothermal system at Roosevelt Hot Springs, using refraction data.

The ratio, K, of P-wave to S-wave velocity may be estimated using a Wadati diagram in which S-P arrival times are plotted versus the P-wave arrival time at many different stations for a single event. From such a plot, a value for Poisson's ratio may be found. Nur and Simmons (1969) observed, experimentally, that fluid saturation in rocks leads to high values of Poisson's ratio ($\sigma \geq 0.25$) while dry rocks exhibit low values of Poisson's ratio ($\sigma < 0.20$). Thus determination of Poisson's ratio in MEQ surveys can conceivably result in determining whether a geothermal reservoir is vapor or water dominated (Combs and Rotstein, 1975; Majer, 1978; Majer and McEvilly, 1979; Gupta et al., 1982).

Table 2 lists values of Poisson's ratio for several geothermal systems. At Baltazor,

TABLE 2

POISSON'S RATIO

GEOTHERMAL SYSTEM	AUTHOR	POISSON'S RATIO
Baltazor	Senturion Sciences	0.22 ?
Coso	Combs and Rotstein	0.16 Steam
Grass Valley	Beyer et al.	0.25 to 0.30 No Anomalies
McCoy	Lange	0.15 Dry or Siliceous Volcanic Fill
		>0.35 Saturated Alluvium
Roosevelt Hot Springs	Ward	0.25 ?
The Geysers	Majer	0.15 to 0.24 Prod. Zone
	Gupta et al.	0.13 to 0.16 Prod. Zone
Tuscarora	Nicholl and Lange	to 0.35 Saturated Allvuvium

Senturion Sciences, Inc. (1977) reported a Poisson's ratio of 0.22. Combs and Rotstein (1975) reported a Poisson's ratio of 0.16 for Coso, a system dominated by vapor, at least in its shallower parts. In Grass Valley, Poisson's ratios of 0.25 to 0.30 were found over the entire region with no apparent anomalies (Beyer et al., 1976). Lange (1980) presented a plan map at McCoy showing contours of Poisson's ratios ranging from 0.15 over the central volcanic fill area, indicating dry or siliceous competent material, to greater than 0.35 over saturated alluvium. P-wave advances accompanied the higher values of Poisson's ratio while P-wave delays accompanied the lower values of Poisson's ratio at McCoy.

I have analyzed microearthquake swarm data apparently related to an east-west fault at Roosevelt Hot Springs and found a Poisson's ratio of 0.25. For the few events directly beneath the geothermal reservoir, a Poisson's ratio of 0.24 was found. Majer and McEvilly (1979) found Poisson's ratios ranging from 0.15 to 0.24 over the production zone at The Geysers, with higher values outside of it. The low Poisson's ratio in part corresponds to a decrease in P-wave velocity. Gupta et al. (1982), in a more extensive study at The Geysers, noted Poisson's ratios of 0.13 to 0.16 over the production zone and values 0.25 and higher outside of it. Nicholl and Lange (1981) reported Poisson's ratios as high as 0.35 due to saturated, fractured, basin fill at Tuscarora. While low values of Poisson's ratio seem to be associated with vapor-dominated systems at Coso and The Geysers, low values at McCoy would appear to be due to silification. A lack of an anomaly in Poisson's ratio at Roosevelt Hot Springs indicates that this parameter may not always contribute useful information about the reservoir.

Amplitude calibration of the microearthquake recording system is essential for meaningful microearthquake surveys. If microearthquake data are recorded on magnetic tape, then amplitude spectra are readily obtained, from which the source parameters seismic moment, stress drop, fault slip, and source radius may be estimated (Majer and McEvilly, 1979). The usefulness of these parameters in reservoir assessment requires extensive study.

For any of the above analyses of microearthquake data, a good model of the subsurface velocity distribution is required. Lack of good velocity control is a principal problem in analysis of MEQ data. Some geothermal systems, such as Roosevelt Hot Springs, have a generally low, episodic level of occurrence of microearthquakes. Swarms of earthquakes occur, but in the intervals between them, insufficient activity may preclude any of the foregoing analyses. Indeed, one can record passive seismic data for a two- or three-week period or longer and come to the conclusion that the geothermal system is unimportant since it is not seismically active.

In some geothermal systems, a fault-plane solution may not be meaningful because the microearthquakes occur not on a single fault, but on several intersecting faults. Caution must be exercised in accepting fault plane solutions in such cases. Further, the active fault(s) might not be related to the fault zone(s) serving as the reservoir.

teleseisms

Steeples and Iyer (1976a,b) found relative P-wave delays of 0.3 sec at stations in the west central part of the Long Valley caldera. Reasenberg et al. (1980) recorded relative P-wave delays of 0.2 sec at Coso. Iyer et al. (1979) found relative P-wave delays as large as 0.9 sec at The Geysers. Robinson and Iyer (1981) reported relative P-wave delays up to 0.3 sec at Roosevelt Hot Springs. Lange (1980) deduced P-wave delays as large as 0.25 sec at McCoy. Berkman and Lange (1980) recorded relative P-wave delays and advances at Tuscarora; the delays were attributed in part to alluvium and in part to zones of hydrothermal alteration, while the advances were attributed to silicification along fracture zones.

While one can speculate that relative P-wave delays are caused by partial melts or magmas, as may be the case at Coso, Long Valley, and The Geysers, they can also be caused by alluvium, alteration, compositional differences, lateral variations in temperature or locally fractured rock (Iyer and Stewart, 1977). Wechsler and Smith (1979) suggest that the P-wave delays found by Robinson and Iyer (1981) at Roosevelt Hot Springs may well be due to fluid-filled fractures or to a compositional change. Thus, teleseismic P-wave delay studies will not always produce conclusive results.

refraction seismology

The seismic refraction method has been used mainly as a geophysical reconnaissance method for mapping velocity distributions and, hence, faults, fracture zones, stratigraphy, and intrusions (Williams et al., 1975; Hill, 1976; Combs and Jarzabek, 1977; Majer, 1978; Ackerman, 1979; Gertson and Smith, 1979). The seismic refraction method does not give resolution of structure as well as does the seismic reflection method. Sentiment today calls for performing seismic refraction at the same time as seismic reflection, with little added cost. Some attempts have been made to map velocity and amplitude attenuation anomalies, of both P- and S-waves, coinciding with a geothermal system (Goldstein et al., 1978b). Beyer et al. (1976), Combs and Jarzabek (1977), Majer (1978), and Gertson and Smith (1979) found anomalous velocities and amplitudes of refracted waves passing through the reservoir region. "The limited results at hand are not easy to explain and are contradictory" (Goldstein et al., 1978b). On the other hand, the potential contribution to the understanding and mapping of the reservoir seems large.

reflection seismology

The seismic reflection method provides better resolution of horizontal or shallow-dipping layered structures than any other method and, hence, is invaluable in mapping stratigraphic geothermal reservoirs of the Imperial Valley type. However, where the structure becomes highly faulted or folded, diffraction of seismic waves occurs at sharp corners and makes the task of interpreting structure difficult.

"Conventional [reflection] seismic surveys appear to give good definition of Basin and Range border faulting and depths to the base of alluvial fill at Roosevelt Hot Springs, UT, Soda Lake, NV, San Emidio, NV and Grass Valley, NV". "One seismic line which crosses the Mineral Mountains at Roosevelt Hot Springs shows little obvious lithologic or structural information within the range itself, or within the reservoir, but substantial structural information along the range front. At Beowawe, extensive and varied digital processing was ineffective in eliminating the ringing due to a complex near-surface intercalated volcanic-sediment section. Majer (1978) found reflection data extremely useful in delineating structure in Grass Valley, NV" (Ward S.H., et al., 1981). At Soda Lake, "in 1977, Chevron obtained modern, 1200% CDP seismic reflection coverage (12 line miles, 48 channel, explosion). The seismic data yielded a complex NE-SW trending graben from the shore of Soda Lake passing south of Upsal Hogback. The reflectors dip to the southwest, consistent with a small basin over the gravity low. The maximum depths of reliable seismic data are governed by a thin basalt unit and vary from 2,400-4,000 ft" (Swift, 1979).

Zoback (1983) has nicely demonstrated the use of seismic reflection data in mapping the style of

initial faulting, infill and subsequent slumping and faulting in some basins in the province.

It is clear from the above remarks that high-resolution reflection seismology is capable of mapping faults, fractures, and stratigraphy in the vicinity of a geothermal system. In the Northern Basin and Range province, it will be useful in mapping range front faults and sedimentary stratigraphy. However, reflection seismology will seldom be of value in outlining reservoirs developed in volcanic, metamorphic, or igneous rocks. It may become almost useless when a volcanic cover or an intercalated volcanic cover is present as at Beowawe. The expense of modern multifold high resolution seismic surveys has deterred their use in geothermal exploration.

gravity

Gravity surveys are used in geothermal exploration as a relatively inexpensive means of obtaining structure and thickness of alluvium. "In the Basin and Range Province, large gravity lows are associated with the low-density basin fill. The gravity anomalies are used to estimate the thickness of the basin fill and the gross structure of the basin, including the location of the major normal faults that are important in understanding a geothermal system. Geothermal-related anomalies in the basins are most commonly residual gravity highs that are interpreted to reflect densification of porous sediments, structural highs, or anomalous geometry of fault zones" (Isherwood and Mabey, 1978). Gravity lows are sometimes found over siliceous magma bodies (Isherwood, 1976). At other times, gravity highs are expected due to rhyolite domes and hydrothermal alteration (Hochstein and Hunt, 1970; Macdonald and Muffler, 1972). Goldstein and Paulsson (1979), Berkman and Lange (1980), and Edquist (1981) found gravity particularly useful in mapping range-front normal faults in the Basin and Range province.

In the above, as in all other geophysical applications, the gravity method is hampered by ambiguity in interpretation. This ambiguity can be reduced by using drill hole, seismic refraction, or seismic reflection data for control. If these additional data are not available, then lateral and vertical resolution of geological features can be quite uncertain.

magnetics

Magnetic surveys, either airborne or ground, have been conducted at many geothermal prospects. Their use can be either for structural mapping or for mapping of changes in the magnetization of rocks caused by hydrothermal fluids. Magnetic anomalies in New Zealand geothermal fields have been interpreted as being due to a conversion of magnetite to pyrite (Studt, 1964). Such an effect would, of course, remain in extinct hydrothermal systems.

"Opinion has been divided on the usefulness of magnetic surveys in geothermal exploration (Cheng, 1970; Banwell, 1970). The magnetization at different rock units may be quite variable, especially in volcanic areas" (Palmason, 1975). "We examine the data from broad magnetic surveys as part of the effort to determine the regional setting ----. Some geothermal anomalies appear to relate to regional magnetic lineaments and zones suggestive of structure within the basement. Regional magnetic data can also be used to estimate the depth to the Curie isotherm by analysis of the spatial wavelengths of the field" (Isherwood and Mabey, 1978).

My own analysis indicates that magnetics have seldom been of major importance in assessing a geothermal reservoir in the Northern Basin and Range province. An outstanding exception appears to occur at Coso, where a magnetic low caused by destruction of magnetite from hydrothermal alteration draws attention, when correlated with other methods, to the heart of the reservoir. A similar magnetic low occurs over a part of the hot spring area at Long Valley (Plouff and Isherwood, 1980), and is interpreted by Kane et al. (1976) as due to magnetite destruction. At the Cove Fort-Sulphurdale KGRA, aeromagnetic data were important for an entirely different reason; structural controls on the potential reservoir could be deduced rather inexpensively from aeromagnetic data.

resistivity

Geothermal reservoirs frequently exhibit low resistivities due to high temperature, enhanced porosity, salinity of the interstitial fluid, and alteration of feldspars and other silicate minerals to clay minerals.

The geothermal use of the Schlumberger and Wenner arrays have been referenced in Banwell and Macdonald (1965), Hatherton et al. (1966), Macdonald and Muffler (1972), Meidav and Furgerson (1972), Zohdy et al. (1973), Arnorsson et al. (1975), Gupta et al. (1975), Stanley et al. (1976), Tripp et al. (1978) and Razo et al. (1980). Dipole-dipole arrays were used in surveys reported by Klein and Kauahikaua (1975), Jiracek et al. (1975), McNitt (1975), Garcia (1975), Beyer (1977), Fox (1978b), Ward, S.H. et al. (1978), Patella et al. (1979, 1980), Baudu et al. (1980), Smith (1980), Wilt et al. (1980a,b), Edquist (1981), and Mackelprang (1982). The bipole-dipole array was first used in geothermal exploration by Risk et al. (1970) and subsequently studied by Bibby and Risk (1973), Keller et al. (1975), Risk (1975a,b), Williams et al. (1975), Beyer et al. (1975), Stanley et al. (1976), Jiracek and Smith (1976), and Souto (1978). The bipole-dipole array achieved early success over broad areas of resistivity lows caused by hydrothermal alteration (Risk et al., 1970; Hohmann and Jiracek, 1979), but it has subsequently fallen into disfavor because of its failure to produce distinctive anomalies over geothermal systems lacking a broad surface manifestation (Dey and Morrison, 1977; Frangos and Ward, 1980).

The Schlumberger array is the most convenient one for depth sounding, i.e. estimation of the thicknesses and resistivities of the layers of a horizontally layered earth. The dipole-dipole array is used for continuous sounding-profiling, i.e. determination of both lateral and vertical variations in resistivity.

Several problems arise with the Schlumberger and dipole-dipole arrays (Ward and Sill, 1982):

1) Natural electric fields constitute noise for resistivity surveys and these result in slower productivity, higher costs, data of poorer quality, or in the extreme, no data at all. Modern data processing reduces but does not eliminate this problem.

2) Cultural features such as fences, powerlines, and pipelines redistribute current from the transmitter electrodes of the resistivity array; spurious resistivity anomalies result.

3) Strong noise voltages are present in the vicinity of powerlines. While notch filtering in the receiver will reduce this noise, it does not eliminate it.

4) Conductive overburden, generally in the form of porous alluvium or weathered bedrock, tends to prevent current from penetrating to the bedrock. Hence detection of bedrock features is less certain when overburden is present than when it is absent. When the overburden is of irregular resistivity, the geologic noise produced by the near-surface features may readily obscure the anomaly due to the target in the bedrock. Of course, this is common to all geophysical methods. Anomalies due to geological heterogeneities of no geothermal significance can also obscure, or partly obscure, the anomaly due to a geothermal system. In the Northern Basin and Range province these usually arise in Quaternary alluvial valley fill, and in salt playas.

5) Much geothermal exploration is done in mountainous terrain where topography can produce spurious resistivity anomalies. In a recent study, Fox et al. (1980) showed that a valley can produce a large, spurious resistivity low which could easily be misinterpreted as evidence for a buried conductor. Similarly, they showed that a hill can produce an apparent resistivity high.

   In general, topographic effects are important where slope angles are 10° or more for slope lengths of one dipole or more. The solution to the problem is to include the topographic surface in numerical models used for interpretation.

6) The practical limitation on the depth of exploration of the Schlumberger array is the large separation needed between current electrodes. A large current electrode separation usually means that lateral resistivity variations outside the array will affect the measurements, thus rendering interpretation difficult. The dipole-dipole array minimizes this difficulty, but introduces a new one; a dipole-dipole array is sensitive to shallow lateral resistivity variations beneath the array whereas a Schlumberger array is not so sensitive (Palmason, 1975).

   The depth of exploration of resistivity arrays is difficult to assess, but values in the range 0.5 km to 1.5 km are common.

controlled source electromagnetic (CSEM) and controlled source audiomagnetotellurics (CSAMT)

The transmitter for a CSEM method consists of either a loop of wire or a grounded bipole. Either source is energized by one or more frequencies in the audio frequency range or by a step current. One or more orthogonal components of magnetic and electric fields are recorded by a receiver located at a distance from the transmitter. The resistivity of the earth is measured by noting the phase and amplitude relationship of the voltage in the receiver to the current in the transmitter. This relationship is termed the impedance and is defined as

$$Z = \frac{V(t + \phi)}{I(t)} \quad , (2)$$

in which both the voltage V and the current I are functions of time. The received voltage is shifted in phase by ϕ relative to the current in the transmitter.

Keller (1970) reviewed the applications of active and passive electromagnetic methods in geothermal exploration. His article constituted a baseline for reference to controlled-source electromagnetic methods (CSEM) in geothermal environments. Subsequent to Keller's review, a number of articles have appeared which illustrate the success and failure of these methods in geothermal exploration. Included are the articles by Lumb and MacDonald (1970), Jackson and Keller (1972), Keller and Rapolla (1974), Jacobson and Pritchard (1975), Morrison et al. (1978), Tripp et al. (1978), Kauahikaua (1981), Wilt et al. (1980c,d), Wilt et al. (1981a,b), Goldstein et al. (1982), and Keller et al. (1982).

The method will suffer all of the problems listed under the *resistivity* section above.

CSAMT is a subset of CSEM, or is a subset of AMT in which the transmitter is a grounded bipole. It is the only CSEM method that does not utilize a loop source. Two orthogonal, horizontal components of electric and magnetic field are measured (as in magnetotellurics). It offers advantages over resistivity methods in that it is faster and suffers less from the effects of lateral resistivity variations when providing

sounding information (Ward, S.H., 1983). The method is used for combined sounding-profiling.

scalar audiomagnetotellurics (AMT)

The AMT method utilizes natural electromagnetic fields in the 10 Hz to 20 kHz band. These natural fields arise in atmospheric lightning discharges worldwide. Hoover et al. (1976), Hoover and Long (1976), Hoover et al. (1978), and Long and Kaufman (1980) described reconnaissance AMT surveys. Keller (1970), Whiteford (1975), Williams et al. (1975), Isherwood and Mabey (1978), and Jackson and O'Donnell (1980) have also reported on its use in geothermal exploration.

Two orthogonal magnetic-field components and two orthogonal electric-field components are measured and the scalar apparent resistivities are computed from the formulae

$$\rho_{a_1} = 0.2T \left|\frac{E_x}{H_y}\right|^2 , \qquad (3)$$

and

$$\rho_{a_2} = 0.2T \left|\frac{E_y}{H_x}\right|^2 , \qquad (4)$$

in which the electric field is measured in mv/km and the magnetic field in gammas; T is the period in seconds. The apparent resistivities are then given in ohm-meters.

The method suffers from all of the problems listed under resistivity, except natural field noise. It exhibits two other problems, however. The first is that the natural fields occasionally are too weak to obtain useful information. The second, and far more important, is that the simple formulae of equations (9) and (10) are totally inadequate for interpretation in two- and three-dimensional terrains, in which the tensor AMT method should be used. However, the scalar AMT method has proven useful for reconnaissance surveys of the type performed by USGS personnel who have fostered its use in this country. Very little application of the method has been made by industry, probably because equipment for the method has not been available commercially.

The CSAMT method is a substantial improvement over scalar AMT insofar as the direction of the inducing fields can be controlled, thus simplifying interpretation in two- and three-dimensional environments. The uncertainty over the strength of the fields used in AMT disappears when CSAMT is used.

MT/AMT

The tensor MT/AMT method utilizes natural electromagnetic fields in the 10^{-4} Hz to 10^{4} Hz band. Below about 1 Hz these fields arise in geomagnetic perturbations brought about by interaction of the solar wind with the main geomagnetic field. Above 1 Hz the natural fields arise in atmospheric discharges worldwide. Three components of magnetic field and two components of electric field are measured. Data acquisition, processing and interpretation must be treated in highly sophisticated ways whose theory is beyond the scope of this paper.

Papers describing application of the tensor MT/AMT method in geothermal areas include Hermance et al. (1975), Hermance and Pedersen (1977), Stanley et al. (1977), Goldstein et al. (1978a), Morrison et al. (1979), Dupis et al. (1980), Gamble et al. (1980), Musmann et al. (1980), Ngoc (1980), Wannamaker et al. (1980), Aiken and Ander (1981), Berktold (1982), Berktold and Kemmerle (1982), Goldstein et al. (1982), Hutton et al. (1982), Martinez et al. (1982), Stanley (1982) and Wannamaker et al. (1983). A comprehensive review of data acquisition, processing, and interpretation for the method, plus a full discussion of the problems it encounters in geothermal exploration, has been prepared by Ward, S.H. and Wannamaker (1983). In the following I seek to summarize their review of these problems.

1) Source dimensions

All of the formulation for interpretation of MT/AMT data over one-, two-, or three-dimensional earths assumes that the MT fields are propagated as plane waves. This assumption was the source of much controversy in the early days of MT, but Madden and Nelson (1964) showed that the field is usually plane wave at frequencies greater than 10^{-3} Hz in mid latitudes.

At frequencies below 1 Hz, the primary concern appears to be whether or not the fields due to equatorial and auroral electrojet ring currents in the E-layer of the ionosphere can be treated as planar. Hermance and Peltier (1970) and Peltier and Hermance (1971) have studied the effects of such ring currents. They conclude that in conductive environments, the plane-wave assumption is valid in the frequency range 10^{-4} Hz to 1 Hz. However, significant errors can occur at frequencies less than 10^{-1} Hz in areas where high resistivities are encountered if measurements are made within 500 km of the position vertically beneath the electrojet.

At frequencies above 1 Hz, the proximity of lightning discharges becomes important. Bannister (1969) studied the fields radiated from a vertical electric dipole over a homogeneous earth and concluded that the plane-wave assumption is valid for distances greater than seven skin depths from the source.

If however, the plane wave assumption is not valid, then the extra field components associated with non-planar waves will be processed so as to produce bias in MT estimates.

2) Random noise

Random noise may arise in a) the electrodes for E-field measurement via chemical disequilibrium, b) movement of the E-field wires in the earth's magnetic field when wind agitates them, c) movement of the H-field sensors in the earth's magnetic field due to wind or seismic activity, d) microphonics in the H-field sensors due to any motion, e) thermal noise in the E- and H-field preamplifiers, f) quantization noise in A/D converters, g) *non-linear* behavior of the total recording system, h) sporadic departure from plane wave propagation, and i) sporadic cultural noise due to power lines, telephone lines, rail electrification, pipeline corrosion protection, radio interference, and the power sources in the recording instrumentation. The processing system must be designed to minimize, evaluate, and place statistical limits on errors introduced into MT transfer functions by *random noise*.

3) Systematic noise

Most of the noise sources described in 2) above are also capable of introducing systematic noise into estimates of the MT transfer functions. As Stodt (1983) points out, the systematic noise must be treated independently of the random noise in any statistical evaluation of noise in MT data. As a result of systematic noise, biased estimates of the MT transfer functions result. To attempt to eliminate this problem, the use of a remote reference has become common practice (Gamble et al., 1979a,b).

4) Geological noise due to overburden

In areas where there is irregular conductive overburden, current channeling into a patch of deeper or more conductive overburden will produce anomalies even to the lowest frequencies. Unless these anomalies are interpreted via 2D or 3D modeling, they can be mistaken for deep-seated features. Wannamaker (1983a) illustrates these effects.

5) Topography

The effect of topography on the results of an MT survey may be significant. Anomalous secondary electric and magnetic fields result. Topography must be included in the numerical modeling used in interpretation to prevent topographic effects from being interpreted as subsurface effects.

6) Depth of exploration and detectability

Depth of exploration is often stated to be one skin depth, δ, where

$$\delta = 500 \sqrt{\frac{2}{\omega \mu \sigma}} \qquad (5)$$

and σ = the conductivity of the earth, ω is the angular frequency of the signal under consideration, while μ is magnetic permeability. This simplification is misleading, because noisy data or surface geological noise can obscure the responses of deep bodies. However, with care in both data acquisition and interpretation, depths of exploration well in excess of 100 km can be achieved for infinite interfaces.

For 2D or 3D bodies, depth of exploration can be considerably less. Newman et al. (1983) have explored the possibility of detecting deep magma chambers with MT. If the magma chamber is electrically connected to a highly conducting layer below it, the magma chamber probably will not be detected. On the other hand, if the basal half-space is resistive or if the earth is not layered, the magma chamber is more readily detected.

self-potential

In principle, self-potential surveys are very simple: two non-polarizing electrodes, a length of wire, and a D.C. voltmeter are all the equipment needed to perform a survey. However, much attention must be paid to details if the desired reproduceability of $\pm$ 5 mV is to be achieved. Two methods of moving the electrodes along the traverse line are used; they are *leapfrog* and *long wire* methods. In the former, the back electrode is leapfrogged past the forward electrode for each move. Only a short wire is required. In the long wire method, the back electrode is left fixed and the forward electrode is moved farther and farther away. A long length of wire is then required.

Corwin and Hoover (1979) reviewed the self-potential method in geothermal exploration. Other pertinent references to the use of the self-potential method in geothermal exploration include Zohdy et al. (1973), Corwin (1975), Anderson and Johnson (1976), DeMoully and Corwin (1980), Hoover (1981), Sill (1982a,b,c), and Sill (1983a,b). Noise in self-potential surveys arises in telluric currents, electrode drift, topographic effects, variations in soil moisture, cultural noise, vegetation potentials, and electrokinetic potentials due to running surface water (Ward, S.H. and Sill, 1982). The cultural noise sources include: radiated fields from power lines, telephone lines, and electrified rails; corrosion potentials from pipelines, fences, and well casings; and spurious potentials from corrosion protection systems associated with pipelines. The following discussions of these problems follow from Ward, S.H. and Sill (1982).

1) Telluric currents

Time-varying voltages induced in the earth by the geomagnetic field, of frequencies within the passband of the voltmeter, may reach several hundred mv/km over resistive terrain (Keller and Frischknecht, 1966). These time-varying voltages constitute noise which inhibits repeatability of a measurement of the steady-state self-potentials. The magnitude of this noise is proportional to the separation between the two electrodes and accordingly is largest for the *long wire* method.

If telluric noise is dominant, then the *leapfrog* method is preferred.

2) Electrode drift

A voltage will be measured across an electrode pair if either or both of the electrodes are not in equilibrium. Departure from zero electrode potential will occur if the electrolyte in the non-polarizing electrode is diluted or contaminated by groundwater or if there is a temperature differential between the two. These effects will vary with time, moisture content of the soil, and ambient temperature. Repeated checks of drift must be made periodically by placing both measuring electrodes in a bath of electrolyte solution and connecting them in order to establish equilibrium. Leapfrog surveys usually result in irregular electrode drift so that long wire surveys are preferred where electrode drift is the dominant source of noise.

3) Topography

Topographic relief will distort self-potentials and this effect must be taken into account in interpretation of field data. Another topographic effect is due to the movement of shallow groundwater. More negative potentials are sometimes correlated with an increase in elevation with observed gradients as large as -6 mv/m (Hoover, 1981).

4) Variations in soil moisture

As noted by Corwin and Hoover (1979), variations in soil moisture often give rise to self-potential variations, with the electrode in the wetter soil usually becoming more positive. Watering of electrodes to improve electrical contact can produce the same effect, but even worse, electrokinetic potentials are generated as the water moves through the soil. Electrode watering should be avoided for self-potential surveys in geothermal areas because the geothermal anomalies frequently are small, so that reducing noise to a minimum becomes essential.

5) Cultural noise

We have noted above some sources of cultural noise encountered when performing S.P. surveys. All of them can lead to potentials, which vary with time, while corrosion potentials and potentials from corrosion protection systems additionally will produce spurious anomalies. Results from self-potential surveys in a developing or developed geothermal field will be quite different from results obtained before well casings were installed.

6) Vegetation potentials

Trees, shrubs, and grasses produce potentials which are commonly of order 10 mv. A technique used to reduce this noise, and noise due to varying soil moisture, involves making five measurements in a star about each observation point. Four readings are offset about 3 m north, south, east, and west of the central point. The five readings are then averaged.

7) Electrokinetic potentials from moving non-thermal water

Potentials generated by the flow of non-thermal surface and subsurface water, i.e. electrokinetic potentials, constitute a noise source in geothermal exploration, and may be a major cause of topographic noise (Corwin and Hoover, 1979) because of water flowing downhill beneath the surface.

tellurics

"---- the telluric method is mainly suitable for reconnaissance of horizontal resistivity variations. It is based on the assumption that telluric currents flowing in extensive sheets are affected by lateral variations in the resistivity structure, which can be caused, for example, by variations in geological structure or by hydrothermal systems. The method requires the simultaneous measurement of the telluric electric field at two stations. From the ratio of the amplitudes of the electric field at the two stations, inferences may be drawn about variations in the underlying resistivity structure. By keeping the base station fixed and moving a field station about, one can thus map resistivity variations in a qualitative way." (Palmason, 1975)

The method has been used in geothermal exploration by Beyer (1977), Isherwood and Mabey (1978), Jackson and O'Donnell (1980), and others. It appears to be a convenient method for regional surveys in order to detect areas worthy of more detailed exploration by resistivity methods (Palmason, 1975).

The method suffers from a number of problems which have already been described under MT/AMT as follows: random noise, geological noise due to overburden, lack of resolution, and effects of topography. Its worst problem is that it is a semi-quantitative method at best. However, Beyer (1977) advocated its use for northern Nevada because of its simplicity, low cost, and ease of interpretation.

heat flow

I will not dwell on the problems encountered with temperature gradient and heat flow measurements since that subject will be treated by D. D. Blackwell in this volume.

5.0 ILLUSTRATIVE RESULTS

Long Valley

Figure 3 presents the generalized geology of the Long Valley caldera, California from Bailey et al. (1976). I wish to draw attention to the resurgent dome depicted by early rhyolite flows,

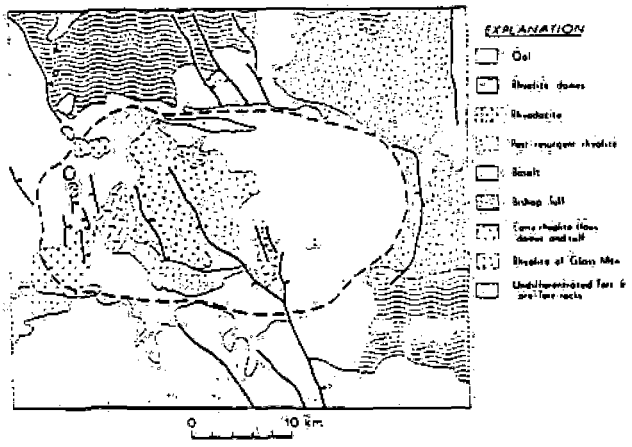

Figure 3. Generalized geologic map of Long Valley caldera (from Bailey et al., 1976).

domes and tuff, and to the medial graben transecting the resurgent dome in a northwest direction. Heat flow has been measured in 29 drill holes from 50 to 300 m deep within the caldera. An additional 11 holes outside, but adjacent to the caldera, were drilled to 150 to 300 m and heat flow was measured in them (Lachenbruch et al., 1976a,b). Temperature at 10 m depth for the drill holes within the caldera is contoured in Figure 4. An outline of the area of

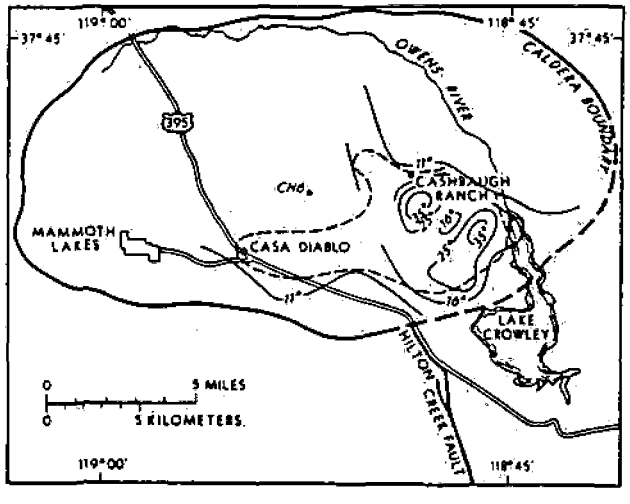

Figure 4. Temperatures at 10 m depth, Long Valley caldera (from Lachenbruch et al., 1976a). The area of hot spring activity is superimposed as a dashed line.

hot springs is included in the figure. There is an obvious correlation between shallow temperature measurements and hot spring activity. Note that drill hole CH6 is the only drill hole within the resurgent dome; it was isothermal at 111°C from about 150 m to 300 m. Ground deformation, enhanced seismicity, and fumarolic activity in the last 5 years, and particularly in the last 2 years, testifies to a modern increase in tectonism and presumed magmatism. The enhanced seismicity appears to lie south of the resurgent dome. Figure 5 shows earthquakes occurring in the region

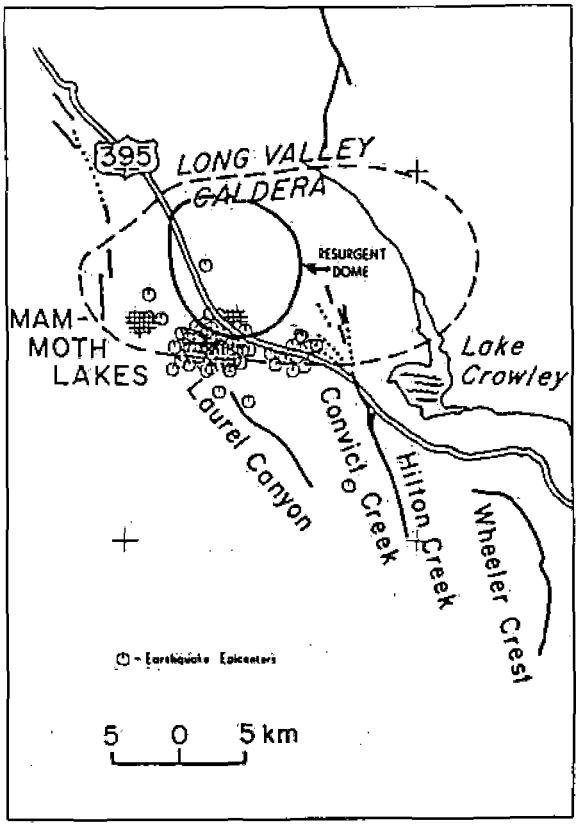

Figure 5. Mammoth Lakes earthquakes July, 1981, (from Miller et al., 1982).

in July, 1981 (from Miller et al., 1982). A tongue of magma is believed to have risen to within 2 to 3 km of the surface beneath the epicenter of the earthquakes shown in Figure 5. Many more earthquakes than are shown in this figure have occurred in the last several years. Ryall and Vetter (1983) indicate that such earthquakes occur as far as 7 km north from the south rim of the caldera and as much as 15 km south of it.

The resurgent dome has bulged upward in recent years (Miller et al., 1982). Steeples and Iyer (1976a) reported a zone of significant

teleseismic P-wave delay, beneath much of the resurgent dome. Hill (1976) found evidence for the roof of a magma chamber in late P-wave arrivals which he identified as reflections from a low-velocity horizon at a depth of 7 to 8 km. Ryall and Ryall (1981) found P- and S-wave attenuation which they attributed to a magma chamber beneath the Long Valley caldera. Ryall and Vetter (1983) reported on the absence of S waves at stations north of the caldera, for events occurring south of it; a magma chamber within the caldera is postulated to account for these observations; the postulated magma chamber roughly coincides with the area of hot spring activity shown in Figure 4.

Figure 6 (from Bailey et al., 1976) portrays a schematic east-west cross section through Long

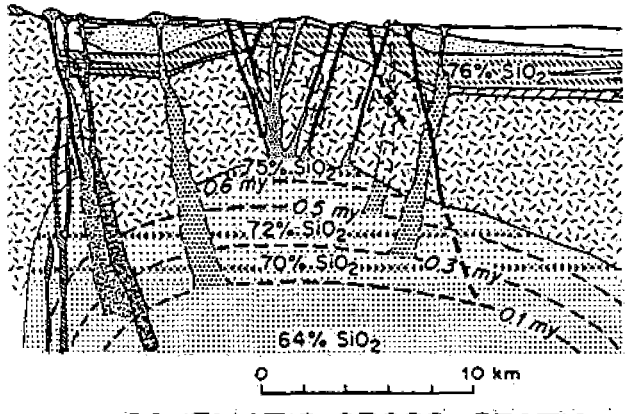

SCHEMATIC CROSS-SECTION

EXPLANATION

- ALLUVIUM, GLACIAL DEPOSITS, AND CALDERA FILL
- HOLOCENE, RHYOLITE-RHYODACITE
- LATE BASALTIC ROCKS
- RIM RHYODACITES
- MOAT RHYOLITES
- EARLY RHYOLITES { TUFFS: FINE DOTTED; FLOWS: COARSE DOTTED
- BISHOP TUFF
- RHYOLITE OF GLASS MTN. { DOME FLOWS: FINE LINED; TUFFS: COARSE LINED
- TERTIARY VOLCANIC ROCKS
- JURASSIC-CRETACEOUS GRANITIC ROCKS

Figure 6. Schematic east-west cross section through Long Valley caldera and its underlying magma chamber (from Bailey et al., 1976).

Valley caldera. As noted by Muffler and Williams (1976) and by Sorey et al. (1978) the prevalent USGS view has been that the geothermal reservoir lies in the Glass Mountain rhyolites and the Bishop Tuff, the two earliest volcanics to infill the caldera.

The caldera fill above the Bishop Tuff consists of a variety of rhyolitic flows and tuffs, rhyodacitic flows, basaltic flows, and in the eastern half, lake, marsh, and periglacial sediments. These rocks are considered to be impermeable except along faults and hence do not form part of the reservoir (Muffler and Williams, 1976). The gravity data of Kane et al. (1976) and the seismic section of Hill (1976) have been used by USGS personnel to define the volume of the proposed reservoir to be 450 km^3.

Resistivity and AMT surveys mapped two near-surface low-resistivity zones associated with hydrothermally altered rocks and/or hot saline water (Hoover et al., 1976; Stanley et al., 1976).

Nine geothermal test wells were drilled near Casa Diablo and one well was drilled about 5 km farther east by Magma Power Company. One well was drilled by Republic Geothermal, Inc. about 4 km south of Cashbaugh Ranch. Union Geothermal drilled two wells, one near a clay pit in the north end of Little Antelope Valley, and one near Casa Diablo. All of the above wells have failed to discover a high temperature geothermal reservoir. None of the wells has been sited near the center of the resurgent dome, especially where transected by the medial graben. The self-potential data of Figure 7 draw attention to the whole of the area of the resurgent dome. W.R. Sill (pers. comm.) advises that cold water inflow from the west-northwest and outflow in the area of the thermal springs could account for the dipolar S.P. pattern. The cold water inflow could readily mask the center of a deep convective hydrothermal system possibly occurring beneath the resurgent dome.

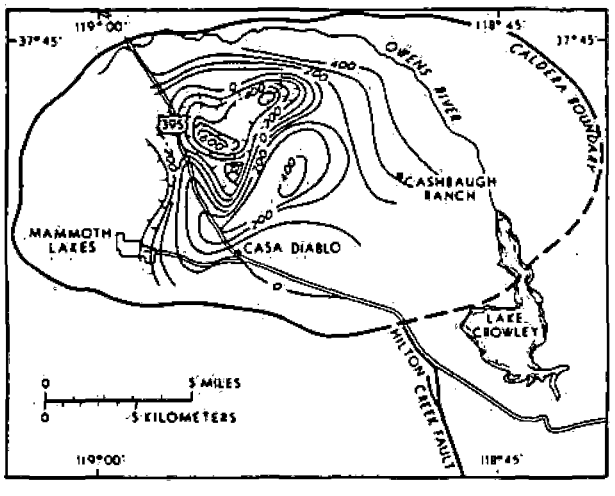

Figure 7. Self-potential map of Long Valley. (after Anderson and Johnson, 1976).

The magma chamber, as determined by the teleseismic P-wave delays, lies directly beneath the resurgent dome. The cross section of Bailey et al. (1976), Figure 6, schematically illustrates a potential fault-controlled reservoir within and below the caldera infill and beneath the resurgent

dome. The problem with this notion is that for calderas elsewhere (e.g. Baca) the resurgent dome may be a poor exploration target because of lack of permeability (D.L. Nielson, 1983, pers. com.).

The resistivity and AMT data draw attention to areas south and east of the resurgent dome, while the aeromagnetic data draw attention to a small region of magnetite destruction around Casa Diablo. Surface manifestations of hydrothermal activity are abundant in these areas. I have downgraded shallow heat flow, magnetics, resistivity, and AMT at this geothermal prospect because drilling to date has not found a commercial reservoir where these methods have produced anomalies. I have up-graded self-potential on the speculation that a commercial reservoir may be found in the central part of the resurgent dome. Gravity and seismic refraction were very useful in delineating the Glass Mountain Rhyolites and Bishop Tuff in the floor of the caldera and were instrumental in quantifying the USGS model of the reservoir. Teleseismic P-wave delays, S-wave attenuation, and S-wave delays seem quite important and reliable indicators of a magma chamber in this setting. Earth noise so far has failed to help us delineate a reservoir. The earthquake epicenter map of Figure 5 may be delineating an east-west fracture zone up which a tongue of lava is believed to have recently intruded. What bearing this would have on a commercial high-temperature reservoir is unknown at present.

Evaluating geophysical methods at Long Valley is a questionable pursuit at present because we do not know where a commercial high-temperature reservoir is located if, indeed, it exists. However, the analysis has been made on the assumption that either the Bishop Tuff or the deeper parts of the medial graben will prove to be commercial. Note that the recent bulging of the resurgent dome would indicate that the medial graben may now be in extension.

Coso

Figure 8 portrays the generalized geology of the Coso geothermal area (Hulen, 1978). "The oldest rocks exposed at Coso are intermediate to mafic metamorphic rocks of uncertain age intruded by dikes and pods of quartz latite porphyry and felsite, and by a small stock of Late Cretaceous (?) granite. These rocks are locally overlain by Late Cenozoic volcanic rocks, which include the domes, flows, and associated pyroclastic deposits of the Coso rhyolite dome field."

"Principal structures in the geothermal area are older high-angle faults of uncertain displacement trending northwest, west-northwest, and east-northeast, and younger high-angle faults with a normal component of displacement trending north-northwest, north-northeast, and (subordinately) northeast. Active surface thermal phenomena and hydrothermal alteration are concentrated along the younger northerly-trending faults, especially where these faults intersect

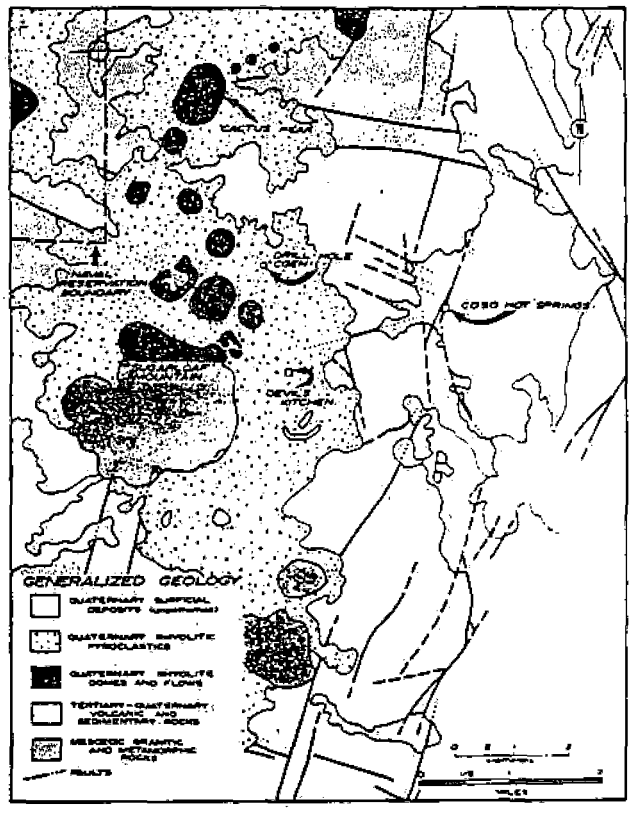

Figure 8. Generalized geologic map of Coso Hot Springs KGRA. (after Hulen, 1978).

older structures. Deep thermal fluid flow at Coso will be controlled entirely by structural permeability developed in otherwise tight and impermeable host rocks."

"Surface alteration at Coso is of three main types: (1) clay-opal-alunite alteration, (2) weak argillic alteration, and (3) stockwork calcite veins and veinlets, which are locally associated with calcareous sinter. Clay-opal-alunite and weak argillic alteration are typically developed around active thermal emissions. These are almost entirely restricted in distribution to an east-northeast-trending belt roughly one mile in width and four miles in length. Calcareous alteration is much more widely distributed, but is confined to a broad zone of anomalous geophysical response interpreted as evidence for a concealed geothermal reservoir" (Hulen 1978).

A low level aeromagnetic map of the area is given in Figure 9 (after Fox, 1978a). The anomalous low which extends southeast from Devil's Kitchen and Coso Hot Springs is attributed, in part, to magnetite destruction by hydrothermal fluids (Fox 1978a).

A resistivity low mapped in the vicinity of Devil's Kitchen and Coso Hot Springs (Figure 10) is attributed, in part, to hydrothermal alteration and hot brines in fractures (Fox, 1978b). The

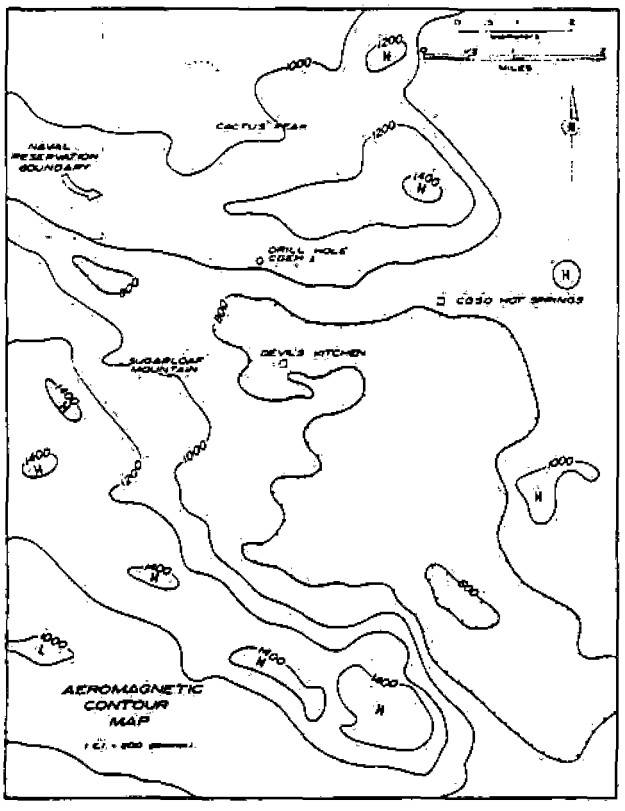

Figure 9. Aeromagnetic residual total field intensity contour map of Coso. (after Fox, 1978a).

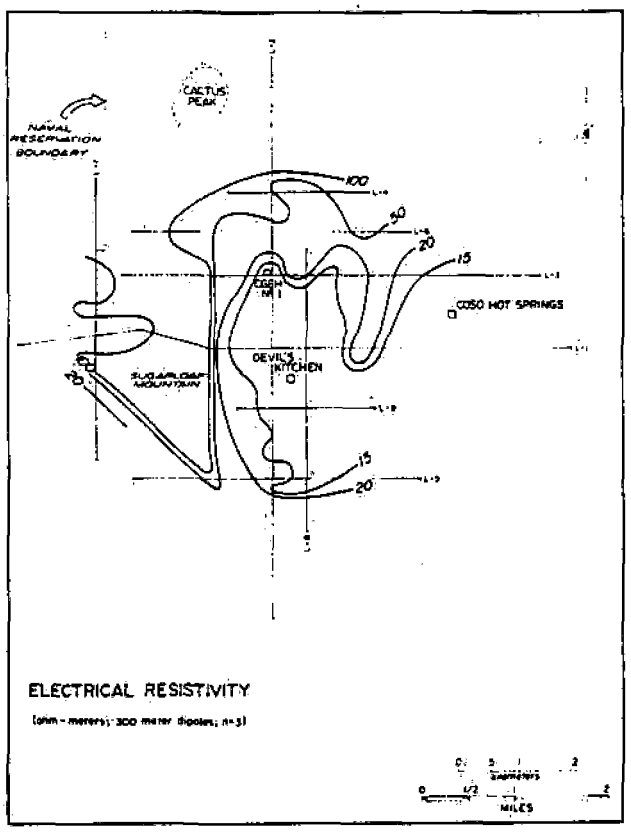

Figure 10. Third separation apparent resistivity map of Coso obtained with 300 m dipole-dipole survey. (after Fox, 1978b).

dipole-dipole array with 300 m dipoles was used. Much the same zone of low resistivity was mapped by AMT earlier. Figure 11 displays the 7.5 Hz AMT apparent resistivity map produced by Jackson and O'Donnell (1980). A telluric J-value map, also produced by these authors, was not nearly as effective in depicting the area of interest around Devil's Kitchen and Coso Hot Springs.

No one of the above geophysical techniques by itself created a confined target for drilling. However, when the resistivity and aeromagnetic data were combined with shallow heat flow data and a map of the hydrothermal alteration, then a target in the general vicinity of Devil's Kitchen was clearly delineated as shown in Figure 12 (from Hulen, 1978). Prior to Hulen producing Figure 12, drill hole CGEH-1 was drilled as a dry hole. Subsequently, all six wells have been producers. The importance of overlapping several data sets prior to spotting the first well on a geothermal prospect is vividly illustrated by this example.

I have not found that earth noise, teleseisms, gravity, or tellurics have contributed much to understanding the reservoir. The earth noise data of Figure 13 (after Combs, 1980) could be aliased and noise power peaks near Coso Hot Springs may, in part, be due to Rayleigh waves in deep alluvium. The teleseismic evidence of a 0.2

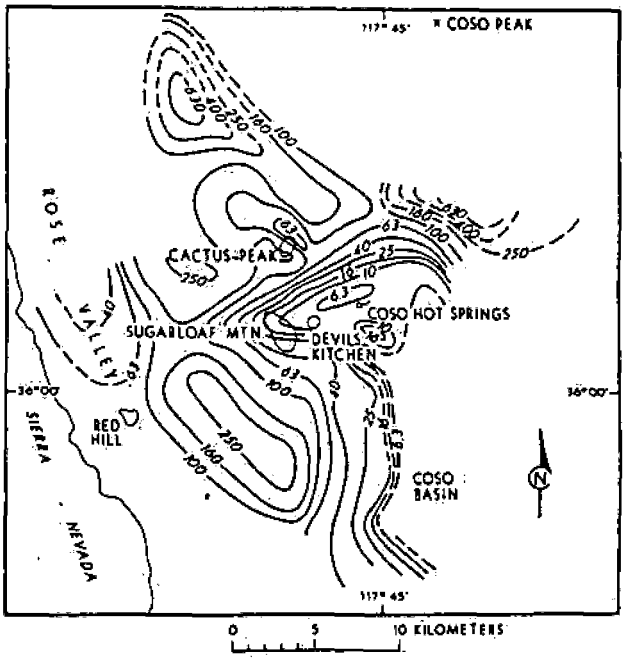

Figure 11. The 7.5 Hz AMT apparent resistivity map of Coso. (after Jackson and O'Donnell, 1980).

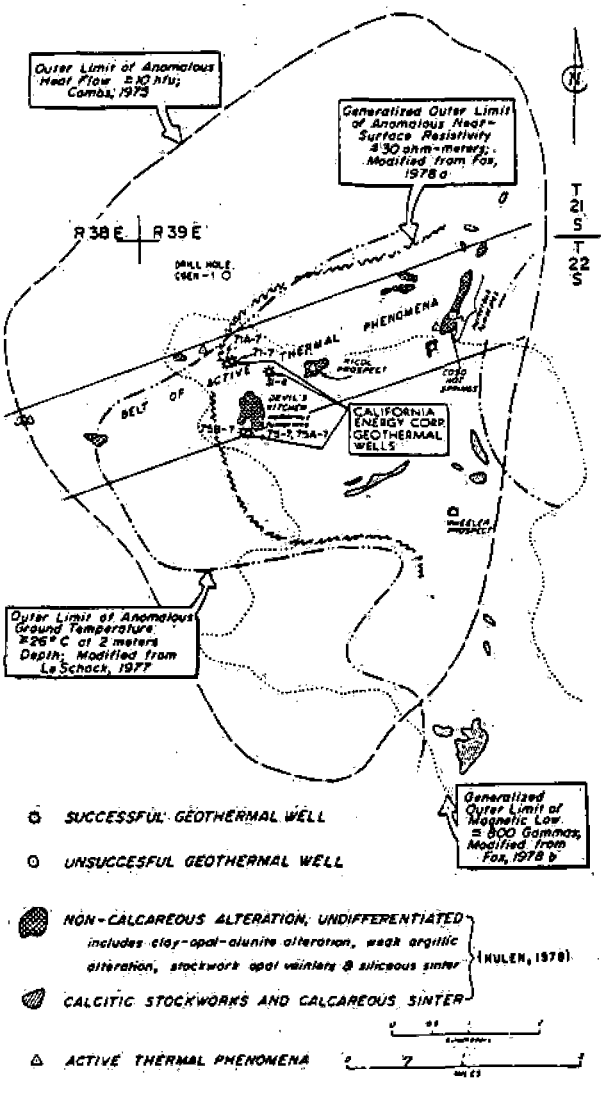

Figure 12. Generalized alteration and geophysical map. (after Hulen, 1978).

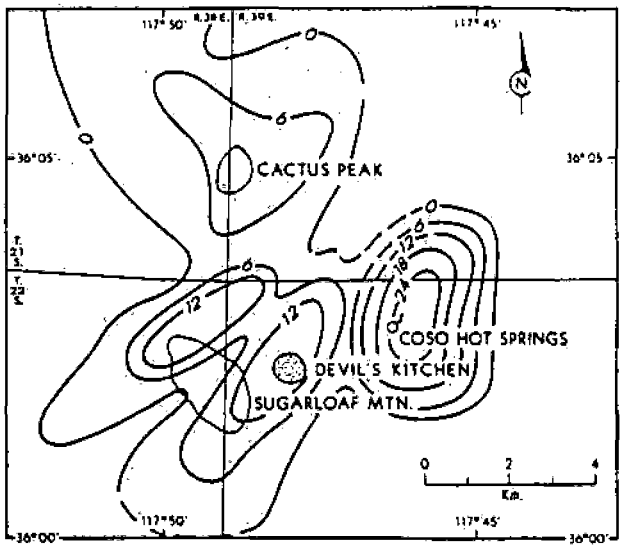

Figure 13. Earth noise power expressed in decibels, Coso. (after Combs, 1980).

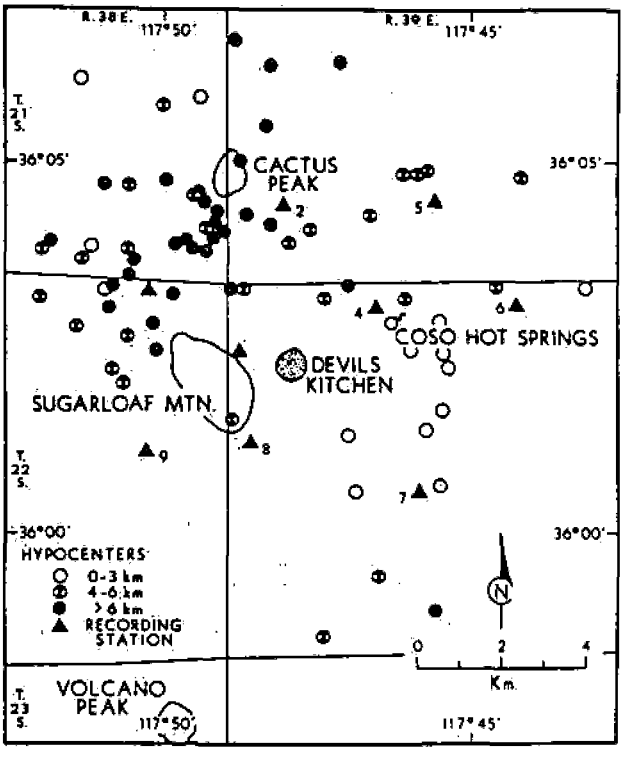

Figure 14. Epicenters of 78 microearthquakes associated with the Coso geothermal area. (from Combs and Rotstein, 1975).

sec P-wave delay is not convincing. The gravity data are relatively featureless in the region between Devil's Kitchen and Coso Hot Springs. The telluric data are too much affected by Coso Basin to be of good quality in the region of interest. Microearthquakes were highly scattered throughout the area as Figure 14 illustrates (after Combs and Rotstein, 1975). No major faults were deduced from the data by Combs and Rotstein. However, the important contribution of microearthquakes at this prospect lies in calculation of a Poisson's Ratio

of 0.16, an indicator of a vapor-dominated system. Based on current knowledge, the shallower parts of the reservoir appear to be vapor dominated (J.A. Whelan, 1983, pers. com.). The refraction method was useful at Coso in suggesting "the existence of a localized body of low velocity material at depth, possibly a magma chamber." (Combs and Jarzabek, 1977)

Roosevelt Hot Springs

Figure 15 portrays the generalized geology at the Roosevelt Hot Springs KGRA (after Sibbett and Nielson, 1980). From Ross et al. (1982) we extract the quotations which follow.

"The geothermal system is a high-temperature water-dominated resource, and is structurally controlled with permeability localized by faults and fractures cutting plutonic and metamorphic rocks."

"The oldest unit exposed in the area of the geothermal system is a banded gneiss which was formed from regionally metamorphosed quartzo-feldspathic sediments." "The rock is compositionally heterogeneous and contains thick sequences of quartzo-feldspathic rocks. The unit also contains metaquartzite and sillimanite schist layers which have been differentiated in the more detailed geologic study (Nielson et al., 1978)."

"The Mineral Mountains intrusive complex is the largest intrusive body exposed in Utah. Potassium-Argon dating and regional relationships suggest that the intrusive sequence is middle to

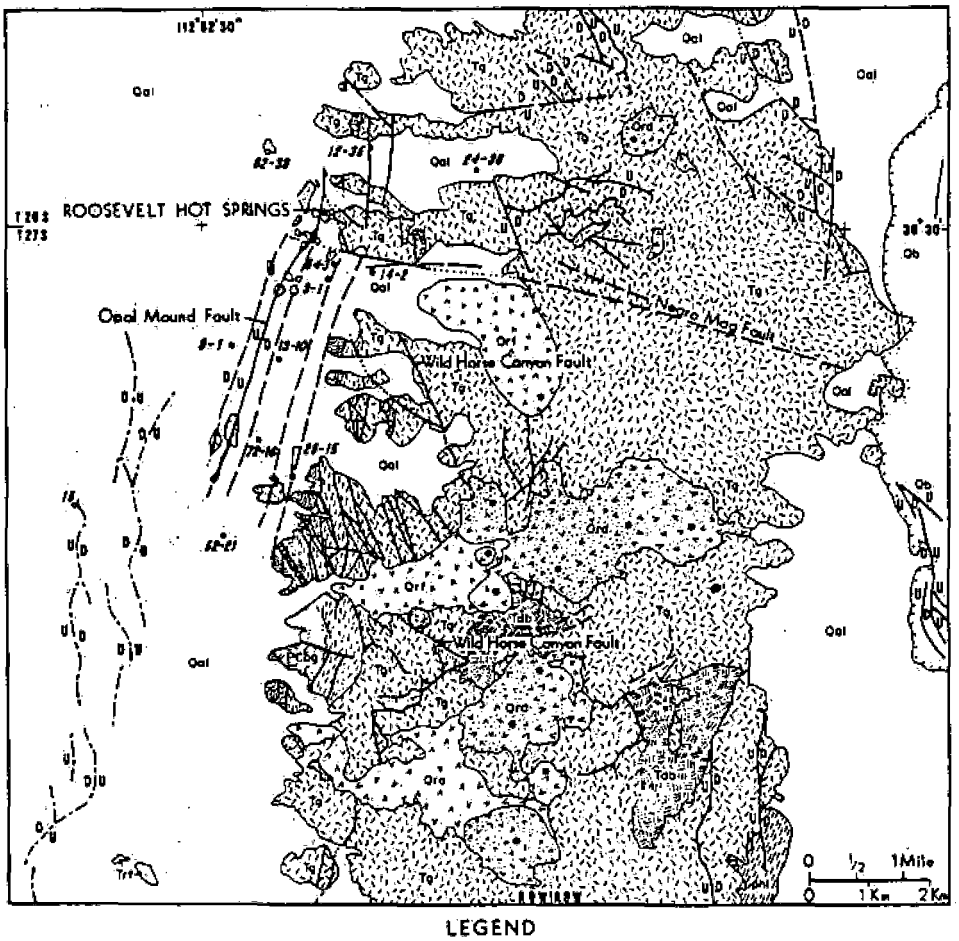

Figure 15. Geologic map of Roosevelt Hot Springs KGRA and vicinity. (after Sibbett and Nielson, 1980).

late Tertiary in age. In the vicinity of the geothermal system, the lithologies range from diorite and granodiorite through granite and syenite in composition.

"Rhyolite flows, pyroclastics, and domes were extruded along the spine of the Mineral Mountains 800,000 to 500,000 years ago (Lipman et al., 1977). The flows and domes are glassy, phenocryst-poor rhyolites. The pyroclastic rocks are represented by air-fall tuff and nonwelded ash-flow tuffs."

"Hot spring deposits in the vicinity of the geothermal system have been mapped as siliceous sinter, silica-cemented alluvium, hematite-cemented alluvium, and manganese-cemented alluvium. The principal areas of hot-spring deposition are along the Opal Mound fault and at the old Roosevelt Hot Springs. In both of these areas, the deposits consist of both opaline and chalcedonic sinter."

The hot spring deposits are depicted in Figure 16. A soil survey within the area of

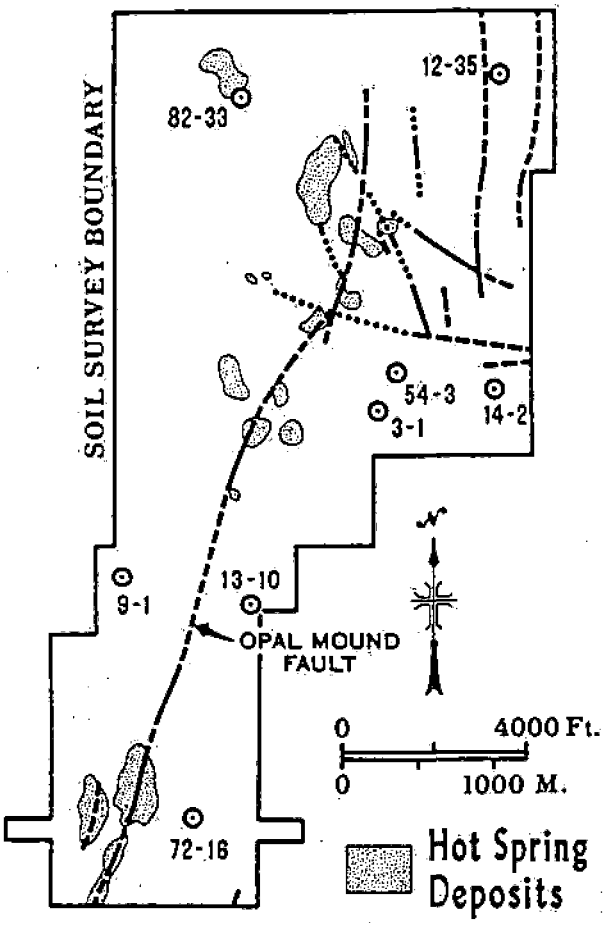

Figure 16. Hot spring deposits, Roosevelt Hot Springs. (after Bamford et al., 1980).

Figure 16 revealed anomalous mercury and arsenic. Hydrothermal alteration in the geothermal system and the adjacent Mineral Mountains is localized along faults and fractures.

"The hydrothermal alteration produced assemblages of quartz + chlorite + epidote + hematite. Hematite is commonly found as specularite veinlets and, where genetic relationships can be observed, hematite mineralization follows sulfide mineralization."

"The hydrothermal alteration assemblages associated with the present geothermal system are crudely zoned with depth. The uppermost assemblage, occurring around the hot-spring deposits and fumaroles, is characterized by quartz, alunite, kaolinite, montmorillonite, hematite, and muscovite. Parry et al. (1980) have studied the near-surface alteration and suggest that these minerals have formed above the water table by downward-percolating acid sulfate waters. Upward-convecting geothermal brines have produced, with increasing depth, alteration assemblages characterized by montmorillonite + mixed layer clays + sericite + quartz + hematite and chlorite + sericite + calcite + pyrite + quartz + anhydrite (Ballantyne, 1978). Thermochemical calculations and petrologic observations suggest that the brines are in equilibrium with the alteration assemblages produced by the upward-migrating fluids (Capuano and Cole, 1982)."

Figure 17 shows the heat flow contours, expressed in mWm^{-2}, over the main prospect area at Roosevelt Hot Springs KGRA. The southern lobe, up to Negro Mag fault, is a legitimate expression of the geothermal reservoir as it is currently known. The northern lobe, northwest of the intersection of the Negro Mag fault and the Opal Mound fault, may in part be an expression of leakage of hot water northwestward out of the reservoir. Wells 82-33 and 24-36 are dry, while well 12-35 is productive.

The resistivity contours of Figure 18 correspond with the heat flow high very nicely. The resistivity low is primarily due to surface conductivity of clay minerals produced in hydrothermal alteration (Ward, S.H. and Sill, 1976). Leakage of brine northwestward out of the reservoir would appear to be saturating valley alluvium leading to low resistivities beyond the heat flow high. The CSAMT apparent resistivities at 32 Hz, shown in Figure 19, also directly correlate with the zone of high heat flow. Quantitative two-dimensional modeling of the resistivity and CSAMT data has yielded high-resolution targets for drilling; such resolution is not afforded by modeling the heat flow data.

The self-potential map of Figure 20 reveals a number of closures, some of which are positive and some negative. Quantitative interpretation of the self-potential data has not yet been made and its contribution to understanding the reservoir is not known.

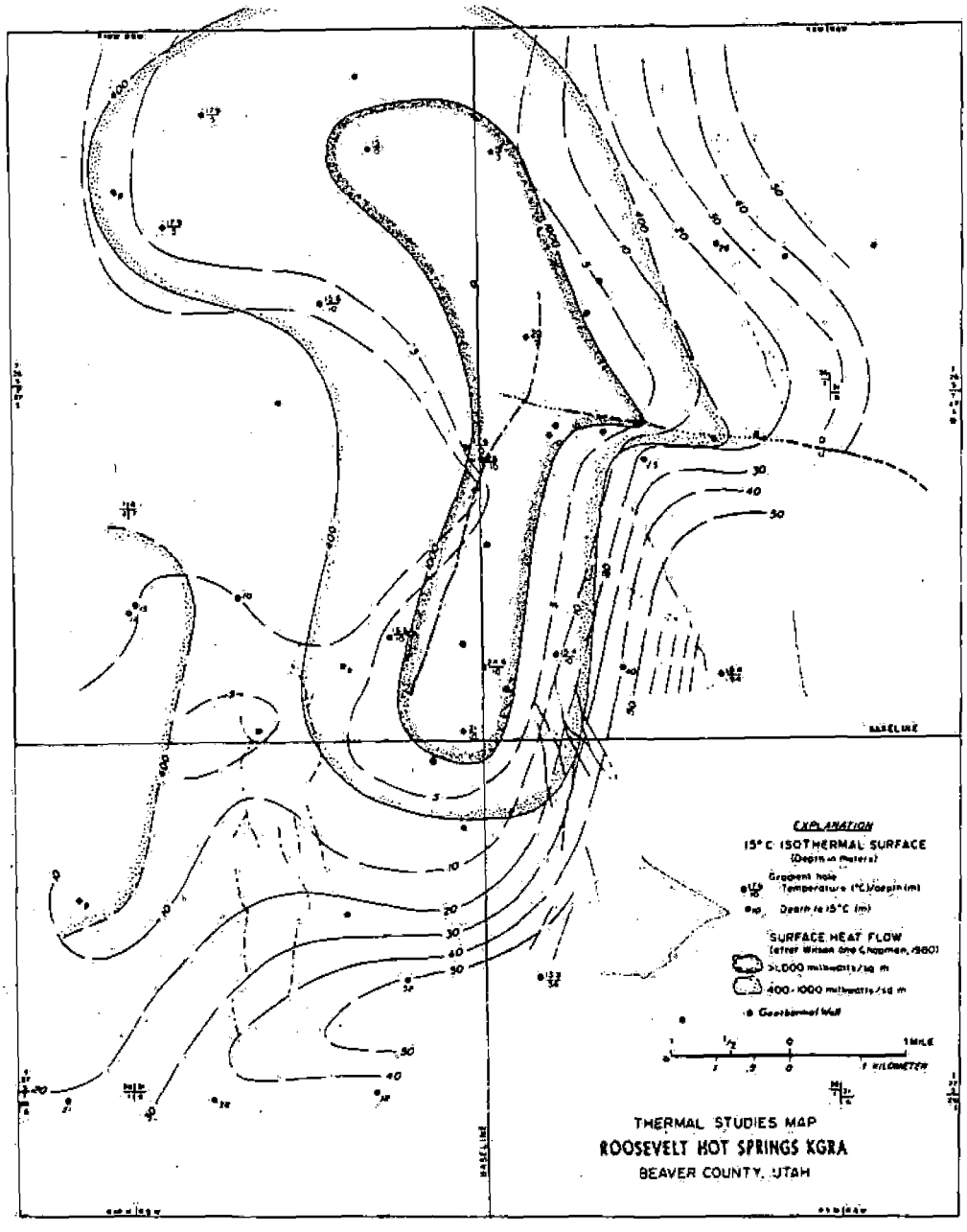

Figure 17. Thermal studies map, Roosevelt Hot Springs KGRA. (from Ross et al., 1982).

Very few microearthquakes have been found beneath wells currently known to be productive. Activity in the region is episodic. During one episode of increased activity, the numerous hypocenters of Figure 21 were located; most occur at a depth of about 5 km. They seem to depict an east-west fault along B-B'. Whether the hypocenters lie on a southward dipping Negro Mag fault, or whether they are associated with another east-west fault is unknown. Research on these microearthquakes and their structural significance is continuing. The Wadati diagram of Figure 22 was developed from the origin times and S- and P-arrival times. A Poisson's Ratio of 0.25 results. Hypocenters occurring beneath the reservoir as currently known, while few in number, yielded a Poisson's Ratio of 0.24. Thus the Poisson's Ratio does not reflect the fact that the reservoir is liquid dominated. It is too early to say whether microearthquakes will contribute to knowledge of the reservoir; to this date they have not.

Douze and Laster (1979) detected no earth

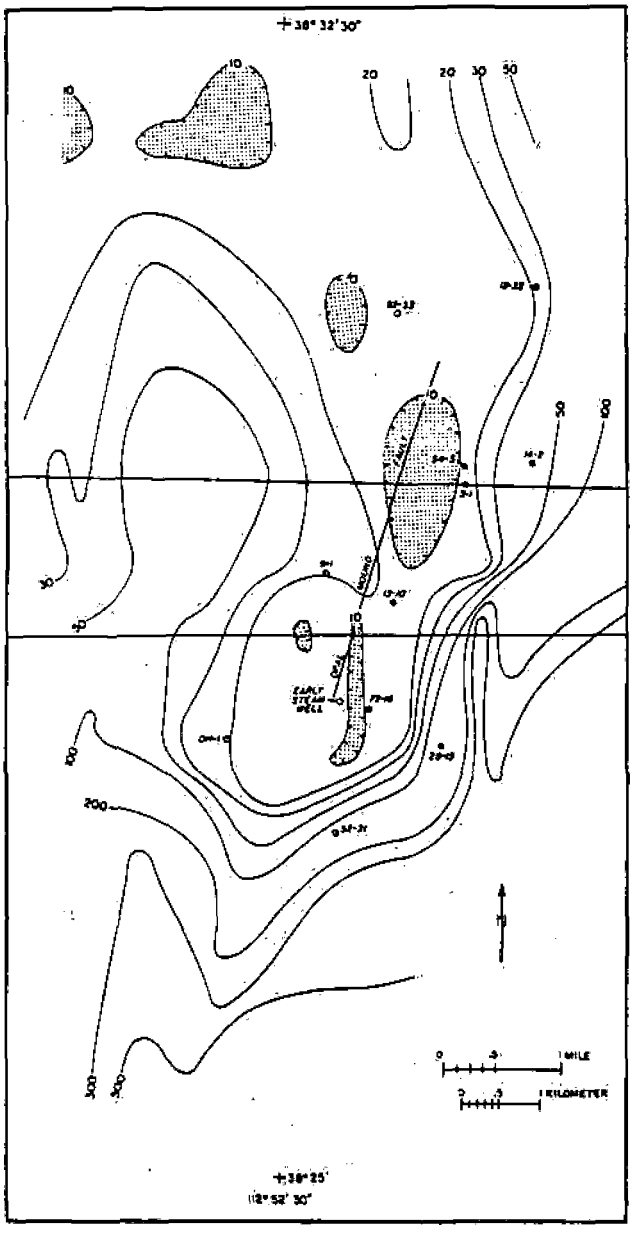

Figure 18. First separation resistivity map from 300 m dipole-dipole survey, Roosevelt Hot Springs KGRA. (after Ward and Sill, 1976).

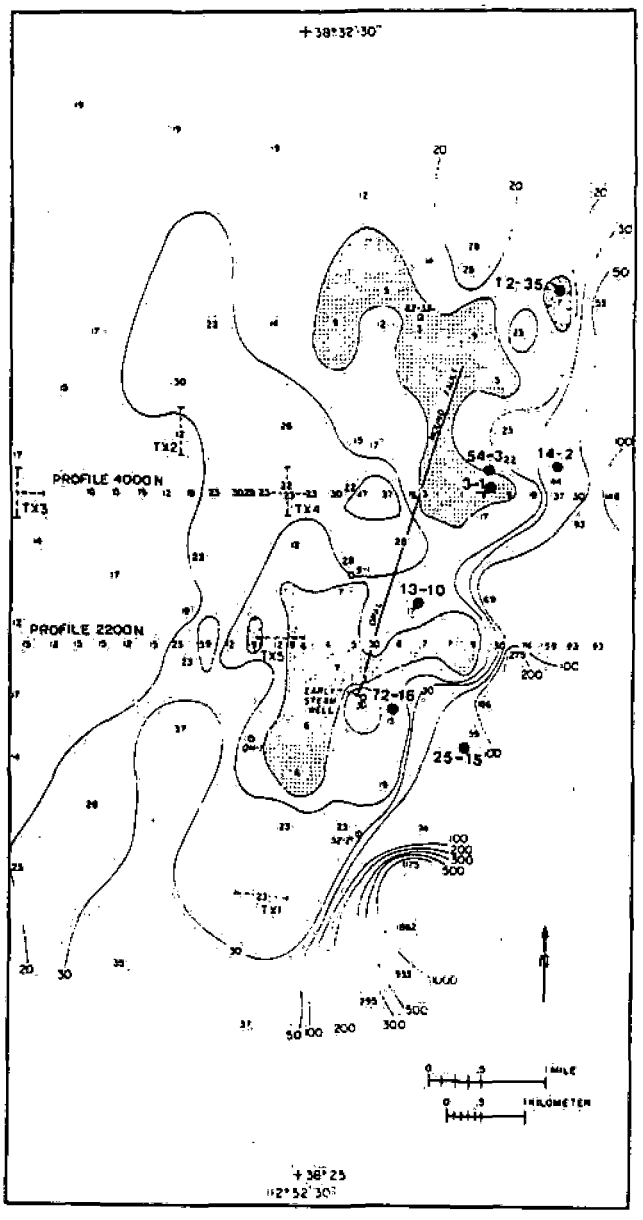

Figure 19. The CSAMT 32 Hz apparent resistivity map of Roosevelt Hot Springs KGRA. (from Sandberg and Hohmann, 1982).

noise that could be related to the geothermal reservoir. Robinson and Iyer (1981) make a modest claim that there is teleseismic evidence for a partial melt at about 15 km depth. Wechsler and Smith (1979) cast doubt on this interpretation and I am inclined to agree with them. Reflection and refraction surveys have yielded information on range front faulting and on depth of valley alluvium, but they have not given any useful information on the reservoir (Ross et al., 1982).

Gravity and magnetic methods have aided in understanding the structure in the vicinity of Roosevelt Hot Springs, but their contribution to understanding the reservoir is nil.

The magnetotelluric method detected the shallow resistivity structure but at great expense. It also detected a partial melt in the upper mantle. Research is continuing to delineate the lateral extent of the partial melt and to determine whether or not it has any significance to the occurrence of the geothermal reservoir. No deep geothermal system and no magma body were

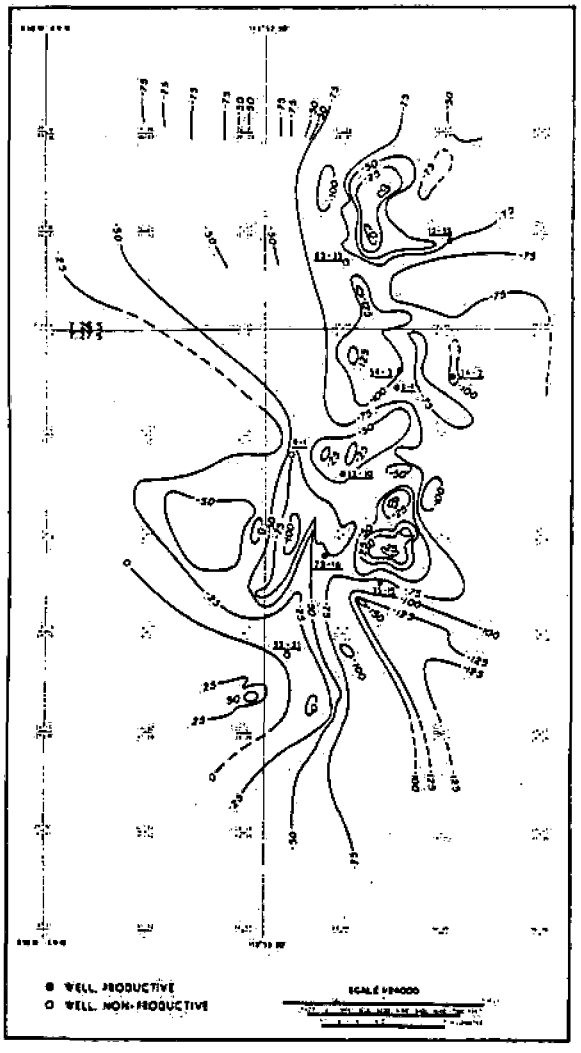

Figure 20. The self-potential map of Roosevelt Hot Springs KGRA (courtesy W. R. Sill).

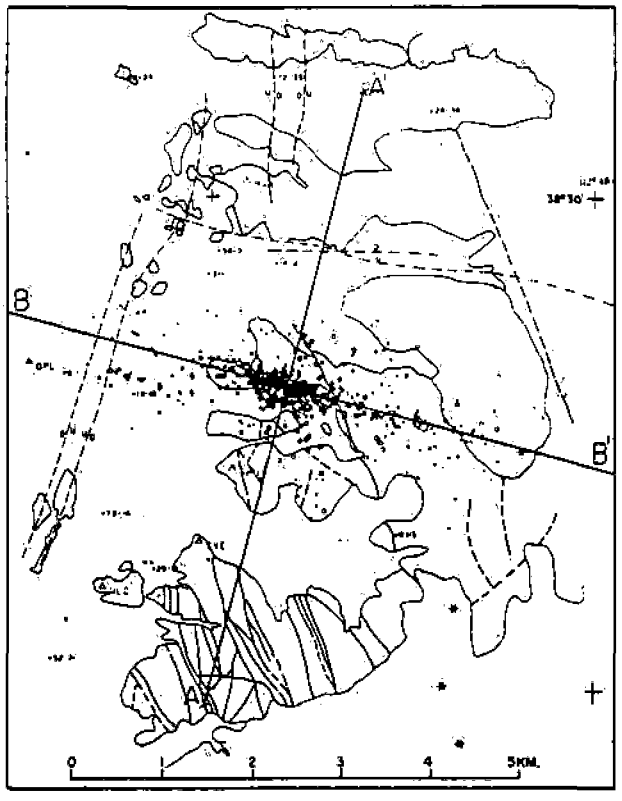

Figure 21. Microearthquakes occurring during swarm, July 1981. (after Zandt et al., 1982).

detected by the MT survey. Detectability of magma chambers by MT is a questionable enterprise as Newman et al. (1983) have demonstrated.

Tuscarora

Pilkington et al. (1980) and Sibbett (1982) have described the geology of the Tuscarora geothermal prospect in Elko County, Nevada. Figure 23 portrays the simplified representation of the geology of the prospect according to Sibbett, who states, "The Tuscarora geothermal prospect is located at the north end of Independence Valley in northern Nevada. Thermal springs issue from Oligocene tuffaceous sediments near the center of an area of high thermal gradient. The springs are associated with a large siliceous sinter mound and are currently depositing silica and calcium carbonate. Measured

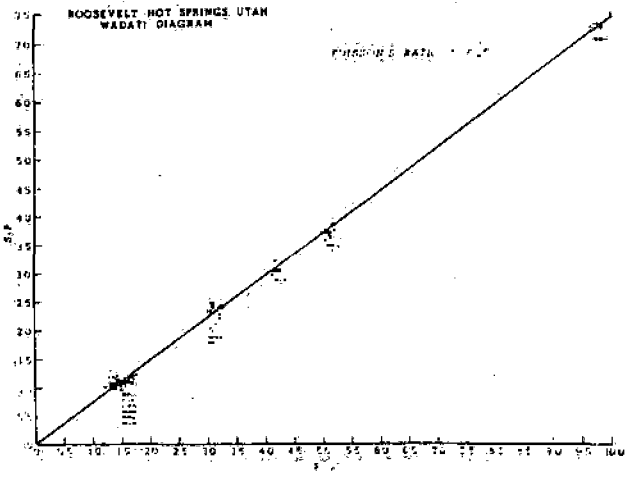

Figure 22. Wadati diagram derived from earthquakes occurring at Roosevelt Hot Springs KGRA during July, 1981.

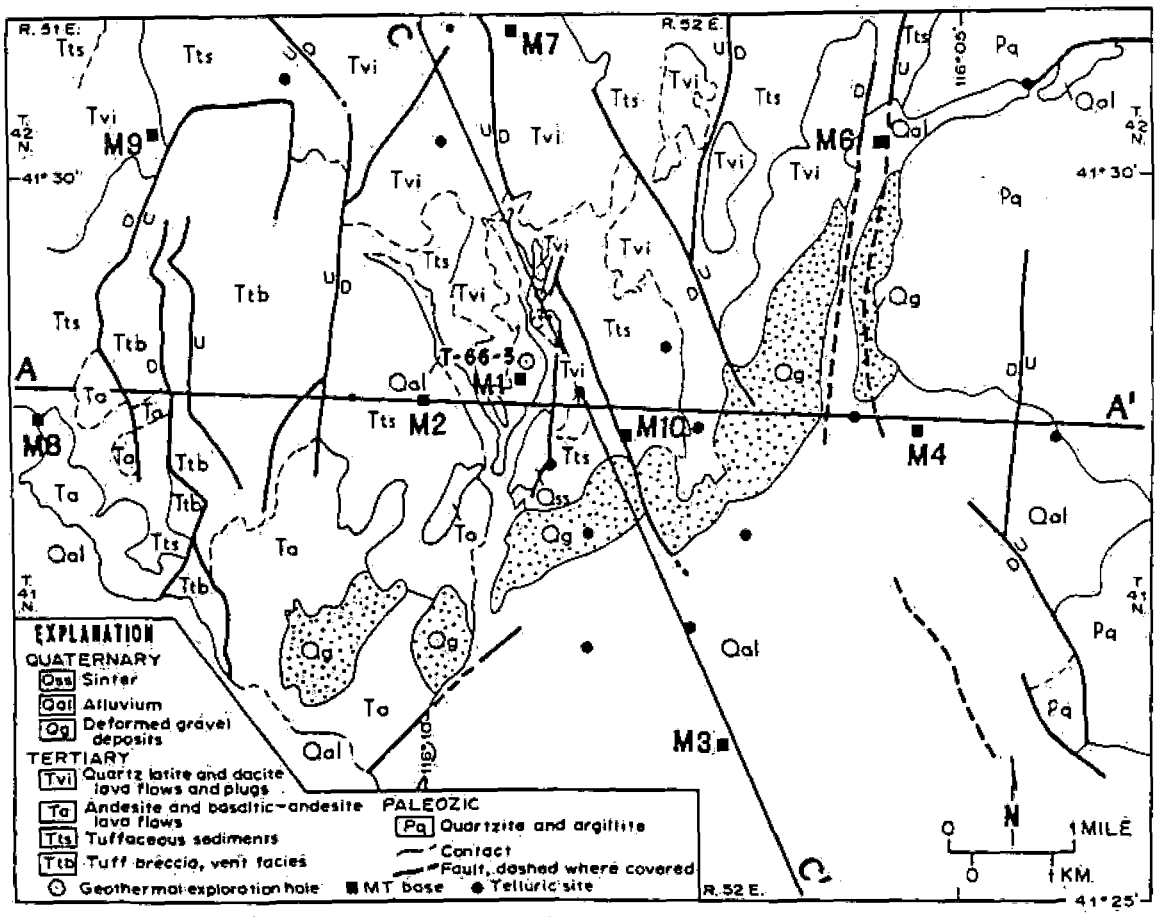

Figure 23. Generalized geology, Tuscarora. (from Sibbett, 1982).

fluid temperatures range up to 95°C, and chemical geothermometers indicate a reservoir temperature of 216°C. The Independence Valley contains 35- to 39-m.y.-old tuffs and tuffaceous sediments which overlie Paleozoic clastic and volcanic rocks and are overlain by Miocene lava and pyroclastic flows. The rocks have been deformed by normal faults trending north-south and northwest and by folds trending north-south which have been active in the Pleistocene."

The heat flow anomaly at the Tuscarora prospect is centered on Hot Sulphur Springs as Figure 24 illustrates (from Pilkington et al., 1980). The north-south faulting is evident in the gravity map of Figure 25 from Pilkington et al., 1980). Meidav and Tonani (1975) observed "that both microearthquake activity and thermal spring occurrences are more commonly associated with that side of the basin which has the steeper gravity gradient". If this is an observation upon which we can rely, let us test it with the available data. From Figure 25 it is evident that the east side of Independence Valley has the steepest gradient of gravity. The range lines in Figures 23 and 25 permit ready correlation of the gravity

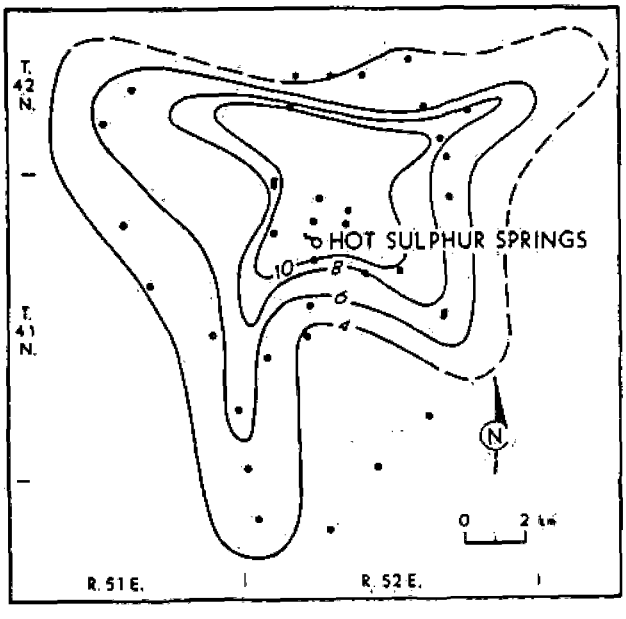

Figure 24. Contours of heat flow at Tuscarora (in HFU). (from Pilkington et al., 1980).

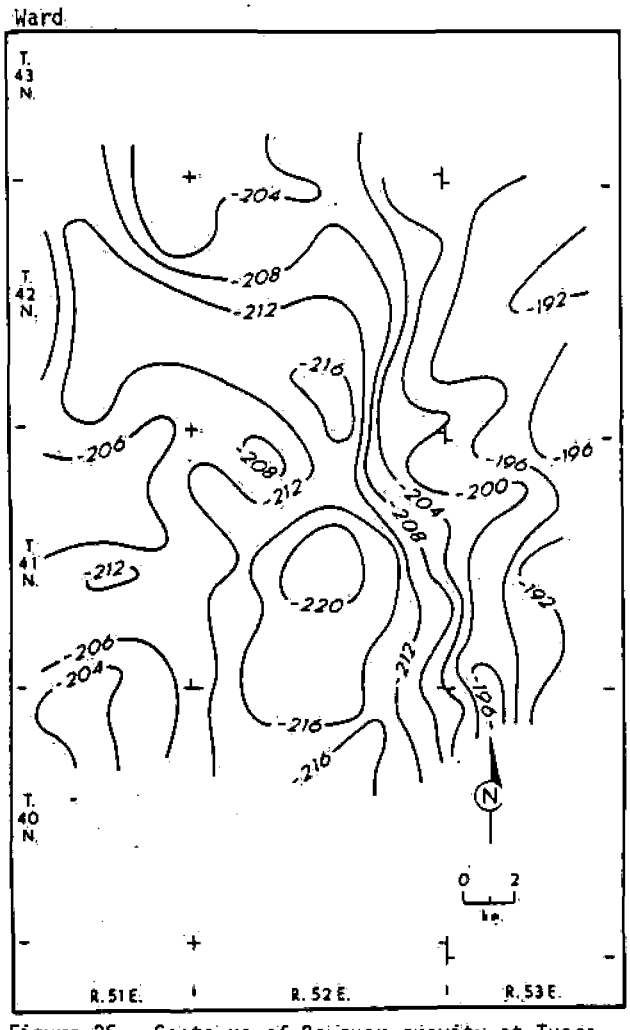

Figure 25. Contours of Bouguer gravity at Tuscarora. (from Pilkington et al., 1980).

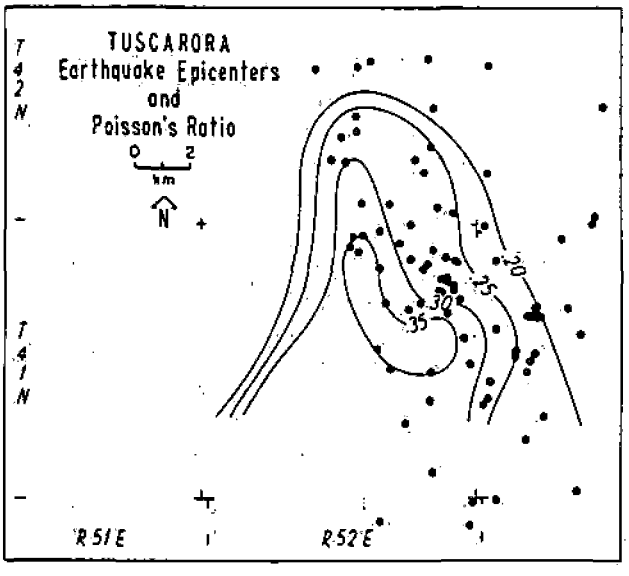

Figure 26. Distribution of microearthquakes and contours of Poisson's ratio. (from Pilkington et al., 1980).

data with the geology. The microearthquakes of Figure 26, as documented by Pilkington et al. (1980), are scattered but clearly follow a range front fault suggested by the steep gravity contours of Figure 25. Contrariwise, Hot Sulphur Springs occur well west of this presumed fault line.

As concluded by Sibbett (1982),

"The surface expression of the Hot Sulphur Springs thermal system is controlled by a fault zone trending N20°E. Exposed argillic alteration produced by the thermal system is limited to the spring area. Quartz-sericite alteration which predates the present thermal system is present along the fault zone."

"The subsurface character of the geothermal system is not known, but the geophysical and geological data are consistent with an interpretation that the reservoir is 3 to 5 km southeast of the hot springs. In this model, meteoric water circulates down along the range-front fault system and is heated at depth. The thermal waters rise along major fractures, perhaps the intersection of the N10°E and N30°W fault zones, into either a solution reservoir in the lower-plate carbonates or a fracture reservoir in the overlying Valmy Group quartzite. The fracture reservoir and feeder channelways may have been formed by brecciation along the thrust fault and by formation of the deep graben. The reservoir cap consists of the incompetent and less permeable Tertiary tuffs and tuffaceous sedimentary rocks, the base being 1,200 m or more below the surface. Some of the thermal fluids migrate up major fractures within the Paleozoic shale, chert and greenstone unit which overlies the Valmy Group quartzite. The fluids probably move updip to the northwest along gravel aquifers either at the base of or within the tuffaceous sedimentary rocks, ultimately reaching the surface along the faults at the hot springs. Cold water aquifers in the thick quartzite gravel overlying the tuffaceous sedimentary rocks apparently mask the thermal anomaly directly above the reservoir."

Drilling on this prospect has been confined to the general vicinity of the heat flow high surrounding Hot Sulphur Springs. If Sibbett's model is correct, and resistivity data (Mackelprang, 1982) would tend to support it, then drilling might recommence along the zone of the eastern range front depicted by the gravity and microearthquake data. In this region, the contoured values of Poisson's Ratio shown in Figure 26 are probably not indicative of the characteristics of the reservoir but rather of the fluid saturated alluvium of Independence Valley (Berkman and Lange, 1980).

Beowawe

Figure 27 depicts the generalized geologic map at Beowawe (from Sibbett, 1983). The Beowawe Geysers have formed a 850 m long sinter terrace at the base of the Malpais scarp.

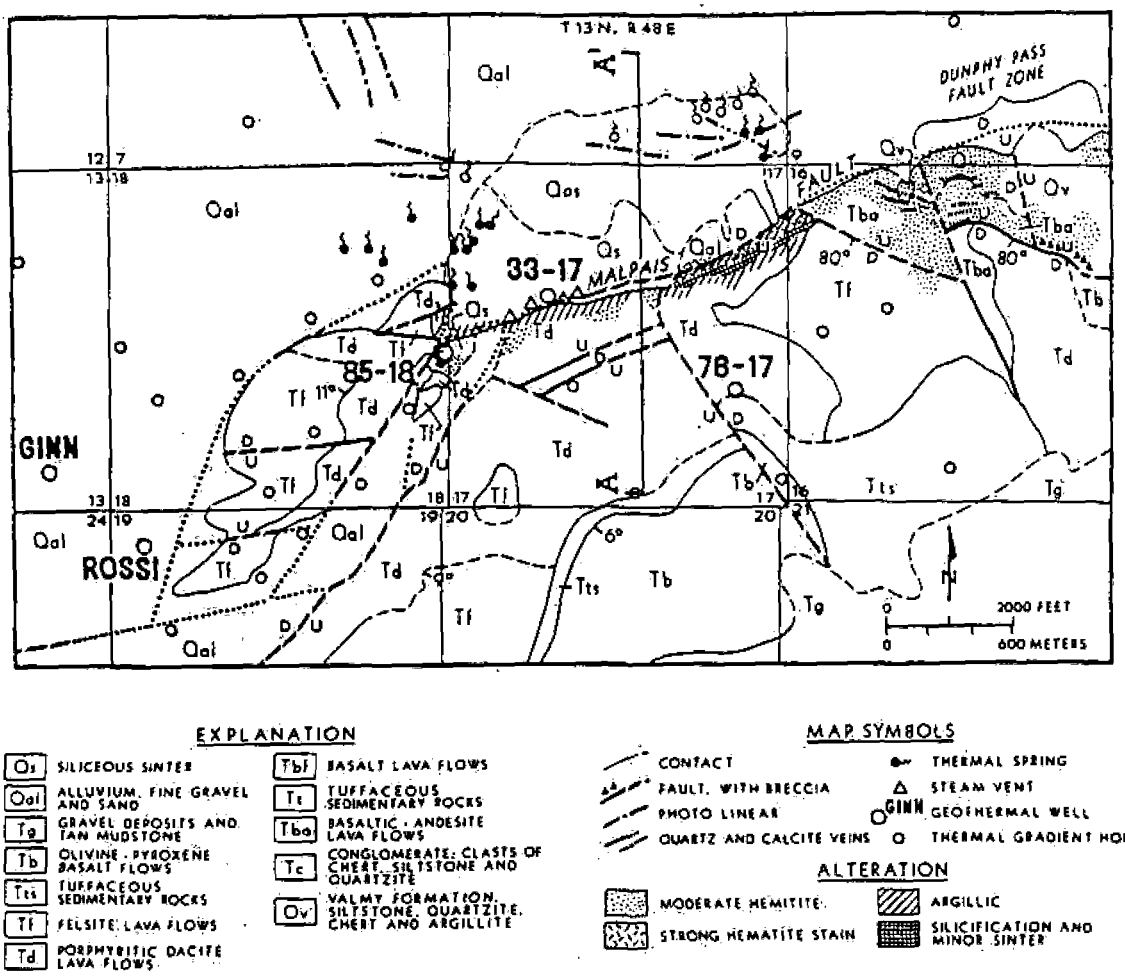

Figure 27. Generalized geology, Beowawe. (from Sibbett, 1983).

"The Beowawe geothermal system in northern Nevada is a structurally controlled, water-dominated resource with a measured temperature of 212°C (414°F). Surface expression of the system consists of a large, active opaline sinter terrace that is present along a Tertiary to Quaternary normal fault escarpment. The thermal system appears to be controlled by the subsurface intersection of the east-northeast trending, north dipping Malpais fault with a pre-existing northwest trending fault which dips south and has 884 m of vertical displacement.

Surface alteration associated with the geothermal system is vertically zoned along the Malpais escarpment with, from base to top: hematite stained, argillized rock along the fault trace; silicification and quartz veining; and argillic, acid leach zone at the top. Subsurface alteration generally increases with depth in the volcanic rocks and is most intense in basaltic-andesite lava flows which are capped by tuffaceous sedimentary rock." (Sibbett, 1983)

Figure 28 presents the contoured heat flow values, which provide a focus for attention to the flexure in the Malpais Fault near well 85-18. Smith (1983) discusses the thermal hydrology and heat flow at Beowawe. Swift (1979) outlined the area of low resistivity, as in Figure 29, and this outline passes through the center of the heat flow high. A dipolar self-potential anomaly, shown in Figure 30, best delineates the convective system at Beowawe (Swift, 1979).

According to Swift (1979), gravity and magnetic data delineate the Malpais Fault and the important north-northwest structures which may control the reservoir at depth. Seismic reflection data are too noisy, because of the interbedded volcanic section, to provide definitive structural information. In contrast, Swift (1979) reports that the Geysers area at Beowawe appears as an earth noise source. Magnetotelluric data seem to have yielded only regional information at Beowawe, based on Swift's remarks.

6.0 COMPARATIVE CASE HISTORIES

An evaluation has been made, in Table 3, of the contribution made by each of 14 geophysical

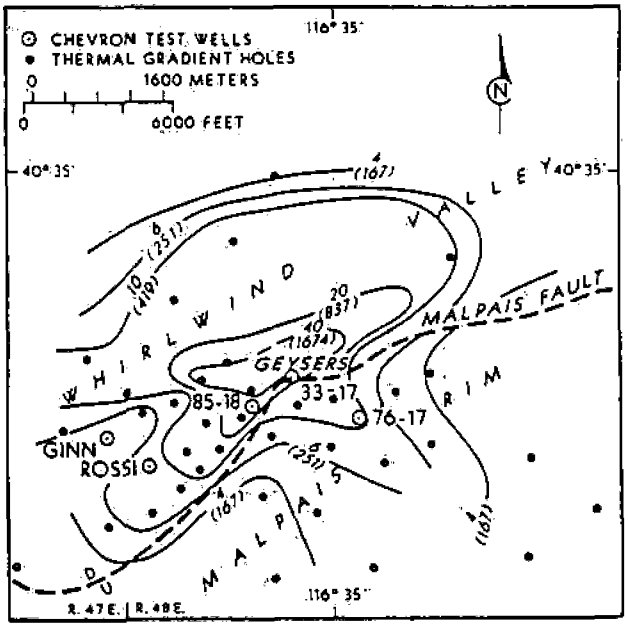

Figure 28. Contours of heat flow at Beowawe (in HFU). (courtesy B. S. Sibbett).

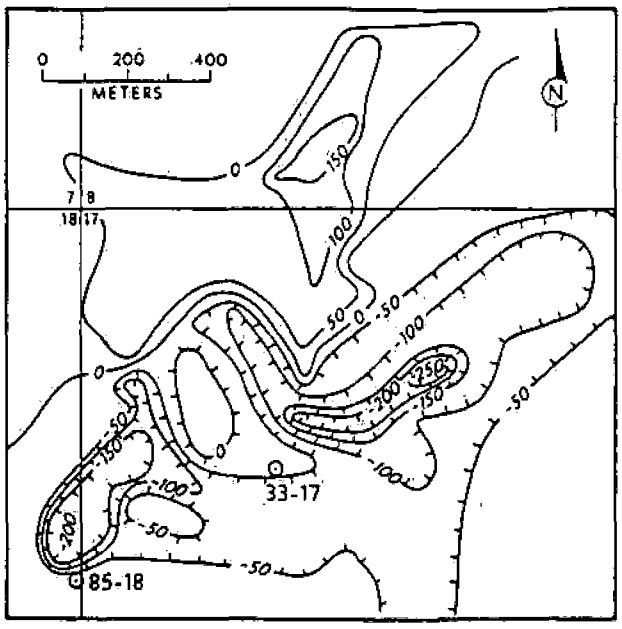

Figure 30. Contours of self-potential at Beowawe. (from DeMoulley and Corwin, 1980).

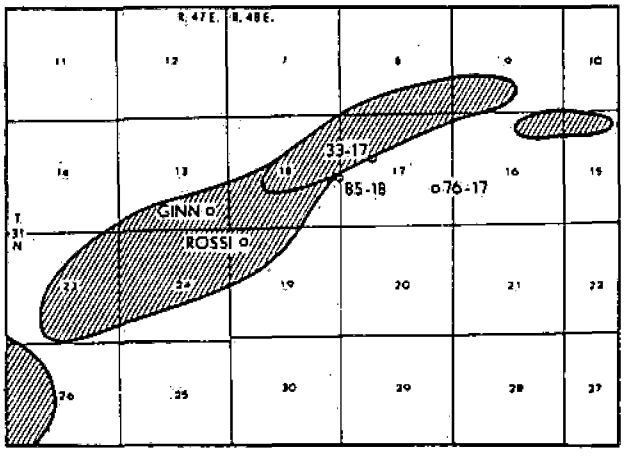

Figure 29. Outline of zone of low resistivity at Beowawe. (after Swift, 1979).

methods to understanding the known or postulated reservoir at each of 13 geothermal prospects. Each method has been rated from 1 (good) through 4 (poor). The rating is subjective, but a serious attempt has been made to apply the rating uniformly throughout the matrix of Table 3. The surprising results of this analysis are that: a) geophysical methods are uniformly inconsistent in performance, b) no geophysical method ranks one, five methods rank about two, eight rank between two and one half and three, while none ranks four, c) no combination of any four methods has been successful at more than one site where "successful" means a ranking of one or two, d) the most useful of the methods, judging by their mean rankings, are heat flow, microearthquakes, gravity, resistivity, and self-potential, e) the least effective methods are earth noise, magnetics, and magnetotellurics. The CSAMT method has been included with CSEM for purposes of the comparative study. There are 23 entries of good (1), 29 of fair (2), 48 of questionable (3), and 10 entries of poor (4) in Table 3. Thus 53% of the time the results of geophysical surveys in geothermal exploration are either questionable or poor.

Overall, this study provides a somewhat discouraging picture. I would tend to use heat flow, microearthquakes, gravity, resistivity (or CSAMT), and self-potential methods at all prospects. Once these data were interpreted and correlated, I would then decide whether or not additional geophysical surveying was justified. All geophysical surveys should be designed with one or more conceptual geological models in mind and the density and extent of the geophysical coverage should be compatible with the range of conceptual geologic models.

Clearly the reader will want to know why each method has performed poorly or questionably under some circumstances. To attempt to satisfy the reader's curiosity, I have prepared Table 4 in which I have indicated my assessment of why a method rated a 3 or a 4 in Table 3. Six categories of answers seem to be sufficient. These are:

TABLE 3 CONTRIBUTION TO UNDERSTANDING RESERVOIR

METHOD	IGNEOUS RELATED: COSO*	LONG VALLEY*	ROOSEVELT HOT SPRINGS*	BALTAZOR	BEOWAWE*	COVE FORT*	DESERT PEAK*	GRASS VALLEY	McCOY	SAN EMIDIO	SODA LAKE*	TUSCARORA	RAFT RIVER	MEAN
EARTH NOISE	3	3	4		1			4	3	3				3.0
MICROEARTHQUAKES	1	3	3	3		2		1	1			1		1.9
TELESEISMS	2	1	3						3			4		2.6
REFRACTION	2	2	3					3					2	2.4
REFLECTION			3		3	4		1		2	2			2.5
GRAVITY	4	2	4	1	2	3	3	1	3	1	2	1	2	2.2
MAGNETICS	1	3	4	3	3	2		4	3		4	3	3	3.0
RESISTIVITY	2	3	1	1	2	1	4	2	3	2	3	2	3	2.2
CSEM & CSAMT		3	1					3	3		2			2.4
SCALAR AMT	2	3		2									3	2.5
MT/AMT			3		3		3	3	3		3	3	3	3.0
SELF POTENTIAL		1	2	3	1			2	2			3	3	2.1
TELLURICS	3			3				2	2					2.5
HEAT FLOW	1	3	1	2	1	2	1	2	3	3	1	3	2	1.9

* EXPECTED TO BE COMMERCIAL IN NEAR TERM
* EXPECTED TO BE COMMERCIAL IN LONG TERM

CODE: 1 GOOD, 2 FAIR, 3 QUESTIONABLE, 4 POOR

TABLE 4 REASONS FOR POOR PERFORMANCE OF GEOPHYSICAL METHODS

METHOD	IGNEOUS RELATED: COSO*	LONG VALLEY*	ROOSEVELT HOT SPRINGS*	BALTAZOR	BEOWAWE*	COVE FORT*	DESERT PEAK*	GRASS VALLEY	McCOY	SAN EMIDIO	SODA LAKE	TUSCARORA	RAFT RIVER	SUMMARY
EARTH NOISE	T_1	T_1	N					N	R	T_1				3T_1,2N,1R
MICROEARTHQUAKES		R	R	R										3R
TELESEISMS	I		I						R			R		2R,2I
REFRACTION			N					N						2N
REFLECTION			N		T_2	T_1								1T_1,1T_2,1N
GRAVITY	N		N			N	N		R					4N,1R
MAGNETICS		R	N	R	R			N	R		R	D	R	6R,2N,1D
RESISTIVITY		R					T_1		D		R		R	3R,1T_1,1D
CSEM & CSAMT		R						I	I					2I,1R
SCALAR AMT		R											R	2R
MT/AMT			N		N		I	I	I		N	I	R	4I,3N,1R
SELF POTENTIAL				T_1								R	R	2R,1T_1
TELLURICS	R			D										1R,1D
HEAT FLOW		R							R	R		R		4R

T_1 - TECHNOLOGY DEFICIENT, HAS BEEN IMPROVED
T_2 - TECHNOLOGY DEFICIENT, HAS NOT BEEN IMPROVED
I - INTERPRETATION PROCEDURE QUESTIONABLE
D - DATA SET INCOMPLETE
N - NO RECOGNIZABLE SIGNATURE OVER RESERVOIR
R - RELATIONSHIP TO RESERVOIR UNCERTAIN

T_1 - technology deficient, but has since been improved,
T_2 - technology deficient, and has not yet been improved,
I - interpretation procedure questionable,
D - data set incomplete,
N - no recognizable signature over reservoir, and
R - relationship to reservoir uncertain.

Table 4 contains 6 T_1, 1 T_2, 12 N, 28 R, 8 I, and 3 D entries. The T_1, I and D entries total 17 (29%), indicating that improvement in equipment or interpretation has or can be made. Unfortunately, we can do nothing about the poor ratings associated with the 41 entries (71%) reporting T_2, N, and R.

The following comments follow on each method:

earth noise

The technology has improved so that the method should perform better when advantage is taken of f-k processing.

microearthquakes

Some geothermal reservoirs do not yield sufficient numbers of microearthquakes to permit the method to be successful.

teleseisms

The method does not always produce useful results.

refraction seismology

The method is not always applicable to reservoir delineation. It should be used late in the exploration sequence.

reflection seismology

Data processing advances in reflection seismology may ultimately permit us to work in volcanic environments and efforts should be directed toward that end. However, the method will not always be applicable to reservoir delineation and should be used late in the exploration sequence.

gravity and magnetics

The main use of the gravity and magnetic methods will continue to be as aids in geological mapping of structure. Gravity seems to be quite useful in mapping range front faults with which some geothermal reservoirs are associated. The magnetic method occasionally will prove useful in mapping zones of magnetite destruction.

resistivity

The technology of data acquisition, processing, and interpretation has been much improved for Schlumberger and dipole-dipole resistivity surveys. Algorithms for 2D modeling of resistivity data are now used routinely. Algorithms for 3D modeling are available. The bipole-dipole method has not proven itself to be satisfactory for reservoir delineation in most cases.

CSEM/CSAMT

These methods have not been sufficiently tested in geothermal environments to be certain of their future. Interpretation procedures for CSAMT are capable of encompassing 2-D and 3-D earth models, although there has been a reluctance on the part of industry to use them. Reliable computer algorithms to permit 2D modeling of CSEM data are only now emerging. Algorithms for 3D modeling are still on the drawing boards.

scalar AMT

Scalar AMT doesn't always produce results that are as good as we prefer and its use should be restricted to reconnaissance surveys.

MT/AMT

There is a tendency to use 1D inversion, only, in interpretation of MT/AMT data. Algorithms for 2D and 3D interpretation are available but industry seems reluctant to use them. This is the weakest link in application of the method. Data acquisition and processing have improved greatly in recent years, to the extent that there is no excuse for data of poor quality.

There is also a tendency by industry to use MT/AMT when it is not warranted. It should be reserved for special situations, usually late in the exploration sequence.

self-potential

The self-potential method shows great promise, if the new quantitative interpretation schemes work as expected. The method doesn't always produce meaningful signatures over geothermal systems.

tellurics

Since it lacks a truly quantitative scheme for interpretation, the method should be used only in reconnaissance.

heat flow

As Blackwell (1983) has indicated, heat flow as measured at surface is not always a reliable indicator of a high quality geothermal resource. Reference should be made to Blackwell's paper for cognizance of the advantages and limitations of heat flow in geothermal applications.

7.0 CONCLUSIONS

The performance of 14 different geophysical methods used at 13 high temperature geothermal

sites in the Northern Basin and Range Province has been somewhat disappointing. Heat flow, microearthquakes, gravity, resistivity and self-potential methods appear to be the most consistently useful, although none of them performs up to expectations all of the time. Recent improvements in interpretation procedures are expected to benefit the resistivity and self-potential methods. The least effective methods at the present time are earth noise, reflection seismology, magnetics, magnetotellurics, and tellurics. Recent improvements in survey design will make the earth noise method much more effective for those reservoirs which emit earth noise. Accomplished improvements in interpretation of magnetotelluric data, if adopted by industry, will improve that method's performance. However, the magnetotelluric method ought to be reserved for those special prospects to which it is applicable. Improvements in processing reflection seismic data in volcanic covered areas may make that method more generally applicable in the late stages of an exploration sequence. The teleseismic method, developed to a reasonable degree of sophistication, may occasionally contribute, in a broad sense, to understanding the reservoir. The refraction seismic method probably ought to be considered a subset of combined reflection-refraction surveys for optimum resolution of subsurface velocity structures. However, refraction seismic surveys should be considered also as an adjunct to microearthquake surveys since they can provide 3D velocity distributions necessary for interpretation of microearthquake data. Controlled source electromagnetic and controlled source audiomagnetotelluric methods require much more exposure in geothermal exploration before they can be evaluated properly. However, the controlled source audiofrequency magnetotelluric method looks very promising, and it may replace resistivity surveying if its cost-effectiveness can be established as is expected. Scalar AMT and tellurics seem destined for use as inexpensive reconnaissance techniques which will find occasional application.

There is evidence of need for improvement in survey design, data acquisition, data processing, and data interpretation in geothermal exploration in the Northern Basin and Range Province. Yet the predominant problems with application of geophysical methods in this environment are related to fundamental limitations of the methods as have been described in the text.

Of the five case histories presented for comparison in this article, we find the following results.

Long Valley

While no high temperature reservoir has been defined, there is a chance that ultimately the teleseismic, microearthquake and self-potential methods may prove to be valuable in delineating a postulated fracture-controlled reservoir beneath the medial graben in the resurgent dome. The existence of such a reservoir probably requires regional faulting through the resurgent dome following the graben, and subsequent extension produced by recent bulging of the dome. Refraction seismology and gravity have been exceptionally useful in quantifying the potential reservoir, advocated by the USGS, to be the Bishop Tuff within the Long Valley caldera. The heat flow anomaly at this site may be misleading.

Coso

The combination of resistivity, scalar AMT, shallow heat flow, and airborne magnetic data, when added to the knowledge of hydrothermal alteration provided by careful geological mapping, have clearly defined the drilling targets. Teleseismic P-wave delays and refraction seismology are methods which have provided information of secondary importance.

Roosevelt Hot Springs

The heat flow pattern at Roosevelt Hot Springs has been fundamental in outlining the reservoir. However, careful application of the resistivity and CSAMT techniques has provided the detail necessary to site wells. Self-potential data at this site have not yet been interpreted quantitatively but ultimately it may prove to be useful in understanding and delineating the reservoir.

Tuscarora

Microearthquakes and gravity draw attention to the eastern margin of Independence Valley, while heat flow and surface manifestations draw attention to a region around Hot Sulphur Springs about 4 km to the west. Drilling has been concentrated in the vicinity of Hot Sulphur Springs whereas our speculation dictates that the reservoir might be along the range front fault bounding the eastern margin of Independence Valley. Dipole-dipole resistivity interpretations would tend to confirm this notion. The heat flow data at this site may be misleading.

Beowawe

The self-potential method has been the best confirmation of the heat flow anomaly which seems to be centered over the shallow reservoir. Dipole-dipole resistivity has provided supporting evidence for the location of the drilling target. Gravity and magnetics have helped to define the Malpais Fault zone while application of MT/AMT was necessary to attempt to delineate the deep reservoir.

From the above comments it should be evident that there is no common denominator of geophysical methods which might lead us to a better record of discovery and delineation of geothermal reservoirs. Exploration for igneous-related geothermal systems is no different from those geothermal systems of no obvious igneous relationship. Exploration for geothermal

resources of any type, those with surface manifestations or those without, is difficult.

8.0 ACKNOWLEDGEMENTS

This review article has only been made possible by my reliance upon the library facilities of the Earth Science Laboratory of the University of Utah Research Institute. I am grateful to C. M. Swift, Jr. and Dennis L. Nielson, for excellent reviews which have markedly improved the manuscript. P. M. Wright kindly provided a final editing of the manuscript. Connie Pixton, Doris Cullen, Pat Daubner, Sandra Bromley, and Paul Onstott prepared the illustrations. Joan Pingree dutifully and superbly turned out draft after draft on her word processor. I am indebted to all of the above mentioned people.

This report has been prepared under DOE Contract No. DE-AC07-80ID12079 with the U.S. Department of Energy.

REFERENCES

Ackerman, H.D., 1979, Seismic refraction study of the Raft River geothermal area, Idaho: Geophysics, v. 44, p. 216-225.

Aiken, C.L.V., and Ander, M.E., 1981, A regional strategy for geothermal exploration with emphasis on gravity and magnetotellurics: J. Volc. and Geotherm. Res., v. 9, p. 1-27.

Anderson, L.A., and Johnson, G.R., 1976, Application of the self-potential method to geothermal exploration in Long Valley, California: J. Geophys. Res., v. 81, p. 1527-1532.

Applegate, J.K., Goebel, V.S., Kallenberger, P., and Rossow, J., 1981, The use of seismic reflection techniques in geothermal areas throughout the U.S.: extended abstract, 5th Annual International Meeting and Exposition, Society of Exploration Geophysicists, Los Angeles, Oct. 11-15.

Arnorsson, S., Bjornsson, A., Gislason, G., and Gudmundsson, G., 1975, Systematic exploration of the Krisuvik high-temperature area, Reykjanes Peninsula, Iceland: Proc. Second U.N. Symposium on the Development and Use of Geothermal Resources, San Francisco, v. 2, p. 853-864.

Bailey, R.A., Dalrymple, G.B., and Lanphere, M.A., 1976, Volcanism structure and geochronology of Long Valley caldera, California: J. Geophys. Res., v. 81, p. 725-744.

Ballantyne, J.M., 1978, Hydrothermal alteration at the Roosevelt Hot springs thermal area, Utah: modal mineralogy and geochemistry of sericite, chlorite, and feldspar from altered rocks, Thermal Power Company well Utah State 14-2: Univ. of Utah, Dept. of Geol. and Geophys. Rept., 42 p.

Bamford, R.W., Christensen, O.D., and Capuano, R.M., 1980, Multielement geochemistry of solid materials in geothermal systems and its application, Part I: The hot-water systems at Roosevelt Hot Springs KGRA, Utah: Univ. of Utah Res. Inst., Earth Sci. Lab., Rept. ESL-30.

Bannister, P.R., 1969, Source distance dependence of the surface-impedance conductivity measurement technique: Geophysics, v. 34, p. 785-788.

Banwell, C.J., 1970, Geophysical techniques in geothermal exploration: U.N. Symposium on the Development and Utilization of Geothermal Resources, Pisa, Geothermics Spec. Issue 2, v. 2, pt.1, p. 32-56.

Banwell, C.J., and Macdonald, W.J.P., 1965, Resistivity surveying in New Zealand thermal areas: Eighth Commonwealth Mining and Metallurgical Congress, Australia and New Zealand, New Zealand Section, p. 1-7.

Baudu, R., Bernhard, J., Georgel, J.M., Griveau, P., Rugo, R., 1980, Application of d.c. dipolar methods in the Upper Rhinegraben: Advances in European and Geothermal Research, Dordrecht, Holland, D. Reidel Co., p. 823-832.

Benoit, W. R., and Butler, R. W., 1983, A review of high temperature geothermal developments in the northern Basin and Range Province: this volume.

Berkman, F., and Lange, A.L., 1980, Tuscarora geophysics - preliminary report: Amax Exploration, Inc. internal report, open filed by Univ. of Utah Res. Inst., Earth Sci. Lab., 7 p.

Berktold, A., 1982, Electromagnetic studies in geothermal regions: Proc. 6th Workshop on Electromagnetic Induction in the Earth and Moon, Dept. Physics, Univ. of Victoria, Canada.

Berktold, A., and Kemmerle, K., 1982, Distribution of electrical conductivity in the Urach geothermal area, a magnetotelluric and geomagnetic depth sounding investigation, The Urach Geothermal Project: Stuttgart, E. Schweizerdort'sche Verlagsbuchhandling, p. 289-300.

Beyer, J.H., 1977, Telluric and D.C. resistivity techniques applied to the geophysical investigation of Basin and Range geothermal systems: Univ. of California, Lawrence Berkeley Lab., Rept. LBL-6325, 461 p., 3 vol.

Beyer, J.H., Morrison, H.F., and Dey, A., 1975, Electrical exploration of geothermal systems in the Basin and Range valleys of Nevada: Proc. Second U.N. Symposium on the Development of Geothermal Resources, San

Francisco, p. 889-894.

Beyer, J.H., Dey, A., Liaw, A., Major, E., McEvilly, T.V., Morrison, H.F., and Wollenberg, H., 1976, Preliminary open file report, geological and geophysical studies in Grass Valley, Nevada: University of California, Lawrence Berkeley Lab., Rept. LBL-5262, 144 p.

Bibby, H.M., and Risk, G.F., 1973, Interpretation of dipole-dipole resistivity surveys using a hemispheroidal model: Geophysics, v. 38, p. 719-736.

Blackwell, D. D., 1983, Heat flow in northern Basin and Range Province: this volume.

Capuano, R.M., and Cole, D., 1982, Fluid-mineral equilibria in high temperature geothermal systems: the Roosevelt Hot Springs geothermal system, Utah: Geochim. et Cosmochim. Acta, v. 46, p. 1353-1364.

Cheng, W.T., 1970, Geophysical exploration in the Tatum volcanic region, Taiwan: Proc. U.N. Symposium on the Development and Utilization of Geothermal Resources, Pisa, Geothermics Spec. Issue 2, v. 2., pt. 1, p. 262-274.

Chu, J.J., Ward, S.H., Sill, W.R., Stodt, J.A., 1983, Induced polarization at Roosevelt Hot Springs Geothermal Area, Utah: unpublished manuscript.

Combs, J., 1980, Heat flow in the Coso geothermal area, Inyo County, California: J. Geophys. Res., v. 85, p. 2411-2424.

Combs, J., and Rotstein, Y., 1975, Microearthquake studies at the Coso geothermal area, China Lake, California: Proc. Second U.N. Symposium on the Development and Use of Geothermal Resources, San Francisco, p. 917-928.

Combs, J., and Jarzabek, D., 1977, Geothermal: State of the Art: Trans., Geoth. Res. Council, v. 1, p. 41-44.

Corwin, R.F., 1975, Self-potential exploration for geothermal reservoirs: Proc. Second U.N. Symposium on the Development and Use of Geothermal Resources, San Francisco, p. 937-946.

Corwin, R.F., and Hoover, D.B., 1979, The self-potential method in geothermal exploration: Geophysics, v. 44, p. 226-245.

DeMoully, G.T., and Corwin, R.F., 1980, Self-potential survey results from the Beowawe KGRA, Nevada: Trans., Geoth. Res. Council, v. 4, p. 33-36.

Dey, A., and Morrison, H.F., 1977, An analysis of the bipole-dipole method of resistivity surveying: Geothermics, v. 6, p. 47-81.

Douze, E.J., and Laster, S.J., 1979, Seismic array noise studies at Roosevelt Hot Springs, Utah, geothermal area: Geophysics, v. 44, p. 1570-1583.

Dupis, A., Marie, Ph., and Petian, G., 1980, Magnetotelluric prospecting of the Mont Dore area: Advances in European Geothermal Research, D. Reidel, Dordrecht, Holland, p. 935-943.

Edmiston, R.C., 1982, A review and analysis of geothermal exploratory drilling results in the northern Basin and Range geologic province of the U.S.A. from 1974 through 1981: Trans, Geoth. Res. Council, v. 6, p. 11-14.

Edquist, R.K., 1981, Geophysical investigation of the Baltazor Hot Springs known geothermal resource area and the Painted Hills thermal area, Humboldt County, Nevada: Univ. of Utah Res. Inst., Earth Sci. Lab., Rept. DOE/ID/12079-29, 89 p.

Fox, R.C., 1978a, Low-altitude aeromagnetic survey of a portion of the Coso Hot Springs KGRA, Inyo County, California: Univ. of Utah Res. Inst., Earth Sci. Lab., Rept. IDO/77.5.7., 19 p.

Fox, R.C., 1978b, Dipole-dipole resistivity survey of a portion of the Coso Hot Springs KGRA, Inyo County, California: Univ. of Utah Res. Inst., Earth Sci. Lab., Rept. IDO/77.5.6., 21 p.

Fox, R.C., Hohmann, G.W., Killpack, T.J., and Rijo, L., 1980, Topographic effects in resistivity and induced polarization surveys: Geophysics, v. 43, p. 144-172.

Frangos, W., and Ward, S.H., 1980, Bipole-dipole survey at Roosevelt Hot Springs thermal area, Beaver County, Utah: Univ. of Utah Res. Inst., Earth Sci. Lab., Rept. DOE/ID/12079-15, 41 p.

Gamble, T.D., Goubau, W.M., and Clarke, J., 1979a, Magnetotellurics with a remote reference: Geophysics, v. 44, p. 53-68.

Gamble, T.D., Goubau, W.M., and Clarke, J., 1979b, Error analysis for remote reference magnetotellurics: Geophysics, v. 44, p. 959-968.

Gamble, T.D., Goubau, W.M., Goldstein, N.E., and Clarke, J., 1980, Referenced magnetotellurics at Cerro Prieto: Geothermics, v. 9, p. 49-63.

Garcia, D.S., 1975, Geoelectric study of the Cerro Prieto geothermal area, Baja, California: Proc. Second U.N. Symposium on the Development and Use of Geothermal Resources, San Francisco, v. 2, p. 1009-1012.

Gertson, R.C., and Smith, R.B., 1979, Interpretation of a seismic refraction profile across the Roosevelt Hot Springs, Utah and vicinity: Univ. of Utah, Dept. Geol. and Geophys., Rept. IDO/78-1701.a.3, 116 p.

Goldstein, N.E., and Paulsson, B., 1979, Interpretation of gravity surveys in Grass and Buena Vista Valleys, Nevada: Geothermics, v. 7, p. 29-50.

Goldstein, N.E., Mozley, E., Gamble, T.D., and Morrison, H.F., 1978a, Magnetotelluric investigations at Mt. Hood, Oregon: Trans. G.R.C., v. 2, p. 219-221.

Goldstein, N.E., Norris, R.A., and Wilt, M.J., 1978b, Assessment of surface geophysical methods in geothermal exploration and recommendations for future research: Univ. of California, Lawrence Berkeley Laboratory, Rept. LBL-6815, 166 p.

Goldstein, N.E., Mozley, E., and Wilt, M., 1982, Interpretation of shallow electrical features from electromagnetic and magnetotelluric surveys at Mount Hood, Oregon: J. Geophys. Res., v. 87, p. 2815-2828.

Gupta, M.L., Singh, S.B., and Rao, B.V., 1975, Studies of direct current resistivity in the Puga geothermal field, Himalayas, India: Proc. Second U.N. Symposium on the Development and Use of Geothermal Resources, San Francisco, v. 2, p. 1029-1036.

Gupta, H.K., Ward, R.W., and Lin, T-L., 1982, Seismic wave velocity investigation at The Geysers - Clear Lake geothermal field, California: Geophysics, v. 47, p. 819-824.

Hamilton, R.M., and Muffler, L.J.P., 1972, Microearthquakes at The Geysers geothermal area, California: J. Geophys. Res., v. 77, p. 2081-2086.

Hatherton, T., Macdonald, W.J.P., and Thomson, G.E.K., 1966, Geophysical methods in geothermal prospecting in New Zealand: Bull. Volcanology, p. 485-497.

Hermance, J.F., and Pedersen, J., 1977, Assessing the geothermal resource base of the southwestern U.S.; status report of a regional geoelectromagnetic traverse: Geophysics, v. 42, p. 155-156.

Hermance, J.F., Thayer, R.E., Bjornsson, A., 1975, The telluric-magnetotelluric method in the regional assessment of geothermal potential: Proc. Second U.N. Symposium on the Development and Use of Geothermal Resources, San Francisco, v. 2, p. 1037-1048.

Hermance, J.F., and Peltier, W.R., 1970, Magnetotelluric fields of a line current: J. Geophys. Res., v. 75, p. 3351-3356.

Hill, D. G., Layman, E. B., Swift, C. M., Jr., and Yungul, S. H., 1979, Soda Lake, Nevada, thermal anomaly: Trans., Geoth. Res. Council, v. 3, p. 305-308.

Hill, D.P., 1976, Structures of Long Valley Caldera, California, from a seismic refraction experiment: J. Geophys. Res., v. 81, 5, p. 745-753.

Hochstein, M.P., and Hunt, T.M., 1970, Seismic, gravity, and magnetic studies, Broadlands geothermal field, New Zealand: Proc. U.N. Symposium on the Development and Utilization of Geothermal Resources, Pisa, Geothermics Spec. Issue 2. v. 2, pt. 1, p. 333-346.

Hohmann, G.W., and Jiracek, G.R., 1979, Bipole-dipole interpretation with three-dimensional models: Univ. of Utah Res. Inst., Earth Sci. Lab., Rept. DOE/ET/28392-29, 20 p.

Hoover, D.B., 1981, Self-potential investigations at Mt. Hood, Oregon, paper presented at the Self-Potential Workshop, Golden, Colorado, March 3-4, 1981.

Hoover, D.B., Frischknecht, F.C., and Tippens, C., 1976, Audiomagnetotelluric soundings as a reconnaissance exploration technique in Long Valley, Calif: J. Geophys. Res., v. 81, p. 801-809.

Hoover, D.B., and Long, C.L., 1976, Audiomagnetotelluric methods in reconnaissance geothermal exploration: Proc., Second U.N. Symposium on the Development and Use of Geothermal Resources, San Francisco, p. 1059-1064.

Hoover, D.B., Long, C.L., and Senterfit, R.M., 1978, Some results from audiomagnetotelluric investigations in geothermal areas: Geophysics, 43, p. 1501-1514.

Hulen, J.B., 1978, Geology and alteration of the Coso geothermal area, Inyo County, California: Univ. of Utah Res. Inst., Earth Sci. Lab., Rept. IDO/78-1701-b.4.1, 28 p.

Hutton, V.R.S., Dawes, G.J.K., Devlin, T., and Roberts, R., 1982, Magnetotelluric and magnetovariational studies in the Travale geothermal field: Report for the Commission of the European Communities, Directorate General for Science, Research, and Development.

Isherwood, W..F, 1976, Complete Bouguer gravity map of The Geysers Area, California: U.S. Geological Survey Open File Report, 76-357.

Isherwood, W.F., and Mabey, D.R., 1978, Evaluation of Baltazor known geothermal resources area, Nevada: Geothermics, v. 7, p. 221-229.

Iyer, H.M., and Hitchcock, T., 1975, Seismic noise as a geothermal exploration tool: techniques

and results: Proc. Second U.N. Symposium on the Development and Use of Geothermal Resources, San Francisco, v. 2, p. 1075-1083.

Iyer, H.M. and Stewart, R.M., 1977, Teleseismic technique to locate magma in the crust and upper mantle, H.J.B. Dick, ed., Magma genesis; Oregon Dept. of Geol. and Min. Ind., Bull. 96, p. 281-299.

Iyer, H.M., Oppenheimer, D.H., and Hitchcock, T., 1979, Abnormal P-wave delays in The Geysers - Clear Lake geothermal area, California: Science, v. 204, p. 495.

Jackson, D.B., and Keller, G.V., 1972, An electromagnetic sounding survey of the summit of Kilauea Volcano, Hawaii: J. Geophys. Res., v. 77, p. 4957.

Jackson, D.B., and O'Donnell, J.E., 1980, Reconnaissance electrical surveys in the Coso Range, California: J. Geophys. Res., v. 85, p. 2502-2516.

Jacobson, J.J., Pritchard, J.I., 1975, Electromagnetic soundings in geothermal exploration: Proc. Second U.N. Symposium on the Development and Use of Geothermal Resources, San Francisco, p. 45-.

Jiracek, G.R., and Smith, C., 1976, Deep resistivity investigations at two known geothermal resource areas (KGRAs) in New Mexico: Radium Springs and Lightning Dock: New Mexico Geol. Soc. Spec. Pub. No. 6, p. 71-76.

Jiracek, G.R., Smith, C., Dorn, G.A., 1975, Deep geothermal exploration in New Mexico using electrical resistivity: Proc. Second. U.N. Symposium on the Development and Use of Geothermal Resources, San Francisco, p. 1095-1102.

Kane, M.F., Mabey, D.R., and Brace, R., 1976, A gravity and magnetic investigation of the Long Valley Caldera, Mono County, California: J. Geophys. Res., v. 81, p. 754-762.

Kauahikaua, J., 1981, Interpretation of time-domain electromagnetic soundings in the East Rift geothermal area of Kilauea volcano, Hawaii: USGS open-file report 81-979.

Keller, B.V., Furgerson, R., Lee, C.Y., Harthill, N., and Jacobson, J.J., 1975, The dipole mapping method: Geophysics, v. 40, p. 451-472.

Keller, G.V., 1970, Induction methods in prospecting for hot water: Proc. U.N. Symposium on the Development and Utilization of Geothermal Resources, Pisa, Geothermics Spec. Issue 2, vol. 2, pt. 1, p. 318-332.

Keller, G.V., and Frischknecht, F.C., 1966, Electrical methods in geophysical prospecting: New York, Pergammon Press, 517 p.

Keller, G.V., and Rapolla, A., 1974, Electrical prospecting methods in volcanic areas: Civetta, K., et al., eds., Physical volcanology: Amsterdam, Elsevier Sci., p. 133.

Keller, G.V., Taylor, K., and Santo, J.M., 1982, Megasource EM method for detecting deeply buried conductive zones in geothermal exploration: Geophysics, v. 47, p. 420 (abstract).

Klein, D.P., and Kauahikaua, J.P., 1975, Geoelectric-geothermal exploration, Hawaii Island, preliminary results: report, Hawaii Institute of Geophysics.

Lachenbruch, A. H., Sorey, M. L., Lewis, R. E., and Sass, J. H., 1976a, The near-surface hydrothermal regime of Long Valley caldera: J. Geophys. Res., v. 81, p. 763-768.

Lachenbruch, A. H., Sass, J. H., Munroe, R. J., and Moses, T. H., Jr., 1976b, Geothermal setting and simple heat conduction models for the Long Valley caldera: J. Geophys. Res., v. 81, p. 769-784.

Lange, A.L., and Westphal, W.H., 1969, Microearthquakes near The Geysers, Sonoma County, California: J. Geophys. Res., v. 74, p. 4377-4382.

Lange, A.L., 1980, The McCoy Nevada geothermal project: Paper delivered at the Fiftieth Annual Meeting of the Society of Exploration Geophysicists, Houston, Texas, 17 November.

Liaw, A.L., and McEvilly, T.V., 1979, Microseisms in geothermal exploration-studies in Grass Valley, Nevada: Geophysics, v. 44, p. 1097-1115.

Liaw, A., and Suyenaga, W., 1982, Detection of geothermal microtremors using seismic arrays: paper presented at 52 Annual International Meeting and Exposition, Society of Exploration Geophysicists, Dallas, Oct. 17-21.

Lipman, P.W., Rowley, P.D., Mehnert, H.H., Evans, S.H., Jr., Nash, W.P., and Brown, F.H., 1977, Pleistocene rhyolite of the Mineral Range, Utah: geothermal and archeological significance: U.S.G.S. J. Res., v. 6, p. 133-147.

Long, C.L., and Kaufman, H.E., 1980, Reconnaissance geophysics of a known geothermal resource area, Weiser, Idaho, and Vale, Oregon: Geophysics, v. 45, p. 312-322.

Lumb, F.T., and Macdonald, W.J.P., 1970, Near-surface resistivity surveys of geothermal areas using the electromagnetic method: U.N. Symposium on Development and Utilization of

Geothermal Resources, Pisa, Geothermics Spec. Issue 2, p. 311-317.

Macdonald, W.J.P. and Muffler, L.J.P., 1972, Recent geophysical exploration of the Kawerau geothermal field, North Island, New Zealand: New Zealand J. Geol. and Geophys., v. 18, p. 303.

Mackelprang, C.E., 1982, Interpretation of the dipole-dipole electrical resistivity survey, Tuscarora geothermal area, Elko County, Nevada: Univ. of Utah Res. Inst., Earth Science Lab., Rept. DOE/ID/12079-59

Madden, T.R., and Nelson, P.H., 1964, A defense of Cagniard's magnetotelluric method: Massachusetts Inst. of Technology, Geophys. Lab., Rept. NR-391-401.

Majer, E.L., 1978, Seismological investigations in geothermal regions: Univ. of California, Lawrence Berkeley Lab., Rept. LBL-7054, 225 p.

Majer, E.L. and McEvilly, T.V., 1979, Seismological investigations at The Geyers geothermal field: Geophysics, v. 44, p. 246-249.

Mansure, A.J., and Brown, G.L., 1982, A forecast of geothermal drilling activity: Geothermal Energy, v. 10, p. 8-18.

Martinez, M., Fabrial, H., and Romo, J.M., 1982, Magnetotelluric studies in the geothermal area of Culiacan, Mexico: Sixth Workshop on Electromagnetic Induction in the Earth and Moon, IAGA., Victoria, British Columbia, Dept. of Physics, Univ. of Victoria (abstract).

McNitt, J.R., 1975, Summary of United Nations geothermal exploration experience, 1965 to 1975: Proc. Second U.N. Symposium on the Development and Use of Geothermal Resources, San Francisco, p. 1137-1134.

Meidav, T., and Furgerson, R., 1972, Resistivity studies of the Imperial Valley geothermal area, California: Geothermics, v. 1, p. 47-62.

Meidav, T., and Tonani, F., 1975, A critique of geothermal exploration methods: Proc. Second U.N. Symposium and the Development and Use of Geothermal Resources, San Francisco, p. 1143-1154.

Miller, C.D., Mullineaux, D.R., Crandell, D.R., and Bailey, R.A., 1982, Potential hazards from future volcanic eruptions in the Long Valley-Mono Lake area, east-central California and southwest Nevada - A preliminary assessment: U.S. Geol. Survey, Circular 877, 10 p.

Morrison, H.F., Goldstein, N.E., Hoversten, M., Oppliger, G., and Riveros, C., 1978, Description, field test, and data analysis of a controlled-source EM system (EM-60): University of California, Lawrence Berkeley Laboratory, Rept. LBL-7088, 150 p.

Morrison, H.F., Lee, K.H., Oppliger, G., and Dey, A., 1979, Magnetotelluric studies in Grass Valley, Nevada: Univ. of California, Lawrence Berkeley Lab., Rept. LBL-8646, 50 p.

Muffler, L.J.P., and Williams, D.L., 1976, Geothermal investigations of the U.S. Geological Survey in Long Valley, California, 1972-73: J. Geophys. Res., v. 81, p. 721-724.

Musmann, G., Gramkow, B., Lohr, V., and Kertz, W., 1980, Magnetotelluric survey of the Lake Laach (Eifel) volcanic area: Advances in European Geothermal Research: D. Reidel Co., Dordrecht, Holland, p. 904-910.

Newman, G.H., Wannamaker, P.E., and Hohmann, G.W., 1983, A two- and three-dimensional magnetotelluric model study with emphasis on the detection of magma chambers in the Basin and Range: Univ. of Utah, Dept. of Geol. and Geophys. Rept.

Ngoc, P.V., 1980, Magnetotelluric survey of the Mount Meager region of the Squamish Valley (British Columbia): Rept. of the Geomagnetic Service of Canada, Earth Physics Section, Dept. of Energy, Mines, and Resources, Ottawa, 26 p.

Nicholl, J.J., and Lange, A.L., 1981, Passive seismic results near the Tuscarora prospect, Nevada; Trans., Geoth. Res. Council, v. 5, p. 197-200.

Nielson, D.L., 1978, Radon emanometry as a geothermal exploration technique; theory and an example from Roosevelt Hot Springs KGRA Utah: Univ. Utah Res. Inst., Earth Sci. Lab Rept. No. 14, 31 p.

Nielson, D.L., Sibbett, B.S., and McKinney, D.B., Moore, J. N., and Samberg, S., 1978, Geology of Roosevelt Hot Springs KGRA, Beaver County, Utah: Univ. of Utah Res. Inst., Earth Sci. Lab., Rept. 12, 121 p.

Nur, A., and Simmons, G., 1969, The effect of saturation on velocity in low porosity rocks: Earth Plan. Sci. Letters, v. 7, p. 183-193.

Palmason, G., 1975, Geophysical methods in geothermal exploration: Proc. Second U.N. Symposium on the Development and Use of Geothermal Resources, San Francisco, p. 1175-1184.

Parry, W.T., Ballantyne, J.M., Bryant, H.L., and Dedolph, R.E., 1980, Geochemistry of hydrothermal alteration at the Roosevelt Hot Springs thermal area, Utah: Geochim. et

Cosmochim. Acta, v. 44, p. 95-102.

Patella, D., Quarto, R., and Tramacere, A., 1980, Dipole-dipole study of the Travale geothermal field: Advances in European Geothermal Research, Dordrecht, Holland, D. Reidel Co., p. 833-842.

Patella, D., Rossi, A., Tramacere, A., 1979, First results of the application of the dipole electrical sounding method in the geothermal area of Travale-Radicondoli (Tuscany): Geothermics, v. 8, p. 111-134.

Peltier, W.R., and Hermance, J.F., 1971, Magnetotelluric fields of a Gaussian electrojet: Canadian Jour. of Earth Sci., v. 8, p. 338-346.

Pilkington, H.D., Lange, A.L., and Berkman, F.E., 1980, Geothermal exploration at the Tuscarora prospect in Elko County, Nevada: Trans., Geoth. Res. Council, v. 4, p. 233-236.

Plouff, D., and Isherwood, W. F., 1980, Aeromagnetic and gravity surveys in the Coso Range, California: J. Geophys. Res. v. 85, p. 2491-2501.

Razo, A., Arellano, F., and Fouseca, H., 1980, CFE resistivity studies at Cerro Prieto: Geothermics, v. 9, p. 7-14.

Reasenberg, P., Ellsworth, W., and Walter, A., 1980, Teleseismic evidence for a low-velocity body under the Coso geothermal area: J. Geophys. Res., v. 85, p. 2471-2483.

Risk, G.F., 1975a, Monitoring the boundary of the Broadlands geothermal field, New Zealand: Proc. Second U.N. Symposium on the Development and Use of Geothermal Resources, San Francisco, p. 1185-1190.

Risk, G.F., 1975b, Detection of buried zones of fissured rock in geothermal fields using resistivity anisotropy measurements: Proc. Second U.N. Symposium on the Development and Use of Geothermal Resources, San Francisco, p. 1191-1198.

Risk, G.F., Macdonald, W.J.P., and Dawson, G.B., 1970, D.C. resistivity surveys of the Broadlands geothermal region, New Zealand: Proc. U.N. Symposium on the Development and Utilization of Geothermal Resources, Pisa, Geothermics, Spec. Issue 2, v. 2, p. 287-294.

Robinson, R., and Iyer, H.M., 1981, Delineation of a low-velocity body under the Roosevelt Hot Springs geothermal area, Utah, using teleseismic P-wave data: Geophysics, 46, p. 1456-1466.

Ross, H.P., Nielson, D.L., and Moore, J.N., 1982, Roosevelt Hot Springs geothermal system, Utah - case study: Bull, Am. Assoc. Pet. Geol., v. 66, p. 879-902.

Ryall, A. S., and Vetter, V. R., 1983, Seismological investigation of volcanic and tectonic processes in the western Great Basin, Nevada and eastern California: this volume.

Ryall, A., and Ryall, F., 1981, Attenuation of P and S waves in a magma chamber in the Long Valley Caldera, California: Geophys. Res. Letters, v. 8, p. 557-560.

Sandberg, S.K., and Hohmann, G.W., 1982, Controlled-source audiomagnetotellurics in geothermal exploration: Geophys, v. 47, p. 100-116.

Senturion Sciences, Inc., 1977, N. W. Nevada, Microearthquake survey report for Earth Power Corporation: DOE Industry Coupled Case Study, Univ. of Utah Res. Inst., Earth Sci. Lab., 61 p.

Sibbett, B.S., 1982, Geology of the Tuscarora geothermal prospect, Elko County, Nevada: Bull. Geol. Soc. America, v. 93, p. 1264-1272.

Sibbett, B.S., 1983, Structural control and alteration at Beowawe KGRA, Nevada: submitted to Trans. Geoth. Res. Council.

Sibbett, B.S., and Nielson, D.L., 1980, Geology of the central Mineral Mountains, Beaver Co., Utah: Univ. of Utah Res. Inst., Earth Sci. Lab., Rept. 33, 42 p.

Sill, W.R., 1982a, Self-potential effects due to hydrothermal convection, velocity cross-coupling: Univ. of Utah, Dept. of Geol. and Geophys., Rept. DOE/ID/12079-61, 15 p.

Sill, W.R., 1982b, Diffusion coupled (electrochemical) self-potential effects in geothermal areas: Univ. of Utah, Dept. of Geol. and Geophys., Rept. DOE/ID/12079-73, 31 p.

Sill, W.R., 1982c, A model for the cross-coupling parameters of rocks: Univ. of Utah, Dept. of Geol. and Geophys., Rept. DOE/ID/12079-69, 29 p.

Sill, W.R., 1983a, Self-potential modeling from primary flows: Geophysics, v. 48, p. 76-86.

Sill, W.R., 1983b, Electrical methods used during injection testing: Univ. of Utah Res. Inst., Earth Sci. Lab., Rept. in preparation.

Smith, C., 1983, Thermal hydrology and heat flow of Beowawe geothermal area, Nevada: Geophysics, v. 48, p. 618-626.

Smith, C., 1980, Delineation of electrical resistivity anomaly, Malpais area, Beowawe KGRA, Eureka and Lander Counties, Nevada: Univ. of Utah Res. Inst., Earth Sci. Lab., Rept. DOE/ID/12079-7, 25 p.

Sorey, M.L., Lewis, R.E., and Olmsted, F.H., 1978, The hydrothermal system of Long Valley caldera, California: U.S. Geol. Survey Prof. Paper 1044A, 60 p.

Souto, J.M., 1978, Oahu geothermal exploration: Trans. Geoth. Res. Council, v. 2, p. 605-607.

Stanley, W.D., 1982, Magnetotelluric soundings on the Idaho National Engineering Laboratory facility, Idaho: J. Geophys. Res., v. 87, p. 2683-2691.

Stanley, W.D., Jackson, D.B., and Zohdy, A.A.R., 1976, Deep electrical investigations in the Long Valley geothermal area, California: J. Geophys. Res., v. 81, p. 810-820.

Stanley, W.D., Boehl, J.E., Bostick, F.X., Jr., and Smith, H.W., 1977, Geothermal significance of magnetotelluric sounding in the eastern Snake River Plain - Yellowstone region: J. Geophys. Res., v. 82, p. 2501-2514.

Steeples, D.W., and Iyer, H.M., 1976a, Low-velocity zone under Long Valley as determined from teleseismic events: J. Geophys. Res., v. 81, p. 849-860.

Steeples, D.W., and Iyer, H.M., 1976b, Teleseismic P-wave delays in geothermal exploration: Proc. Second U.N. Symposium on the Development and Use of Geothermal Resources, San Francisco, v. 2, p. 1199-1206.

Stodt, J.A., 1983, Magnetotelluric data acquisition, reduction, and noise analysis: Proc. Workshop on "Electrical Methods in Oil and Gas Exploration", Univ. of Utah Res. Inst., Earth Sci. Lab., Salt Lake City, Utah, (January).

Studt, F.E., 1964, Geophysical prospecting in New Zealand's hydrothermal fields: Proc., United Nations Conference on New Sources of Energy, v. 2, pt. 1, p. 380.

Swift, C.M., Jr., 1979, Geophysical data, Beowawe geothermal area, Nevada: Trans., Geoth. Res. Council, v. 3, p. 701-703.

Tripp, A.C., Ward, S.H., Sill, W.R., Swift, C.M., and Petrick, W.R., 1978, Electromagnetic and Schlumberger resistivity sounding in the Roosevelt Hot Springs KGRA: Geophysics, v. 43, p. 1450-1469.

Wannamaker, P.E., 1983a, Interpretation of magnetotelluric data: Proc. Workshop on "Electrical Methods in Oil and Gas Exploration", Univ. of Utah Res. Inst., Earth Sci. Lab., Salt Lake City, Utah, (January).

Wannamaker, P.E., 1983b, Resistivity structure of the Great Basin and its tectonic implications: this volume.

Wannamaker, P.E., Ward, S.H., Hohmann, G.W., and Sill, W.R., 1980, Magnetotelluric models of the Roosevelt Hot Springs thermal area, Utah: Univ. of Utah Res. Inst., Earth Science Lab., Rept. DOE/ET/27002-8, 213 p.

Wannamaker, P.E., Ward, S.H., Hohmann, G.W., and Sill, W.R., 1983, Deep resistivity structure in S.W. Utah and its geothermal significance: Univ. of Utah Res. Inst., Earth Sci. Lab. Report DOE/ID/12079-89, 95 p.

Ward, P.L., Palmason, G., and Drake, C., 1969, Microearthquake survey and the Mid-Atlantic Ridge in Iceland: J. Geophys. Res., v. 74, p. 665-684.

Ward, P.L., and Bjornsson S., 1971, Microearthquake swarms and the geothermal areas of Iceland: J. Geophys. Res., v. 76, p. 3953-3982.

Ward, P.L., 1972, Microearthquakes: prospecting tool and possible hazard in the development of geothermal resources: Geothermics, v. 1, p. 3-12.

Ward, R.W., Butler, D., Iyer, H.M., Laster, S., Lattanner, A., Majer, E., and Mass, J., 1979, Seismic Methods: D.L. Nielson, ed., Program Review Geothermal Exploration and Assessment Technology Program, Rept. DOE/ET/27002-6, Univ. of Utah Res. Inst., Earth Sci. Lab., 128 p.

Ward, S.H., 1981, Gamma-ray spectrometry in geologic mapping and uranium exploration: Economic Geology, 75th Anniversary Volume, p. 840-849.

Ward, S.H., 1983, Controlled source electromagnetic methods in geothermal exploration: U. N. Univ. Geothermal Training Programme, Iceland, Rept. 1983-4, 46 p.

Ward, S.H., Parry, W.T., Nash, W.P., Sill, W.R., Cook, K.L., Smith, R.B., Chapman, D.S., Brown, F.H., Whelan, J.A., and Bowman, J.R., 1978, A summary of the geology, geochemistry, and geophysics of the Roosevelt Hot Springs thermal area, Utah: Geophysics v. 43, p. 1515-1542.

Ward, S.H., Ross, H.P., and Nielson, D.L., 1981, Exploration strategy for high-temperature hydrothermal systems in Basin and Range Province: Bull, Am. Assoc. Pet. Geol., 65, p. 86-102.

Ward, S.H., and Sill, W.R., 1976, Dipole-dipole resistivity delineation of the near-surface zone at the Roosevelt Hot Springs area: Univ. of Utah, Dept. of Geol. and Geophys., Tech Rept. 76-1, 7 p.

Ward, S.H., and Sill, W.R., 1982, Resistivity, induced polarization, and self-potential methods in geothermal exploration: Univ. of

Utah Res. Inst., Earth Sci. Lab., Rept. DOE/ID/12079-90, 100 p.

Ward, S.H., and Wannamaker, P.E., 1983, The MT/AMT electromagnetic method in geothermal exploration: U.N. Univ. Geothermal Training Programme, Iceland, Rept. 1983-5, 107 p.

Wechsler, D.J., and Smith, R.B., 1979, An evaluation of hypocenter location techniques with applications to Southern Utah: Regional earthquake distributions and seismicity of geothermal areas: Univ. of Utah, Dept. of Geol. and Geophys., Rept. IDO/DOE/ET/28392-32, 131 p.

Whiteford, P.G., 1975, Assessment of the audiomagnetotelluric method for geothermal resistivity surveying, Proc., Second U.N. Symposium on the Development and Use of Geothermal Resources, San Francisco, p. 1255-1261.

Williams, P.D., Mabey, D.R., Zohdy, A.R., Ackerman, H., Hoover, D.B., Pierce, K.L., Oriel, S.S., 1975, Geology and geophysics of the southern Raft River valley geothermal area, Idaho, USA: Proc. Second U.N. Symposium on Development and Use of Geothermal Resources, San Francisco, v. 2, p. 1273-1282.

Wilt, M.J., Goldstein, N.E., and Razo, A., 1980a, LBL resistivity studies at Cerro Prieto: Geothermics, v. 9, p. 15-26.

Wilt, M., Beyer, J.H., and Goldstein, N.E., 1980b, A comparison of dipole-dipole resistivity and electromagnetic induction sounding over the Panther Canyon thermal anomaly, Grass Valley, Nevada: Trans., G.R.C., 4, p. 101-104.

Wilt, M., Goldstein, N.E., Stark, M., and Haught, R., 1980c, An electromagnetic (EM-60) survey in the Panther Canyon area, Grass Valley, Nevada: Univ. of California, Lawrence Berkeley Lab., Rept. LBL-10993, 97 p.

Wilt, M. J., Haught, J. R., and Goldstein, N. E., 1980d, An electromagnetic (EM-60) survey of the McCoy geothermal prospect, Nevada: Univ. of California, Lawrence Berkeley Lab., Rept. LBL-12012, 115 p.

Wilt, M., Goldstein, N.E., Stark, M., Haught, J.R., and Morrison, H.F., 1981a, Experience with the EM-60 electromagnetic system for geothermal exploration in Nevada: University of California, Lawrence Berkeley Lab, Rept. 12618.

Wilt, M. J., Stark, M., Goldstein, N. E., and Haught, J. R., 1981b, Electromagnetic induction sounding at geothermal prospects in Nevada: Univ. of California, Lawrence Berkeley Lab, Rept. LBL-12100.

Wollenburg, H.A., 1975, Radioactivity of geothermal systems: Proc. Second U.N. Symposium on the Development and Use of Geothermal Resources, San Francisco, p. 1282-1292.

Zandt, G., McPherson, L., Schaff, S., Olsen, S., 1982, Seismic baseline and induction studies, Roosevelt Hot Springs, Utah, and Raft River, Idaho: Univ. of Utah Res. Inst., Earth Sci. Lab., unnumbered report, 59 p.

Zoback, M. L., 1983, Style of Basin and Range faulting as inferred from seismic reflection data in the Great Basin, Nevada and Utah: this volume.

Zohdy, A.A.R., Anderson, L.A., and Muffler, L.J.P., 1973, Resistivity, self-potential, and induced polarization surveys of a vapor-dominated geothermal system: Geophysics, v. 38, p. 1130-1144.

BS

Reconnaissance geophysics of a known geothermal resource area, Weiser, Idaho and Vale, Oregon

C. L. Long* and H. E. Kaufmann*

Audio-magnetotelluric (AMT) and telluric current soundings were made in a study of the geothermal potential of the area between Weiser, Idaho and Vale, Oregon, during the spring and fall of 1974. The electrical surveys covered an area on the western edge of the Snake River plain of approximately 3500 km² with 89 AMT and 31 telluric current stations at approximately 6-km spacings.

The AMT method used the natural electromagnetic (EM) field from 7.5 Hz to 6.7 kHz (10 frequencies) with two VLF radio sources at 10.2 and 18.6 kHz, while the telluric method utilized geomagnetic micropulsations, band-limited from 0.02 to 0.1 Hz. Maps were compiled using both methods to outline major high- and low-resistivity features.

Major high-resistivity zones appear to trend northwest on the AMT apparent resistivity maps. These zones parallel structural trends between Vale and Weiser. The lowest apparent resistivities are associated with the known geothermal hot springs in the Vale and Weiser areas.

The telluric ratio map shows lowest values at the eastern side of the area, and a low trend extending through Vale and to the northeast.

INTRODUCTION

During a period of 14 days in the spring and 10 days in the fall of 1974, 89 audio-magnetotelluric (AMT) and 32 telluric current soundings at a station spacing of approximately 6 km were made in a study of the geothermal potential of the area between Weiser, Idaho and Vale, Oregon. Combining these two geoelectric methods improved data correlation and interpretation of the geophysical trends. The areas near Weiser, Idaho and Vale, Oregon have now been designated as Known Geothermal Resource Areas (KGRAs). The electrical surveys cover an area on the western edge of the Snake River plain of approximately 3500 km².

GEOLOGY

The geomorphic setting in this area is a terrain of alluvial terraces with low gentle slopes dissected by many drainage systems, as shown in the map of Figure 1 adapted from Newton and Corcoran (1963). The western Snake River plain is underlain by a thick section of principally nonmarine Cenozoic sediments and sedimentary rocks. The area covered by the electrical surveys, as shown on Figure 1, is mostly the Pliocene and Pleistocene Idaho group which contains gravel, sand, silt, clay, and ash. The Idaho group is at least 1.2 to 1.5 km thick in the center of the survey area; these depths were taken from logs of a number of petroleum exploration wells drilled in the basin. Older rocks outcrop around the edges of this region with the principal unit being the Miocene and Pliocene Columbia River basalt group. In Oregon the Deer Butte formation (Kittleman et al, 1965) and in Idaho its equivalent (the Poison Creek formation), both of the Idaho group, vary from place to place; however, in general each contains a section of fine-grained tuffaceous sediments with a few intercalated basalt flows in their lower part, grading upward into the sandstone layers and conglomerates. Vales Buttes and Mitchell Butte are formed by massive sandstones (Figure 1) in the Poison Creek formation. In the sur-

Manuscript received by the Editor December 3, 1976; revised manuscript received July 6, 1979.
*U.S. Geological Survey, M.S. 964, Box 25046, Denver Federal Center, Denver, CO 80225.
0016-8033/80/0201—312$03.00.

very area, structural trends are northwesterly, with a few exceptions which are north to south as shown in Figure 1.

AMT RESISTIVITY

For the AMT method the natural electromagnetic (EM) field from 7.5 Hz to 6.7 kHz (10 frequencies) with two VLF radio sources at 10.2 and 18.6 kHz was used. The AMT method is useful in searching for conductive bodies such as hot saline water concentrations because it is an inductive method. The method itself has been described by Strangway et al (1973) in relation to mineral exploration, and the reader is referred to this paper for more details and references. A description of a reconnaissance method similar to the one used in this study was given by Hoover and Long (1975). Three methods of AMT data presentation are given below, namely, resis-

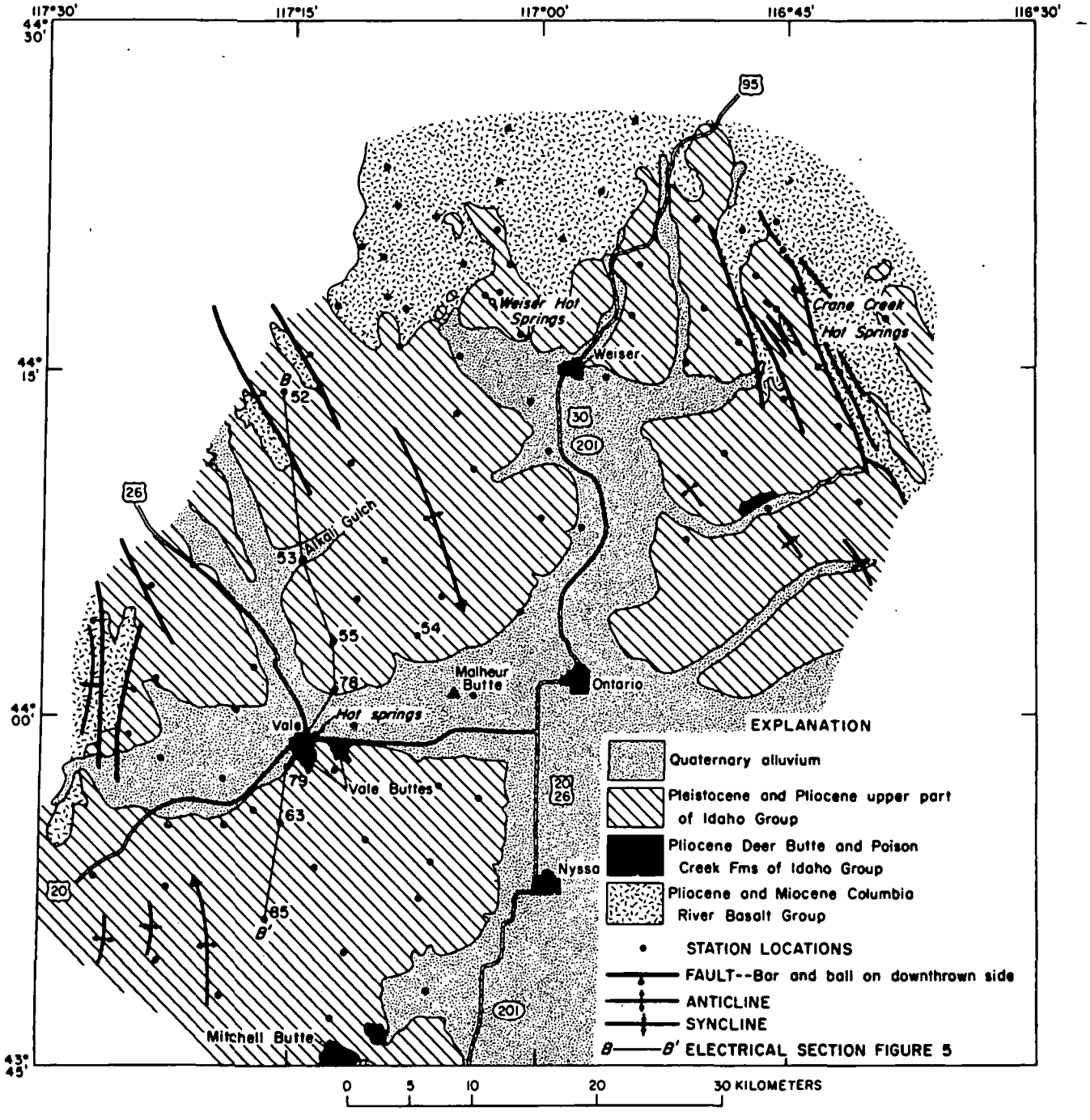

FIG. 1 Audio-magnetotelluric station location and general geology, Weiser, Idaho to Vale, Oregon.

tivity maps, resistivity soundings, and theoretical one-dimensional (1-D) models.

Figure 2 is a 7.5-Hz AMT apparent resistivity map of the Vale-Weiser area. The apparent resistivity values on this map are computed from the logarithmic average of the north-south and east-west scalar impedances. Averaging of values for the two sounding directions is necessitated by a fairly high degree of scatter in the scalar impedances and as a means of summarizing the data at 7.5 Hz. The maximum penetration depth, in meters, of the survey is given approximately by "skin depth" $= 503\sqrt{\rho_a/f}$, where ρ_a is apparent resistivity and f is the frequency. Due to the low resistivities in the basin, at 7.5 Hz the maximum penetration depth was approximately 200–300 m, which in most cases is much less than the thickness of the sediments. The map (Figure 2) shows the highest resistivities in the northern part of the area. The large resistivity gradients are related to thinning of conductive sediments and to the

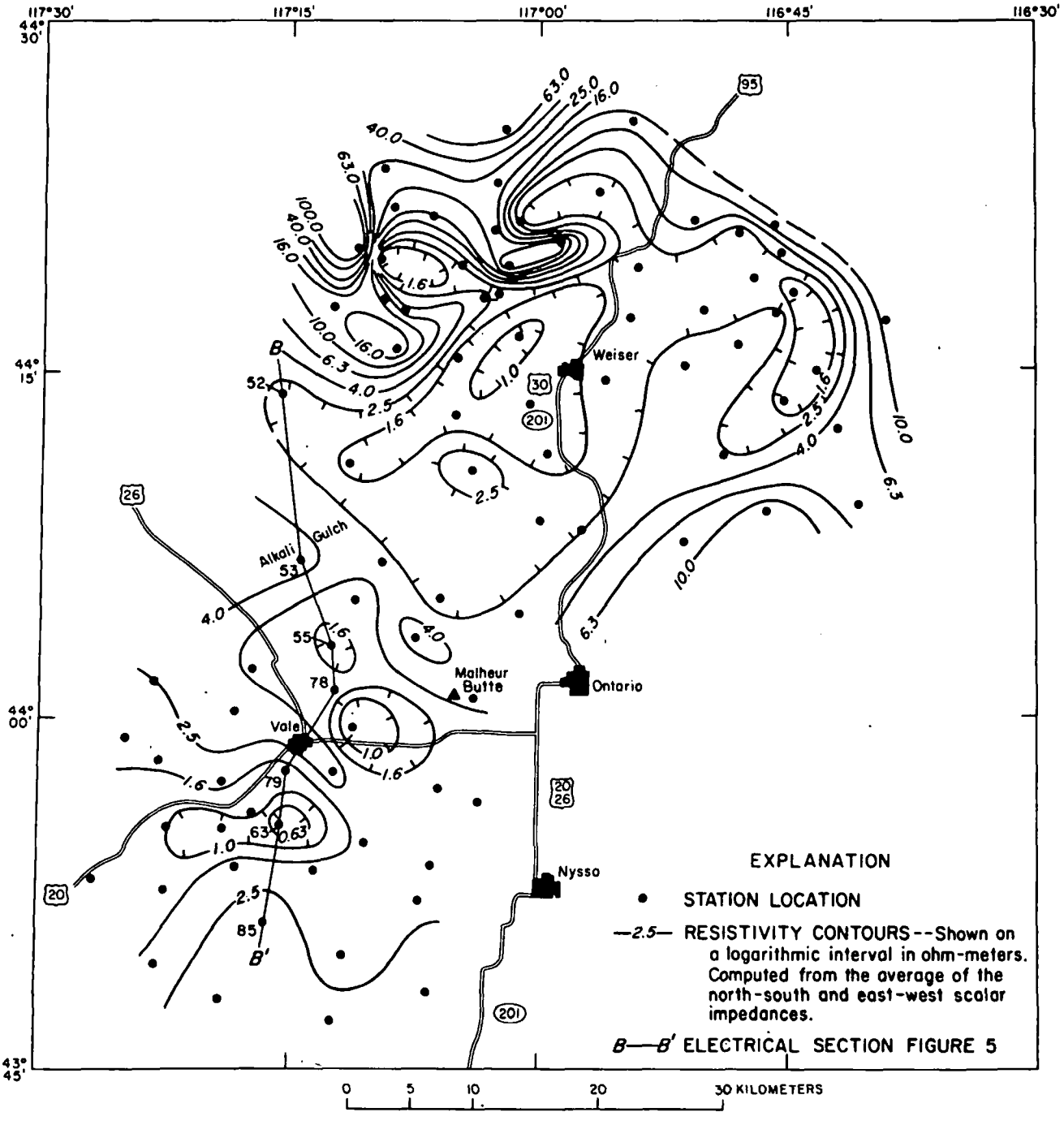

FIG. 2. Audio-magnetotelluric (7.5-Hz) apparent resistivity map, Weiser, Idaho to Vale, Oregon.

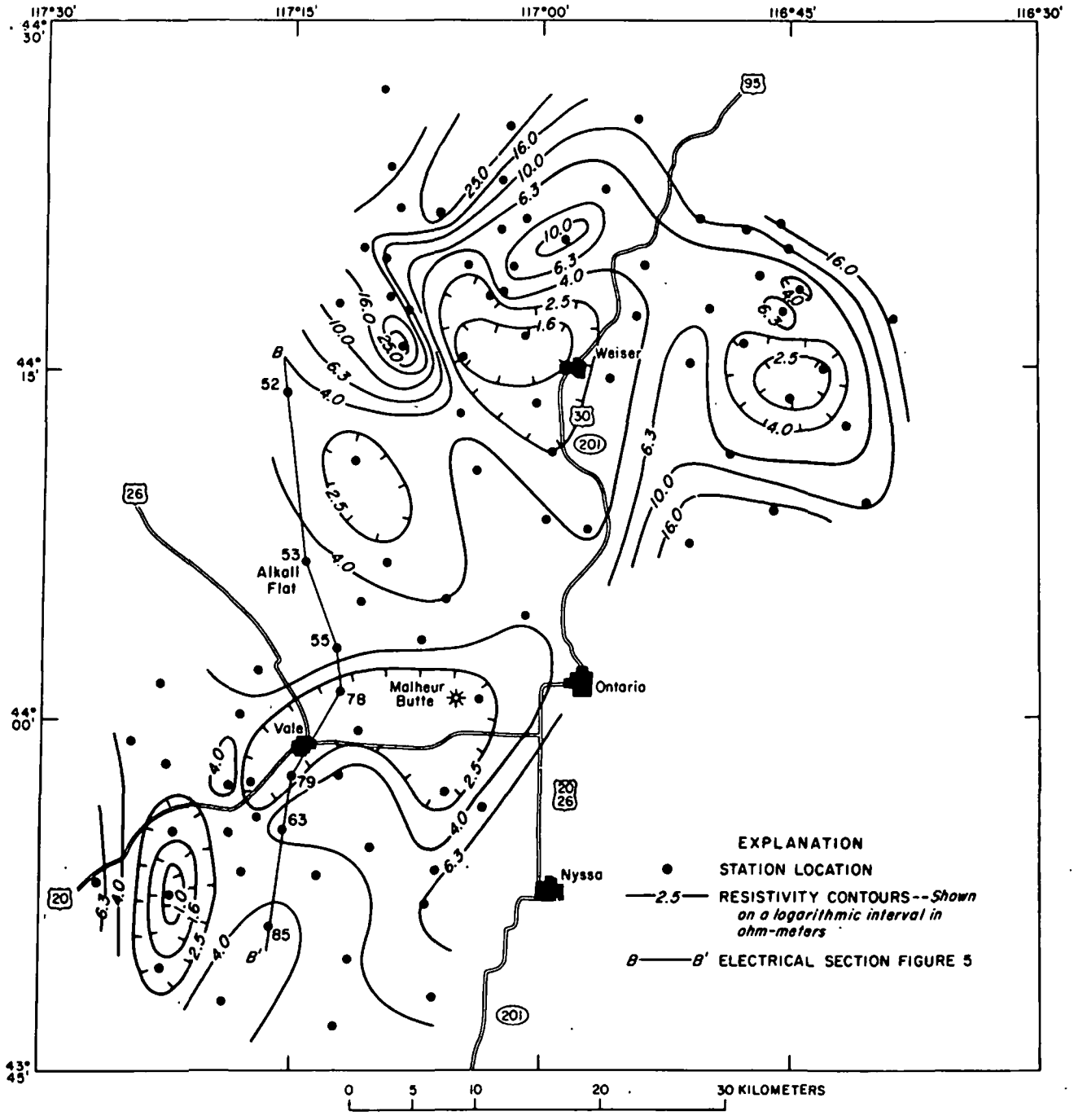

FIG. 3a. North-south telluric line (27-Hz) and audio-magnetotelluric apparent resistivity map, Weiser, Idaho to Vale, Oregon.

presence of near-surface Columbia River basalts and intrusives. Within the basin there is a general trend of low resistivities from south of Vale, Oregon extending to the Crane Creek area in Idaho. Small highs finger into this low and have a northwesterly orientation similar to the structural trend on the geologic map. Despite the low station density, the trends are very descriptive of the local features. The station density is not adequate to define all the lows, and the details of the contouring would be different with more stations.

Comparing the two AMT 27-Hz apparent resistivity maps in Figure 3, one sees that the low-resistivity trend covers the same areas as were shown on the 7.5-Hz AMT map (Figure 2). On the 27-Hz east-west telluric line orientation (Figure 3b), we can see some of the nearer surface lateral effects described by Strangway et al (1973). The best example of this

effect is a localized 16 Ω-m high, which is an expression of the higher-resistivity material comprising Malheur Butte. The volcanic material of Malheur Butte may be structurally related to a dike in Alkali Flat to the northwest; there is a general high-resistivity trend in that direction as can be seen on both 27-Hz maps as well as the 7.5-Hz map (Figure 2). At 27 Hz, the skin depth is about 120 m in the basin areas and increases to a maximum of about 2–3 km near the northern edge of the project area.

Figure 4 illustrates three bidirectional AMT soundings taken, respectively, at stations 53, 54, and 69; the station locations are shown on Figure 1. These soundings are representative of the AMT data of this survey. On Figure 4a, station 69 shows the similarity in apparent resistivity at the lower frequencies

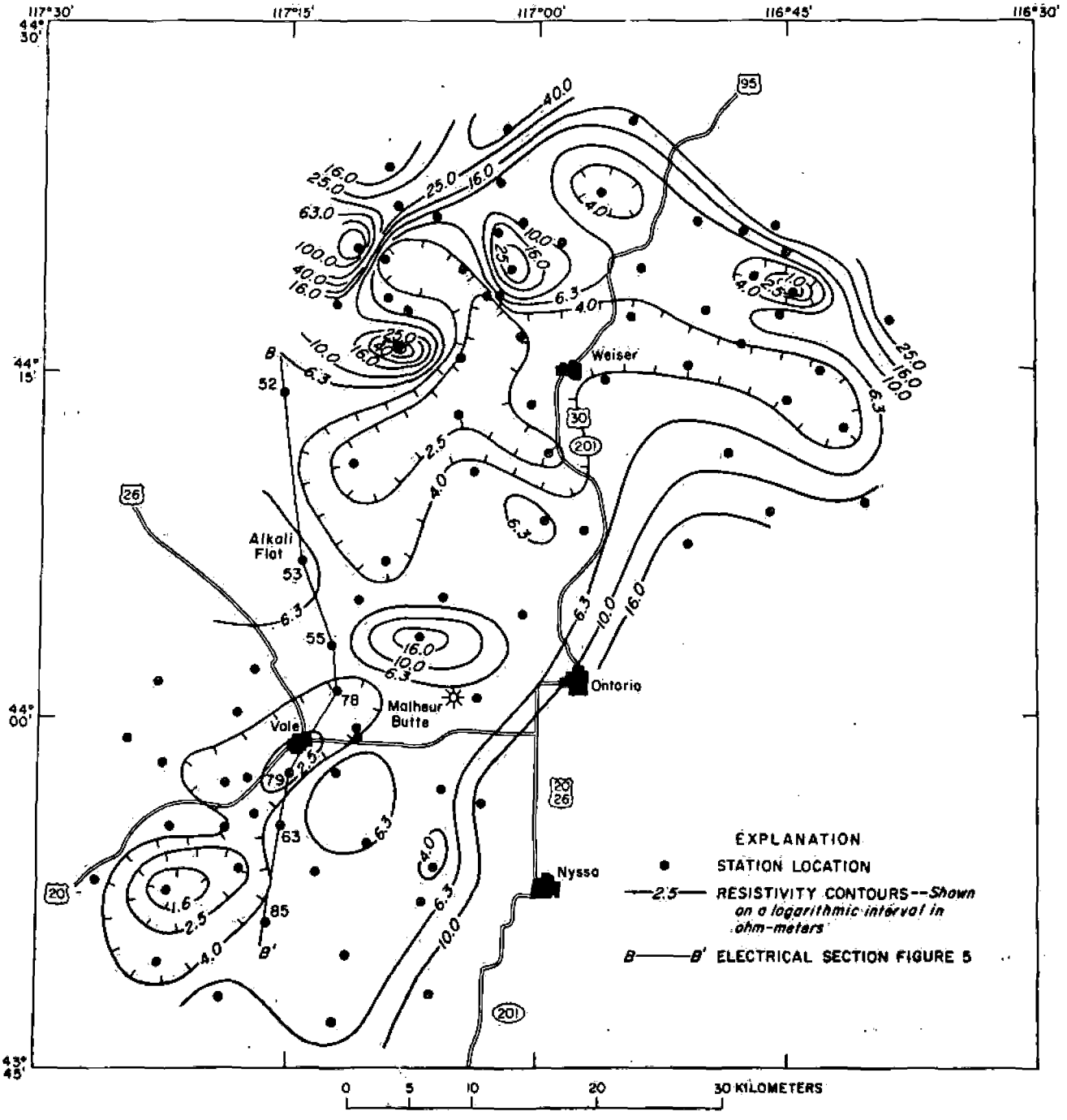

FIG. 3b. East-west telluric line (27-Hz) and audio-magnetotelluric apparent resistivity map, Weiser, Idaho to Vale, Oregon.

of the two sounding orientations (north-south, east-west). There is little evidence of lateral effects, and the variation between soundings is not much greater than the standard deviation (described in Hoover and Long, 1975) shown by the vertical bars.

The sounding curves for station 53 (Figure 4b) show almost no separation, but there is a definite break in the trend of the curves, perhaps due to a vertical dike located a few hundred meters from the station. The strike of the dike is at a 45-degree angle to both telluric lines, affecting the two telluric directional measurements equally.

In Figure 4c (station 54), we see evidence of a lateral effect which is almost constant at the lower frequencies, due to the inhomogeneity near Malheur Butte. The dip in the east-west sounding curve at 76 Hz is due to changing polarization of the incident field over inhomogeneous media. The separation

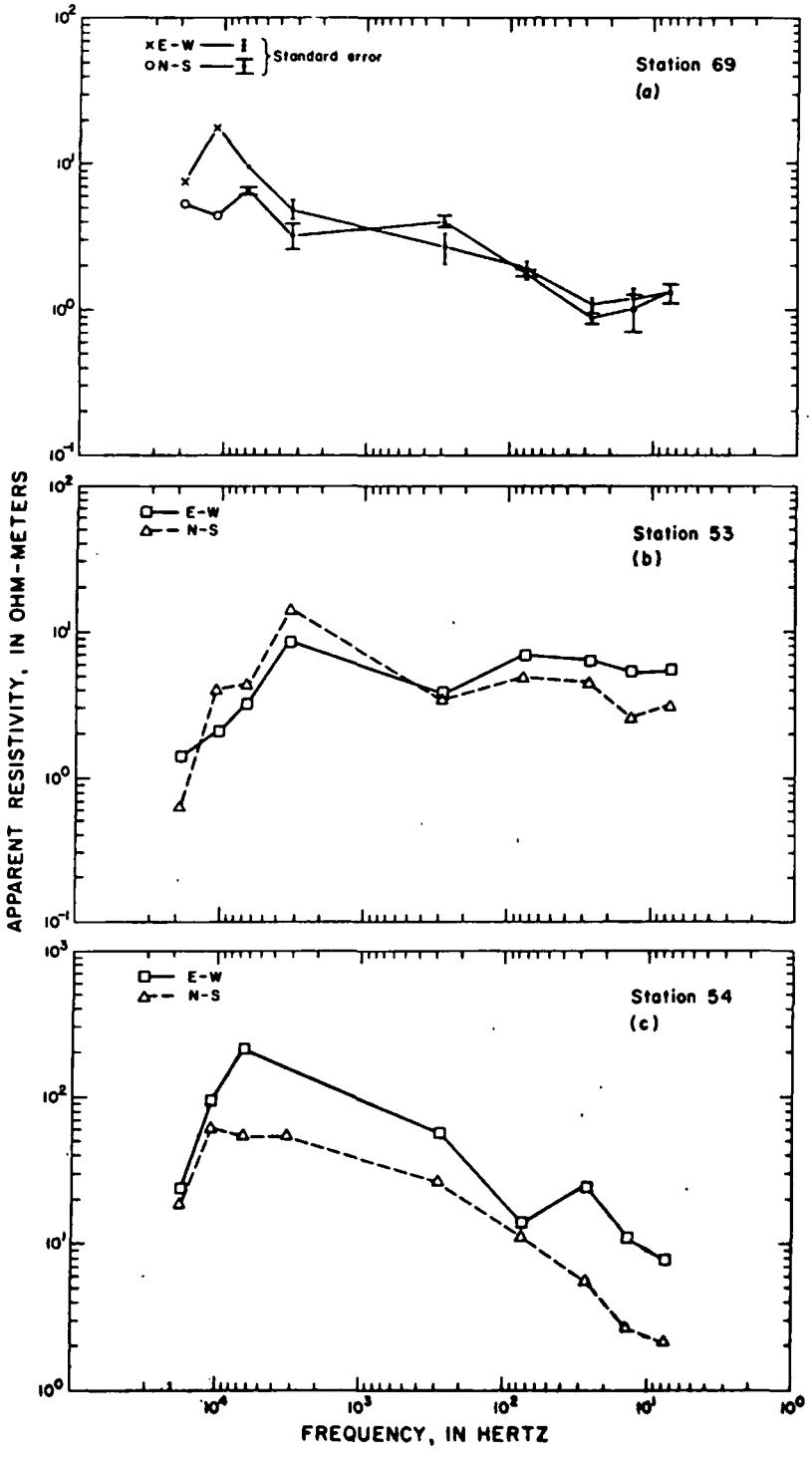

FIG. 4. Three bidirectional AMT soundings.

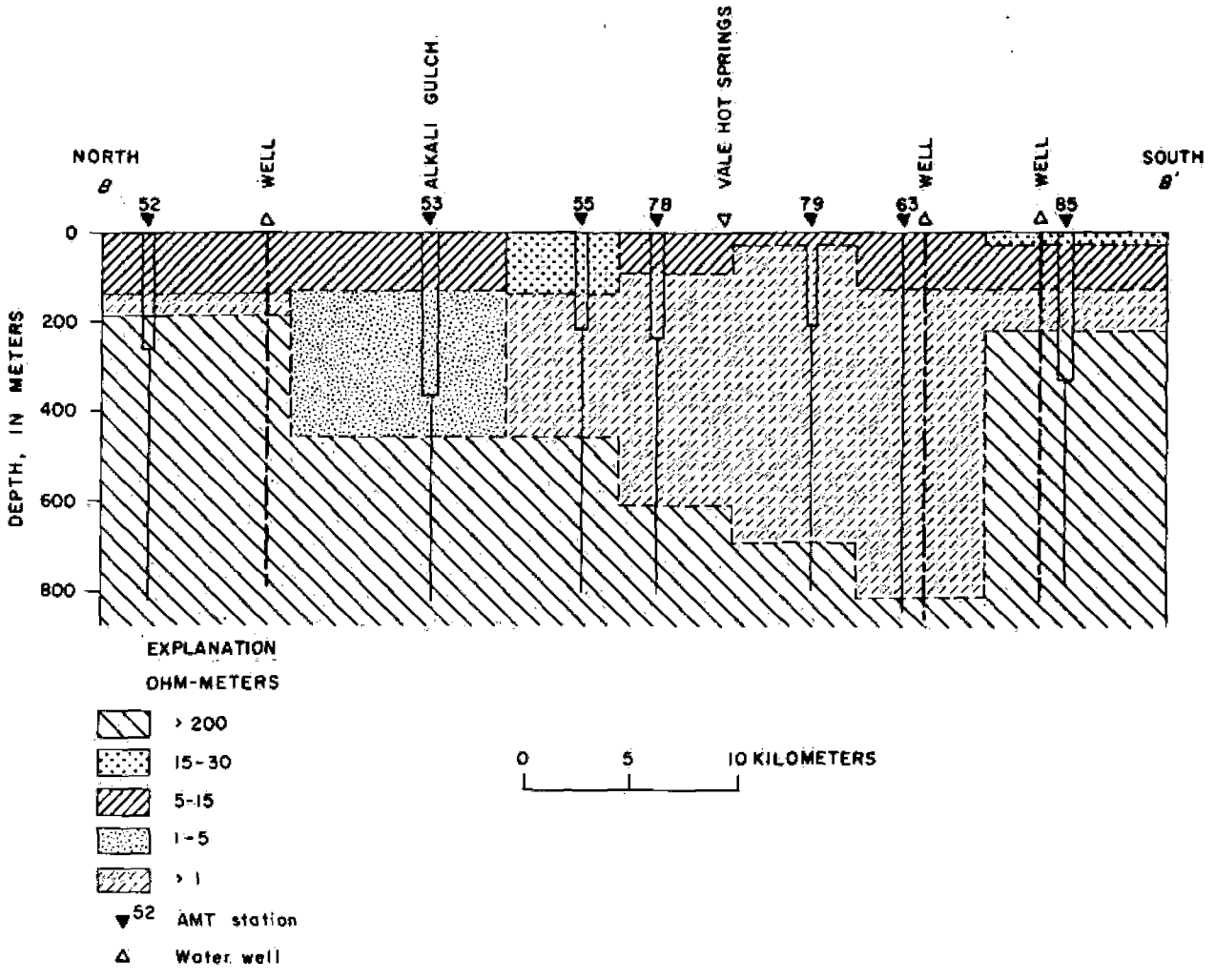

FIG. 5. Electrical cross-section.

between the curves is less at 10.2 and 18.6 kHz, indicating minimal lateral effects in the near-surface.

Assuming a 1-D model, we inverted data along profile B-B' (Figure 1) by computer (Smith, 1975) to obtain an electrical cross-section (Figure 5). Well logs along the profile provided information on rock depth and types. The rectangular area below each AMT station is the skin depth at 7.5 Hz plotted to scale vertically and horizontally to show roughly the maximum area sampled by the AMT method. The vertical scale exaggeration is about 60 to 1. The basement, indicated by the material of resistivity greater than 200 Ω-m, is a basaltic layer which was identified from well logs. With the depth to the basalt fixed from various well logs and for an assumed resistivity of greater than 200 Ω-m for the basalt, the other layer thicknesses and resistivities were allowed to vary until a good fit to each sounding curve was found. A qualitative comparison of AMT and telluric current data (Figure 8) was used for additional guidance in preparing this resistivity section. In most cases, a four-layer model was required; however, for station 52, a three-layer model fit was adequate. In general the AMT method was unable to penetrate the low-resistivity layer of sediments shown by less than 1 Ω-m material on the section (Figure 5), except at station 85 where basement of resistivity greater than 200 Ω-m was detected. Model fits to most of the sounding curves were very good, except at station 53 near the dike. The dike seemed to influence the model as evidenced by the zone of 1–5 Ω-m material.

TELLURIC CURRENT RESULTS

The telluric current method utilized micropulsation data, band-limited from .02 to .1 Hz and recorded using *x-y* plotters (Yungul, 1966). A contoured telluric current map of *J* values is shown in Figure 6. The *J* values were obtained by taking a ratio of rover

to base station (fixed position) ellipse areas (Yungul, 1968). As seen in Figure 6, the J values of less than 10 indicate an area of lower resistivity relative to the base. The lowest resistivities are found in the east-central part of the area, near Ontario, and extend west across the map and just north of Vale. The most outstanding anomaly on Figure 6 is a ridge of higher resistivity trending to the north and west from Vale. This trend follows the basic grain of the geologic structures and reflects basement topography, but does not agree with the overall trends displayed by the 7.5-Hz AMT map (Figure 2). The low surface resistivities (shown by AMT data) do influence the telluric current data, but the deeper part of the section has enough influence on the telluric current results to change the trend of the contours.

In Figure 7 we show the normalized ellipses for 31 telluric stations in the Vale-Weiser area. At each

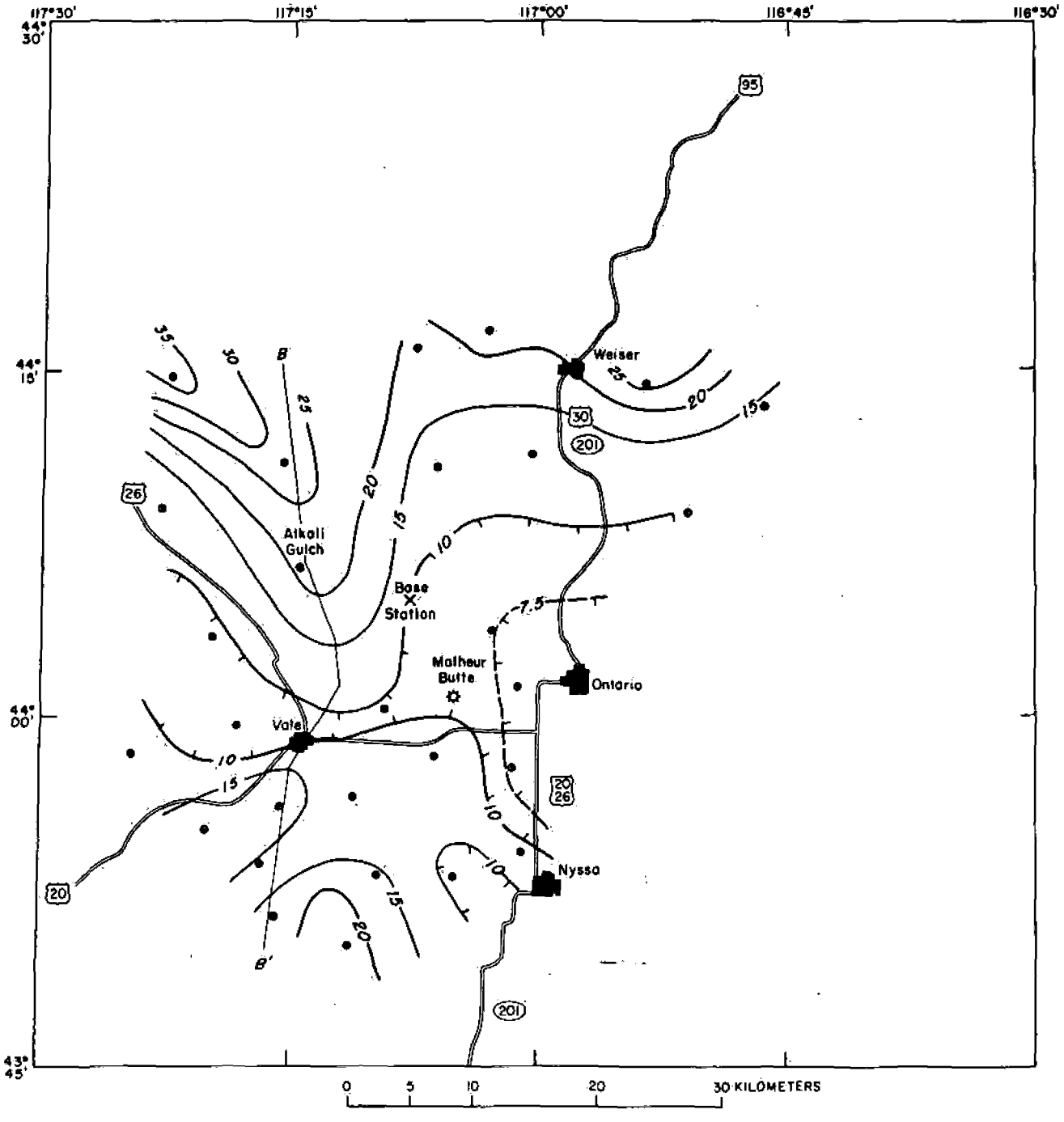

FIG. 6. Telluric anomaly map at 20–30 sec period. Contour interval in J values varies from 2.5 to 5, Weiser, Idaho to Vale, Oregon.

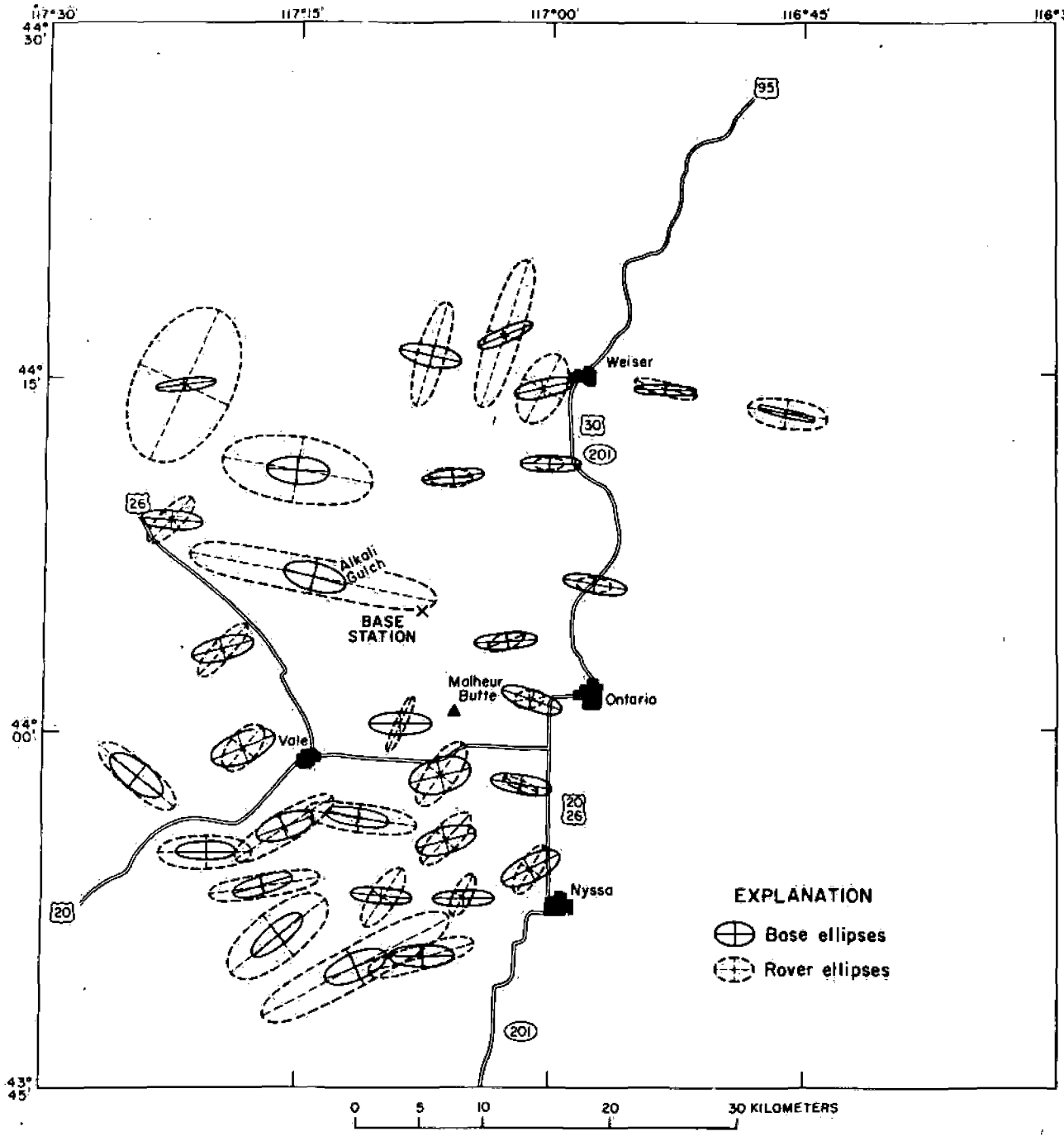

FIG. 7. Correlations of rover-to-base orientations and current amplitudes, Weiser, Idaho to Vale, Oregon.

rover station, the relative area and estimated orientation of base and rover ellipses are indicated. The rover ellipse outline is dashed, and the base ellipse outline is solid. At three stations west of Weiser, the axis of the rover ellipse is shifted almost 90 degrees with respect to that of the base ellipse, and larger amplitudes are indicated by the larger size of the form. This implies a major structure to the north, changing direction of telluric current, and also a decreasing distance to basement. The three large rover ellipses in the northwest corner reveal very large changes in electric field current with respect to the base station. The three stations along highway 26 show a significant shift of the electrical axis from Vale to the northwest. This may be indicative of local features related to the northwest-trending resistivity high seen on Figure 2 between Malheur Butte and Alkali Gulch. The rover ellipse with the small amplitude and large electrical axis shift with respect to the base, seen near Malheur Butte northeast of

Vale, is another good example of a local effect of high-resistivity material. South and east of Vale, we see numerous changes in orientations and amplitudes. While most of the changes are smaller than the ones described to the north, they help illustrate the complexity of the local area.

Figure 8 illustrates a qualitative comparison of the AMT and telluric current data along the same profile as the AMT 1-D section. The apparent resistivity profile was computed from the AMT horizontally layered model for a frequency of .04 Hz. The telluric profile was obtained directly from the contoured telluric current J value map (Figure 6). The telluric current and AMT data correlate well on this profile, despite the lateral variation in the electrical section at depths greater than those probed by the AMT method.

CONCLUSIONS

Highly conductive sediments restricted the exploration depth of the AMT method to a few hundred meters over much of the area. Nevertheless, high-conductivity anomalies were mapped with the method in an area near prominent hot springs. The limited extent of these anomalies suggests that near-surface thermal waters are restricted to a few narrow fault zones in the immediate vicinity of the hot springs. Scattered dikes and volcanic rocks which cut through the sediments and are exposed at the surface locally cause large differences between the north-south and east-west scalar resistivities.

The telluric current data are strongly influenced by the highly conductive near-surface layers which affect the AMT results, but the telluric current results do reflect the presence of deeper structures and basement

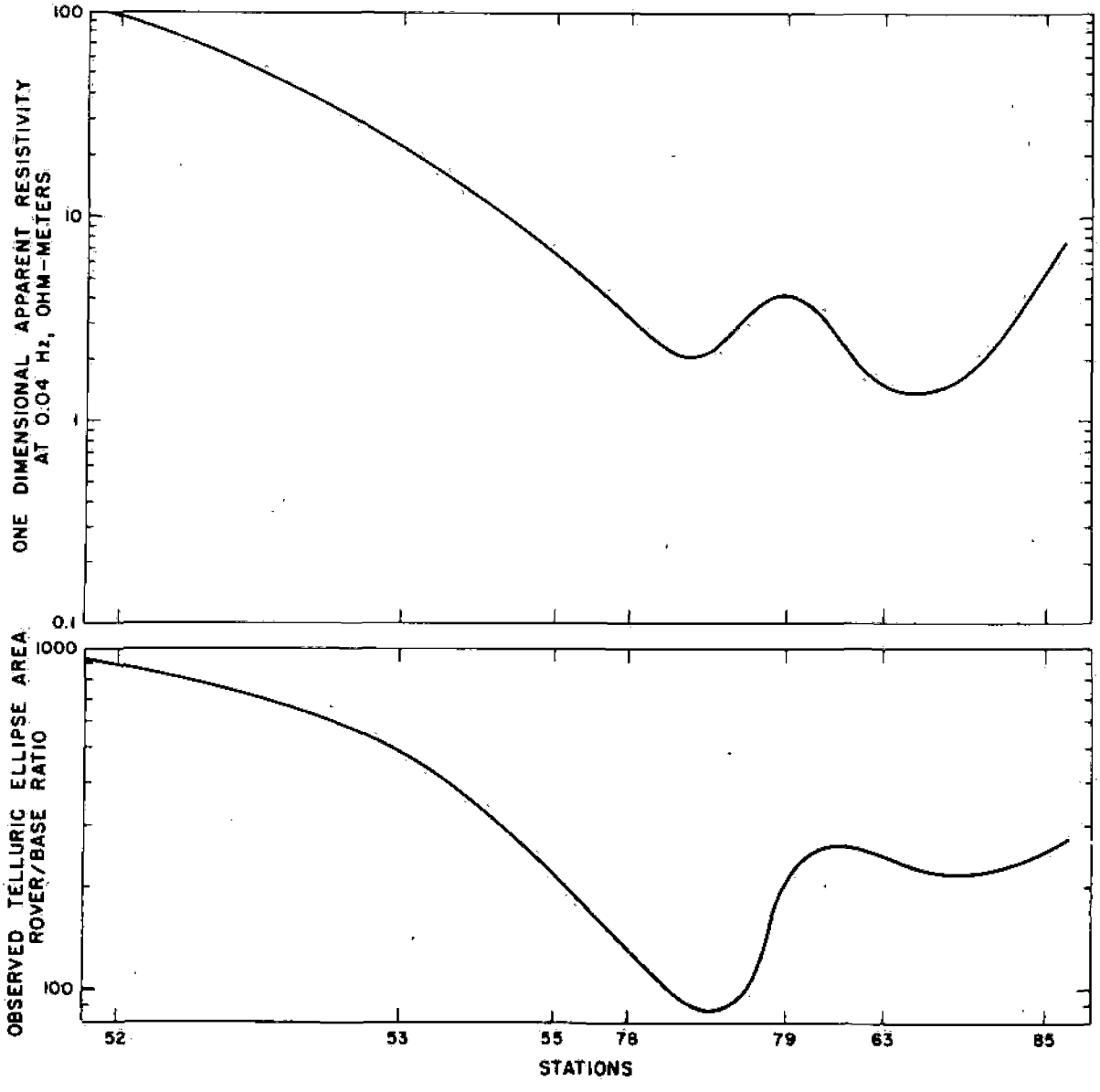

FIG. 8. Qualitative comparison of AMT and telluric current data.

topography, at least in the northwest part of the area.

The station density for both methods was too sparse to locate and define accurately all of the small anomalies which exist in the area. In particular, additional measurements are needed in the Crane Creek, Weiser, and Vale Hot Springs areas to delineate more closely the low-resistivity anomalies associated with those "hot spots." Despite the need for some additional work, the AMT and telluric current methods were effective in covering a large area rapidly and at low cost.

REFERENCES

Hoover, D. B., and Long, C. L., 1975, Audio-magnetotelluric methods in reconnaissance geothermal exploration: U.S.G.S. open file rep. 75–362.

Kittleman, L. R., Green, A. R., Hagood, A. R., Johnson, A. M., McMurray, J. M., Russell, R. G., Weeden, D. A., 1965, Cenozoic stratigraphy of the Owyhee region, southeastern Oregon: Univ. of Oregon Mus. Nat. Hist. Bull., no. 1.

Newton, V. C., and Corcoran, R. E., 1963, Petroleum geology of the western Snake River basin, Oregon, Idaho: Oil and Gas Investigations no. 1, State of Oregon, Dept. of Geol. and Mineral Ind.

Smith, B. D., 1975, Computer program: U.S.G.S., unpublished.

Strangway, D. W., Swift, C. M., Jr., and Holmer, R. C., 1973, The application of audio-frequency magnetotellurics (AMT) to mineral explorations: Geophysics, v. 38, p. 1159–1175.

Yungul, S. H., 1966, A magnetotelluric method without magnetic measurements: Geophysics, v. 31, p. 185–191.

——— 1968, Measurements of telluric relative ellipse area by means of vectograms: Geophysics, v. 33, p. 127–131.

mostly BS

A Coordinated Exploration Program for Geothermal Sources on the Island of Hawaii

AUGUSTINE S. FURUMOTO

Hawaii Institute of Geophysics, University of Hawaii, 2525 Correa Road, Honolulu, Hawaii 96822, USA

ABSTRACT

Staff members of the Hawaii Institute of Geophysics carried out an exploration program for geothermal sources on the island of Hawaii by using all relevant geophysical and geochemical methods. Infrared scanning surveys by aircraft followed by reconnaissance-type electrical surveys and ground-noise surveys narrowed down the promising area to the east rift of Kilauea.

The surveys carried out over the east rift included magnetic, gravity, and electrical surveys by various methods; microearthquake surveillance; temperature profiling of wells; and chemical analysis of water samples. Aeromagnetic, regional gravity, and crustal seismic refraction data were available in the published literature.

A model of the thermal structure of the east rift was put together to account for the data. The dike complex through which magma from the central vent of Kilauea travels laterally occupies a zone 3 km wide extending from a depth of 1 to 5 km. On the south side of the dike complex, there may be a self-sealing geothermal reservoir where ground water heated by the dike complex is trapped. Not all of the dike complex is hot; hot sections seem to occur in patches.

INTRODUCTION

The active volcanoes of Kilauea and Mauna Loa on the island of Hawaii indicate the existence of a large amount of thermal energy. Because these volcanoes are surface manifestations of thermal processes, geologists and laymen have speculated whether that energy could be harnessed for the generation of electrical power. The high porosity and permeability of the basaltic rock that makes up the volcanoes has been the major obstacle so far. As the lateral flow of ground water is consequently rather swift, even with the existence of fumaroles and warm springs, it has been generally considered that geothermal reservoirs do not exist in the Hawaiian Islands.

Most of the world's geothermal power development is located in continental areas. Even the geothermal field in Iceland is located among acidic volcanoes which resemble continental rather than oceanic volcanoes. Because of these negative facts, it was deemed necessary to do rather comprehensive research on the volcanoes on the island of Hawaii to see whether geothermal sources do exist there.

On the other hand, there are some encouraging speculations that have been proposed since the mid-60s. The concept of a self-sealing geothermal reservoir (Facca and Tonani, 1967) could very well apply to basaltic rocks in Hawaii. Furthermore, in recent years we have seen progress in experiments attempting to utilize hot rock or magma. Because of these developments, a research program was conceived to determine whether Hawaii had a conventional type of geothermal reservoir brought about by a self-sealing mechanism or whether thermal energy was limited to hot rock and magma. If the latter were the case, then the research program should determine the utilizable energy content of the sources.

Although Hawaiian volcanoes have been investigated more than any others in the world, examination of the literature showed it would be necessary to carry out a coordinated series of surveys in order to define the thermal processes associated with the volcanoes. With this in mind, a proposal was submitted to the U.S. National Science Foundation for support of the research. The proposal was accepted and funded.

EXPLORATION PROGRAM

The coordinated exploration program as carried out is shown in schematic form in Figure 1. The actual program differed from that planned because of the funding level, and the slow delivery of equipment and instruments from manufacturers. When the program was begun in May 1973, the USA was facing an acute shortage of material, especially electronic and electrical components and parts.

The persons involved in the exploration program from the Hawaii Institute of Geophysics (HIG) were: Professors A. S. Furumoto and A. T. Abbott; Associate Professor P. F. Fan; Graduate Assistants W. Suyenaga, D. P. Klein, J. Halunen, E. Epp, G. McMurtry, and J. Kauahikaua; Research Associate R. Norris; and Electronics Technician C. Dodd.

In addition, G. V. Keller of the Colorado School of Mines was engaged to conduct an electrical resistivity survey over the summit area and east rift of Kilauea. Throughout the survey he kept in contact with the HIG group and provided timely inputs. Independent of the HIG effort, C. Zablocki of the U.S. Geological Survey was carrying out self-potential surveys in areas of mutual interest. In exchange for field assistance, Zablocki made his data available to the HIG exploration program.

The island of Hawaii is composed of five volcanoes,

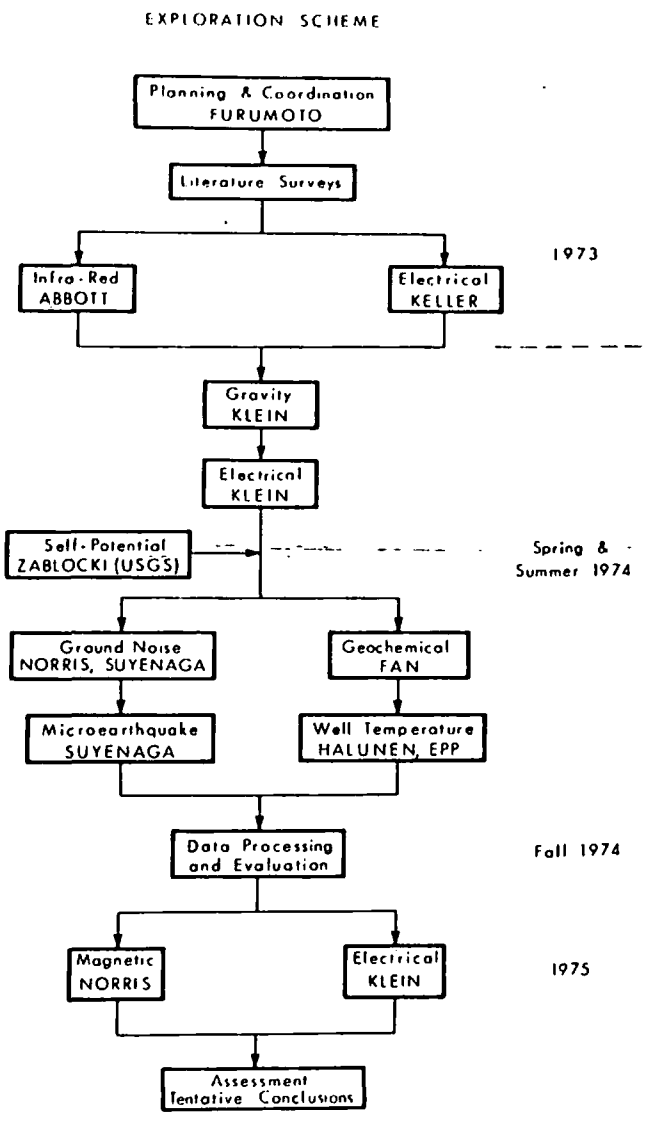

Figure 1. Exploration scheme.

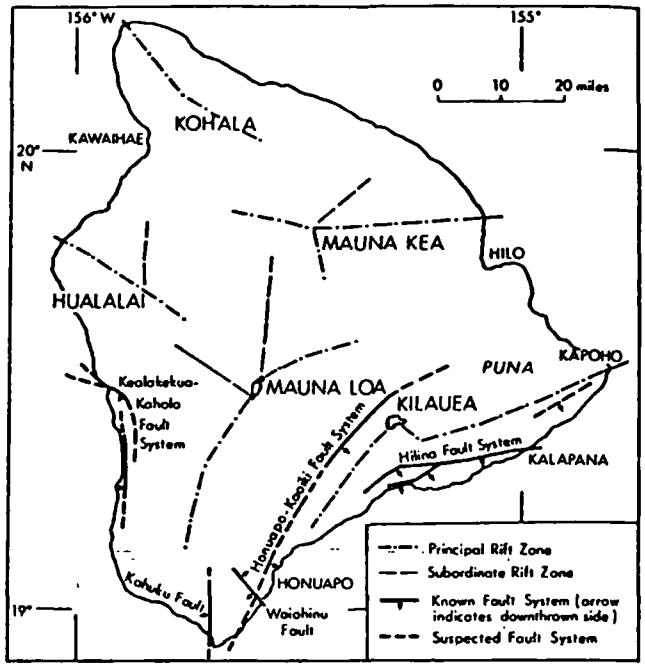

Figure 2. Map of the island of Hawaii showing volcanoes and associated rift zones.

namely Kohala, Hualalai, Mauna Kea, Mauna Loa, and Kilauea (Fig. 2). Of these, Mauna Loa and Kilauea are considered active. Associated with each volcano are rift zones that are named for the direction in which they extend. The exploration program started out with infrared scanning surveys over the rift zones. The results showed that temperatures over the east and southwest rifts of Kilauea and the southwest rift of Mauna Loa were above normal. The other rift zones of the active volcanoes as well as those of the inactive volcanoes showed no temperature anomaly.

With the information provided by the infrared surveys, the three prospective rift zones were examined by reconnaissance-type electrical and ground-noise surveys. The results showed that the east rift of Kilauea was by far the best prospect as a geothermal source. In the spring of 1974 we therefore decided to concentrate on the east rift of Kilauea, which is located in the Puna district. The central vents of Kilauea and Mauna Loa volcanoes were excluded from consideration because they are within the confines of the Hawaii National Park.

Upon making the decision to concentrate on the east rift of Kilauea, electrical surveys were carried out in greater detail. However, after the anomalous areas of low resistivity were delineated, we found it difficult to interpret the data in terms of thermal processes because of our limited knowledge of the structure of the east rift. Hence, gravity, magnetic, and microearthquake surveys were carried out. The exploration scheme of Figure 1 shows the manner in which the results from one survey provided information or incentive for the others. From time to time, data were assessed and plans were revised.

At this writing (May 1975), the active exploration program has come to a pause, but not necessarily to completion. Although enough data have been gathered to justify a drilling program, further surveys are being planned—especially seismic refraction, gravity, and magnetic surveys—in order to better understand the hydrothermal process.

As part of the broader geothermal project for the island, a site selection committee for a drilling program was set up independent of the exploration program. Although the committee did consider input from the exploration program, it selected a drill site at an early stage before the exploration program could satisfactorily analyze the data collected. There are some misgivings concerning the site chosen.

The next section will present a brief summary of the geophysical data obtained to date.

GEOPHYSICAL DATA

Our discussion is limited to data on the east rift of Kilauea, as the east rift is the only area adequately surveyed so far.

Electrical Surveys

The electrical surveys were conducted by Keller (1973) and Klein and Kauahikaua (1975). The techniques used included dipole-bipole mapping, line-loop time-domain inductive sounding, galvanic sounding, and loop-loop fre-

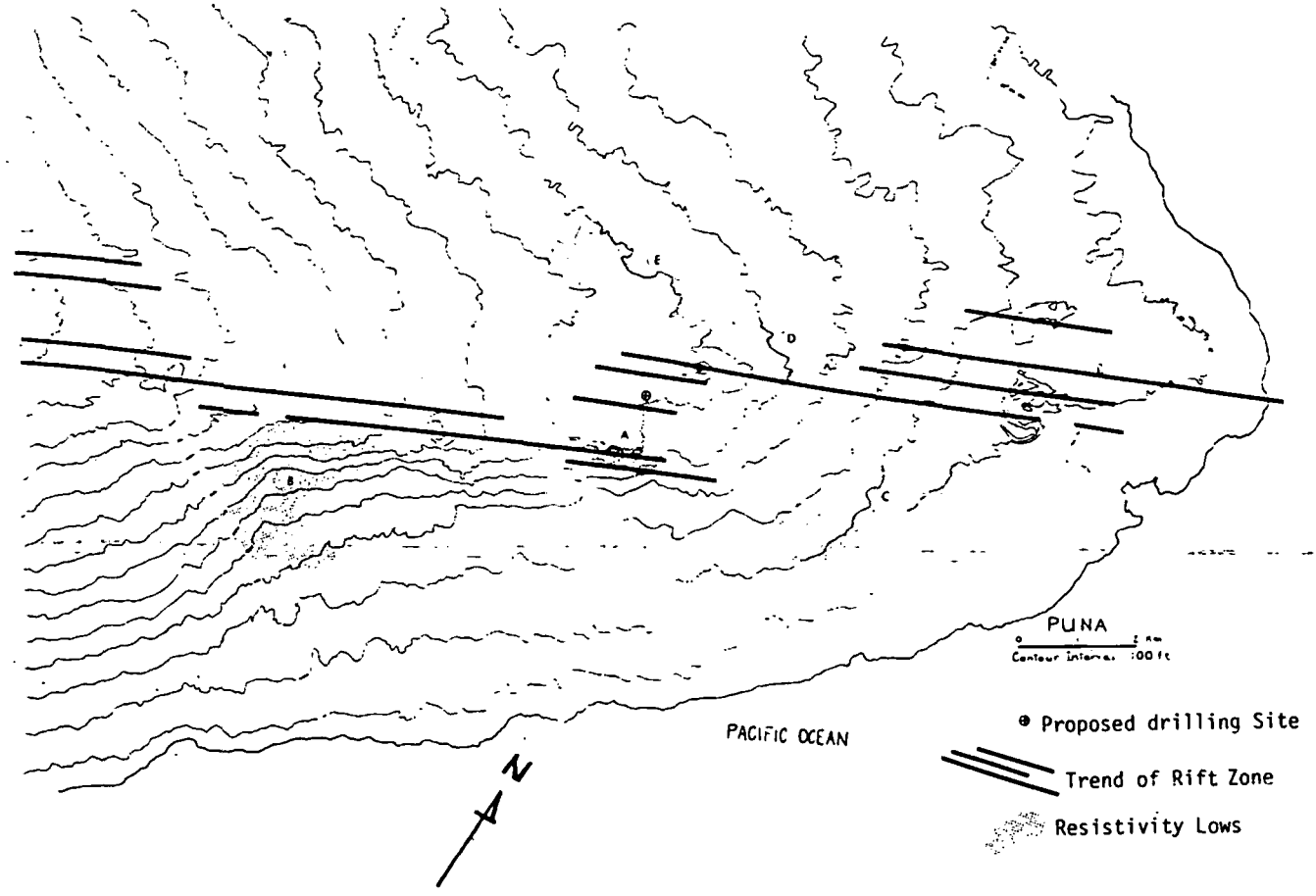

Figure 3. Contour map of Puna area showing trend of rift zone and areas of low electrical resistivity.

quency-domain sounding. The composite results of the surveys given in Figure 3 show five areas (A, B, C, D, and E) of low resistivity. Also shown is the generalized trend of the line of vents to illustrate the geographical relationship of the rift with the areas of low resistivity. Of these, area E is considered the result of cultural sources such as water pipes, sewer pipes, and cables. The low-resistivity zone in area B, which was outlined by Keller (1973), was estimated to exist from a depth of 700 to 2100 m. As outlined by Keller the original area for B was larger; in the map it has been trimmed to exclude those portions thought to be caused by salt water intrusions from the sea. Even so, area B is still much larger than area A.

Attempts have been made to interpret the resistivity data in terms of Archie's Law. The conclusion, although admittedly hazardous, is that the upper limit of the temperature of hot water in the areas under consideration is about 140°C.

Gravity Survey

The available Bouguer gravity map of the island published by Kinoshita (1965) was not particularly useful to the geothermal project because the gravity stations were confined to highways and were spaced at 2-km intervals; for this reason, a more detailed survey was carried out in April 1974 over a stretch of Highway 13 in the Puna district (Fig. 4). For analysis of the data, Bouguer corrections were added and the values were projected along a line that ran perpendicular to the line of vents along the Puna east rift. On incorporating Kinoshita's data, a gravity profile crossing the east rift was obtained, as shown in Figure 5.

To analyze the data, we assumed that the subsurface feature causing the gravity profile was a two-dimensional body. Also, in order to use simplified methods of analysis, we considered the body to cause a symmetrical profile around the maximum value which is shown as 275.3 mgal in Figure 5. We assumed the high gravity values to the right of that point to be caused by a separate body. Upon using the simplified methods as proposed by Skeels (1963) we obtained the values for the gravity anomaly shown in Table 1.

Of the density contrast values given in Table 1, we prefer the value of 0.6 g/cm^3 since this is the value Strange et al. (1965) chose for analysis of volcanic intrusives in the Hawaiian Islands. From the gravity surveys the following conclusions can be drawn:

1. The width of the anomalous body, which we identify as a dike complex, is 3.2 km. This agrees with topographic expression.
2. The vertical dimension of the anomaly is about 3 to 4 km. The anomaly extends from a depth of 1 km to about 4 km.
3. The dike complex exists below the line of vents known as the east rift of Kilauea and trends N65°E.

Magnetic Surveys

An airborne magnetic survey map published by Malahoff and Woollard (1965) showed the east rift as a magnetic low of about 100 gammas trending in an east-west direction.

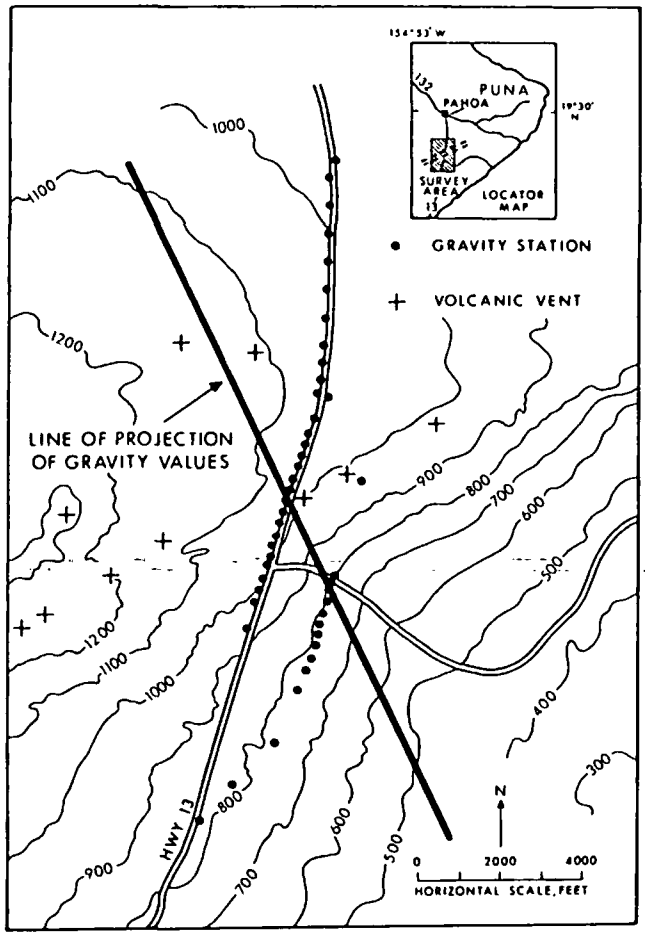

Figure 4. Survey area and gravity stations.

As data are sparse over the Puna district, a ground survey was carried out in January 1975 (Fig. 6). Although the amount of data gathered was large, only the traverse between the areas of Pahoa and Kaimu (Fig. 6) has been processed to date. The profile is given in Figure 7, and its interpretation in Figure 8.

In the interpretation of the data, we assumed that nonmagnetic areas are regions whose temperatures are above the Curie point, and areas of intense magnetization are relatively cool regions. This meant that along the line from Pahoa to Kaimu, only the southern section of the dike complex has temperatures above the Curie point and that some of the adjacent nondike rocks are also hot. Data from other traverses also showed that not all of the dike complex is hot, and that hot sections occur in patches. Of particular concern to the project is that the spot which the drilling committee has selected for its first drill hole is in one of the relatively cool areas.

Table 1. Dimensions of an assumed rectangular prism anomaly.

Density contrast (g/cm^3)	Depth to top (km)	Depth to bottom (km)	Width (km)	Depth to center (km)
0.6	1.0	3.4	3.2	2.2
0.5	.87	3.6	3.2	2.2
0.4	.69	4.0	3.2	2.3

Temperature Measurements in Wells

In 1961 three wells were drilled in the Puna district in search of geothermal sources. All three, together with irrigation wells were measured with a temperature probe to obtain thermal profiles with depth. The location of the wells is shown in Figure 9 and temperature profiles of five of these wells in Figure 10. The most prominent profile is that obtained from geothermal test well No. 3. The temperature in the well rises to a high of 92°C, but the hot water layer is rather thin and the water table practically at sea level. This thinness of the hot water layer confirms the rather high permeability of the rocks in the area, which is due not so much to porosity, but to the cracks between successive layers of volcanic flows.

Microearthquake Surveys

An array of seven geophones was set up over the Puna district with signals from all seven telemetered to one central recording station, three of them by hard wire and the other four by radio. The survey covered a period of two weeks and the number of earthquakes detected was not large. Figure 11 shows epicenteral locations and Figure 12, focal depths projected onto cross section AA′ of Figure 11. On the left side of the latter figure is given the velocity structure which we have used to obtain epicenters and focal depths. Notice in Figure 12 that there is a cluster of earthquakes concentrated in the shallow depth between the surface to 5 km. Below the 5-km depth earthquakes are few. One interpretation from these data is that the dike complex, or the active part of the dike complex, is limited to a depth of 5 km. This inference is in accord with our gravity survey which determined the bottom of the dike complex at about 4 km.

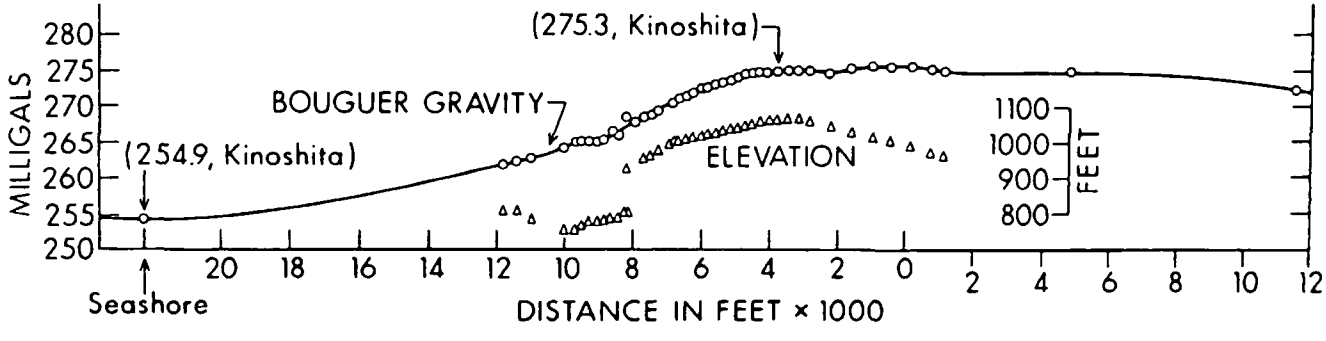

Figure 5. Gravity profile.

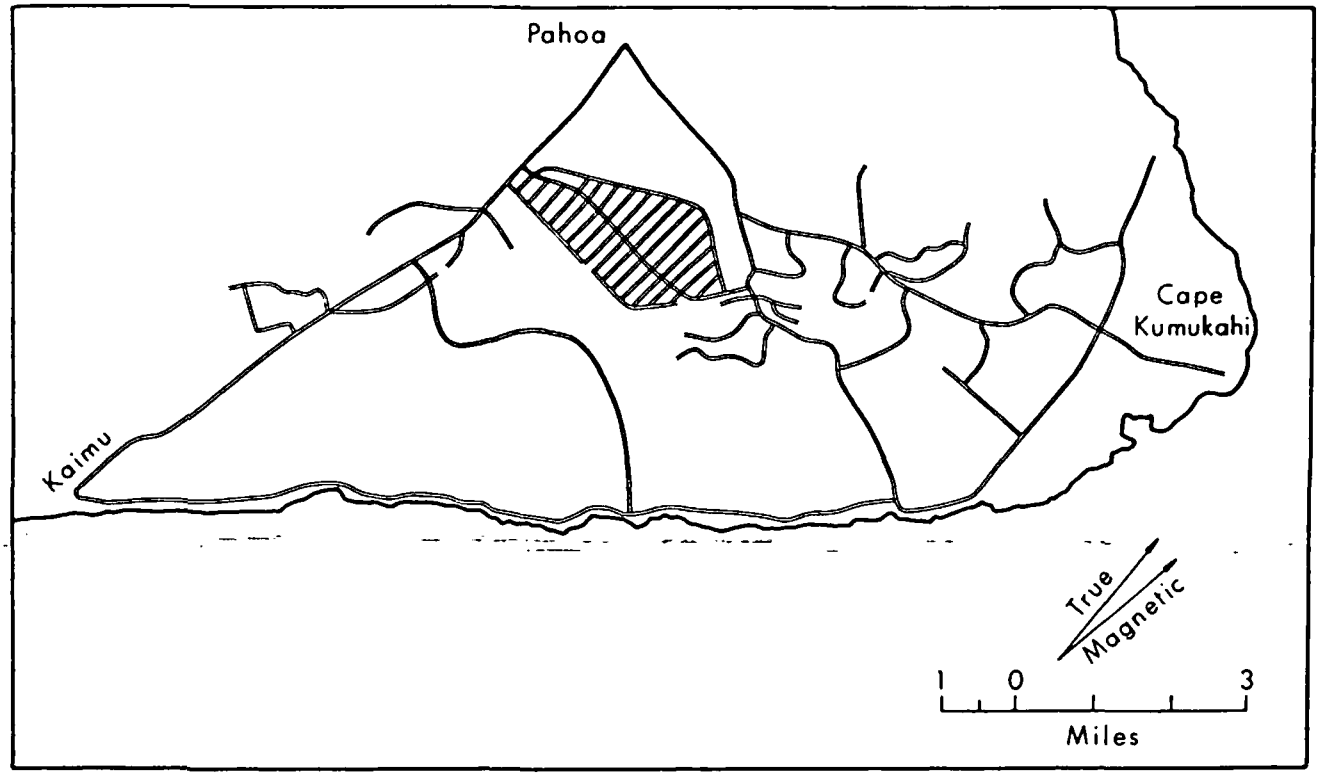

Figure 6. Tracks of magnetic measurements in Puna area.

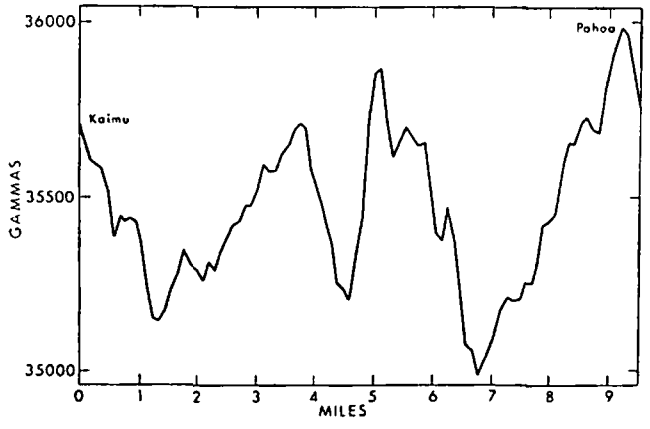

Figure 7. Space-filtered magnetic profile from Kaimu to Pahoa.

Ground-Noise Survey

A ground-noise survey using a 1-Hz geophone was carried out in August 1974. Recording was done on an FM tape recorder. After taking into consideration such things as diurnal variation, meteorological factors, and so forth, a ground-noise intensity map centering on 4 Hz was obtained as shown in Figure 13. Other frequency ranges were analyzed with similar results.

Geochemical Surveys

Water samples from the wells throughout the Puna area were collected and analyzed for oxygen isotope content. Chemical analysis showed that silica content in some of the wells was rather high although the basaltic rock is undersaturated in silica. The significance of the chemical survey is not fully understood at the present time because the use of isotope data as a geothermometer has not been worked out for basaltic rocks. We are seriously looking into this problem.

INTEGRATION OF GEOPHYSICAL DATA

Each of the geophysical tasks provides, in its own way, part of the structure of the east rift of Kilauea and the hydrothermal processes associated with it. When the parts are assembled, a composite picture of the thermal processes emerges. However, the picture obtained is not entirely clear.

The location, shape, and size of the dike complex were determined by gravity and seismic data. Interpretation of magnetic data led to the conclusion that only parts of the dike complex are hot enough to be above the Curie point, but a hot section can heat up adjacent nondike rocks to temperatures above the Curie point. The dike complex in Figure 14 is shown in its geographical relation to the line of vents of the east rift and to the electrically anomalous areas. One of the hot sections inferred from magnetic data is also shown in the figure.

The map of Figure 15 shows that although the dike complex and the line of vents trend N65°E, the magnetic lineaments trend east-west. The magnetic data are from the aeromagnetic surveys of Malahoff and Woollard (1965). The east-west trends are probably ancient remnants of the Molokai fracture zone, as mapped by Malahoff and Woollard (1968). These lineaments are disturbed by hot intrusives, a good example of which is the summit area of Kilauea (Fig. 2). The hot area which we have found by surface surveys also disturbs the lineaments.

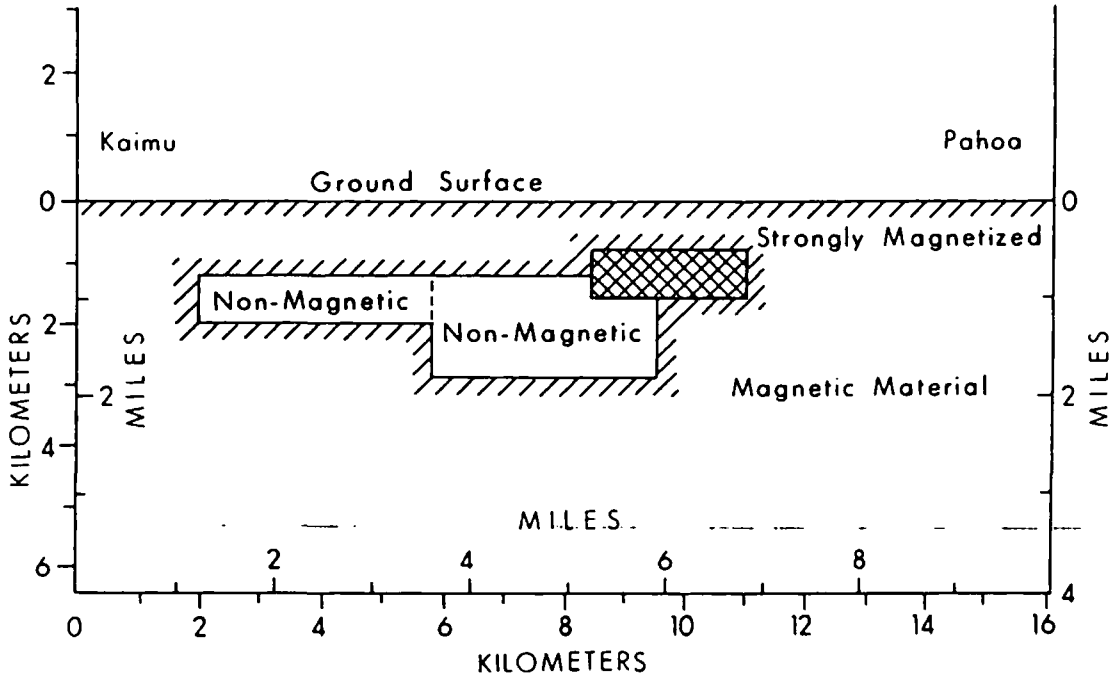

Figure 8. Magnetic anomalies inferred from magnetic profile.

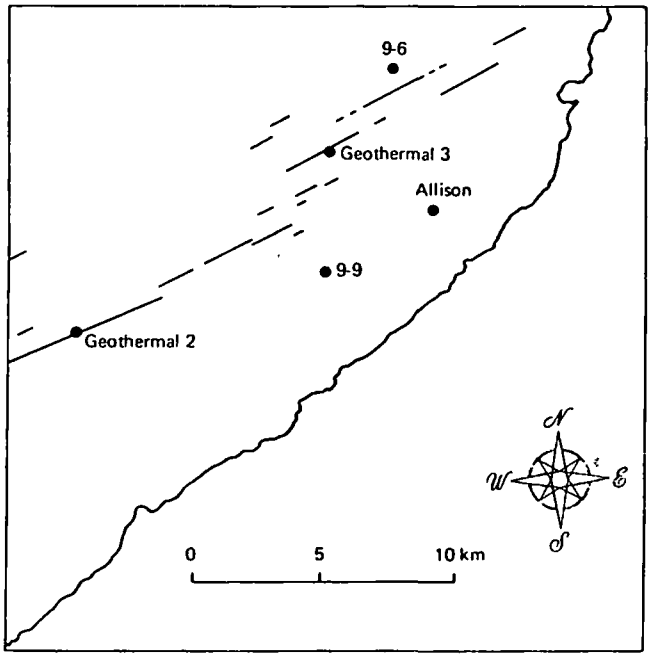

Figure 9. Location in Puna area of wells discussed in the text.

Let us consider first the hot area of Figures 14 and 15 which also corresponds to area B of low electrical resistivity. Keller (1973) calculated that the low-resistivity zone here extends from a depth of 700 m to a depth of 2100 m. Keller (personal commun., 1975) also found from earthquake data that rocks in this area have high Poisson's ratio, about 0.4, and also that small earthquakes here have fault plane solutions which dip southward at angles from 45 to 70 degrees. A high Poisson's ratio is indicative of fractured rocks. Another bit of geophysical data for this area is that of Hill (1969) who, using seismic refraction methods, found a layer with a seismic velocity of 3.1 km/sec at a depth of 700 m, coinciding with the low-resistivity layer of Keller.

We shall now attempt to assemble these seemingly disparate bits of geophysical parameters into a coherent model, which is shown in Figure 16. The source of heat for the rift zone is the dike complex, but hot material whether magma or hot water leaks off into the southern flank of the rift zone. The fractured rocks have cracks dipping south 45 to 70 degrees, as the fault plane solutions indicate. The hot material heats up brine seeping in from the sea, in the manner of the Ghyben-Herzberg hypothesis. Now if the brine is heated, how are we to account for the low resistivity at 700 m depth? We account for it by saying that the 3.1-km/sec seismic velocity represents a pore-filled rock layer. The 3.1-km/sec velocity is peculiar in that it cannot be produced by compressing low-velocity surface basalts with pressures equivalent to 700 m depth. Since some other mechanism is needed, we propose that filling of rock pores and crevices by precipitates from the hot brine changed the seismic velocity to 3.1 in analogy to the self-sealing theory of Facca and Tonani (1967). The pore-filled layer then acts as a caprock to confine the hot brine below 700 m. The pore-filled layer is not very thick, perhaps just thick enough to be a wave guide for seismic waves. In brief, we propose a self-sealing geothermal reservoir for area B.

The model proposed here then accounts for electrical, seismic, magnetic, and gravity data. Admittedly it is highly speculative; the association of the 3.1-km/sec velocity with a pore-filled layer is the weakest link in the series of arguments. But the self-sealing geothermal reservoir model is compatible with all the data that we have so far gathered over this area.

One hazy point in this model is that we do not know how far we can extend it laterally, since electrical data become diffused because of the proximity of this section to the sea.

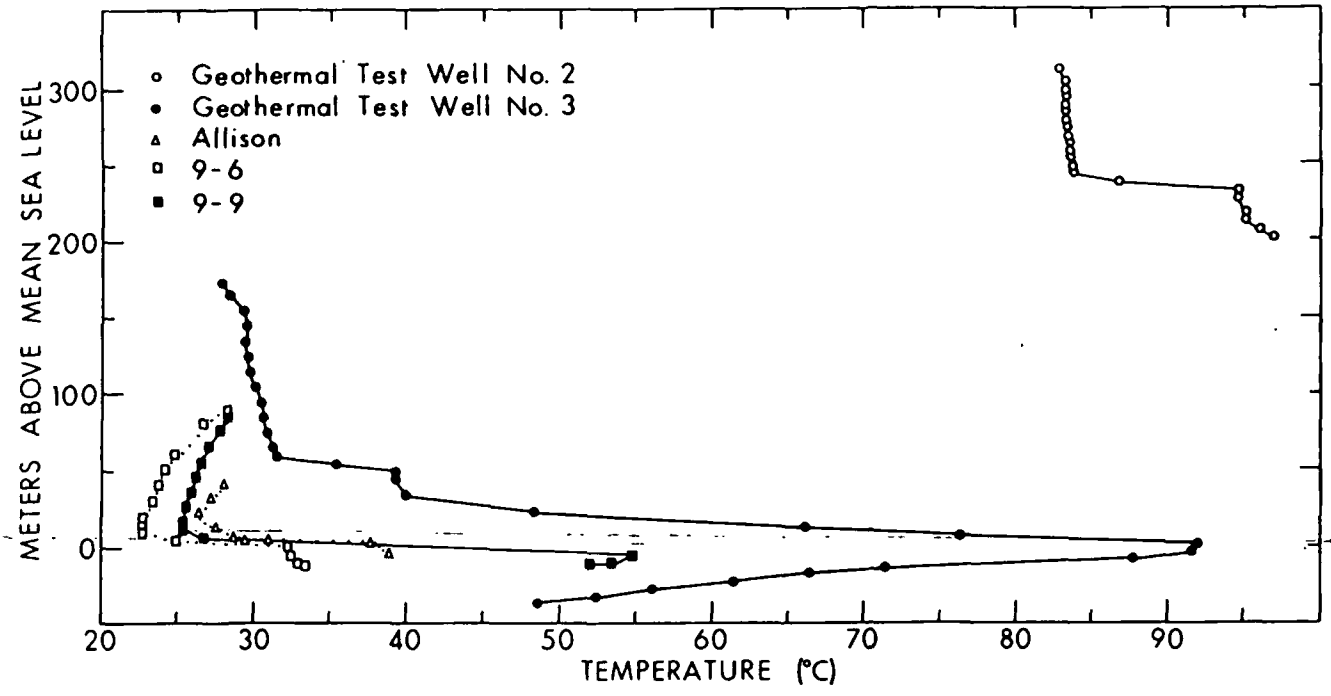

Figure 10. Temperature profiles of the five wells in Puna area.

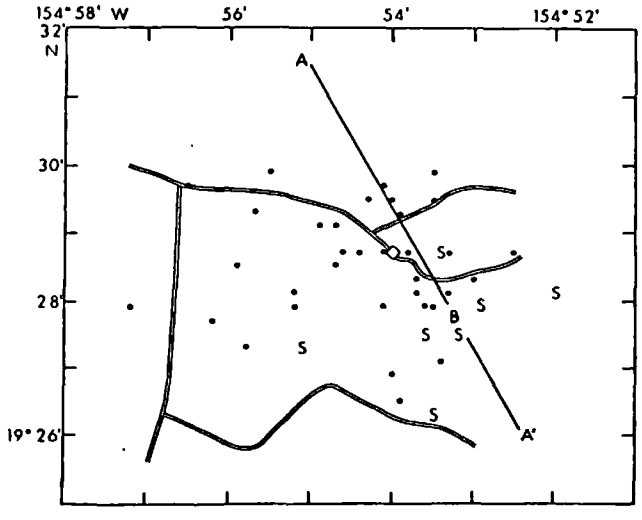

Figure 11. Epicenters of observed earthquakes, S: seismograph stations; B: base station.

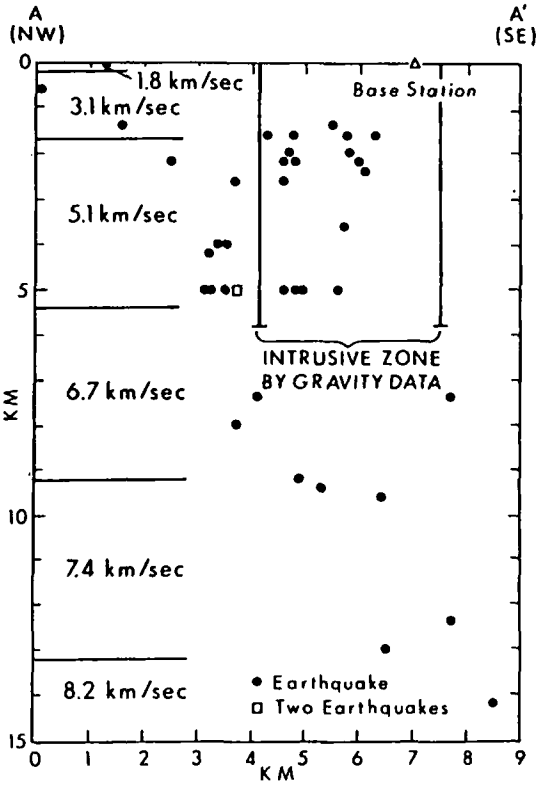

Figure 12. Depth of foci of earthquakes as projected onto plane A–A' shown in Figure 11.

There are other low-resistivity areas in Figure 14, such as areas A, C, D, and E. Area E can be explained by cultural sources such as sewer pipes and cables; area C is quite similar to area B and may be an extension of area B; area A and C are on the dike complex. Area A has been chosen for a drill site by the site selection committee of the geothermal project. It has the following favorable geophysical data: a self-potential anomaly, a low-resistivity area, a ground-noise high, and hot water (92°C) in a nearby well. But the drawbacks are several: aeromagnetic and surface magnetic surveys do not indicate hot intrusions; the low resistivity occupies relatively a small area so that even if a hot water or vapor system were present, the volume would not be commercially viable; the hot water in the nearby well is limited to a thin layer of about 7 m, and below that the water temperature drops off considerably. The motivation of the site selection committee seems to be the hope of hitting hot rock or magma, but even this hope may turn out to be in vain, as magnetic data would appear to forecast.

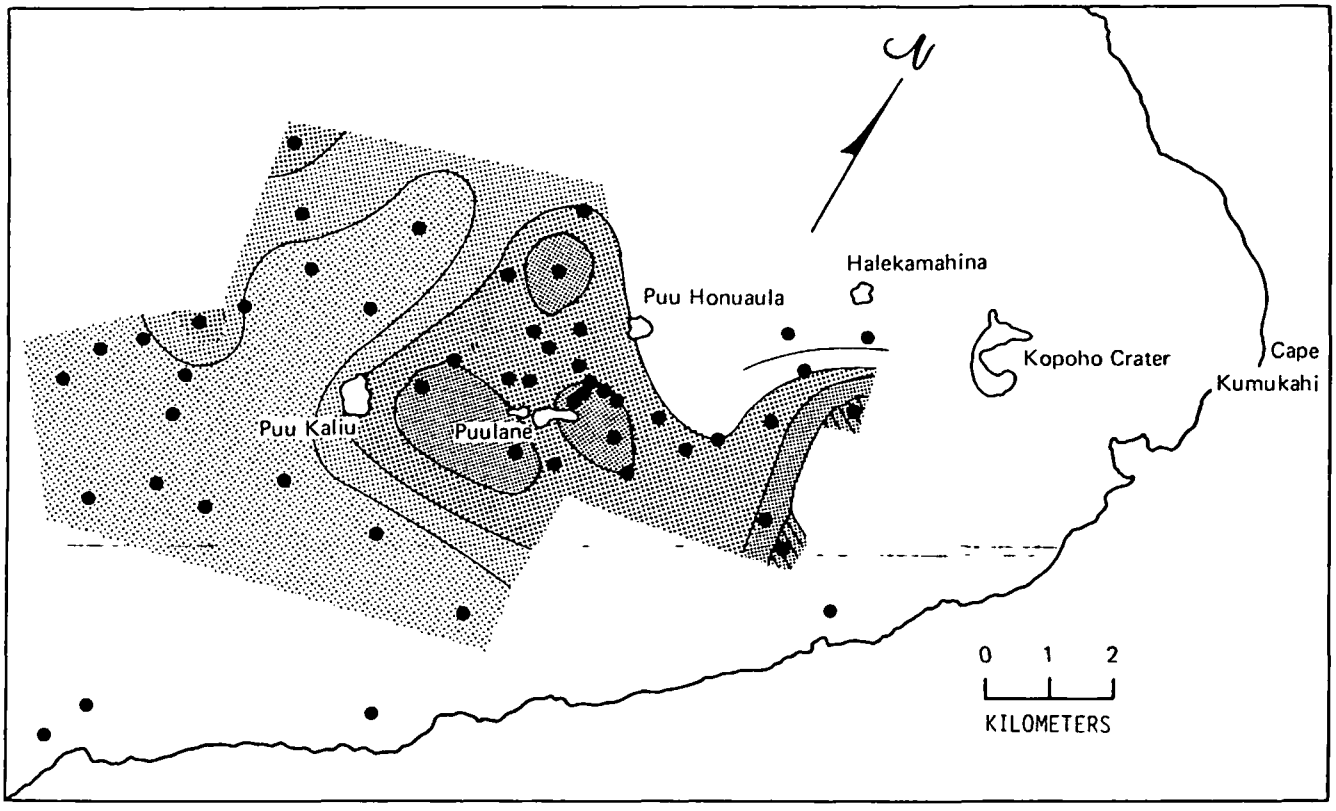

Figure 13. Three db interval contours of 4 Hz noise. The darker the area, the higher the amplitude.

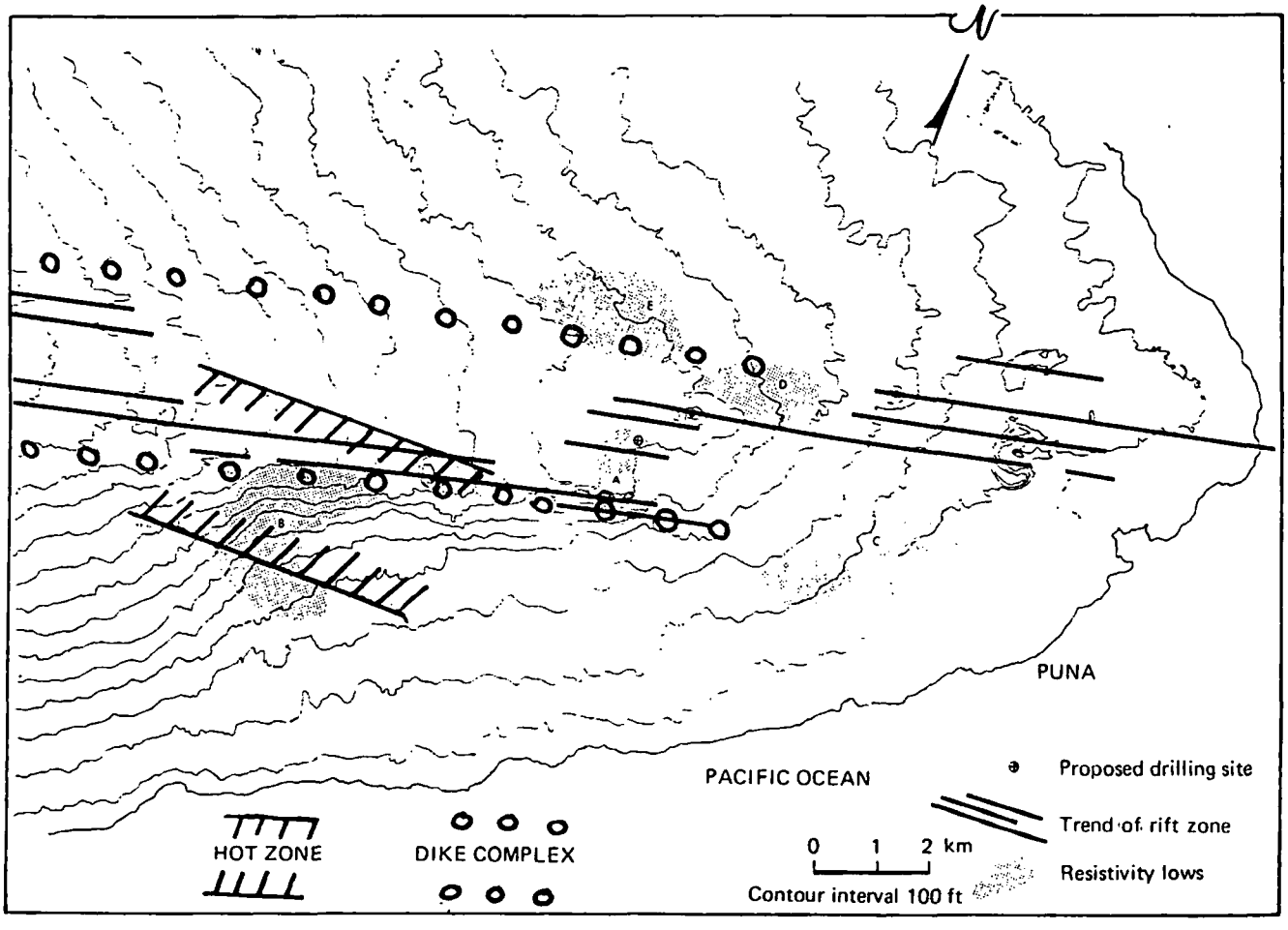

Figure 14. Location of dike complex and hot section of east rift of Kilauea.

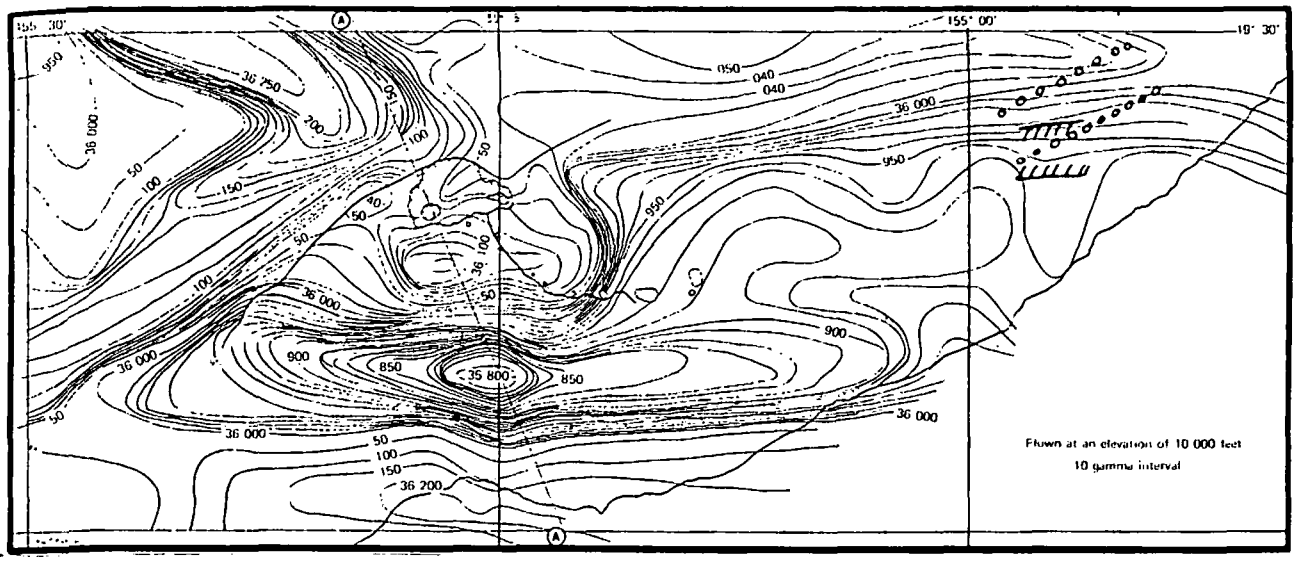

Figure 15. Magnetic map of Kilauea and Puna areas with dike complex and hot area of Figure 14 superimposed.

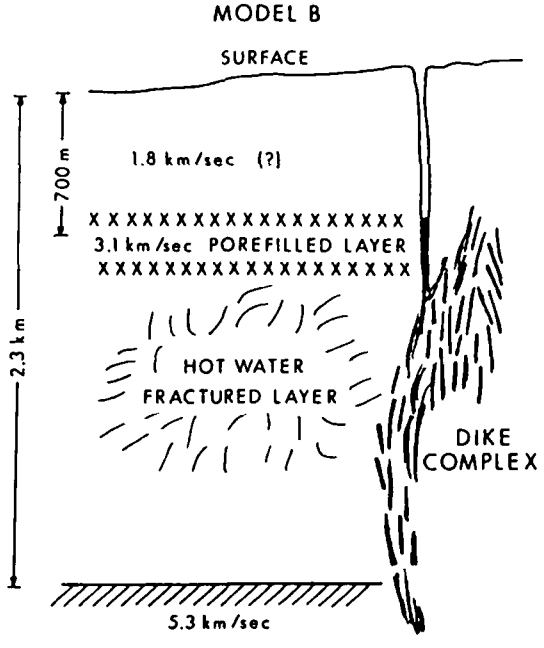

Figure 16. Hydrothermal process of area B. The model is very conjectural.

CONCLUSIONS

Electrical methods are generally considered the most powerful tool for geothermal exploration. But for basaltic rocks with high permeability, the nature of low resistivity areas found by electrical methods cannot be determined unless the ultimate source of heat is found. Usually the source is a dike complex or plug, which can be clearly outlined by gravity and seismic methods. The dike complex is not uniformly hot; hot areas occur in patches which can be found by magnetic methods. Surface magnetic surveys are more effective than aeromagnetic surveys.

We are still assessing the value of geochemical data for resource location.

ACKNOWLEDGEMENTS

Gratitude is hereby expressed to the project participants P. F. Fan, D. P. Klein, J. Kauahikaua, W. Suyenaga, R. Norris, and G. McMurtry, who made their data available for this paper. All of the illustrations used in this paper, except Figure 15, have appeared in a final report to the National Science Foundation under Grant GI 38319. This grant is gratefully acknowledged. This paper constitutes Hawaii Institute of Geophysics Contribution No. 673.

REFERENCES CITED

Facca, G., and Tonani, F., 1967, Self-sealing geothermal field: Bull. Volcano., v. 30, p. 271-273.

Hill, D., 1969, Crustal structure of the island of Hawaii from seismic refraction measurements: Seismol. Soc. America Bull. v. 50, p. 101-130.

Keller, G. V., 1973, An electrical resistivity survey of the Puna and Kau districts: Report submitted by Group 7 to the Research Corporation of the University of Hawaii.

Kinoshita, W. T., 1965, A gravity survey of the island of Hawaii: Pacific Sci., v. 19, p. 339-340.

Klein, D. P., and Kauahikaua, J., 1975, Geothermal-geoelectric exploration on Hawaii Island, preliminary report: Hawaii Inst. Geophysics Report, HIG 75-6.

Malahoff, A., and Woollard, G. P., 1965, Magnetic surveys over the Hawaiian ridge: Hawaii Inst. Geophysics Report, HIG-65-11.

Malahoff, A., and Woollard, G. P., 1968, Magnetic and tectonic trends over the Hawaiian ridge: Am. Geophys. Union Geophys. Mon. 12, p. 241-276.

Skeels, D. C., 1963, An approximate solution of the island of Hawaii: Pacific Sci., v. 19, p. 339-340.

Strange, W. E., Woollard, G. P., and Rose, R. C., 1965, An analysis of gravity field over the Hawaiian Islands in terms of crustal structure: Pacific Sci., v. 19, p. 381-389.

51st Annual meeting SEG, 1981

Pub Ap 1982

Geothermal Exploration Session

Thursday Morning

Geothermal Energy Resources In the Eastern United States: Atlantic Coastal Plain GE.1

John K. Costain and Lynn Glover, III, Virginia Polytech Inst. and State Univ.

Optimum sites for the development of geothermal energy resources in the eastern United States will probably be associated with the Atlantic coastal plain sediments. The low thermal conductivity of these sediments requires relatively high geothermal gradients even for normal heat flow. Where these sediments are thick and where they blanket radioactive, heat-producing granitoids in the basement rocks, isotherms are warped upward and higher temperatures occur at shallower depths. During 1976-80, heat flow determinations were made at drill sites in the Piedmont and on the Atlantic coastal plain from New Jersey to North Carolina. On the Atlantic coastal plain, gradients between Crisfield, Maryland and Oak Hall, Virginia are greater than 40° C/km; the thickness of the sediments here is more than 1.2 km.

Geothermal resources in the Appalachian Mountain system and the Atlantic coastal plain can be grouped into four types: (1) radioactive heat-producing granite buried beneath a thick blanket of sediments of low thermal conductivity (a sedimentary insulator), (2) normal geothermal gradient resources, (3) warm water emanating from fault zones, and (4) hot-dry-rock in regions of abnormal geothermal gradients without associated water reservoirs.

Resource 1 is the principal subject of this abstract. Resource 2 (normal gradient) is widely available throughout much of the U.S. (Sammel, 1979). Resource 3 (hot springs) could be important locally in the eastern U.S. Perry et al (1979) proposed a model for the origin of the hot springs in Virginia that may apply to many of the hot springs in the eastern U.S. In this model, meteoric water at high elevations enters nearly vertical permeable Silurian quartzites and possibly adjacent fractured carbonate units along steep to vertical bedding, extends to depths (3 km) sufficient to heat water, and then rises rapidly along local east trending transverse fracture zones which intersect the bedding permeability at depth. Groundwater flow lines are essentially vertical beneath the recharge areas and diverge at depth to intersect the transverse fracture zones. Resource 4 (hot-dry-rock) is described by Pettitt (1979). It is unlikely to be economic in the near future for the eastern U.S.

Resource 1 has been the principal focus of the geothermal program at VPI&SU, and we explain its existence by the "radiogenic model" (Figure 1), (Costain et al. 1980). For the development of a geothermal resource, the combination of high heat flow, low thermal conductivity, and low rates of groundwater flow will result in the highest subsurface temperature at the shallowest depths. High heat flow in the eastern U.S. is associated with relatively young, unmetamorphosed granite plutons. Birch et al (1968) showed that the local heat flow has a well-defined relation to the concentration of uranium (U), thorium (Th), and potassium (K) in

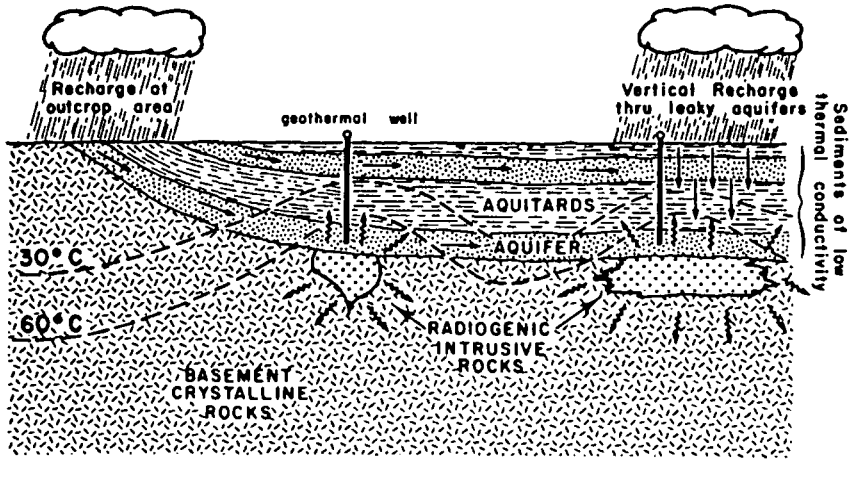

FIG. 1. The radiogenic model.

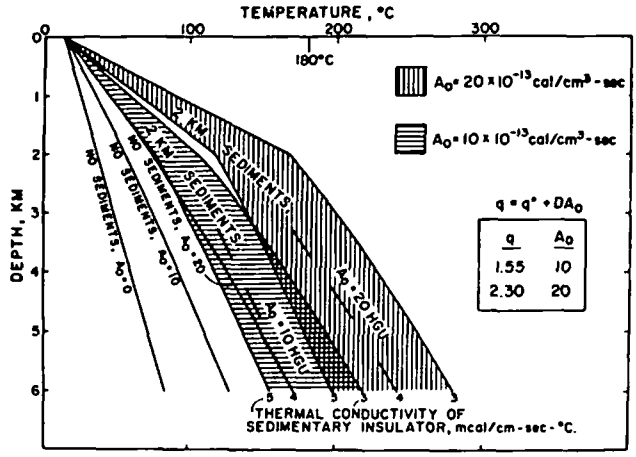

FIG. 2. Insulating effect of a sedimentary blanket.

the upper crust. The distribution of U and Th in the upper 10 km or so of the earth's crust is primarily responsible for lateral variations in surface heat flow in the eastern U.S. Most of the heat produced comes from U and Th; only about 10-15 percent comes from K. Optimum sites for the development of geothermal energy in the eastern U.S. are associated with the flat-lying, relatively unconsolidated sedimentary blanket beneath the Atlantic Coastal Plain that overlies heat-producing granitoids in the basement. At many locations, the overlying sediments yield large quantities of water that can be used for the effective transfer of heat to the surface.

One of the principal objectives of the geothermal program at VPI&SU has been to locate and study relatively young, (254-330 Ma.) unmetamorphosed heat-producing U- and Th-bearing granitoids such as those in the exposed basement rocks of the Piedmont province adjacent to the Atlantic coastal plain (Glover, 1979). Results of studies of the granite petrology were reported by Speer et al (1980) and Speer et al (in press).

The basement rocks are concealed to the southeast by the sediments of the Atlantic coastal plain which comprise the seaward-thickening sedimentary insulator. Sediment thickness is known to be about 3 km at Cape Hatteras, NC.

Figure 2 illustrates the effect on subsurface temperature where crystalline rocks are blanketed by a sedimentary insulator. The leftmost curve in Figure 2 is the temperature-depth profile in unblanketed basement crystalline rocks devoid of U and Th. As U and Th are added to produce 10 HGU (1 HGU = 1 heat generation unit = 10^{-13} cal/cm³) and 20 HGU, the subsurface temperature and geothermal gradient increase. Finally, if U- and Th-bearing granite is blanketed by sediments that have a relatively low thermal conductivity, the subsurface temperature is increased further.

The locations of our heat flow sites in the eastern U.S. were chosen on the basis of gravity data, magnetic data, thickness of coastal plain sediments; apparent thermal anomalies, available basement core data, suitable sites for the evaluation of the radiogenic pluton model, and proximity to energy markets.

Lambiase et al (1980) discussed the distribution and values of geothermal gradients obtained in the holes drilled on the northern Atlantic coastal plain. One promising area appears to be between Crisfield, Maryland and Oak Hall, Virginia, on the Eastern Shore. Higher gradients (48°C/Km) were found elsewhere, for example, on the west side of Chesapeake Bay within the large negative gravity anomaly in the vicinity of the bay, but the depth to basement there is less. A test hole was drilled on the Eastern Shore at Crisfield.

The temperature predicted at the base of the coastal plain sediments (1.42 km) at Crisfield was about 16 percent less than the actual temperature as a result of the uncertainty in predicting the thermal conductivity of coastal plain sediments at depths below the drill hole. Limited pump tests were made at Crisfield to estimate potential fluid production. Laczniak (1980) modeled the response of a leaky aquifer system to be a single dipole (pumping plus injection well) using the results from the Crisfield tests. The model was run for a simulated period of 15 years or until steady-state thermal and fluid flow were reached.

Important conclusions of Laczniak's study were: (a) direct injection back into the reservoir may be necessary to maintain sufficient fluid pressure at the production well for systems with a low permeability, (b) temperature distribution within the system is only slightly affected by changes in permeability in the range 10-100 md, (c) resting the system for periods of 6 months does not result in a significant recovery of heat at the production well, and (d) a doublet system with thermal and hydrologic conditions similar to those encountered at Crisfield, a well spacing of 1000 m, a permeability of 100 md, and a pumping-injection stress of 500 gpm (injection temperature 44° C) could produce 5.5 million Btu's per hour over a period greater than 15 years.

References

Birch, F., Roy, R. F., and Decker, E. R., 1968, Heat flow and thermal history in New England and New York, *in* Studies of appalachian geology: E. Zen, W. S. White, J. B. Hadley, and J. B. Thompson, Jr., editors, Interscience, New York, p. 437-451.

Costain, J. K., Glover, III, L., and Sinha, A. K., 1980, Low-temperature geothermal resources in the eastern United States: *EOS*, Trans. AGU, v. 61, p. 1-3.

Glover, L., III, 1979, General geology of the east coast with emphasis on potential geothermal energy regions: A detailed summary: *in* A symposium of geothermal energy and its direct uses in the eastern United States: Geother. Res. Coun., spec. rep. no. 5, Davis, CA.

Laczniak, R. J., 1980, Analysis of the relationship between energy output and well spacing in a typical Atlantic Coastal Plain geothermal doublet system: M.S. thesis, VA Polytech. Inst. and State Univ.

Lambiase, J. J., et al, 1980, Geothermal resource potential on the northern Atlantic Coastal Plain: Geology, v. 8, p. 447-449.

Perry, L. D., Costain, J. K., and Geiser, P. A., 1979, Heat flow in western Virginia and a model for the origin of thermal springs in the folded Appalachians: J. Geophys. Res., v. 84, p. 6875-6883.

Sammel, E. A., 1979, Occurrence of low-temperature geothermal waters in the United States, *in* Assessment of geothermal resources of the United States—1978: L. J. P. Muffler, ed., U.S.G.S. circ. 790.

Speer, J. A., Becker S. W., and Farrar, S. S., 1980, Field relations and petrology of the postmetamorphic, coarse-grained granitoids and associated rocks of the southern Appalachian Piedmont, in The caledonides in the U.S.A. IGCP Project 27: Caledonide Orogen, Dept. of Geol. Sci, VPI&SU, Blacksburg, VA, 24061.

Speer, J. A., Solberg, T., and Becker, S. W., (in press) Petrography of the U-bearing minerals of the Liberty Hall Pluton, South Carolina: Phase assemblages and migration of U in granitoid rocks: Econ. Geol.

Search for Geothermal Heat Sources in the Oregon Cascades by Means of Teleseismic P-Residual Technique GE.2

H. M. Iyer, A. Rite, Chevron International Oil Co.; and S. M. Green, U.S.G.S.

The geothermal potential of the Oregon Cascades is considered to be high in view of its tectonic setting, the presence of young volcanoes, and high heat flow. Geophysical techniques, however, have failed to provide unambiguous evidence for the presence of large crustal magma bodies, unlike at some other rhyolitic volcanic centers in the western United States. Teleseismic residual studies at Mount Hood and Newberry volcano show no evidence for crustal magma chambers of detectable size under these vol-

canoes; the same situation seems to prevail in the California Cascades as well. However, results of drilling at Newberry indicate that high-temperature water is present at a depth of 1 km and suggest that a magmatic heat source exists. Teleseismic-residual studies, using a 32-station seismic network encompassing the whole of the Oregon Cascades, give some clues as to the nature of the heat sources in the region. A velocity model derived from the teleseismic data shows a zone of relatively low velocity in the crust and upper mantle under the High Cascades, in comparison with higher velocities beneath the Western Cascades. We interpret these results as indicating the presence of low-density high-temperature rock to great depths. Intrusion of magma related to subduction of the Juan de Fuca plate is apparently responsible for this and results in the observed high heat flow. The presence of numerous small pockets of magma, as well as favorable hydrologic circulation patterns, may give rise to high-temperature water at shallow depths, such as at Newberry volcano.

It is generally believed that the Oregon Cascades have high geothermal potential. The tectonic setting of Oregon over the subducting Juan de Fuca plate, the abundance of Quaternary volcanism, the presence of numerous hot springs, and high measured heat flow suggest that an extensive geothermal resource may exist. However, unlike at many other geothermal areas in the Western United States where detectable low-velocity anomalies that can be interpreted as magma bodies seem to be present in the crust (Iyer, 1980), our efforts to detect such bodies in the Oregon Cascades have consistently met with negative results. The fact that magma is, indeed, locally present at shallow depths is evidenced by the recent eruption of Mount St. Helens and the building of a massive lava dome in the newly formed crater.

In this paper we present results of teleseismic P-residual measurements around Mount Hood and Newberry volcano in Oregon. In addition, we also present a three-dimensional *P*-wave-velocity model for the whole of the Oregon Cascades. These results, together with other available geophysical data, are interpreted to explain the geothermal enigma of the Oregon Cascades, namely, high apparent geothermal potential but the absence of detectable magma chambers.

Mount Hood

A detailed analysis of *P*-wave residuals from 55 teleseisms recorded by a 16-station seismic network around Mount Hood show a total regional variation of 0.7 sec (Figure 1a). There is no evidence, however, for a localized high or low-velocity anomaly (negative or positive relative residuals) that could be related to a magma chamber under the volcano (The teleseismic technique is capable of detecting magma bodies of 5 km or more in diameter.). Analysis of gravity data by Couch and Gemperle (1979), although showing regional structural trends and lateral and vertical variations in the density of pyroclastic flows, also shows no evidence for a magma chamber. Several drill holes around Mount Hood do not show any abnormally high bottom-hole temperatures or thermal gradients (Robinson et al, 1981; Ehni, 1981). Mount Hood, however, like other Quaternary volcanoes in the Oregon Cascades, is situated on a ridge of high heat flow that coincides with the High Cascades. Heat flow jumps by a factor of almost 2.5 from 40 mW/m² (1 HFU) in the Western Cascades to 105 mW/m² (2.5 HFU) in the High Cascades (Blackwell et al, 1978).

Newberry volcano

Newberry volcano in west-central Oregon presents a more promising geothermal picture than the Mount Hood area. Test drilling by the U.S. Geological Survey near the center of New-

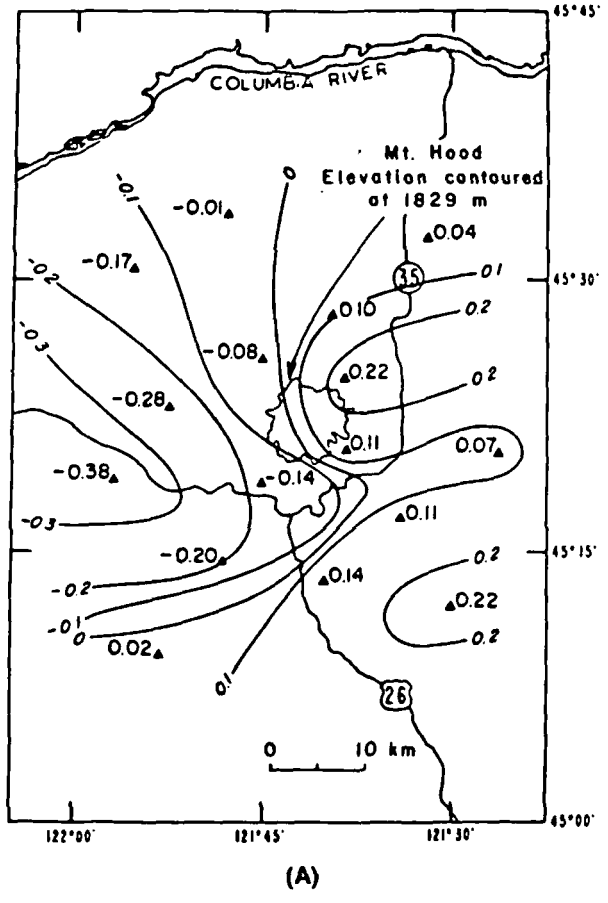

(A)

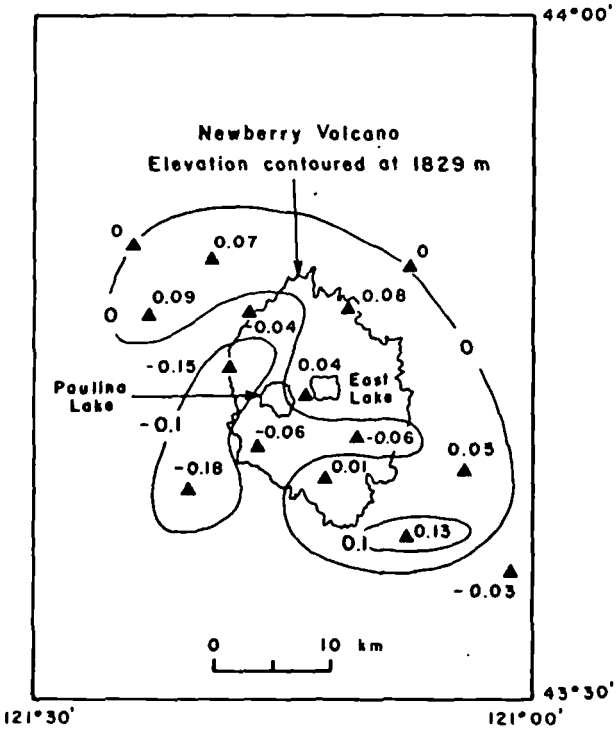

(B)

FIG. 1. Relative teleseismic residual contours. Units are in seconds. (A) Mount Hood (B) Newberry volcano.

berry caldera encountered high temperatures (265°C) at a depth of 930 m (Sammel, 1981). A teleseismic study by the U.S.G.S., however, showed no evidence for a low-velocity anomaly that could be interpreted as a magma body under the volcano. Teleseismic residuals were generally of low amplitude and independent of azimuth. The average relative residuals, contoured in Figure 1b, show only a negative residual anomaly of about 0.2 sec to the west of the caldera. This can be interpreted as a shallow high-velocity intrusion and is somewhat similar to an interpretation of gravity data by Williams and Finn (1981).

Oregon Cascades

Available evidence from several other cascade volcanoes, such as Mount St. Helens, Mount Shasta, and Lassen Peak (personal communication from various individuals), also seems to follow the pattern at Mount Hood and Newberry volcano, in that no detectable magma chambers of finite dimensions (diameter greater than 5 km) seem to be present in the crust or mantle. The obvious question, therefore, is: What is the nature of the geothermal heat source responsible for the elevated regional heat flow in the High Cascades (see Figure 2)?

The regional nature of the High Cascade heat source is corroborated by a teleseismic study using a 32-station seismic network being operated in Oregon by the U.S.G.S., under its Volcano Hazards Program. The teleseismic residuals show large azimuthally dependent variations with amplitudes of about 0.5 sec. The relative-residuals (average of 82 teleseisms) contoured in Figure 2 reveal the following features: (1) a ridge of positive residuals (indicating lower than normal velocities) over the High Cascades; (2) a sharp west-to-east transition from an average of −0.3 to +0.3 sec in the central area; and (3) a large regional delay (positive residuals) around Newberry volcano. The region of high heat flow (greater than 100 mW/m²) is shaded in Figure 2 for comparison with the area of positive residuals.

We have used the inversion technique developed by Aki et al (1977) to obtain a 3-D velocity model of the area contoured in Figure 2. The block sizes used in the inversion are 50 km × 50 km horizontally and 20, 20, 75, 100, 100 km, vertically. The results (not shown here) indicate considerable complexity in structure of the northern Oregon Cascades within the top 20 km of the crust. In the central and southern cascades there is a change in velocity from higher to lower values by about a 10 percent from west to east. In the lower crust and upper mantle, the main feature throughout the model is this west-to-east change from high to low velocities. There is also some indication that this transition boundary migrates eastward with increasing depth. Figure 3 is a northwesterly cross-section of a highly idealized velocity model. Two important features of this model are relevant to volcanism in Oregon: (1) the inclined boundary between the high- and low-velocity zones suggests a subducting plate, and (2) the entire High Cascades region seems to be underlain by relatively low velocity material (Note that the cross-section is perpendicular to the direction of plate convergence and at 45 degrees to the axis of the volcanic chain.).

Regional-gravity data in Oregon also show this deficiency in mass under the High Cascades. Dehlinger et al (1968) and Thiruvathukal et al (1970) interpreted this phenomenon as due to a drastic increase in crustal thickness under the High Cascades. Crustal thickening would also result in a pattern of residuals similar to that shown in Figure 2. However, inversion of residual data computed using reasonable crustal-thickening models show that this effect alone cannot explain the results summarized in Figure 3. We conclude that the velocities in the crust and lower mantle are indeed lower in the High Cascades compared to the Western Cascades. We interpret this contrast as due to the presence of hot rock and pockets of magma.

Thus, our model for the deep structure of the High Cascades resembles that proposed by Karig (1971) for marginal basins behind island arcs. In such regions, above the underthrusting lithosphere, shear-heated material rises buoyantly and results in a wedge of low-density high-temperature upper mantle. A petrogenetic model, in which intrusion of calc-alkaline magmas occurs in the wedge-shaped region above a subducting plate, was postulated by Ringwood (1977). Further confirmation for the existence of such a structure under the High Cascades will require seismic-refraction surveys to constrain crustal effects and Q measurements on a regional scale. Magma pockets under the volcanoes may themselves be too small to be detectable by existing teleseismic techniques and other high-resolution seismic techniques will be needed to locate them.

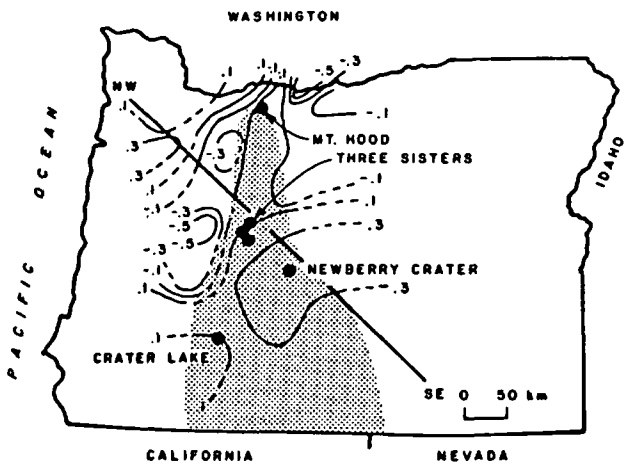

FIG. 2. Relative teleseismic residual contours in western Oregon. Units are in seconds. Stippling, area where heat flow exceeds 100 mW/m² (adapted from Blackwell et al, 1978). Dots denote selected volcanoes. Velocity cross-section shown in Figure 3 is along northwest-southeast line.

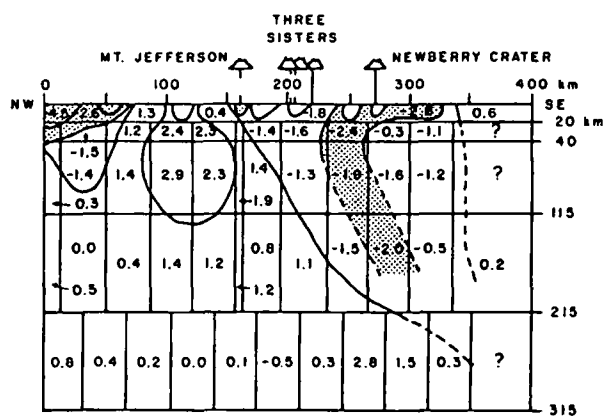

FIG. 3. Velocity cross-section along a northwest-southeast profile indicated in Figure 2. Numbers show relative velocity variation (in percent). Contour interval is 2 percent. Cells show block sizes used in inversion. Shaded area is where velocity decrease is greater than 2 percent.

References

Aki, K., Christoffersson, A., and Husebye, E. S., 1977, Determination of the three-dimensional structure of the lithosphere: J. Geophys. Res., v. 82, p. 277-296.

Blackwell, D. D., Hull, D. A., Bowen, R. G., and Steele, J. L., 1978, Heat flow of Oregon: Oreg. Dep. of Geol. Miner. Ind. Spec. pap. 4, 42 p.

Couch, R., and Gemperle, M., 1979, Gravity measurements in the area of Mt. Hood, Oregon, *in* Geothermal resource assessment of Mt. Hood: Oreg. Dep. of Geol. Miner. Ind. Open-file rep. 0-79-8, p. 137-189.

Dehlinger, P., Couch, R. W., and Gemperle, M., 1968, Continental and oceanic structure from the Oregon coast westward across the Juan de Fuca Ridge: Can. J. Earth Sci., v. 5, p. 1079-1090.

Ehni, W. J., 1981, Summary of 1980 geothermal drilling in western United States: Geotherm. Energy, v. 9, p. 4-15.

Iyer, H. M., 1980, Magma chambers and geothermal energy (abs.): Presented at the 50th Annual International SEG Meeting, Houston.

Karig, D. E., 1971. Origin and development of marginal basins in the western Pacific: J. Geophys. Res., v. 76, p. 2542-2561.

Ringwood, A. E., 1977. Petrogenesis in island arc systems, *in* Island arcs, deep sea trenches, and back-arc basin: M. Talwani and W. C. Pitman III (editors), AGU, Washington, D.C., p. 311-324.

Robinson, J. H., Forcella, L. S., and Gannett, M. W., 1981, Data from geothermal test wells near Mt. Hood, Oregon: U.S. Geol. Surv. Open-file rep. 81-1002, 24 p.

Sammel, E. A., 1981, Results of test drilling at Newberry Volcano, Oregon: Geotherm. Resour. Counc. Bull., v. 10, no. 11, p: 3-8.

Thiruvathukal, J. V., Berg, Jr., J. W., and Heinrichs, D. F., 1970, Regional gravity of Oregon: GSA Bull., v. 81, p. 725-738.

Williams, D. L., and Finn, C., 1981. Gravity anomalies in sub-volcanic intrusions in the Cascades Range and elsewhere (abs.): Presented at the 51st Annual International SEG Meeting, Los Angeles.

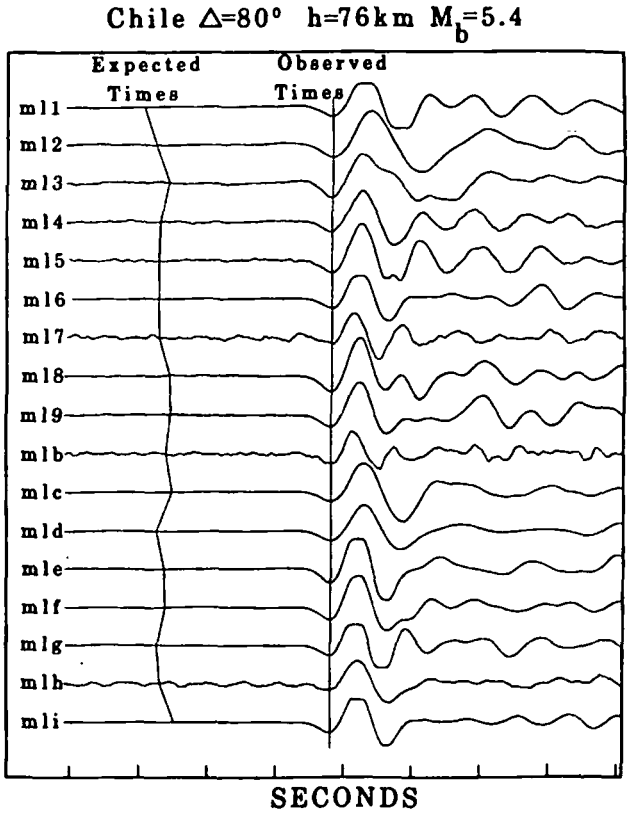

FIG. 1. An example of teleseismic data aligned by picks to show signal coherence across the array. The differences between these observed relative times and the expected arrival times (less the average difference for the event) are relative traveltime residuals. Picks were actually made in the first half cycle of narrow band-filtered copies of these traces.

Compressional-Wave Velocity Structure of the Medicine Lake Volcano and Vicinity from Teleseismic Relative Traveltime Residuals — GE.3

John R. Evans, U.S.G.S.

Teleseismic *P*-wave relative traveltime residuals from an array spanning the Medicine Lake volcano, California, reveal high-velocity anomalies in the crust and upper mantle extending from very shallow depths to at least 100 km beneath the volcano. These preliminary data also suggest the presence of a shallow low-velocity feature beneath a young lava flow on the southeast flank of the volcano. This low-velocity feature may be associated with the source of the flow and is the most promising geothermal prospect seen from these preliminary data. The absence of any other significant low-velocity region, of even a mantle low-velocity source anomaly, suggests that any melt or partial-melt pockets forming prior to an eruption must either be very small, very short lived, or both. The high-velocity main anomaly contrasts sharply with those in other volcanic areas such as Yellowstone and The Geysers.

Method

Teleseismic *P*-wave relative traveltime residuals have been used in many areas to map the 2-D or 3-D compressional-velocity structure of the crust and upper mantle (for example, Iyer et al, 1981; Steeples and Iyer, 1976; Evans, 1982; Reasenberg et al, 1980; Oppenheimer and Herkenhoff, 1981). This technique can resolve features at least as small as a few kilometers across (Stauber, 1982) and has the unique ability to resolve complex structure to depths exceeding several hundred kilometers. In addition, resolution of the study volume is relatively uniform and is quantitatively described through a damped least-squares inversion technique (Aki et al, 1977).

Relative residuals are computed as follows:

(1) Accurate relative arrival times are determined for numerous teleseisms ($\Delta \geq 25$ degrees) at the stations in a 1-D or 2-D array. First peak, trough or zero-crossing times (Figure 1) of narrow band-filtered traces provide relative times usually accurate to ±0.05 sec.

(2) Theoretical arrival times based on a standard earth model (e.g., Herrin, 1968) and on hypocenters determined from world-wide networks (e.g., *Preliminary Determinations of Epicenters*, a regular publication of the U.S. Geological Survey) are subtracted from the observed times to produce traveltime residuals.

(3) Errors in hypocenters, departures from the standard earth model (including some large-scale structures near the array), and use of different earth models for locating the events and calculating expected arrival times all introduce large traveltime residuals. Since these effects are the same or nearly the same at all stations within a compact array, the average traveltime residual for each event is subtracted from each residual to give relative residuals.

Relative residuals contain information on relative-velocity structures smaller than the sampled volume under the array. Information on absolute velocities and on uniform structures spanning the sampled volume is lost when an event's average residual is removed, whereas information on velocity variations is retained.

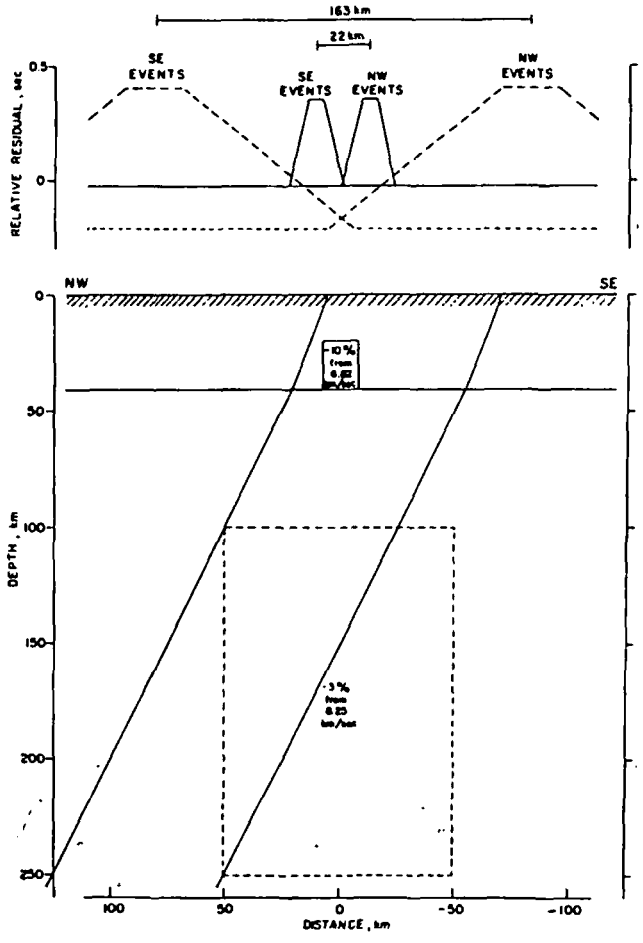

FIG. 2. Schematic illustration of the means of vertical resolution with teleseismic relative residuals. The relative residual patterns move roughly as far horizontally as the body is deep when the azimuth of ray approach is reversed.

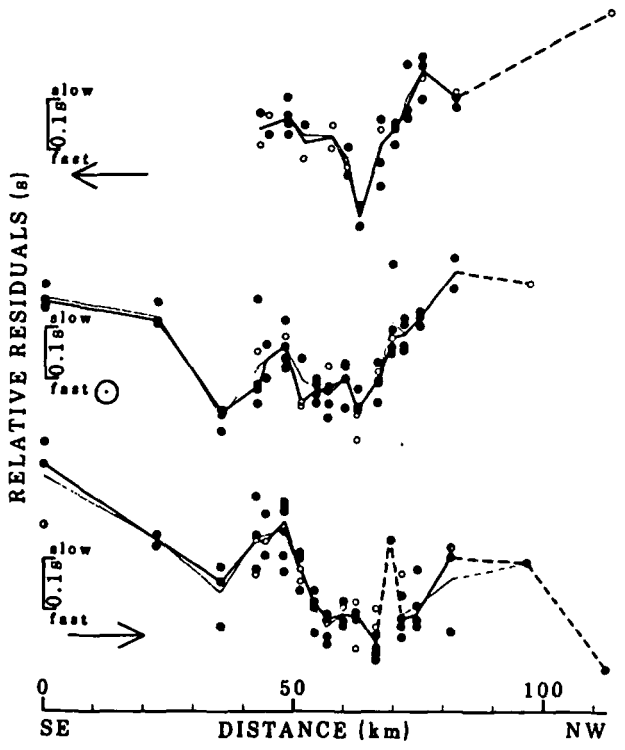

FIG. 4. Relative residuals for each of three ray azimuths plotted as a function of positions of stations in the array. Directions of ray travel are indicated by the arrow. Solid dots are good quality data, open circles are lesser quality data. Heavy lines connect the median relative residual at each station; narrow lines connect mean relative residuals weighted in favor of the better data. Lines are dashed where based on a single datum. Positive (slow) direction is up on all traces.

Horizontal resolution of anomalous bodies is better than vertical resolution because raypaths are within 30 degrees of vertical in the upper crust. Nevertheless, substantial vertical resolution is obtained, as illustrated in Figure 2. For a low-velocity body, for example, the peak in relative residuals occurs at different parts of the array for different ray azimuths and for different distances to the events (different incidence angles). This peak in relative residuals moves farther if the body is deeper.

Results

The Medicine Lake volcano in central northern California, 40 km east of Mt. Shasta, is a broad shield volcano with numerous flow and cone features. It exhibits basaltic, andesitic, dacitic, and rhyolitic volcanism of Pliocene through Holocene age (Anderson, 1941). It is underlain by a shallow high-density, high-velocity body previously observed with gravity and seismic refraction technique (C. Finn, personal communication, 1982; J. Zucca, personal communication, 1982). In order to explore deeper crustal and upper-mantle structure associated with the volcano, a 100 km-long 1-D array was deployed across the area during June and July 1981 (Figure 3). Three-kilometer station spacing in the center of the array was sufficient to resolve features 3 km across or smaller at any depth in the crust; larger station spacing at the ends of the array provide reconnaissance of larger features to a depth of 100 km. The array was oriented northwest to southeast to take advantage of the distribution of teleseismic events and allow inversion of these data for a 2-D section of velocity structure.

Preliminary data from this array are shown in Figure 4 for each of three ray azimuths. Several features are clearly shown:

(1) A large high-velocity feature (negative relative residuals) between distance 35 to 80 km coincides with the topographic expression of the volcano. The minimum residual (distance 60 to 70 km), centered just northwest of the Medicine Lake caldera, moves only slightly with changing ray azimuth and is therefore caused largely by features shallower than about 3 to 6 km.

(2) The region between 40 and 50 km distance is of lower velocity than areas on either side and produces a relatively positive residual. This feature is also independent of azimuth and therefore caused by a shallow body. Coincidentally, it occurs near one of the youngest lava flows on the volcano (J. Donnelly-Nolan, personal communication, 1982) and is the only candidate for a currently hot volcanic source region yet seen with these data.

(3) Although sparse northwest of the volcano, these data com-

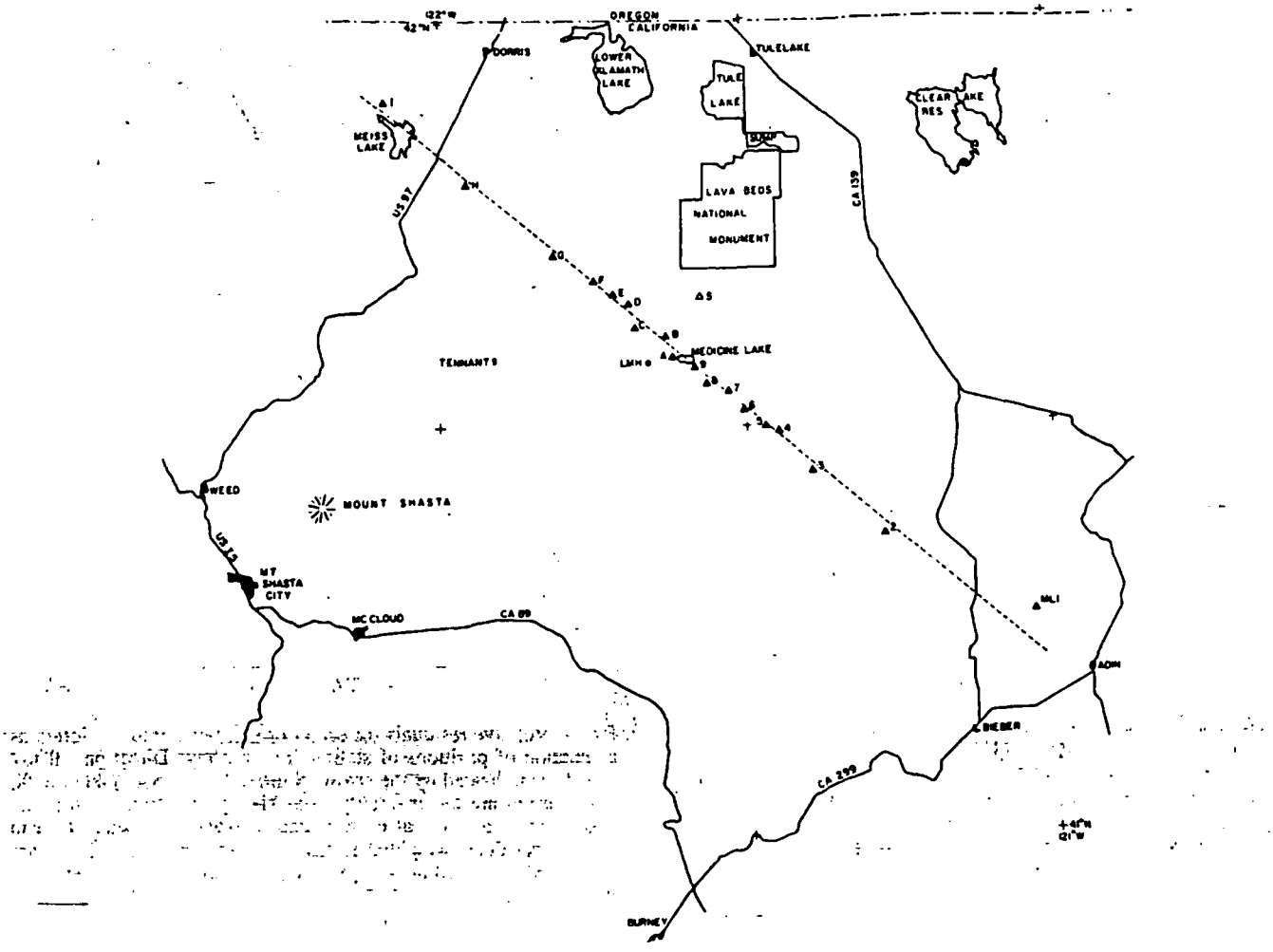

FIG. 3. The 110 km long Medicine Lake array (triangles) showing the array's location relative to towns and other features. Open triangle S is location of smoked paper monitor; dots are stations of permanent network. Station spacing in the center of the array averages 3 km; it strikes northwest to take advantage of the uneven distribution of teleseisms.

bined with data from stations southeast of the volcano suggest that the shallow part of the high-velocity body is confined to the area directly under the volcano.

(4) Relative residual features with large linear dimensions indicate the presence of high-velocity material in the lower crust and upper mantle as well. Events from the southeast (bottom of Figure 4) generate earlier arrivals northwest of the volcano than southeast of it; events from the southwest (center of Figure 4) give about equal relative residuals on both ends of the array; and northwestern events (top of Figure 4) generate larger residuals northwest of the volcano. This "seesaw" pattern suggests a large, high-velocity body extending to depths of at least 100 km.

In most volcanic regions, volumes thought to be composed of melt or partial melt produce low-velocity bodies (e.g., Iyer et al, 1981). With the possible exception of the small shallow feature between 40 and 50 km distance, no such low-velocity volcanic source volume has yet been identified under the Medicine Lake volcano. The ubiquitous high-velocity features may represent melt residuum (in the mantle) and cooled mafic material emplaced into the crust. These results do suggest that any melt or partial-melt pockets that form prior to eruptions must either be very small, very short lived, or both.

Firm results await processing of the rest of the available data and inversion of the final data set; this inversion is expected to reveal any subtle velocity structures not readily visible in the relative residual data. Additional data from other networks in the area will also be inverted with the Medicine Lake volcano data to produce a (less-detailed) 3-D model of the Mt. Shasta-Medicine Lake region.

References

Aki, K., Christoffersson, A., and Husebye, E. S., 1977, Determination of the three-dimensional seismic structure of the lithosphere: J. Geophys. Res., v. 82, p. 277.

Anderson, C. A., 1941, Volcanoes of the Medicine Lake highland: Univ. of Calif. Pub. Bull. Dept. of Geol. Sci., v. 25, p. 347.

Evans, J. R., 1982, Compressional-wave velocity structure of the upper 350 km under the eastern Snake River Plain near Rexburg, Idaho: J. Geophys. Res., (in press).

Herrin, E. (ed.), 1968, 1968 seismological tables for *P* phases: Bulletin SSA, v. 58, p. 1193.

Iyer, H. M., Evans, J. R., Zandt, G., Stewart, R. M., Coakley, J., and Roloff, J., 1981, A deep magma body under the Yellowstone caldera: Delineation using teleseismic *P*-wave residuals and tectonic interpretation: GSA Bull., v. 92, pt. I, p. 792; part II, p. 1471.

Oppenheimer, D. H. and Kerkenhoff, K. E., 1981, Velocity-density properties of the lithosphere from three-dimensional modeling at the Geysers-Clear Lake region, California: J. Geophys. Res., v. 86, p. 6057.

Reasenberg, P., Ellsworth, W., and Walter, A., 1980, Teleseismic evidence for a low-velocity body under the Coso geothermal area: J. Geophys. Res., v. 85, p. 2471.
Stauber, D. A., 1982, Two-dimensional compressional wave velocity structure under San Francisco volcanic field, Arizona, from teleseismic *P* residual measurements: J. Geophys. Res., (in press).
Steeples, D. W., and Iyer, H. M., 1976, Low-velocity zone under Long Valley as determined from teleseismic events: J. Geophys. Res., v. 81, p. 849.

Induced Seismicity at The Geysers, California GE.4

David Oppenheimer and Donna Eberhart-Phillips, U.S.G.S.

A simultaneous inversion for hypocenters, velocity, and station delays was performed from *P*-wave arrival times of microearthquakes and explosions at The Geysers geothermal area in northern California. The resulting 1-D layered model was used to relocate over 5000 earthquakes occurring May 1975 through December 1981. The relocated hypocenters are spatially clustered near production wells in the steam field, not apparent in earlier studies. Following the expansion of power production in 1979-80, new seismic activity is observed near the new, previously aseismic production areas. Statistical correlations of seismicity rate and both steam withdrawal and injection volume rates were calculated. Significant negative correlations were found between steam production and seismicity rate with a one month time lag. Both negative and positive correlations were found for injection volume rate. The most significant correlation coefficient, 0.68, was obtained for seismicity surrounding a well that commenced injection in April 1979. We infer from the spatial and temporal pattern of seismicity that earthquakes at The Geysers are induced by geothermal-production activities, but neither steam production nor fluid injection can directly be shown to be the inducing mechanism.

The Geysers geothermal steam field, located 130 km north-northwest of San Francisco is one of the more seismically active regions in California, with on average 10 microearthquakes $M \geq 0.5$ occurring each day and 8 earthquakes $M \geq 3$ occurring during the past 10 years. Previous studies of the seismicity in the area noted an apparent coincidence between earthquake locations and geothermal steam production sites (Marks, et al, 1978; Ludwin and Bufe, 1980) and suggested that the seismicity may be induced by geothermal steam production activities. However, adequate seismic coverage existed only after 1975, 15 years after active steam withdrawal began, and the preproduction seismicity is unknown. Peppin and Bufe (1980) failed to see a distinction in the seismic source characteristics between "induced" earthquakes at The Geysers and "tectonic" earthquakes occurring outside The Geysers. In this study we pursue the question of induced seismicity at The Geysers by precisely relocating the seismicity at The Geysers and examining the spatial-temporal correlations of the seismicity to the geothermal production activities.

Relocations

To precisely relocate microearthquakes in the study area, an improved velocity model was determined from simultaneous inversion of *P*-wave arrival times from local microearthquakes and explosions following Crosson (1976). The model consists of six constant velocity layers with velocity increasing with depth from 4.4 km/sec at the surface to 5.9 km/sec at 8 km depth and delay terms for each station. The model reduces the variance of travel-time residuals by approximately 70 percent in comparison to that of locations obtained from previous velocity models. Comparison of computed locations of explosions with their known coordinates indicates mislocation biases less than 0.3 km using this model.

Figure 1 shows the relocated seismicity for $M \geq 1.2$ occurring at The Geysers during 1976 and 1981. In 1976 the areas about power units 13, 14, and 15 were essentially aseismic. In 1979 and 1980 steam production began near these units, and within 6 months after production commenced microseismicity appeared near these units. By contrast, the seismicity near unit 12 which also began production in 1979 did not increase. Since unit 12 is located in a region of the steam field with production dating to 1972, the lack of new seismicity may indicate that this area has already adjusted to previous steam withdrawal.

Seismicity at The Geysers does not generally exceed 6 km depth (Figure 1). This unusually shallow range of earthquake depths may reflect elevated temperatures at depth, such that deformation occurs aseismically. Alternatively, if the seismicity is induced by production activities, then this depth may indicate the maximum depth of influence of production. Projections of surface locations of the steam and fluid injection wells to their reported total depths show a marked correspondence between hypocenters and well location. Equally significant is the absence of seismicity observed in areas of no production. Most events occur in clusters with horizontal and vertical dimensions of 0.5 and 1.0 km, at corresponding depths of well penetration (0.5-3.0 km), except for one cluster at a depth of 3.0-5.0 km beneath units 7 and 8, which is deeper than the total depths of all wells.

Correlations

To quantify the apparent correspondence between microseismicity and geothermal production, statistical correlations (C) were calculated between the monthly number of earthquakes and fluid injection and steam production volume (State of California, Division of Oil and Gas open-file information). Injection volume correlations with microseismicity located within a 1 km radius of 8 injection wells are significant ($-.037 \leq C \leq 0.68$) at 5 of the 8 wells. The largest correlation (0.68) occurs for a well which began injection in 1979. From the change in sign of C we conclude that either the correlation results are spurious or indicate that the microseismicity is not simply dependent on fluid injection volume. In fact, the seismicity about all injection wells has increased with time, while the monthly variability of injection volume explains the difference in sign of correlation.

Similar analyses were performed using the monthly volume of steam withdrawn from 80 percent of the wells about units 1-10, the oldest steam-producing region of The Geysers. Significant negative correlations occur only for one month time lag of seismicity following steam withdrawal. The negative correlations reflect the steady increase in seismicity in contrast to the overall decline in volume of steam withdrawn due to the corresponding decline in steam pressure (Lipman et al, 1978). The negative correlations also conflict with the observation that seismicity commences in new production areas (Figure 1). A more reasonable interpretation is that the seismic response to variations in steam withdrawal in these areas of long-standing production can no longer be recognized.

Conclusions

We infer from the spatial and temporal pattern of seismicity that earthquakes are induced by geothermal production activities at The Geysers. However, the mechanism responsible for inducing seismicity is not clear. Thermal contraction of the reservoir rock due to steam withdrawal or fluid injection may be a factor (Denlinger, 1980), but we observe little positive correlation between the volume of cold water injected or steam withdrawn and the number of earthquakes per month. Similarly, seismicity resulting from a vol-

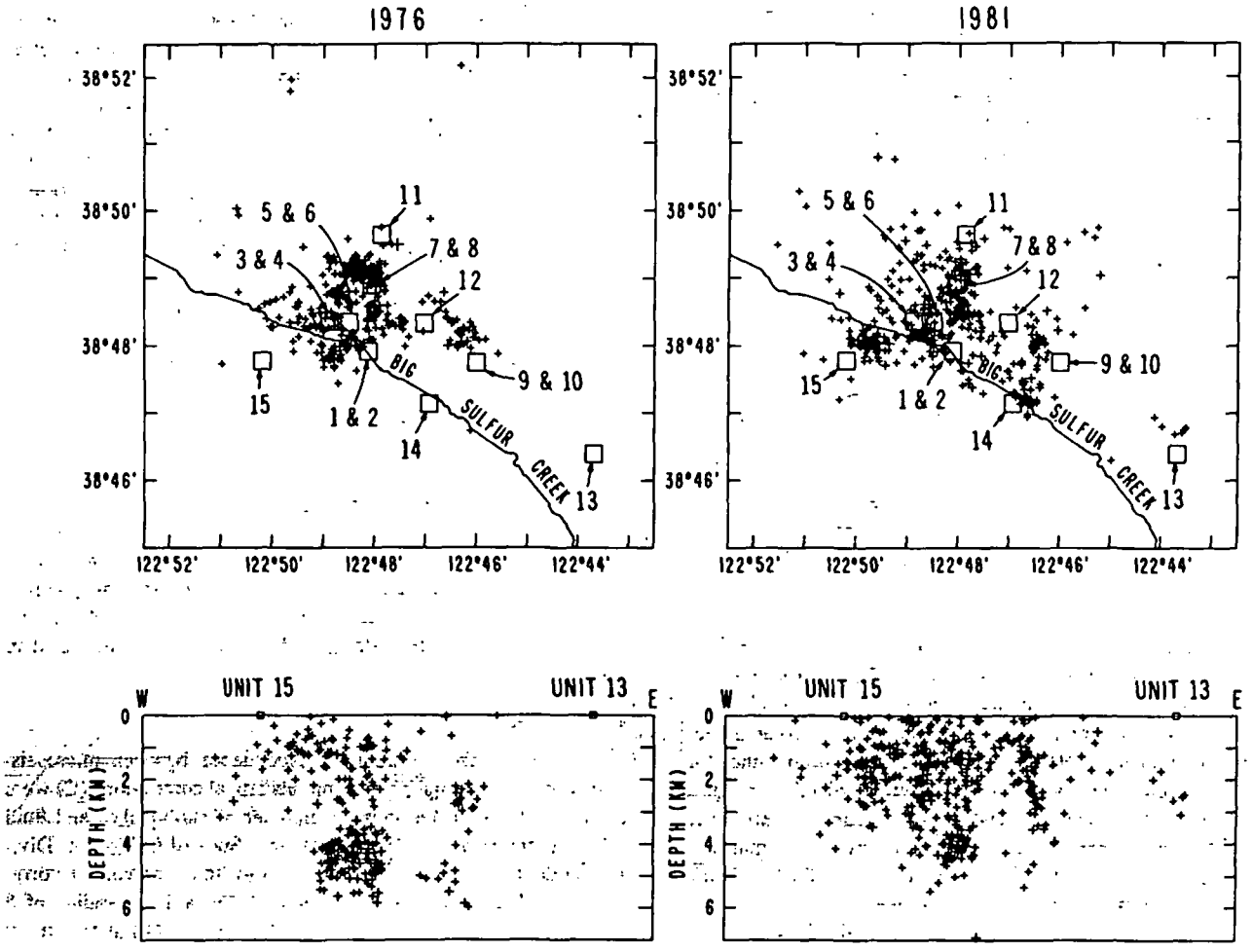

FIG. 1. Comparison of all $M \geq 1.2$ earthquakes at The Geysers in 1976 and 1981. Power units are indicated by boxes. Cross-sections are projections of all seismicity onto east-west plane.

umetric change associated with steam withdrawal (Majer and McEvilly, 1979) is not directly observable in the data. Alternatively, Allis (1981) proposed hardening of the reservoir rock due to pore pressure decline or increase in the coefficient of friction, thereby favoring unstable sliding to deformation by creep. The present data are insufficient to distinguish between these hypotheses, but do clearly demonstrate that the seismicity at The Geysers is induced by production-related activities.

References

Allis, R. G., 1981, Comparison of mechanisms proposed for induced seismicity of The Geysers geothermal field: Proc. 1981 New Zealand geother. workshop, p. 57-61.

Bufe, C. G., Marks, S. M., Lester, F. W., Ludwin, R. S., and Stickney, M. C., 1981, Seismicity of The Geysers-Clear Lake region: U.S.G.S. prof. paper 1141, p. 129-137.

Crosson, R. S., 1976, Crustal structure modeling of earthquake data 1. Simultaneous least squares estimation of hypocenter and velocity parameters: J. Geophys. Res., v. 81, p. 3036-3046.

Denlinger, R. P., and Bufe, C. G., 1980, Seismicity induced by steam production at The Geysers steam field in northern California: Trans. AGU, v. 61, p. 1051.

Lipman, S.C., Strobel, C. J., and Gulati, M. S., 1978, Reservoir performance of The Geysers field: Geothermics, v. 7, p. 209-212.

Ludwin, R. S., and Bufe, C. G., 1980 Continued seismic monitoring of The Geysers, California geothermal area: U.S.G.S. open-file rep. 80-1060.

Majer, E. L., and McEvilly, T. V., 1979, Seismological investigations at The Geysers geothermal field: Geophysics, v. 44, p. 246-269.

Marks, S. M., Ludwin, R. S., Louie, K. B., and Bufe, C. G., 1978, Seismic monitoring at The Geysers geothermal field: U.S.G.S. open-file rep. 78-798.

Peppin, W. A., and Bufe, C. G., 1980, Induced (?) versus natural earthquakes: search for a seismic discuminant: Bull. SSA, v. 70, p. 269-281.

Detection of Geothermal Microtremors Using Seismic Arrays GE.5

Alfred Liaw and Wayne Suyenaga, Arco Oil and Gas

Two passive seismic studies were conducted in the Basin and Range province of the western United States, using state-of-the-art multichannel seismic array data acquisition and frequency-wavenumber processing techniques. The purpose of our studies is to investigate the correlation between low frequency microtremor activity and existing geothermal reservoirs. A 256-element modified eight-arm geophone array, with 1823 ft diameter, was deployed to monitor microtremors in the vicinity of Roosevelt Hot Springs, Utah. Coherent 2Hz microtremors were detected intermittently in four of the six recording sites; however, directions of

microtremor propagation did not indicate the existing production reservoir system to be the common source. The microtremor data in Beowawe geothermal area, Nevada, were acquired by a 120-element 2000 ft diameter cross array located to the west of the geyser. Low frequency (2 to 10 Hz) microtremors clearly appear on every record. These microtremor activities are associated with the geothermal system at depth, as indicated by seismic body wave components propagating with extremely high apparent velocities.

Microtremor, or seismic noise generated by a geothermal reservoir, has been considered a direct indicator in geothermal exploration. But in spite of a number of studies on this topic, the subject is still controversial. It is clear that a prime assumption has yet to be proved: that geothermal reservoirs produce a detectable seismic signal. Physical mechanisms that might produce seismic noise include pressure variations, with or without changes of state, and microcracking. These mechanisms seem plausible but will remain pure speculation until there is an unambiguous recording of microtremors originating from a geothermal reservoir. Experiments designed to detect microtremors with geophone array and frequency-wavenumber (*f-k*) processing have been conducted in several geothermal areas in the western U.S. Not all studies were successful in correlating microtremor with a geothermal reservoir, however. In this paper we present results of the use of state-of-the-art data acquisition capabilities, with the potential of using several hundred data channels, and *f-k* processing techniques to correlate microtremor activities in two known geothermal areas, Roosevelt Hot Springs, Utah and Beowawe, Nevada.

Roosevelt hot springs area

The geothermal field at Roosevelt Hot Springs is delineated by production tests which agree with geophysical and geochemical data. The top of the geothermal reservoir ranges between 3000 to

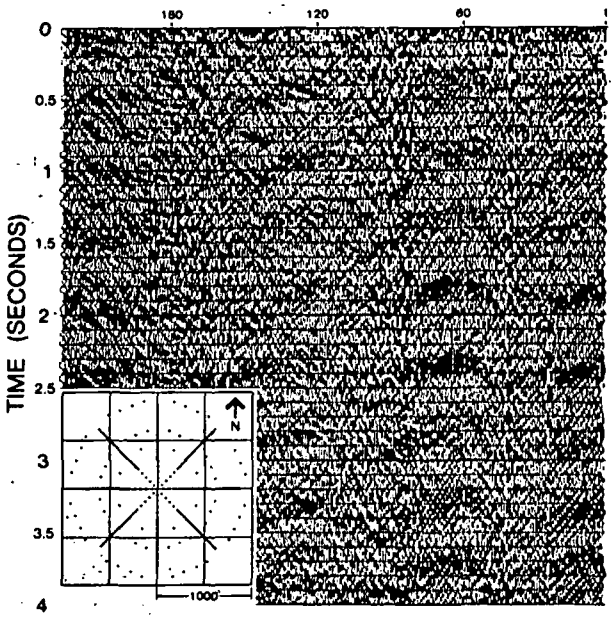

FIG. 2. Sample record of microtremor showing 2 Hz component and the geometry of seismic array.

5000 ft deep. Figure 1 shows approximate limits of the Roosevelt field as defined by well tests; also shown are six sites selected for the microtremor field tests. Two sites are directly over the reservoir, three are just outside the boundaries of the field, and the last site is about 7 miles south-southwest of the producing field. The microtremor field test took place while the field was shut down during January and February 1980. A 256-element, modified,

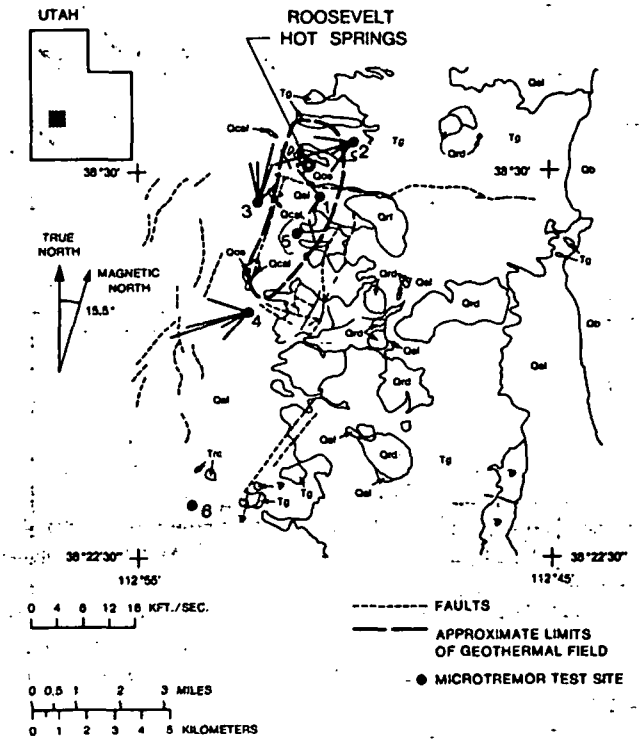

FIG. 1. Geologic map of Roosevelt Hot Springs geothermal area, depicting locations of seismic array as well as azimuths and apparent velocities of 2 Hz microtremor wave field. Lines radiating from sites have length proportional to velocity.

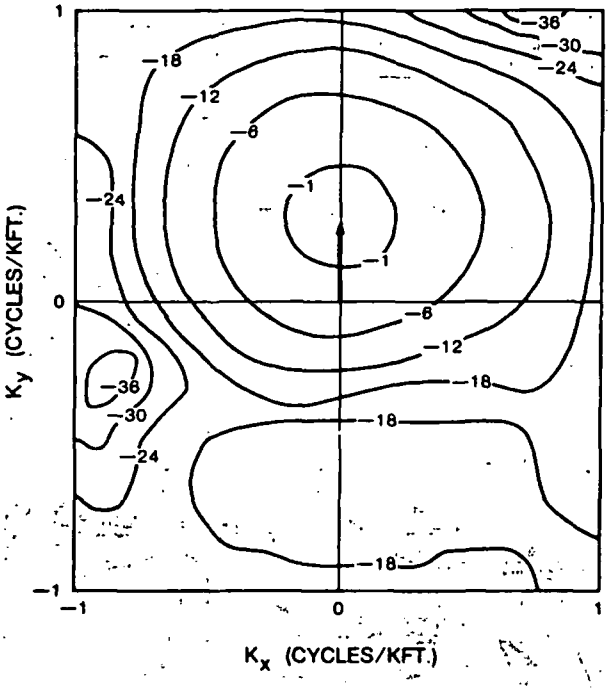

FIG. 3. 2-D wavenumber power spectral density contour plot at 2 Hz for microtremors recorded at Roosevelt Site no. 3. Arrow points toward source of wavefront.

eight-arm array (Figure 2), with 1823 ft diameter, was deployed at each recording site. Data were recorded by a GUS-BUS system during the early morning when wind noise was generally at a minimum.

After editing, array data were transformed to the frequency-wavenumber domain. The apparent velocity and azimuthal angle of the propagating wave fields were determined according to the peak of the power spectral contours on the two-dimensional wavenumber domain for the dominant frequency component. The dominant frequencies of the seismic noise field recorded in the Roosevelt area are at 15, 40, and 78 Hz. The *f-k* analysis indicates coherence is significant but apparent velocities are low, implying surface waves. The 2 Hz coherent microtremors were observed sporadically at sites 1, 2, 3, and 4. Figure 2 is a sample record from site 3, showing coherent 2 Hz microtremor. For site 3, the azimuth ranged from 350 to 53 degrees, and apparent velocities ranged from 5590 to 6910 ft/sec. Figure 3 shows one of the power spectral contours plotted in terms of wavenumbers for the 2 Hz component. Similar observations were made at other sites: the 2 Hz component came in a duration of several minutes sporadically during the recording period but, with one exception, at consistent wavenumber and azimuth. However, the 2 Hz signal was not observed at all of the sites, and at those that it was, the incoming azimuth did not indicate a common source. On Figure 1, we see that at site 1, the 2 Hz component came in at widely varying azimuths. At site 5, which was located directly over the geothermal field, no significant 2 Hz was recorded.

Beowawe geothermal area

The Beowawe geothermal area is located within the Battle Mountain heat flow high in north-central Nevada. The geothermal system consists of a shallow aquifer at about 1000 ft depth which directly feeds the geysers and hot springs there. The shallow hydrothermal system is connected by faults to a reservoir at several thousand feet depth. The deep reservoir is probably in fractured Paleozoic carbonates, with heat supplied by the enhanced subcrustal heat flow.

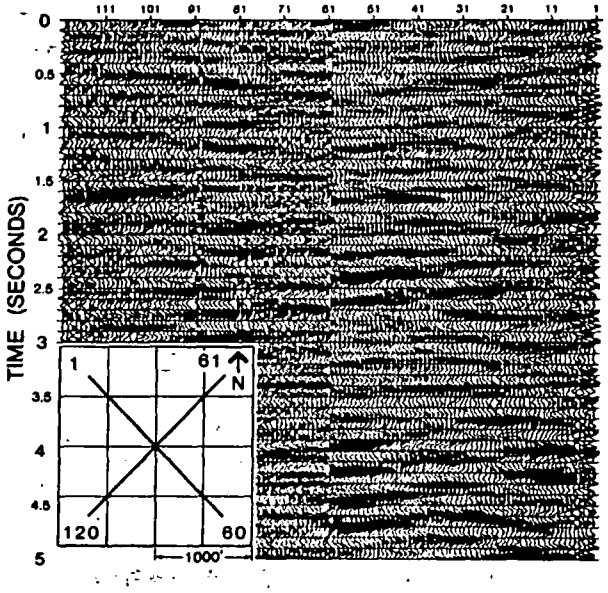

FIG. 5. Sample record of microtremor showing low frequency components and the geometry of seismic array.

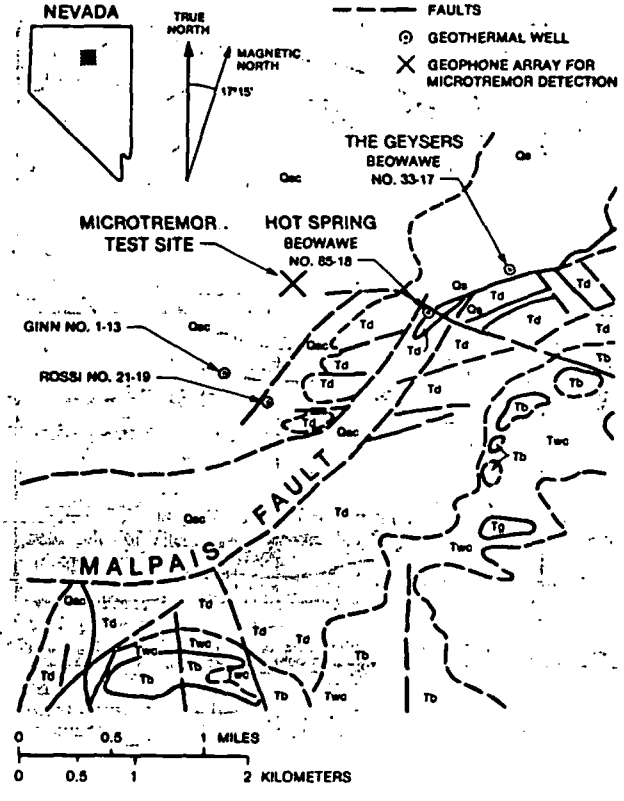

FIG. 4. Geologic map of Beowawe geothermal area, showing location of microtremor test sites.

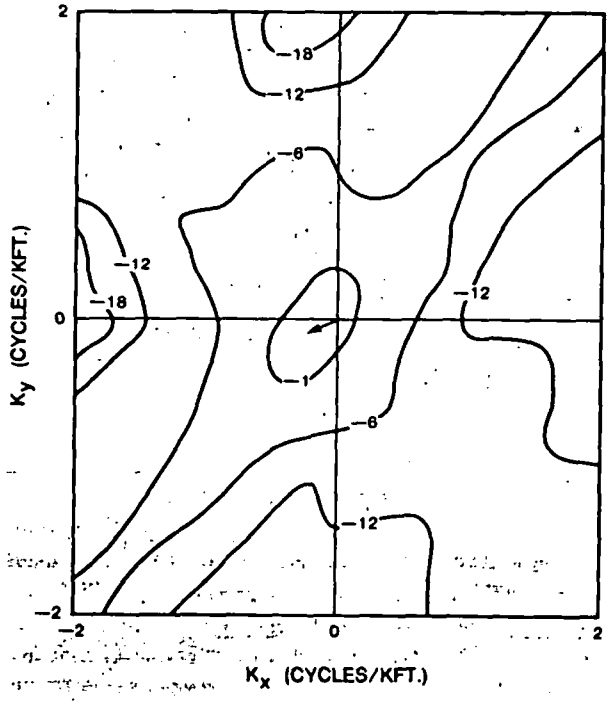

FIG. 6. 2-D wavenumber power spectral density contour plot at 4 Hz for microtremors recorded at Beowawe test site. Arrow points toward source of wavefront.

The microtremor experiment was conducted by Chevron Resources Co. in August 1978, at a site about a half mile northeast of exploration well Ginn 1-13, (Figure 4). The test site was occupied by a 120-element cross array, with 2000 ft diameter (Figure 5). Data were recorded with a 120-channel DFS V system.

The microtremors at the Beowawe test site are consistently dominated by 2 to 10 Hz coherent seismic noise (Figure 5). The results of *f-k* analyis reveal that the predominant coherent microtremors propagate through the test site with azimuths ranging from 225 and 333 degrees. The apparent velocities of 2, 3, and 4 Hz components range from 10,000 to 20,000 ft/sec across the geophone array. On the other hand, the 10 Hz components propagate with apparent velocities from 15,000 to 69,000 ft/sec. Figure 6 shows a typical contour plot of two-dimensional wavenumber power spectral density for a 4 Hz microtremor coming from 245 degree azimuth with 17,600 ft/sec velocity. Azimuthal angles for incoming microtremors do not correlate with any surface geothermal manifestation. The extremely high apparent velocity indicates that the detected microtremors are largely body wave components emanating from the buried sources.

Conclusions

The sources of the intermittent 2 Hz component microtremor in the Roosevelt area are not clear. One thing is definite: it does not originate from the existing geothermal system. The *f-k* analysis with array used in this study should have been sufficient to detect body waves emanating from the geothermal reservoir. We conclude that the geothermal reservoir at Roosevelt either (a) does not produce any microtremor event, or (b) it produces one that is too small to be detected by the *f-k* method. The low frequency microtremors detected in Beowawe geothermal area do not correlate with surface manifestation. The high apparent velocity body wave components imply that those microtremors are emanating from the buried sources at depth.

Acknowledgments

The authors acknowledge with thanks, permission of the management of Arco Oil and Gas Co., Arco Exploration Co. and Chevron Resources Co. to publish this paper.

Deep Electromagnetic Sounding In Central Nevada GE.6

M. Wilt, N. E. Goldstein, J. R. Haught, and H. F. Morrison, Lawrence Berkeley Lab

Sixteen shallow and deep controlled source electromagnetic soundings were performed in Buena Vista Valley, near Winnemucca, Nevada, to investigate an intrabasement conductor previously detected with magnetotellurics. The survey was carried out with the LBL EM-60 system using a remote magnetic reference for low-frequency geomagnetic noise cancellation, 100 m and 2.8 km diameter transmitter loops, and a minicomputer for in-field processing. EM soundings were made at distances from 0.5 to 30 km from three loops over the frequency range 0.02 to 500 Hz. Data were interpreted by means of 1-D inversions and the resulting layered models were pieced together to yield an approximate 2-D geoelectric model along the north-south axis of the valley. The EM soundings and one MT sounding show a 3 to 7 Ω-m zone at a depth of 4 to 7 km. The conductor appears to be deepest at the northern end of the valley and shallowest beneath a basement ridge that seems to divide Buena Vista Valley into two basinal structures. Similar intrabasement conductors are also reported 50-75 miles south in the Carson Sink-Fallon areas, suggesting a common source, probably related to an anomalously hot, thin crust.

During the Spring of 1981 a deep electromagnetic sounding survey was undertaken by Lawrence Berkeley Laboratory (LBL) in Buena Vista Valley, Nevada to confirm the presence of a relatively shallow intrabasement conductor, first detected with magnetotelluric measurements, and to delineate the conductor by means of the LBL controlled-source system, modified for deep sounding work. Shallow crustal conductors have been reported at various places within the Basin and Range province and they are presumed related to the heat source that causes numerous hot springs, high regional heat flow, and widespread epithermal gold and mercury mineralization.

Sixteen controlled-source electromagnetic soundings and one magnetotelluric sounding were made in Buena Vista Valley, Pershing County, Nevada (Figure 1). The EM soundings were made relative to three loop sources with source-receiver separations ranging from 0.5 to 30 km. Two of the loops were four-turns and 100 m in diameter, similar to those we used previously for investigations to depths of about 2 km. The other was a 6.25 km^2, single-turn large-moment source capable of providing signal for deeper exploration. This large-diameter source had a moment of 2 $\times 10^8$ mks, approximately 80 times greater than the smaller loops.

Features of the system, shown schematically in Figure 2, include an 8-channel multiplexer, a 2-channel digital oscilloscope for digitization, storage and display, and an HP 9835 minicomputer for data processing. Phase reference between loop current and observed magnetic fields was maintained by means of oven-controlled quartz clocks.

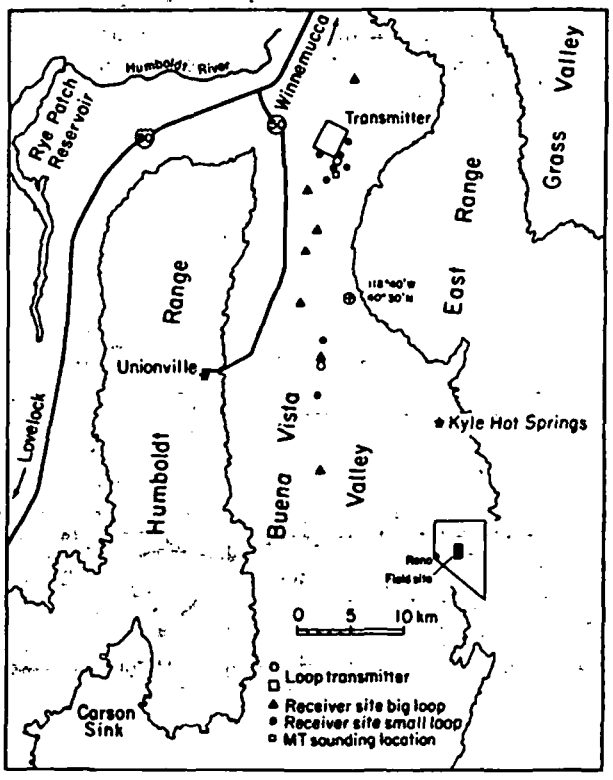

Fig. 1. Location map of the deep electromagnetic soundings, Buena Vista Valley, Pershing County, Nevada.

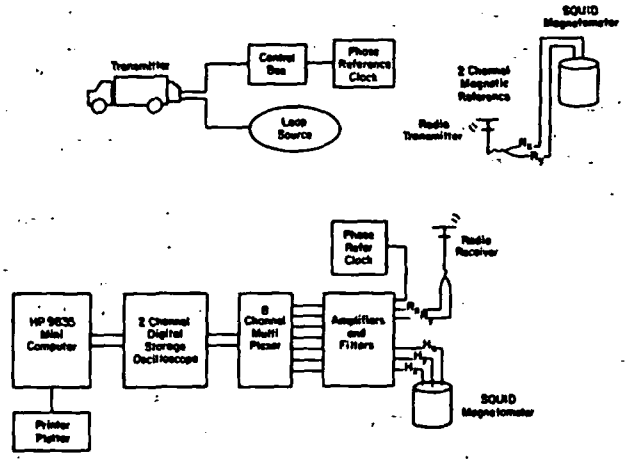

FIG. 2. Schematic diagram of the EM-60 controlled-source EM system.

A remote reference magnetometer, shown in the upper right corner of Figure 2, was used for noise cancellation during both the MT and controlled-source EM surveys. The MT noise cancellation technique was described by Gamble et al (1979). In the controlled-source work, a distant reference magnetometer provides signals to buck-out the natural geomagnetic variations at the receiver station. Our experience shows that a simple procedure of analog scalar subtraction performed with the transmitter off will reduce the geomagnetic "noise" by about 20 dB, thereby extending the useful frequency range down to ~0.02 Hz. The more elegant noise cancellation technique based on finding the tensor coefficients did not work as well because of the large amount of time needed to obtain the coefficients, and the instability of the coefficients over longer time intervals.

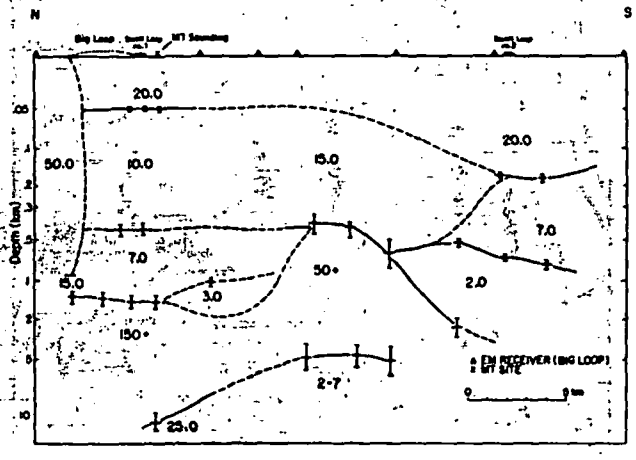

FIG. 3. Geoelectric cross-section showing interpreted resistivities along the axis of Buena Vista Valley, Pershing County, Nevada. Error bars are the standard error for the layer thickness.

Results

We performed 1-D inversions on all 16 EM soundings and the one MT sounding. The data for most stations fitted well to 1-D models, and these layered models were reasonably consistent from station to station (Figure 3).

The low resistivity (10-20 Ω-m) of the upper km presents some problems for deep electromagnetic sounding. Although signals could be received at up to 30 km from the source, the higher frequencies were severely attenuated by the conductive surface layer, making it impossible for us to get useable data above about 5 Hz when source-receiver separations exceeded 15 km. The low resistivity surface also limited penetration of EM waves, thus making low frequency data collection mandatory. Without noise cancellation, collection at low frequency data would have been very difficult.

Figure 3 is a composite of 1-D interpretations along a north-south line paralleling the valley. According to our convention, the layered-model interpretation is plotted at a point midway between the transmitter and the receiver. The resistivity cross-section reveals that the shallow portion of the crust beneath Buena Vista Valley can be approximated by 4 or 5 layers. The parameters of the top layer are resistivity of 20 Ω-m and a thickness of between 50 and 200 m. These parameters seem to be fairly consistent at most locations in the valley. This layer most likely represents partially saturated Quaternary alluvium. The second layer is some 200 to 500 m thick and approximately 10 Ω-m in resistivity. This unit is thickest in the northern and southern parts of the valley and may be absent in the center of the valley; it likely represents saturated Tertiary sediments and volcanics. Deeper parts of the section indicate conductive sediments overlying resistive basement. Basement depth ranges from 0.5 to 2.5 km with a basement high which suggests that the valley may be subdivided structurally into two basins, a northern one 1 to 1.5 km deep and a southern one 2 to 2.5 km deep. The resistivity of the basement is poorly resolved with EM and MT soundings because it carries relatively little current and therefore does not contribute greatly to the received signals.

Evidence for a conductor within the basement was found on three EM soundings and the MT sounding. For the EM soundings, a good electrical conductor (3 to 7 Ω-m) was indicated 4 to 7 km beneath the central portion of the valley. The MT sounding indicated a good conductor (approximately 25 Ω-m) 11 km in depth beneath the northern end of the valley. Fifty to 75 miles to the south in the Carson Sink, experiments by Keller et al (1981) and by the U.S.G.S. (Stanley et al, 1976) have indicated conductors at about 5 km in depth. It is tempting, therefore, to speculate on whether the conductors are related geologically, constituting a regional feature. On the basis of geothermal evidence, Stanley et al (1979) proposed that the conductor is caused by Tertiary and pre-Tertiary marine sediments saturated with water at 150° C or greater and with salinities of about 20,000 ppm. The widespread occurrence of the conductor seems to confirm that a broad area of the shallow crust is anomalously hot.

Although there are other surveys supporting the intrabasement conductor, our subsurface electrical model is only preliminary. The irregular valley shape, variable basement depth, and the anomalously small radial fields and large tangential fields observed suggest 3-D complexities. 2-D modeling suggests that the depth to the conductor may be underestimated in the 1-D inversions.

Acknowledgment

The work was supported by the Director, Office of Energy

Research, Office of Basic Energy Sciences, Division of Engineering, Mathematics and Geosciences of the U.S. Department of Energy under Contract DE-AC03-76SF00098.

References

Keller, G. V., Taylor, K., and Souto, J. M., 1981, Megasource EM method for detection of deeply buried conductive zones in geothermal exploration (Abst): Geophysics, v. 47, p. 420.

Stanley, W. D., Wahl, R. R., and Rosenbaum, J. G., 1976, A magnetotelluric study of the Stillwater-Soda Lakes, Nevada geothermal area: U.S.G.S. open-file rep. 76-80, 38 p.

Gamble, T. D., Goubau, W.. M., and Clarke, J. 1979, Magnetotellurics with a remote reference: Geophysics, v. 44, p. 53-68.

Depth to Curie Isotherm In Arizona by Magnetic Anomaly Inversion GE.7

M. R. Hong, C. L. V. Aiken, Univ. of Texas at Dallas; and W. J. Peeples, Univ. of Texas at El Paso

Modeling sources of magnetic anomalies as variable magnetic layers with lateral susceptibility changes allow the depth to the Curie isotherm to be interpreted. If the Curie temperature isotherm depths are mapped, information as to the present thermal condition of the crust is obtained. A Backus-Gilbert method is used to solve for the lower boundary of 2-D bodies (models) which cause magnetic anomalies and to assess vertical accuracy (variance) and lateral resolution (spread). The lower boundary can be considered a continuous function. A depth to Curie isotherm map of Arizona is obtained from analysis of the state aeromagnetic map. Results are compared to other Curie depth studies as well as available geologic and geophysical data. The results agree in general with Curie depth investigations which employed spectral matching, but not with other types of magnetic anomaly analyses. Shallow depths (5–9 km below sea level) are indicated along the transition between the Colorado plateau and the Basin and Range provinces, in the White Mountains in east-central Arizona, in southwest Arizona, and in the Tucson area of southeast Arizona. Curie depths in central and south-central Arizona are 20 km below sea level which is unexpectedly deep for the Basin and Range. The results can be an aid in determining geothermal potential of the area when used in an integrated analysis.

Estimates of the thickness of the magnetized portion of the earth's crust suggest that magnetization boundaries can correspond to changes in composition within the crust or higher temperatures at depth which cause the rocks to lose their magnetism (the depth to Curie isotherm). It may be possible to locate a point on the isothermal surface by determining the depth at which the rock is no longer magnetic. If a sufficient number of Curie depths are obtained in an area, an isothermal surface at the Curie temperature would be defined and temperatures at other depths could be determined.

The general linear geophysical problem relates observation data with the unknown function and its defining kernels through an integral transform equation. A solution is estimated by the method suggested by Backus and Gilbert (1970). The quality of the solution can be expressed by the trade-off of spread versus variance and the average solution for the model. This approach is used for inversion of magnetic anomalies, being applied directly to the observed magnetic data with no manipulation of the data, such as reduction-to-pole processing. A known variable upper boundary of the magnetic body can be used to take into account magnetic terrain effects and different magnetic survey parameters. Lateral susceptibility contrast variations can be incorporated so that adjacent body interference can be considered.

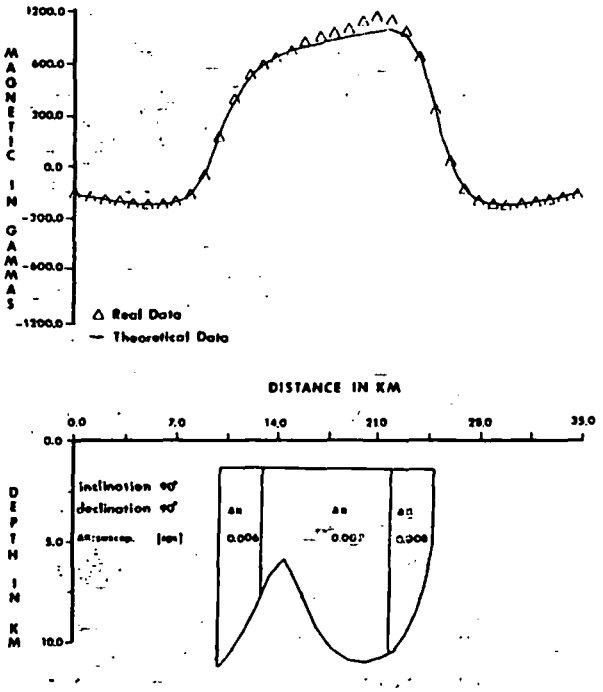

FIG. 1. Inversion of magnetic anomaly of synthetic model with incorrect assumption.

Synthetic data were calculated for models and then inverted to determine the lower boundary solution. In Figure 1, boundaries and values of the lateral susceptibility contrasts were incorrectly placed. The fit between synthetic noise-free data and computed magnetic effects is considered insufficient. A change of susceptibility contrasts and block widths is considered necessary by the radical thinning of the lower boundary.

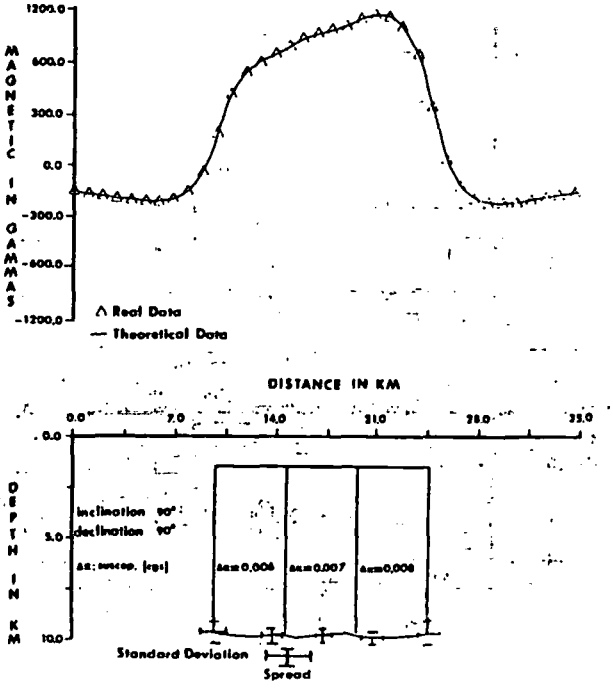

FIG. 2. Inversion of magnetic anomaly of synthetic model with correct assumption

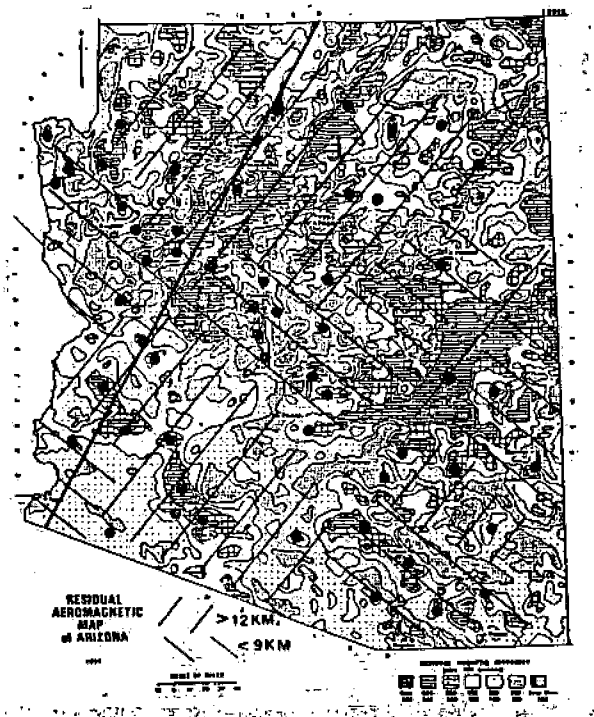

FIG. 3. The distribution of Curie isotherm depths determined from Backus-Gilbert inversion.

A good fit occurs with correct susceptibility describing the structure (Figure 2). The solution has a standard deviation of less than 0.3 km. Only when all the free parameters were correctly supplied can the Backus-Gilbert method converge closely to the solution.

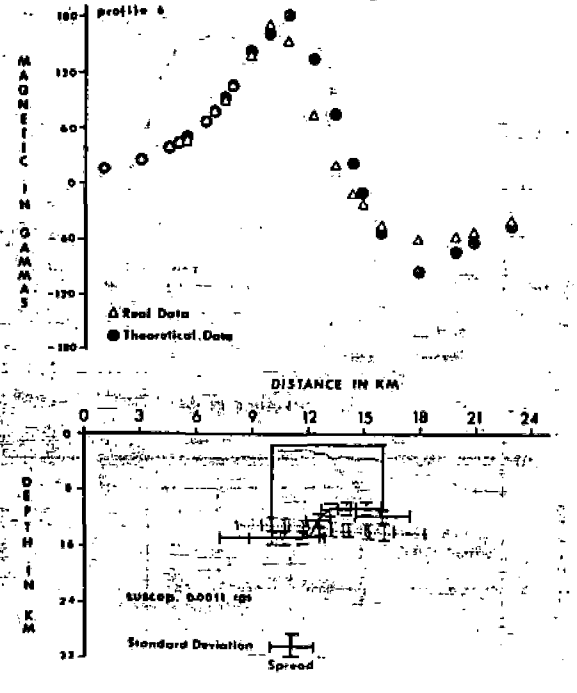

FIG. 4. Inversion for Curie depth estimation south of Tucson, Arizona. Theoretical (computed) data shown only for flat top assumption.

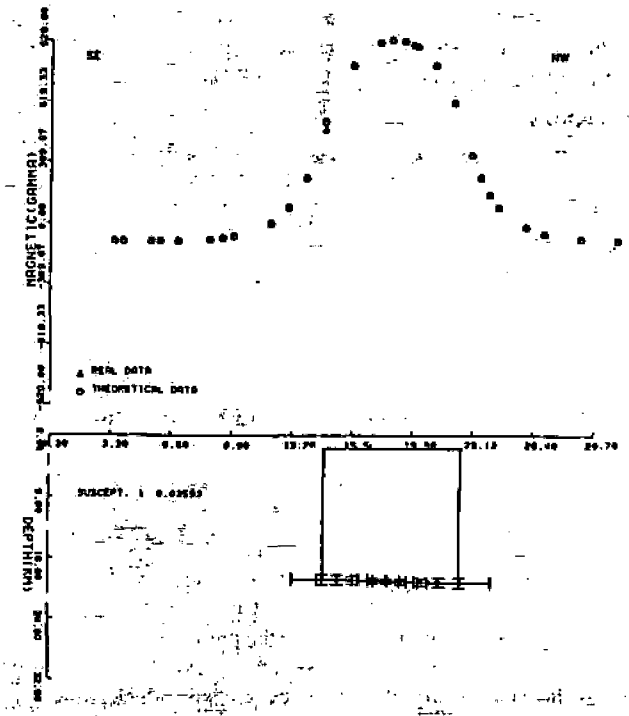

FIG. 5. Inversion for Curie depth estimation in Colorado Plateau near Juniper Mountains east of Kingman, Arizona.

Magnetic data over Arizona are available from a regional magnetic survey (Sauck and Sumner, 1970). These magnetic anomalies were studied previously for Curie depth by the method of spectral matching (Byerly and Stolt, 1977), anomaly amplitudes (Sauck, 1972), and spectral analysis (Shuey et al, 1973). Constraints on the upper boundaries of the sources of magnetic anomalies are taken from geologic maps, depths to bedrock maps, drill hole information, and geophysical interpretations. The deepest part of the resultant model from inversion is then chosen as a point estimate for the depth to the Curie isotherm within a vertical accuracy determined by statistics. A total of 58 profiles over the state

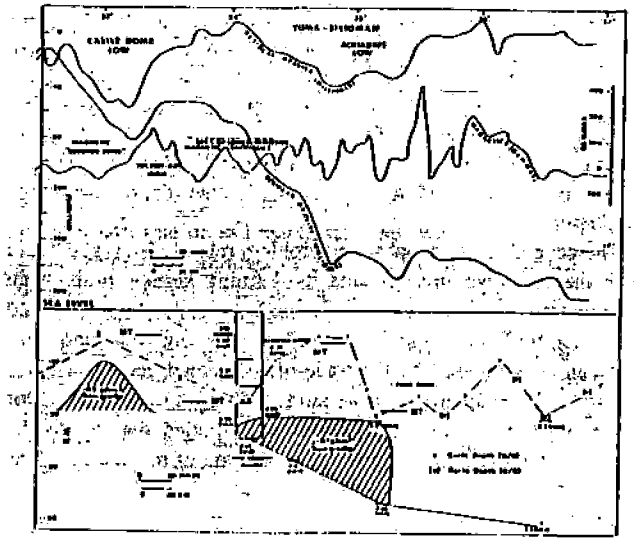

FIG. 6. A regional profile study from combined geophysical information

have been inverted to date, and areas of deep and shallow Curie depths have been defined (Figure 3). The Curie map in this study covers a larger area than the Byerly and Stolt (1977) map, extending into the southern part of the state. This new map shows more variations than the Byerly and Stolt (1977) map, but their region of shallow Curie depth in central Arizona does correspond well with this new map.

A profile located near the Sierrita Mountains to the south of Tucson in the Basin and Range province was inverted, and a solution was first obtained assuming that the model had a flat upper boundary (Figure 4). The result is an abruptly irregular lower boundary, and computed values do not fit the observations very closely. The upper boundary of this magnetic block was then determined by geophysical analysis and drill hole control (see dotted upper boundary). The final depth to Curie isotherm solution is similar (dotted lower boundary), about 12 km below sea level, but the lower boundary is remarkably flat and the fit to the observed anomaly is significantly better, within less than one gamma.

Figure 5 shows a typical anomaly in the Colorado plateau near the Juniper Mountains. The source apparently is an intrusive body below a relatively flat crystalline basement. The depth to the Curie temperature is defined with a flat surface. Also note the extremely large effective susceptibility, 0.0059 cgs, indicating a very mafic rock type.

A profile extending from southwest Arizona northeastward to Utah is shown in Figure 6. In a gravity analysis of Arizona, two prominent residual gravity lows occur: (1) in northwest Arizona, the Aquarius area, and (2) in southwest Arizona, the Castle Dome area (Aiken and Ander, 1981). These have been interpreted as possibly related to high temperatures, but the sources of the anomalies are modeled as low-density lower crust. These two gravity lows agree in general with the location of the shallow Curie depths on the new map. The shallow Curie depth in the southwest correlates with the so-called subdued zone thought to be related to shallow Curie depths (Sauck, 1972). The other supposed subdued zone (near 34°N. latitude) thought by some to be related to a shallow isotherm does not correlate with an interpreted shallow Curie depth or gravity lows. These lower magnetic anomaly amplitudes reflect a lithologic change in the crust, not significantly higher crustal temperatures. Other seismic information between the Castle Dome and Aquarius areas indicate an anomalously low *P*-wave velocity of 7.65 km/sec, possibly related to melt conditions (Sinno et al, 1980). Heat flow maps from Shearer (1980) and others show the relatively lower heat flow of the inner Colorado plateau and higher heat flow of the Basin and Range province, but the data coverage is sparse and uncorrected. The combined geophysical information seems to indicate the possibility of shallow geothermal resources at both the Castle Dome and Aquarius areas, but the shallow depth at the north end near the Grand Canyon in the Colorado plateau could be related to a lithologic lower boundary. Whether the magnetic layer is defined lithologically or thermally is dependent on an integrated analysis.

References

Aiken, C. L. V., and Ander, M. E., 1981, A regional strategy for exploration with emphasis on gravity and magnetotellurics: J. Volcano. Geoth. Res., v. 8.

Byerly, P. E., and Stolt, R. H., 1977, An attempt to define the Curie isotherm in northern and central Arizona: Geophysics, v. 42, p. 1394-1400.

Lysonski, J., Sumner, J. S., Aiken, C. L. V., and Schmidt, J. S., 1980, Complete residual Bouguer gravity map of Arizona: Bur. Geol. and Min. Tech., Tucson.

Sauck, W. A., and Sumner, J. S., 1970, Residual aeromagnetic map of Arizona: Univ. of Arizona, Tucson.

Sauck, W. A., 1972, Compilation and preliminary interpretation of Arizona aeromagnetic map: Unpublished doctoral dissertation, Univ. of Arizona, Tucson.

Shearer, C., 1980, A regional terrestrial heat flow study in Arizona: Unpublished doctoral dissertation, New Mexico Institute of Mining and Technology, Socorro.

Sinno, Y. A., Keller, G. R., and Sbar, M. L., 1981, A crustal seismic refraction study in west central Arizona: J. Geophys. Res., v. 86, p. 5023-5038.

Shuey, R. T., Schellinger, D. K., Johnson, E. H., and Alley, L. B., 1973, Aeromagnetics and the transition between the Colorado Plateau and Basin and Range provinces: Geology, v. 1, p. 107-110.

Terrane Correction for Terrestrial Heat Flow GE.8

Steven G. Henry, Conoco Inc.; and Henry N. Pollack, Univ. of Michigan

We present a method of estimating true regional heat flow in the presence of perturbing topography, variable surface temperatures, and subsurface thermal conductivity contrasts. The method involves the solution of the steady-state three-dimensional heat conduction equation by finite difference numerical techniques. The topography is represented by an irregular upper boundary and the variable surface temperature as a boundary condition along the irregular upper surface. Internal structural configurations and conductivity contrasts are easily accommodated. The principal variable input into the system is the basal unperturbed heat flow. The best value of heat flow is obtained by minimizing, in a least-squares sense, differences between observed and calculated temperatures. Temperature observations commonly are distributed throughout the near-surface (perturbed) environment, in multiple boreholes, tunnels, and/or mine galleries. The method is particularly suited to the simultaneous analysis of an ensemble of distributed observations, in contrast to other methods that focus on perturbation to the temperature gradient in the vicinity of a single borehole. We have used the method to reduce data obtained at 15 newly established heat flow sites in the Bolivian and Peruvian Andes. We illustrate the application of the method to observations made in the Bolivar mine in Bolivia. Temperature measurements there were obtained in two vertical and two inclined boreholes drilled from within the underground mine. The observations were distributed horizontally over 1200 m and vertically from 100 to 650 m beneath the topographic surface.

We present here the results of an investigation into a method of terrane correction which models the subsurface temperature distribution and provides an estimate of the reliability of the heat flow determined by the method. The necessity of terrane corrections to measured temperature gradients in regions of topographically perturbed heat flow has long been recognized as a problem in geothermal investigations. A recent treatment of the terrane correction by Blackwell et. al (1980) provides references to all the major investigations of the topographic disturbance to the near surface temperature distribution. The early methods of terrane correction involved an approximation of the actual topography with a geometric form for which an exact solution to the heat conduction equation could be determined. Birch (1950) developed an improved method which allowed for a numerical representation of the topography. His method involves defining a reference plane on which the temperature varies in proportion to the overlying topography. Recent methods of calculating terrane corrections utilize modern computational power and are able to calculate the entire subsurface temperature field. The method of Blackwell et al, for example, represents the local topography and surface temperature distribution by Fourier series, and via potential theory solves for

temperatures in the subsurface. The method which we present is similar to that of Blackwell et al, except that the heat conduction equation is solved by finite difference numerical techniques under more general conditions.

In order to deal with terrane corrections numerically, sufficient information must be collected from the field area of the heat flow sites. Data which enter into terrane calculations are the topographic configuration, the temperature distribution over the surface, and the distribution of thermal conductivity. A model is constructed by partitioning the region surrounding the site with a 2-D or 3-D rectangular grid. The local topography may be approximated by a series of steps up or down in the grid. The temperatures on this irregular surface then define an upper boundary condition to which the subsurface temperature distribution most come into equilibrium. The subsurface temperature distribution is determined by the heat flow which enters the region from below (an experimental input variable), the distribution of thermal conductivities, and the surface temperature boundary condition. Subsurface temperatures are calculated iteratively, and as the iterations proceed, the effect of the surface boundary condition relaxes into the subsurface until an equilibrium temperature distribution is achieved.

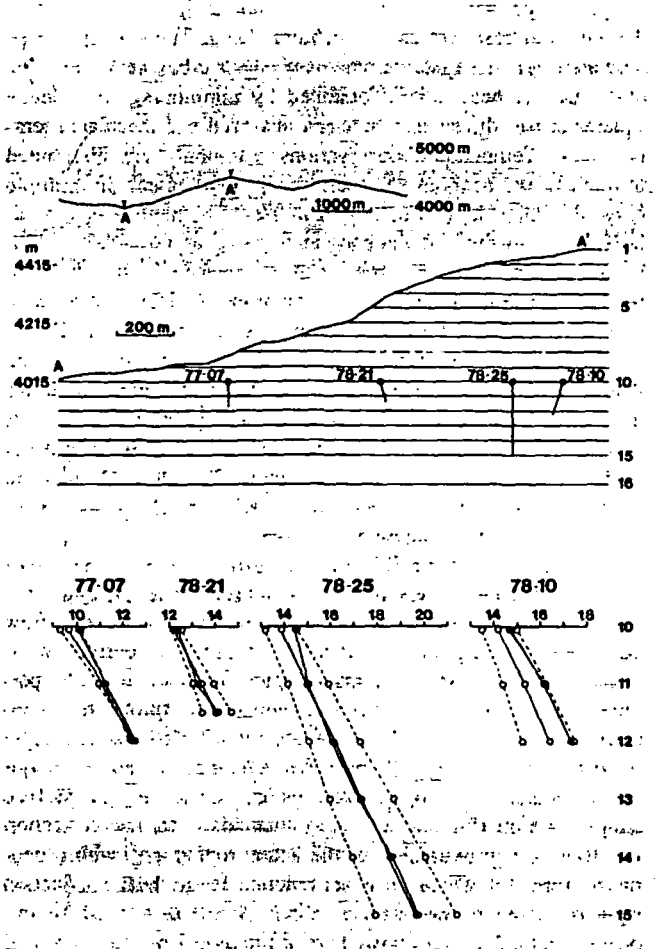

FIG. 1. Above, Cross-section through the Bolivar mine, Bolivia. Regional cross-section is shown above mine cross-section. Mine section shows location of boreholes as solid heavy lines. Elevations on left are in meters with no vertical exaggeration; grid element numbers are on right. Below, open circles are calculated temperatures, solid circles are observed temperatures. For each borehole, dashed line to left is for basal heat flow of 100 mW m^{-2}, dashed line to right is for 150 mW m^{-2}, solid line is a close fit of 125 mW m^{-2}.

Computing the differences between observed and calculated temperatures and minimizing these differences in a least-squares sense allows for establishment of the basal heat flow which best satisfies the observed temperatures. The ability to match closely the calculated temperature field to measured temperatures is primarily a function of the quality and distribution of the field observations.

The following illustrative example is from one of 15 newly established heat flow sites in the Bolivian and Peruvian Andes (Henry, 1981). All of these sites required terrane corrections, and most required 3-D models. The Bolivar mine in Bolivia, however, is adequately represented with a 2-D model due to the structurally controlled topography which follows the long axial anticlines and synclines in folded Devonian shales. The topographic profile and measured temperature-depth plots are shown in Figure 1. Effects of varying the basal heat flow are illustrated by the temperatures shown with open circles. However, to determine precisely the best fitting value of basal heat flow, it is necessary to calculate the mean-squared differences of the observed and computed temperatures. The mean difference between the 15 observed and the corresponding computed temperatures for basal heat flows of 100 and 150 mW m^{-2} are approximately 1.6°C, whereas for 125 mW m^{-2}, the mean difference is about 0.5°C. The computed best fit was 128 mW m^{-2}, with about 0.3°C mean deviation, indicating the sensitivity of the method. If the observed temperatures are of moderate to poor reliability, then a larger range of basal heat flow will yield calculated temperature distribution which match the observations roughly equally, resulting in a broad minimum of differences. We estimate the quality of a heat flow site on the basis of the range of basal heat flow which results in a doubling of the minimum mean deviation. Determination of the quality of the site allows for better evaluation and can provide the necessary basis for the elimination of sites with possible disturbed or unreliable temperature measurements.

The modeling procedure presented here has proven useful in interpreting subsurface temperature distributions in regions which require terrane corrections. The best fitting basal heat flows determined by terrane modeling in a number of different areas revealed that the regional variability of heat flow in the Andes was much less than uncorrected heat flow estimates had suggested.

References

Birch, F., 1950, Flow of heat in the Front range: GSA Bull., v. 61, p. 567-630.

Blackwell, D. D., Steel, J. L., and Brott, C. A., 1980, The terrain effect on terrestrial heat flow: J. Geophys. Res., v. 85, p. 4757-4772.

Henry, S. G., 1981, Terrestrial heat flow overlying the Andean subduction zone: Ph.D. dissertation, Univ. of Michigan, Ann Arbor.

GEOPHYSICS, VOL. 48, NO. 5 (MAY 1983); P. 618-626, 11 FIGS.

Thermal hydrology and heat flow of Beowawe geothermal area, Nevada

Christian Smith*

ABSTRACT

Inflections in temperature-depth profiles from forty 150 m thermal gradient holes define a shallow thermal flow system in the Whirlwind Valley near the Beowawe Geysers. U.S. Geological Survey hydrologic data reveal the vertical and west-to-east components of cold water flow at the water table above the thermal flow system. The temperature inflections break most abruptly in areas with a downward component of flow at the water table. The inflections are thought to indicate the level where the buoyant thermal water maintains a dynamic equilibrium with the overlying cold water. Combining these geophysical and hydrologic data suggests areas away from The Geysers where thermal water may rise from the deep reservoir into the alluvium. These leakage areas may be viable geothermal exploration targets. Even if the temperatures of the leakage were subeconomic, knowledge of where upwelling occurs could be helpful in assessing the potential for energy production. The systematic acquisition of hydrologic data is recommended as a standard component of hydrothermal resource exploration programs.

Measurements of thermal conductivity from chip samples from the shallow holes and from Chevron Resources Company's Ginn 1-13 geothermal exploration hole (2917 m T.D.) enable inferences based on heat flow. The average heat flow east of the Dunphy Pass fault zone, 110 mW/m^2, may be representative of background in this portion of the Battle Mountain high heat flow province. Thermal gradient and conductivity data from the deep well have a wide range of values (65–144°C/km, 1.59–5.95 $Wm^{-1}K^{-1}$) but produce a relatively constant heat flow of 235 mW/m^2 above a depth of 1600 m. The shallow data indicate that the area with similarly high surficial heat flow extends as far east as the Dunphy Pass fault zone, suggesting that this Miocene rift boundary may form the eastern margin of the Beowawe hydrothermal system.

INTRODUCTION

The geysering action of vandalized wells drilled in the late 1950s for geothermal exploration at Beowawe, Nevada, may have been the most spectacular hydrothermal phenomenon created artificially in the United States. The location of the blowing wells, known as The Geysers, is shown in Figure 1. They were spudded in a 1 km long opaline sinter terrace on the south flank of the Whirlwind Valley in Eureka and Lander Counties, Nevada, approximately 50 km east of the town of Battle Mountain. At this time (spring 1981), The Geysers play intermittently.

Struhsacker (1980) gave the most thorough description of the stratigraphic and structural framework of the Beowawe area. Other recent geologic summaries were given in Zoback (1979) and Garside and Schilling (1979). As shown in Figure 1, The Geysers lie along the Malpais fault zone at the base of the Malpais Rim. The steep fault-scarp slope faces north-northwest towards the Whirlwind Valley. Tertiary lava flows and tuffaceous sediments crop out on the Malpais dip slope. The Malpais scarp exposes an older normal fault system, the Dunphy Pass fault zone, that has a northwest trend. This Oligocene to Miocene fault zone forms the eastern margin of a major northwest-trending graben that is part of the southern extension of a 750 km long linear aeromagnetic and structural feature called the Oregon-Nevada lineament (Stewart et al, 1975).

The Tertiary volcanic section within the graben is approximately 1400 m thick; east of the Dunphy Pass fault zone, it is only 100 m thick. The detailed volcanic stratigraphy of Struhsacker (1980) is included in Figure 2. The underlying Ordovician Valmy formation is a shattered sequence of siliceous eugeosynclinal sediments that are part of the Roberts Mountains thrust sheet. Carbonaceous siltstone, chert, and quartzite of the Valmy formation crop out along the Malpais east of the Dunphy Pass fault zone and are encountered by the deep geothermal test wells in the Whirlwind Valley. Tertiary diabase dikes that intrude both the Valmy and the volcanic rocks are thought to be the source for the pronounced aeromagnetic anomaly associated with the Oregon-Nevada Lineament and

Presented at the 50th Annual International SEG Meeting, November 18, 1980, in Houston. Manuscript received by the Editor April 29, 1981; revised manuscript received June 24, 1982.
*Formerly Earth Science Laboratory, University of Utah Research Institute, Salt Lake City; presently Chevron Resources Co., P.O. Box 7147, San Francisco, CA 94107-7147.

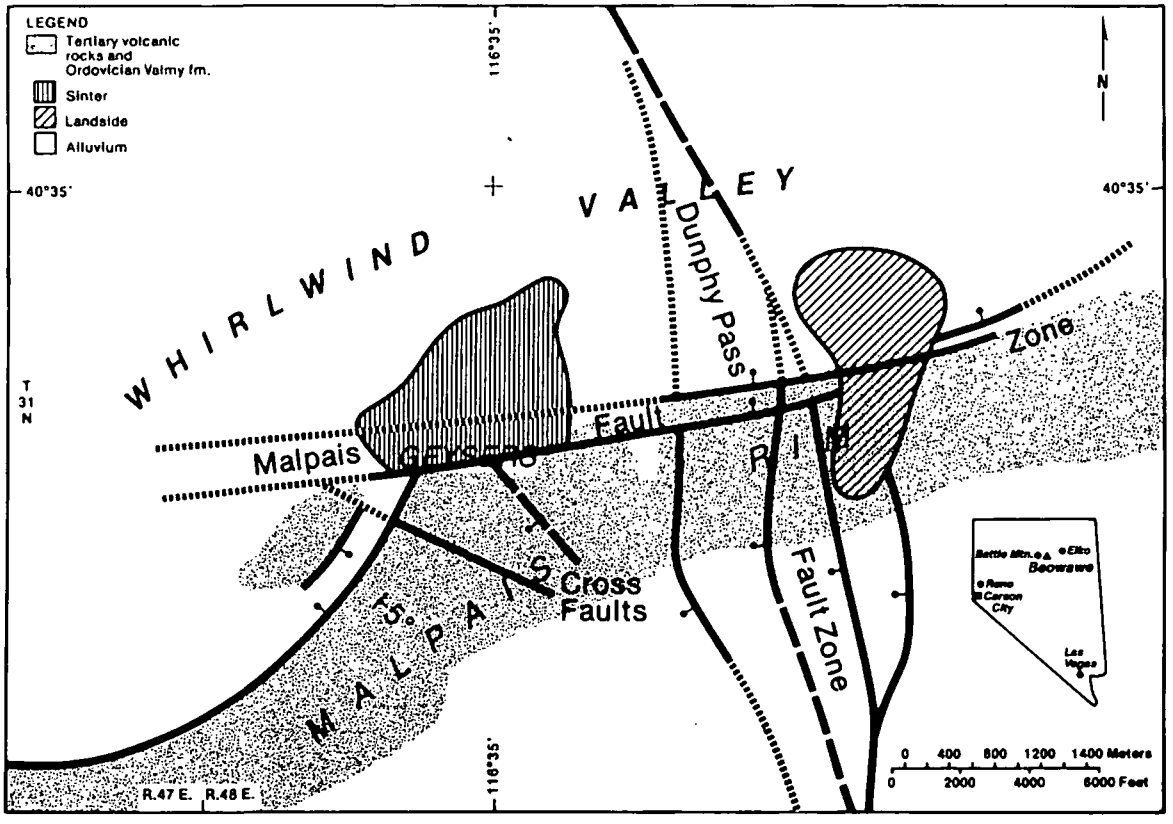

FIG. 1. Location and generalized structure of the Beowawe area (after Struhsacker, 1980).

the feeders for the Tertiary volcanic sequence filling the graben (Robinson, 1970).

In the 1970s, exploration for a hydrothermal resource capable of sustaining electrical power generation was conducted by Chevron Resources Co. and Getty Oil Co. Much of their geophysical data has been acquired and made available through the Dept. of Energy, Division of Geothermal Energy Industry Coupled Program (Chevron Resources Co., 1979; Getty Oil Co., 1981). Included in these data packages are the temperature-depth profiles and drill-chip cuttings from the forty 150 m thermal gradient holes shown in Figure 3. The temperature-depth profiles provide a three-dimensional (3-D) view of the coupled heat and water flow in the shallow subsurface. Mapping these flows can contribute to the exploration effort by locating upflow zones or widespread horizons with enhanced permeability.

THERMAL HYDROLOGY

The geothermal industry has generally neglected to include groundwater studies in their exploration programs even though water is the resource being sought. The typical program has looked at water only with an eye to its chemistry. Geothermal exploration geophysicists can remedy this omission by including piezometers in their shallow drilling plans.

A piezometer is a small-diameter pipe open to a waterbearing formation at one depth only, generally at the bottom, as schematically shown in Figure 4. The annulus between the drilled hole and the pipe or casing is usually grouted to ensure that there can be no vertical fluid flow within the hole. The elevation at which water stands in the piezometer indicates the total hydraulic head at the point of measurement. The hydraulic head H is the sum of two components, the pressure head $P/\rho g$ and the elevation head z:

$$H = z + \frac{P}{\rho g}, \tag{1}$$

where z is the elevation above an arbitrary datum (usually sea level), P is the fluid pressure, ρ the fluid density at ambient temperature, and g the acceleration due to gravity.

Under nonisothermal conditions, observed head values are corrected for density differences. In most groundwater studies these differences are small enough to be neglected. At geothermal areas with cold water aquifers, the less dense thermal water generally plumes upward to float on the colder water or emerge as hot springs. Where the thermal water is not sufficiently hot and buoyant, the weight of the overlying cold water may hold it down. The result can be a temperature inversion within the aquifer.

Water flows from areas of higher hydraulic head to areas of lower hydraulic head. Figure 4 is a sketch of the relation given

MAP CODE		LITHOLOGIC UNIT	THERMAL CONDUCTIVITY Mean ± Std. Dev. ($W \cdot m^{-1} K^{-1}$)	NUMBER SAMPLES
Qs		Opaline Sinter	——	——
Qls		Landslide	——	——
Qal		Alluvium	1.68 ± 0.11	8
Tv	Tg	Coarse Gravel	1.60	1
	Tb	Basalt	1.60	2
	Twc	Tuffaceous Sediment of White Canyon		
		glassy	1.33 ± 0.12	3
		silty	1.65 ± 0.08	9
	Td	Dacite		
		porphyritic	2.02 ± 0.13	9
		vitrophyric	1.20	2
		argillized	1.67 ± 0.22	4
	Tba	Basaltic Andesite	2.26 ± 0.06	5
	Tts	Early tuffaceous material	1.58 ± 0.01	4
	Tha	Hornblende Andesite	1.90 ± 0.17	5
	Ti	Diabase dikes	2.09 ± 0.17	3
Ov		Valmy Formation	4.44 ± 1.01	6

FIG. 2. Stratigraphy of Beowawe area with measured thermal conductivity values.

by equation (1). The elevations of standing water (corrected for temperature where necessary) in a number of piezometers completed in the same horizon and distributed over an area, as in Figures 5a and 5b, are used to produce maps of hydraulic head. The differences in water levels seen in plan view can be used to compute the horizontal component of hydraulic gradient and, in isotropic media, the direction of water flow.

A cross-section of hydraulic heads can be generated if water levels are measured in adjacent piezometers completed at different depths, illustrated by Figures 5c and 5d. The difference in elevation of standing water in adjacent piezometers can be used to compute the vertical hydraulic gradient. Since elevation is positive upward, a negative vertical hydraulic gradient implies that there is a downward component of groundwater flow at that location. A positive value is computed wherever water rises from depth.

In areas where water flow affects heat flow, hydraulic head data should be able to delineate zones of upwelling hot water. Since hot water is the hydrothermal resource, water levels and vertical hydraulic gradient data should be gathered as part of any geothermal exploration program. Data from Beowawe demonstrate the utility of incorporating groundwater hydrology into thermal gradient surveys.

BEOWAWE GROUNDWATER

The U.S. Geological Survey, Water Resources Division, has drilled piezometers at several northern Nevada geothermal areas (e.g., Welch et al, 1981). Their data for the water table in the Whirlwind Valley are shown in Figure 3. The elevation of the water table appears to decrease systematically down the valley from west to east, reflecting the topography. It is within a few meters of the surface in the center of the valley. Much of the groundwater in the valley is presumably discharged by evapotranspiration at a playa lake beyond the eastern edge of Figure 3. Some may reach the Humboldt River farther to the east.

Water levels in the paired piezometers allow the computation of the vertical hydraulic gradient. Near The Geysers the vertical gradients are negative; water at the water table flows downward as well as toward the center of the valley. The

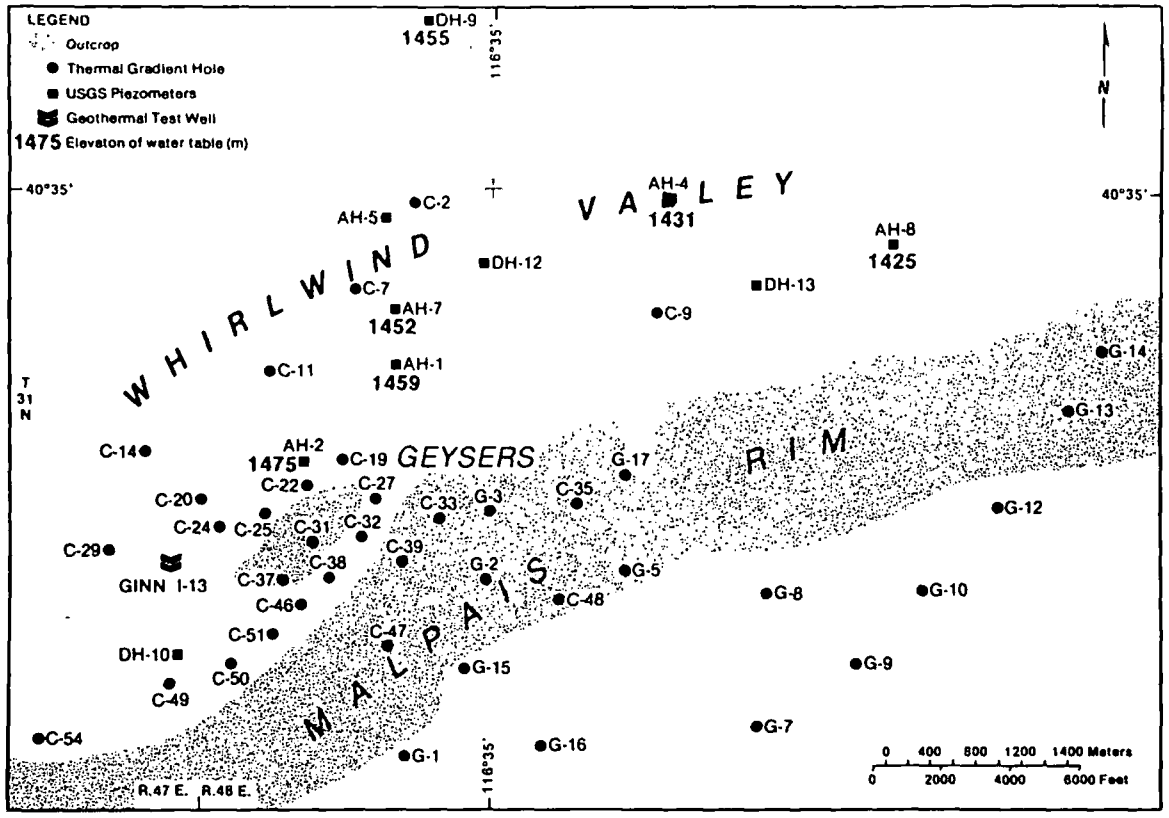

FIG. 3. Map of Beowawe area showing thermal gradient holes, piezometers, and elevation of water table.

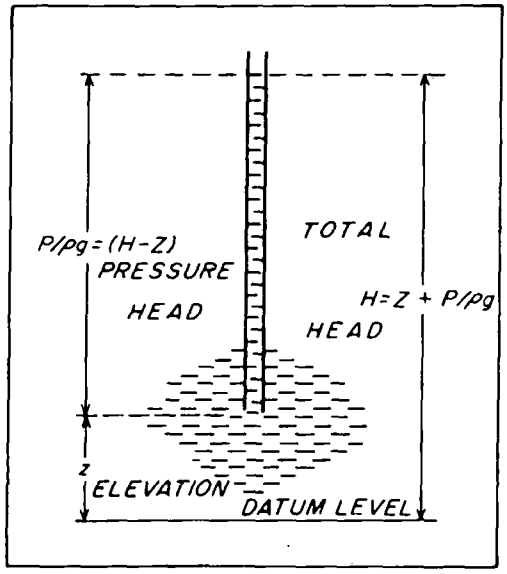

FIG. 4. Relation between total head, pressure head, and elevation (after Hubbert, 1940).

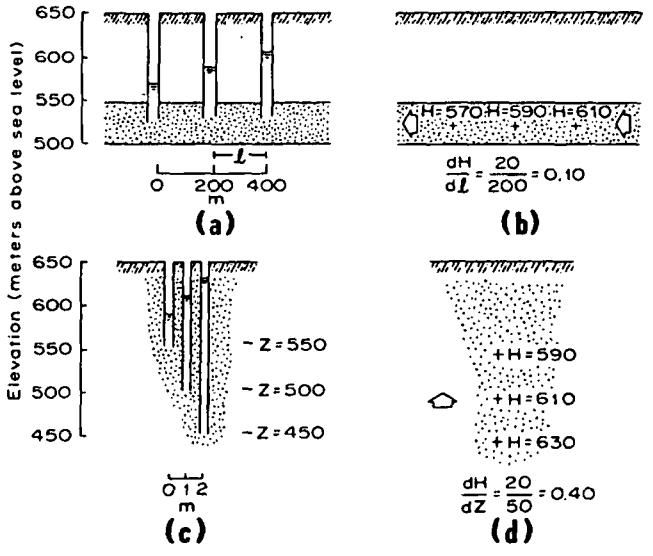

FIG. 5. Theoretical cross-section showing piezometers, head distribution, flow pattern, and hydraulic gradients (after Freeze and Cherry, 1979).

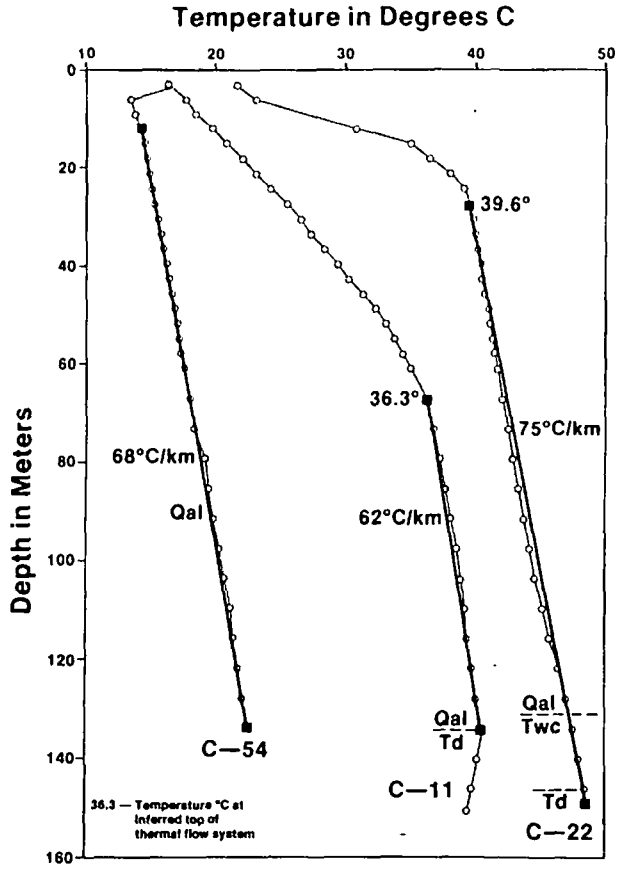

FIG. 6. Temperature-depth profiles with similar thermal gradients, Whirlwind Valley, with inferred depths to top of thermal flow system. Lithologic symbols given in Figure 2.

vertical gradient is positive in the piezometer pairs in the center of the valley. In this area, water flows upward as well as eastward, perhaps responding to evaporation at the water table.

The vertical flow measured in the shallow piezometers is indicated at greater depths by curvature and inflections in temperature-depth profiles. Figure 6 presents examples. Hole C-22 is near piezometer pair AH-2 which has a strong negative gradient; its temperature profile is concave upward, reflecting the downward flow of water (Sorey, 1971). Upward fluid flow is shown by the concave downward profile of hole C-11 near the center of the valley.

The 68°C/km gradient in hole C-54 is similar to those in holes C-11 and C-22, but its linearity for the length of the hole and low temperature are unlike the other profiles in Figure 6. The temperature-depth profile in hole C-54 is one of the few in the Whirlwind Valley that shows little disturbance by groundwater flow and may be representative of regional conductive heat flow. If 68°C/km were a background gradient in alluvium, the regional conductive heat flow would be approximately 118 mW/m^2. This heat flow is within the range of values given by Sass et al (1971a) for this portion of the Basin and Range province, allowing hole C-54 to serve as the reference for an arbitrary definition of *cold* and *thermal* for the Beowawe area: water less than 7°C above the temperature in C-54 at the same

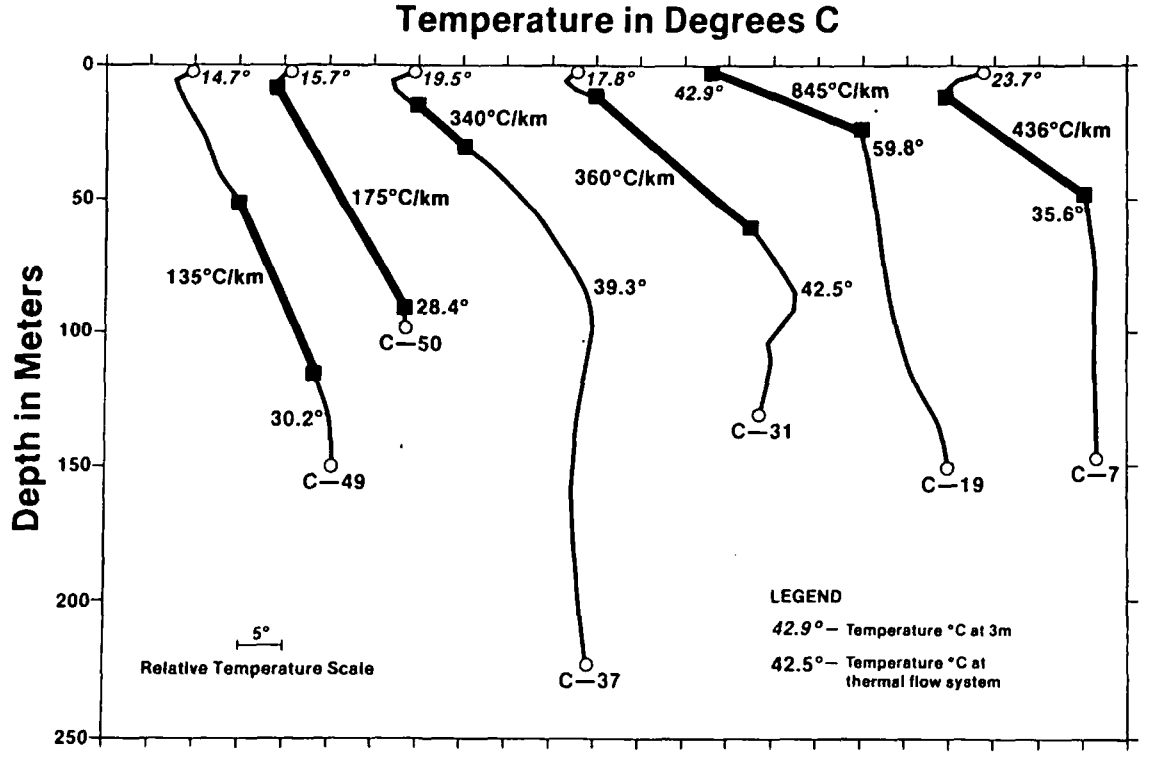

FIG. 7. Representative temperature-depth profiles in Whirlwind Valley.

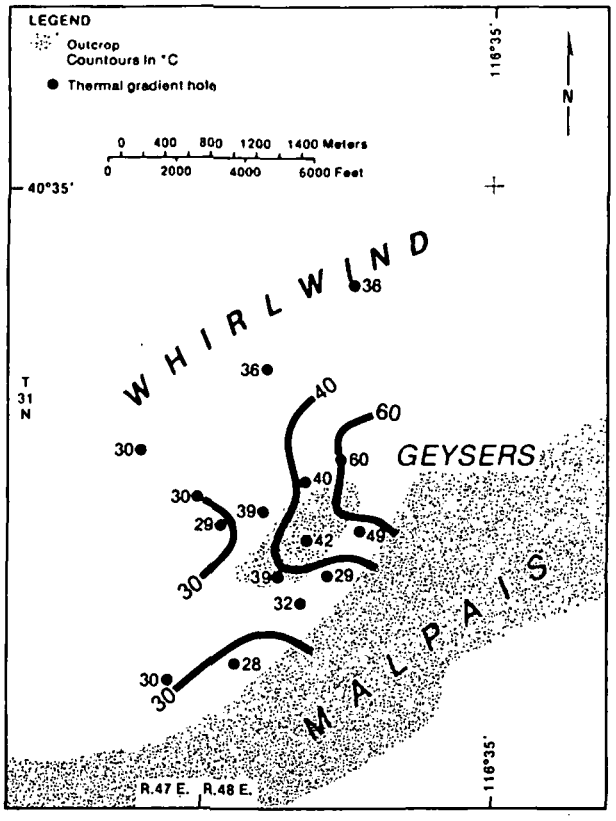

FIG. 8. Map of temperature at top of thermal flow system, contours in °C.

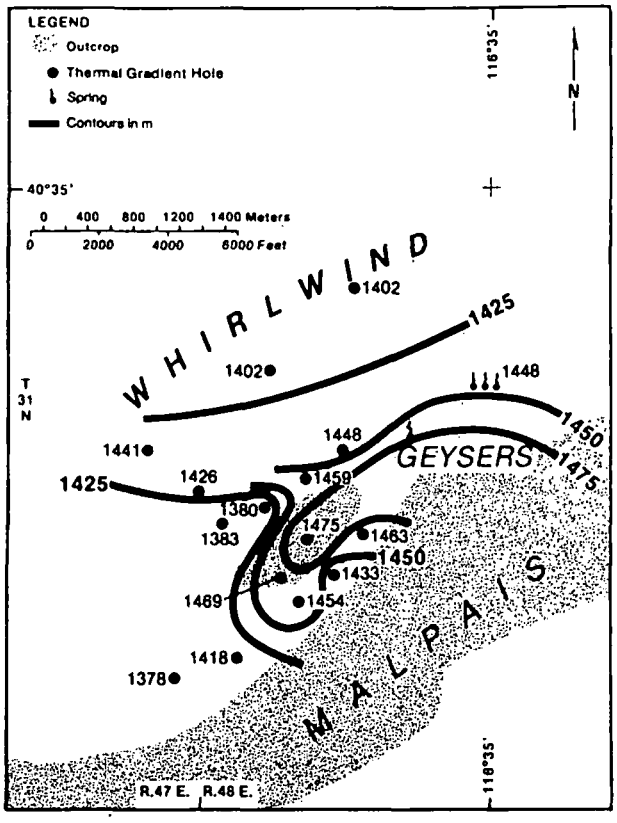

FIG. 9. Map of elevation at top of thermal flow system, contours in meters.

depth is said to be cold; water at higher temperatures is thermal.

Many of the temperature-depth profiles in the Whirlwind Valley contain abrupt downward inflections that are diagnostic of vertical transport of heat by groundwater. The inflections occur at depths ranging between 24 and 134 m and at temperatures from 28°C to 60°C. The relative temperature scale of Figure 7 is used to avoid overlap of several of these profiles. The inflections are keyed with their temperatures. Including the measured temperature at the shallowest depth permits the reconstruction of the actual temperature profiles.

The inflections in the temperature profiles are caused by fluid flow largely within the open annulus of these economically completed exploration holes. To minimize drilling costs, the annulus between the 0.12 m (4.75 inch) drilled hole and the 0.03 m (1 inch) pipe was not grouted. This method of hole completion is not recommended because the open hole forms a conduit for vertical flow. The annulus becomes a poor piezometer, open to the formation over the length of the hole instead of at one isolated interval. Differences in hydraulic head within the formation drive the vertical flow. The temperature inflections are interpreted to occur where the buoyant head of thermal water balances the gravitational head of the column of cold water above. They indicate the level where a dynamic equilibrium is maintained in the hole between rising thermal water and heavier cold water. Their depths probably do not strictly correlate to the top of a particular aquifer or to a true hydraulic head. These data are not optimal but they are usable. They form a mappable horizon interpreted to represent the top of the thermal flow system.

Figure 8 is an illustration of the temperature at the top of the thermal flow system as inferred from inflections like those in Figures 6 and 7. The hot springs around the base of the sinter terrace at The Geysers provide additional data. The near radial symmetry of the temperature distribution suggests that the area of The Geysers contains the principal source of thermal water flowing into the alluvium of the Whirlwind Valley. This symmetry also suggests that the temperature inflections reveal a single, laterally continuous flow system.

The elevation of the top of the thermal flow system is shown in Figure 9. These elevations cannot be corrected for density since the thermal gradient holes are not true piezometers and the inflections are not true hydraulic heads. The contours of Figure 9 reveal the levels to which the buoyant water rises. They reflect neither the radial pattern of the temperature map nor the west-to-east hydraulic gradient of the water table. Thermal water levels are higher within the bedrock southwest of The Geysers than they are in the adjacent alluvium. The high water levels may indicate that upwelling occurs in this area. It is also possible that water from The Geysers is perched above a less permeable horizon of volcanic rock.

Relatively high thermal water levels are sustained within the

alluvium along the buried extension of the Malpais fault zone to the west of The Geysers (Smith, 1979). Since water level and vertical hydraulic gradient data are not available there, it is not possible to decipher the hydrologic system that sustains the high thermal water levels. One plausible flow system would limit the source of thermal water to The Geysers and suggest that it preferentially flows laterally along the fault zone. If this were the case, vertical hydraulic gradient data would probably show only a small vertical component of groundwater flow.

An alternative flow system that would account for the high thermal water levels in the alluvium suggests that the western extension of the Malpais fault zone may be a channel for rising thermal water. If this buried structure were a local source of thermal water, vertical hydraulic gradients along its trace would indicate an upward flow of water.

A few strategically placed piezometers could determine whether the western extension of the Malpais fault zone allows water to rise from depth. If it does, it may prove to be a viable geothermal exploration target or the key to the location of a deep permeable reservoir.

HEAT FLOW

Figure 2 summarizes the mean and standard deviations of the measured thermal conductivities for each of the major rock units in the Beowawe area. All thermal conductivity values were determined using a modified divided bar apparatus at the University of Utah (Chapman et al, 1981). Computations of the thermal conductivities of the 61 drill-chip samples were made using the cell technique of Sass et al (1971b) but were not corrected for in-situ porosity. Uncertainty about the in-situ porosity is the major source of error in the computation of surface heat flow. The porosity of the alluvial and tuffaceous materials may exceed 30 percent; if so, the conductivities mea-

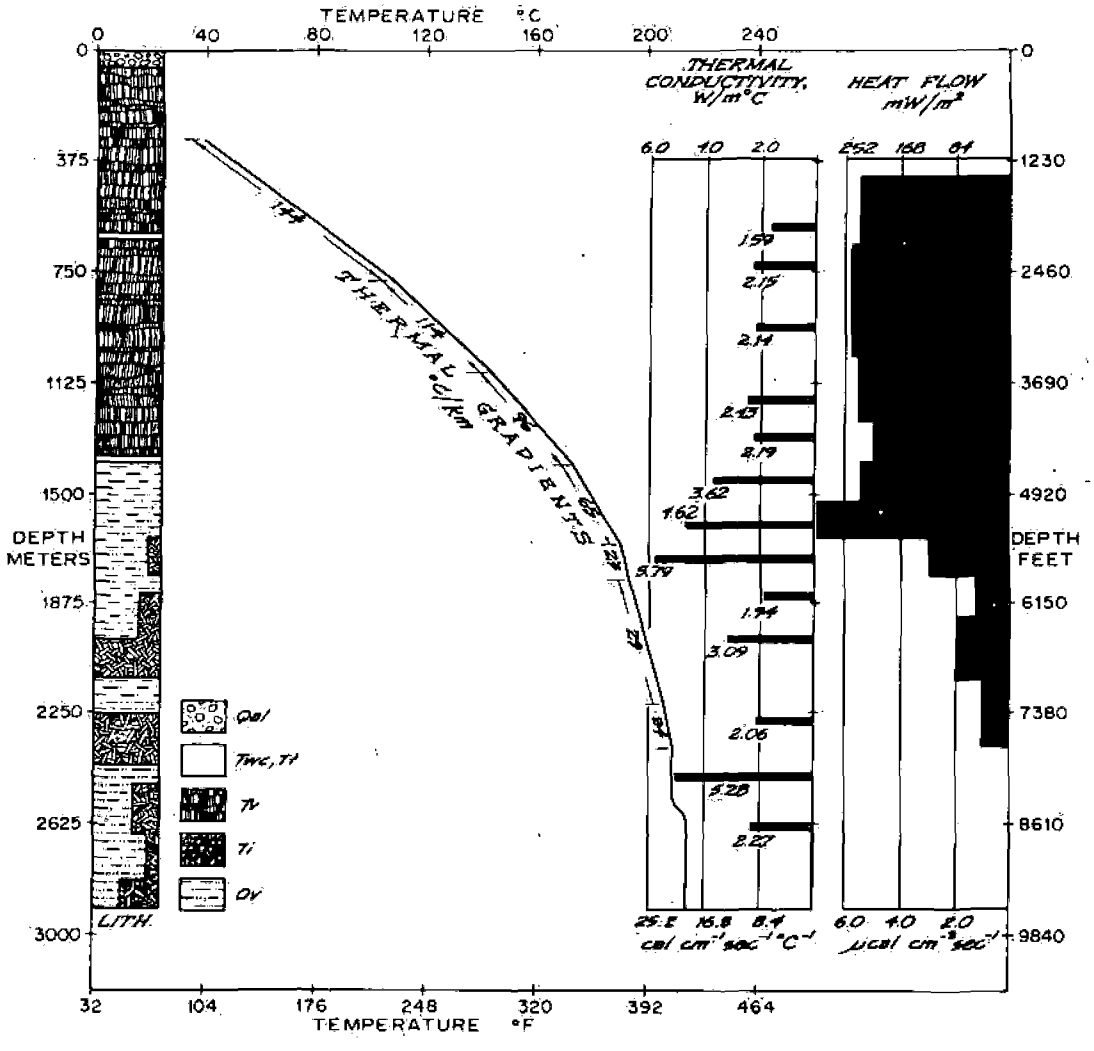

FIG. 10. Generalized lithology, thermal gradients and conductivities, and computed heat flow, Chevron Resources Co. Ginn 1–13 geothermal test well, Whirlwind Valley. Lithologic symbols given in Figure 2.

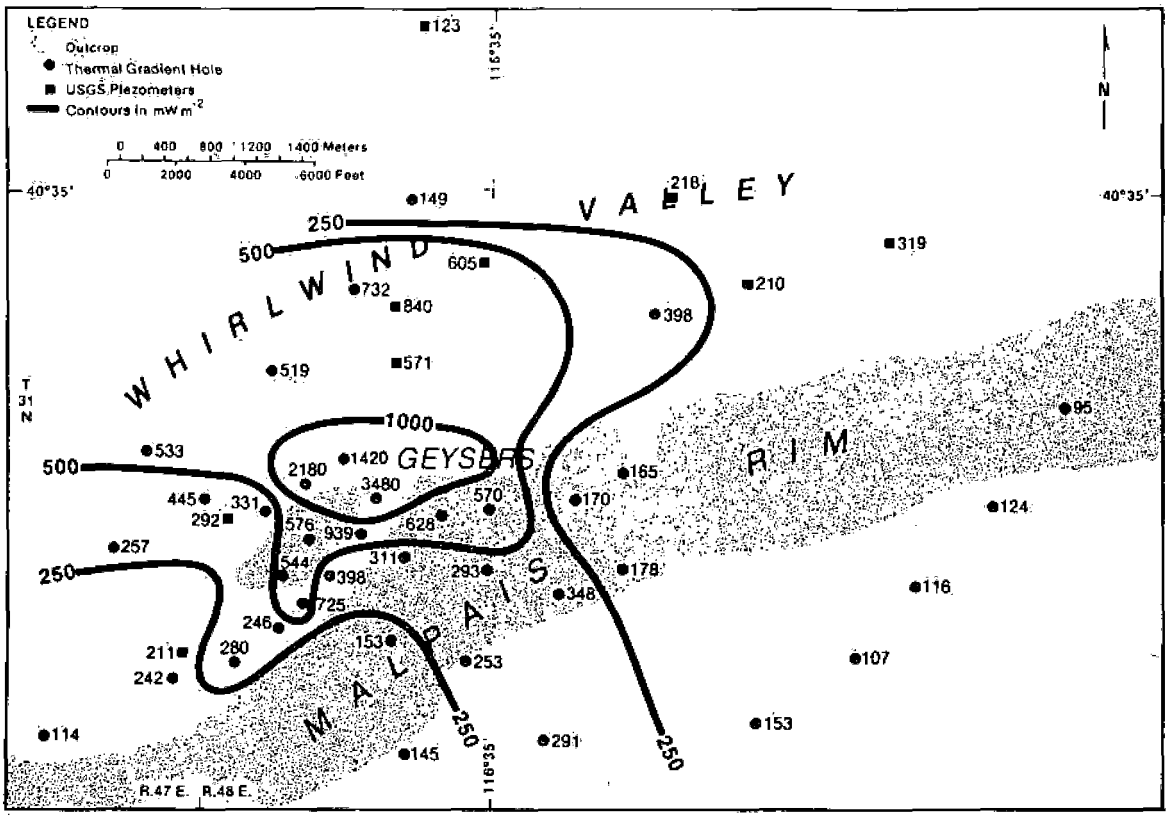

FIG. 11. Map of shallow heat flow, with generalized, variable contour interval in mW/m^2. Discrepancies among neighboring values have been ignored. These differences may be due to the wide range of depths over which the thermal gradient is calculated.

sured for these sedimentary units may be 20–30 percent too large. The matrix porosity of the competent rocks probably averages less than 10 percent and the required correction less than 15 percent.

The low thermal conductivities of the vitrophyric dacite flow and shard-rich tuffaceous sediments reflect their high glass content. The thermal conductivities of the volcanic flow and intrusive rocks cluster around 2 $Wm^{-1}K^{-1}$, but argillization of some of the dacite flows reduces their conductivity significantly. The high thermal conductivity and standard deviation computed for the Valmy formation reflect the preponderance of quartzite in the measured sample and a highly variable lithology.

An equilibrium temperature log of the Ginn 1-13 geothermal test well is shown in Figure 10 (Chevron Resources Co., 1979). The total depth of the well is approximately 2900 m and the bottom-hole temperature 213°C. It is essentially isothermal below a depth of 2400 m within the Valmy formation. Between 1600 and 2400 m, the temperature gradient decreases systematically. The hole either penetrates a hot water-bearing structure or a permeable formation. Given the fractured character of the Valmy (Evans and Theodore, 1978), it is likely that it could contain a high-temperature hydrothermal reservoir.

Above 1600 m, thermal gradients range from 23 to 144°C/km and thermal conductivities from 1.59 to 5.79 $Wm^{-1}K^{-1}$. The inverse relationship between the gradients and conductivities produces a nearly constant conductive heat flow averaging 235 mW/m^2. The uniformity of the heat flow above the inferred deep reservoir indicates that the Tertiary volcanic section acts as a relatively impermeable cap. The thermal water must find permeable structures to rise from depth.

Values of surficial heat flow were computed using linear segments of the shallow temperature-depth profiles like those shown in Figures 6 and 7. As shown in Figure 11, the heat flow generally exceeds the 235 mW/m^2 found in the Ginn test well. Most of the Whirlwind Valley and much of the Malpais Rim appear to receive heat not only from the deep reservoir but also from additional shallower sources. In the Whirlwind Valley, the shallow thermal flow system is a supplemental source of heat.

Along the Malpais Rim, the shallow heat flow exceeds the value from the Ginn well in the area between the two southeast-striking cross faults shown in Figure 1. While it is possible that this area contains conduits for upwelling thermal water, hydraulic head data would be required to resolve whether the fault zone channels water to or away from The Geysers.

A different thermal regime is apparent east of the Dunphy Pass fault zone. Four of the values of heat flow along the Malpais Rim average 110 mW/m^2, near the background value given by Sass et al (1971a) for this portion of the Basin and Range province. The Dunphy Pass fault zone appears to form

the eastern margin of the Beowawe hydrothermal system. The 110 mW/m^2 average value may be realistic for background heat flow.

RECOMMENDATIONS

The hydraulic head of the shallow thermal flow system at Beowawe and most other hydrothermal exploration targets could be readily obtained by converting existing thermal gradient holes to piezometers. The conversion would consist of perforating the casing below the top of the thermal aquifer. In addition, a shallower companion piezometer open below the water table would make it possible to compute the vertical hydraulic gradient at these locations. Even if conduits for upwelling hot water were not located, the hydrologic data would surely augment the existing thermal data and refine the conceptual model of the resource.

Converting ungrouted thermal gradient holes to piezometers may not provide reliable hydraulic head values because of the difficulty of ensuring that the perforated interval is open to only an isolated portion of the aquifer (Benson et al, 1980). However, it should be possible to obtain both hydrologic and thermal data from piezometers that are later converted to thermal gradient holes. In areas where shallow drilling is planned, holes that intersect an aquifer could be initially completed as piezometers. A screen and a wellpoint would be attached to pipe and set at the bottom of the hole, the annulus filled with gravel to the top of the screen and grouted to the surface. After the static hydraulic head is obtained, the screen could be plugged with cement and the hole filled with water, converting it to a thermal gradient hole. Companion piezometers would be needed to obtain vertical hydraulic gradient data. This procedure is recommended as an integral part of future hydrothermal exploration programs.

At any geothermal prospect where drilling encounters water, the water is a source of data. The hydrologic-thermal field procedure recommended here requires repeated site visits and the drilling and completion of additional shallow, thin holes. This expanded exploration program is predicated on the assumption that it is worthwhile to gather as much meaningful data as possible at a reasonable price. The possibility of locating viable deep drilling targets with groundwater hydrology should encourage geothermal exploration managers to incorporate hydrologic data acquisition in their exploration plans.

ACKNOWLEDGMENTS

Funding for this project at the Earth Science Laboratory of the Univ. of Utah Research Institute came from the Dept. of Energy/Division of Geothermal Industry Coupled Program contract DE-AC07-80ID12079. E. M. Struhsacker and J. L. Iovenitti provided geologic guidance. F. H. Olmsted and M. L. Sorey of the U.S. Geol. Survey contributed piezometer data and excellent reviews. Dr. David Chapman and Dr. Leslie Smith of the University of Utah helped develop the ideas about combining thermal and groundwater data.

REFERENCES

Benson, S., Goranson, C., Noble, J., Schroder, R., Corrigan, D., and Wollenberg, H., 1980, Evaluation of the Susanville, California geothermal resource: Lawrence Berkeley lab rep. LBL-1187, 100 p.

Chapman, D. S., Clement, M. D., and Mase, C. W., 1981, Thermal regime of the Escalante Desert, Utah, with an analysis of the Newcastle geothermal system: J. Geophys. Res., v. 82, p. 11735–11746.

Chevron Resources Co., 1979, Open-file data released by Earth Science Laboratory, Salt Lake City.

Evans, S. G., and Theodore, T. G., 1978, Deformation of the Roberts Mountains allochthon in north-central Nevada: U.S.G.S. prof. paper 1060, 18 p.

Freeze, R. A., and Cherry, J. A., 1979, Groundwater: Englewood Cliffs, New Jersey, 604 p., Prentice-Hall, Inc.

Garside, L. J., and Schilling, J. H., 1979, Thermal waters of Nevada: Nevada Bur. Mines Geol., Bull. 91, 163 p.

Getty Oil Co., 1981, Open-file data released by Earth Science Laboratory, Salt Lake City, Utah.

Hubbert, M. K., 1940, The theory of groundwater motion: J. Geology, v. 48, p. 785–944.

Oesterling, W. A., 1962, Geothermal power potential of northern Nevada: Southern Pacific Co. report.

Robinson, E. S., 1970, Relations between geologic structure and aeromagnetic anomalies in central Nevada: GSA Bull., v. 81, p. 2045–2060.

Sass, J. H., Lachenbruch, A. H., Munroe, R. J., Greene, G. W., and Moses, T. H., Jr., 1971a, Heat flow in the western United States: J. Geophys. Res., v. 76, p. 6376–6413.

Sass, J. H., Lachenbruch, A. H., and Munroe, R. J., 1971b, Thermal conductivity of rocks from measurements on fragments and its application to heat flow measurements: J. Geophys. Res., v. 76, p. 3391–3401.

Smith, C., 1979, Interpretation of electrical resistivity and shallow seismic reflection profiles, Whirlwind Valley and Horse Heaven areas, Beowawe KGRA, Nevada: Univ. of Utah Research Inst., Earth Science Lab, rep. no. 25, 43 p.

Sorey, M. L., 1971, Measurement of vertical groundwater velocity from temperature profiles in wells: Water Resources Res., v. 7, p. 963–970.

Stewart, J. H., Walker, G. W., and Kleinhampl, F. J., 1975, Oregon-Nevada lineament: Geology, v. 3, p. 265–268.

Struhsacker, E. M., 1980, The Geology of the Beowawe geothermal system, Eureka and Lander counties, Nevada: Univ. of Utah Research Inst., Earth Science Lab, rep. no. 37, 78 p.

Welch, A. H., Sorey, M. L., and Olmsted, F. H., 1981, The hydrothermal system in Southern Grass Valley, Pershing County, Nevada: U.S.G.S. open-file rep. 81-915, 193 p.

Zoback, M. L. C., 1979, A geologic and geophysical investigation of the Beowawe geothermal area, north-central Nevada: Stanford Univ. Publ., Geological Sciences, v. 16, 79 p.

Geophysical methods in geothermal exploration

C. J. Banwell
Consulting Geophysicist
(New Zealand)

Introduction

Geophysical prospecting may be defined as the art of detecting and interpreting anomalies in the local pattern of certain physical quantities, as measured by suitable sensing equipment and techniques. It is only to be expected that the presence of a geothermal field will affect or distort some of the local physical quantities, and geophysical aids have in fact proved to be of considerable value in the detection and interpretation of geothermal fields.

Geophysical work, however, should not be regarded in total isolation from other subjects. It must proceed in close coordination with geology, hydrology and geochemistry, so that physical measurements may constantly be interpreted and checked. For example, geochemistry can be used as a convenient *physical* instrument, like a sophisticated thermometer or steam detector, valuable both for planning and interpreting geophysical programmes. The location of promising drilling sites is an act of complex *detection that* must eventually be checked by actual drilling; but the intelligent weaving together of *all* survey data, geophysical and other, can often permit the drill holes to be sited to the best advantage. No single method of survey, be it geophysical, geochemical or geological, can be expected to yield a unique and unambiguous result, and the erall picture of a geothermal field and reservoir is built by a continuous process of cooperative data synthesis cross-checks. It will thus be necessary in the course of article sometimes to stray beyond the subject of 'geo-cs' in the strictly limited sense.

inary evidence eothermal field

mal reservoir may be defined as a zone in the st where the temperature, fluid pressure and y are sufficient to permit efficient exploitation, e, the size of the reservoir must be great enough to maintain the desired energy output for a long enough period, and the depth must be shallow enough to keep drilling costs within reasonable economic bounds. In terms of figures, this means that the mean reservoir temperature should generally be of the order of 200 °C or higher, the depth not more than about 2 km, and the volume at least 2 km³. The fluid filling the pore spaces in the reservoir, if steam, would then have a pressure equal to or less than that of saturated vapour at the reservoir temperature (e.g. some 225 psia for 200 °C); or, if hot water, a base pressure of the order of the cold water hydrostatic—say, about 3,000 psia. In practice, a reservoir at the maximum depth and minimum temperature, as quoted above, would seldom be economic to develop: all reservoirs now being exploited on a significant scale lie at depths less than half the maximum and have temperatures appreciably above 200 °C.

A reservoir of even marginal size, temperature and depth would produce a steady state thermal anomaly at the surface, which could readily be measured by present techniques. It can therefore be said, at least in principle, that any reservoir of economic significance can be detected by surface exploration involving no more than shallow drilling and temperature measurements. In practice, heat transfer effects by fluid convection often modify the conductive temperature distribution to an important degree. Movement of cold surface water through permeable formations near the surface can sometimes distort, or almost obliterate, the conductive anomaly, so that gradient holes may have to be deepened sufficiently to allow the necessary temperature measurements to be made below the level of the disturbance. However, the great majority of hydrothermal systems known and explored up to the present are associated with extensive deep circulatory systems which result in discharges of hot water and steam at the surface, accompanied by strong surface temperature anomalies. They are thus readily detected by casual observation; and so many of these zones of surface manifestations are known in various parts of the world that it seems very probable that geothermal exploration, for some time to come, will be mainly concerned with the investigation of

reservoirs whose presence has been betrayed by visible activity. This, however, does not necessarily mean that important thermal reservoirs may not exist without any significant surface evidence, or that they should not be sought by more refined methods of exploration.

World distribution of hydrothermal systems

Attempts have been made by investigators (Banwell, 1967) to define those regions of the earth that offer reasonable promise of geothermal exploitation. Areas believed to have sufficient potential to warrant power development consist of island arcs in the circum-Pacific belt, continental margins bordering the Pacific, parts of Southern Europe and Asia Minor, and transitional rock suites in South-west Italy, Sicily, Iceland, Jan Mayen, Spitzbergen and Central Africa. These areas are of course not necessarily exhaustive, but they contain 'prima facie' evidence of economic geothermal potential.

Most of these fields are associated in some way with vulcanism, although the connection is not always very close, as can be seen from the following list of fields already explored:

Field	Fluid	Source rocks
Larderello	Steam	Fractured limestones; dolomite.
New Zealand, Japan	Hot water	Acid volcanics.
The Geysers, California	Steam	Fractured greywacke.
Cerro Prieto, Mexico; Niland, California	Hot water	River delta sediments.
Pathé, Mexico	Hot water	Fractured middle tertiary volcanics.
Iceland	Hot water	Fractured cavernous basaltic lavas.
Northern Taiwan	Hot water	Acid volcanics and some sedimentaries.

There is no clear correlation either with particular rock types or with geological period, and it seems possible that geothermal fields are better sought on some non-geological basis. Possibly the common factor, if one indeed exists, lies in processes in the upper mantle or crust which in turn lead to areas of high tectonic activity, where magma bodies are injected into the crust and where continual crustal fracturing provides paths by which surface water can penetrate freely to heating zones, and also provides permeable reservoirs in which large quantities of heat and hot fluid (steam or water) can be stored. Fracturing may also result in the escape of some of the heat to the surface, thus providing direct indications of the presence of a hydrothermal system. It should however be mentioned that the deposition of minerals (especially quartz and calcite) from hot water systems will tend to seal the escape paths some distance below the surface, thus increasing the retaining capacity of the reservoir. Storage in *steam* systems, however, may sometimes be dependent on the presence of a pre-existing impermeable capping formation of suitable thickness: this possibly explains why hot water reservoirs of adequate size seem to be more common than steam systems.

Heat flow studies made by other investigators are also of great interest in that they indicate certain other regions where geothermal activity is apparent, though not necessarily of sufficient intensity to justify power generation. Lee and Uyeda (Lee, 1965) have demarcated certain areas of the globe where heat flow is abnormally high. These areas show no evident correlation with the distribution of geothermal areas mentioned in the early part of this section of the article. The most conspicuous zone of maximum heat flow is located over the eastern central part of the African continent. The maximum value is about 1.5 times the global average, and the maximum includes the zone of Ethiopian vulcanism and the Gulf of Aden, where high heat flows have been found on the sea floor. The thermal areas of Italy and Turkey lie near its northern margin, and an area of somewhat lower values extends into Hungary, where significant heat flow anomalies have also been observed. At the present time, little geothermal exploration data from Africa are available, and it would be premature to say whether this major anomaly has any significance of its own for power production.

Preliminary data required

For the initial planning of geothermal exploration before the execution of any true geophysical work, and for the preliminary selection of localised fields for detailed study, it is extremely useful to have a catalogue of basic physical and geochemical data from all the suspected fields. The compilation of a comprehensive catalogue of this sort could well be a major undertaking that would take too long to complete. But advance work in selected areas, where other considerations (e.g. economic, lack of alternative power sources, or special uses for geothermal heat) support early development, would greatly assist in the programming of further stages of the work. The preliminary data in question are those than can be collected fairly quickly, at low cost, and without the necessity for setting up an elaborate field establishment for each promising area. The information required is briefly listed below:

a) *Geographical*

i) Location of field and apparent size of active area.
ii) Topography. Access, roads, land ownership, special problems.
iii) Hydrology. Drainage pattern, rivers, lakes, watersheds.

iv) Climate. Mean temperature and annual range, seasonal distribution of rainfall and annual total.

) *Physical*

i) Location map of thermal features, hot springs, fumaroles, mud volcanoes, steaming ground, hot seepages into rivers and lakes.
ii) Temperatures and estimated discharges from all major features, overall heat and mass discharge.
iii) Suitability of area for shallow surveys (e.g. possible difficulties in penetrating hard surface rocks, disturbance of surface temperature pattern by surface run-off, etc.).

c) *Geochemical*

i) Sampling of principal thermal features (hot springs, geysers, fumaroles, etc.) for the determination of concentrations and ionic ratios of important dissolved and gaseous constituents; the selection of constituents to be determined being in accordance with the most recent recommendations and established methods of interpretation.
ii) Preparation of geochemical maps, showing the distribution of the more important element concentrations and ionic ratios over the whole field.
iii) Sampling of rivers and streams, where appropriate to determine the total rate of discharge of chemical constituents from the field.

The potential importance of the geochemical work as an indirect physical instrument can be very great. It has been shown that the concentrations of certain compounds and elements (e.g. SiO_2 and magnesium) and ionic ratios (e.g. Na/K) in the hot water can give useful preliminary indications of reservoir temperature. In addition, certain chemical equilibria (e.g. CO_2, H_2, CH_4, H_2O) in the gases discharged, and associated carbon isotope exchanges, are temperature-sensitive and can again be used for estimating underground temperatures. It may also be possible to use sulphur isotope equilibria in the same way. Thus several more or less independent ways of making preliminary estimates of reservoir temperature are available, and these may be used to check one another as well as the inferences from purely physical measurements. The presence or absence of certain other mineral constituents in the surface activity can also sometimes be used to discriminate between steam and hot water systems, and this kind of information is obviously very useful both for planning further survey work and for subsequent exploitation programmes.

For the planning and conduct of the next, more detailed, stages of geophysical survey it is of course necessary to give thought to the possible or probable ultimate purpose to which a useful geothermal field, if discovered, would be put. Points to be considered include whether there is a need for electric power only, or whether industrial or other uses could be developed—at least from low grade or waste heat; the minimum acceptable economic life of the field; whether the recovery of chemical components from the geothermal fluids could be economic; whether any special problems arise in the disposal of waste water; etc. Consideration of these problems could influence the choice between two or more promising fields on which exploratory efforts should first be concentrated.

First stage survey

GENERAL

Assuming that a review of the preliminary data has led to the conclusion that a potentially useful geothermal field has apparently been identified, the next object of exploration is to define its location, area and depth; also, if necessary, to improve the precision of some of the preliminary data, such as the heat and mass flows, and to carry out more detailed geochemical work.

MAPPING AND AERIAL SURVEYS

For the efficient performance of this stage of the work it is very desirable to have available good topographic maps, on a scale of 1 : 100,000 or larger and a set of recent stereoscopic aerial photographs on a scale of 1 : 10,000 for survey planning and positional control. Normal and infra-red colour photographs on the same scale can also be useful for outlining possible hot areas in the office before proceeding to the field. If the field is situated close to large bodies of water (lakes or the sea) or on the banks of a river, long wave infra-red scanner images of the area may be of value for mapping hot water seepages as well as the areas of intense ground surface activity. Recent experimental work shows that areas having a heat discharge of about 350 $\mu cal/cm^2s$ (roughly 230 times normal) and upwards can be identified with reasonable certainty. However, it is usually possible to map heat flow anomalies down to much lower levels by shallow surface thermometry, and a special aerial infra-red survey would be justified only in exceptional circumstances. Preferably, surveys of this kind, if they are to be made, are best undertaken at the same time as other aerial mapping and photographic projects.

At the outset of all field work it is important to set up a survey network and a system of benchmarks and permanent blocks at a sufficient number of points to allow all maps resulting from the surveys to be related to a common grid. Also it is very helpful for correlating the data collected to have all maps either on the same scale or, if this is inconvenient for some surveys, on the smallest possible number of different scales. If a precise regional map reference grid exists, maps should be related to this if practicable; otherwise a provisional local grid should be set up for later tying in to the principal network. Field parties should be provided with copies of printed or duplicated map blanks with the grid and showing the positions and levels of all reference blocks, trig points and major topographic features.

SURFACE TEMPERATURE AND SHALLOW RESISTIVITY SURVEYS

The object of this survey is to delineate the hot area and its margins more precisely, with a view to determining the conductive heat discharge, the location of the less conspicuous anomalies, and the correlation of the heat flow pattern with local topography, drainage, etc. The choice of method will depend on the type of surface cover predominant in the area. If it is mainly of loose pumice soil, ash or sediments, the 'one metre probe' method, using a perforating tool and bi-metallic thermometer, is both rapid and inexpensive. If the terrain is rocky or covered with hard sintered deposits it would be better to substitute shallow resistivity measurements in place of direct temperature readings. Since ground resistivity is influenced by temperature (Keller, 1970), the discovery of a resistivity anomaly can be indicative of a temperature anomaly. (Figures of only a few ohm-metres may be recorded in hot water reservoirs, as compared with several hundred ohm-metres or more in 'normal' areas.) The so-called 'electromagnetic gun', a portable inductive device, is convenient for carrying out a resistivity survey with a penetration of 25 to 30 m.

Subject to topography, it is generally convenient to carry out either type of survey (temperature or resistivity) with station spacings of 50 to 100 m. The larger spacing should still be close enough to avoid missing any features of importance, since a geothermal field of minimum economic size is unlikely to cover less than 2 or 3 km^2.

The form and position of an anomalous area should be considered in relation to possible direction of ground water movement, as indicated by the topography and general drainage direction through the area. If disturbances of this kind are large, the true position of the reservoir at depth may be considerably displaced upstream from the surface patterns, and possibly also from the area of surface activity.

ESTIMATION OF ENTHALPY

In most known hydrothermal systems, surface radiation and conduction account only for a negligible fraction of the total natural heat discharge from a thermal area. Practically all this discharge is brought up from below by convecting hot water or steam. Provided that the total mass and heat content of all fluids escaping from the area are accurately measured, and provided that proper correction is made for dilution by local cold surface water (and this can be done by chemical means—see Mahon, 1970), then it is possible to deduce the enthalpy of the fluid at depth from the ratio of heat flow to mass flow. It is important, for this purpose, to include the heat and mass losses from all warm springs and river seepages round the margins of the area. Some of these marginal seepages may be well disguised in rivers, lakes or general ground water movements across the area.

Physical enthalpy, measured in this way, may be compared with the value derived from geochemical estimates of reservoir temperature. If agreement is good, the result may be regarded as satisfactory; but if poor, a more careful check should be made of all possible routes of surface heat loss. An interesting example of this occured in the Broadlands field in New Zealand. Enthalpy calculated from observed heat and mass flows was at first much lower than that derived from drillhole temperature data. Further measurements revealed a large additional heat flow into the Waikato River from warm springs discharging very low chloride water made up of ground water heated by sub-surface steam. Because the chloride content of this water was much lower than that of the reservoir water, it had been missed in the earlier chemical measurements made in the river upstream and downstream of the thermal area: only the physical measurements (precise temperature and flow measurements in the river) revealed the missing heat. With this correction the different estimates of enthalpy came into much closer agreement.

Second stage survey

GENERAL

This stage will probably proceed as a continuation of the first stage, or may even begin before the first stage is completed as soon as some preliminary data become available as to size and location of the shallow temperature anomaly.

DEEP ELECTRICAL EXPLORATION

This means resistivity measurements by electrical techniques involving current injection and voltage measurements by means of separate sets of electrodes in contact with the ground (as distinct from electromagnetic or induction methods which do not involve the drilling of any holes or even making electrical contact with the ground at any point). Most commonly used are the Schlumberger or Wenner electrode arrangements, which differ only in the spacing of the current and voltage electrodes in a single line.

The recommended method will generally be a series of Schlumberger traverses (van Nostrand and Cook, 1966) over the area of the surface thermal anomaly and as far outside as may be necessary to find apparently normal resistivity values. A 'traverse' is made by selecting a fixed electrode spacing and taking successive readings by shifting the whole set of electrodes along the survey line.

In addition to the traverses a number of soundings should be made at selected points to determine the vertical resistivity distribution and possible layering of different formations. A 'sounding' is made by keeping the centre of the electrode system at a fixed point and increasing the linear scale of the electrode pattern from low to high values.

'Traverses' are used for mapping the horizontal variations of the mean resistivity (taken over some chosen range

of depths depending on the electrode spacing used) over the survey area. 'Soundings' give the variations of average resistivity as an increasing range of depths is included in the average. The graph of apparent resistivity against electrode spacing ('sounding curve') can be used to calculate the parameters (thickness and electrical resistivity) of the layers of a hypothetical underground model made up of a series of horizontal beds.

A supplementary geological survey may be of value at this stage if it can suggest the probable thickness and compositions of these layers. If clay, or clay-bearing formations, of significant thickness are present in the survey area, these may give low resistivity zones which are not associated with thermal anomalies. A geological study which can predict such formations and give their depth and thickness with reasonable precision can be of considerable value for interpretation.

The effective depth of penetration of resistivity traverses and soundings in low resistivity formations can sometimes be seriously limited by 'skin effect' if alternating current, or switched direct current of too short a period, is used. It is generally advisable to use direct current methods where possible. But if the equipment available permits only the use of alternating current, the penetration should be calculated from the frequency used and the measured resistivity, in order to avoid possible erroneous interpretations of the sounding profiles. It should also be noted that sounding profiles can be distorted if the soundings are carried out in a field of limited size, or too close to the boundary, the effect usually being to give an apparent increase of resisitivity at maximum spread.

Subject to these limitations the soundings should be carried out up to theoretical penetrations of about 3 km so as to obtain as complete a profile as possible. From the soundings it should be possible to deduce whether the reservoir is filled principally with steam or with hot water, thus checking earlier preliminary conclusions. In a hot water field the resistivity pattern takes the form of a central 'low', representing the porous reservoir rocks filled with hot chloride water, surrounded by a region of rapidly increasing resistivity outside the hot area. In a steam field, on the other hand, there would probably be a central resistivity 'high', because the reservoir rocks are now filled with steam which has low electrical conductivity, surrounded or overlain by lower resistivity zones containing steam-heated ground water and condensate. In actual fields, things are seldom quite so simple, and resistivity alone will seldom give a complete answer. As already stated, the presence of clay formations can behave deceptively like hot water reservoirs. Resistivity 'highs' within one area of low values can also sometimes be due to buried masses of impermeable rocks such as rhyolite domes, massive lava flows, etc.: these can sometimes be detected and mapped by seismic (refraction) surveying, by gravity or magnetic mapping, or from geological evidence. Thus evidence based on resistivity should always be cross checked against evidence based on other methods.

An apparent hot water reservoir can be readily mapped by means of traverses, using a current electrode spacing of about 500 m, giving an effective penetration of some 250 m. With a steam reservoir it is possible that overlying confining formations will have a lower resistivity than the reservoir rocks, which may therefore be identified by a resistivity rise in the soundings. Owing to the limitations mentioned above, however, checks by thermal gradient measurements are advisable.

Before leaving the subject of deep resistivity measurements, it may be mentioned that variants of the electrode arrangement (e.g. the so-called 'dipole-dipole system') can be used with good effect for mapping horizontal discontinuities (e.g. faults, boundaries of hydrothermal systems, geological contacts, etc.) and this can often serve for checking proposed geological models. Geological models can also sometimes be used for the preliminary interpretation of sounding curves.

Electromagnetic methods have also been proposed for deep resistivity surveys, though rather different approaches would be needed (Keller, 1970; Strangway, 1970). These may have useful application after further development, but not much use has yet been made of them for geothermal exploration. (See also Meidav, 1970.)

THERMAL GRADIENT DRILLING

Holes for thermal gradient measurement must be drilled deep enough to penetrate any surface formations liable to be disturbed by ground water movement, and they should extend far enough into the undisturbed zone below to give reliable gradients. Although it may sometimes be possible to estimate the thickness of the disturbed layer from geological or other evidence, it is very desirable to check whether a hole is deep enough by measuring temperatures at multiple points spaced about 2½ m apart over the bottom 20 m of the hole. If the measured temperatures fall on a straight line when plotted against depth, the deduced gradient is probably reliable; otherwise, the hole must be deepened or the area avoided. In general, very little will be learned by drilling gradient holes too close to the areas of surface activity; the gradient will be subject to disturbance by upward movement of hot water or steam, and the holes will be liable to erupt.

If gradient holes are drilled on a regular grid pattern with a spacing of 1 km, a thermal anomaly of reasonable size (covering, say, 10 km^2), could be mapped, inclusive of margin areas, with an array of 20 to 30 holes. A hole density of this order should suffice for all but the most detailed mapping, since experience has shown that lateral temperature variations below the surface convective zone are generally not very rapid. Additional holes could, however, be necessary in some fields if marked discontinuities in the temperature pattern indicate corresponding structural features, such as faults, contacts, etc., which might in some cases also be checked against geological data. As a general rule these gradient holes would be too shallow (30 to 40 m) to provide much new information about structure, but

coring for geophysical or geological information could be profitable, at least on a trial basis, in a few holes.

For actual temperature measurements various instruments may be used. For temperatures much over 100 °C a geothermograph or Amerada gauge is suitable. For lower temperatures it may be convenient to use thermo-couples, thermistors, platinum resistance thermometers, or even mercury maximum thermometers with proper precautions. Electrical instruments can be wired up differentially so as to measure the gradient directly, though this is seldom done in practice. Care must be taken, with electrical instruments, to ensure that the cable insulation is suited to the temperatures to which it is exposed. Nylon or pvc is suitable for moderate temperatures, while mineral insulation or such materials as 'Teflon' may be required for higher temperatures.

Third stage survey

SUNDRY GEOPHYSICAL AIDS

Little or nothing has hitherto been said of the following geophysical techniques which have been used or recommended from time to time for geothermal exploration:

Dipole resistivity
Magnetic
Gravity
Seismic (reflection or refraction)
Microwave
Radio-frequency interference
Ground noise
Micro-seismicity

. This is because it will often be unnecessary to use any of these aids to bring the investigation to the point where a deep exploratory hole can be planned and sited. On past occasions there has perhaps been a tendency to undertake some of these specialised surveys solely in the belief that they may perhaps be useful in some way or another. In this way, considerable expenditure can be incurred of money, time and effort in producing maps which, though of potential *research* value, may do little or nothing to promote the search for an exploitable geothermal reservoir.

Nevertheless, in an actual survey problems could arise which some of these techniques could help to resolve; they could perhaps account for anomalies in the temperature or resistivity patterns. But the choice of technique, and the justification for using it at all, must arise in, and be defined by, the progress of the basic survey. Thus a seismic survey could be of possible value if it permitted any discontinuities or other features of the resistivity soundings to be identified in terms of other physical properties, or if it enabled their depths, extent and thickness to be checked. Seismic surveying could also have potential value in locating zones of low velocity, low wave frequency or high attenuation, which could be associated with a steam or hot water reservoir (Hayakawa, 1970). Similarly a ground noise survey, though its precise application is still under trial at present, might be used to check the reservoir location suggested by other surveys; and a geological study would be of value if it could provide relevant advance information about the physical properties of the underground formations (porosity, permeability, density, seismic velocity, depth thickness and continuity).

ESTIMATION OF RESERVOIR CAPACITY

Completion of this stage of the exploration programme should enable a first estimate to be made of the power potential, using the family of curves published by Banwell (1964). Taking the area indicated by the deep resistivity and surface gradient measurements, and the reservoir temperature implied by the geochemical studies, it is possible to deduce from the curves the approximate field potential in megawatt-years. Thus, for example, a thermal anomaly with a horizontal area of 10 km^2 and an inferred reservoir temperature of 260 °C would have an estimated potential of about 4,000 MW-years, or sufficient to maintain an output of 200 MW for 20 years. This estimate is believed to be conservative, as it assumes a hot water system with a boiling point/depth distribution and an energy yield of only 25% of the theoretical.

Fourth stage survey: deep exploratory drilling

The foregoing programmes should have outlined the surface projection of the presumed steam or hot water reservoir, its depth and probable temperature, and the sequence of formations to be traversed, together with some indication of their physical properties. The value of a deep hole is to test the proposed model by providing quantitative data, first from cores and later from temperature measurements, followed by production tests if the hole taps a productive zone. Projected drilling depth will depend on expected reservoir depth and thickness, but it is suggested that a minimum of 1 km should be planned for unless special circumstances should suggest otherwise.

If it is thought important that steam should be produced from the first hole, it will be desirable to try to locate it so as to intersect permeable formations at reservoir depth. A connection between surface fault traces and the existence of permeable zones has been claimed in some fields. It has also been suggested that the presence of both vertical and horizontal fissures, which could provide gas or steam paths, can be predicted by seismic records. The use of the surface fault criterion, taken alone, is apt to be severely limited by the fact that in most areas a very large number of fractures and fault traces can be mapped from aerial photographs and surface surveys, whereas very few, if any, of these may prove to have any immediate connection with thermal activity or reservoir permeability. There may perhaps be some general connection between surface faulting and reservoir permeability in that the presence of numerous

young faults above the reservoir could indicate a good probability of drillholes intersecting permeable zones in the reservoir, but it would be unwise to depend on any closer relationship. In the absence of more definite information on the distribution of reservoir permeability, holes may be sited in relation to surface fault traces as well as by any other means; but the success or failure of the first few holes, however sited, to give satisfactory production, can give only very limited information about overall reservoir permeability.

Possibly, the only general criteria for the siting of deep exploration holes are as follows:

(i) The sites should be far enough away from areas of surface activity and hot ground to avoid the risk of blow-outs at shallow depth in the early stages of drilling and casing;

(ii) Subject to (i), most holes should be located well within the boundaries of the reservoir as indicated by deep resistivity and gradient surveying;

(iii) Despite (ii), some test holes should be drilled well out on the boundary of the apparent reservoir, to check the correctness of its limits and the form of the temperature/depth curve near the boundary;

(iv) Holes should be well distributed over the reservoir area, without too many in one line, so as to permit a three-dimensional 'model' of the reservoir to be prepared as early as possible.

The coring programme for these holes should be planned to provide enough samples to allow the relevant physical properties of each of the formations identified by the preceding surveys to be determined. In addition, samples are needed from zones characterised by their physical state —e.g. temperature, presence of steam or water in the pores, or cementation by mineral deposition or transformation. Petrological examination of core material can also show significant mineral changes due to hydrothermal alteration, and the nature and extent of these changes can give an indication of the temperature at which they took place.

The core data can now be used, in conjunction with the models derived from the previous surveys, to construct a series of sections showing the distribution of physical properties through the volume surveyed. These sections can then be used to interpret and refine the earlier survey data and possibly to suggest other surveys that could be profitable. It could be decided, for example, whether any features of the density distribution are important for the further evaluation of the field, and whether they will give large enough anomalies at the surface to justify a gravity survey. Core data can of course also be used to construct geological sections if required.

After completing each hole, temperature measurements should be made at regular intervals over the full depth until stable values are reached. Aquifer pressure measurements should also be made at several levels, assuming the hole is partly filled with water, and chemical samples taken from levels of interest. After this, the hole, if hot enough, should be allowed to discharge, the output should be measured, and the steam and water should be sampled for chemical analysis.

Data from the first few holes will have an increasing influence on the siting of those to follow. Also, if reservoir conditions prove favourable, an increasing number of these holes will be available for production, with the result that the diameter, depth and placing of many new holes will be decided by engineering and field layout considerations. However, data from some of these production holes will still be worth gathering to improve the picture of the field and of reservoir geometry and conditions; while the chemistry of the water and steam produced, and the changes in this chemistry that occur as exploitation proceeds, will give further important information about the reservoir, its relation to its surroundings, and its probable useful life.

Effects of exploitation on the field

As the exploitation of the field proceeds, the withdrawal of steam or water from the reservoir and the inflow of recharge fluid from outside will affect the hydraulic balance and pressure distribution, both in the reservoir and in the surrounding areas. Pressure changes can be monitored by regular measurements in the various prospecting and production holes, while the mass balance can be checked by surface gravity measurements. To do this satisfactorily, it is advisable to set up a network of permanent gravity stations over the area, preferably before production begins, and to carry out precision gravity surveys (to within about $\pm$ 0.01 milligal, or better) at intervals of approximately one year. Comparisons between the gravity values from these annual surveys will show within quite close limits whether the reservoir is being depleted by draw-off, and to what extent the fluid removed by exploitation is being replaced. The exploitation of a field can eventually result in measurable ground level changes.

Bibliography

BANWELL, C. J. 1961. Geothermal drill-holes: physical investigations. *Proc. U.N. Conf. on new sources of Energy. Rome, 1961*, vol. 2, p. 60-72 (E/CONF 35/G/53). New York, United Nations.

——. 1967. Geothermal power. *Impact Sci. Soc.*, Paris, vol. 3 XVII (1967) no. 2, p. 149-166, table 2.

DOBRIN, Milton B. 1960. *Introduction to geophysical prospecting*. New York, Toronto, London, McGraw Hill. i-ix + 446 p.

HAYAKAWA, H. 1970. The study of underground structure and geophysical state in geothermal areas by seismic exploration. *U.N. Symp. on Geothermal Energy. Pisa, 1970.*[1]

HUNT, T. M. 1970. Net mass loss from the Wairakei geothermal field, New Zealand. *U.N. Symp. on Geothermal Energy. Pisa, 1970.*[1]

KELLER, G. V. 1970. Induction methods in prospecting for hot water. *U.N. Symp. on Geothermal Energy. Pisa, 1970.*[1]

LEE, W. H. K. 1965. *Terrestial heat flow.* Washington, American Geophysical Union (Monograph no. 8). See map, fig. 44, by Lee and Uyeda.

MAHON, W. A. J. 1970. Chemistry in the exploration and exploitation of hydrothermal systems. *U.N. Symp. on Geothermal Energy. Pisa, 1970.*[1]

MEIDAV, T. 1970. Application of electrical resistivity and gravimetry in deep geothermal exploration. *U.N. Symp. on Geothermal Energy. Pisa, 1970.*[1]

NOSTRAND, R. G. van; COOK, K. L. 1966. Interpretation of resistivity data. *Prof. Pap. U.S. geol. Surv.*, 499. Washington, U.S. Government Printing Office. (Library of Congress catalog-card no. GS 65-322. For sale by Superintendent of Documents, U.S. Government Printing Office, Washington D.C. 20402.) i-xi + 310 p.

STRANGWAY, D. W. 1970. Geophysical exploration through geologic cover. *U.N. Symp. on Geothermal Energy. Pisa, 1970.*[1]

1. Published by the Istituto Internazionale per le Ricerche Geotermiche, Lungarno Pacinotti 55, Pisa.